WADC TECHNICAL REPORT 54-557

STUDY ON A-C GENERATING MACHINE CHARACTERISTICS FOR AIRCRAFT ELECTRIC SYSTEMS

HERMAN J. BRAUN
HOMER B. JAMES
RAYMOND P. JUDKINS
RICHARD E. KLOKOW
CHARLES F. YOHE

WESTINGHOUSE ELECTRIC CORPORATION

31 DECEMBER 1954

[redacted]

EQUIPMENT LABORATORY
CONTRACT No. AF 18(600)-402
RDO No. R-656-2112A-9

WRIGHT AIR DEVELOPMENT CENTER
AIR RESEARCH AND DEVELOPMENT COMMAND
UNITED STATES AIR FORCE
WRIGHT-PATTERSON AIR FORCE BASE, OHIO

Carpenter Litho & Prtg. Co., Springfield, O.
100 - June 1957

FORWARD

This report was prepared by the Aviation Engineering Department, Westinghouse Electric Corporation, Lima, Ohio, under Contract No. AF 18(600)-402. The contract was initiated under Research and Development Order No. R-656-2112A-9 and was administered under the direction of the Equipment Laboratory, Directorate of Laboratories, Wright Air Development Center, with Mr. Earl Rowland acting as project engineer.

This report was under the supervision of H. J. Braun. The report was prepared by H. B. James, R. P. Judkins, R. E. Klokow, and C. F. Yohe. Also assisting with the material was P. F. Boggess and H. K. Omer.

ABSTRACT

The results of a study of the characteristics of aircraft alternating-current generators are presented in this report. Emphasis has been placed on the transient performance of the generator in conjunction with other elements of isolated electric power systems. Other topics covering a-c generators and their exciters are also included.

Test methods are given which are used to obtain the pertinent characteristics and parameters of aircraft a-c machines.

From these studies it is concluded that a-c generator parameters cannot be absolutely specified, for these factors are dependent upon other conditions in the generator-regulator system.

PUBLICATION REVIEW

The publication of this report does not constitute approval by the Air Force of the findings or the conclusions contained therein. It is published only for the exchange and stimulation of ideas.

FOR THE COMMANDER:

J. E. ROWLAND
Chief, Systems & Power
Conversion Section
Electrical Branch
Equipment Laboratory

TABLE OF CONTENTS

TABLE OF CONTENTS (Continued)

TABLE OF CONTENTS (continued)

TABLE OF CONTENTS (continued)

TABLE OF CONTENTS (continued)

LIST OF ILLUSTRATIONS

CHAPTER III

CHAPTER IV

CHAPTER V

APPENDIX A

APPENDIX B

APPENDIX C

APPENDIX D

APPENDIX E

LIST OF TABLES

CHAPTER I

INTRODUCTION

I-A PURPOSE

This report gives the results of a study of the characteristics of rotating alternating-current electric machines for aircraft electric systems. This study was undertaken to determine specification requirements for these characteristics and to establish standard methods for measuring these characteristics. These a-c generator characteristics, which would be recommended as specification requirements, were to be optimum values which would assure stable and reliable operation of all components as an integrated electric system.

After the work of this project had progressed to a considerable degree, it was determined that specific recommendations were practically impossible. This was true because of two reasons. First, it was evident that there were different and conflicting requirements in the specifications covering various types of aircraft electrical systems. Second, within the requirements of any one specification, it is possible to satisfactorily meet the required performance with an infinite number of possible designs of the a-c generator and other components of the system. This latter reason was most important and was a result of a considerable amount of study by means of analogue computer techniques. This method of study demonstrated the difficulty involved in attempting to arrive at an optimum value for any of the various characteristics or constants which describe an a-c generator. It was felt that the most useful service would be provided by determining the performance for various system component parameters. With such information at hand, the electric systems designer can select the type of power supply which best suits his needs.

I-B SCOPE

This study was undertaken, as stated above, to specify standard requirements and standard test procedure for the characteristics and parameters of the a-c machine. These parameters and characteristics were selected because of their importance to the transient performance and the stability of the electrical system. These were as follows:

A-C Generator Reactances

Direct-axis synchronous reactance
Direct-axis transient reactance
Direct-axis subtransient reactance
Quadrature-axis synchronous reactance
Quadrature-axis transient reactance
Quadrature-axis subtransient reactance

A-C Generator Symmetrical Component Impedances

Positive sequence impedance
Negative sequence impedance
Zero sequence impedance

A-C Generator Time Constants

Direct axis transient open-circuit time constant
Quadrature axis transient open-circuit time constant
Short circuit time constant of armature
Direct axis transient short-circuit time constant
Direct axis subtransient short-circuit time constant
Quadrature axis transient short-circuit time constant
Quadrature axis subtransient short-circuit time constant

Miscellaneous

Exciter response
Voltage regulator time constant
Overload ratings
Ceiling voltage-speed characteristics
Excitation data

A number of the listed characteristics and parameters are of little interest when the study is restricted to conventional a-c synchronous generators. For example, the quadrature-axis time constants are of little value where salient-pole machines are used since their value is negligible. Also the subtransient quantities, both reactance and time constants, have been of little importance in most of the aircraft systems because of the

short duration of this component.

By using only zero-power-factor loads it was possible, while studying the transient performance, to eliminate the quadrature-axis reactance from the problem. Some comments are made on this parameter, however, under parallel operation. Some of the miscellaneous parameters were considered, to a degree, under transient performance. Overload ratings are covered in the chapter on a-c generators.

It is pointed out that the systems studied were those which utilize carbon-pile voltage regulators. The magnetic-amplifier-type voltage regulator has become the newest addition to aircraft electrical systems. The significance of this type regulator is now recognized, but at the time the work was outlined for the project such regulators were in the development stages and were therefore not included in the transient performance studies. The parallel system tests did include the newer regulator, however. This test data, given in Appendix D, presents a comparison between the two regulators.

Further statement with regard to the scope of this report is necessary. It was felt that most of the requirements in existing specifications concerning steady-state operation of the a-c electric systems have been adequately taken care of in the past, and that the most important remaining problems exist in the transient performance of these systems. Therefore, a major part of the time devoted to this project was used to study by means of computer techniques, the transient phenomena of the three major systems which were a part of the report. The manner in which this work was accomplished was to establish on the computer the dynamic relationships which exist in the actual machine as presently built. This was done by mathematical analysis, investigation of laboratory test data, and work on the computer in an empirical manner. When finally the performance on the computer matched that which was obtained from actual test machines, parametric studies were made on this "base" system. Most of these investigations concern the constants and characteristics of the a-c generator with some work on the other elements in the system. As pointed out in the outline of material in this chapter, most of the results obtained from this computer study are found in Appendix A of the report. Conclusions based on this data are found in the last chapter of the main body.

The approach here is to also recount some of the more important known considerations in designing a-c machines. For this reason one will find, in all the chapters of the main body of the report, material which is available from other sources. These considerations, however, are felt to be

important in the design of a-c machines. This treatment of available material is by no means exhaustive, but it is hoped that enough information is presented to enable the reader to gain an insight into these factors. Reference is made throughout the report to significant literature on the various topics covered.

I-C METHOD

The method of attack used to study the characteristics of a-c electric machines was multiple.

(1) Analogue computer techniques were utilized to study the transient performance of the complete system: a-c generator, d-c exciter, carbon-pile regulator, and the feedback circuits.

(2) Mathematical analyses of idealized circuits were used to augment the computer results.

(3) Test results on actual machines and actual systems were used as a basis for comparison with computer data and calculated data.

(4) Other studies were made which would reduce the theoretical results to a practical level, one which can be achieved with known techniques and materials.

(5) A survey of the aircraft electrical industry was made to determine the desires of those persons concerned with a-c system performance.

I-D OUTLINE OF MATERIAL

The report is divided in the following manner:

(1) Chapter II covers a-c synchronous generators, both under steady-state and transient operating conditions. A review of existing literature is augmented with special treatments of such factors as the voltage recovery after removal of load and the effect of winding and dimensional changes on machine parameters.

(2) Chapter III deals in a general manner with the d-c integral exciters which were used in the systems studied. A clarification of the problem of eddy-currents in the exciter is presented.

A brief treatment of the voltage regulators which were employed in this study is given at the end of this chapter.

(3) Chapter IV presents the test methods and test procedures used to measure the various a-c generator characteristics and constants. Various tests on the exciter are also considered.

(4) Chapter V is a brief treatment of parallel operation of a-c generators.

(5) Chapter VI is devoted to the conclusions and recommendations based on material in the main body of the report and in the appendixes.

To substantiate the main body of the report and also to add background material of interest to the reader, there are six appendixes. Appendix A covers the analogue computer studies and the results of this work. Appendix B covers four separate sections: (1) a mathematical treatment of overvoltage resulting from load removal, (2) a resume of the equations used by Kilgore to relate a-c generator constants to the magnetic circuit geometry and winding configurations, (3) material on the effect of variations of machine dimensions and windings on the weight, reactances, time constant and gain of the a-c generator and (4) a treatment of the calculations used to describe the eddy-current phenomena in d-c exciters. Appendix C presents actual data obtained on five different a-c generators; this data was used to set up the computer for the studies in Appendix A. Appendix D is concerned with actual mock-up test results of a parallel a-c systems using 40-Kva a-c generators. A comparison between the carbon-pile voltage regulator and the magnetic amplifier voltage regulator is given for most of the conditions which may exist on a parallel system. Appendix E deals with a survey made of the aircraft industry to determine what requirements are desired from a-c systems and a-c generators. Appendix F is a glossary of definitions and symbols pertinent to the report.

CHAPTER II

A-C SYNCHRONOUS GENERATORS

II-A INTRODUCTION

The purpose of this chapter is to discuss various aspects of the a-c synchronous generator as used in aircraft electric systems. Both steady-state and transient characteristics are treated. Saturation affects are pointed out at various conditions where they apply.

Under the category of steady-state characteristics a method is given for calculating the zero power-factor saturation curve including the affect of pole leakage flux. There are brief discussions on field form, harmonics at balanced loads, and overload capacity. Considerable attention is given to the determination of terminal voltages with unbalanced loads using symmetrical component analysis.

In the section on transients there is an explanation,in terms of the constant-flux-linkage theorem, of the flux and current relationships when a three-phase short circuit is applied. The discussion also pertains, with slight modification, to other zero power-factor loads. Some of the transient mathematical treatments which have been made in the past are reviewed. New work is presented on the overvoltages which occur when load is removed from an a-c generator.

The remainder of the chapter deals with the affect of generator design changes upon the machine constants. The reactances, open-circuit time constant, gain, and weight are given for a number of generators all of the same steady-state rating. This work should be very useful in designing new aircraft electric systems.

II-B SYNCHRONOUS MACHINE STEADY-STATE CHARACTERISTICS

The general theory for salient pole machines at steady-state operation is well covered in the literature [1, 2, 3]. The material included here is intended to briefly review the major characteristics and to supplement other portions of this report.

II-B-1 Saturation Curves - Figure II-1, curve A, shows a typical no-load saturation curve. The curve data may be readily determined by test, as described in Chapter IV, or calculated with a fair degree of accuracy. A good basic procedure is given in Kuhlman's text [4]. The zero power-factor, rated current, saturation curve may also be obtained by test or be calculated. For a salient pole machine, the calculation must take into account the increase in pole leakage flux under load conditions. The method described in the following paragraphs was used in connection with this study and the results obtained agree very well with those obtained by test.

The general calculation procedure is as follows:

(a) Obtain a no-load saturation curve corrected for increased pole leakage corresponding to rated load current at zero power-factor as indicated by curve A' in Figure II-1.

(b) Calculate the armature demagnetizing mmf at rated current and zero power-factor, which is represented by line a-b on the diagram.

(c) Calculate the armature leakage reactance drop for rated current indicated by line a-c on the diagram.

(d) Move the triangle a-b-c so that c traces curve A', holding line a-b parallel to the horizontal axis, then the zero power-factor, curve B, is generated by b.

The armature leakage reactance, x_ℓ, is readily calculated as outlined in Appendix B-2, and the armature demagnetizing equation (given in reference 4) is easily applied. Determining the corrected no-load saturation curve A', however, is somewhat tedious.

For example, a correction will be made at voltage E_1 and the corresponding field excitation of F_1. The pole leakage flux at no load $\phi_{\ell 1}$, is calculated using the leakage path permeance and the field mmf F_1. At rated current zero power-factor load, the field excitation, F_a, is estimated for a generated voltage of E_1 (anticipating that it will be larger than F_a'), and the leakage flux is again calculated giving $\phi_{\ell 1a}$. The relationship between the machines generated voltage and air-gap flux per pole is obtained from the voltage equation and a flux no-load saturation curve is drawn as shown in Figure II-2. On this figure the saturation curve for

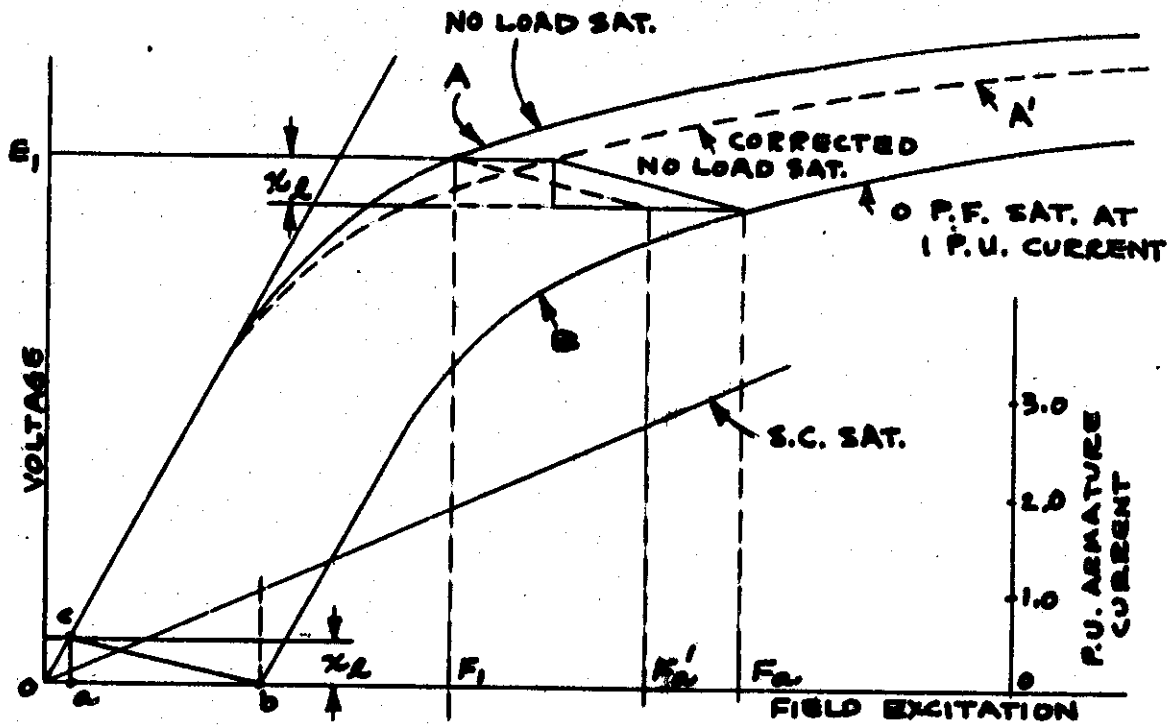

Figure II-1. Synchronous Machine Saturation Curves

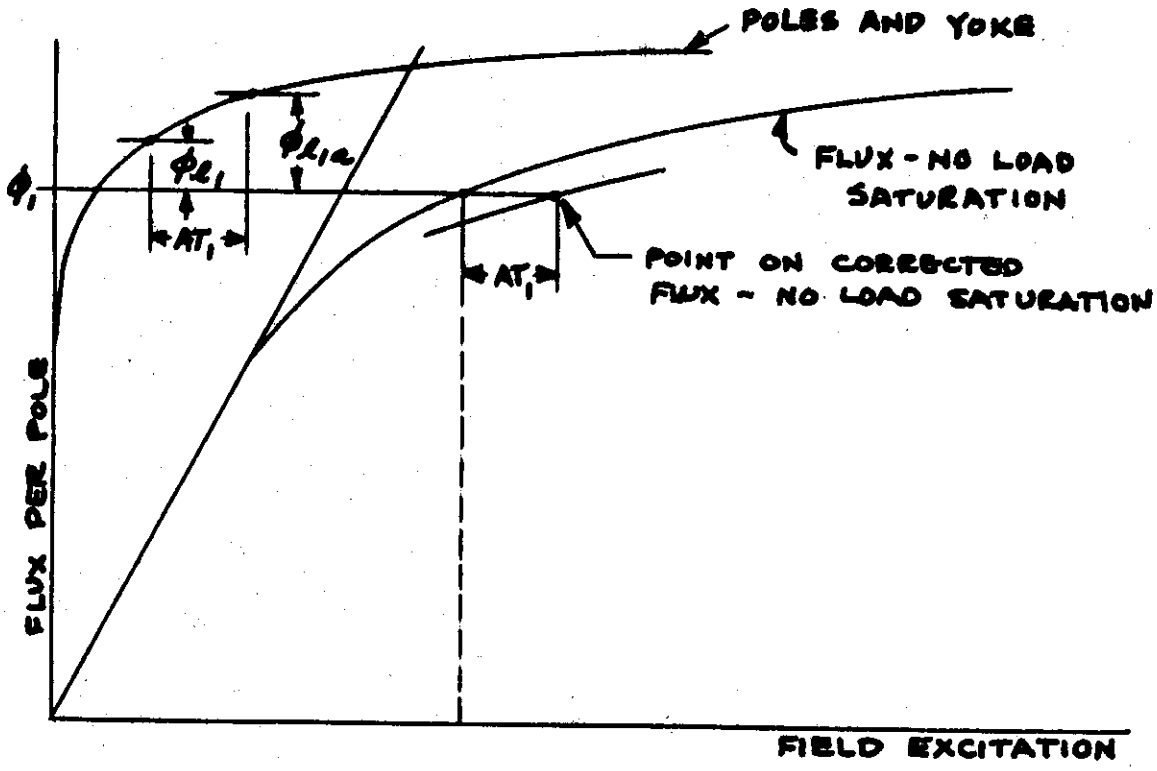

Figure II-2. Flux Saturation Curves

the poles and yoke are also drawn. The total flux through the pole will be $\phi_1 + \phi_{\ell 1}$ at no-load, and $\phi_1 + \phi_{\ell 1a}$ at the load condition. It is apparent that a greater mmf is required to drive the flux through the field structure, with the increased leakage, by the amount shown as AT_1. A point on the corrected flux saturation curve is obtained at the ϕ_1 value by merely adding AT_1 to F_1. In a similar manner other points in the saturation region are obtained and the whole curve may be drawn. The flux curve is then converted back to a voltage curve shown as A' on Figure II-1. Applying the triangle a-b-c it is determined whether the original estimate for F_a was sufficiently accurate. A considerable error will only affect the value of AT_1 a slight amount. It should be mentioned that a portion of the pole leakage flux does not pass through the full length of the pole and therefore, does not contribute to saturation in all portions to the same degree. This can be taken into account graphically and be reflected in the value obtained for AT_1.

The zero power-factor curve was of particular interest in performing the work described in other chapters of this report because the transient study was made assuming zero power-factor loads. The two-reaction theory should be applied for salient pole machines at other power-factors to determine the excitation requirements. The AIEE empirical method for calculating regulation gives the excitation requirements sufficiently accurate for uniform air-gap machines. It gives fair accuracy for salient pole machines at power-factors below .8 lagging.

II-B-2 Air-Gap Flux Distribution and Voltage Harmonics

The air-gap of salient pole machines is usually uniform only in the vicinity of the center of the pole and gradually increases toward the pole tips. The purpose is to obtain an approximate sinusoidally distributed flux wave which favors generating the highest fundamental voltage while limiting the harmonic voltages. Even with ideal flux distribution at no-load, there may be harmonic voltages generated under balanced load conditions unless special precautions are taken. The difficulty arises from the armature mmf distorting the field form. Great effort in designing and manufacturing a certain shape pole head is, therefore, hardly justified.

Selecting the proper winding pitch [5] will effectively reduce the lower order voltage harmonics. A two-thirds pitch winding is often used to reduce the third harmonic to zero. Figure II-3 shows how all harmonics are affected by the pitch. Table II-1, taken from the Standard Handbook for Electrical Engineers, shows how the harmonics are reduced by the distri-

Figure II-3 Pitch Factor (K_p) for Odd Harmonics

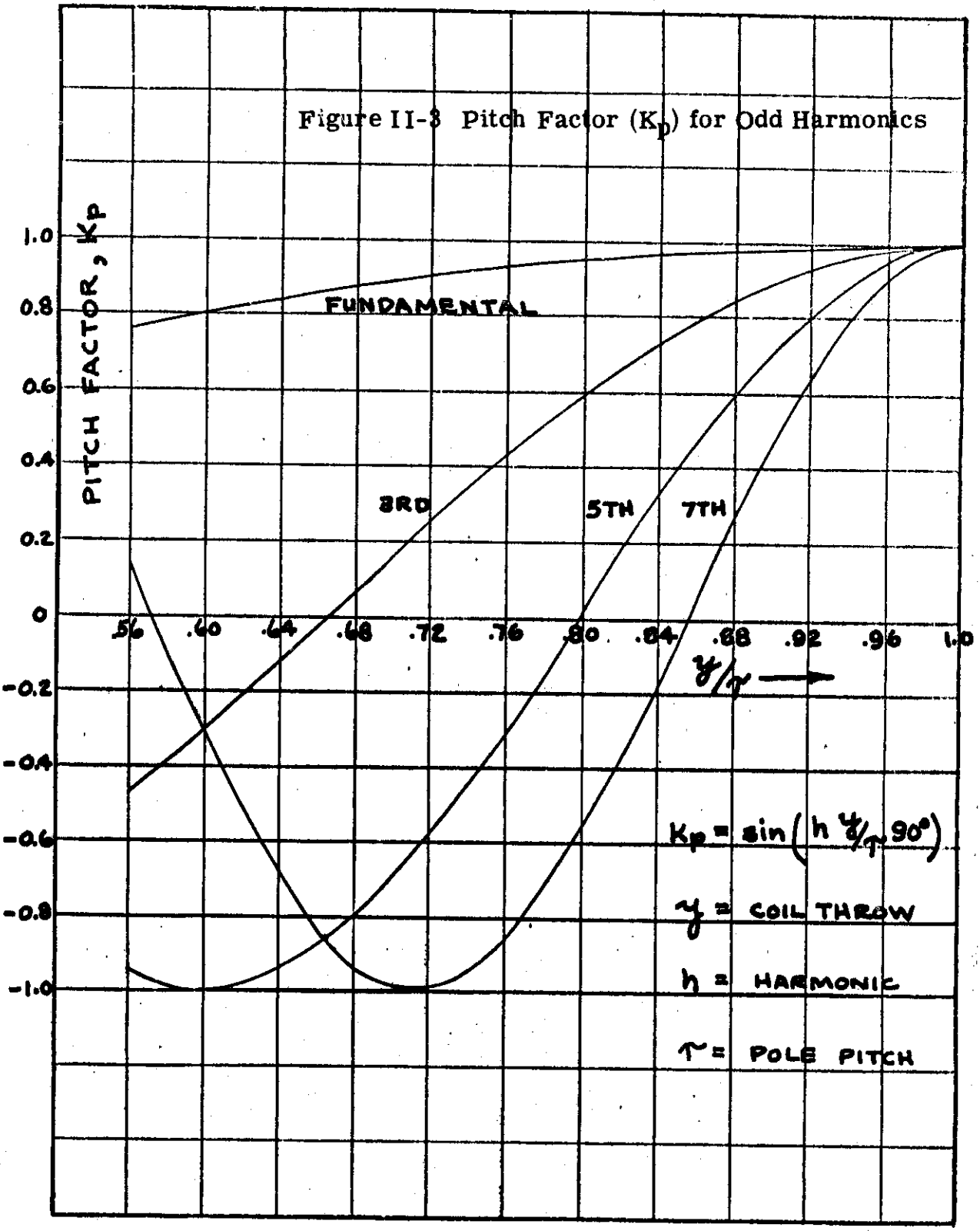

TABLE II-1

Distribution Factors for the Fundamental and Odd Harmonics Corresponding to Various Numbers of Slots per Phase (Nsp). 60 Degree Phase - Belts Three -Phase.

Nsp → / h ↓	3	6	9	12	15	18	21	24	∞
1	1.00	+0.966	+0.960	+0.958	+0.957	+0.956	+0.956	+0.956	+0.955
3	1.00	+0.707	+0.667	+0.653	+0.647	+0.644	+0.642	+0.641	+0.637
5	1.00	+0.259	+0.218	+0.205	+0.200	+0.197	+0.196	+0.194	+0.191
7	1.00	-0.259	-0.177	-0.157	-0.149	-0.145	-0.143	-0.141	-0.136
9	1.00	-0.707	-0.333	-0.270	-0.248	-0.236	-0.229	-0.225	-0.212
11	1.00	-0.966	-0.177	-0.128	-0.109	-0.102	-0.097	-0.095	-0.087
13	1.00	-0.966	+0.218	+0.128	+0.102	+0.091	+0.086	+0.083	+0.073
15	1.00	-0.707	+0.667	+0.270	+0.200	+0.173	+0.159	+0.149	+0.127
17	1.00	-0.259	+0.960	+0.157	+0.102	+0.084	+0.075	+0.070	+0.056
19	1.00	+0.259	+0.960	-0.205	-0.109	-0.084	-0.072	-0.066	-0.050
21	1.00	+0.707	+0.667	-0.653	-0.248	-0.173	-0.147	-0.127	-0.091
23	1.00	+0.966	+0.218	-0.958	-0.149	-0.091	-0.072	-0.063	-0.041
25	1.00	+0.966	-0.177	-0.958	+0.200	+0.102	+0.075	+0.063	+0.038
27	1.00	+0.707	-0.333	-0.653	+0.647	+0.236	+0.159	+0.127	+0.071

bution of the windings for 60 degree phase belts. The fifth and seventh harmonics are reduced to below 25 per cent for six or more slots per pole. The table also applies to a fractional-slot winding if the numerator of the improper fraction "slots per pole" is reduced to its lowest terms and used with the table for Nsp.

Integral-slot windings are likely to give troublesome slot harmonics. The fractional slot winding gives an equivalent effect of a large number of slots. This is beneficial in reducing the distribution factor and the magnitude of the slot flux ripple. A slight amount of skew is commonly used to limit the slot harmonic, particularly with integral-slot windings. Figure II-4 shows the reduction of voltage harmonics by skewing.

Figure II-4 Skew Factor (C_{SK}) for Odd Harmonics

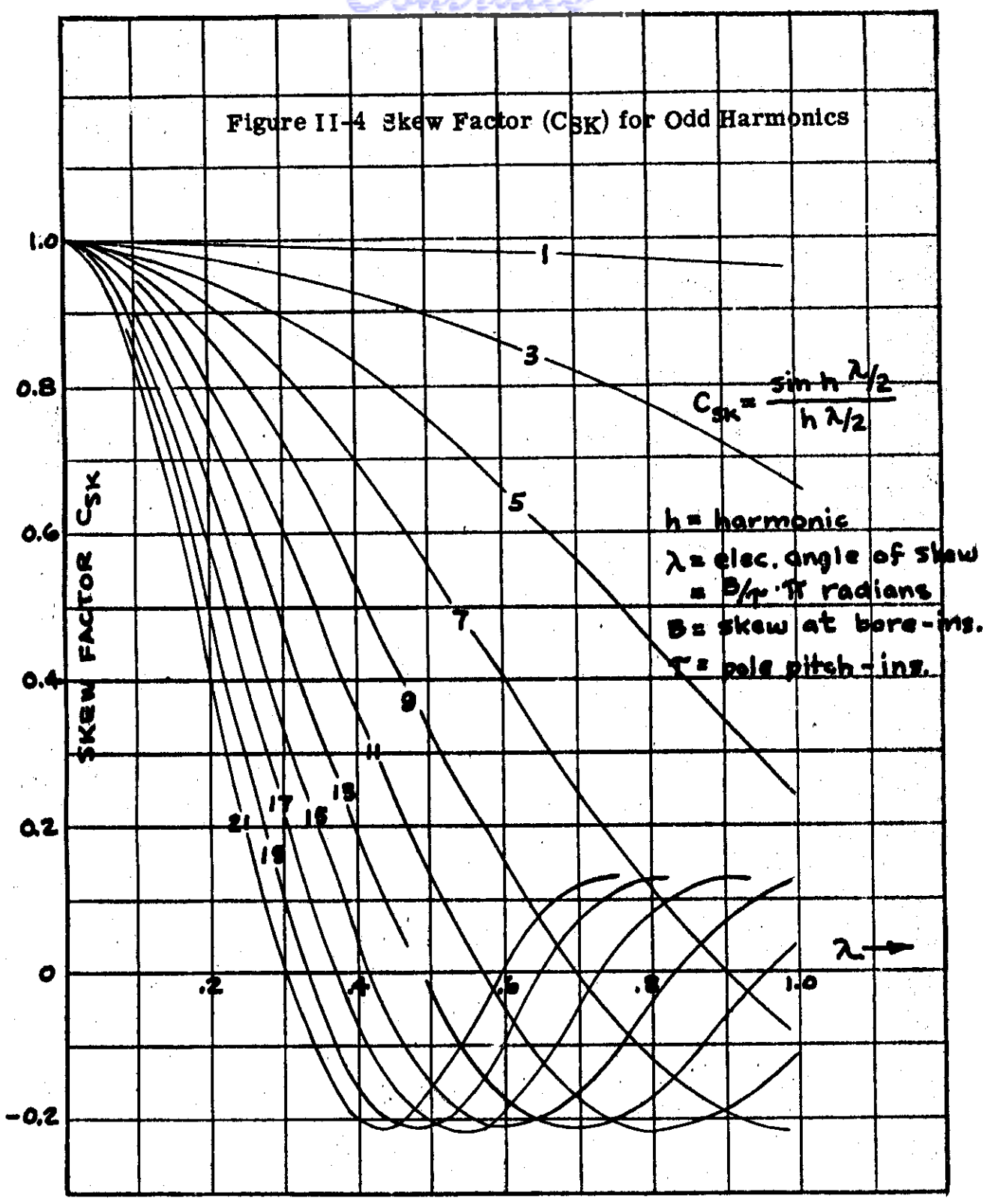

II-B-3 The Effect of Unbalanced Operation on Terminal Voltage and Harmonics.

The problem of determining the performance of a three-phase a-c generator operating under unbalanced load conditions has been solved by various writers using the method of symmetrical components. The writings of Fortescue [6], Wagner and Evans [7], Lyon [8] and Clarke [9, 10] cover the general theory and specific problems. These references also contain bibliographies on this widely discussed subject. A recent paper by Wilson [11] covers the case of unbalanced aircraft generator operation taking into account the characteristics of the regulator sensing circuit, regulator and exciter. Stineman's [12] discussion of reference [11] gives a shorter method which is based upon the assumption that the regulator will hold the average terminal voltage at a constant value until ceiling excitation is reached. No attempt will be made in this report to reproduce this previous work.

The purpose of the following qualitative discussion is to describe the internal reactions of the a-c generator. In general, under unbalanced conditions all sequence (positive, negative, and zero) currents exist in the armature windings of the a-c generator. Neglecting saturation, each sequence system can be considered separately.

II-B-3-a Positive Sequence System

Consider first only the fundamental frequency stator currents. The positive sequence currents produce a fundamental space mmf and a series of odd harmonic space mmfs. The magnitude of each space component depends upon the pitch and distribution of the winding. The net result of considering all three phases is as follows:

The space fundamental mmf is constant in amplitude (3/2 times the peak space fundamental of any one phase) and rotating forward at synchronous speed with respect to the stator and is stationary with respect to the rotor.

The third harmonic space mmf is zero.

The fifth harmonic space mmf is constant in amplitude. This amplitude is $1/5 \frac{K_{p5} K_{d5} K_{s5}}{K_{p1} K_{d1} K_{s1}}$ times the amplitude of space fundamental,

where K_p, K_d, K_s are the pitch, distribution and skew factors, respectively, and the numerical subscript refers to the order of the space harmonic. This component rotates backwards at 1/5 synchronous speed with respect to the armature and at 6/5 synchronous speed with respect to the rotor.

The seventh space harmonic of mmf has a constant amplitude of

$1/7 \quad \frac{K_{p7}\ K_{d7}\ K_{s7}}{K_{p7}\ K_{d7}\ K_{s7}}$ times the amplitude of the space fundamental and rotates forward at 1/7th synchronous speed with respect to the armature and at 6/7 speed with respect to the rotor.

The ninth space harmonic mmf is zero, etc.

The magnitude of the space harmonics of mmf are small compared with the fundamental for two reasons. First, the magnitude of the n^{th} space harmonic is $1/n^{th}$ the magnitude of the fundamental; second, the magnitude is multiplied by $\frac{K_{pn}\ K_{dn}\ K_{sn}}{K_{p1}\ K_{d1}\ K_{s1}}$. The reduction factors for pitch, distribution and skew for the harmonics are much smaller than the reduction factors for the fundamental. Thus these harmonic mmf waves are neglected in most analysis of unbalanced operation entirely or at most the fundamental voltage induced by the flux set-up by these harmonics is included in the leakage reactance.

The effect of the space harmonics of mmf are analyzed by Doherty and Nickle. Their paper [14] shows that in cylindrical rotor machines, each space harmonic wave of mmf produce a corresponding space harmonic of flux. In salient pole machines each harmonic space wave produces a series of odd harmonic flux waves which induce odd harmonic (including fundamental) voltages in the stator. The effect of damper bars on the rotor is not considered.

This entire phenomenon exists not only for the time fundamental, but there is also a similar situation for each harmonic current.

Consider the space fundamental of mmf due to the fundamental of positive sequence currents. This constant amplitude wave travels at synchronous speed with respect to the armature and is stationary with respect to the rotor. In a uniform air-gap machine the flux produced by this space

fundamental would be a sinusoid of the same wave length. However, in a salient pole machine the flux is not sinusoidally distributed in space, but consists of a fundamental and space harmonics. Actual numerical calculation of the flux distribution is best made by resolving the stator mmf into direct-axis and quadrature-axis components and calculating the flux waves in the two axes separately. It should be noted that there is a pronounced third harmonic flux in space due to the quadrature-axis mmf. In cases of high reactance machines operating at full load, this magnitude could be as high as 50% of the fundamental. These space harmonics of flux induce corresponding time harmonic voltages. The magnitude is reduced by the reduction factors.

If all the space harmonics of flux and the corresponding time harmonics of induced voltage are neglected there is only left a space fundamental of flux in the direct- and quadrature-axis. The ratio of the voltage induced by the space fundamental direct-axis flux to the direct-axis component of current is the familiar reactance of armature reaction x_{ad}. A similar situation in the quadrature-axis results in a physical picture of x_{aq}. Lyon analyzes the salient pole machine under unbalanced operation taking account of the saliency in the positive sequence system. Most writers neglect the effect of saliency. The synchronous reactances $x_d = x_\ell + x_{ad}$ and $x_q = x_\ell + x_{aq}$ are considered equal. This approximation is not too severe for short-circuit problems where the stator mmf is centered near the direct-axis.

Next consider the action of the field winding mmf. With direct currents in the field winding a stationary field is set up in the direct-axis. The fundamental of this field produces positive sequence voltages in the stator. The harmonic voltages are reduced by their respective reduction factors. No negative sequence or fundamental frequency zero-sequence voltages are induced.

The 3rd harmonic is a zero-sequence voltage in time phase in the three stator phases.

With the assumption of no saturation, the voltages induced by the field and armature mmfs can be superimposed. Thus, the positive sequence system is usually represented by an emf (generated by the space funda-

mental field mmf) in series with a synchronous reactance.

II-B-3-b Negative Sequence System

The negative sequence armature currents are balanced and of opposite phase sequence from the positive sequence currents. This set of currents produces a series of space mmf waves similar to the positive sequence except for relative velocities.

Again the harmonic mmfs are small compared to the fundamental so they will be neglected in the following. The action of the space fundamental of the negative sequence mmf is not as simple to consider as its positive sequence counterpart; because, while the latter is stationary with respect to the rotor, the former rotates at twice synchronous speed past the pole structure. This space fundamental of mmf meets a rapidly varying permeance. The resultant flux in the air-gap is due to the action of both stator and rotor mmfs. This phenomenon can be viewed qualitatively as being similar to the action in a three-phase induction motor operating at a slip of two per-unit. One difference is that in an induction motor (neglecting armature resistance and leakage reactance) the air-gap flux is determined by the magnitude of the applied voltage; whereas in this case the stator mmf is constrained by the a-c generator terminal load so that the flux is determined by the net mmf. Another difference is that the rotor winding of an a-c generator without damper bars is a single-phase winding, unlike the polyphase induction motor rotor winding. Consequently, the double frequency current which exists in the field winding due to the rate of change with respect to time of the net backward flux wave sets up an mmf which is stationary in space with respect to the rotor and pulsating at twice rated frequency in time. This pulsating field can be resolved into forward and backward rotating fields. These constant amplitude fields are of fundamental space wave length and rotate at constant speeds. The speed of the forward field is twice synchronous speed with respect to the rotor and three times synchronous speed with respect to the stator.

The backward field rotates at twice synchronous speed with respect to the rotor and backward at synchronous speed with respect to the stator. The backward component reacts with the backward field set up by the negative sequence stator currents to determine the net backward flux in the air-gap.

The forward field set up by the field currents induces third harmonic voltages in the armature winding. These third harmonic voltages are 120° out of phase and of positive sequence and consequently will appear in the line-to-line voltages. Also, these third harmonic voltages are not reduced

in magnitude by the third harmonic pitch, distribution and skew factors but by the fundamental reduction factors.

The difference in the third harmonic voltages generated by a space fundamental of flux rotating at three times synchronous speed and those induced by a third harmonic in space rotating at synchronous speed should be noted.

A solution to two of the problems just mentioned lies in the use of damper bars which were omitted from the previous discussion.

A continuous damper winding when acted upon by the resultant backward rotating flux wave, has voltages induced in it and currents existing which set up a space mmf which is rotating backward at twice synchronous speed with respect to the rotor and fixed in space relative to the backward rotating field set up by the negative sequence stator currents.

If the leakage reactance and resistance of the damper circuits are small, the net backward air-gap flux will be small. Two important consequences of this fact are: first, the voltage unbalance is reduced, and second, the third harmonic armature voltage is reduced. The voltage unbalance is reduced because the negative sequence voltage induced by the net backward field is small if the flux is small. In terms of machine reactances, the negative sequence reactance is small since it consists of the armature leakage reactance plus a reactance which could be defined as the ratio of the voltage induced by the backward rotating flux wave to the negative sequence armature current. This latter component is reduced if the net backward flux is reduced due to the action of the damper bars. Notice that even in the limiting case of perfect damping; i. e., when the backward field is reduced to zero, the negative sequence reactance still consists of the armature leakage component.

The third harmonic armature voltage is reduced because the field set up by a continuous damper winding is rotating at synchronous speed in the backward direction. It is not a pulsating mmf, hence, there is no component field rotating at three times synchronous speed with respect to the armature. The field winding still has a pulsating mmf but the magnitude is reduced since the resultant backward field is reduced by the mmf of the damper bars. Therefore, there will still be a second harmonic field current and a third harmonic stator voltage but the magnitudes will be smaller. With perfect damping, the magnitude would be zero.

Thus, in so far as obtaining low unbalanced voltages and low third harmonic stator voltages during unbalanced operating conditions, a machine should have continuous dampers with small resistance and leakage reactance. The dampers should be large in cross-section and close to the air-gap.

Also, this type of damper will provide large damping torques during disturbances on multimachine systems.

This type of winding would not provide as large starting torque as a higher resistance damper would on machines which may be used as both motors and generators.

Quantitatively the negative sequence reactance is considered equal to the average of the direct-and quadrature-axis subtransient reactances.

II-B-3-c Zero-Sequence System

The zero sequence currents are in time phase in each stator winding. These currents set up an mmf which is pulsating in time at fundamental frequency and stationary in space. The spatial distribution consists of a series of harmonics: the third and triple multiples of the third. There is no fundamental field. The zero-sequence reactance consists of the zero sequence leakage reactance (which is different from the positive sequence leakage reactance,especially at armature winding pitches different than unity) and a component which could be defined as the ratio of the voltage induced by the triple pole air-gap flux to the zero-sequence current. This latter component is termed "belt-leakage" by some writers.

II-B-3-d Quantitative Expressions for Reactances

Expressions for the various reactances in terms of machine dimensions and constants is given in Appendix B-2.

II-B-4 Short-Circuit and Overload Capacity - Short-circuit capacity of an a-c generator is usually specified to insure that a fault in the system will be properly cleared with fuses and limiters. The time interval that this current is needed is probably not more than two or three seconds and the heating of the generator is not important from this consideration. The main magnetic circuit of the generator is normally not saturated under short-circuit, but rather the exciter is at ceiling output and thus limiting the magnitude of the current. For a given excitation, reducing the machines main air-gap or the number of armature conductors will give a greater short-circuit capacity. Reducing the number of conductors reduces x_d, of course.

Overload capacity at normal voltage is affected by heating and saturation in addition to the previously mentioned factors. The most difficult load requirement specified is that the machine must be capable of delivering 150 per cent load at minimum speed and minimum rated lagging power-factor for a period of five minutes. An exciter with capacity to supply the necessary short-circuit current probably will meet the five-minute overload condition without difficulty. Trouble is often encountered in keeping the field winding from overheating. A well-designed machine will operate under this condition at a moderate amount of saturation, the field winding will approach its maximum allowable temperature, and the exciter will be operating considerably below its maximum capacity.

II-B-5 Affects of Saturation at Steady-State - Saturation of the main magnetic circuit of the generator is apparent from the no-load saturation curve. The per-unit saturated direct-axis synchronous reactance is computed as the field current necessary to circulate rated three-phase current on short-circuit divided by the field current necessary to give rated terminal voltage at no-load. For the unsaturated value the field current for rated voltage on the air-gap line is used. Saturation has no appreciable affect upon the leakage reactance x_ℓ. This reactance results from leakage flux crossing air paths. The reluctance of the air paths is so much greater than those in the iron that the saturation of the iron is insignificant.

II-C SYNCHRONOUS MACHINE TRANSIENTS

The theory for salient pole generators under transient condition is well covered in the literature [14, 15]. Only partial treatment is given here.

II-C-1 Application of a Three-Phase Short-Circuit

Suppose a salient pole generator without damper bars is running at no-load and rated voltage. Let it be assumed that the excitation voltage will remain constant during the transient to be considered, and a three-phase short-circuit is suddenly applied. Applying the constant-flux-linkage theorem, the field and each armature winding maintain constant flux linkages the instant the short-circuit is applied. The armature currents increase practically instantaneously giving a resultant mmf that opposes the air-gap flux. The field current also increases instantaneously in its effort to maintain constant flux linkages. The armature currents go up to a value corresponding to e/x_ℓ, where e is the voltage generated by the air-gap flux and x_ℓ is the armature leakage reactance. The value of e is less than the no-load voltage before short-circuit was applied. Even though the flux linkages are essentially the same, the flux redistributes itself to give less flux across the air-gap and a greater pole leakage flux. Had the air-gap flux remained constant during the transient then the voltage generated in each armature winding would be the same as at no-load and the transient reactance x_d' would simply be x_ℓ. The air-gap flux is less, however, and consequently the alternating current is less so it is concluded that x_d' must be greater than x_ℓ. x_d' is a reactance that includes the affect of the increased field leakage occasioned by the increase of field current. It is further defined as the voltage before application of the short-circuit divided by the initial peak of the transient alternating current. Figure IV-6 shows the manner in which these quantities are related. The field winding current jump is in proportion to that of the armature symmetrical current jump. The field current cannot be maintained at this peak value, however, and it decays according to the transient time constant down to the steady-state value. The symmetrical alternating currents of the armature windings follow the same rate of decay down to their sustained value.

There is an asymmetrical, or d-c, component of current in each of the armature windings. This is the result of a certain amount of flux being trapped in each phase winding when the short-circuit was applied. The phase windings, being 120 electrical degrees apart, will very likely each trap a different amount of flux. To maintain constant flux linkages the alternating armature currents may be considered as having d-c components. These d-c components decay according to the armature time constant T_a. The affective inductance related to T_a is $x_2/2\pi f$ and the resistance is that of the armature r_a.

The subtransient affects are dependent upon the amortisseur windings. Figure IV-6 shows that the symmetrical short-circuit current jumps to e/x_d''. If there is no amortisseur winding, the current only reaches e/x_d'. The greater value in the former case is due to the amortisseur winding being physically near the air-gap and tending to hold the flux constant in that region. The figure also shows that the subtransient armature currents decay relatively fast according to the time constant T_d''. This is the result of the armortisseur currents decaying and having the same time constant.

II-C-2 Mathematical Relationships

A logical approach to the study of transients in synchronous machines would follow the procedures used in studying transients in static networks. However, even with the simplified assumptions made to idealize the machine, the resulting differential equations are difficult to solve analytically, since they contain time-varying coefficients. These coefficients result from the variable mutual inductances between stator and rotor circuits and between the different circuits on the stator.

To avoid the difficulty of time-varying coefficients, the actual voltages, currents and flux linkages are transformed to new quantities which result in differential equations with constant coefficients. The transformation of variables is not unique and no analytical method exists whereby a particular transformation is obtained. Rather the transformation comes from physical insight into the problem or ability to look at a set of equations and see what transformation to use.

Two such transformations which have been developed are the change from actual quantities to:

(a) Direct-and quadrature-axis quantities.
(b) Symmetrical components.

These are not the only possible changes of variables, but will suffice for the purpose of this section. Method (a) is discussed by R. H. Park, B. Adkins and C. Concordia in References 16, 17 & 18 and Method (b) by Y. H. Ku and W. V. Lyon in References 19 and 20 . For more literature on the subject, see the bibliography of the references given.

Since the complete derivation of the machine equations in terms of the new variables is given in the references, only a brief summary of the methods will be given here.

II-C-2-a Assumptions [20, 21]

(1) Neglect eddy-current and hysterisis.
(2) Neglect saturation.
(3) The effect of stator slots is neglected.
(4) The self and mutual inductances are constant or vary sinuosidally with rotor angle or are a combination of both.

II-C-2-b Transformation of Variables

(1) Direct and Quadrature-axis components.

The actual phase currents i_a, i_b, i_c, are transformed into the new quantities i_d, direct-axis component; i_q, quadrature-axis component; and i_o, zero sequence component as follows:

$$i_d = 2/3[(i_a \cos \theta + i_b \cos (\theta - 120) + i_c \cos (\theta - 240)]$$

$$i_q = -2/3[(i_a \sin \theta + i_b \sin (\theta - 120) + i_c \sin (\theta - 240)]$$

$$i_o = 1/3 (i_a + i_b + i_c)$$

Where θ is the angle between the axis of phase "a" and the axis of the field winding,

The inverse of equation 1 gives:

$$i_a = i_d \cos \theta - i_q \sin \theta + i_o$$

$$i_b = i_d \cos (\theta - 120^o) - i_q \sin (\theta - 120^o) + i_o$$

$$i_c = i_d \cos (\theta - 240^o) - i_q \sin (\theta - 240^o) + i_o$$

Similar relationships are defined for voltages and flux linkages.

The resulting Kirchhoff equations in terms of the direct and quadrature-axis components are linear differential equations with constant coefficients provided the speed ($\frac{d\theta}{dt}$) is constant.

(2) Symmetrical Components

Here the actual stator currents i_a, i_b, i_c are transformed into positive, negative and zero sequence components, respectively, of i_a.

$$i_{a1} = 1/3 (i_a + e^{j120} i_b + e^{j240} i_c)$$

$$i_{a2} = 1/3 (i_a + e^{j240} i_b + e^{j120} i_c)$$

$$i_{a0} = 1/3 (i_a + i_b + i_c)$$

The stator currents are given by:

$$i_a = i_{a0} + i_{a1} + i_{a2}$$

$$i_b = i_{a0} + e^{j240} i_{a1} + e^{j120} i_{a2}$$

$$i_c = i_{a0} + e^{j120} i_{a1} + e^{j240} i_{a2}$$

Similar relations are defined for voltages.

Kirchhoff's equations in terms of symmetrical components are again linear with constant coefficients.

The two forms of Kirchhoff equations are the same except for the variables used. Lyon shows this correspondence and gives the relationship between the direct-and quadrature axis components and the symmetrical components:

$$i_d = i_1 e^{-j\theta} + i_2 e^{j\theta}$$

$$i_q = -j i_1 e^{-j\theta} + j i_2 e^{j\theta}$$

Thus either transformation results in a set of linear differential equations with constant coefficients which can be solved analytically. However, literal solutions are unwieldly when damper windings are considered and various approximations have been made to obtain relatively simple expressions for the currents.

One such approximation, i.e., neglect of resistances except where they affect damping leads to the constant flux linkage approach which is described in References 13, 22 and 23.

The references show what assumptions are made in going from the "exact" equations to the various approximate solutions.

No complete solution is given for all transient problems because the approximations used depend upon the problem.

II-C-2-c Saturation

Saturation is included in some treatments by appropriately adjusting the constants used in the linear theory.

Rudenberg[24] presents graphical methods for dealing with transients in saturated machinery based on the assumption that the change with respect to time of the envelope of a-c voltages and currents is slow compared to the system frequency. This is the method used in the subsequent section for calculating the terminal voltage rise upon removal of load from a saturated machine.

II-C-3 Effect of Machine Parameters on Transient Performance - To analytically study the effect of the a-c generator parameters on transient performance it is necessary to fix certain variables of the complete electric system. In the following study of transient performance this method is employed to simplify the problem.

II-C-3-a Analytical Study of the Effect of Machine Parameters on Voltage Peaks and Dips - Papers by Harder and Cheek,[25] Anderson,[26] Rosenberg[27] and Chapter 9 of Concordia's book[18] cover the analytical study of voltage dips after sudden application of load to an ideal synchronous machine. The above mentioned articles give results showing the affect of the machine parameters on the voltage dip and will not be repeated here. It should be mentioned however that some of the conclusions in these papers which hold for large central station machines do not hold for aircraft machines. For example, the affect of the synchronous reactance, x_d, is small for machines with open circuit time constants greater than 1 second, whereas its affect is significant for machines with open circuit time constants in the order of 0.1 second.

The problem of removing load is treated in Appendix B-1 for the assumed linear case. Equation (9) of this appendix, which is an analytical expression for the maximum terminal voltage after suddenly removing load, is:

$$e_t \max = e_q(0) + i_d(0) - k \left\{ T_{do}' \ln \left[\frac{x_d - x_d'}{k} \frac{i_d(0)}{T_{do}'} + e^{t_1/T_{do}'} \right] - t_1 \right\}$$

$e_q(o)$ = quadrature-axis component of terminal voltage in steady-state before load is removed.

$i_d(o)$ = direct-axis component of armature current in steady-state before load is removed.

Both $e_q(o)$ and $i_d(o)$ are determined from the steady-state vector diagram and are functions of both the magnitude and power-factor of the load in addition to x_q, the quadrature-axis synchronous reactance.

Appendix B-1 covers the assumptions used in obtaining the desired results.

(1) Effect of the Various Factors

(a) Power Factor - Physically, the power factor of the load determines the position of the armature mmf wave with respect to the position of the rotor in space. For large inductive reactance loads, the stator mmf is practically in line with and in opposition to the field mmf. This means that more field ampere-turns are required under a low power-factor load in the steady-state and consequently the terminal voltage without exciter action will rise to a higher value in the new steady-state condition of no load.

The transient in terminal voltage consists of an abrupt change from the former steady-state value followed by an exponential rise, with a time constant determined by the inductance and resistance of the field winding, to the new steady-state condition. Figure II-5 shows the effect of power factor on the envelope of the terminal voltage following sudden removal of loads with the exciter voltage held constant. Note that for unity power factor load, the terminal voltage actually jumps in a negative direction at the instant of switching. Figure I I-6 shows the results obtained by considering an exciter response, k, of 100. As can be seen, the maximum value of terminal voltage decreases with increase in power-factor. The change is not great for power factors in the range of 0 to . 5, but decreases rapidly after . 5.

(b) Regulator Time Delay t_1, and Exciter Response, k - The regulator-exciter combination is assumed to vary as shown in Figure II-7.

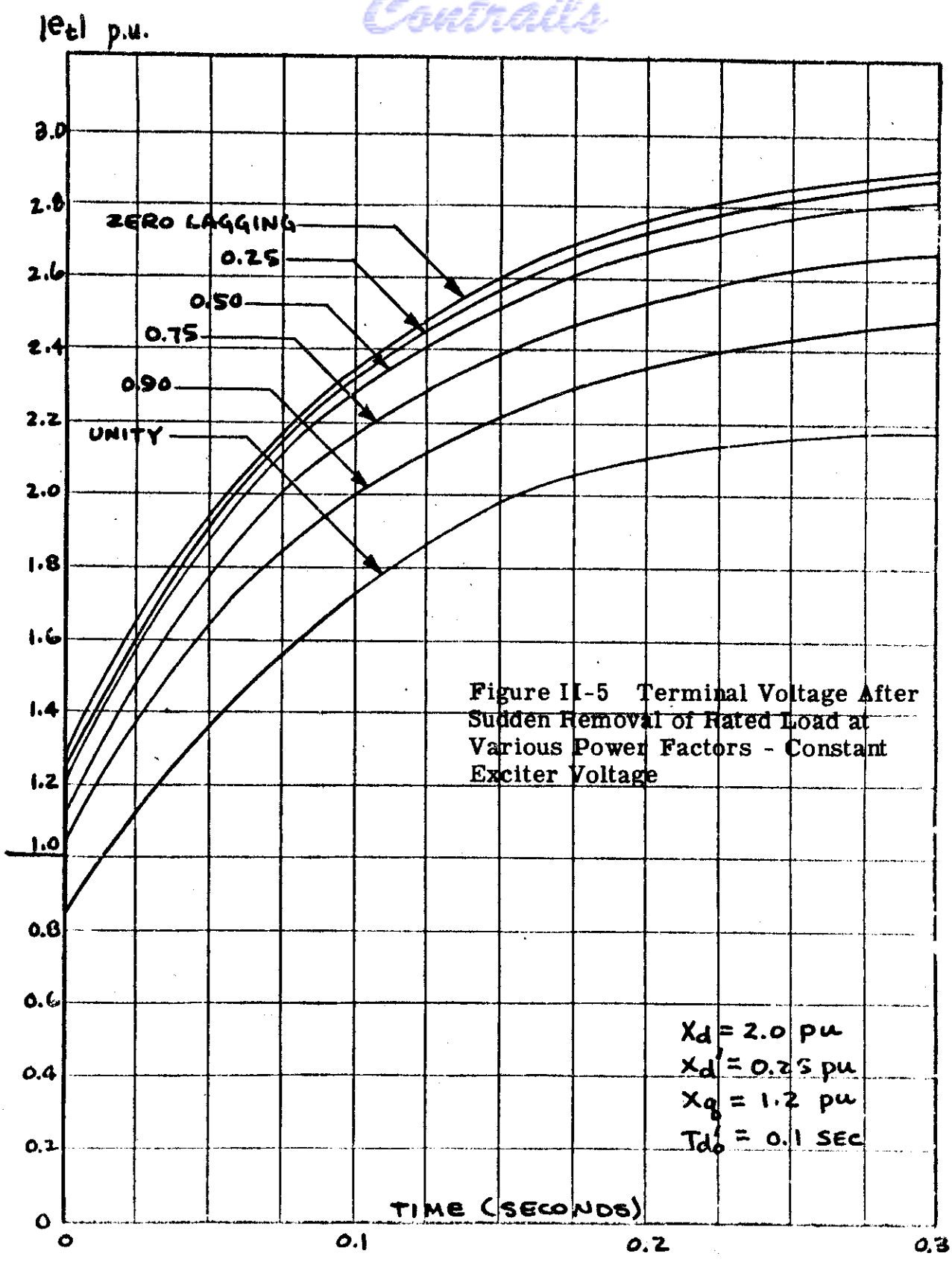

Figure II-5 Terminal Voltage After Sudden Removal of Rated Load at Various Power Factors - Constant Exciter Voltage

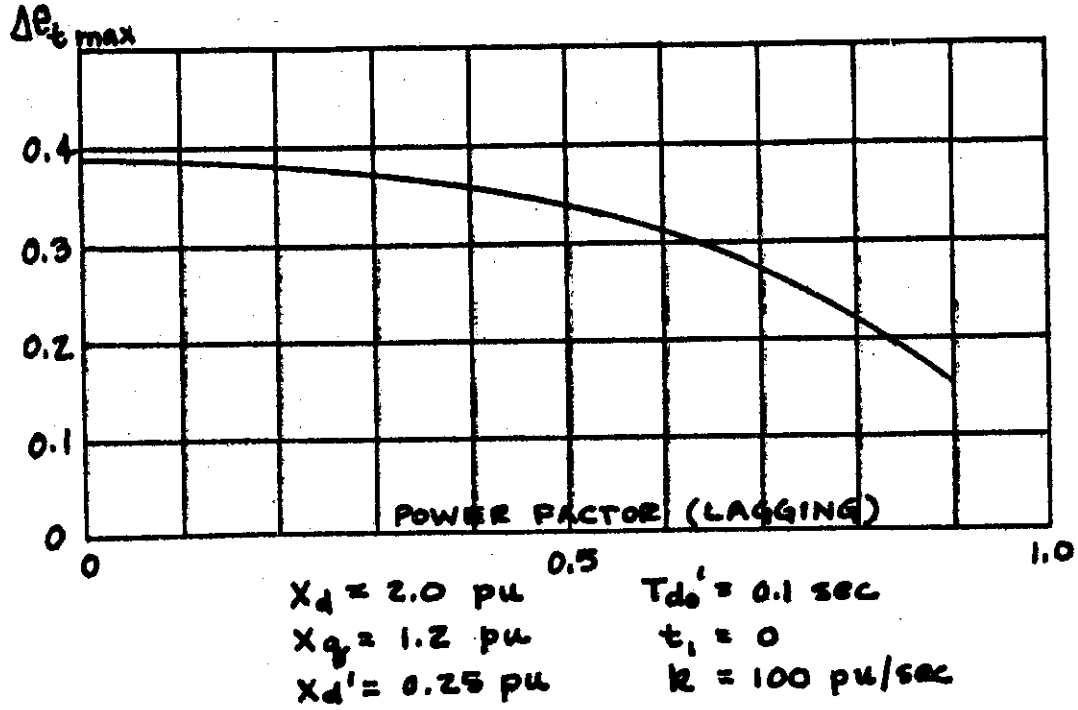

Figure II-6 Maximum Overvoltage as a Function of Power-Factor of Suddenly Removed Load.

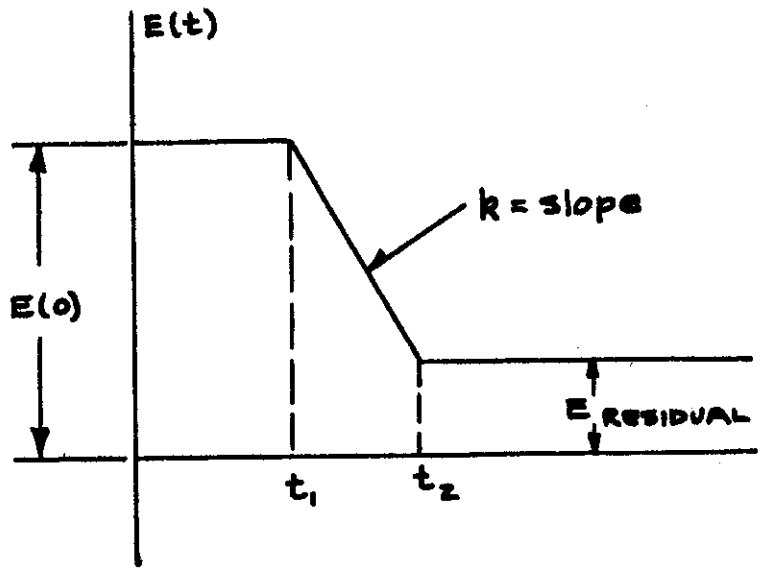

Figure II-7 Assumed Variation of Excitation Voltage as a Function of Time

The reasons for this simplifying assumption is that it permits study of the machine without including the complete overall closed-loop system.

The effect of regulator time delay on the maximum overvoltage after sudden removal of load is shown in Figure II-8, while the effect of exciter response is shown in Figure II-9.

As would be expected, increasing the regulator time delay makes the maximum overvoltage greater whereas increasing the exciter response decreases the maximum overvoltage.

(c) Machine Parameters - Figure II-10 shows the effect of the direct-axis synchronous reactance x_d; the direct-axis transient reactance, x_d' and the open-circuit field time constant, T_{do}' on the maximum overvoltage.

The effect of x_d is relatively large for aircraft machines with time constant under .2 second, whereas its effect at larger time constants diminishes.

x_d' has a greater effect at the larger time constants than it does at time constants near those of present aircraft machines.

The effect of T_{do}' is very significant in the range of present aircraft machines and its effect levels off at higher values.

As can be seen from Figure II-10, the maximum overvoltage is decreased as both x_d and x_d' are decreased and as T_{do}' is increased.

(2) Effect of Saturation - The previous work neglected the influence of saturation on the results. Saturation affects the results in two ways:

(a) The values of the machine parameters are not constant but vary with saturation.

Figure II-8 Maximum Overvoltage as a Function of Regulator Time Delay

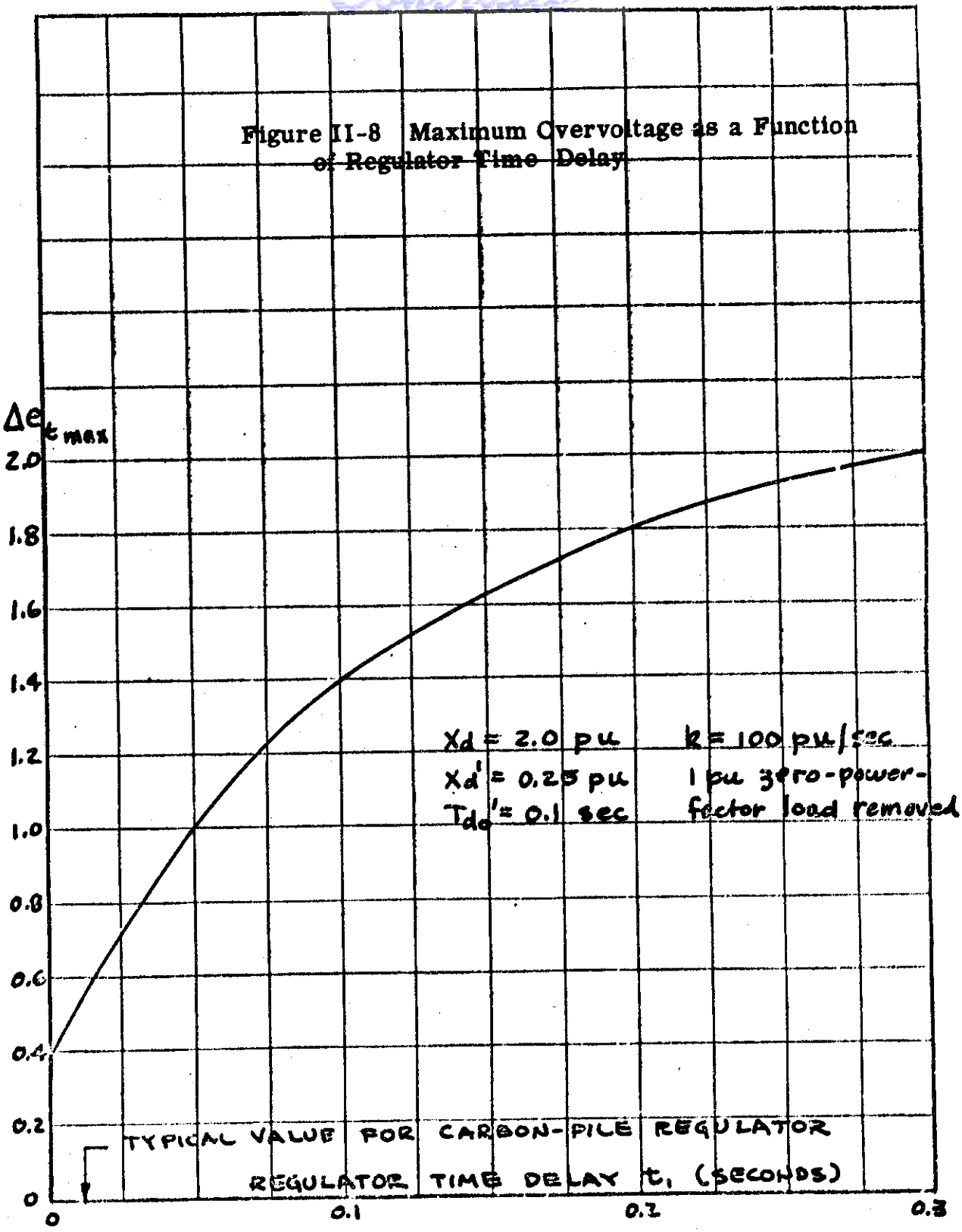

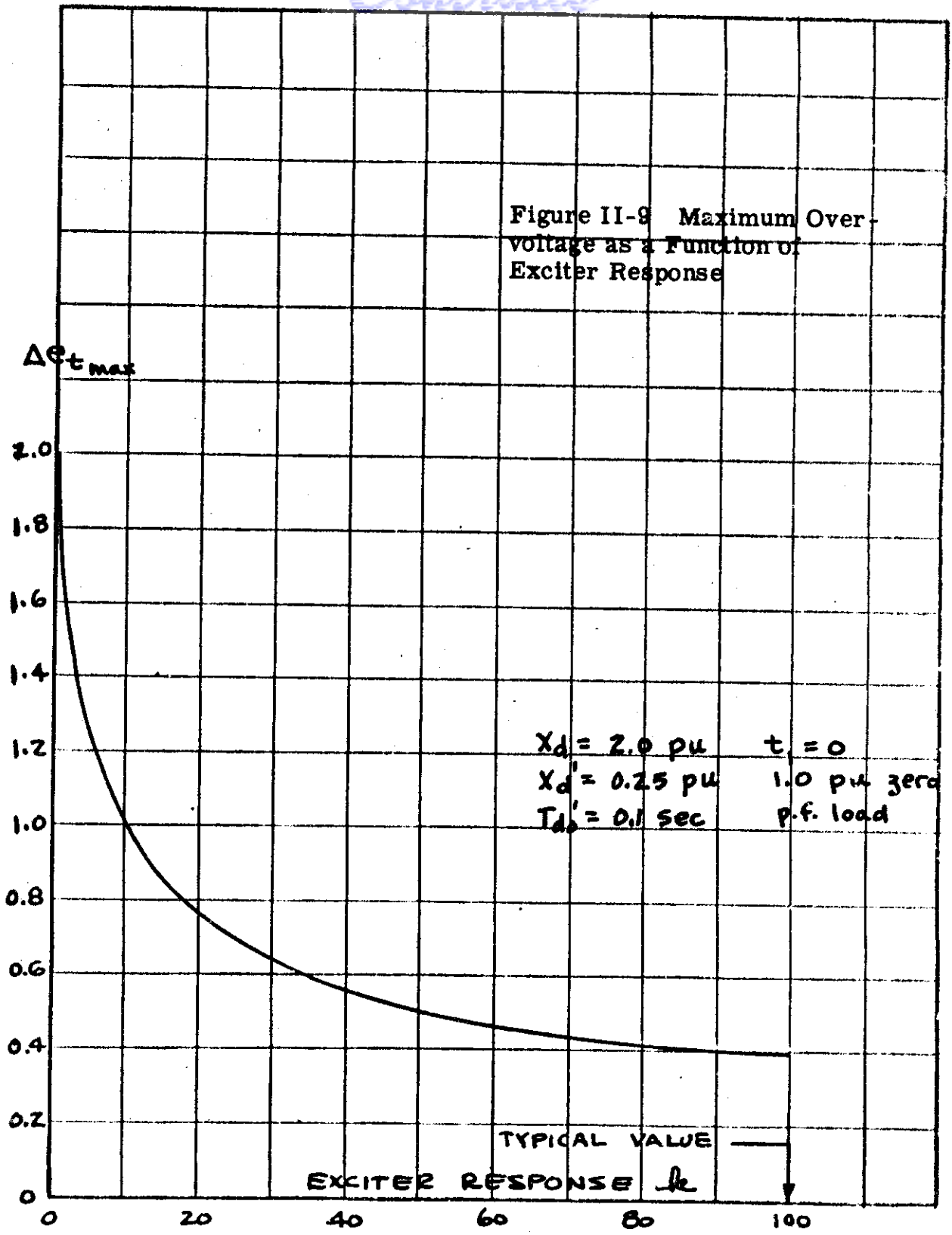

Figure II-9 Maximum Over-voltage as a Function of Exciter Response

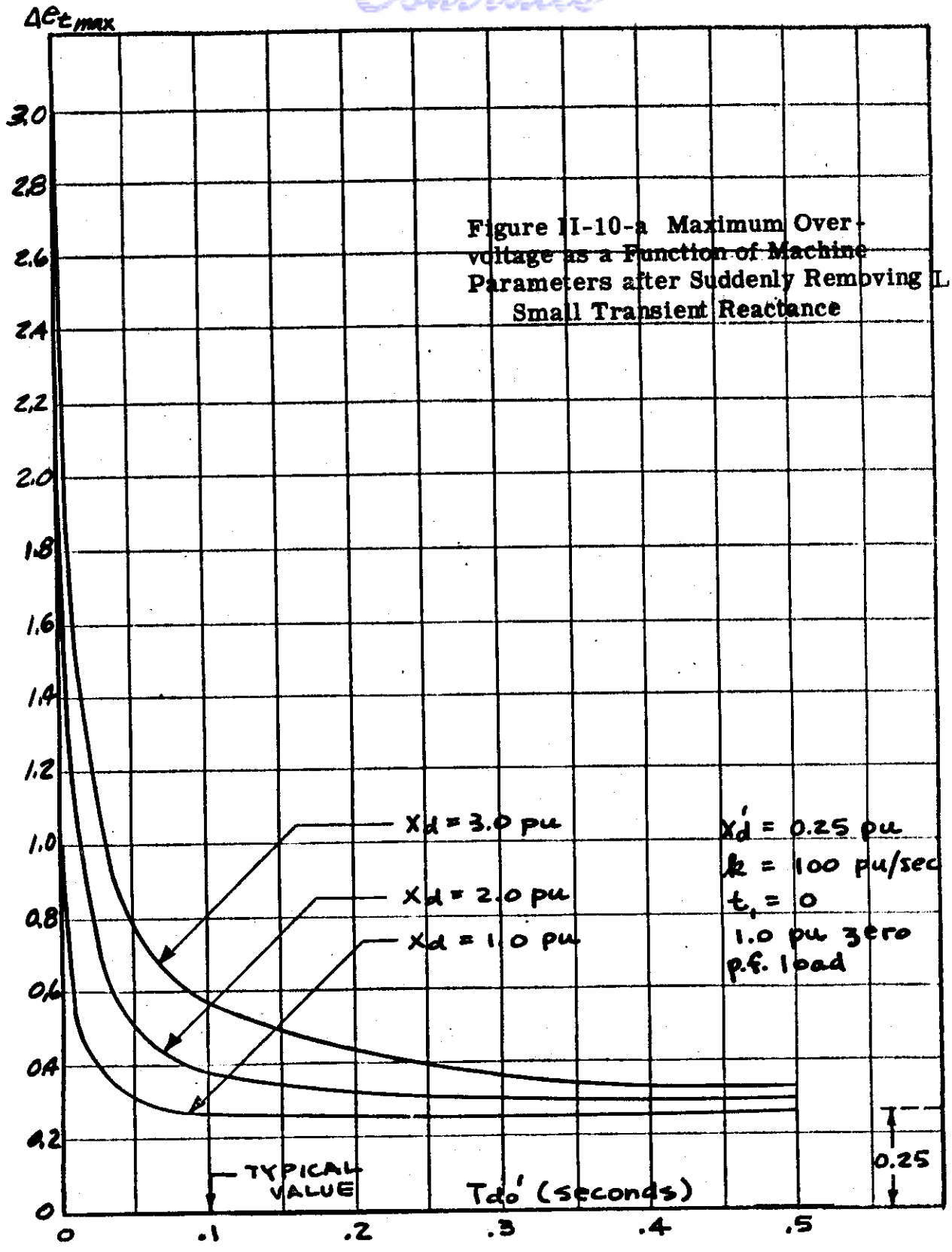

Figure II-10-a Maximum Over-voltage as a Function of Machine Parameters after Suddenly Removing Load Small Transient Reactance

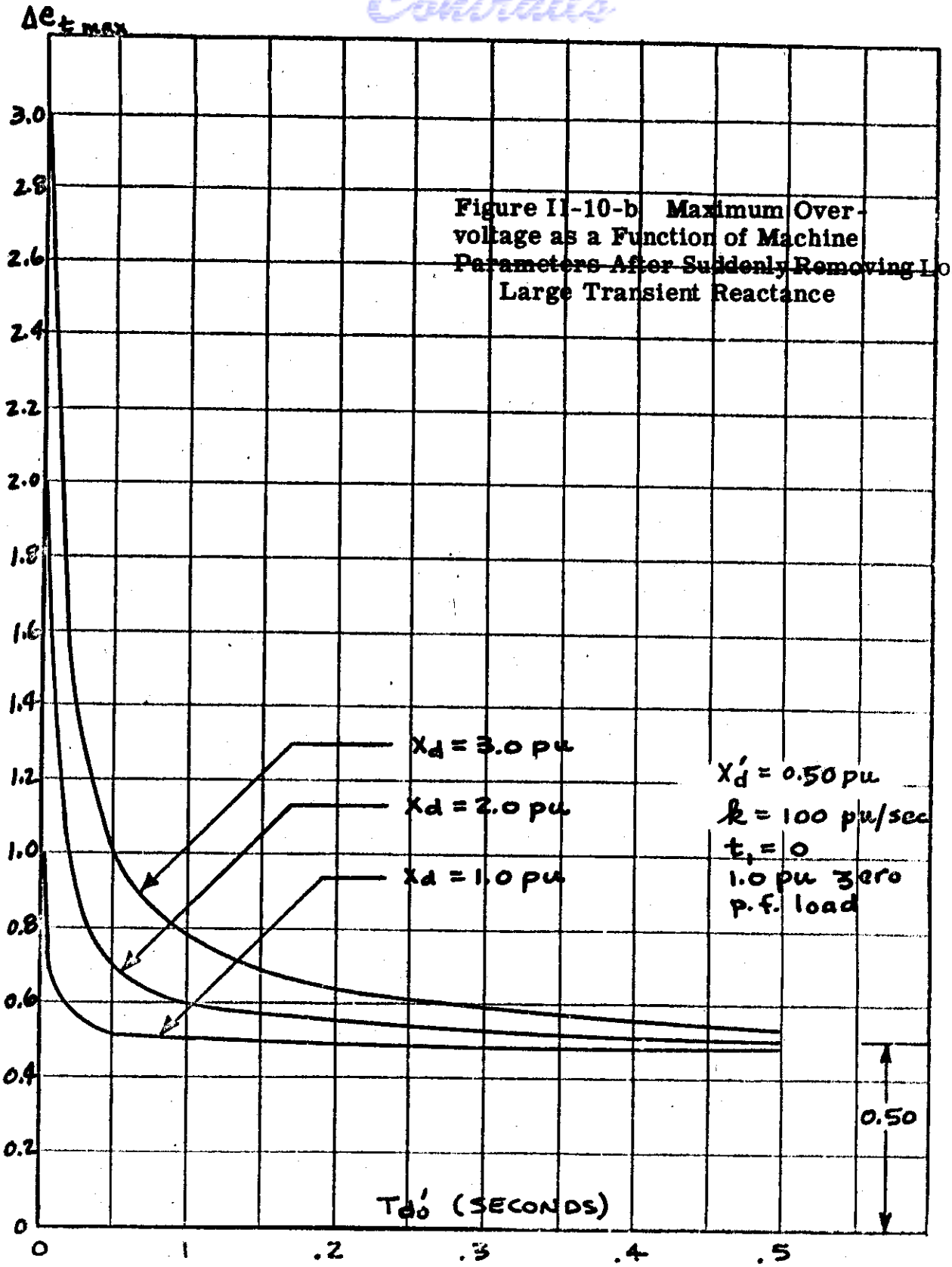

Figure II-10-b Maximum Over-voltage as a Function of Machine Parameters After Suddenly Removing Load
Large Transient Reactance

(b) The voltage induced in the a-c generator at no load is not a linear function of the field current. For example, in cases where the maximum overvoltage is calculated to be 2.0 to 3.0 p.u. these results would not be correct in a saturated machine. The results do hold more closely for wide speed range aircraft machines operating at the higher speeds. However, even where the results are not quantitatively correct, they do show qualitatively the effect of the various parameters.

In a particular case saturation can be included by a graphical method given by Rudenberg [24]. This method was used to calculate a curve of terminal voltage versus time (Figure II-11) following removal of load using the no-load saturation curve of a 60 kva a-c generator. A test curve of this generator and one given from the results of Appendix B-1 are also shown for comparison in Figure II-11.

II-C-3-b Effect of Machine Parameters on Recovery Time - The analytical study of system recovery time is extremely difficult if not completely impossible due to the many variables which influence its value. Feedback circuits and nonlinearities all tend to complicate the problem. Furthermore, one cannot isolate the a-c generator or even the generator and its exciter and then talk about time of recovery, for the entire system must be considered. The study of the effect of machine parameters on recovery time is shown in detail in Appendix A.

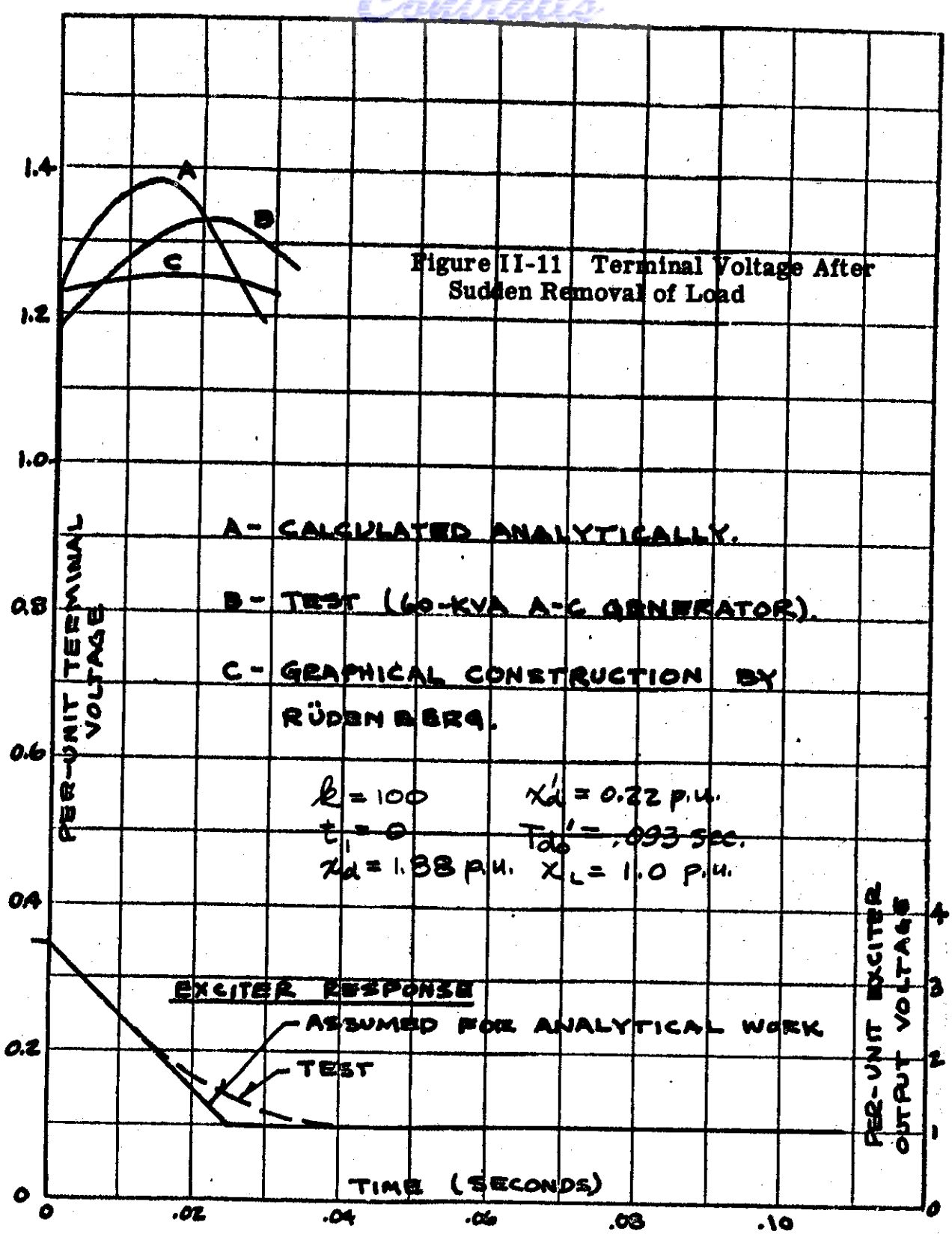

Figure II-11 Terminal Voltage After Sudden Removal of Load

II-D A-C GENERATOR DIMENSION AND WINDING VARIATIONS

Aircraft a-c generator machine constants are often set directly by specifications or indirectly by performance requirements such as output, speed, harmonic level, and maximum allowable weight. The designer, for lack of a better method, proceeds by the trial-and-error process to obtain the desired constants. In connection with this study, the results obtained from analogue computer and analytical work had to be correlated with a practical range of machine constants. Certain constants can hardly be changed in a practical machine design without affecting others. As an approach to the problem it was decided to make a number of design calculations for practical machines to determine how the constants are affected by variations of certain dimensions and winding. For direct comparison purposes, all of the new designs were calculated to meet the same speed-load requirement. The rating is the same as that of an existing machine: 60 kva, .75 power factor, 120/208 volts, 5400/6600 rpm, 360/440 cps, and an overload capacity of 50 percent at minimum speed for five minutes. The actual machine is called the "reference" machine in this study.

Appendix B-3 gives the assumptions and calculating procedure for this portion of the study. Appendix B-2 gives a resume of Kilgore's machine constant equations[28]. These equations and some of Alger's work[29] are used to calculate the constants.

II-D-1 A-C Generator Physical Variations - The new designs differ from the reference machine in one of the following respects:

(a) length of air gap
(b) ratio of copper to magnetic material
(c) number of armature conductors, and
(d) cross-sectional dimensions keeping the configuration proportions constant.

Two calculations were made for each of these variations, one on either side of the reference machine. An objective in selecting the values for each variation was to use the practical limit. In several cases, however, there appears to be no limiting consideration except the resulting machine constants or excessive weight of the generator.

II-D-1-a Air Gap Length Calculations - The minimum gap calculation was made at .0185 inches and the maximum gap calculation was made at .043 inches, the reference machine being .043 inches. Considering manufacturing tolerances, flexibility of the shaft between bearing supports,

and mass and diameter of the rotor, the .0185 inch gap is probably a reasonable lower limit. The upper limit is only governed by the characteristic and weight of the machine. Probably a greater gap than .043 inches would result in a machine too heavy for aircraft applications.

II-D-1-b Ratio of Copper to Magnetic Material Calculations - Designers of industrial a-c generators have long made use of empirical data, such as a constant "ampere-conductors per inch", in obtaining satisfactory proportion of copper to magnetic material. To the writer's knowledge, such data has not been published for aircraft generators. The pole body may be slender with a relatively large winding, as indicated in Figure II-12(a). With such proportioning of the pole, the armature teeth would also have a small cross-sectional area and allow a large number of armature conductors in a practical design. The wide-pole machine shown in Figure II-12(c) would require a small field winding and a relatively small number of armature conductors. The practical limits can hardly be set by any criteria other than the resulting performance and weight of the machines. The designs were arbitrarily made at plus and minus 15 per cent of the iron cross-sectional area of the reference machine.

II-D-1-c Number of Armature Conductors Calculations - The designer has considerable leeway in choosing the total armature conductors. Supposing the cross-sectional area of the magnetic circuit has been selected, more conductor space can be obtained by increasing the depth of the slots. The reference machine has two conductors per slot. Considerations here will be confined to the same number, since it is desired to make only one physical change at a time, if possible. More than two conductors per slot will give a better space factor and result in a lighter generator. The leakage reactance would increase however, since it varies with the square of the conductors per slot and only directly with the total number of conductors.

For this portion of the calculations the field structure is unchanged except for stack length. One calculation is made for 115.3 per cent of the reference machine slots, resulting in narrower, deeper slots, and a greater outside diameter for the stator. Another calculation is made for 84.7 per cent of the reference machine slots.

II-D-1-d Variations of Dimensions Perpendicular to the Shaft Holding the Same Proportions - Specifications often give the maximum permissible diameter for the a-c generator, as well as the maximum allowable overhung moment from the mounting flange In effect, this influences the

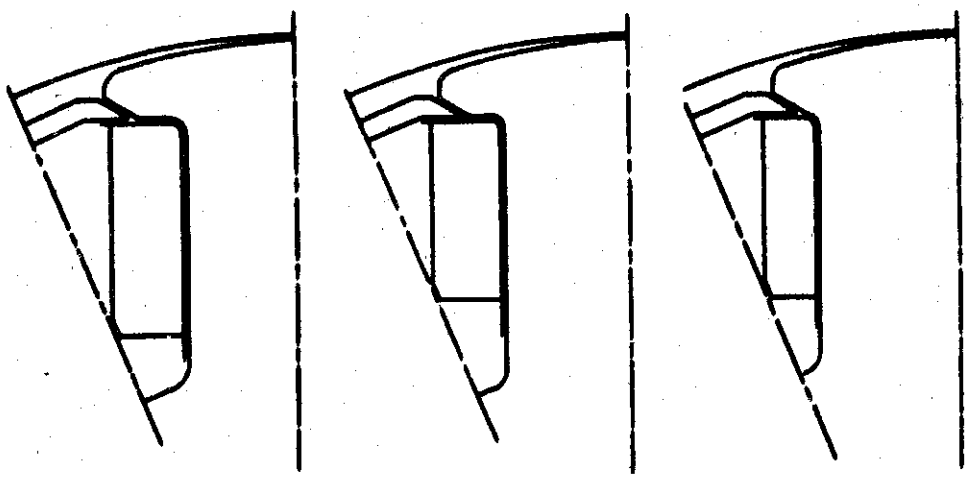

(a) 85 per cent of reference machine magnetic material/inch

(b) reference machine

(c) 115 per cent of reference machine magnetic material/inch

Figure II-12 Field Pole Configuration

ratio of the generator diameter to stack length. Several texts (by Kuhlemann [4], Still [30], Slichter [31], and others) have discussed the optimum ratio. It appears that a simple equation cannot be written. An approximate relationship would be for the pole pitch times the chording factor to equal the stack length. This would permit a given length armature coil to encircle the greatest cross-sectional area of magnetic material. For the reference machine, the rotor "diameter/length" from this consideration would be 2.80, whereas it is actually 2.38. The above authors point out that the centrifugal forces must be considered. This is probably always a limitation in aircraft generators of about the size and speed of the reference machine. A design has been made here for all "active" material dimensions, in a plane perpendicular to the shaft, increased to 107.5 per cent of that of the reference machine. Another calculation was made to decrease the dimensions to 92 per cent.

II-D-2 Weight Considerations - Calculation of accurate weights was not considered justified here since the approximations used for the designs are somewhat inaccurate. Instead "$D^2\ell$" values are calculated for the a-c generator and the exciter on each design. The "$D^2\ell$" for the reference machine exciter was known. The values for the other exciters was obtained by multiplying by the ratios of the a-c generator field requirements. Figures II-13 through II-16 give the sum of the generator and exciter "$D^2\ell$" values.

II-D-3 Conclusions - The design and machine constants for all generators considered here are given in Tables B-1 and B-2 of Appendix B-3. The effect of dimensional and winding changes upon the major machine constants is shown in the form of curves, Figures II-13 through II-16.

Factors Affecting A-C Generator and Exciter Weight:

It is apparent that all of the general variations of design considered have a pronounced effect upon the weight of the machines, as shown by Figures II-13 through II-16. Any one of the changes affects a number of other constants, however, and this must be kept in mind. The lightest-weight a-c generator and exciter will result from: using a minimum air gap, keeping the ratio of copper to magnetic material high, and judiciously choosing the ratio of the rotor diameter to length. Centrifugal forces at overspeed often limit the rotor diameter.

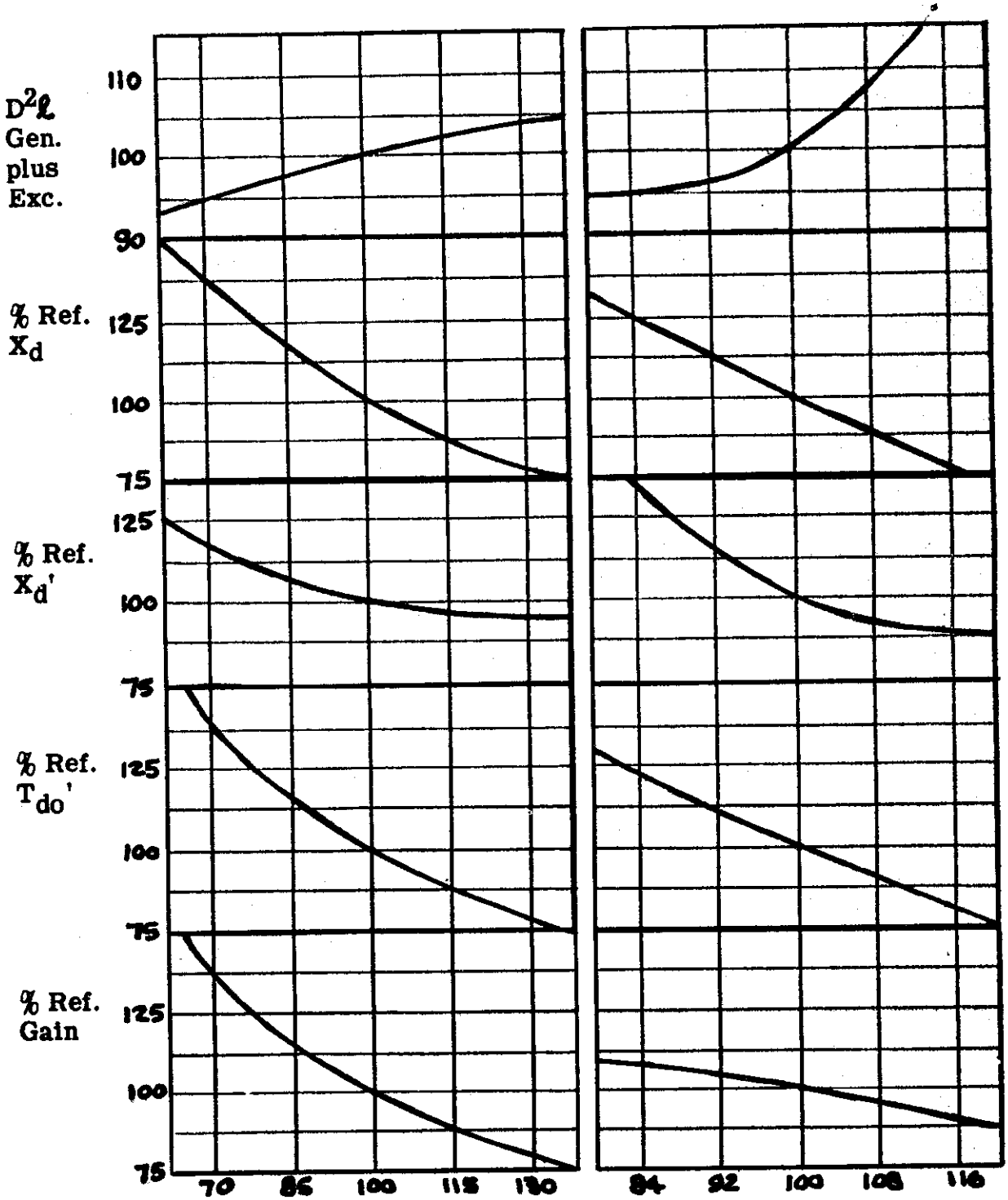

Figure II-13 Variation of Gen. Air-Gap

Figure II-14 Variation of Ratio of Copper to Magnetic Material

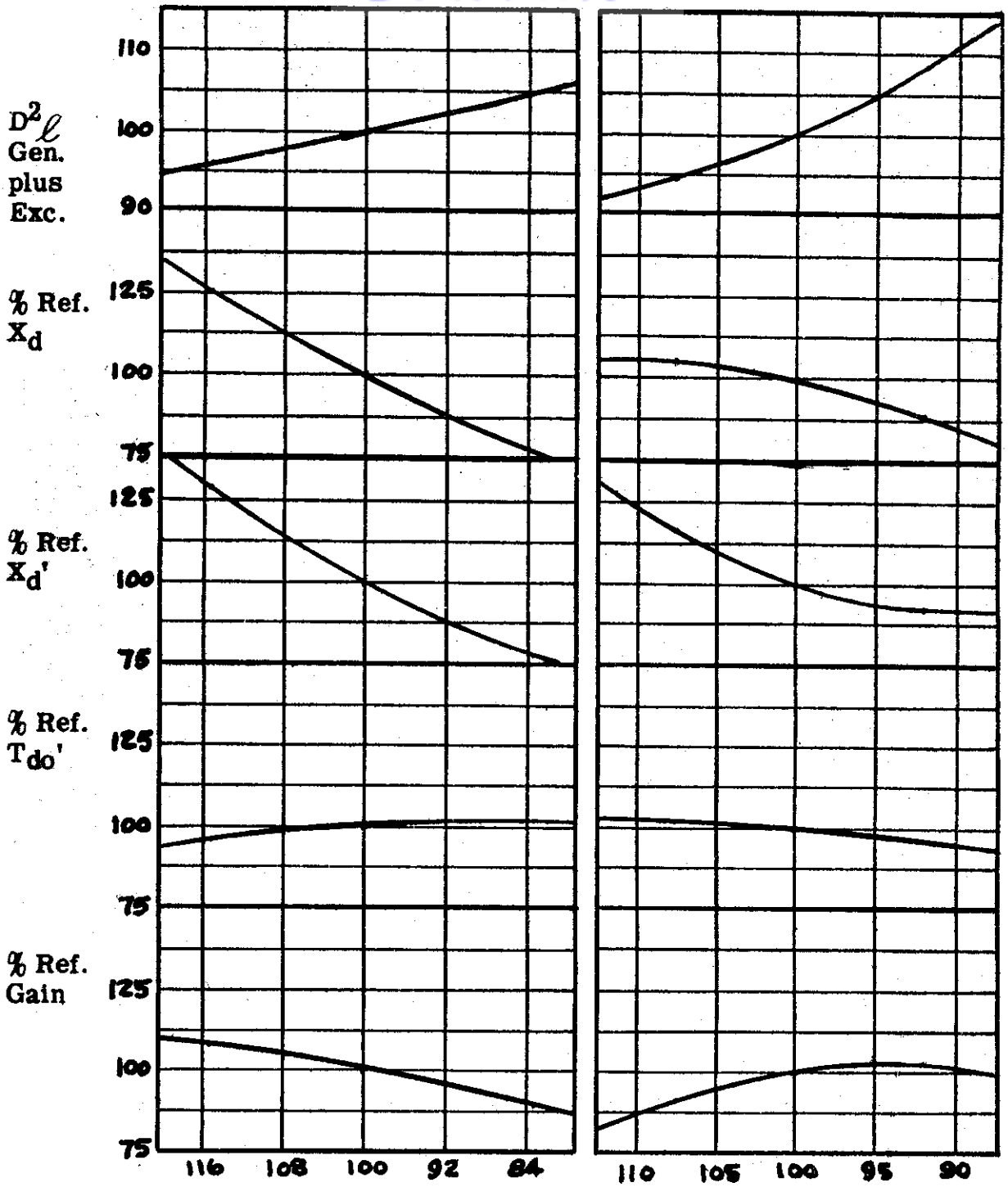

%Ref. Gen. Arm. Conductors

Figure II-15 Variation of Gen. Arm. Conductors

%Ref. Gen. Cross-Sect. Dimen.

Figure II-16 Variation of Gen. Cross-Sectional Dimensions

Factors Affecting x_d:

Figures II-13 through II-16 show that changing the air-gap causes the most drastic change in x_d. The number of armature conductors are changed the same amount for "ratio of copper to magnetic materials" and "armature conductor" variations. Since the effect upon x_d is essentially the same, it is concluded that the armature conductor change is the prime factor. Figure II-16 shows that the change of cross-sectional dimensions, keeping the same proportions, has no appreciable effect.

Factors Affecting x'_d:

x'_d was calculated following Kilgore's paper (see Appendix B-2 for equations). His equations show that x_d and x'_d are both greatly affected by the reactance factor, X, and the air-gap permeance, λa. If it were not for the variation of λ_f in the designs, the curves for x_d and x'_d would be very similar. It was not expected that x'_d would be so great for the narrow-pole calculation as indicated in Figure II-14. It must be caused primarily by the increased amount of field winding offsetting the increase in distance between the pole sides.

Factors Affecting T'_{do}:

This time constant is most affected by changes in air-gap as shown by Figure II-13. The "ratio of copper to iron" variation, figure II-14, has considerable effect, since the field-winding cross section was varied as well as the stack length.

Factors Affecting the Gain (per cent air-gap voltage/ampere turn/pair of poles):

The air-gap variation has the most effect upon no-load gain, as shown by Figure II-13, and the other variations have very little effect.

Combinations of Design Variations Studied Here:

A designer probably would not choose to use any one of the outside variation limits considered here to obtain a given set of machine constants. It would probably be preferred to use two or more. Time did not permit making combination calculations of the various physical changes. It is believed, however, that constants can be predicted from a given design, when more than one variation is made, by use of the curves. It is to be kept in mind that the "ratio of copper to magnetic material" study

has the same changes in the number of armature conductors as the "armature conductor" study. A designer may use both of them to reduce weight, for example, but he probably would be increasing the number of armature conductors beyond a reasonable limit.

BIBLIOGRAPHY FOR CHAPTER II

1. Liwschitz, Garik and Whipple. Electric Machinery Volume II. First Edition. D. Van Nostrand Company, Inc., New York, 1946. Chapter 9.

2. Puchstein, Lloyd, Conrad. Alternating Current Machinery. Third Edition John Wiley and Sons, Inc., New York, 1954. Chapter 14.

3. McFarland, T. C. Alternating Current Machinery. First Edition. D. Van Nostrand Company, Inc., New York, 1948. Chapter 7.

4. Kuhlmann, J. H. Design of Electrical Apparatus. Second Edition. John Wiley and Sons, Inc., New York, 1946

5. Knowlton, A. E. Standard Handbook for Electrical Engineers Seventh Edition. McGraw-Hill Book Company, Inc., New York, 1941. pp 635-642.

6. Fortescue, C. L. Method of Symmetrical Coordinates Applied to the Solution of Polyphase Networks. AIEE Transactions, Vol. 37, Pt. II, 1918, pp. 1027-1140.

7. Wagner, C. F. and Evans, R. D. Symmetrical Components First Edition. McGraw-Hill Book Company, Inc., New York, 1933.

8. Lyon, W. V. Applications of the Method of Symmetrical Components First Edition. McGraw-Hill Book Company, Inc., New York, 1937

9. Clark, E. Circuit Analysis of A-C Power Systems, Vol I. First Edition. John Wiley and Sons, Inc., New York, 1943.

10. Clarke, E. Circuit Analysis of A-C Power Systems, Vol. II. First Edition. John Wiley and Sons, Inc., New York, 1950.

11. Wilson, B. J. Methods for Predication of Steady-State Performance for Unbalanced Regulated 3-Phase Generators. AIEE Transactions, Vol. 73, Part II, Applications and Industry, 1954, pp. 413-421.

12. Stineman, R. W. Discussion of Reference 11, AIEE Transactions, Vol. 73, Part II, Applications and Industry, 1954 pp. 421-422.

13. Westinghouse Authors, Electrical Transmission and Distribution Reference Book, Fourth Edition, Westinghouse Electric Corporation, East Pittsburgh, Pa., 1950, Chapters 2 and 6.

14. Doherty, R. E. A Simplified Method of Analyzing Short-Circuit Problems. AIEE Transactions. Volume 42, 1923 pp. 841-849.

15. Westinghouse Authors. Electrical Transmission and Distribution Reference Book. Fourth Edition. Westinghouse Electric Corporation, East Pittsburgh, Pa., 1950. pp. 153-155.

16. Park, R. H. Two-Reaction Theory of Synchronous Machines- Generalized Method of Analysis Part I. AIEE Transactions, Vol. 48, 1929. pp. 716-727.

17. Adkins, B. Transient Theory of Synchronous Generators Connected to Power Systems. Proceedings of the Institute of Electrical Engineers, 1951. pp. 510-528

18. Concordia, C Synchronous Machines First Edition. John Wiley and Sons, Inc., New York, 1951.

19. Ku, Y. H. Transient Analysis of A-C Machinery AIEE Transactions, Vol. 48, 1929. pp. 707-715.

20. Lyon, W. V. Transient Analysis of Alternating Current Machinery First Edition. John Wiley and Sons, Inc., New York, 1954.

21. Park, R. H. Definition of an Ideal Synchronous Machine and Formula for the Armature Flux Linkages General Electric Review, Vol. 31, June 1928. pp. 332-334.

22. Doherty, R. E. and Nickle, C. A. Synchronous Machines V - Three Phase Short Circuits AIEE Transactions, Vol. 49, 1930. pp. 700-714

23. Fitzgerald, A. E. and Kingsley, C. Electric Machinery First Edition McGraw-Hill Book Company, Inc., 1952.

24. Rudenberg, R. Transient Performance of Electric Power Systems First Edition. McGraw-Hill Book Company, Inc., 1950.

25. Harder, E. L. and Cheek, R. C. Regulation of A. C. Generators with Suddenly Applied Loads AIEE Transactions, Vol. 63, 1944. pp. 310-318.

26. Anderson, H. C. Jr. Voltage Variation of Suddenly Loaded Generators General Electric Review, August 1945 pp. 25-33.

27. Rosenberg, L. T. A Semiempirical Approach to Voltage Dip-With Suddenly Applied Loads on A. C. Generators. AIEE Transactions, Vol. 68, 1949 pp. 160-166.

28. Kilgore, L. A. Calculation of Synchronous Machine Constants AIEE Transactions Vol. 50, 1931. pp. 1201-1213.

29. Alger, P. L. Calculation of Armature Reactance of Synchronous Machines AIEE Transactions, Vol 47. pp. 493.

30. Still, Alfred. Elements of Electrical Design Second Edition. McGraw-Hill Book Company, Inc., New York, 1932. pp. 180

31. Slichter, W. I. Design of Electrical Machinery First Edition John Wiley and Sons, Inc., New York, 1926. pp. 148-149.

CHAPTER III

EXCITERS AND VOLTAGE REGULATORS

III-A INTRODUCTION

It has been common knowledge for some time that an important part of a generator-regulator system, so far as transient performance is concerned, is the excitation means. In general this is defined as the exciter, the voltage regulator and the feedback stabilizing circuit. In this report the latter two portions are combined under the common heading of voltage regulators.

Since the main purpose of the work described in this report was to study a-c generator characteristics, the role of the excitation means was given secondary consideration. This is not to say that it was disregarded, but rather only a limited number of variations were studied.

A common procedure in the development of a new generator system is to first establish the main generator design and then adjust the excitation system to give the necessary transient performance. The approach here is somewhat different in that the excitation system is fixed and the a-c generator constants are varied to determine what factors may ease the requirements for the excitation system.

This chapter will therefore cover the exciter and voltage regulator only to the extent necessary to understand the viewpoint taken in other portions of this report. The exciter is treated under steady-state conditions, taking up saturation curves and compounding effects. Under exciter transients,time constants, performance definitions and eddy currents are discussed. A section is also included for practical methods of dealing with non-linearities in the exciter. Finally voltage regulators and their feedback circuits are briefly discussed.

III-B EXCITER STEADY-STATE CHARACTERISTICS

D-C generators are commonly used as exciters for a-c synchronous machines. Shunt field windings are employed and often a cumulative series winding is added. Other special windings, such as a differential shunt, may be included for various reasons.

III-B-1 **No-Load Saturation Curves** - A typical no-load saturation curve is shown in Figure III-1 as curve A. It is readily determined by test or it may be calculated with a fair degree of accuracy. If there were no saturation in the iron of the magnetic circuit, the curve would fall on the air gap line. The calculation procedure involves determining the flux density for all sections of the magnetic circuit, for a particular air gap flux, and from the B-H curves for the respective section materials the ampere-turns per unit length is read. Each value is multiplied by its length and finally the total ampere-turns is obtained by adding that for each section to that for the air gap. An accurate calculation takes into account the pole leakage, the air gap between the poles and the frame, a non-uniform main air gap and a number of other factors. Load saturation curves are calculated using the no-load curve as a starting point. Armature reaction tends to decrease the net air gap flux unless 100 percent compensation is employed. With no pole-face windings the armature mmf peaks midway between the main poles and is zero at the center of the poles. This increases the flux density on one side and decreases it on the other. In the high density regions the pole tips and armature teeth tend to saturate and thus the flux increase does not make up for the flux loss on the low density side of the poles. The result is a loss of net air gap flux. Pole face windings are commonly used in exciters to nullify from 60 to 100 percent of the armature mmf. A' of Figure III-1 is a corrected no-load saturation curve for a machine not fully compensated, corresponding to a particular load current.

III-B-2 **Fixed Resistance Load Saturation Curves** - The exciter load, which is the field winding of the main generator, has a considerable resistance change under operating conditions because of the variation of temperature. In problems of other sections of this report the resistance is considered constant at a value corresponding to an average field temperature. A typical fixed resistance saturation curve is shown as B in Figure III-1. It may be obtained from test data or calculated with a fair degree of accuracy. The load saturation curve normally falls below the no-load curve because of the resistive drop through the exciter and the compounding effects from commutation. The resistive drop includes that for the armature, the brush contact, the interpole and compensating windings and the series windings when used. All of the winding resistances are affected by temperature. As in the case of the main generator field, they are considered fixed at a compromise value in the problems of this report. With this assumption the load current is linear with the exciter output voltage and thus the resistive drop would also be linear as indicated in the figure by curve C.

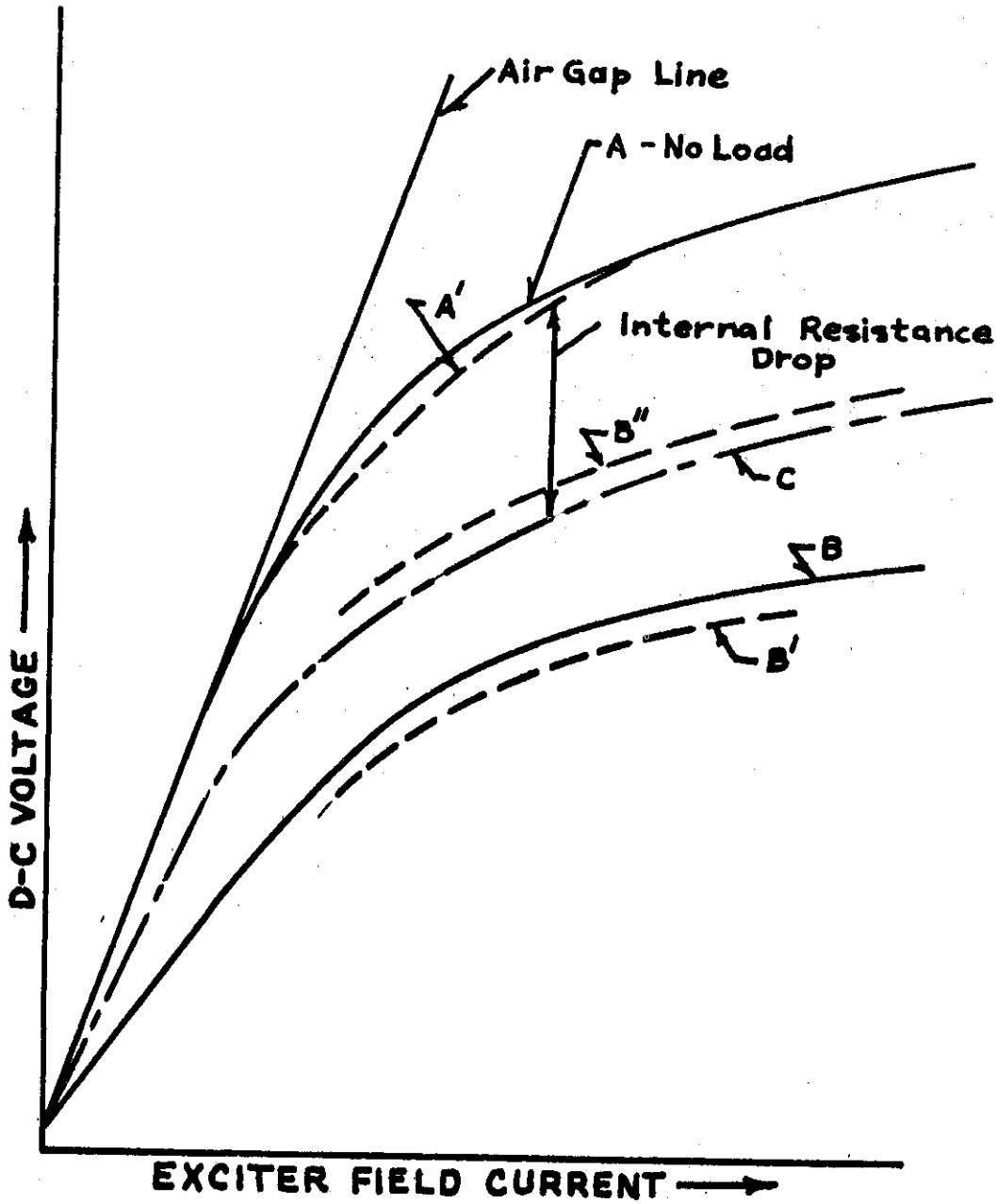

Figure III-1 Exciter No-Load and Fixed–Resistance Load Saturation Curves

With no series winding curve C should ideally coincide with curve B. In actual practice this is usually not realized, however, as there is some compounding effect from the armature conductors undergoing commutation. Where the interpole winding mmf is too weak or the brushes are set off neutral in the direction of armature rotation, differential compounding results. Curve B of Figure III-1 exemplifies this condition. Similarily, where an interpole winding is too strong or where the brushes are shifted against armature rotation, cumulative compounding results. The load saturation curve for such an exciter would be drawn above curve C in the figure. This subject is given excellent treatment in Langsdorf's text[1].

III-B-3 Compounding Effects Resulting From The Use Of Altitude Treated Brushes - Considerable progress has been made the last five years in obtaining satisfactory brush life for aircraft machines operating above 35,000 feet altitude. This has come about by developing special treated brushes. The new brushes still have some objectionable features however. One difficulty is obtaining satisfactory brush life at low altitude operation. At sea level the brushes tend to build up a relatively thick commutator film at the trailing edge of each bar. This film continues to grow and the commutation grows progressively worse. The bars are seldom badly burned or pitted but the brushes last a very short time after the film begins to form on the edges of the bars. The purpose of the discussion here is to point out that the contact drop of the brushes and the compounding effects from the conductors undergoing commutation vary widely with the build-up of the film. Also, these effects vary appreciably with the temperature of the commutator. For the work covered in this report it was assumed that the load saturation curve was a mean curve lying between the extremes as shownin Figure III-1 by curve B' for a cold commutator and B" for a hot commutator.

III-C EXCITER TRANSIENTS.

The exciter is now recognized as an important component of the a-c generator system from a transient performance standpoint. The time constant of the main shunt field is an important parameter of the exciter. In some approximate analyses it is considered the only delay in the exciter. An idealized exciter is shown in Figure III-2. Assume it has no saturation, no resistance drop in the armature, and no compounding effects.

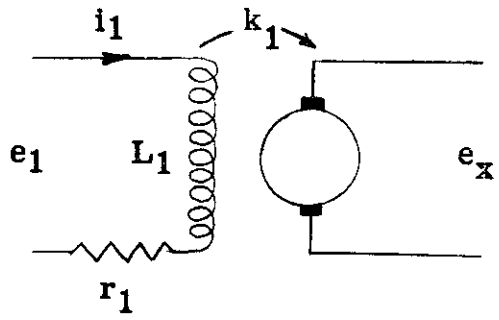

Figure III-2. An Idealized Exciter

This is a one-delay component with a transfer function of

$$\frac{e_x}{e_1} = \frac{k_1}{r_1 (1 + T_1 p)}$$

where: k_1 is the output voltage generated per ampere of field current,
$T_1 = L_1/r_1$ or the time constant of the field and
p is the differential operator d/dt.

A fundamental relationship has been pointed out recently by different authors [2, 3, 4] for the ratio of the machine power amplification to the field time constant. This is sometimes called "The Figure of Merit". It means that a required power amplification (output power divided by field input power) can only be obtained subject to a time constant which cannot be reduced below a certain value without increasing the weight of the exciter. The figure of merit is given by the equation

$$M = \frac{.57\ s\ q}{g'\ B}$$

where: s = peripheral speed of armature - ft./min.,
q = ampere - conductors per inch of armature periphery,
g' = effective length of air gap - inches, and
B = air gap flux density - lines/in.^{2}

This equation, in regard to power output, includes the total generated value, i.e., the resistance losses are included. There are limits for s, q, and g' in an attempt to increase M because of mechanical and thermal considerations. B can be decreased, however, at the expense of an increase in weight.

Another useful definition for describing exciter performance is the "Response Ratio". It is defined[5] as the ratio of the output voltage change, volts per second, to rated-load field voltage, which response if maintained constant would develop in one-half second the same excitation voltage-time area as attained by the actual exciter. The response is determined with no exciter load, with the output voltage initially equal to the rated-load field voltage and then suddenly establishing circuit conditions to obtain nominal exciter ceiling voltage. Figure III-3 illustrates this definition.

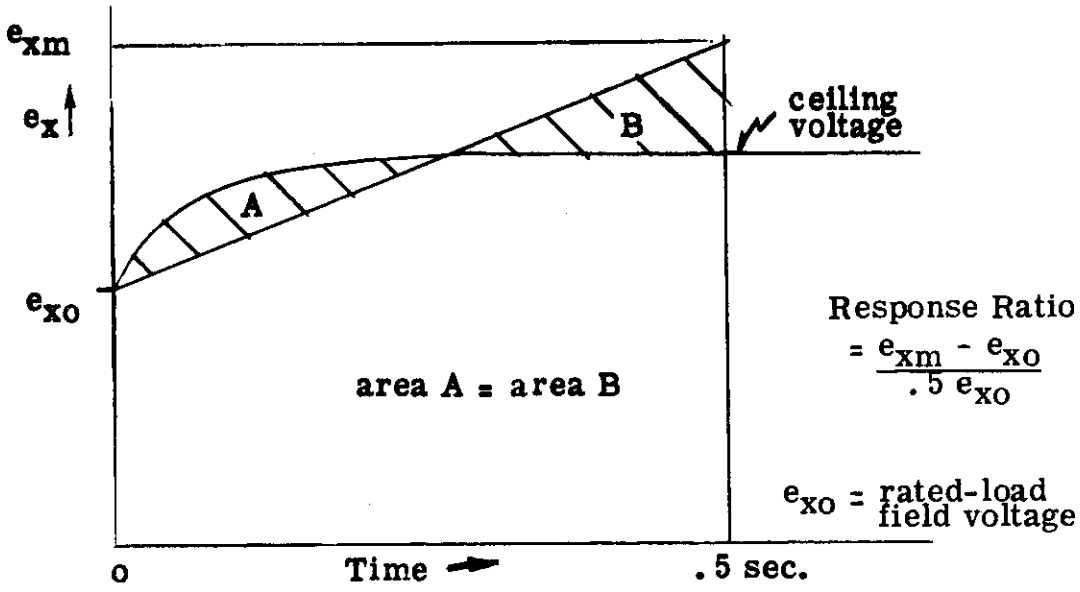

Figure III-3. Response Ratio

It is apparent that the response ratio reflects the effective time constant of the exciter and the ceiling voltage. The half-second time should be changed to about .05 seconds for aircraft exciters since they are normally a fraction of the size of industrial exciters and have a much smaller time constant. If the half-second value is used it reflects primarily the exciter ceiling voltage and gives little weight to the response.

III-C-1 Saturation Effect Upon Exciter Transients

Saturation at steady-state conditions is significant primarily because it increases the excitation. This also applies under transients. Reconsider the idealized exciter with transients extending into the saturation region. The self-inductance of the field winding may be expressed

$$L_1 = Pn_1 \frac{d\phi}{di_1} 10^{-8} \text{ henrys}$$

where: P is the number of exciter poles,
n_1 is the winding turns per pole,
ϕ is the flux per pole - lines and
i_1 is the shunt field current.

From the flux saturation curve, Figure III-4, the slope of a tangent to the curve gives $d\phi/di_1$. At point f, for example, $d\phi/di_1$ can be determined and the inductance may then be calculated.

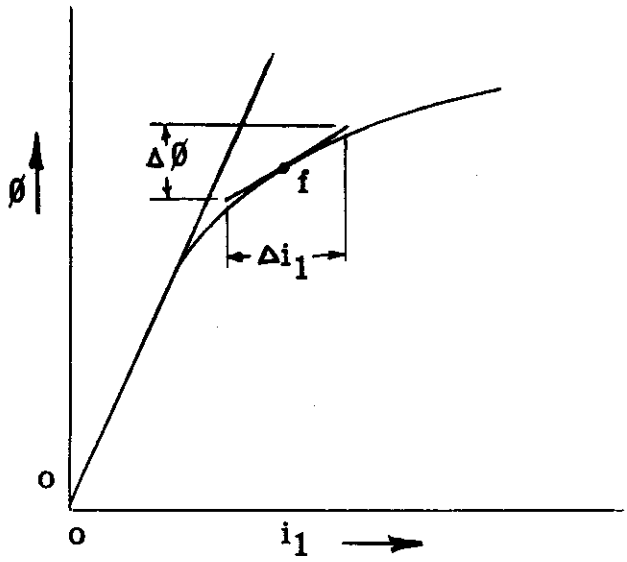

Figure III-4. Determination of $d\phi/di_1$

A rigorous analysis would treat L_1 as a variable which is dependent upon the degree of saturation. The exciters considered in the work related to this study have negligible saturation at the operating conditions of interest. L_1 was therefore considered a constant in all cases.

III-C-2 Exciter Effective Time Constant

The exciters considered in this report have eddy-current time constants in the order of twenty percent of the respective main shunt field values. Rudenberg shows[6] that the effective time constant of a machine with eddy currents is the sum of the exciting winding time constant and the eddy current time constant.

III-C-3 Eddy-Current Effects In Exciters. The frame of exciter stators are often made from solid iron and the main poles are attached by bolts. The poles may be made from laminations and held together by weld beads along the sides. The frame would contribute the major portion of the eddy-current effects, but there may be minor effects from circuits such as those caused by the welds on the side of the poles or burrs on the punchings.

An approach to the eddy-current problem is given in a British paper[7] by Pohl. First, the equations for the eddy-current demagnetizing flux are developed for a sheet of iron of infinite width. The net flux through the iron, perpendicular to the thickness and width directions, has a constant rate of change. It is assumed at the instant impact excitation is applied that counter flux, to offset the eddy-current flux, appears instantaneously and dies out with the eddy-current time constant.

Equations are next developed for a winding (one turn) outside the solid iron that would give the same demagnetizing flux as the actual eddy-currents. It is shown that the substitute winding must have about 22 per cent leakage in order for the time constant to check that for the actual eddy-currents. Pohl indicates that the leakage flux for the infinitely wide sheet of iron and for a round cross-section of iron should each have about 22 per cent leakage. This is accepted here as correct for a rectangular cross-section also.

The reference paper gives an equation for the conductance of the substitute winding where the solid iron is rectangular. The reciprocal of this is the resistance. Applying to an exciter, the value should be multiplied by "2P" to give the total resistance where "P" is the number of

poles. The equation is:

$$r_2 = 2P\rho \frac{(12b + 20a)}{\ell_2 a} \quad \text{ohms}$$

where: r_2 = effective resistance of eddy-current circuits - ohms,
ρ = resistivity of frame material - ohm-cm,
a = thickness of frame - cm,
b = width of frame - cm, and
ℓ_2 = length of solid iron section or one-half the distance on the frame between poles - cm.

Usually the self-inductance of the main shunt field is known from calculations or from test data. Using this the self-inductance of the eddy-current circuits may be calculated as:

$$L_2 = 1.22 \frac{\phi\ 12}{\phi\ 11} \cdot L_1 \frac{(n_2)^2}{(n_1)^2} \quad \text{henrys}$$

where: a 22 percent leakage factor is included to account for the substitute winding normally having less leakage than the actual eddy-current circuits,

ϕ_{12} = flux caused by the main shunt winding flux linking the substitute winding,
ϕ_{11} = total flux linking the main shunt winding,
L_1 = self-inductance of the main shunt winding - henrys,
n_1 = number of turns/pole on main shunt winding and
n_2 = number of turns/pole on substitute winding.

The ratio of ϕ_{12}/ϕ_{11} can be obtained from a flux map of the exciter stator interpolar space.

The eddy-current time constant T_2, is simply L_2/r_2. Values obtained by the above method were checked against the results obtained using Rudenberg's equation[8] and fair agreement was obtained.

Appendix B-4 elaborates upon some parts of Pohl's paper and gives a sample calculation of the eddy-current constants for an exciter.

III-C-4 Exciter Non-Linearity Approximations.

Exact equations expressing the relationship of currents, voltages, and flux in exciters cannot be written for the non-linear regions of operation, or at best, they are tedious and approximate. The assumptions and approximate mathematical expressions defining exciter non-linear characteristics as used in the work related to this report are given in this section.

III-C-4-a Voltage-Excitation Non-Linearity.

Saturation of the iron of the main magnetic circuit accounts for the non-linearity of the generated voltage excitation curve as shown in Figure III-5.

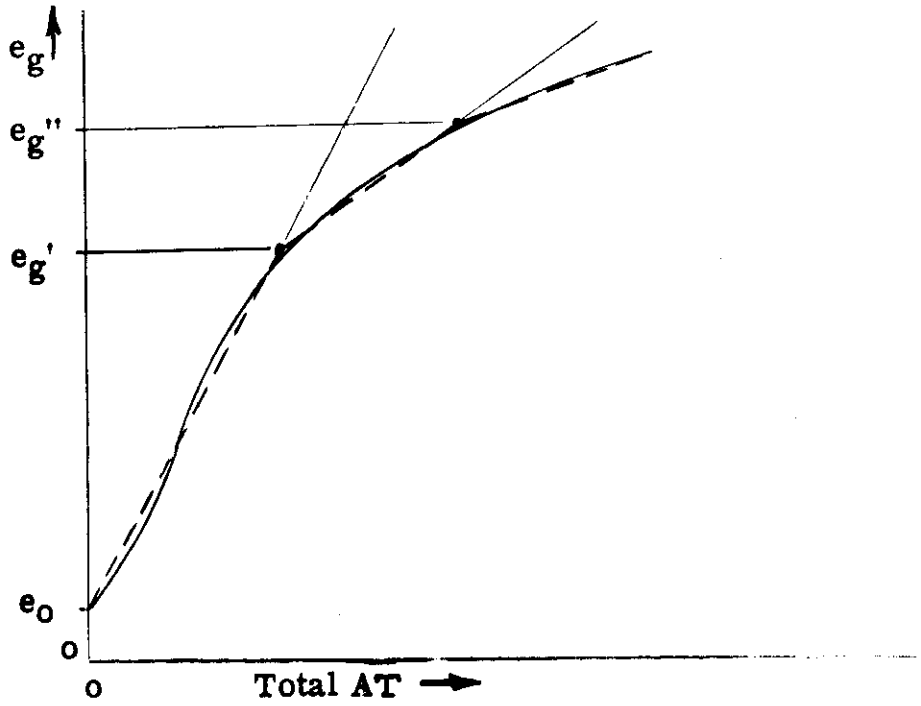

Figure III-5. No-Load Saturation Characteristic Approximation

The curve is approximated by a number of straight line segments. The residual voltage is assumed constant as indicated by e_o. An expression for the approximate curve is:

$$e_g = \gamma k AT_t + e_o$$

where: k is a constant - volts/ampere-turn ,
AT_t is the total instantaneous field excitation - ampere-turns,
$\mathcal{T}$ is a saturation factor and
e_o is the residual voltage.

The saturation factor for a curve as shown in the figure is

$$\mathcal{T} = 1 \quad \text{(for values of } e_g \text{ below } e'_g\text{)}$$
$$= 1 - k' (e_g - e'_g) \quad \text{(for values of } e_g \text{ between } e'_g \text{ and } e''_g\text{)}$$
$$= 1 - k' (e_g - e'_g) - k'' (e_g - e''_g) \quad \text{(for values of } e_g \text{ above } e''_g\text{)}$$

where: k' and k'' are constants related to the slope of the straight-line segments.

Though it was not necessary in the problem studied in this report to include exciter saturation, the above equations are in a convenient form for simulating an exciter using an analogue computer and diode-limiter sections to introduce the non-linearity.

III-C-4-b **Non-Linearity Associated With Exciter Load Current.**

The effect of load current was discussed in Section III-B-2 and III-B-3 for steady-state conditions. The effects of the load current are the same at transient conditions if the instantaneous values of currents are applied. An expression for the exciter output voltage is:

$$e_x = \mathcal{T} k AT_t + e_o - i_f r_3 \quad \text{or}$$
$$e_x = \mathcal{T} k (AT_1 + AT_2 - \delta i_f) + e_o - i_f r_3$$

where: AT_1 and AT_2 are the ampere-turns from the main shunt field and eddy-currents respectively,
δ is the effective turns for the compounding effect,
r_3 is the internal resistance of the exciter armature circuit and
i_f is the a-c generator field current.

It was mentioned previously that the generator field resistance was assumed to be a constant and therefore under steady-state conditions there is a fixed relationship between the exciter output voltage and its load current. From the saturation curves, as shown in figure III-1, the field current ordinate may be readily converted to ampere-turns per pole. Since the exciter load current is proportional to exciter output voltage at steady-state the relation between the generated voltage from the series or com-

pounding ampere-turns may be related to the load current. That is, the generated voltage, the calculated resistive drop, and the compounding-effect voltage must add algebraically to give the output voltage. The relation between the compounding-effect generated voltage to load current is thus determined from the steady-state conditions. The relationship would hold for transient conditions, however.

Suppose the compounding ampere-turns versus load current relationship is as shown in figure III-6, where δi_f is the ampere-turns.

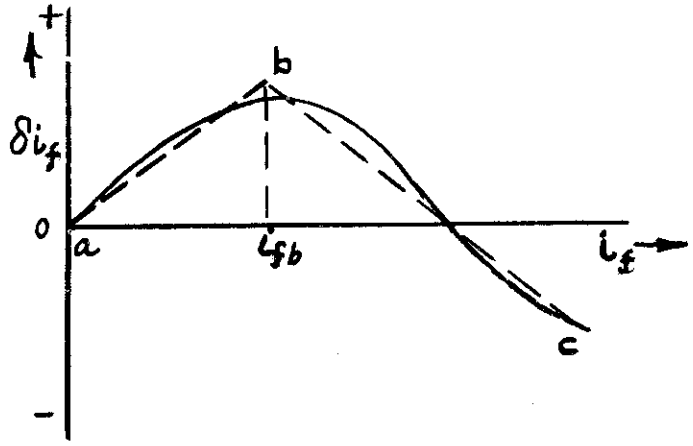

Figure III-6. Compounding Ampere-Turns vs. Load Current

δi_f is obtained by dividing the corresponding generated voltage, taken from the saturation curves, by k. δi_f is approximated by straight line segments a-b and b-c. The equation for the approximation may be written:

$$\begin{aligned} \delta i_f &= c' i_f, && \text{for } i_f \text{ currents below } i_{fb} \\ &= c' i_f - c'' (i_f - i_{fb}), && \text{for currents above } i_{fb} \end{aligned}$$

where: c' and c'' are constants.

It is emphasized that the compounding effect curve shown in Figure III-6 is not the general shape for all exciters. δi_f may be positive or negative for low values of load current. Usually, however, it is either zero or positive in this region and usually goes negative at the higher values of i_f.

III-D VOLTAGE REGULATORS

As stated in the introduction, the systems which were studied for this report all employed carbon-pile voltage regulators. Though in the past year the magnetic-amplifier voltage regulator is found on most of the new designs of a-c systems, there are many installations in military aircraft utilizing the carbon-pile regulator, and it is therefore important to consider the performance of the a-c system with such a control device.

There is considerable material in the literature on the operation and the details of carbon-pile regulators [9-18]. There is no attempt here to cover this phase of the a-c system. It is felt that the regulators used for this report are representative of those being produced and used at the present time, and can therefore be considered as a base by which to judge the remainder of the electric power system.

Little work has been done in the past on the problem of parametric-forcing type of voltage control. Previous stability investigation for voltage regulation systems are concerned with controls which vary the voltage applied to a separate field on the exciter. This is much easier to treat mathematically, which accounts for its popularity. This difficulty in describing carbon-pile regulators mathematically is one of the main reasons why the actual regulators were used in the analogue computer studies. Rather than suffer the loss of many of the important characteristics of the carbon-pile regulator, they are used in their normal manner. Refer to Appendix A for the details on how the regulators were operated. Appropriate voltages were applied to three inputs of the regulator: (1) the voltage coil, (2) the carbon-pile, and (3) the feedback stabilizing transformer.

The only important change made in the voltage regulators during the transient performance studies was the strength of the feedback signal. It is shown in Appendix A how this affects the influence of the other parameters on system performance. With weaker feedback one observes variations which greatly change the system recovery time, for example. With stronger feedback these same variations will cause practically no change in the system recovery time.

In Chapter II and Appendix B the regulator time delay is treated briefly in an analytical manner for the case of sudden removal of loads from the system.

Though it was not possible to go into a study of the magnetic amplifier regulator and the differences in performance between it and the carbon-pile regulator, there was a large amount of data taken on a mock-up of a two-generator system using both regulators. Appendix D presents this data for all types of transients and fault conditions.

Summarizing, the voltage regulator was definitely an important factor in the studies made for this report, but it was considered as a fixed design in most cases since the emphasis is on the a-c generator.

BIBLIOGRAPHY FOR CHAPTER III

1. A. S. Langsdorf, Principles of Direct Current Machinery; McGraw-Hill Book Company, Inc., New York, N. Y., 1940 Fifth Edition, Chapter XII.

2. H. C. Bourne, Jr., Alexander Kusko, Determination of Optimum Excitation and Voltage Control Systems For A-C Generators; Air Force Technical Report No. 6652, 30 September 1953, pp 107-111.

3. H. C. Bourne, Jr., David C. White, Study of Voltage Regulating Systems For Aircraft Alternating Current Generators, Air Force Technical Report No. 54-298, Part I, August 1954, pp 15-22.

4. A. Tustin, Direct Current Machines For Control Systems; The Macmillan Company, New York, N. Y., 1952, pp 63-66.

5. Westinghouse Authors, Electrical Transmission and Distribution Reference Book; Fourth Edition, Westinghouse Electric Corporation, East Pittsburgh, Pa., 1950, Chapter 7.

6. R. Rudenberg, Transient Performance of Electric Power Systems; McGraw-Hill Book Company, Inc., New York, N. Y., 1950, Chapter 8, Chapter 46.

7. R. Pohl, Rise of Flux Due to Impact Excitation; Retardation By Eddy-Currents in Solid Parts; Proceedings, Institute of Electrical Engineers, Vol. 96, Part 2, 1949.

8. R. Rudenberg, Ibid, Chapter 10.

9. R. L. Mills, Dynamic Characteristics of Carbon-Pile Voltage Regulators; AIEE Transactions, Vol. 69, Part II, 1950, pp 1347-53.

10. D. G. Scorgie, Transient Analysis of Voltage-Regulated Aircraft D-C System; AIEE Transactions, Vol. 69, Part II, 1950, pp 1318-23.

11. B. O. Austin and H. H. C. Richards, Aircraft Carbon-Pile Regulators, Fundamentals and Design Improvements; AIEE Transactions, Vol. 68, Part II, 1949, pp 983-87.

12. H. H. C. Richards, Carbon-Pile Regulator Theory, Calibration, Adjustment and Factors Effecting Its Operation; AIEE Transactions, Paper No. 54-356, October, 1954.

13. John Hopkins University, The Analysis of the Carbon-Pile Voltage Regulator for Continuous Potential Aircraft Generators; Navy Dept., Bureau of Aeronautics, Contract No. NOa(s)4574, February 28, 1946.

14. W. G. Nield, Carbon-Pile Voltage Regulators for Aircraft; AIEE Transactions, Vol. 63, 1944, pp 839-43.

15. W. B. Kouwenhoven, G. J. Thaler, Analysis and Redesign of a Carbon-Pile Voltage Regulator for Aircraft Generators; AIEE Transactions, Vol. 67, Part II, 1948, pp 1197-203.

16. D. G. Scorgie, D. H. Schaefer, Steady-State Characteristics of Carbon-Pile Voltage Regulators; AIEE Transactions, Vol. 70, Part II, 1951, pp 1572-77.

17. H. C. Bourne, Jr., Alexander Kusko, Determination of Optimum Excitation and Voltage Control Systems for A-C Generators; Air Force Technical Report, No. 6652, 30 September 1953, pp 211-240.

18. G. N. Patchett, Automatic Voltage Regulators and Stabilizers; Sir Isaac Pitman and Sons, Ltd. London, England, 1954.

CHAPTER IV

TEST METHODS

FOR MEASURING MACHINE CONSTANTS AND CHARACTERISTICS

IV-A INTRODUCTION

This chapter contains a general discussion of testing methods to determine the a-c generator constants and characteristics which are of primary importance to system performance. Also included are integral-exciter testing methods for determining those exciter characteristics and constants which are commonly used for design verification and analytical studies. A detailed test procedure for each test is given.

These machine constants and characteristics are normally required for analytical investigation of transient stability, parallel operation, fault characteristics, unbalanced loading, and verification of machine design.

Past experience has shown that machine constants determined by test at two different locations may differ by rather large percentages. Therefore, standard test procedures should be employed to reduce the discrepencies that may occur; for with unreliable machine constants one has a very difficult problem trying to determine whether the analytical techniques or the machine constants are in error. Refinement and improvement of analytical techniques can only be made after the source of discrepancy is determined.

It is important to analytical studies,therefore, that complete and accurate information be available. However, the required completeness and accuracy of machine constants and characteristics depend on the range and types of analytical investigation to be conducted. To assure that the required information for analytical studies is available always necessitates co-ordination between testing and analytical groups.

It is the purpose of this chapter to describe these testing procedures in a manner which can be understood by the personnel actually performing the testing. By this it is hoped to emphasize the necessity for accurate testing at the most effective point.

IV-B SUMMARY OF FACTORS AFFECTING MACHINE CONSTANT TESTING

Inconsistency of machine constants results from many sources. Such factors as temperature variation between tests, saturation effects, inadequate testing equipment, poor testing techniques, errors in the analysis of test information, and inherent errors of the test,all contribute.

The following is a discussion of standard testing practices which should be followed to insure that most of the discrepancies in test results will be eliminated. Some of the points of discussion may be considered as obvious, but they are of primary importance and worthy of statement.

IV-B-1 Saturation - Normal practice is to define the machine constants determined by test as either rated voltage or rated current values. All aircraft a-c generators operating at rated minimum speed, many operating at rated nominal speed, and even some operating at maximum rated speed,will have saturation at rated voltage conditions. Hence, tests taken at rated voltage will usually yield saturated machine constants.

In general, the machine constants based on the linear or unsaturated regions of generator operation are more desirable. These unsaturated parameters are of more universal use, and standard testing procedures should, therefore,yield values in the linear region.

This means that standard tests should be taken at either rated-current conditions which are ordinarily unsaturated, or at less than rated-voltage conditions.

Saturation is dealt with usually by empirical factors which are determined over long periods of time on a great number of machines. Another method which can often be used is to decrease the unsaturated value of the parameter by a factor equal to the ratio of the voltage on the no-load saturation curve to the corresponding voltage on the air-gap line for a given excitation.

When conditions warrant it, specific testing conditions can be employed to give the desired degree of saturation and its resultant affect on the machine parameters.

IV-B-2 Temperature Variation - Machine temperatures should be

measured for all tests where the winding resistances are an appreciable factor of the machine parameter. This is especially important in determining machine time constants since the time constant is inversely proportional to resistance.

IV-B-3 Metering - Meters should be selected so that all readings can be taken on the upper portion of the scale, preferably greater than half scale deflection. Comparison of meter impedance to the circuit impedance in which the meter is being used will indicate if consideration should be given to meter loading affects. In general, ammeters are more likely to introduce appreciable error in low impedance circuits while voltmeters are troublesome in high impedance circuits. Preferably, meter impedances should be at least in a one to one hundred ratio to test circuitry impedances.

IV-B-4 Oscillographs - Oscillographs should be treated with extra care and the instruction manual should be referred to for proper adjustment and set-up. It will be necessary in most cases to make repeated tests to obtain suitable oscillograms to determine machine constants. Each of the oscillograms taken should contain the following:

(1) Magnitude Calibration - Each trace must have a magnitude calibration. This calibration, in many cases, may be obtained by simply recording the steady-state meter reading before and after the oscillogram is taken. When the initial values are zero and the steady-state values are not shown on the oscillogram, it will be necessary to take a calibration oscillogram. In these cases, it is sufficient to merely take a second oscillogram of the final steady-state conditions. Each calibration trace must have sufficient deflection, preferably greater than one inch, to accurately determine the units per inch deflection.

(2) Zero Lines - Each trace must also have a clearly indicated zero line. These lines are placed on the oscillogram by taking a double exposure when no signal is being applied to the oscillograph elements.

(3) Magnitude of Deflection - The deflections should be made as large as possible without exceeding the limits of the oscillograph. All traces must stay on the film and must not intermesh to a degree where one trace cannot be distinguished from another. Oscillograph adjustments and developing procedure should be done carefully to make the traces as fine as possible, assuring that they can be readily distinguished at all points.

(4) Time Calibration - All oscillograms taken for the determination of machine constants should have a time calibration. The generator output voltage serves as a good time calibration signal if a suitable speed or frequency indicating device is available. A 60 cps signal may be used, but the peaks are not well defined for the fast film speeds used in aircraft machine constant tests.

(5) Oscillogram Inspection - Each oscillogram which is to be analyzed for determination of machine constants should be inspected for all of the above mentioned conditions of calibration, adequate deflection, and legibility. Some discontinuities may be present in time constant tests due to the eddy-currents and damper windings which cause an initial jump in current. If unexplainable jumps are present, the set-up should be examined for relay contact bounce or similar phenomena.

IV-B-5 Transient Tests - Additional consideration should be given to transient tests, such as those for the determination of time constants, to insure that the circuitry added to facilitate taking the test does not alter the transient performance of the machine under test. Each circuit loop should be checked to determine if meter impedances, shunts, rheostats, and power source impedances are not appreciable in comparison to the impedance of the respective circuit loops in which they are used. The exciter time constant test may be cited as an example. For this test the power source used to supply the step function voltage to the shunt field should not have an effective internal impedance which is appreciable in comparison to the shunt field inductance and resistance. The affect of resistance in the test circuitry may be checked by comparing its voltage drop to normal circuit voltage. The voltage drops may be measured by a suitable high impedance low voltage reading voltmeter.

IV-B-6 Testing Limits - No clear cut rule can be given as to the maximum electrical limits that should be used in taking machine characteristic tests except that the name plate rating should be exceeded. For no-load characteristics the excitation field temperature is the limiting factor, while for load characteristics the limiting factors may be the field windings, the brushes, or some mechanical part. A commonly used rule-of-thumbis that the machine life is halved for each twelve degrees centigrade increase in ambient temperature if operation is continuous at this increased ambient. Since these overload tests can be made of short duration when testing for machine characteristic, the decrease in machine life will be small.

The exciter rated load can be taken normally as the a-c generator field requirements for rated load at rated nominal speed and rated cooling on the a-c generator. Exciter testing limits may be compared to this rated value. Discretion must be exercised to determine these maximum over-load testing limits.

IV-B-7 Per-Unit Impedance - Common practice is to express all a-c generator constants in per-unit values. The per-unit impedances may be obtained by multiplying the ohmic value by rated current and dividing by rated line-to-neutral voltage.

IV-C WINDING RESISTANCE MEASUREMENTS

IV-C-1 General Remarks - There are two commonly used methods of measuring field resistances: The resistance bridge method and the volt-ampere method. The resistance bridge method is recommended for determining winding resistances where a known winding temperature exists since it eliminates the difficulties of brush drop on rotating field measurements and winding temperature variations encountered in the volt-ampere method. Standard practice is to use a Wheatstone bridge for resistance measurements greater than 5 ohms and a Kelvin bridge for resistance measurements less than 5 ohms. The volt-ampere method should be used only where windings are carrying current and the resistance measurement is desired for a particular operating condition.

The winding temperatures should be allowed to stabilize in a constant ambient before taking resistance measurements. It may be assumed that winding temperatures are equal to the ambient temperature after the machine has remained in the constant ambient for eight hours. The temperature stability of the windings may be checked by taking resistance readings at time intervals. At normal ambient temperatures, a 2.6 degrees centigrade change in winding temperature will give an approximate one per cent change in resistance.

IV-C-2 Test Procedure

IV-C-2-a Stationary Windings - Stationary winding resistances are measured by referring to the machine wiring diagram and placing the probes at the terminals of the winding to be tested. Caution should be taken that the probes make good contact and that there is no parallel "sneak" circuits.

This may require lifting all the exciter commutator brushes, all the generator slip ring brushes, and disconnecting the regulator.

IV-C-2-b A-C Rotating Field - Sufficiently accurate measurements of the generator field resistance are obtained by firmly placing soft solder-tipped probes on the slip rings outside the brush raceway and recording the indicated resistance.

IV-C-2-c Exciter Armature Resistance - A convenient method of measuring the exciter armature resistance of a wave wound armature is to first lift all of the commutator brushes, then rotate the armature a fraction of a bar to a position where bars are nearly centered under two adjacent brushholders. The armature resistance is then measured by placing the soft solder-tipped probes on each of the bars under the adjacent brushholders.

IV-C-2-d Effective Armature Resistance - The most straight forward method of determining the effective armature resistance is to measure the input shaft power when the a-c generator is short-circuited and separately excited. For accurate results the torsion dynamometer head must be capable of measuring the relative small torques involved. The test procedure is described below.

(a) Connect the a-c generator as shown in Figure IV-1 and provide for a separate source of excitation. Make the terminal shorting resistance negligible in comparison to the armature resistance.

(b) Operate the a-c generator at rated nominal speed and rated cooling.

(c) Increase the field excitation to obtain rated armature current and allow the machine temperature to stabilize.

(d) Measure the input torque. Reduce the armature current to zero and measure the no-load input torque.

(e) Compute the effective armature resistance by the following equation:

$$r = \frac{W_{SC} - W_{NL}}{3I_a^2} \quad \frac{\text{ohms}}{\text{phase}}$$

r = Effective armature resistance

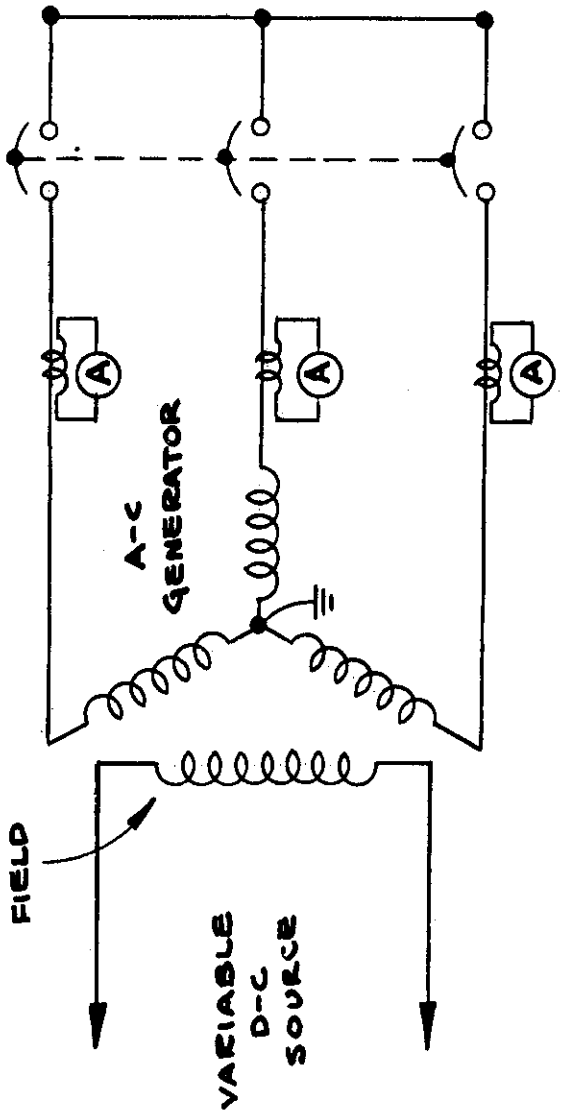

Figure IV-1 Test Set-up to Determine the A-C Generator Effective Armature Resistance

W_{SC} = Input watts with generator short-circuited (stator copper plus friction plus windage losses)

W_{NL} = Input losses at no-load (friction plus windage losses)

I_a = Armature phase current.

IV-D A-C GENERATOR SATURATION CHARACTERISTICS

IV-D-1 No-Load Saturation Characteristic

IV-D-1-a General Remarks - This test is taken to verify the magnetic circuit design and serves as a basis for computing load characteristics and machine constants. This test is usually taken at average rated speed. The no-load characteristic for any other speed may be obtained by scaling the average rated speed curve.

IV-D-1-b Test Procedure

(1) Connect the circuit as shown in Figure IV-2. It will be convenient, in most cases, to use the exciter to supply the generator field power. The wattmeters, load, and load ammeters shown in Figure IV-2 are not required for the no-load characteristics test.

(2) Operate the generator at average rated speed, rated cooling, and no-load. Increase the a-c generator field current in approximately fifteen equal increments and record a-c generator field current and line-to-neutral voltages. The generator residual voltage and hysteresis affects will usually be negligible.

IV-D-2 Rated Power Factor and Zero Power Factor Saturation Characteristics

IV-D-2-a General Remarks

Either a second a-c generator or a static-load circuit may be used to provide machine loading. This choice is a matter of convenience. Initial generator temperature stabilization is not necessary unless excitation requirements other than generator field current are to be determined.

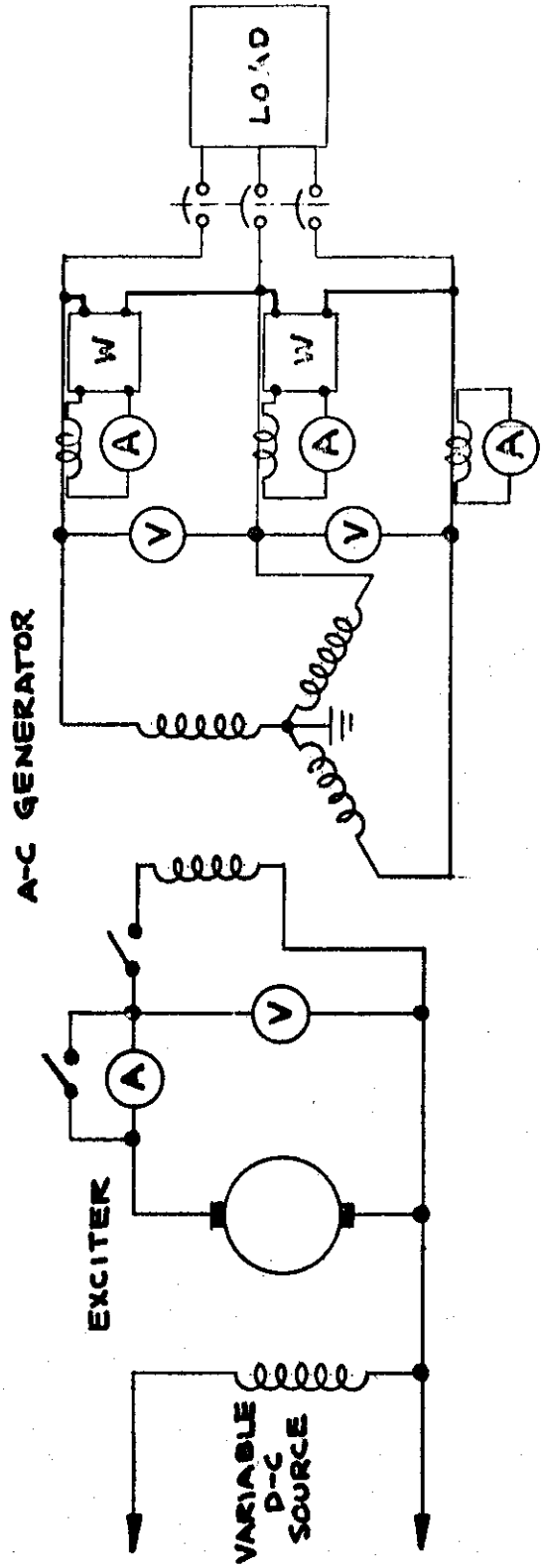

Figure IV-2 Test Set-up to Determine the A-C Generator No-load and Load Saturation Characteristics

IV-D-2-b Test Procedure (static type load)

(1) Connect the a-c generator as shown in Figure IV-2.

(2) Operate the a-c generator at average rated speed and rated cooling with no field excitation.

(3) Set the load impedance to its minimum value for the rated power factor load. Increase the a-c generator field excitation to produce rated current. Record a-c generator field current, load current, terminal voltage and load watts.

(4) Maintain rated current and rated power factor as the load impedance is increased in increments to give approximately ten points on the curve.

(5) Repeat (1) through (4) using a zero (lagging) power factor load.

IV-D-3 Short-Circuit Saturation Characteristics

IV-D-3-a General Remarks - These characteristics determine the short-circuit current versus excitation requirements for the a-c generator and are practically independent of speed and temperature. The three-phase symmetrical short-circuited characteristic is required to determine the synchronous impedance.

IV-D-3-b Test Procedure

(1) Connect the a-c generator as shown in Figure IV-3 for a three-phase symmetrical short-circuit. Operate the a-c generator at rated nominal speed and provide for rated cooling.

(2) Increase the a-c generator field voltage to produce rated armature current. Take a voltage reading of the short-circuited terminal voltage with a suitable low voltage reading voltmeter to assure a solid short. This voltage should be less than 2 volts and may be r duced by decreasing the short-circuit impedance.

(3) Record the a-c generator field current and armature short-circuit current. In many cases, it will be desirable to continue the test for 2.0 and 3.0 per-unit short-circuit currents, but someone

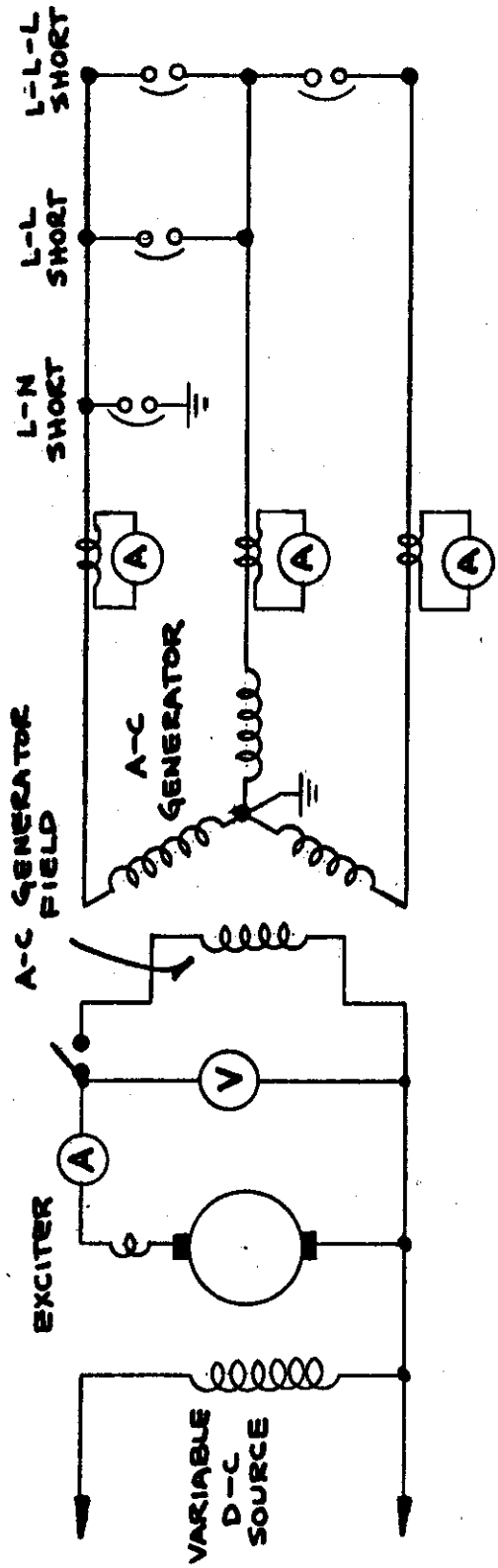

Figure IV-3 Test Set-up to Determine the A-C Generator Short-Circuit Saturation Characteristics

familiar with the machine should decide if this overload test is feasible. Overload testing time may be minimized if separate people read each meter and provide switching. High short-circuit currents should be released by opening the a-c generator field to prevent overloading circuit breakers.

(4) Repeat paragraphs (1), (2), and (3) for the line-to-line short-circuit. This short-circuit is shown as L-L in Figure IV-3.

(5) Repeat paragraphs (1), (2), and (3) for the line-to-neutral short-circuit. This short-circuit is shown as L-N in Figure IV-3.

IV-D-4 Synchronous Impedance and Curve Plotting

It is preferable to plot a-c generator terminal voltage and armature short-circuit current in per-unit values. Figure IV-4 shows a method of presenting a-c generator characteristics.

The per-unit unsaturated synchronous impedance is obtained by dividing the a-c generator field current required to produce rated three-phase symmetrical short-circuit current by the field current required to produce rated terminal voltage on the air-gap line. These excitation currents are shown in Figure IV-4. The saturated synchronous reactance is obtained by taking I_{FG} from the no-load characteristic instead of the air-gap line.

$$Z_d = \frac{I_{FSI}}{I_{FG}} \text{ (per-unit)}$$

$$x_d = \sqrt{Z_d^2 - r^2} \text{ (per-unit)}$$

Z_d = Per-unit synchronous impedance

I_{FSI} = A-C generator field current required to produce rated three-phase symmetrical short-circuit current

I_{FG} = A-C generator field current required to produce rated terminal voltage on the air-gap line.

x_d = Per-unit synchronous reactance

r = Per-unit effective armature resistance

Figure IV-4 A-C Generator Saturation Characteristics

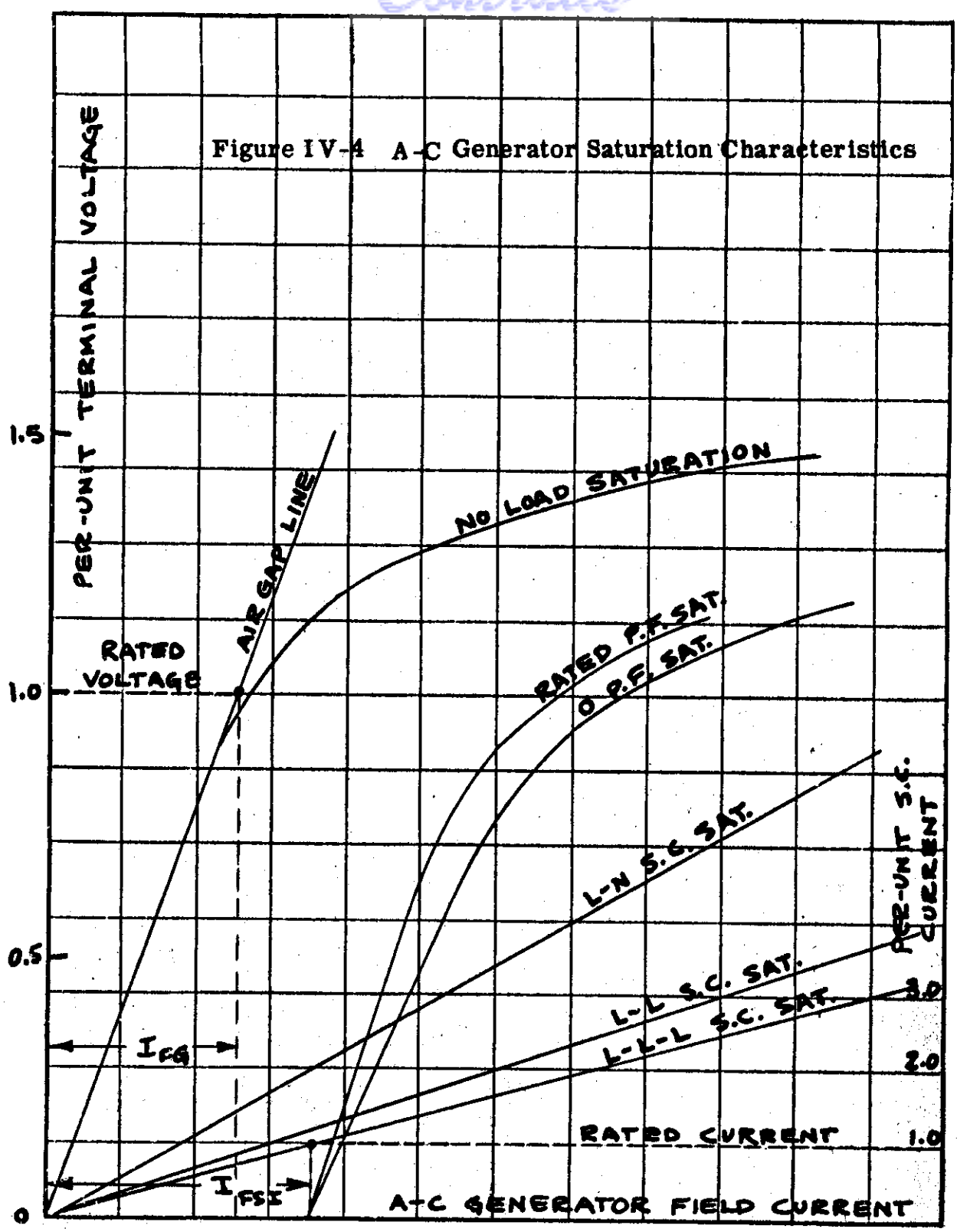

IV-E Direct-Axis Short-Circuit Reactances and Time Constants

IV-E-1 General Remarks - The direct-axis short-circuit constants: T_d'' - subtransient time constant, x_d'' - subtransient reactance, T_d' - transient time constant, x_d' - transient reactance, and T_a - armature time constant are obtained by a graphical analysis of the armature short-circuit current wave following a sudden application of a three-phase short-circuit from no-load with constant field excitation. The asymmetrical short circuit current is analyzed by resolving the short-circuit current wave into three symmetrical components (sustained, transient, and subtransient) and one unidirectional component.

The subtransient, transient and unidirectional current components are approximately exponential functions of time; hence, these curves appear as straight lines when plotted on a semi-log scale as shown in Figures IV-5 and IV-6. These straight lines are extrapolated to zero time to determine the initial current values. The subtransient reactance is determined by dividing the open-circuit voltage by the sum of the initial values of the sustained, transient, and subtransient components. The transient reactance is obtained in a similar manner except the subtransient component is neglected. Each of the time constants are determined by the time required for the respective current components to decay to .368 of the initial value.

The symmetrical current components (sustained, transient, and subtransient) produce a rotating mmf which is stationary with respect to the field poles while the unidirectional component produces an mmf which is stationary in space. The transient component of armature current has a related d-c current component in the rotor field circuit which is proportional and decays with the same time constant [1]. Impedance added to the a-c generator field circuit will alter the transient performance and will yield erroneous results for the transient time constant and transient reactance.

Appreciable subtransient currents do not persist after the first few cycles;hence, insufficient points are available to accurately extrapolate the A curve shown in Figure IV-6, to zero time. Errors are also introduced when the three contacts of the circuit breaker do not close at the same instant. This results in an initial single-phase short-circuit. Furthermore, some breakers will exhibit contact bounce on closing which further accentuates single-phase action.

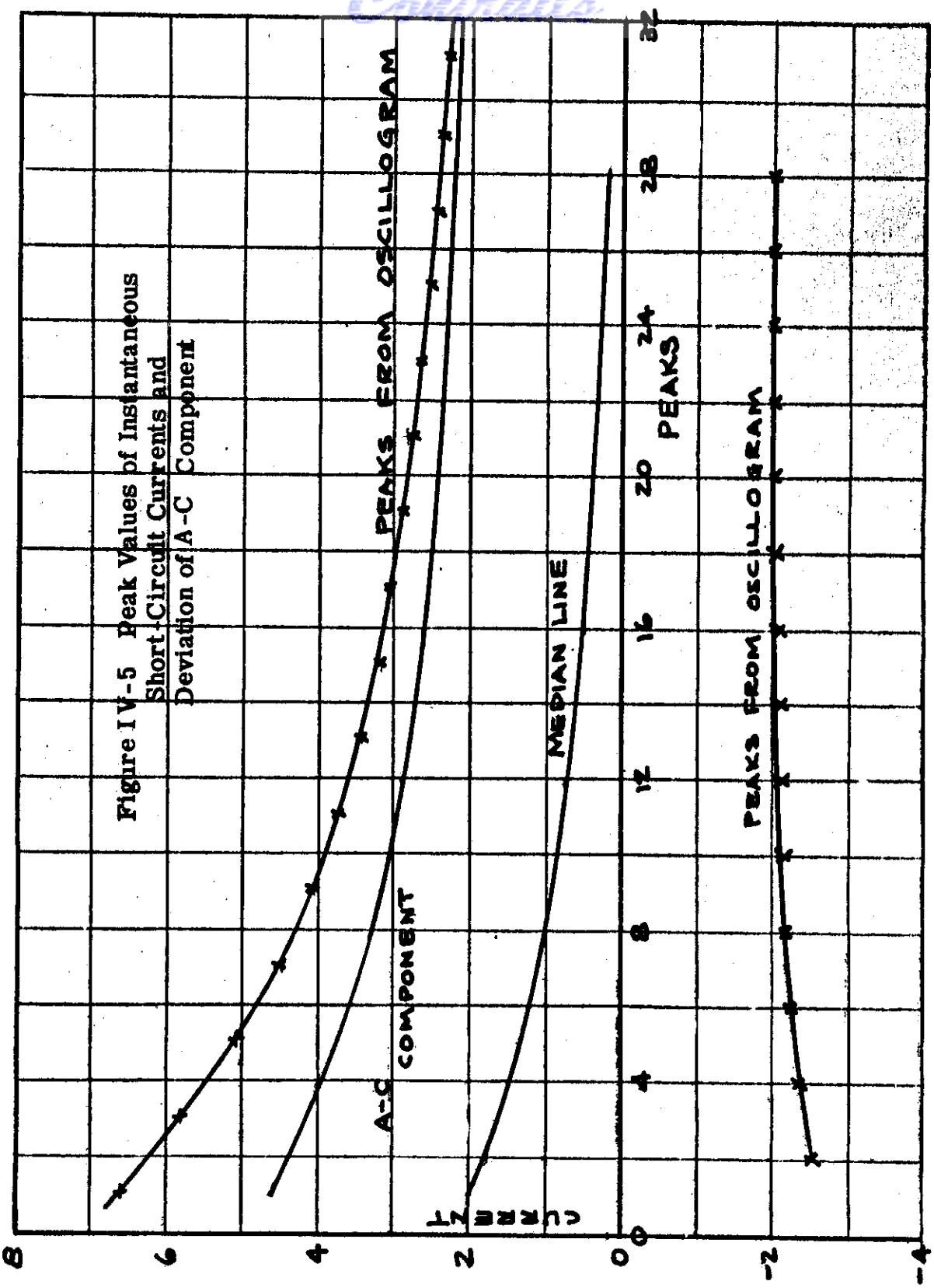

Figure IV-5 Peak Values of Instantaneous Short-Circuit Currents and Deviation of A-C Component

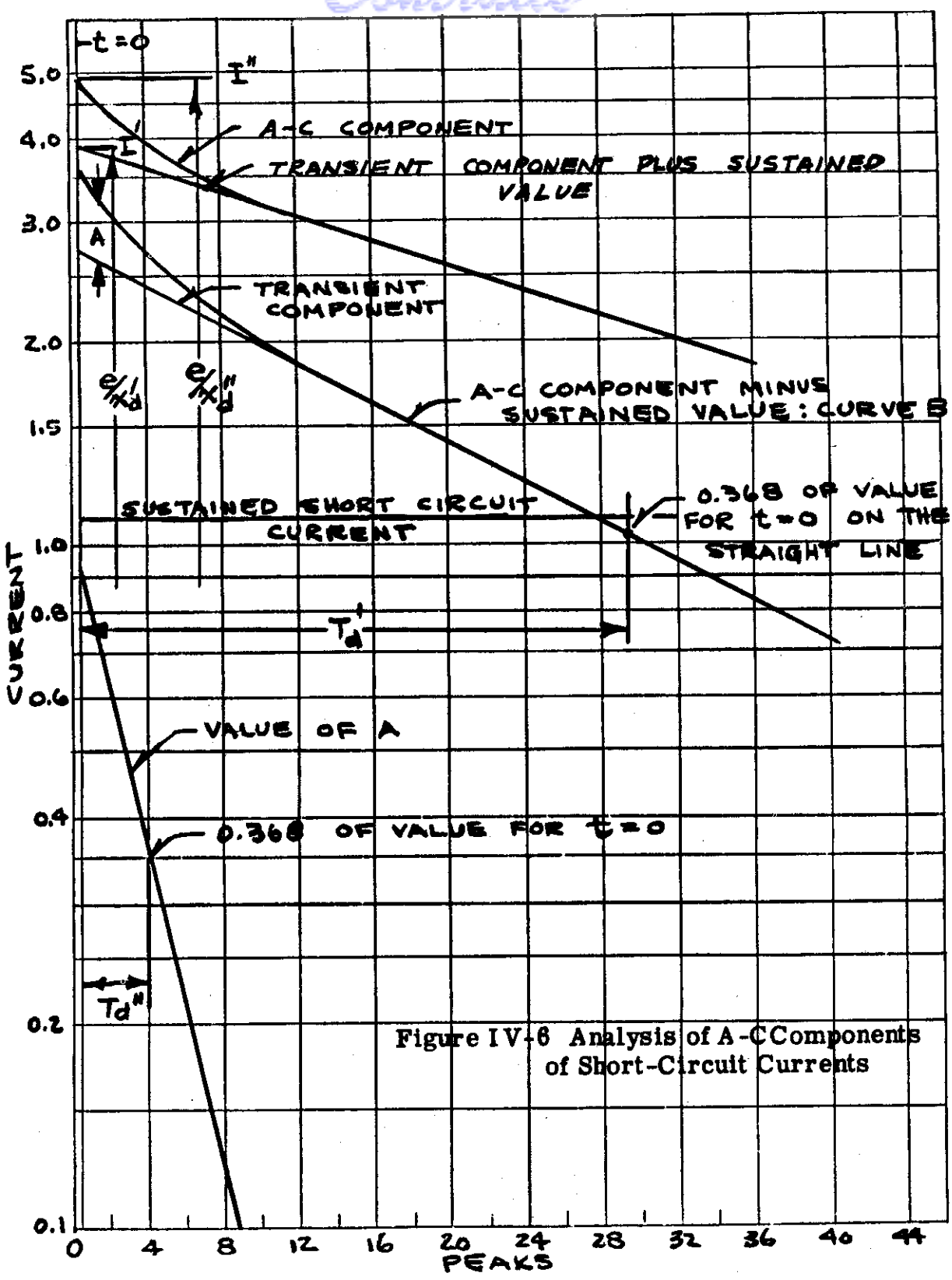

Figure IV-6 Analysis of A-C Components of Short-Circuit Currents

In many cases, it is found that the short-circuit resistance will introduce appreciable error in the value obtained for the armature time constant. The armature time constant is equal to the negative sequence reactance divided by $2\pi f\ r_a$ where r_a is the direct-current armature resistance and f is the frequency at which the negative sequence reactance has been determined [1]. The armature resistance is usually in the order of a few hundredths of an ohm; hence, a short-circuit resistance of a hundredth of an ohm will have an appreciable affect on the value obtained for the armature time constant. In order to obtain results consistent with the computing method, the short-circuit terminal voltage must be small in comparison to the armature resistance voltage drop.

Consideration should be given to the circuit breaker closing performance, short-circuit resistance, and excitation source impedance to insure consistent results. In most cases, it will be necessary to obtain a factory adjusted circuit breaker if nearly simultaneous closing of the breaker contacts is to be achieved. Results of repeated tests will tend to average out the inherent errors of this test.

IV-E-2 Test Procedure - Average rated speed and unsaturated conditions are recommended for this test. The initial temperature conditions are determined by measuring the a-c generator field resistance by the volt-ampere method prior to application of the short-circuit.

(1) Connect the a-c generator as shown in Figure IV-7. Use resistive shunts to obtain the short-circuit current signals for the oscillograph. Current transformers or current shunts may be used with indicating ammeters to meter the sustained short-circuit current and calibration currents.

(2) Operate the a-c generator at average rated speed with rated air flow cooling. Use a suitable speed indicating device so that the a-c generator frequency may be used as a time calibration signal.

(3) Choose a shorting breaker which exhibits no contact bounce on closing and one which allows the last two contacts to mate at nearly the same instant. The allowable delay between the closing of the last two contacts will depend upon the ratio of subtransient quadrature-axis reactances to direct-axis subtransient reactance and the desired accuracy of the machine constants. A delay less

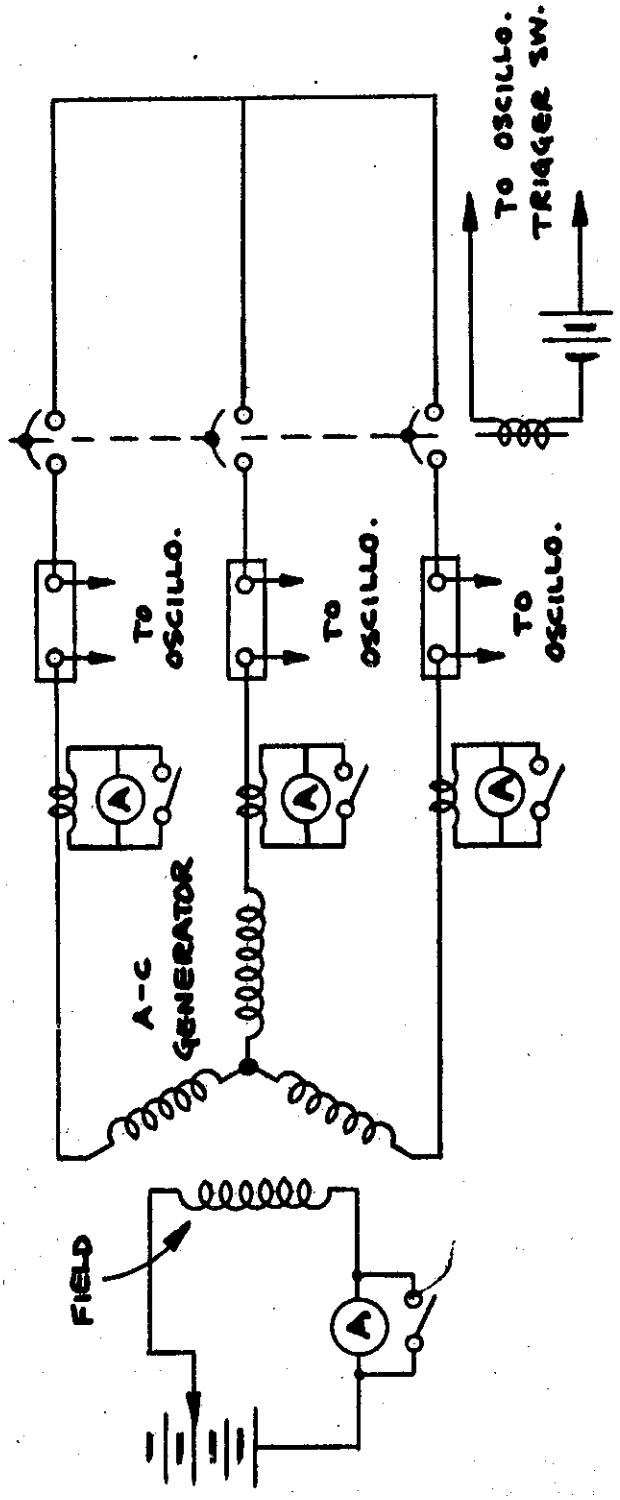

Figure IV-7 Test Set-up to Determine the A-C Generator Short-Circuit Constants

than one-fifth of a cycle can be used as a rule-of-thumb to meet a desired accuracy of five per cent if the generator being tested has a x_q'' / x_d'' ratio less than one and a half [2].

(4) Tap the storage battery cells to obtain approximately the maximum open-circuit terminal voltage on the air-gap line or follow the instructions given in the AIEE Test Code 503, paragraph 1.841 for determining the rated current constants. Record the open-circuit terminal voltage, a-c generator field current, and a-c generator field voltage.

(5) Short the ammeters for protection against the high transient currents. Take an oscillogram of the three-phase short-circuit currents when a three-phase short-circuit is suddenly applied to the a-c generator. Make the deflections as large as possible but keep the peaks on the film. Run the film at approximately five feet per second. It will be necessary to cut-and-try until the best film speed, deflections, and oscillograph trigger switch settings are found.

(6) Record the short-circuit terminal voltage and sustained short-circuit current. If accurate results for the armature time constant are expected, the short-circuit terminal voltage must be negligible in comparison to the internal armature resistive voltage drop. The sustained short-circuit current is required for the analysis of the oscillograms.

(7) Take a calibration film. If equipment heating and film space allow, make the calibration traces at least 150 per cent of the sustained short-circuit current as determined in part (6). This can conveniently be done by increasing the a-c generator field voltage by the proper amount and taking an oscillogram of the sustained short-circuit currents, recording the ammeter readings.

IV-E-3 Method of Analyzing the Short-Circuit Current Wave to Determine the Direct-Axis Short-Circuit Reactances and Time Constants

The following procedure used to analyze the current wave to determine the machine constants is taken from the AIEE Test Code for Synchronous Machine No. 503, dated June 1, 1945. See the Glossary, Appendix F, for the definition of the various terms used in this chapter.

IV-E-3-a Direct-Axis Transient Reactances (x_d') - The direct-axis transient reactance is determined from the current waves of a three-phase short-circuit suddenly applied to the machine operating at no-load and rated speed. The direct-axis transient reactance is equal to the ratio of the no-load voltage to the corresponding value of the armature current given by the extrapolation of the envelopes of the a-c components of the armature current waves to the instant of the sudden application of the short-circuit, neglecting the high decrement currents during the first few cycles. Figures IV-5 and IV-6 illustrate this method of determining the direct-axis transient reactance.

In plotting the current values from the oscillogram, the first peak should be plotted at the abscissa 1, and subsequent peaks numbered consecutively. The positive peaks will be odd numbers, and the negative peaks will be even numbers, or vice versa. The current values from the oscillograms should be plotted first, and then the median line and the a-c component. These curves are usually plotted on standard rectangular co-ordinates, and are most conveniently analyzed if the currents are expressed in per-unit values, with the unit value equal to the peak value of the rated current wave (see Figure IV-5).

The a-c component should then be re-plotted on semi-log scales with the current on the logarithmic scale together with a plot of the a-c component minus the sustained short-circuit current. (Curve B, Figure IV-6.) These curves should pass through the ordinates for peak 1. Since the first peak is plotted at abscissa 1, the abscissa for the time of application of the short-circuit is usually not at zero, but a time which can be readily determined from the oscillogram. This zero time line should be plotted on the semi-log plot, and extrapolations of the current curves are extended to this line. It is important in plotting the first several cycles (a-c components minus the sustained value) to choose current and time scales that will avoid a steep slope during the first three or four cycles. It will usually be found that curve B can be very closely represented by a straight line and a curve for several cycles at the beginning of the short circuit. The curves for the tests and analysis should be carried out for sufficient cycles to establish definitely the straight line part of curve B. The difference A (see Figure IV-6) between curve B and extension of the straight part to t = 0, when plotted on the semi-log scales, will also be closely represented by a straight line. (This straight line should always be plotted to pass through the ordinate for peak 1.

The ordinate for curve B at t = 0 is equal to the sum of the ordinates at t = 0 from the two straight lines. The ordinate for the a-c component at t = 0 is then determined by adding the sustained short-circuit to the ordinate of curve B at t = 0. The curve for the transient component plus the sustained value of the current is determined by adding the sustained short-circuit current to the extended straight line part of curve B.

$$x_d' = \frac{e}{I'} \text{ (per-unit value)}$$

Where e = the open-circuit voltage of the machine before the short-circuit, expressed in per-unit based on rated voltage.

I' = per-unit current from the transient component plus the sustained value at t = 0 (Figure IV-6).

IV-E-3-b Direct-Axis Subtransient Reactance (x_d'') - The direct-axis subtransient reactance is determined in a similar manner as the transient reactance. In this case, however, the full value of the a-c component of the armature current is used, including the high decrement currents during the first few cycles.

$$x_d'' = \frac{e}{I''} \text{ (per-unit value)}$$

Where e = the open-circuit voltage of the machine before the short-circuit, expressed in per-unit based on rated voltage.

I'' = per-unit current from the a-c component curve at t = 0 (Figure IV-6).

IV-E-3-c Direct-Axis Transient Short-Circuit Time Constant (T_d') The direct-axis transient short-circuit time constant (T_d') is determined from the short-circuit test data plotted as illustrated in Figure IV-6. It is the time required for the transient component of the current minus the sustained value (represented by the straight line part of the curve B, and its extension to t = 0) to decrease to 0.368 of its initial value.

IV-E-3-d Direct-Axis Subtransient Short-Circuit Time Constant (T_d'') The direct-axis subtransient short-circuit time constant (T_d'') is determined from the short-circuit test data plotted as illustrated in Figure IV-6. It is the time required for the difference A to decrease to 0.368 of its initial value.

IV-E-3-e Short-Circuit Time Constant of Armature Winding (T_a) - The short-circuit time constant of armature winding is obtained from the current waves of a three-phase short-circuit suddenly applied to the machine operating at no-load and rated speed. It is obtained from the waves which have asymmetrical components. The test results are plotted as shown in Figure IV-5, and the asymmetrical components (median lines) are replotted on semi-log paper as in Figure IV-8. The short-circuit time constant of armature winding is the time for the asymmetrical component to decrease to 1/e or 0.368 of its value at the instant of short-circuit. This initial value is determined by the extrapolation of the first straight line part of the curve in Figure IV-8 to the time of application of the short-circuit. The time in peaks is 2.2 - 0.1 = 2.1 and in seconds (for 400 cycles) is .0026. The average of the time constants obtained from the test shall be taken as the time constant of the machine.

IV-F A-C GENERATOR OPEN-CIRCUIT TIME CONSTANT (T_{do}')

IV-F-1 General Remarks - The direct axis open-circuit time constant is the time in seconds required for the a-c generator terminal voltage to decay to .368 of its initial value when the field circuit is suddenly short-circuited with no-load on the a-c generator.

The time constant obtained by this test will depend upon the degree of saturation and field temperature of the a-c generator. To obtain consistent results it is recommended that the open-circuit voltage for this test should not exceed the maximum unsaturated point on the a-c generator no-load saturation characteristic. To approximately determine the a-c generator temperature at the time of the test, the a-c generator field resistance should be measured by the volt-ampere method prior to taking the oscillogram.

IV-F-2 Test Procedure

(1) Connect the a-c generator as shown in Figure IV-9. Other field switching circuitry can be used, but caution should be taken to insure that the circuitry used does not alter the transient performance.

(2) Operate the a-c generator at nominal rated speed and rated cooling. Use a suitable speed indicating device so that the a-c generator terminal voltage may be used as a calibration of the time scale on the oscillogram.

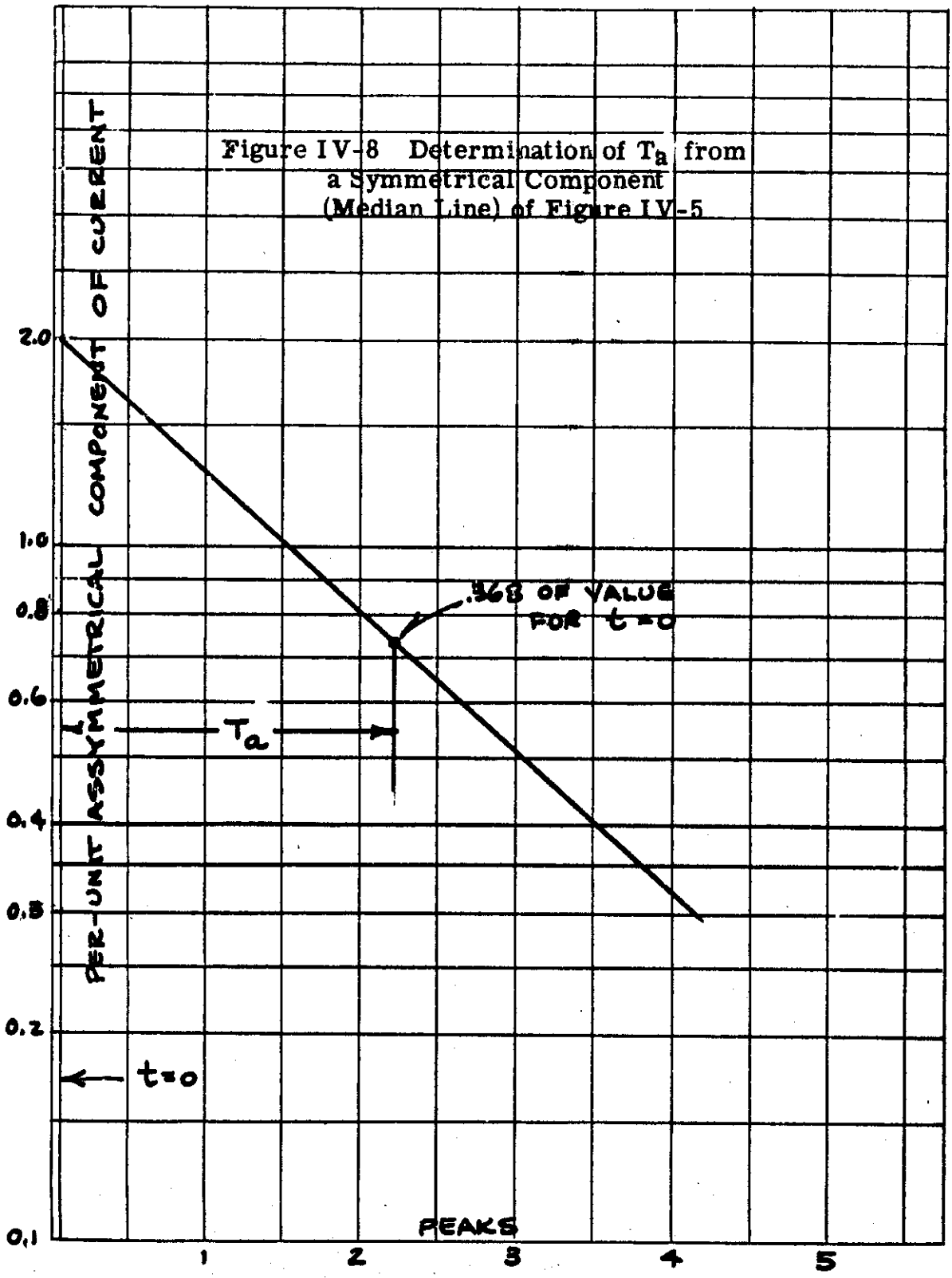

Figure IV-8 Determination of T_a from a Symmetrical Component (Median Line) of Figure IV-5

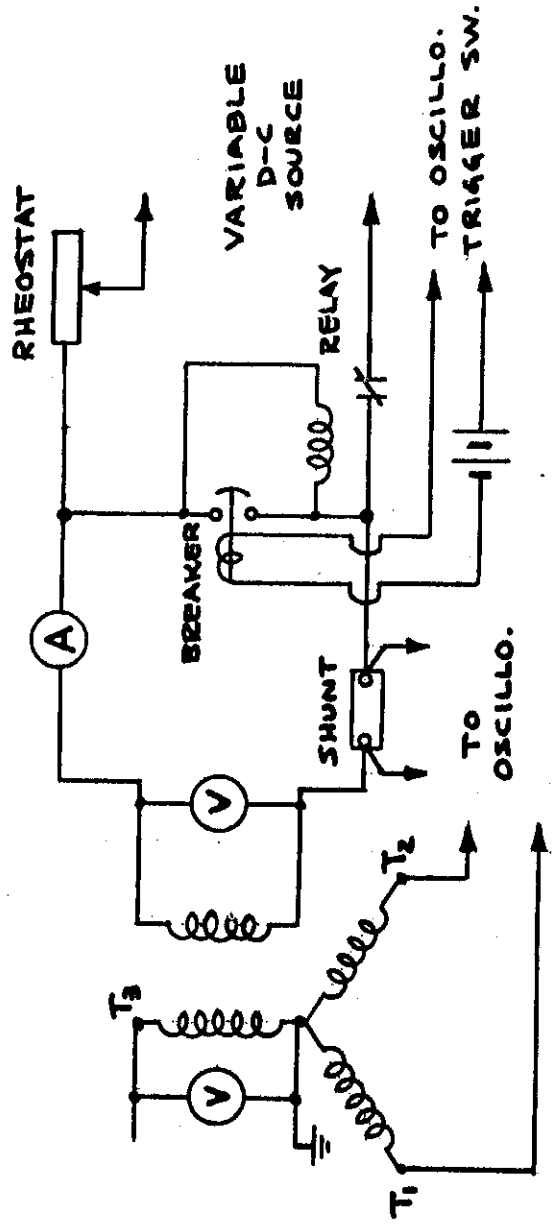

Figure IV-9 Test-up to Determine the A-C Generator Open-Circuit Time Constant

(3) Adjust the field rheostat and tapped battery voltage to give an a-c generator terminal voltage near the maximum operating point on the no-load saturation characteristic and a rheostat setting which sufficiently limits the battery current after the a-c generator field is short-circuited.

(4) Set the relay by manually closing and adjusting the drop-out voltage until the a-c generator field voltage is just sufficient to hold the relay in the closed position. This insures a rapid clearing of the battery circuit after the short is applied. The breaker contact voltage drop may influence the a-c generator field current decay if the battery circuit is not cleared rapidly and the battery current is not sufficiently limited by the rheostat setting after the a-c generator field short-circuit is applied. A fast clearing fuse may be used instead of a relay to clear the battery circuit. An additional oscillogram trace of the voltage across the breaker contacts may be used to check for contact bounce and the affect of battery current after the field is short-circuited.

(5) Record the a-c generator terminal voltage, field current and field voltage.

(6) Take an oscillogram of the a-c generator terminal voltage and field current when the field is suddenly shorted. A film speed of five feet per second will record the transient on approximately one foot of film.

(7) Record the a-c generator terminal voltage (residual voltage) immediately after taking the oscillogram with the field shorted.

IV-F-3 Method of Analyzing the Test Data - The envelope of the a-c terminal voltage is plotted on semi-log graph paper as shown in Figure IV-10. The residual voltage is subtracted from the values given by the oscillogram. The initial high decrement is neglected and the straight line curve is extrapolated to zero time. The a-c generator open-circuit time constant is taken as the time required for the voltage to decay to .368 of the initial value obtained by extrapolating the straight line to zero time.

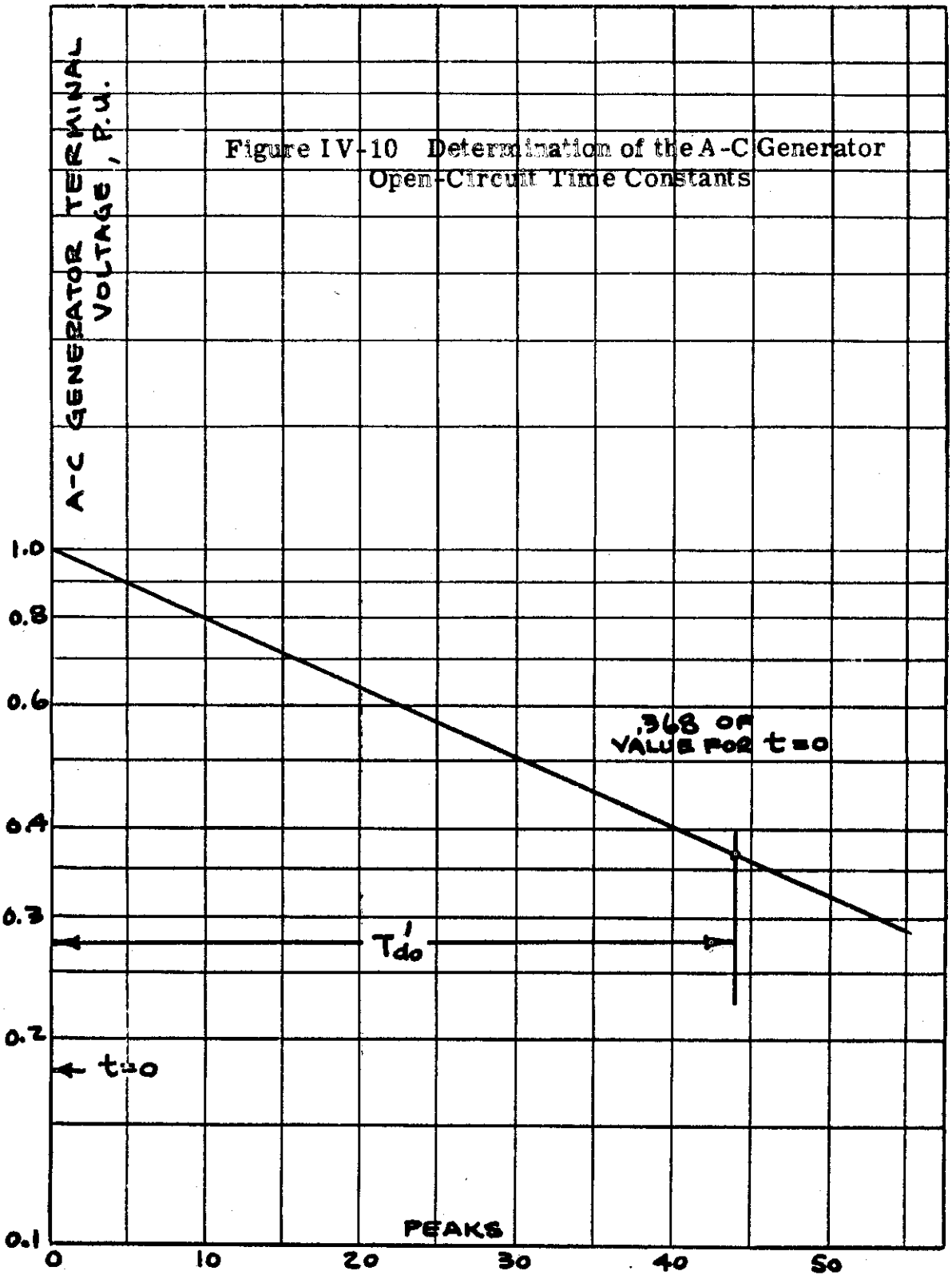

Figure IV-10 Determination of the A-C Generator Open-Circuit Time Constants

IV-G QUADRATURE-AXIS SYNCHRONOUS IMPEDANCE

IV-G-1 General Remarks - The quadrature-axis impedance is used to approximate the affect of the non-uniform air-gap of an a-c salient pole synchronous generator. The armature mmf is resolved into the direct-axis and quadrature-axis components to determine its demagnetizing affect. The quadrature-axis impedance is used to compute the internal angle and the excitation requirements of an a-c salient pole a-c generator under load.

There are two commonly used test methods for determining the quadrature-axis impedance. One method is to supply the armature with rated voltage of nominal rated frequency with the rotor driven at a slight slip frequency. Thus, the armature mmf will encounter a varying reluctance as the pole passes alternately from a direct-axis and quadrature-axis position. An oscillogram is taken of armature voltage and current. The quadrature-axis impedance is the minimum ratio of voltage to current. It is important in this test to have a minimum slip frequency to insure that negligible currents are induced in the amortisseur windings. Past experience has shown that sufficiently small slip is not usually obtained with commonly used test equipment. Difficulties are encountered due to the mechanical drive clearances, the overriding clutch if one is used, and the electrical torque pulsation associated with the slip frequency. These factors give the rotor a tendency to mechanically oscillate. For this reason, it is usually necessary to make the test at high slip frequencies and the value of quadrature impedance obtained from this test will be at error due to the armortisseur winding currents. Hence, the second method of obtaining the quadrature-axis synchronous impedance by operating the generator as a synchronous motor is considered the more preferable. Only the synchronous motor test procedure will be given.

To measure the quadrature-axis synchronous impedance, the generator is operated as a synchronous motor with the proper polarity of the field excitation. The excitation is increased until the poles reach their maximum stable position. The quadrature-axis impedance is determined by taking the ratio of phase voltage to phase current at this critical point.

IV-G-2 Test Procedure

(1) Connect the generator and source supply as shown in Figure IV-11. The source supply should be of equal or greater rating than the test machine.

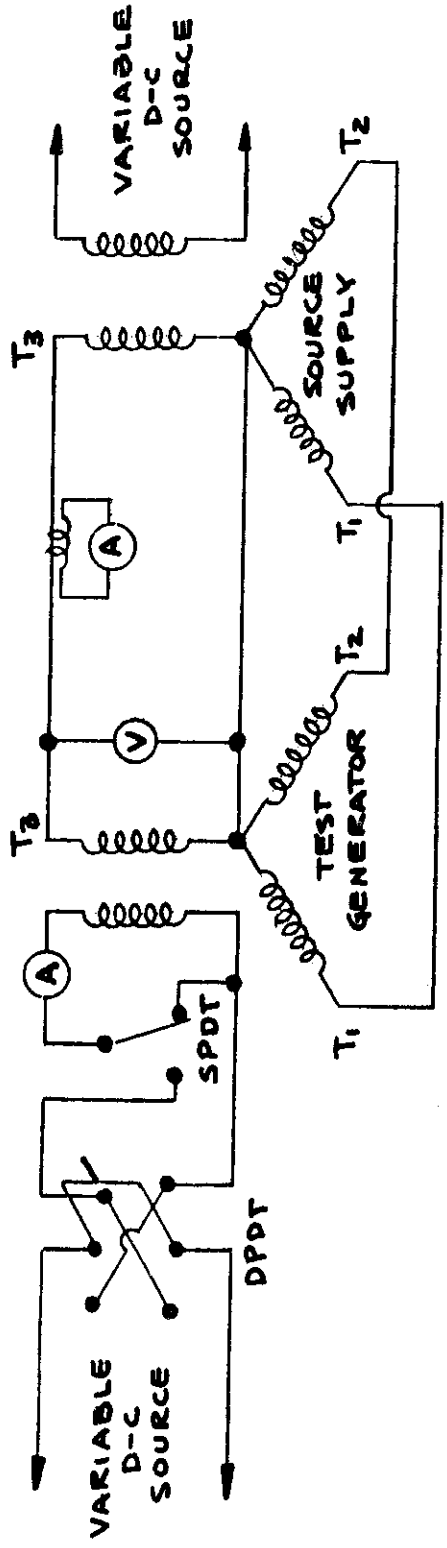

Figure IV-11 Test Set-up to Determine the A-C Generator Quadrature-Axis Impedance

(2) Drive the source generator with no field current at a speed to give the rated frequency of the test machine.

(3) With the shaft of the test generator free, short its field and slowly increase the source voltage until rated voltage is applied to the test generator.

(4) When the test generator comes up to synchronous speed apply a small excitation voltage to its field. *

(5) Position the DPDT switch, such that, an increase in field current will cause an increase in armature current.

(6) Maintain rated terminal voltage on the test machine. Increase the field current slowly and determine the approximate values where a further increase in field current causes a rapid decrease in armature current.

(7) Reduce the field current and switch the DPDT switch to reverse polarity of the test generator field voltage.

(8) Bring the field current up to the approximate range as determined in paragraph (6).

(9) Maintain rated terminal voltage on the test generator and record armature current and field current as the field current is increased in very small increments. Take readings until the critical point is passed.

IV-G-3 Computation of the Quadrature-Axis Synchronous Impedance:

$$Z_q = \frac{V}{I\,(max.)} \quad \frac{ohms}{phase}$$

Z_q = Quadrature-axis synchronous impedance in ohms per phase

V = line-to-neutral test voltage

I(max) = maximum stable armature current.

* If test generator will not accelerate beyond one-half synchronous speed, insert a small resistor in the generator field circuit.

IV-H NEGATIVE SEQUENCE IMPEDANCE

IV-H-1 General Remarks - The negative sequence impedance is determined with the a-c generator operating at rated speed with a sustained line-to-line short-circuit. During this test double frequency currents will be induced in the field winding and any impedance added to the field circuit will alter the results. Realistic results may be obtained by providing the a-c generator field excitation from the integral exciter. This test can conveniently be conducted in conjunction with the line-to-line short-circuit characteristics since the test set-up is similar except for the addition of a voltmeter and wattmeter.

An alternate method for checking the negative sequence impedance of the above test is to compute the arithmetical mean of the quadrature-and direct-axis subtransient reactances obtained from the locked rotor test as described in part IV-J of this chapter.

IV-H-2 Test Procedure

(1) The generator armature windings are connected in Y with a line-to-line short-circuit and the meters arranged as shown in Figure IV-12.

(2) The generator is operated at rated speed and rated cooling.

(3) The exciter shunt field excitation is increased until rated line-to-line short-circuit current is obtained.

(4) Allow the generator temperature to stabilize and record the open-phase voltage, line-to-line short-circuit current and watts.

(5) Compute the negative sequence impedance by:

$$Z_2 = \frac{E}{\sqrt{3}\, I}$$

$$X_2 = \frac{E}{\sqrt{3}\, I} \cos\theta \quad \text{where:} \quad \cos\theta = \frac{\text{Watts}}{EI}$$

$$R_2 = \frac{E}{\sqrt{3}\, I} \sin\theta$$

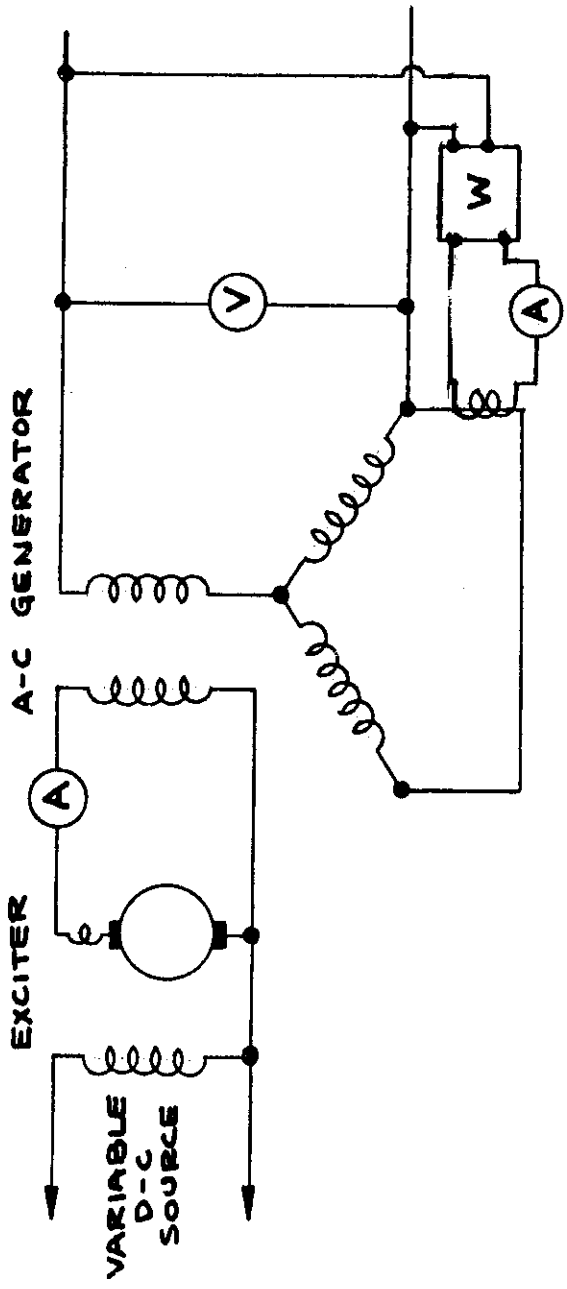

Figure IV-12 Test Set-up to Determine the A-C Generator Negative Sequence Impedance

Z_2 = Negative sequence impedance

X_2 = Negative sequence reactance

R_2 = Negative sequence resistance

E = Open-phase voltage

I = Line-to-line short-circuit current

IV-I ZERO SEQUENCE IMPEDANCE

IV-I-1 General Remarks - There are two commonly used test methods for determining the zero sequence impedance. The test procedure for each method is given. Comparison of the results obtained by both methods indicates that method (2) gives slightly large values for the zero sequence impedance.

IV-I-2 Test Procedure (Method 1)

(1) Connect the a-c generator as shown in Figure IV-13. The three armature windings are connected in series and the generator field is short-circuited.

(2) Operate the a-c generator at rated nominal speed and rated cooling.

(3) Increase the single phase supply voltage to produce rated armature current and allow the generator temperature to stabilize.

(4) Record the applied voltage and armature current.

(5) Compute the zero sequence impedance by:

$$Z_0 = \frac{V}{3I} \quad \frac{\text{ohms}}{\text{phase}}$$

Z_0 = Zero sequence impedance

V = Applied voltage

I = Armature current

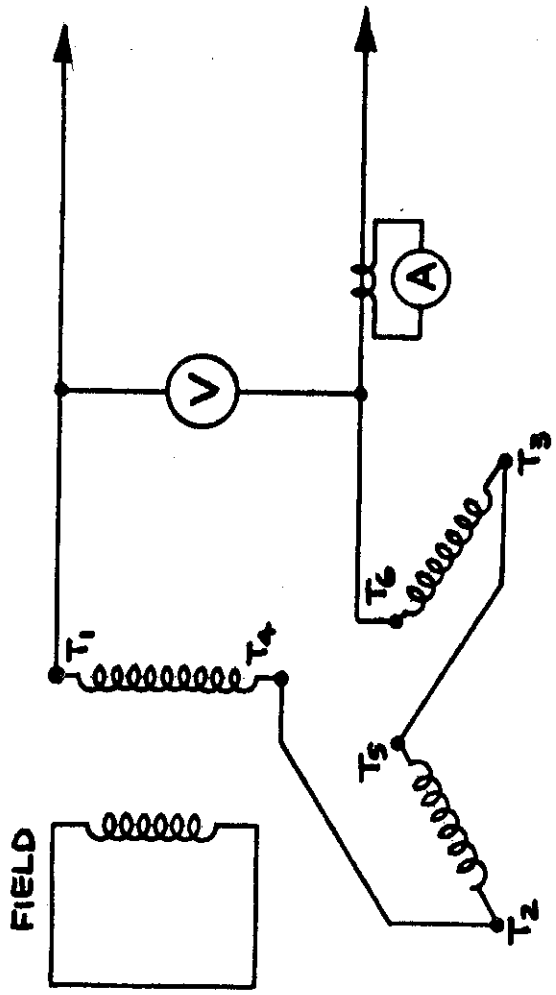

Figure IV-13 Test Set-up to Determine the A-C Generator Zero Sequence Impedance (Method 1)

IV-I-3 Test Procedure (Method 2)

(1) Connect the a-c generator as shown in Figure IV-14.

(2) Operate the a-c generator at rated nominal speed and rated cooling with a (L-L-N) short-circuit and no field excitation.

(3) Increase the a-c generator field excitation to produce rated current and record the watts, neutral current, and the open-phase voltage. The rated current value of the zero sequence impedance will correspond to three per-unit neutral current. Caution should be taken to minimize testing time if the test is continued to three per-unit neutral current.

(4) Compute the zero sequence impedance by:

$$Z_0 = \frac{V}{I} \quad \frac{\text{ohms}}{\text{phase}}$$

$$X_0 = \frac{V}{I} \sin \theta \quad \frac{\text{ohms}}{\text{phase}}$$

$$R_0 = \frac{V}{I} \cos \theta \quad \frac{\text{ohms}}{\text{phase}} \quad \text{where: } \cos \theta = \frac{\text{Watts}}{EI}$$

Z_0 = Zero sequence impedance

X_0 = Zero sequence reactance

R_0 = Zero sequence resistance

V = Open-phase voltage

I = Neutral short-circuit current

IV-J DIRECT AND QUADRATURE-AXIS SUBTRANSIENT REACTANCES

IV-J-1 General Remarks - For reasons given in the discussion of the three phase short-circuit test, it is advisable to verify the direct-axis subtransient reactance by a second method. The locked rotor test is relatively simple and can be used to verify the subtransient reactance.

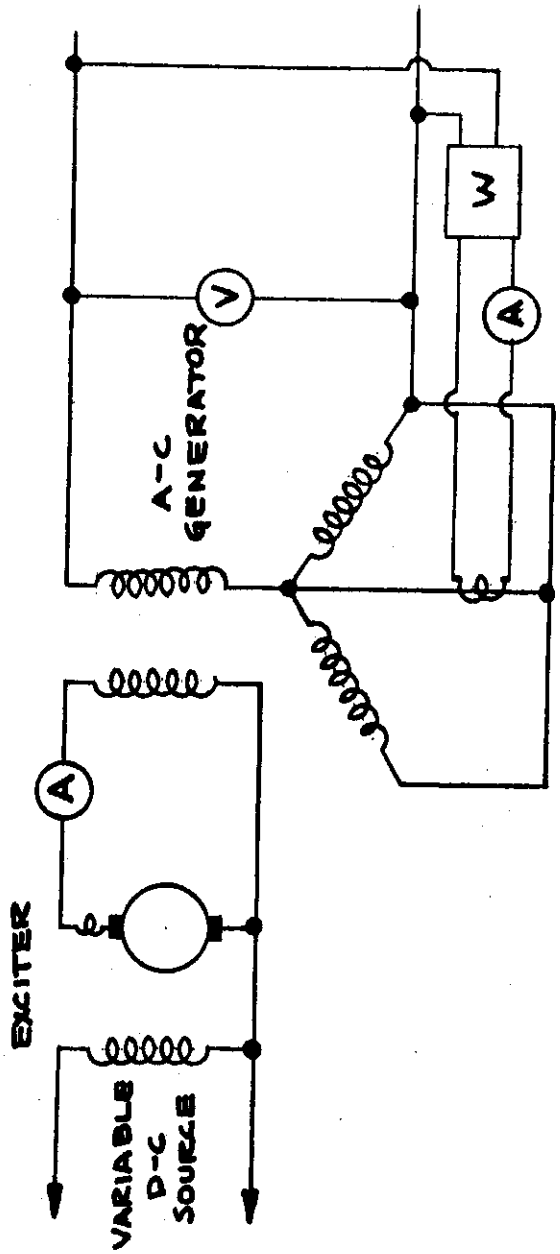

Figure I V-14 Test Set-up to Determine the A-C Generator Zero Sequence Impedance (Method 2)

The arithmetical mean of the quadrature-and direct-axis reactances can also be used as a further check of the negative sequence impedance.

IV-J-2 Test Procedure

(1) Connect the generator as shown in Figure IV-15.

(2) Clamp a lever to the drive spline so that the rotor may be held at any desired position.

(3) Hold the lever by hand and increase the single phase supply voltage of rated frequency until approximately .25 per-unit armature current is obtained.

(4) Rotate the rotor through 90 electrical degrees to determine the rotor position where the ratio of the generator a-c field current to applied voltage is a maximum.

(5) Hold the rotor at this position and increase the applied voltage until rated armature currents is obtained. Record the applied voltage, armature current, and a-c field current. Allow rated current to persist only for the time required to record the data.

(6) Repeat (1) through (6) except adjust the rotor position for the minimum ratio of generator a-c field current to applied voltage.

(7) Compute the constants by:

(a) D-axis subtransient reactance

$$x_d'' = \frac{E}{21}$$

Where: $\left(\frac{\text{generator a-c field current}}{\text{applied voltage}}\right)$ is a maximum

(b) Q-axis subtransient reactance

$$x_q'' = \frac{E}{21}$$

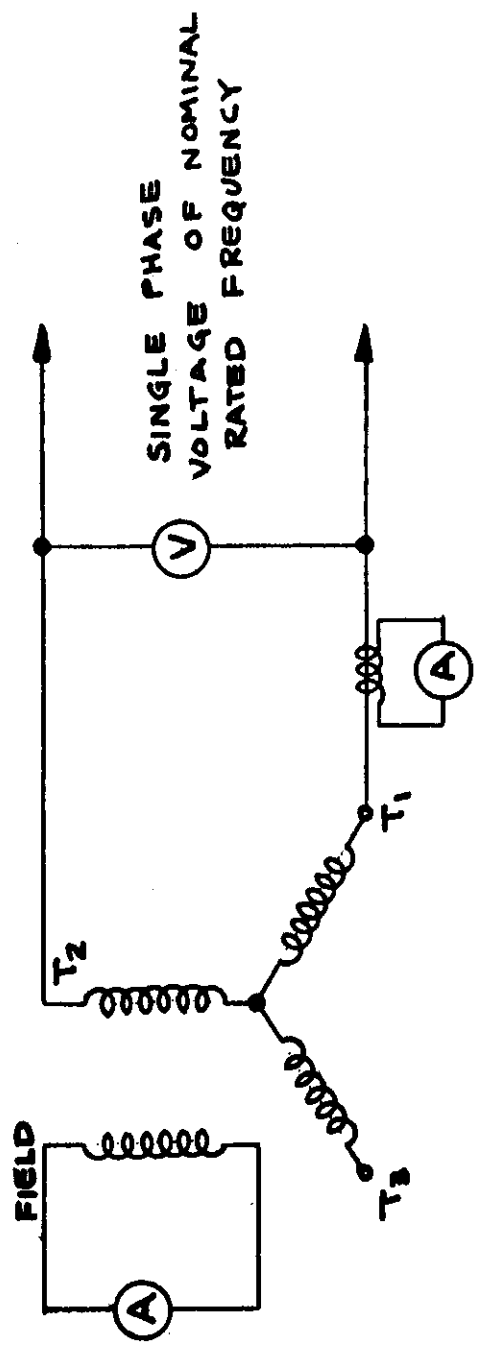

Figure IV-15 Test Set-up to Determine the A-C Generator Direct-Axis and Quadrature Axis Subtransient Reactances

Where: $\left(\frac{\text{generator a-c field current}}{\text{applied voltage}}\right)$ is a minimum

(c) Negative sequence impedance

$$Z_2 = \frac{x_d'' + x_q''}{2}$$

IV-K EXCITER SATURATION CHARACTERISTICS

IV-K-1 Exciter No-Load Characteristics

IV-K-1-a General Remarks - This test is taken to determine the generated voltage versus field excitation at rated speed. Since the generated voltage is proportional to speed, curves at other speeds may be obtained by scaling the curve taken at rated speed. This test information is commonly used for verification of the magnetic circuit design and serves as a basis for calculating load characteristics.

IV-K-1-b Test Procedure

(1) Connect the exciter as shown in Figure IV-16, except leave the simulated load disconnected. Provide for a suitable separate source of excitation.

(2) Operate the exciter at rated speed and rated cooling. Reduce the residual voltage to zero. Increase the exciter shunt field current in approximately 15 equal increments to the maximum point of interest. Record the exciter output voltage, field current and field voltage at each point.

(3) Reduce the exciter field current back to zero in approximately 15 equal increments. Care must be taken to increase or decrease the exciter field current in continuous unidirectional increments, to insure that a definite hysteresis path is traversed. By closing the ammeter shorting switch, ammeter scales or meters may be changed without interrupting the circuit.

IV-K-2 Exciter Load Characteristics

IV-K-2-a General Remarks - This test is taken to determine the exciter terminal voltage versus field current relationship when a load is connected.

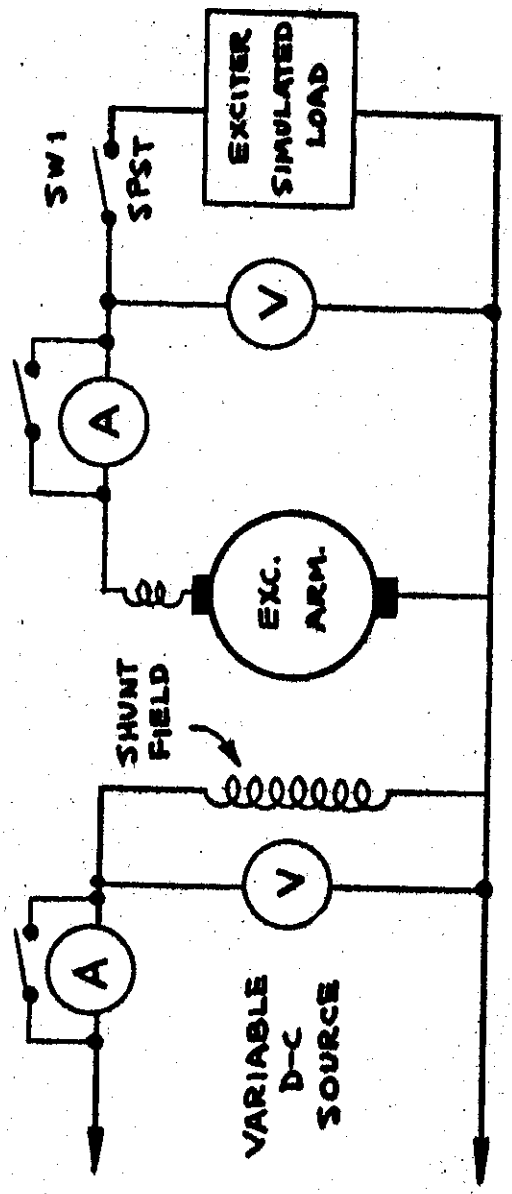

Figure IV-16 Test Set-Up to Determine the Exciter No-Load and Load Saturation Characteristics

The a-c generator field resistance may vary by a ratio of two from its minimum to maximum temperature condition. Thus, the exciter load characteristic will be appreciably affected by the a-c generator field temperature. A simulated load is chosen for the exciter which simulates the desired a-c generator field temperature condition.

Some aircraft integral d-c exciters will have a relatively large load characteristic hystersis loop due to the compounding action of the interpoles. This compounding action will accentuate variations of commutator brush drop and may produce some irregularity in the exciter load characteristic.

IV-K-2-b Test Procedure

(1) Connect the exciter to the simulated load as shown in Figure IV-16.

(2) Operate the exciter at rated speed and rated cooling.

(3) Increase the exciter shunt field voltage in approximately 15 equal increments to the maximum point of interest and record the exciter output voltage, load current, field current, and field voltage at each point.

(4) Decrease the shunt field voltage back to zero following the same procedure. Care should be taken to increase and decrease the excitation in continuous unidirectional increments to insure that a definite hystersis path is traversed.

IV-L EXCITER SHUNT FIELD TIME CONSTANT

IV-L-1 General Remarks - The shunt field time constant is the time required for the exciter output voltage to reach .632 of its final steady-state value when a constant voltage is suddenly applied to the shunt field circuit.

IV-L-2 Test Procedure

(1) Connect the exciter as shown in Figure IV-17. Isolate the exciter by disconnecting its load, other exciter windings, and regulator. Refer to the wiring diagram for multiple exciter

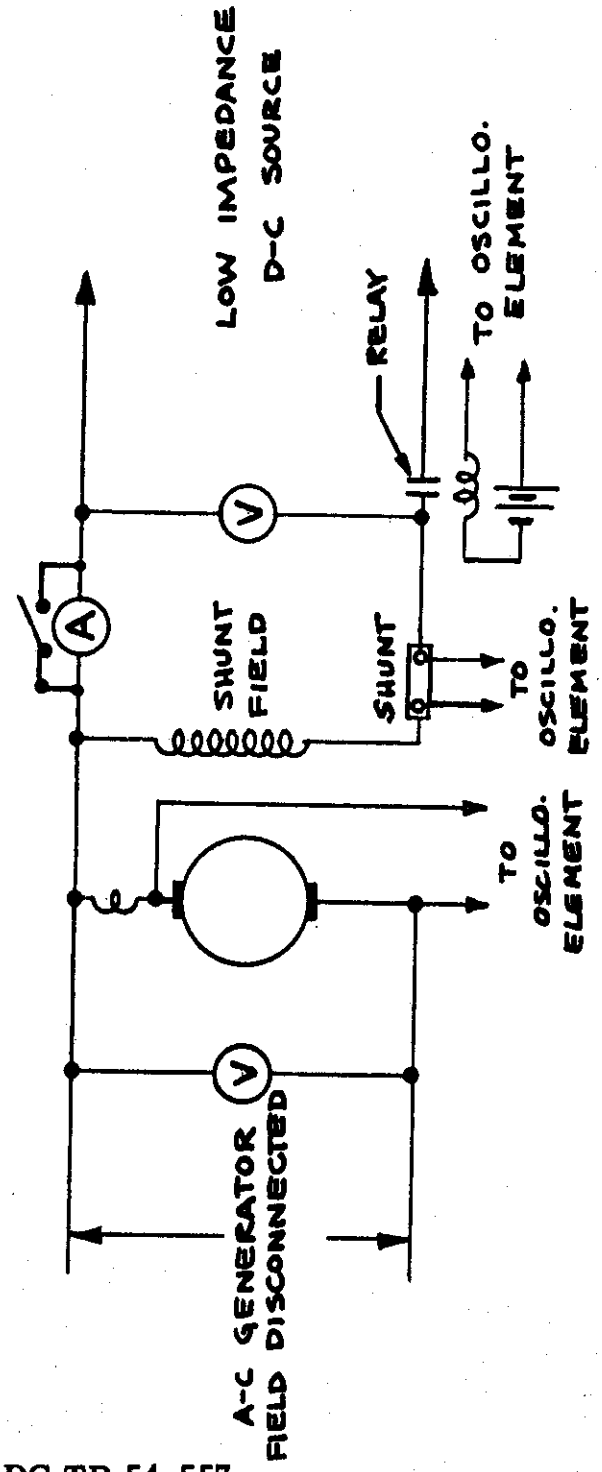

Figure IV-17 Test Set-up to Determine the Exciter Shunt Field Time Constant

windings. It may be necessary to disconnect the other exciter fields by lifting the slip-ring brushes and disconnecting the commutator brush shunts.

(2) Operate the exciter at rated speed and rated cooling. Use a suitable speed indicating device so that the a-c generator terminal voltage may be used as the time scale calibration signal on the oscillogram. If necessary, apply separate excitation to the a-c generator to obtain a trace of the a-c generator output voltage.

(3) Tap the battery cells to give a field current slightly below saturation on the exciter no-load saturation curve.

(4) It will usually be necessary to cut-and-try until the proper adjustment of film speed and oscillograph trigger switch setting is obtained. Start with an oscillograph film speed of about 2 feet per second and advance the film speed and readjust the oscillograph trigger switch setting as indicated by the previous oscillograms. This problem can be avoided by using a continuous film. For this case, the film speed should be approximately 10 feet per second. The optimum film speed will depend upon the time constant of the exciter being tested.

(5) Allow the shunt field temperature to stabilize and measure its resistance immediately prior to taking the oscillogram.

(6) Take an oscillogram of the exciter output voltage, exciter field amperes and timing wave, when the battery voltage is suddenly applied to the shunt field circuit. Double expose the film with the steady-state value of the field current and armature voltage for the magnitude calibration. Do not double expose the timing wave trace.

(7) Open the shunt field circuit and record the exciter output residual voltage.

IV-L-3 Method of Analyzing Test Data - The exciter output voltage trace from the oscillogram is plotted on semi-log graph paper. The residual voltage is subtracted from this curve. The straight line is extrapolated to zero time. The exciter shunt field time constant is taken as the time required for the exciter output to reach .632 of its final steady-state value.

BIBLIOGRAPHY FOR CHAPTER IV

1. Westinghouse Authors, Electrical Transmission and Distribution Reference Book; Fourth Edition, Westinghouse Electric Corporation, East Pittsburgh, Pa., 1950, pp 148-56.

2. Concordia, C and Maginnis, F. J., Inherent Errors in the Determination of Synchronous-Machine Reactances by Test; AIEE Transactions, Vol. 64, pp 288-94, discussion p. 492.

3. Anonymous, Aircraft A-C Generator Test Manual; Part II, Naval Research Laboratory, January 1953.

4. Anonymous, Test Code for Synchronous Machines; No. 503, American Institute of Electrical Engineers, New York, N. Y., June 1945.

5. Holloway, V.C., Transient Characteristics of Aircraft A-C Generators; Applications and Industry, Americal Institute of Electrical Engineers, New York, N. Y., September 1954, pp 187-190.

CHAPTER V

PARALLEL A-C GENERATOR OPERATION

V-A INTRODUCTION

The operation of an a-c generator in a parallel system can be analyzed by single generator theory if certain assumptions are made and if the effects of real and reactive load unbalance between generators are taken into account.

In the preceding chapters, an evaluation of the a-c generator design and system operation has been studied as the generator constants are varied. Emphasis is again called to the fact that these parameters or constants are not truly constants since they are affected by generator load and excitation. The designer can control the constants and thus the generator performance by his choice of dimensions, winding configurations, materials, slot depths, etc., but once the generator is built the constants are fixed for specific load and excitation values. Approximate generator performance can be determined on the basis of fixed values for the constants if correction for saturation is taken into account, but accurate performance is found only by tests.

Included in this chapter is a discussion of the effects upon system operation when real and reactive load unbalance occurs between generators in a parallel a-c system. Figure V-1 represents the typical parallel a-c system.

V-B LOAD VARIATIONS

Since real power output of an a-c generator is a function of the torque input, and reactive power output is a function of excitation, a-c generators in a parallel system may be required to carry a variety of loads even though a constant load is connected to the bus. For instance, if no load is on the bus, one generator may be supplying an inductive reactive load while the other is supplying a capacitive reactive load. One may be operating as a motor while the other is supplying the system losses and power to the motor. The problem of load division becomes more important when a relatively large load is connected to the bus. Figure V-2 shows vectorially the possible load variations on each generator of a two generator system when a constant bus load of 40-kva at 75% power factor is maintained and extreme unbalances in excitation occur.

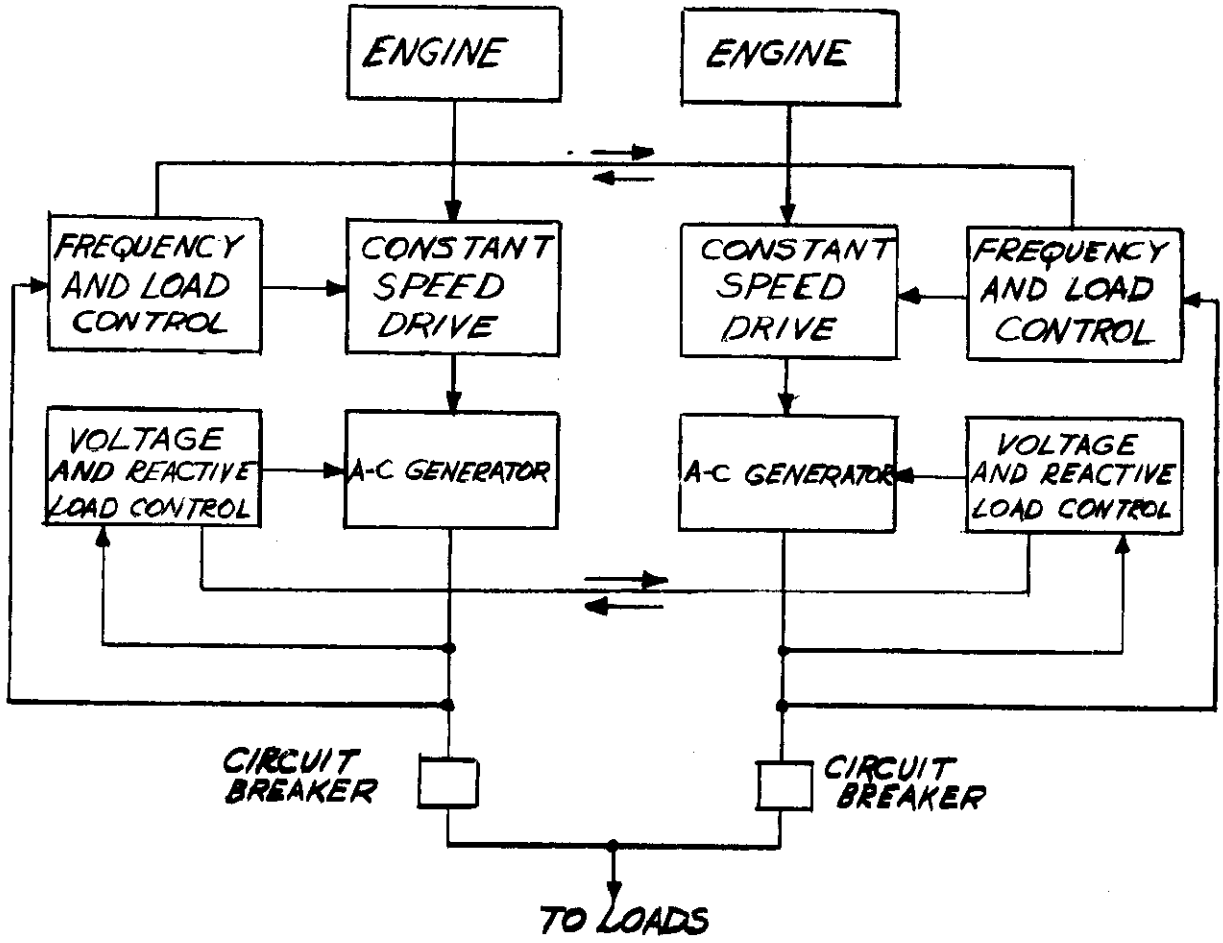

Figure V-1. A Block Diagram of a Two Generator Parallel A-C System

Two kilowatts of reverse power is assumed to be sufficient to motor the generator on the line and supply its losses. From zero to any point in the shaded area represents possible loads on either generator. The vectorial difference between the total load vector and the number 1 generator load vector represents the load on number 2 generator.

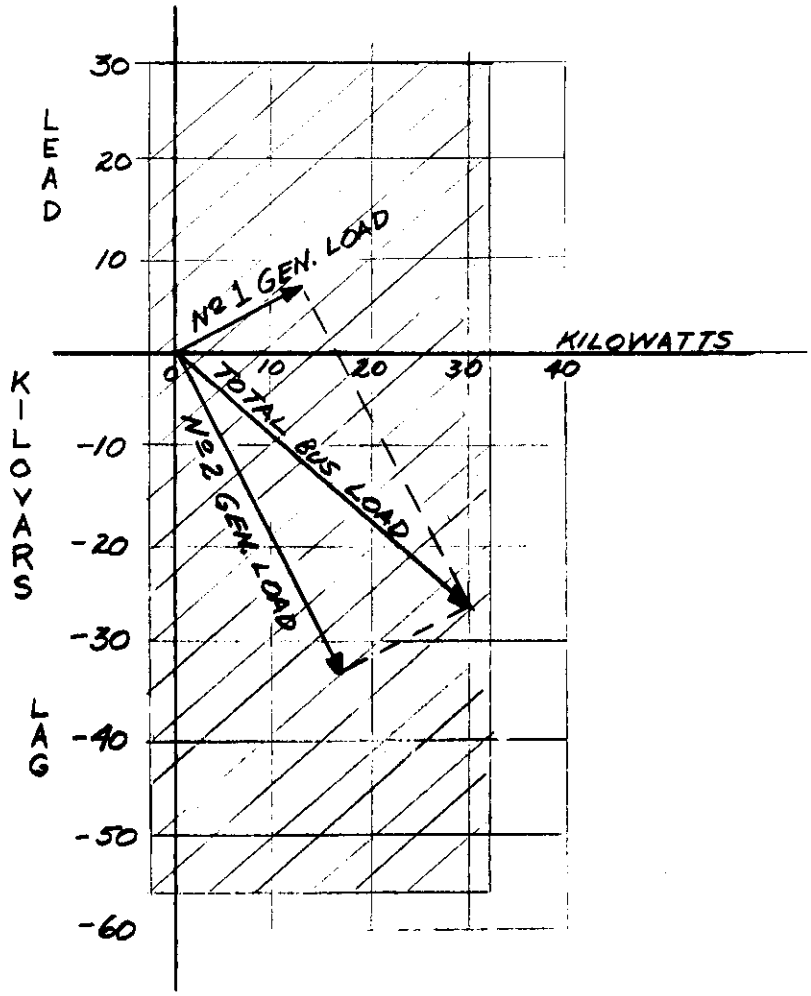

Figure V-2. Possible Load Variations on a Two Generator System with a 40 KVA - 75% PF Bus Load. Shaded Area Defines Possible Load Extremes

V-C LOAD CARRYING CAPABILITIES

Since a generator in a parallel system may be required to carry a variety of loads even though a constant load is applied to the bus, its load carrying capabilities become important. The method shown below can be used to determine the approximate torque angle or load carrying capabilities of a generator with a given value of excitation and terminal voltage. From figure V-3 the following equations can be derived:

(1) $E_o = V \cos\delta + I_q r + I_d X_d$
(2) $I_q X_q = V \sin\delta + I_d r$
(3) $P = V (I_q \cos\delta + I_d \sin\delta)$
(4) $I_d = E_o X_q - V (X_q \cos\delta + r \sin\delta)$
(5) $I_q = E_o r + V (X_d \sin\delta - r \cos\delta)$
(6) $P = V (E_o (r \cos\delta + X_q \sin\delta) + V (X_d - X_q) \sin\delta \cos\delta - V_r)$

Where δ = the torque or power angle

If r is neglected in comparison with X_d and X_q

$$(7)\quad P = \frac{VE_o \sin\delta}{X_d} + \frac{V^2 (X_d - X_q) \sin 2\delta}{2 X_d X_q}$$

$$(8)\quad \delta = \tan^{-1} \frac{I_a (X_q \cos\theta - r \sin\theta)}{V + I_a (X_q \sin\theta + r \cos\theta)}$$

The first term of equation (7) is the same for both round rotor and salient pole a-c generators, however, the second term appears only in salient pole machines. For this reason it is sometimes referred to as the "saliency effect". A plot of power as a function of torque angle δ, as in figure V-4, shows that peak power occurs at an angle less than 90 degrees. The maximum torque angle can be determined by differentiating equation (7) with respect to δ and setting equal to zero. For most aircraft generators δ max is usually between 65 and 75 degrees.

$$(9)\quad \frac{dP}{d\delta} = 0 = \frac{VE_o \cos\delta}{X_d} + \frac{V^2 (X_d - X_q) \cos 2\delta}{X_d \quad X_q}$$

$$(10)\quad \delta \text{ max} = \cos^{-1} \left[\frac{E_o X_q \pm \sqrt{(E_o X_q)^2 + 8V^2 (X_d - X_q)^2}}{4V (X_q - X_d)} \right]$$

The preceding equations indicate that the load carrying capabilities of an a-c generator are a function of the generator constants, X_d and X_q, and the relative excitation level. After the machine constants are established

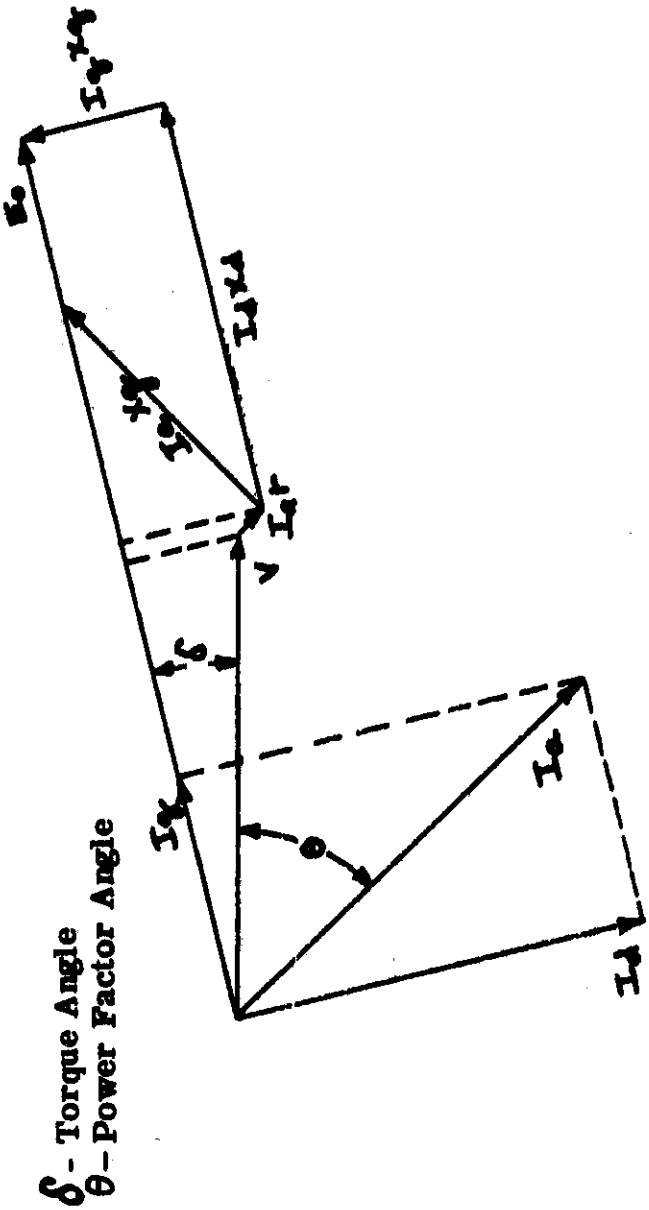

Figure V-3 A Two Reaction Diagram For a Salient Pole a-c Generator

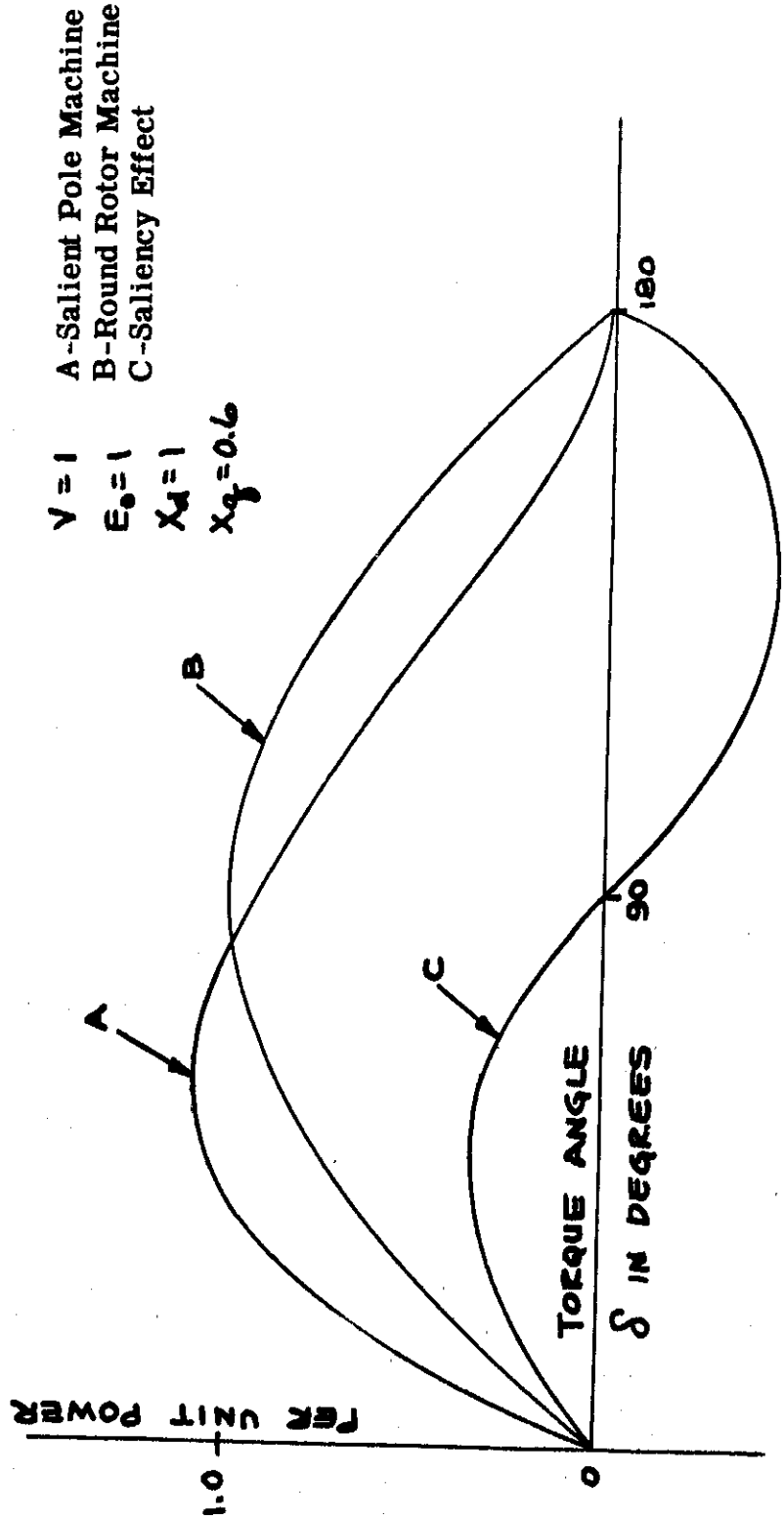

Figure V-4 A Plot of Power VS a-c Generator Torque Angle δ

by the design, the voltage regulator and drive performance should be co-ordinated so that possible pole slippage or unstable operation does not result.

To demonstrate the effects of real and reactive power unbalance on a parallel system figures V-5 and V-6 are shown. Figure V-5 represents the case when real load is unbalanced with reactive load balanced and figure V-6 represents the case where real load is balanced with reactive load unbalanced. In each figure the torque angle of one generator is greatly affected by the unbalance and is approaching the maximum power angle or point where synchronism is lost.

V-D TORQUE ANGLE MEASUREMENTS

A means for the measurement of the torque angle of a generator can be accomplished with the use of a dual channel oscilloscope and a small permanent magnet generator. Connect the rotating portion of the permanent magnet generator to the shaft of the a-c generator and the stationary position to the frame of the generator. Connect the output of the small generator into one channel of the oscilloscope.

The voltage output of the permanent magnetic generator will be in phase with the internal voltage of the a-c generator. Into the other channel of the oscilloscope feed the a-c generator terminal voltage. The oscilloscope should be synchronized from the terminal voltage of the test machine. With no load on the generator under test, adjust the two waves on the oscilloscope so they lie on top of one another. As load is applied, the two waves will move with respect to one another proportional to the torque angle.

V-E REAL AND REACTIVE LOAD DIVISION

The division of real and reactive power between generators in a parallel system can be accomplished in several ways. One method is to divide the real load according to the droop characteristics of the drive and reactive load according to the inherent droop in the generator. This method, however, produces wide variations in frequency and voltage which cannot be allowed on most present day aircraft. The present practice is to use automatic frequency and voltage regulators to maintain an almost constant value of frequency and voltage. By biasing the frequency regulators with signals proportional to real load unbalance and the voltage regulator with a signal proportional to reactive load unbalance, real and reactive load division is accomplished. Both direction and magnitude of flow of both real

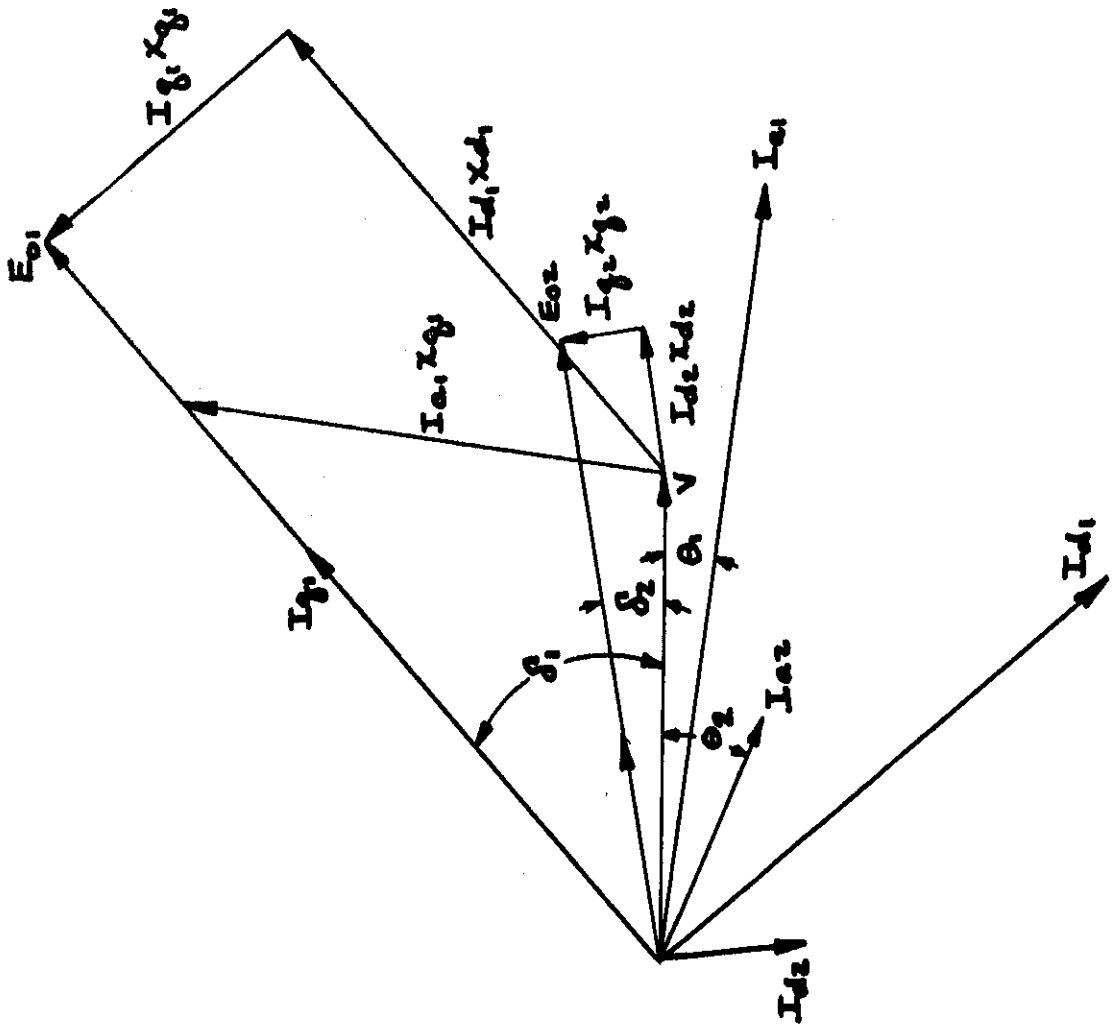

Figure V-5 A Two Reaction Diagram of Two Generators in Parallel with Real Load Unbalanced Between Generators

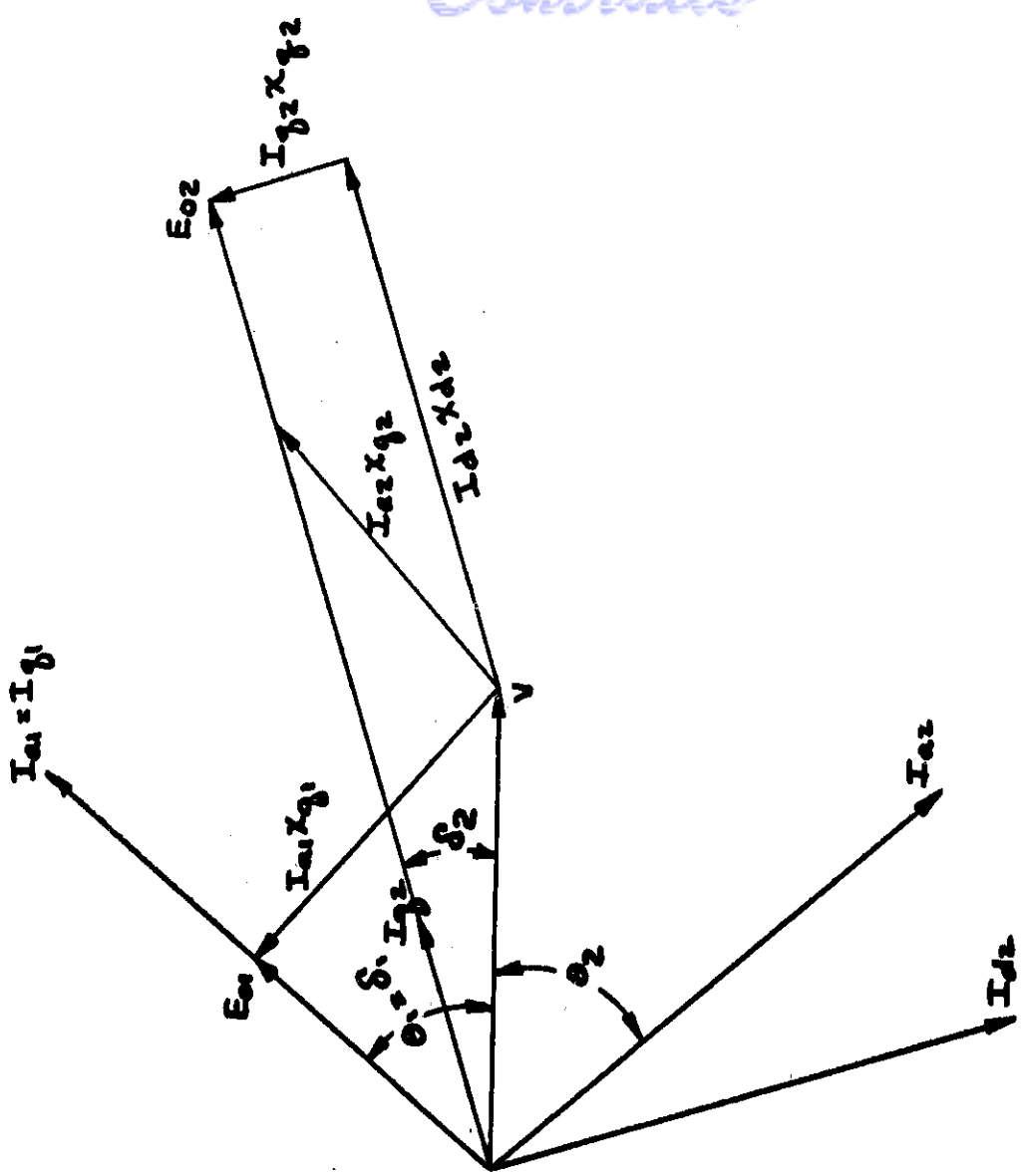

Figure V-5 A Two Reaction Diagram of Two Generators in Parallel With Reactive Load Unbalanced Between Generators

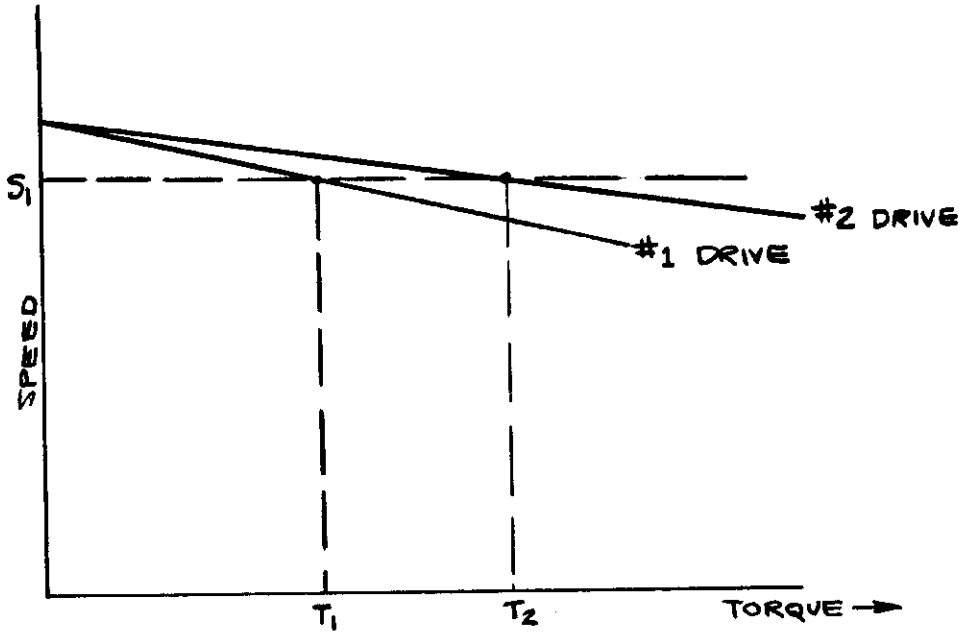

Figure V-7. Load Division Between Two Un-Regulated Drives Which Have Different Torque-Speed Characteristics

and reactive power are required to produce the proper amount of correction. The equalizer circuits employed are of the droop type but since the automatic regulators maintain an almost constant value of frequency and voltage, only small amounts of droop are required to provide the proper division of real and reactive load. Therefore, the system frequency and voltage are maintained more nearly constant by this method than by the first method described.

The equalizer circuits serve a two fold purpose. The first purpose is the reduction of circulating current between generators in a parallel system to prevent the overheating of generators. The second purpose is to accomplish proper load division so that synchronous stability or synchronizing torque is maintained. In general, the strength of the real power and reactive power equalizer loop is determined from the standpoint of maintaining system capacity or preventing the overheating of generators.

If the maximum reactive load difference between any two generators is maintained at 10% of the system capacity and if the voltage regulator maintains 200 volts $\pm$ 2-1/2% on the bus, then for a two generator system the sensitivity of the reactive load division circuit would be

$$\frac{10 \text{ volts}}{.2 I_{pu}} = \frac{50 \text{ volts}}{I_{pu}} .$$

In a similar manner if the real load division between any two generators is maintained to within 10% of the system capacity and if the frequency regulator maintains 400 cps $\pm$ 1/2% on the bus then for a two generator system the sensitivity of the real load division circuit would be

$$\frac{4 \text{ cps}}{.2I_{pu}} = \frac{20 \text{ cps}}{I_{pu}} .$$

I_{pu} is rated line current of the generator.

V-F. CONCLUSIONS

1. Synchronous stability is a function of the generator constants X_q and X_d, the excitation level and the terminal voltage.
2. During a steady state system operation, the possibility of pole slippage or synchronous instability is remote if the strength of the equalizer circuits are maintained as defined in paragraph V-E.
3. On over-excitation faults if the reactive load division circuit is properly co-ordinated, the loss of synchronism will not result.
4. During under-excitation faults the faulted generator may fall out of step with the rest of the system but synchronizing power is low and system disturbances are not severe. The a-c generator protection will remove the faulted generator from the bus.

CHAPTER VI

CONCLUSIONS AND RECOMMENDATIONS

VI-A INTRODUCTION

As stated in the introductory chapter to this report, it was originally intended that specific recommendations be made of the a-c generator characteristics. Based on the work performed, this ideal cannot be attained unless one is willing, simultaneously, to restrict the operation of the system in many other ways. This does not seem wise,for all aircraft electric systems certainly do not require the same performance. Therefore, this study shows the relationships that exist between the machine performance and the machine parameters. Toward this end certain specific machines were studied, and various curves and tables are presented.

Throughout the course of work on this report it was held that one of the most troublesome phases of a-c system performance was that of transient stability. This can be described partially by the system recovery time and this was the criterion used to judge the transient performance of the systems.

A great deal of emphasis was placed on the analogue computer as a suitable tool to facilitate the study of a-c generator parametric changes. Therefore the appendix on analogue computer studies and results (Appendix A) constitutes a large part of the original work done for this report.

In order to properly integrate data obtained from the computer, other factors than transient stability were considered. The steady-state performance of both the a-c generator and the exciter was investigated. Simultaneously, a survey was made of the aircraft industry, the military services, and the accessory manufacturers to determine the requirements for a-c electric system performance. Test methods used to obtain the characteristics of the a-c generator and the other elements of the system were evaluated.

The following sections summarize the different phases of the study separately.

VI-B TRANSIENT PERFORMANCE

To draw any definite conclusions on the transient performance of electric power systems in general is quite difficult, if by conclusions one means a clear-cut recommendation for the magnitudes of the major parameters of the system, and in particular with regard to this report, those associated with the a-c generator. The problem is still complex even when confined to selected systems, such as was done in this study. There are so many possible combinations to study that it becomes necessary to apply constraints to certain portions of the total system. The disadvantage with this is obvious, for any generality is eliminated at once. This nevertheless is necessary in order to solve the particular problem.

First, one portion of the overall problem is studied and then another, eliminating the unimportant factors as one progresses. The approach to this study, so far as the transient performance of the a-c system was concerned, was to more or less fix the remainder of the system (i.e., exciter and voltage regulator) while investigating the affects of all the a-c machine parameters. Even this restriction on the excitation means was not enough, for in order to solve the problem in a manner compatible with the analogue computer, it was necessary to consider only zero-power-factor loads. Thus the results obtained have only a qualitative value if one considers the loads normally encountered in aircraft electric systems. No attempt was made to study loading conditions other than full-load zero-power-factor. Perhaps, if one neglects the vectorial relations, making suitable adjustments to the magnitude of the zero-power factor load, a fair degree of simulation can be achieved at loads which are more nearly normal.

VI-B-1 Comparison to Other Transient Studies - Other investigators, also using the zero-power-factor loading, have studied the problem of system recovery time. Statements are presented in these works regarding the influence of such a-c machine parameters as the open-circuit transient time constant T_{do}' and the a-c machine reactances x_d and x_d'. However, the work accomplished for this report does not confirm these previous investigations. The inconsistency between the observations made for this report and the results reported previously is due in a large part to the fact that the earlier work was performed on the basis of large central-station size machines and systems. Thus, time constants for the main generator and for the exciter were ten times greater than those encountered in aircraft practice. Also, the values of x_d and x_d' were different, usually lower than those found in aircraft a-c machines. The most important dif-

ference which exists between central-station systems and aircraft systems, however, is the ratio of the time constants of the a-c machine to the exciter and to the voltage regulator, and the time constant of the exciter to that of the voltage regulator, too. These ratios are considerably lower in aircraft electrical system practice than in those systems encountered in the commercial field. These enumerated differences make the transient stability problem more difficult in the aircraft system.

VI-B-2 Excitation System - One very important point of agreement between this work and previous studies is that the most important factors which govern the time of recovery of the system voltage are found in the excitation portion of the total system and especially in the feedback circuits associated with this part of the overall system.

The emphasis in this report was always on the a-c generator and its parameters, but various limited studies were made of such factors as exciter gain, exciter time constant, and the feedback circuit in the voltage regulator.

It was apparent in the studies made on the 20-kva a-c system that the strength of the feedback signal was all-important in determining the sensitivity of parametric variations of both the a-c generator and the exciter. With a weaker feedback signal one would easily conclude that the a-c machine constants are very important in the determination of transient stability, yet with a stronger signal in the stabilizing circuit this is not the case. Under these conditions very little influence is observed in the system recovery time as the various parameters are varied.

It is recommended that more work be directed along this approach to the problem of transient performance. Attention is directed to some work dealing with the contribution of the regulator and the feedback stabilizing circuit in WADC Technical Report 54-298, cited in Chapter III.

VI-B-3 Problem of Obtaining Optimum Values - The conclusions reached in Appendix A for all three systems studied (20 Kva, 60 Kva, and 40 Kva) show that there are no optimum numerical values which hold in all cases for the a-c generator characteristics and parameters. The restrictions which were necessary to effect a solution prevented this. In each case a specific system was used and many of the factors in the exciter and the voltage regulator which are vital to the transient performance were held constant during the investigations. Information was obtained from these studies and it is reported in detail in Appendix A, but it applies to the

particular system rather than systems in general.

Further work in this field might yield a general solution to the problem of transient stability in aircraft a-c electric systems. The studies made for this report did not reveal more than a particular solution. It was possible to see what happened for a specified set of values in the system but often the next set gave different results, or it would show negligible effect where previously a significant change had been observed.

VI-B-4 Significance of Analogue Computer Techniques Compared to Previous Methods - The practice in the past has often been to let the machine designer have full freedom in the a-c generator design; simultaneously the exciter and the voltage regulator were designed. Only meager steady-state requirements determined the necessary interrelationships between all three major elements of the system.

After the first samples were built, the real work was accomplished at the time of the preliminary tests. Various feedback circuits were employed and after a "cutting-and-trying" process, the system exhibited a satisfactory transient performance.

The techniques of simulation using the analogue computer are certainly a stride forward in understanding the transient problem and in producing better and more reliable aircraft electric systems. The circuits shown in Appendix A can be readily adapted to any system with similar components, and the circuits can also be used for other voltage regulators (i.e., magnetic-amplifier type) with only minor adaptations.

This method of analoging the electric system allows one to study the stability problem far in advance of the actual components, or one can couple the computer to existing physical elements as was done with the regulator in this report.

Even though the computer is employed in an empirical manner similar to the previous "cut-and-try" method, the time required to arrive at a satisfactory solution is reduced tremendously. Also, by means of electronic simulation, one can explore the permutations of the system over wide ranges, far beyond that possible when working with actual components.

VI-B-5 Summary - The difficulty encountered in attempting to recommend specific values for the various parameters in an electric power system is discussed. Comparison is made to other work on time of recovery. The

advantage of simulation methods over previous "cut-and-try" method is discussed.

Reference is made to the individual conclusions on transient performance found in Appendix A.

VI-C STEADY-STATE PERFORMANCE

It was mentioned previously that greater emphasis was placed on transient performance than on steady-state performance in the work reported here. Steady-state performance has always been of primary importance, however. Certain aspects of steady-state performance were considered in Chapter II and the conclusions and recommendations from this work are given in the following paragraphs.

VI-C-1 Load-Speed-Cooling Considerations - The size of an a-c generator is set mainly by the maximum load at minimum speed requirement. The cooling provisions of the machine are very important as they determine the maximum allowable current densities of the windings without overheating. Machine constants may vary considerably in different designs for the same steady-state rating. This is discussed in Chapter II, section D.

VI-C-2 Harmonics at Balanced Load Conditions

The pole heads of salient pole a-c generators should be shaped to give approximately sinusoidal flux distribution. Under load conditions this is not sufficient to control the harmonics, however, and other measures must be taken. It is recommended that two-thirds coil throw be used to reduce the triplen harmonics (i.e., the third and odd multiples of the third harmonic). The number of slots per pole may be selected to limit the fifth and seventh harmonics. Other harmonics above the ninth are seldom troublesome except those which are a result of the slot ripple flux. The frequencies of the slot harmonics are two times the effective slots/pole plus and minus one. It is advantagous to use a large number of slots which decreases the magnitude of the slot ripple flux. When this cannot be done the armature punching may be skewed to control the harmonics. In general, fractional slot windings are recommended because they give a greater number of effective slots per pole.

VI-C-3 Unbalanced Load Terminal Voltages and Harmonics - The two-thirds pitch winding cannot eliminate the triplen harmonics with unbalanced

load conditions as the voltages are induced in the armature windings by transformer action from the pulsating air-gap flux. It is recommended that amortisseur winding be used with connections between poles. The leakage reactance and d-c resistance of the circuits should be kept as low as is practicable. These windings are also effective in controlling the unbalance of the terminal voltage under unbalance loads. The armature leakage reactance enters into this later consideration and it should be kept as low as possible. It is recommended that further work be done on the two performance considerations mentioned above. Such a study may lead to better amortisseur windings than those now in use.

VI-C-4 Short-Circuit and Overload Capacity - The short-circuit capacity of an a-c generator is not determined by the machine constants alone but also by the excitation capacity. The matter is largely one of providing enough excitation for a given short-circuit current. Overload capacity involves the heating of the windings and saturation as well as the capacity of the exciter. These problems must be taken into account in the basic design of the main generator and exciter.

VI-C-5 Efficiency - The efficiency can only be improved above a certain point at the expense of the weight and size of the machine. Using lower current and flux densities usually leads to improved efficiency. Eddy-current losses may be excessive if solid iron poles are used or if the laminations of the armature or field have excessive burrs. Excessive slot ripple flux is also objectionable from the losses standpoint. It may give relatively high amortisseur winding losses and high localized core losses.

VI-D TESTING AND TEST METHODS

Test methods used to obtain the characteristics and parameters of aircraft a-c generators are outlined in Chapter IV. These should be adequate for most general purposes. It should be restated, however, that standard tests, no matter how well defined, can still produce inconsistent results if care is not exercised at all times. Since testing is always dependent to a degree on the facilities which are available, there is always then, a matter of discretion, common sense, and good judgement.

By following the procedures given, there is every reason to expect reliable test results, providing the testing group and the ultimate users of the test information have properly coordinated their efforts.

In addition, by using these methods as a guide, one can readily understand the requirements for special tests and the precautions which are necessary.

VI-E PARALLEL OPERATION

Since the major portion of the work accomplished for this report deals with isolated power systems, the conclusions on this phase of electric system study are necessarily limited. Chapter V, Section F, presents a summary of these conclusions.

The study of a-c generator characteristics with respect to parallel operation is a field by itself. As stated in the introductory chapter the scope of the work was limited to isolated systems except for the parallel system mock-up tests and the treatment of the subject in Chapter V.

It is recommended that more work be done on the problem of parallel operation of a-c generators. Such topics as real load division, reactive load division, paralleling, fault conditions, voltage recovery after removal of faults have been treated previously, but further investigation is warranted.

VI-F A-C SYSTEM SURVEY

At the outset of the work on this project it was felt that information on aircraft a-c electric system performance from the air-frame manufacturers, utilization equipment and systems manufacturers, and branches of the military services would form.

The response to the questionnaire was not sufficient to provide conclusive statements, but in general, for the answers received, the requirements as specified in MIL-E-7894 and MIL-G-6099 were acceptable.

Many organizations in the aircraft industry are not too clear on what the requirements for a-c power should be, and they are therefore willing to accept these military specifications.

It is recommended that the specifications for electric power systems be studied, first, from an electric-system viewpoint, second, from the power, distribution, and utilization system viewpoint. Only then should the detailed apparatus specifications be issued to support the system-conceived major specifications.

APPENDIX A

ANALOGUE COMPUTER STUDIES AND RESULTS

A-1 INTRODUCTION

This appendix describes the studies and the results of the studies made with an analogue computer on three separate a-c generator-regulator systems. These were a 20-kva single-phase system, a 60-kva three-phase system and a 40-kva three-phase system. The transient performance was the only phenomena which was given any consideration during these studies and in particular the attention was focused on the system recovery time. This system recovery time T_R is the time required for the output voltage of the main generator to return to and remain within a given band around a fixed level. In all the cases studied here this band was plus or minus 2.5 percent, and the level was established as that voltage to which the system stabilized after the disturbance. This then does not account for the increase in recovery time due to shift of the regulator between full-load and no-load voltage levels.

First, we will cover the particular circuits used to analogue the a-c synchronous generator, both a passive circuit for the linear case and a more elaborate circuit which includes saturation. Then we will discuss the individual studies made on each of the systems.

It will be noted that in all of these studies the parameters used are sometimes far beyond the range of practicality. However, the idea for this transient study was to cover the complete field. The largest and the smallest values for X_d and X_d' known for any aircraft a-c generator were used and rather wide limits were made of the other parameters. Due to the advantages of the analogue computer running large amounts of data presents no obstacle.

A-1-a Consideration of Load-On and Load-Off Transients - In most of the previous studies made of the transient performance of electric power systems, the emphasis was always on the voltage transient following a load application. The literature on this subject reveals little work on the case of the transient following load removal, and yet this phenomena is quite important, particularly in aircraft electric systems. The effect of overvoltage transients on a few remaining loads, or even on the protective devices, such as overvoltage relays, creates serious problems to the system design engineer. Therefore, both the load-on and the load-off conditions have been considered in all the studies.

A-1-b Data Smoothing - A word about the data presentation should be made before making any conclusions or recommendations. The curved surfaces which show system response time T_R as a function of various independent system parameters were smoothed out considerably from the actual values obtained on the computer. A true curve of response time versus some variation in a closed-loop system is quite discontinuous, and, therefore, when used in its original state, is difficult to interpret. Optimum conditions in limited regions may give a completely false impression. For purposes of better showing the major change in the response time then, these irregularities have been eliminated and smooth curves used instead.

A-2 ANALYSIS OF ANALOGUE COMPUTER REPRESENTATIONS FOR A-C SYNCHRONOUS MACHINES

A-2-a Linear Simplified Representations - The circuit used to represent the a-c synchronous generator in linear simplified analogues is drawn in Figure A-1.

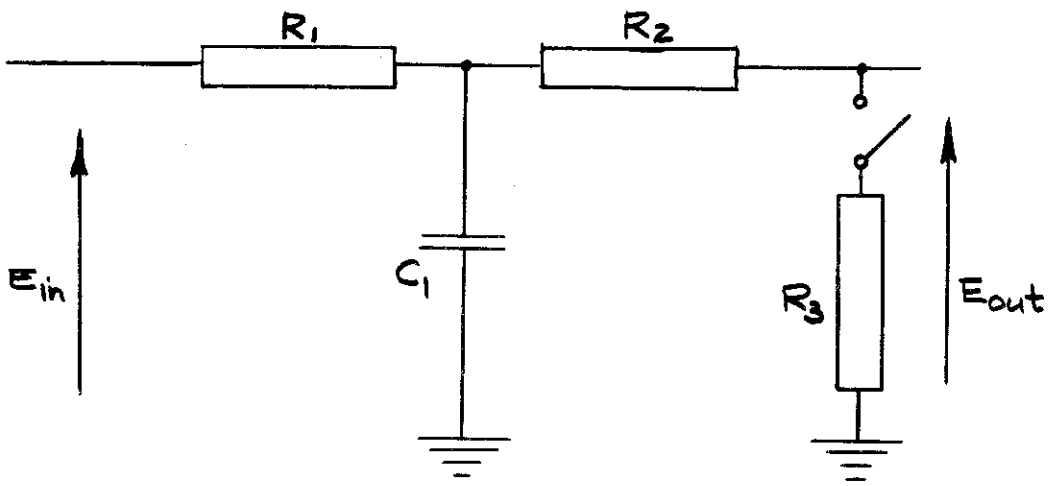

Figure A-1. Simple Passive Network Used to Represent a Linear A-C Generator

Solving the circuit for the output voltage E_{out} as a fraction of E_{in} we obtain the following expression.

$$E_{out} = \left(\frac{R_3}{R_1 + R_2 + R_3}\right)\left(\frac{1}{1 + \frac{R_1 C_1 p (R_2 + R_3)}{R_1 + R_2 + R_3}}\right) E_{in} \qquad (1)$$

Recalling that the usual expression for the time constant of an a-c generator with inductive reactance loading is

$$T_{dz'} = T_{do'} \frac{(X_{d'} + X_L)}{(X_d + X_L)} \tag{2}$$

and further that the total equation for this machine is

$$\text{Generated voltage} = e_g = \left(\frac{K_g}{1 + T_{dz'} p} \right) e_x \tag{3}$$

$$\text{Terminal voltage} = e_t = \left(\frac{X_L}{X_d + X_L} \right) \left(\frac{K_g}{1 + T_{dz'} p} \right) e_x \tag{4}$$

Comparing equation (1) and (4) it can be seen that the correct analogy exists if the following conditions are met:

(1) $R_1 C_1 = T_{do'}$
(2) $R_1 R_2 = X_d$
(3) $R_2 = X_{d'}$
(4) $R_3 = X_L$
(5) $\left(\frac{R_2 + R_3}{R_1 + R_2 + R_3} \right) \left(R_1 C_1 \right) = T_{dz'}$

One important point should be emphasized when using this circuit shown in Figure A-1. At no-load condition conditions the factor relating a-c generator terminal voltage to exciter voltage is unity. If we wish to provide for a value other than unity, this must be done through an additional d-c amplifier in the analogue computer.

This arrangement alone does not provide a signal proportional to the field current under all steady-state and transient conditions. Therefore, we add another section to the circuit above. Figure A-2 shows this schematic.

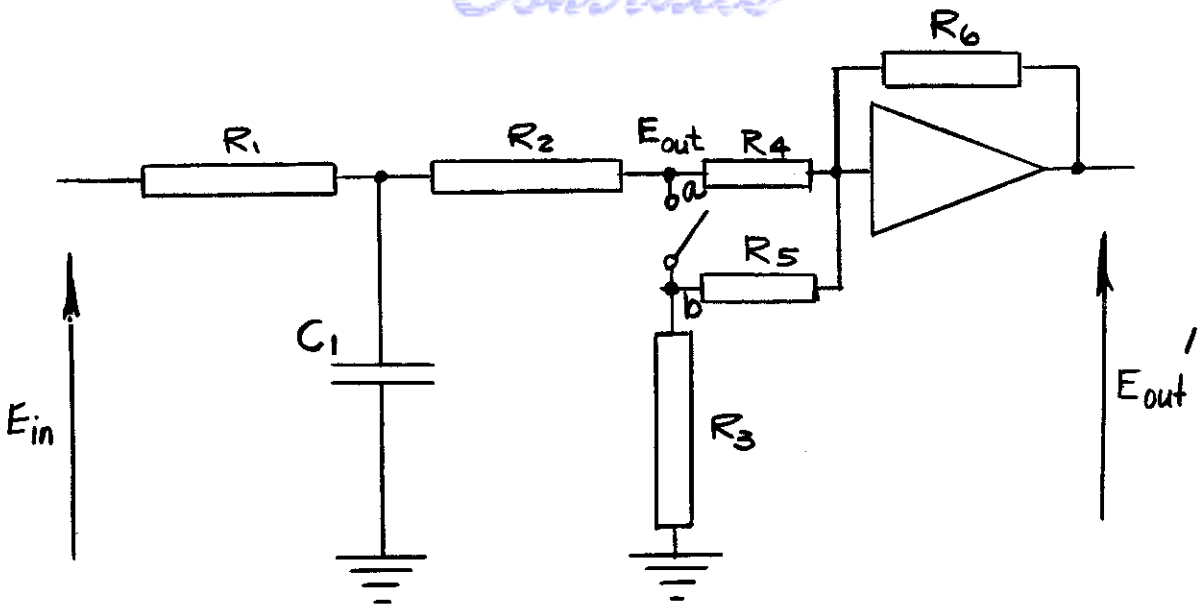

Figure A-2. Complete Passive Network Used to Represent a Linear A-C Generator

One can readily see that through input a to the amplifier we obtain a signal proportional to the generated voltage or the voltage with no-load applied. Under these conditions input b is not connected. The output of the amplifier is simply

$$E_{out}'\Big|_{NL} = \left(\frac{-R_6}{R_4}\right) \qquad E_{out} = \left(\frac{-R_6}{R_4}\right) E_{in} \tag{5}$$

By proper choice of the ratio of R_6 to R_4 we can use E_{out}' as a field current signal for no-load.

Now let us consider what happens when we apply load. First, however, we should look at the relationship between the generator output voltage at no-load and under rated load conditions (zero p.f.). See Figure A-3.

When a zero-power-factor load is suddenly applied to a synchronous machine the voltage drops instantaneously by a certain amount from 1 to 2 and simultaneously the field current increases instantaneously from 1 to 2, the phenomena being due to the principle of constant flux linkages as explained in Chapter II. Referring to the analogue in Figure A-2, it can be seen that the combination of R_4 and R_5 in parallel (producing a smaller input resistor) will increase the gain of the amplifier instantaneously as the switch is closed. Thus we choose R_5 such as to give the desired increase in field current. Under load conditions we have (at steady-state)

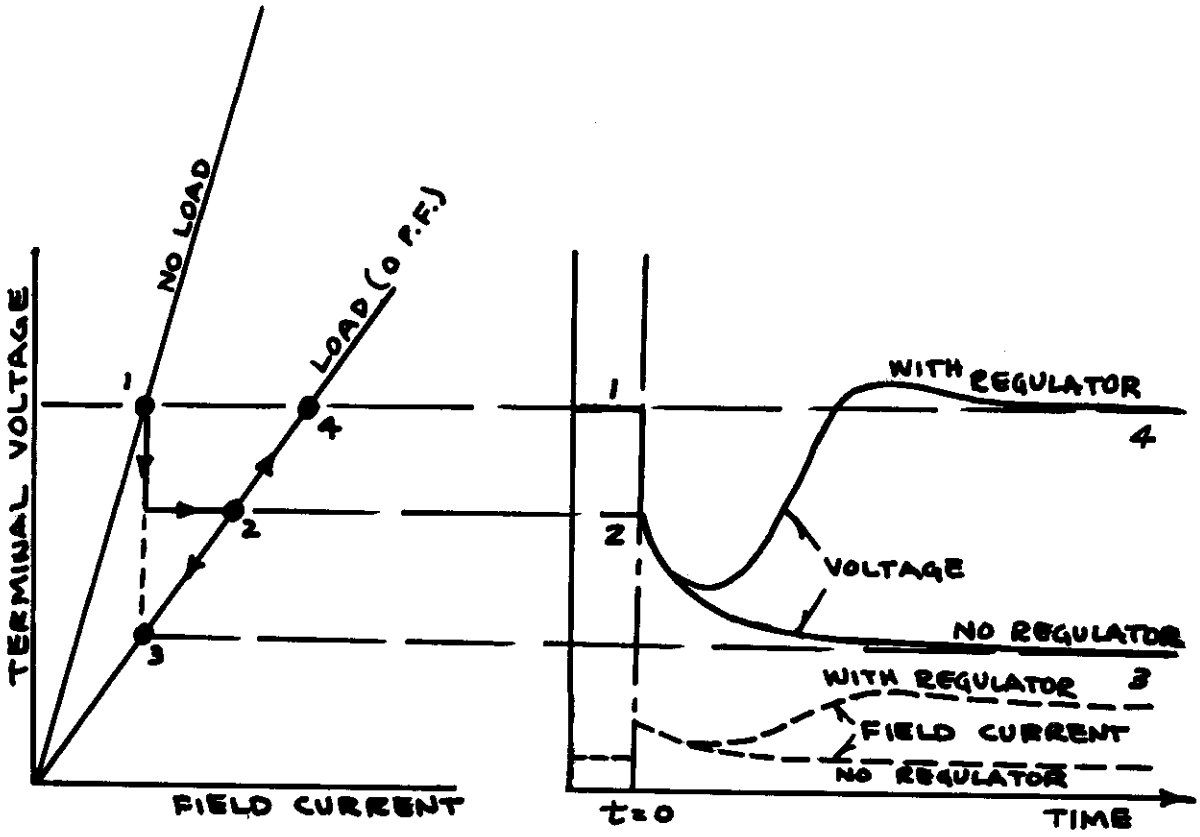

Figure A-3 Effect of Applying Load to an A-C Machine

$$E_{out}' \Big|_{Load} = \left(\frac{-R_6 (R_4 + R_5)}{R_4 R_5} \right) E_{out} \qquad (6)$$

$$E_{out}' \Big|_{Load} = \left(\frac{R_3}{R_1 + R_2 + R_3} \right) \left(\frac{-R_6 (R_4 + R_5)}{R_4 R_5} \right) E_{in} \qquad (7)$$

Naturally, this analogue in Figure A-2 has limited use, but when studying wide-speed systems which operate at high speed it can produce the desired results. The 20-kva system study used this circuit as can be seen in Figure A-9.

A-2-b Representation to Include Saturation - A very useful circuit which is much more flexible and also allows the introduction of saturation to the analogue has been reported in WADC Technical Report 54-298, Part 1, pp 25-32. This circuit in block form is shown in Figure A-4.

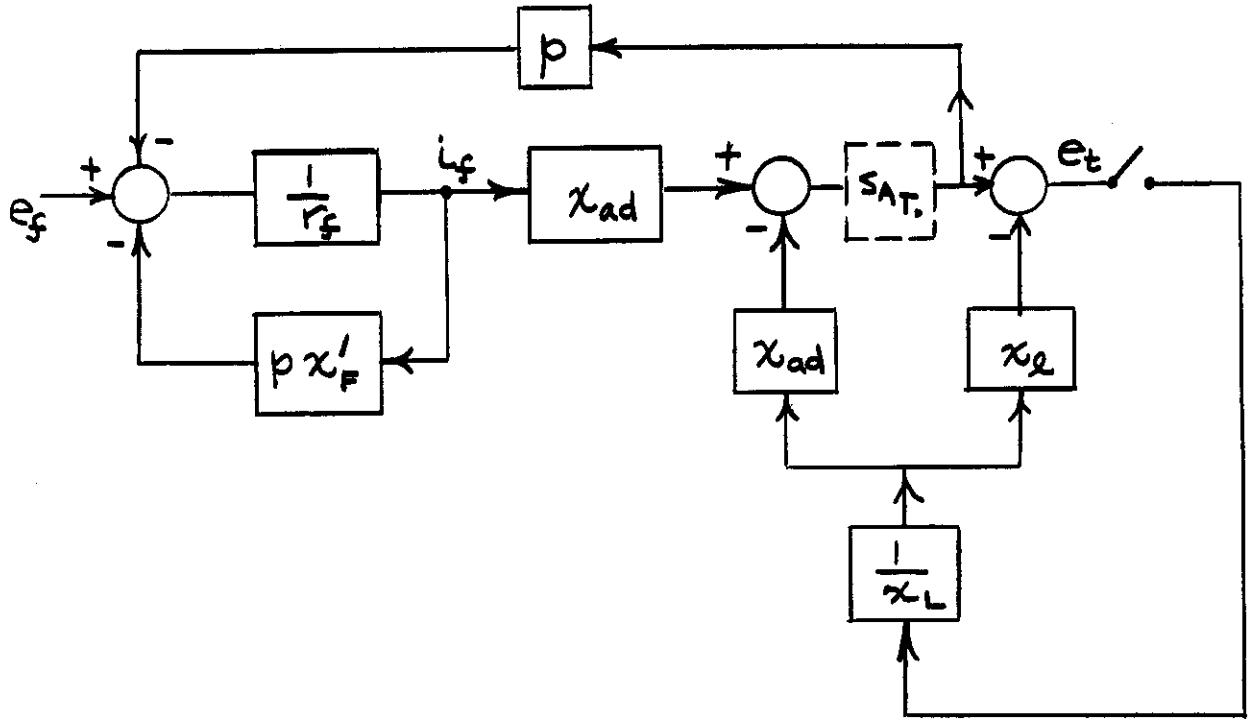

Figure A-4. Block Diagram of A-C Synchronous Machine (Fig. 1, Chapter 3, WADC Technical Report 54-298, Part I)

Since the process of differentiation is very difficult to perform with an analogue computer, this block diagram shown above must be translated into terms which provide integration operations. This is usually a simple process and one which is familiar to those working in the field of d-c analogue computers. Reference to a number of excellent papers and books is given at the end of this appendix which provide the processes by which this is accomplished. Figure A-5-a and Figure A-5-b show respectively the new block diagram and the actual analogue circuit used to provide these operations.

An examination of the two portions of Figure A-5 will show that the following relationships exist between the machine parameters and the components used in the analogue.

(1) No-load gain (unsaturated), G_{NL}

$$G_{NL} = \frac{R_8\, P_1\, R_{10}\, R_{12}\, R_{17}\, R_2}{R_6\, P_4\, R_1\, R_9\, R_{11}\, R_{14}}$$

(2) Direct-axis transient open-circuit time constant (unsaturated), T_{do}'

$$T_{do}' = C_1 \left[\frac{(R_4\, R_{12}\, R_{17} + R_5\, P_2\, R_{11}\, P_4\, R_{14})(R_2\, R_3\, R_{10})}{R_4\, R_5\, R_9\, R_{11}\, P_4\, R_{14}} \right]$$

(3) Load gain (unsaturated), G_L

$$G_L = G_{NL} \left(\frac{X_L}{X_L + X_d} \right) = G_{NL} \left(\frac{1}{1 + \frac{X_d}{X_L}} \right)$$

$$G_L = G_{NL} \left[\frac{1}{1 + \frac{R_8\, R_{17}\, R_{12}}{R_6\, R_{14}\, R_{13}} \frac{P_5}{P_4} + \frac{R_8}{R_7} P_3} \right]$$

(4) Reactance of armature reaction (unsaturated), X_{ad}

$$X_{ad} = \frac{1}{P_4}$$

(5) Armature leakage reactance, X_ℓ

$$X_\ell = \frac{R_6\, R_{14}\, R_{13}}{R_7\, R_{17}\, R_{12}} \left(\frac{P_3}{P_5} \right)$$

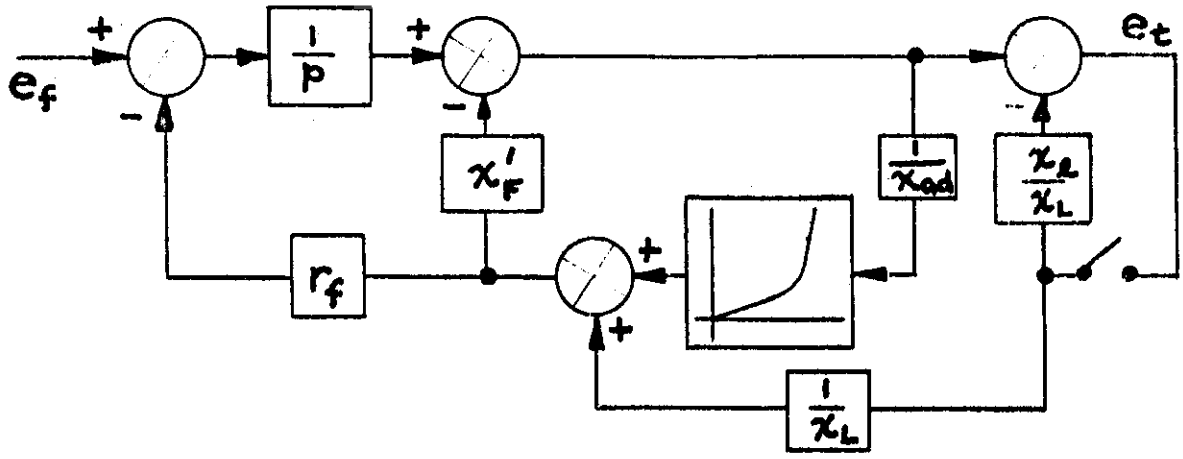

Figure A-5-a Block Diagram of a-c Generator Including Saturation

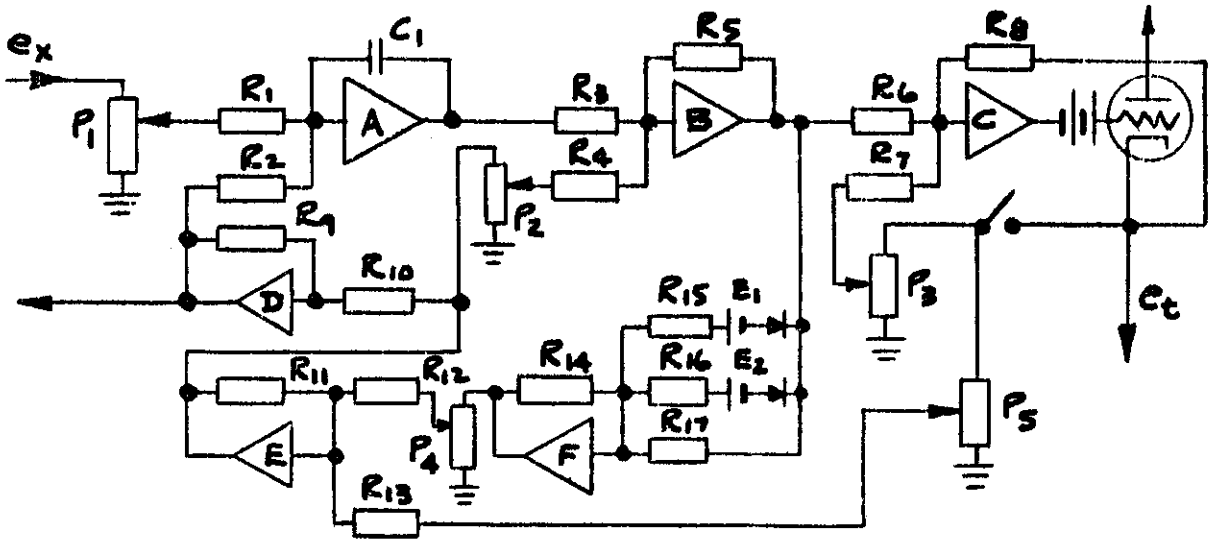

Figure A-5-b Analogue Computer Circuit for a-c Generator Including Saturation

(6) Load reactance, X_L

$$X_L = \left(\frac{R_6 R_{14} R_{13}}{R_8 R_{17} R_{12}} \right) \frac{1}{P_5}$$

(7) Synchronous reactance (unsaturated), X_d

$$X_d = X_\ell + X_{ad}$$

$$X_d = \frac{R_6 R_{14} R_{13}}{R_7 R_{17} R_{12}} \frac{P_3}{P_5} + \frac{1}{P_4}$$

(8) Effective field leakage reactance (saturated), X_F'

$$X_F' = \frac{1}{2} P_2$$

(9) Direct-axis transient reactance (unsaturated), X'_d

$$X'_d = X_\ell + \frac{1}{\frac{1}{X_{ad}} + \frac{1}{X_{F'}}}$$

$$X'_d = \frac{R_6 R_{14} R_{13}}{R_7 R_{17} R_{12}} \left(\frac{P_3}{P_5} \right) + \frac{1}{P_4 + 2 \frac{1}{P_2}}$$

A further consideration is that of saturation. This is taken into account by means of biased-diode elements associated with the input of amplifier F in Figure A-5-b. First, it is customary to set the ratio of R_{14} to R_{17} equal to unity. This then corresponds to the air-gap line of the a-c generator saturation curve. Then R_{15} and R_{16} with bias voltage sources E_1 and E_2 constitute inputs which are "switched in" at the proper voltage appearing at the output of amplifier B. This effectively increases the gain of amplifier of F as each new input is added. More inputs can be used than those shown in Figure A-5-b, depending upon the severity of the saturation curve. Refer to the end of the appendix for the actual settings used in the study of the 60-kva and 40-kva systems. Again there is a great deal of material in the literature on nonlinear representation in analogue computers.

It should be apparent that there must always be a certain degree of experimentation with the analogue before a satisfactory compromise can

be achieved commensurate with available data on test machines and actual calculations. As with any other tool, the analogue computer will only do what the operator commands of it. If certain parameters vary in a complicated fashion but they are set as constants instead of variable, one cannot expect the solution to be a mirror-image of the true phenomena.

As techniques for multiplication at higher speeds and presentation of nonlinearities improve so will the results of studies made on physical systems. But there will always be the problem of judgement and discretion on the part of those using the analogue computer.

A-3 STUDY OF SINGLE-PHASE ISOLATED ELECTRIC POWER SYSTEM (CARBON-PILE REGULATOR)

The system used for this part of the report was a single-phase, 20-kva a-c generator-regulator, operating isolated. The load used was 1.0 per unit, zero power-factor lagging, the condition requiring the greatest excitation for a given speed. Since the actual system operates at a relatively high speed 90% of its operating time (i.e., 8000 rpm), linearity was assumed for both the exciter and a-c generator magnetic circuits. This assumption holds very closely with actual conditions. Figure A-6 shows a block diagram of the generator-regulator system.

It might be well to point out that a rather ideal a-c generator has been assumed for this study in that it is linear and also has no armature leakage drop, but in spite of the simplicity of the system, there is very good correlation with the data obtained from actual machines. Figure A-7 shows the relationship used between the a-c generator voltage and the field current at no load and under a zero power factor load.

The exciter is also idealized to some extent, but as can be seen in the block diagram, Figure A-6, the following factors have been included:

A. Shunt field excitation (many analyses of generator-regulator systems neglect this factor and choose a separate excitation analysis because of the advantage of simplicity and avoidance of "parametric forcing.")
B. Eddy-current effect.
C. Voltage drop in the armature circuit.
D. Cumulative (or differential) compounding due to interpolar windings, compensating or series windings.
E. Residual voltage.
F. Effective over-all gain (See figure A-8).

Figure A-8 shows the static relationship between exciter-output voltage and the net excitation. Note the manner in which the residual voltage is changed when the gain is changed.

The voltage regulator and feedback stabilizing network were used in their real form, operating in their normal manner.

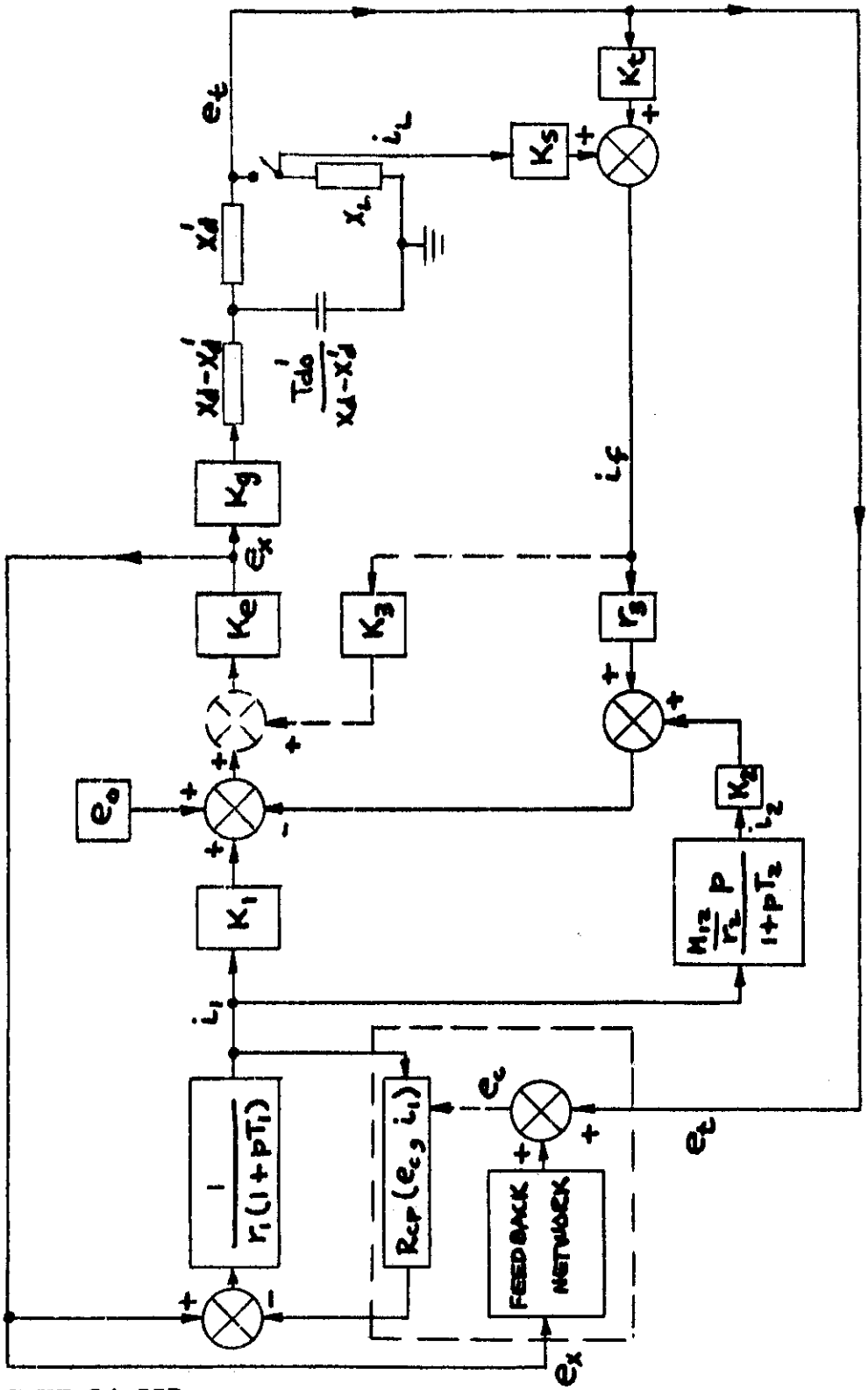

Figure A-6. Block Diagram of 20- Kva Generator - Regulator System

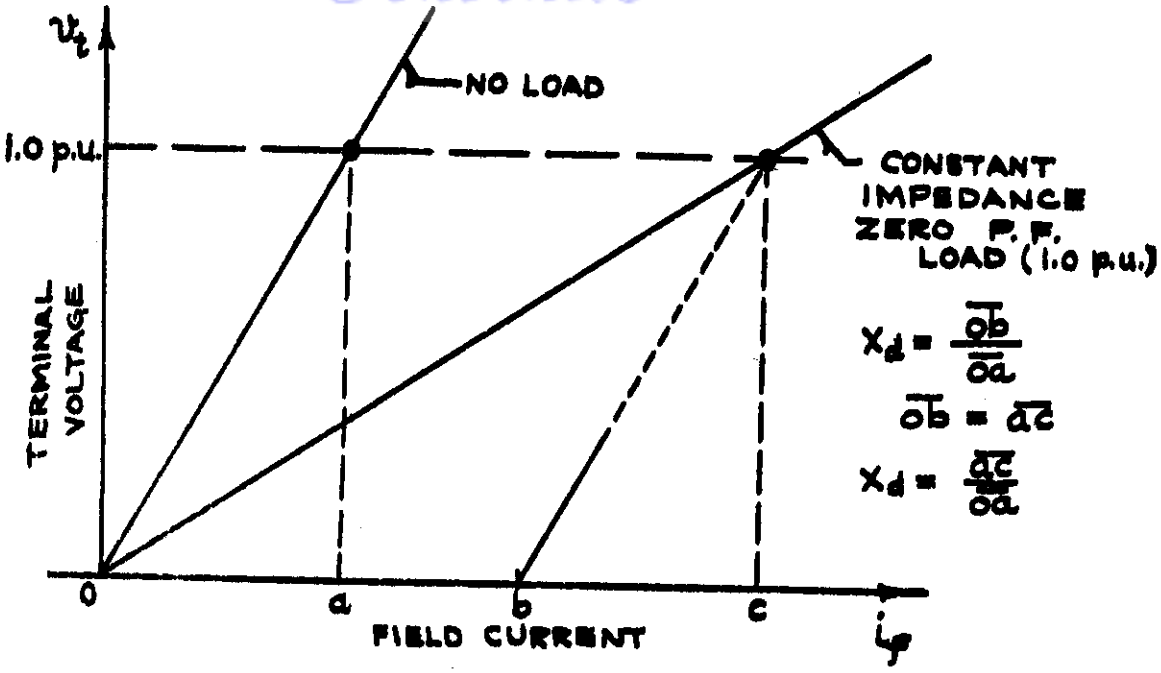

Figure A-7.

Relationship Between A-C Generator Voltage and the Field Current at No Load and Under a Zero Power Factor Load

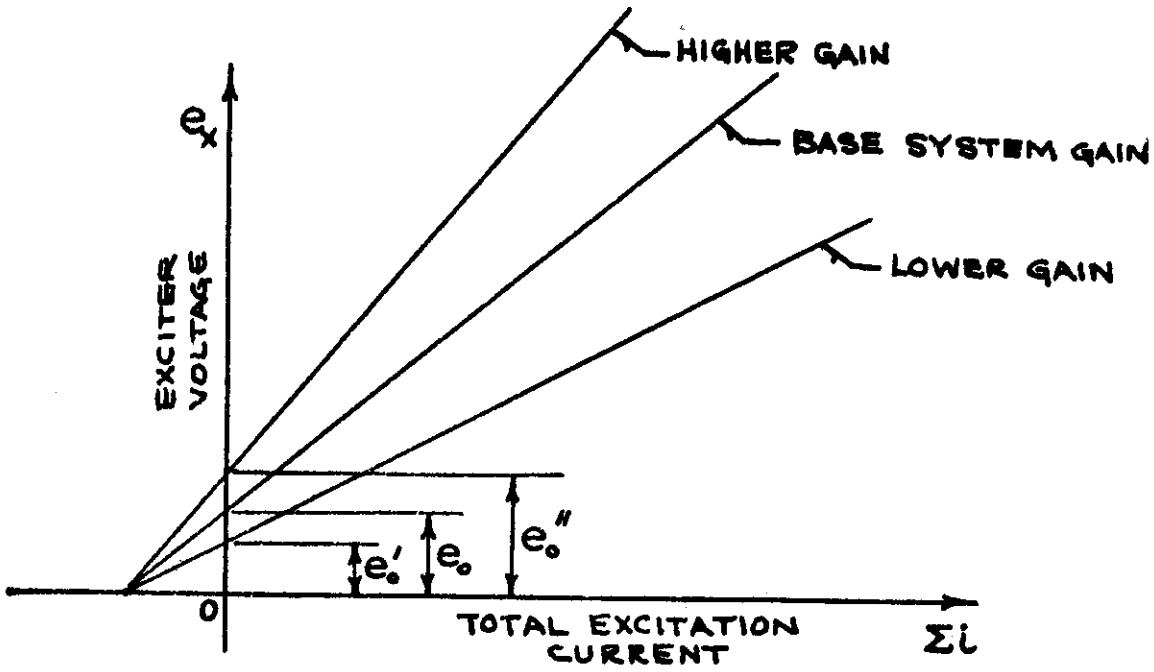

Figure A-8.

Relationship Between Exciter Output Voltage and Summation of Exciter Field Currents

A-3-a General Discussion

(1) Purpose and Scope - The purpose of such a transient study as this is to determine the general relationship between the transient behavior of the system (i.e., time of recovery T_R) and various major parameters in the system. For this study, the following parameters were chosen as the independent variables:

(a) Synchronous Reactance, X_d
(b) Transient Reactance, X'_d
(c) Open-Circuit Time Constant, T'_{do}
(d) Exciter Gain
(e) Exciter Time Constant, T_1
(f) Feedback Stabilizing Transformer

Selected investigations under limited conditions were made using the following variables:

(a) Residual voltage in the exciter, e_o
(b) A-C Generator Gain, K_g
(c) Series-compounding effect in the exciter, K_3
(d) Feedback stabilizing network

(2) Computer Set-up - Figure A-9 shows a diagram of the complete analogue which was used for this study.

Table A-1 gives the purpose of each amplifier in the analog. Table A-2 lists the various types of exciter and regulator combinations. By comparing Figure A-6 to Figure A-9, the analog between all important variables and independent parameters can be easily seen. Note that the voltage regulator is operated by three separate cathode followers: one for the regulating coil current, another for the carbon-pile circuit, and a third to drive the feedback stabilizing transformer.

A-3-b Conclusions

(1) Effect of Changing T'_{do} Recovery Time - The system recovery time T_R has no established pattern or variation with respect to the main generator time constant T'_{do} such as has been reported in previous investigations. It depends on the relationship between other parameters in the system, the most important of which are:

(a) Feedback stabilizing network characteristics

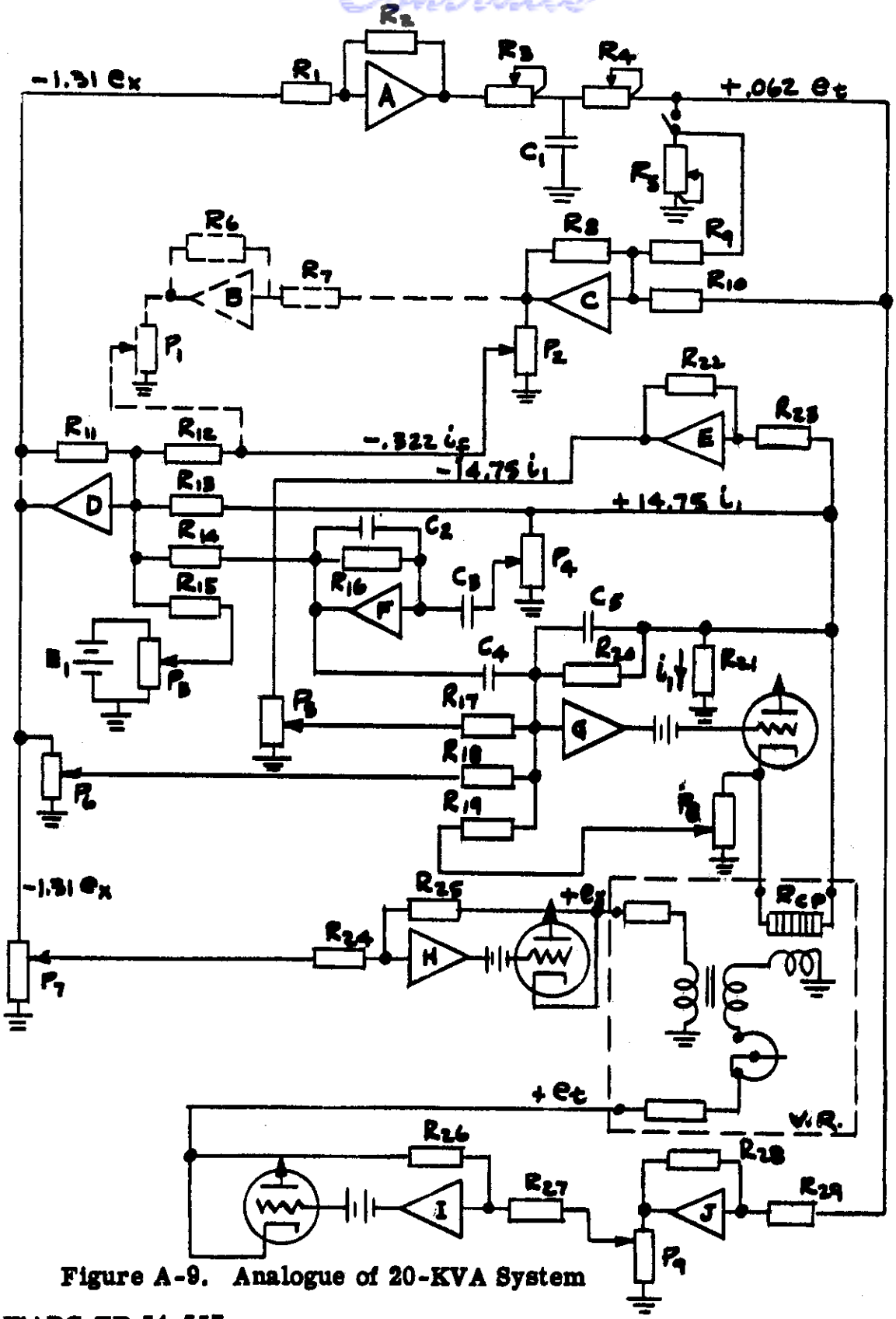

Figure A-9. Analogue of 20-KVA System

Table A-1

Purpose of Each Amplifier in 20-Kva System Analogue

Amplifier	Purpose
A	Sign inversion.
B	Sign inversion.
C	Change main-generator terminal voltage to main-generator field current.
D	Summation of various inputs to exciter fields plus residual voltage input.
E	Sign inversion.
F	Eddy-current generator.
G	Shunt-field-current generator.
H	Sign inversion.
I	Amplification and sign inversion.
J	Amplification and sign inversion.

Table A-2

Exciters Used in the 20-Kva System Study

Exciter	Gain, p.u.	T_1, Sec.	Residual Volts
A	1.00	.0215	3.00
*A'	1.00	.0215	3.00
B	0.75	.0215	2.23
C	1.25	.0215	3.78
D	1.00	.0356	3.00
E	1.00	.0100	3.00

Regulators Used in the 20-Kva System Study

Regulator	(approx) t_1, Sec.	Description
A	.013	Weaker feedback
B	.013	Stronger feedback

The following values were used in exciter A' instead of the values shown in Table A-3:

$R_{12} = 9.90$ $P_1 = .923$

$R_{18} = 0.25$ $P_3 = .559$

$C_1 = .006$ $P_4 = .505$

$C_3 = .002$ $P_5 = .796$

$C_4 = .003$ $P_6 = .927$

$P_8 = .791$

Table A-3

Values of Analogue Computer Elements Used For the Base 20-Kva System

A. Resistors

The values are given in megohms, except for R_{21} which is in ohms. Reactances are in per-unit quantities.

R	Value	R	Value
1	1.000	16	1.000
2	1.000	17	0.164
3	$0.271(x_d-x'_d)$	18	0.100
4	$0.271\ x'_d$	19	0.163
5	$0.271\ x_L$	20	1.000
6	1.000	21	14.75 ohms
7	1.000	22	1.000
8	5.02	23	1.000
9	$5.605(x_L/x_d)$	24	1.000
10	5.605	25	1.000
11	1.000	26	5.50
12	1.95	27	1.000
13	0.76	28	9.60
14	1.000	29	2.99
15	9.60		

Table A-3 Continued

B. Potentiometers

Values are given in per-unit quantities.

P	Value
1	(only used for exciter A')
2	.458
3	.840
4	.803
5	.859
6	.400
7	.764
8	.853
9	.912

C. Condensers

The values are given in micro farads. Reactances are in per-unit quantities. Time constants are in seconds.

C	Value
1	$\left(\frac{T_{do'}}{.0136(x_d - x'_d)}\right)$
2	.015
3	.01
4	.01
5	T_1 (exciter field time constant)

D. Voltage Sources

E	Value
1	45 volts

Figure A-10 Effect of Exciter Time Constant on System Recovery Time

(20-KVA System)

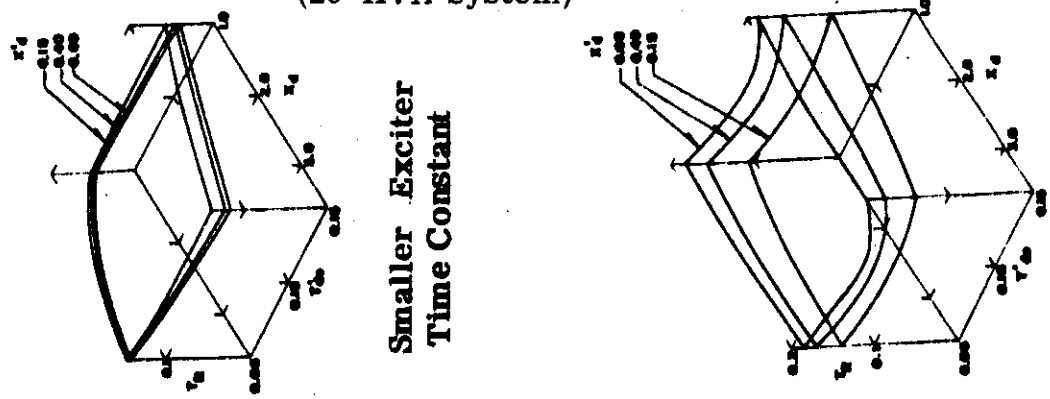

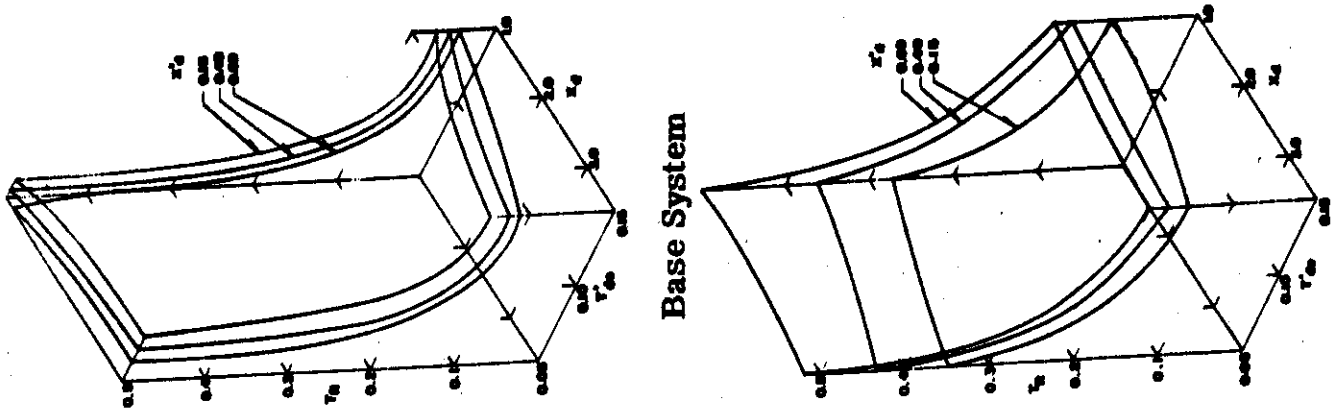

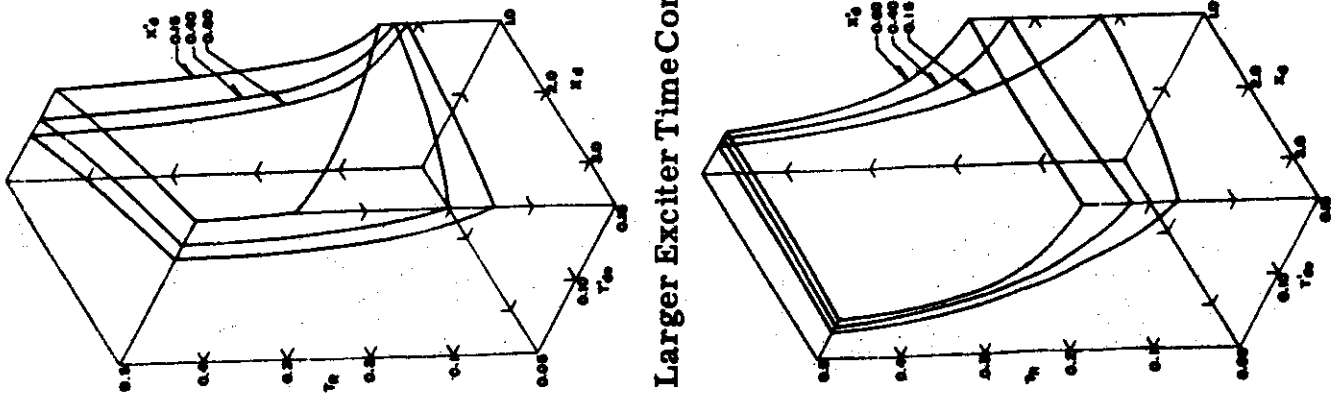

Figure A-11 Effect of Exciter Gain on System Recovery Time (20-KVA System)

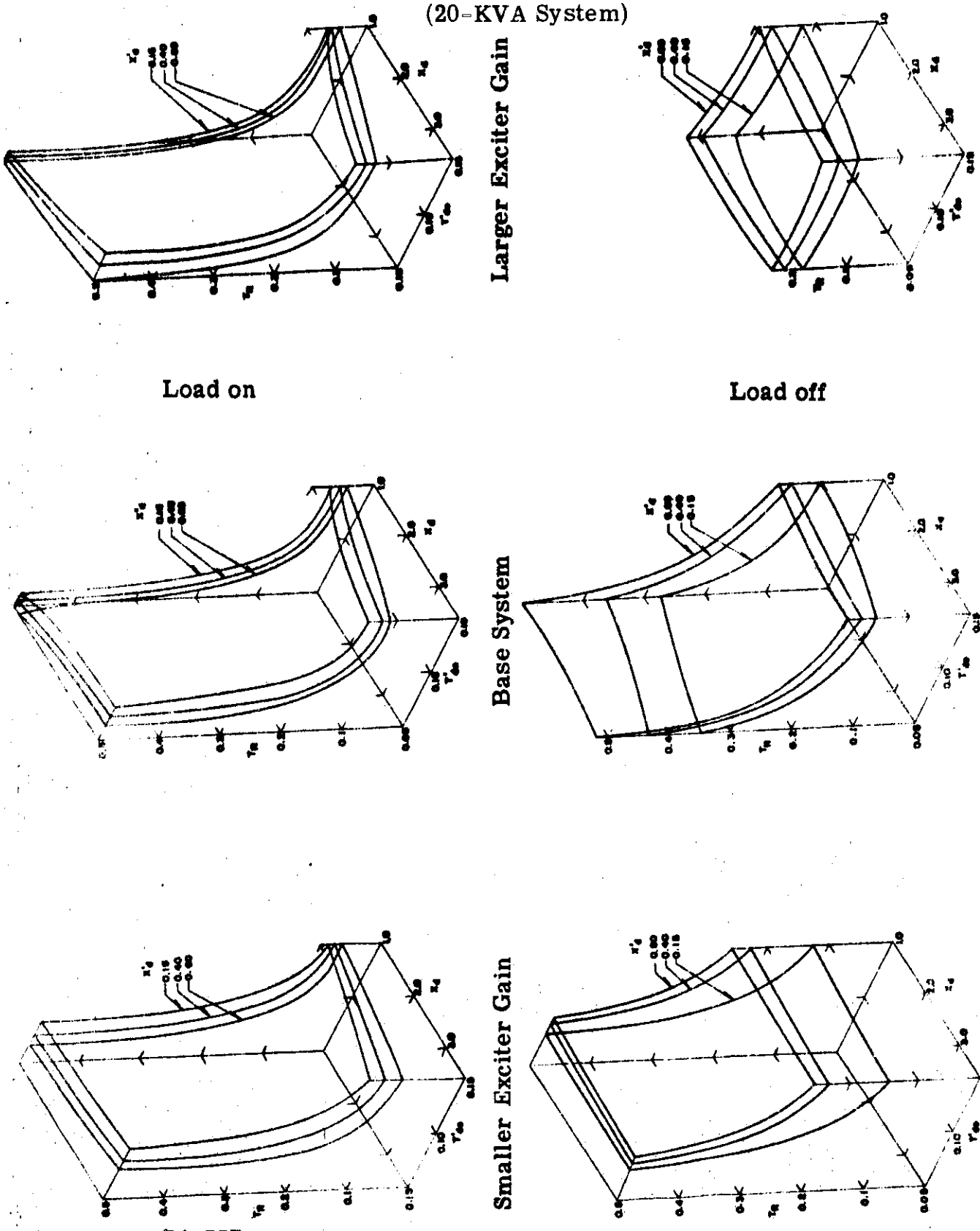

Figure A-12 Effect of Feedback Strength on System Recovery Time

(20-KVA System)

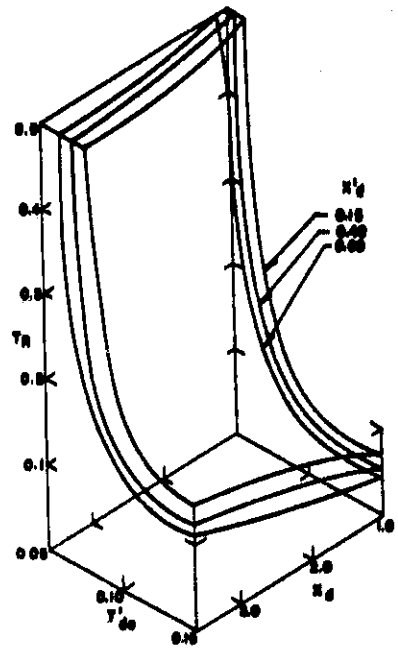

Load on

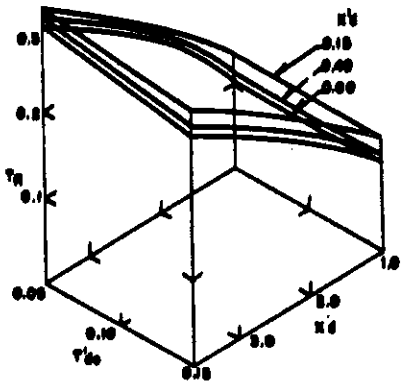

Weaker Feedback

Stronger Feedback

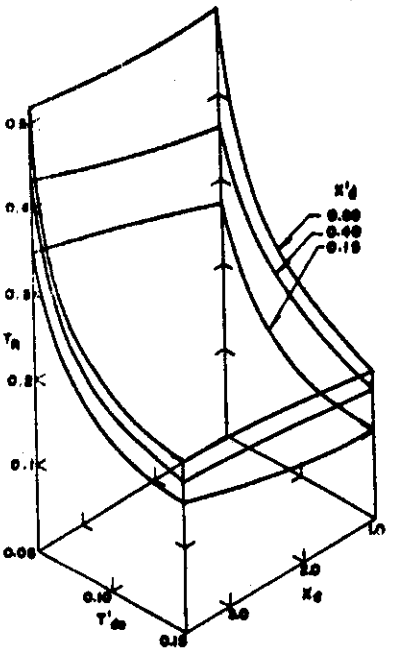

Load off

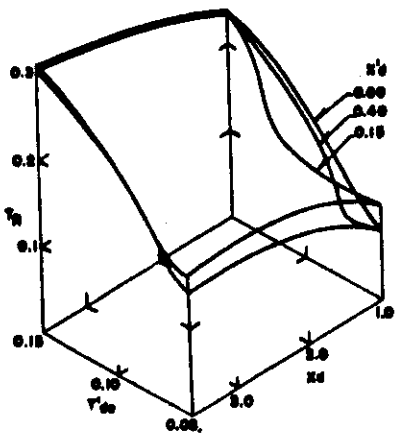

Figure A-13 Effect of Exciter Series Compounding on System Recovery Time

(20-KVA System)

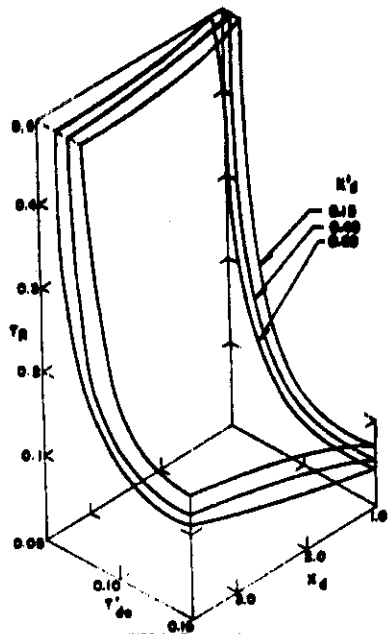

Without Cumulative Feedback

Load on

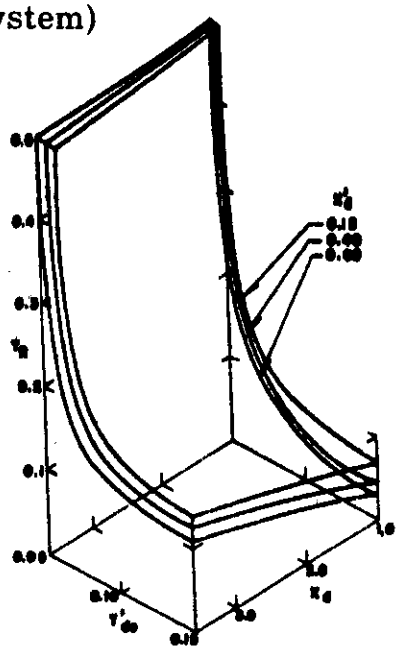

With Cumulative Feedback

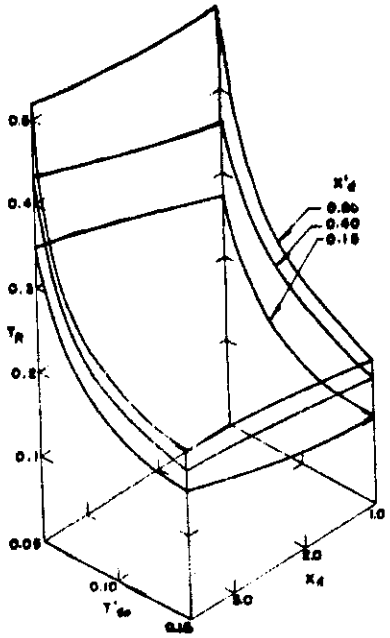

Load off

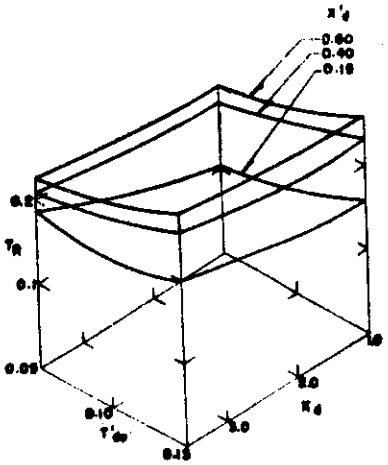

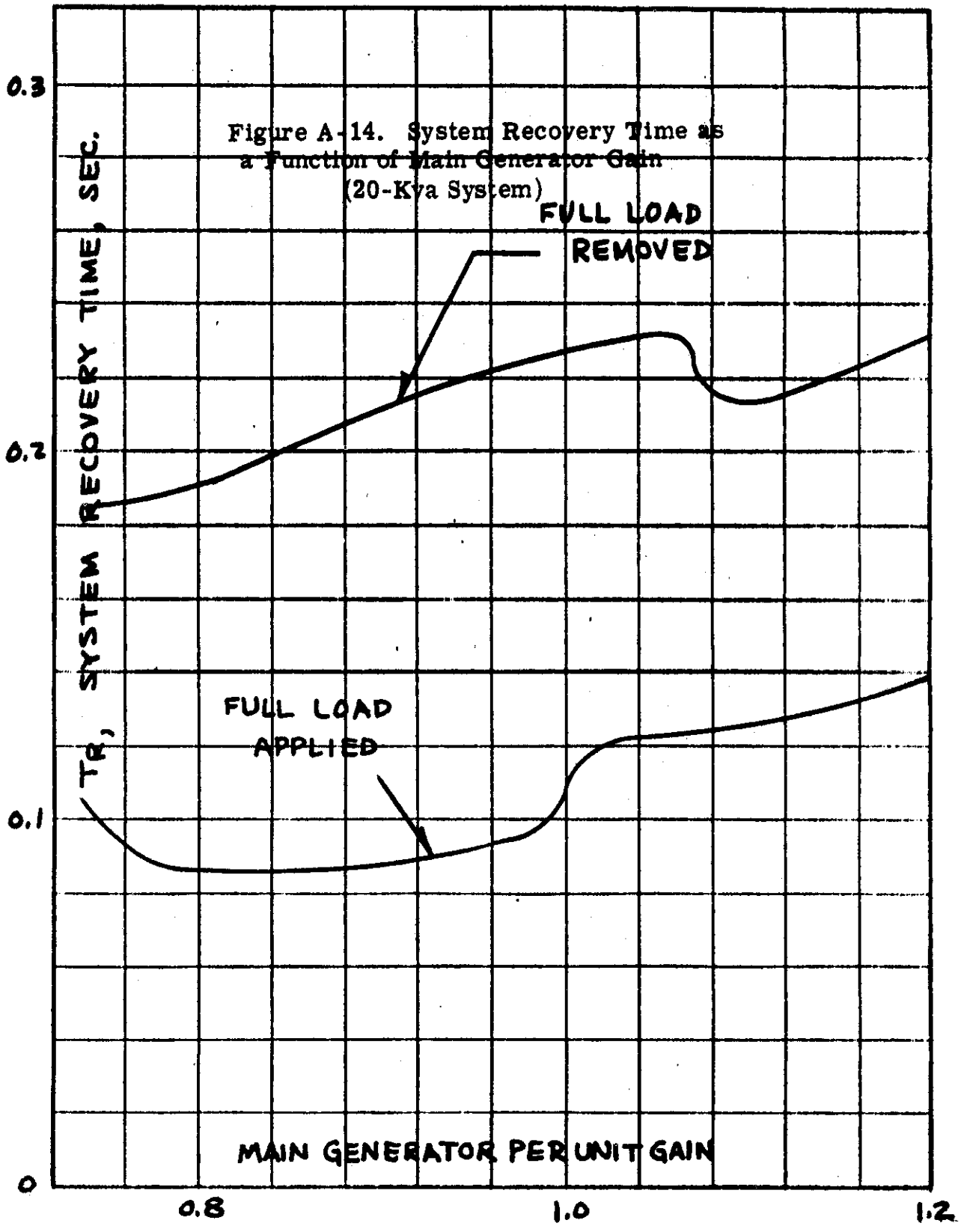

Figure A-14. System Recovery Time as a Function of Main Generator Gain (20-Kva System)

Figure A-15. System Recovery Time as a Function of Exciter Series Compounding (20-Kva System)

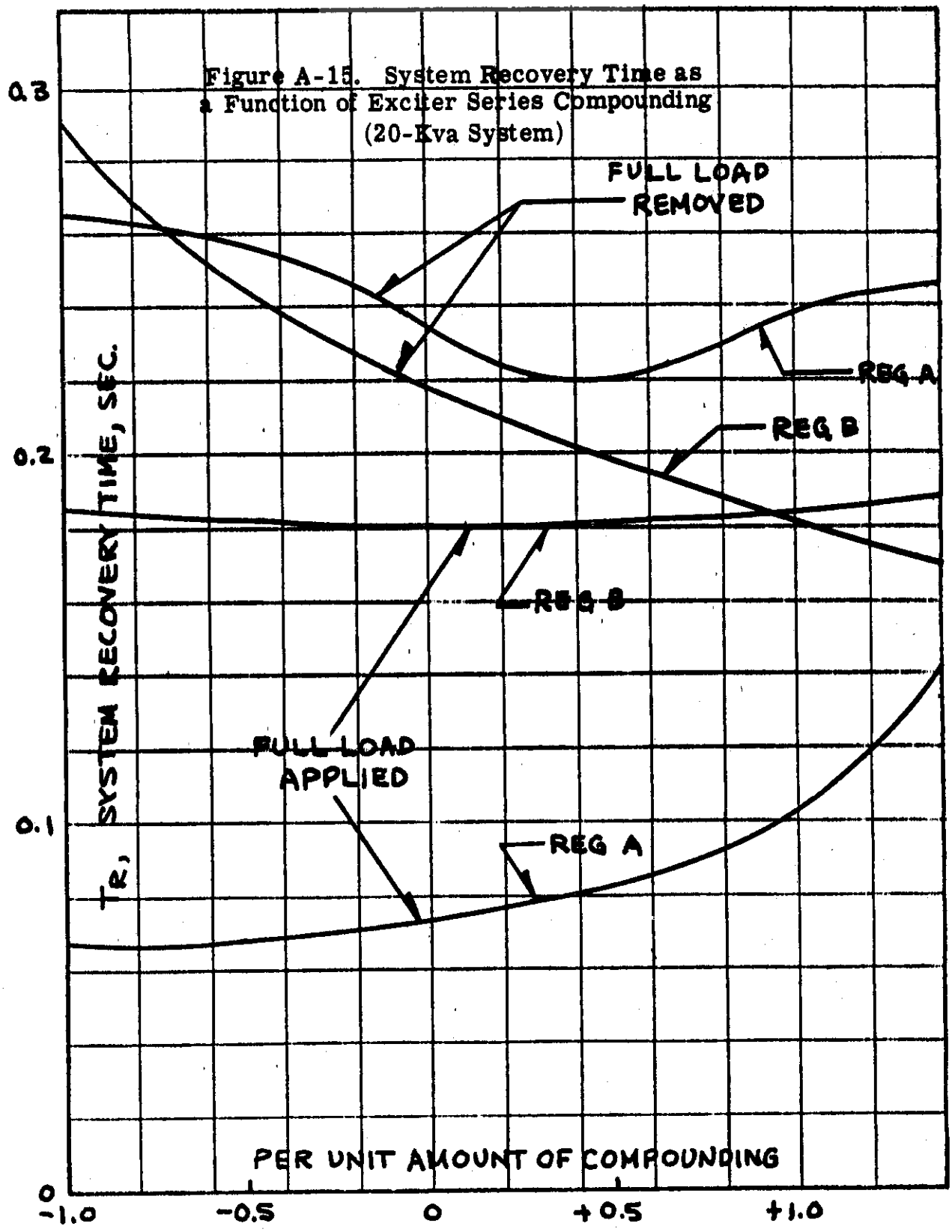

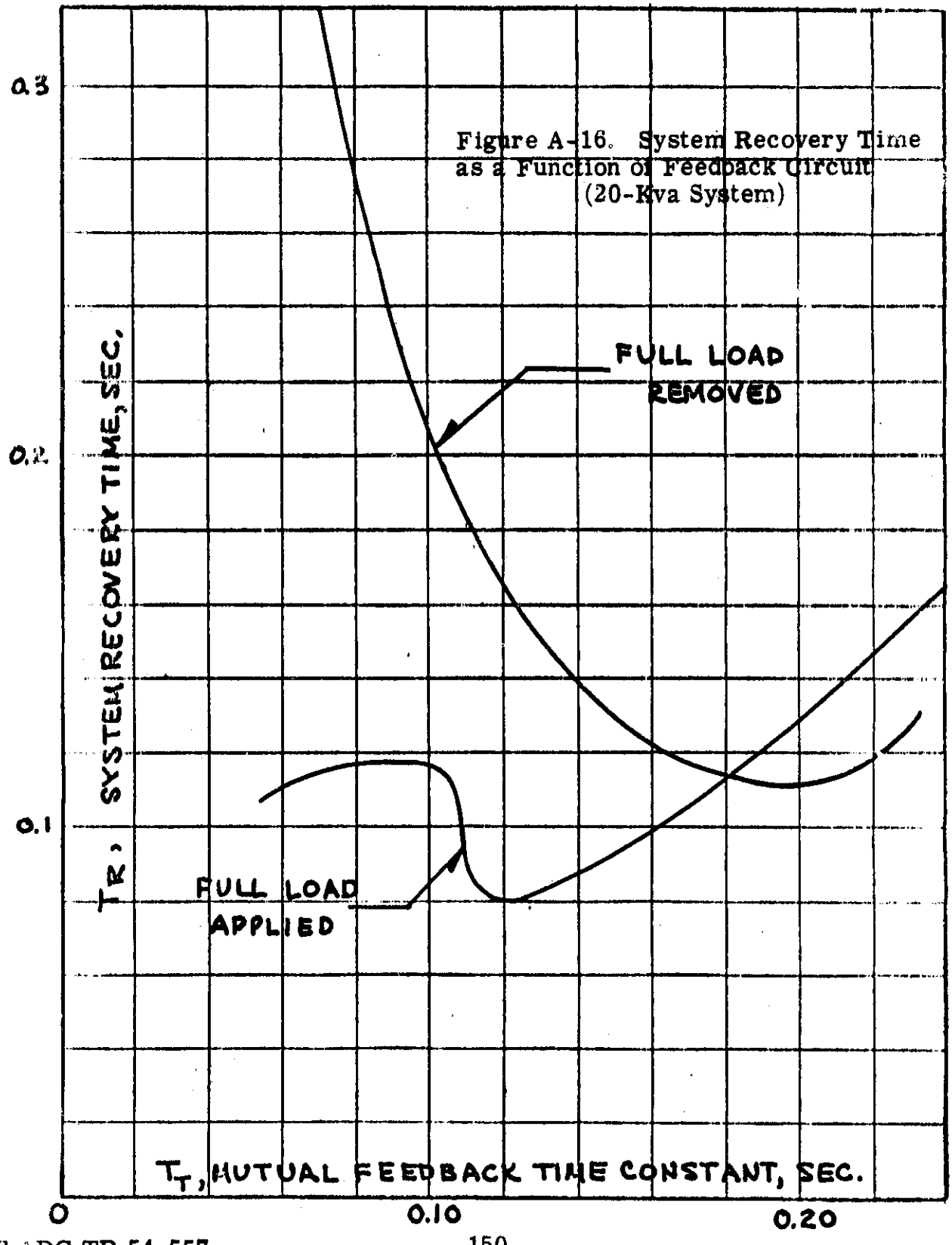

Figure A-16. System Recovery Time as a Function of Feedback Circuit (20-Kva System)

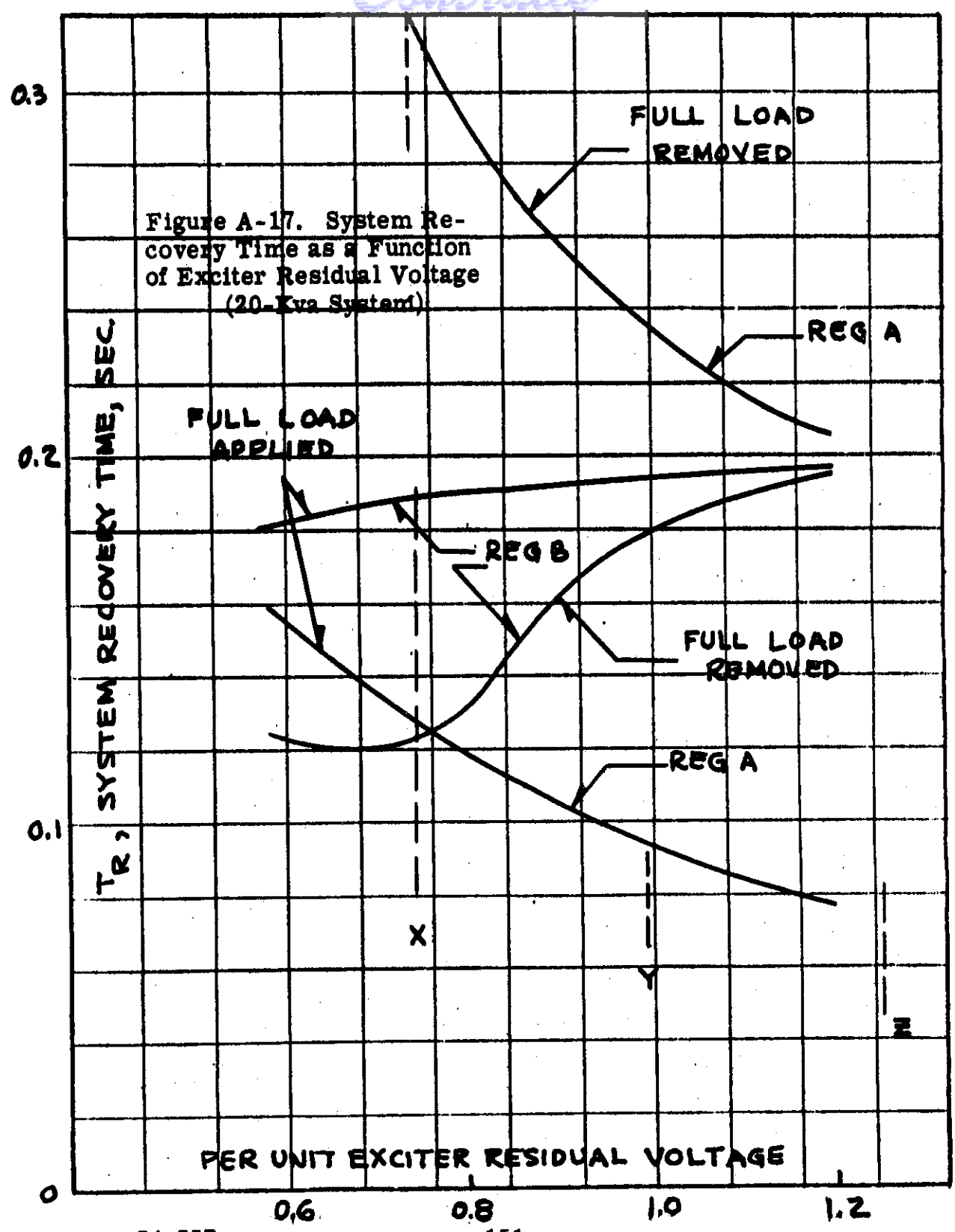

Figure A-17. System Recovery Time as a Function of Exciter Residual Voltage (20-Kva System)

(b) Exciter time constants
(c) Exciter gain and amount of residual voltage
(d) Other exciter characteristics such as exciter compounding

If we first look at Figure A-10 or A-11, we see that there is usually a definite improvement in the system recovery time T_R when the time constant T'_{do} is increased; at least it can be said that we obtain either a shorter recovery time or there is negligible effect. Figure A-6 would also confirm this observation, but unfortunately, if we are looking for hard and fast rules, when we look at Figure A-10 we see that a stronger feedback signal causes the opposite to be true, at least for the case of load-off. (Note: The lower right-hand block in Figure A-10 has an important difference over all other blocks in Figures A-10 through A-13; the direction of the axis for T'_{do} has been reversed to better show the variation in recovery time.) So we see that it makes a difference what the rest of the system is when we describe the effect of variations in T'_{do}.

Also, we can see that there is a different degree of effectiveness in changing T'_{do} depending on other factors besides feedback signal strength. It is felt that further work in this field, augmented by the analogue-computer tools, may eventually show the true cause for some of these phenomena.

(2) Effect of Changing Machine Reactances on Recovery Time

(a) Synchronous Reactance, X_d - In general, we can say that Figures A-10 through A-13 show little change in the recovery time as the synchronous reactance X_d is varied over very wide limits. If any statement be made, one could say that there is a slight improvement at the lower values of X_d, and, also, this improvement is more apparent in the case of load-on than in the case of load-off. In addition, it seems to effect the system more when strong feedback is present, as evidenced by Figure A-12.
(b) Transient Reactance, X'_d - The spread of X'_d from 0.15 per unit to 0.60 per unit covers a wide range of machines, yet there is little significance in its effect on the recovery time. The change which does result from this parameter is different in the case of load-on compared to the case of load-off. The system recovery time improves when load is removed if the transient reactance is smaller, whereas when load is applied, this parameter should be larger.

(3) Effect of Changing Exciter Parameters on Recovery Time

(a) Exciter Time Constant - As can be readily seen from Figure A-10, the greatest improvement on recovery time was made with a reduction in the exciter time constant; this applies to both load-on and load-off. One note of caution should be added, however. Figure A-10 applies to the system with a feedback signal which, for purposes of comparison, we term "weak". It is very significant that when "strong" feedback is used, as shown in Figure A-12 there is no difference when the exciter time constant is changed.

The right-hand side of Figure A-12 applied for all three cases of exciter time constant. See Table A-2 for the data on the various exciter combinations used in this study.

(b) Exciter Gain and Residual Voltage - Examination of Figure A-11 shows a definite improvement in recovery time when the exciter gain is increased, especially in regions of smaller values of T'_{do}. Also, there is more effect on the load-off case. Again, as pointed out above under "Exciter Time Constant", the system with "strong" feedback reacts the same regardless of the exciter gain.

Figure A-9 shows three different conditions of gain in the exciter, and it also shows how the residual voltage changes at the same time. This is important because Figure A-17 shows the variation of system recovery time as a function of the exciter residual voltage only. There is very good reason to believe that the variations in response which are shown for the three cases of gain in Figure A-11 are really due to the residual change instead. On Figure A-17 there is shown three lines, X, Y and Z; these correspond respectively to lower gain, base system gain and higher gain. Regulator A refers to the same regulator used for the studies in Figure A-11.

Later tests on other machines have somewhat confirmed this observation.

Referring again to Figure A-17, the effect of a different feedback signal can be seen in the comparison between regulator A and regulator B.

(c) Exciter Compounding - The curves in Figure A-13 show the effect of over-all recovery when cumulative compounding is added to the exciter. Actually, at the standard conditions, there was

little difference, but as T'_{do} is varied, the recovery is nearly independent of this variation when cumulative compounding is present. Figure A-15 also shows the results, at base conditions, of variations in compounding both positive and negative. In this case, the results are a bit harder to interpret. In the case of the weaker feedback, it seems that recovery time increases with an increase in cumulative compounding. Per unit compounding refers to the degree of positive compounding used in Figure A-13.

(4) Effect of Different Feedback Strength - Figure A-16 shows the results of an investigation of different types of feedback stabilizing transformers. The various designs used in this study have been resolved in terms of a mutual feedback time constant, T_t.

Figure A-12 has been discussed already under other categories, but a further comment should be made. The difference between the weak and the strong feedback shows that neither condition was optimum for the middle of the range (i.e., T'_{do} equal to 0.10 seconds). The long recovery time with weaker feedback is due to excessive oscillations, while the long recovery time with strong feedback is due to over-damping and sluggish response. The system is very stable, but it is too slow. This can be just as detrimental as the high oscillatory case. Note again that the direction for T'_{do} has been reversed for the load-off case with stronger feedback.

(5) Effect of Main Generator Gain - The effect of the main generator gain on the system recovery time is shown in Figure A-14. Little can be concluded from the study made, except to say that a slight improvement in recovery time results from lowering the gain. But even this statement is questionable, however, because the load-on case is apparently getting worse at gains around 0.75 per unit. Per unit gain is the gain used for the base system.

A-3-c Additional Data

Figures A-18 through A-31 are included to show in greater detail the data used for the composite figure discussed above. The captions on each figure are self-explanatory.

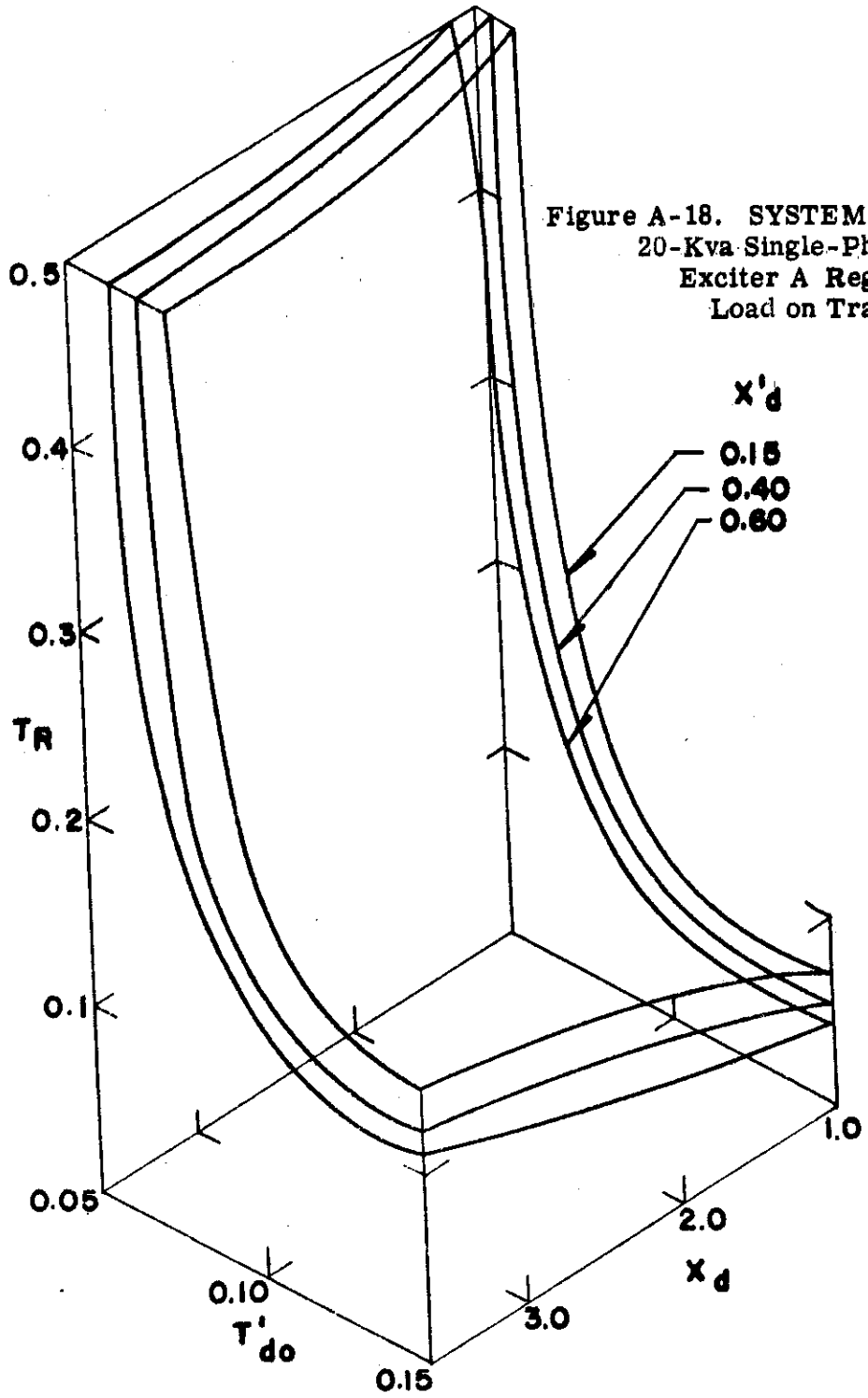

Figure A-18. SYSTEM RECOVERY TIME
20-Kva Single-Phase System
Exciter A Regulator A
Load on Transient

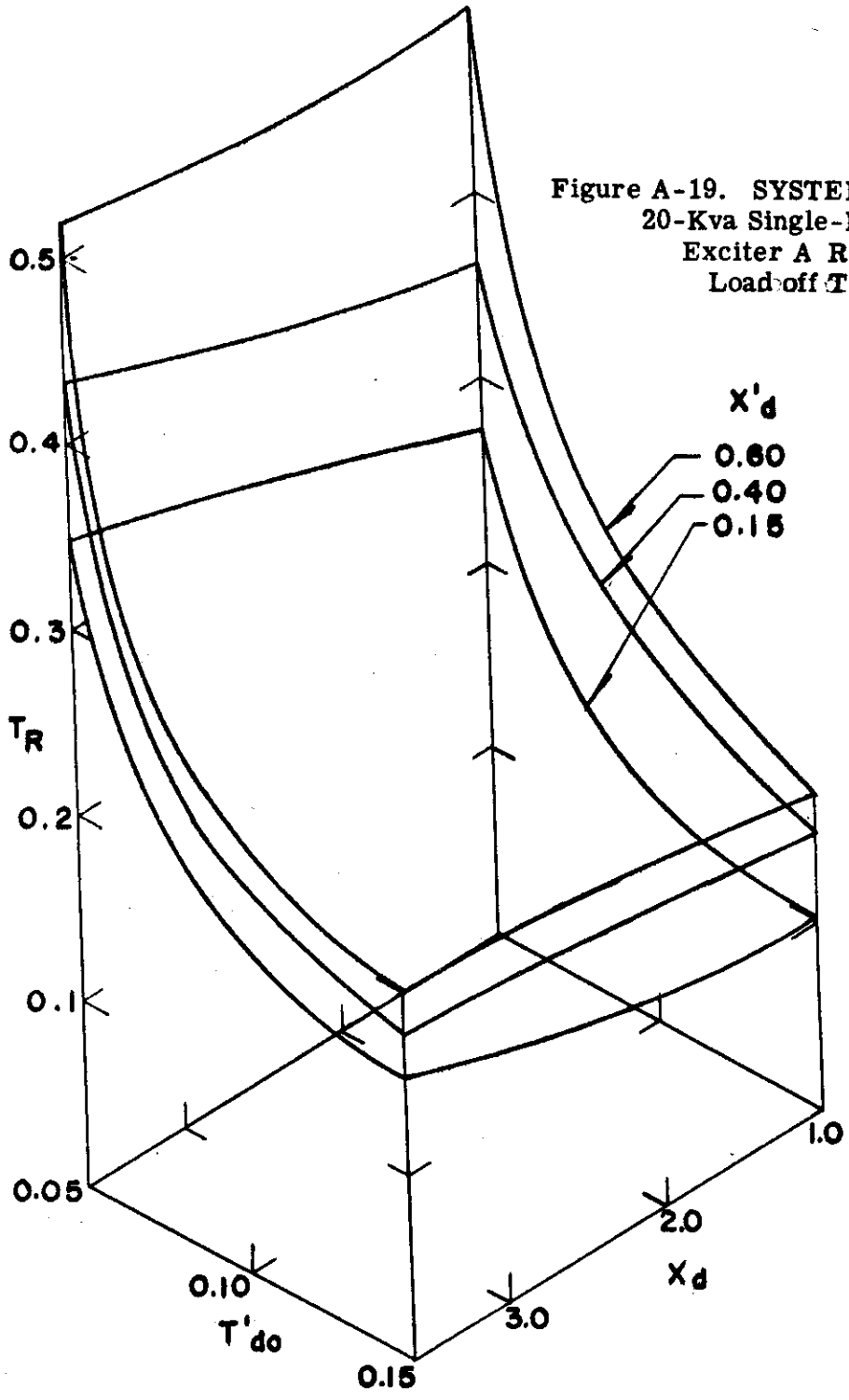

Figure A-19. SYSTEM RECOVERY TIME
20-Kva Single-Phase System
Exciter A Regulator A
Load-off Transient

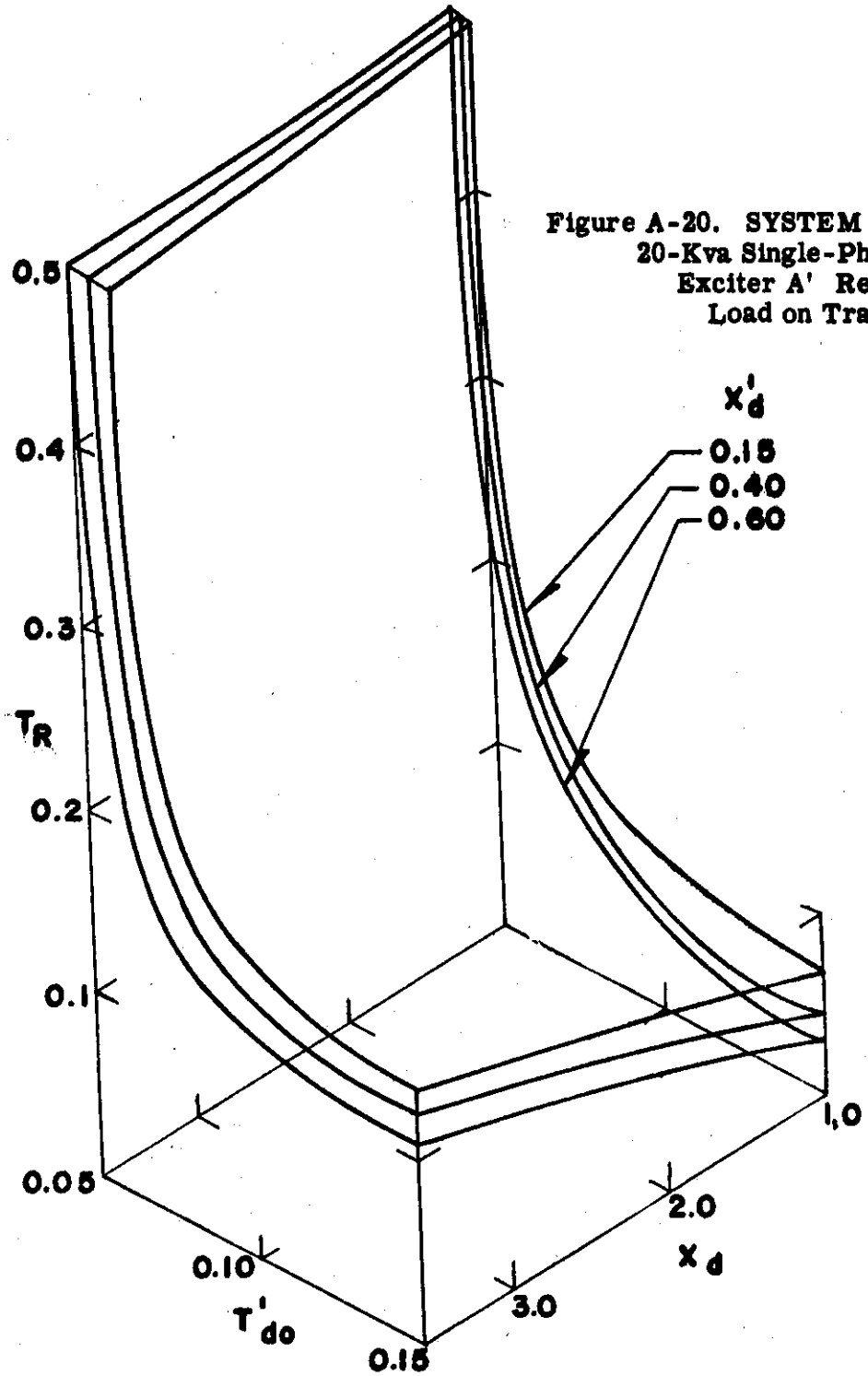

Figure A-20. SYSTEM RECOVERY TIME
20-Kva Single-Phase System
Exciter A' Regulator A
Load on Transient

Figure A-21. SYSTEM RECOVERY TIME
20-Kva Single-Phase System
Exciter A' Regulator A
Load off Transient

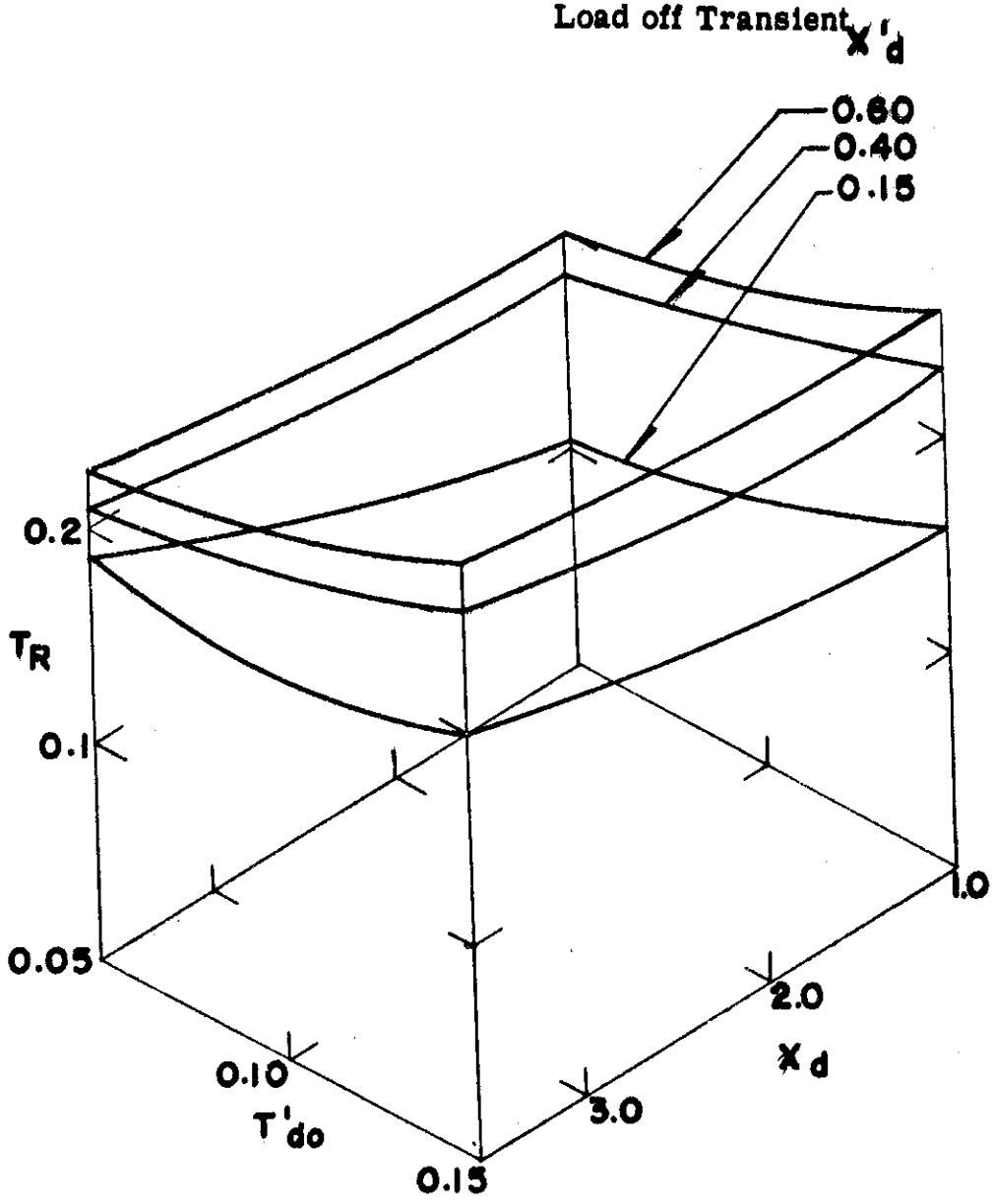

Figure A-22. SYSTEM RECOVERY TIME
20-Kva Single-Phase System
Exciter B Regulator A
Load on Transient

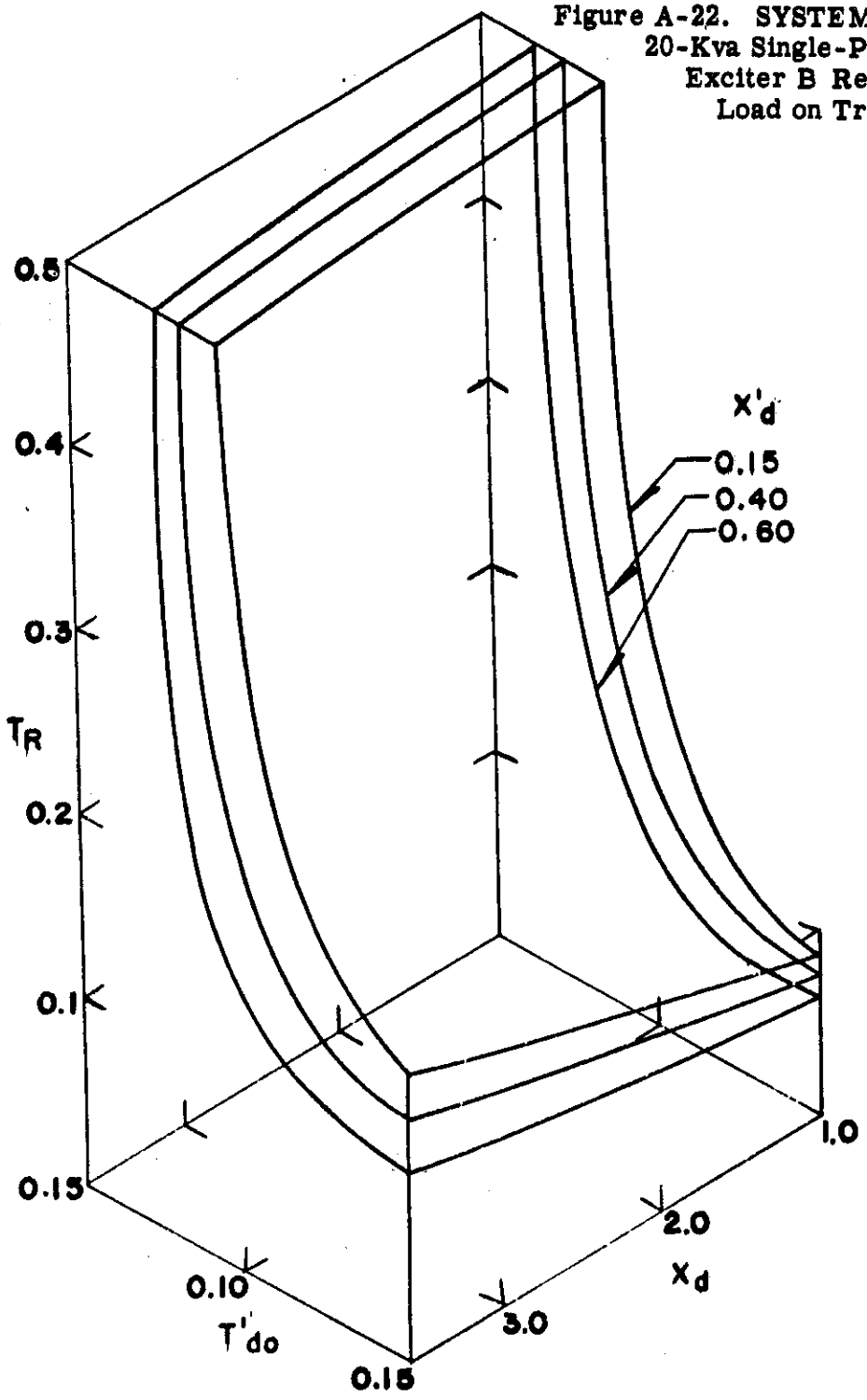

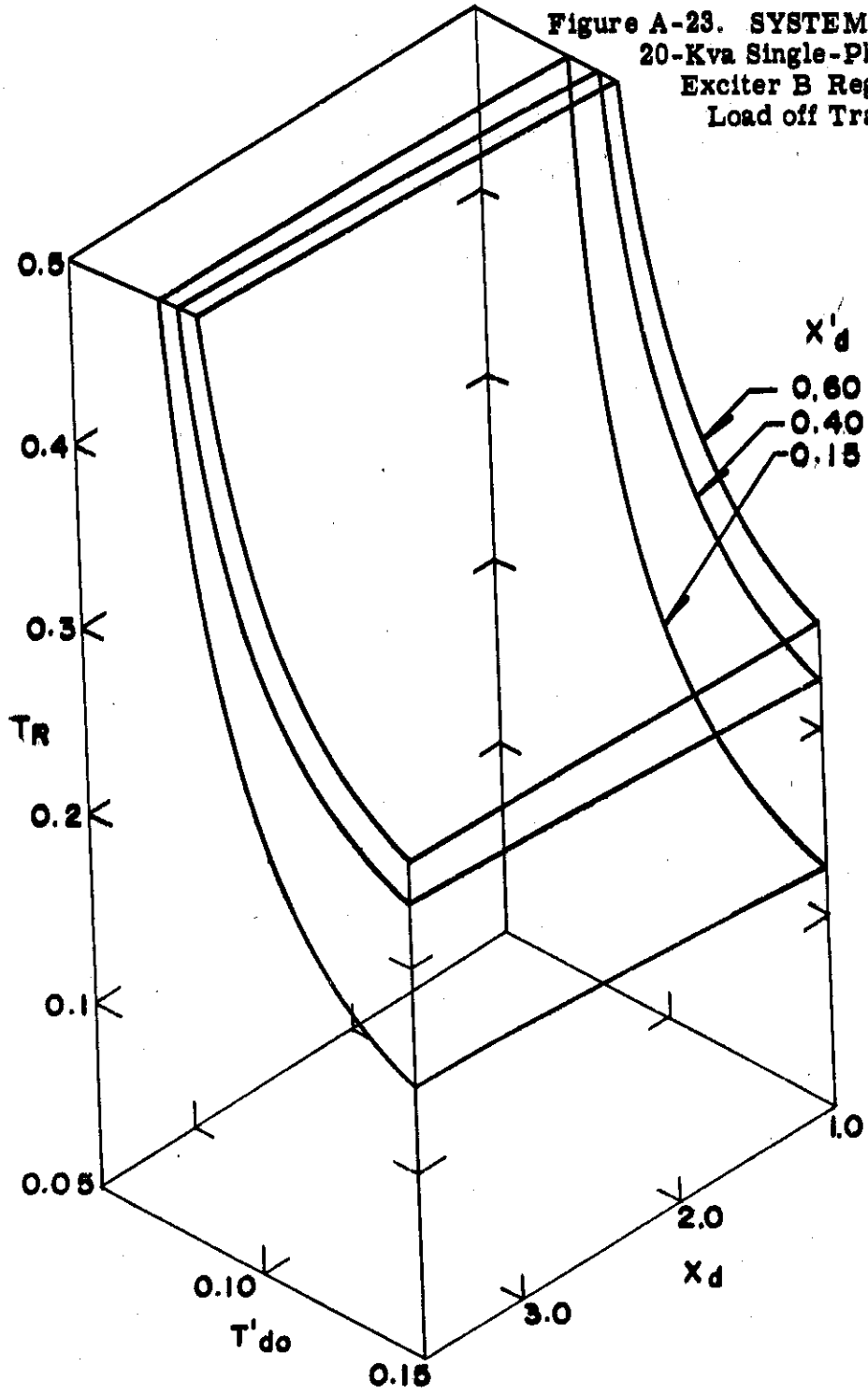

Figure A-23. SYSTEM RECOVERY TIME
20-Kva Single-Phase System
Exciter B Regulator A
Load off Transient

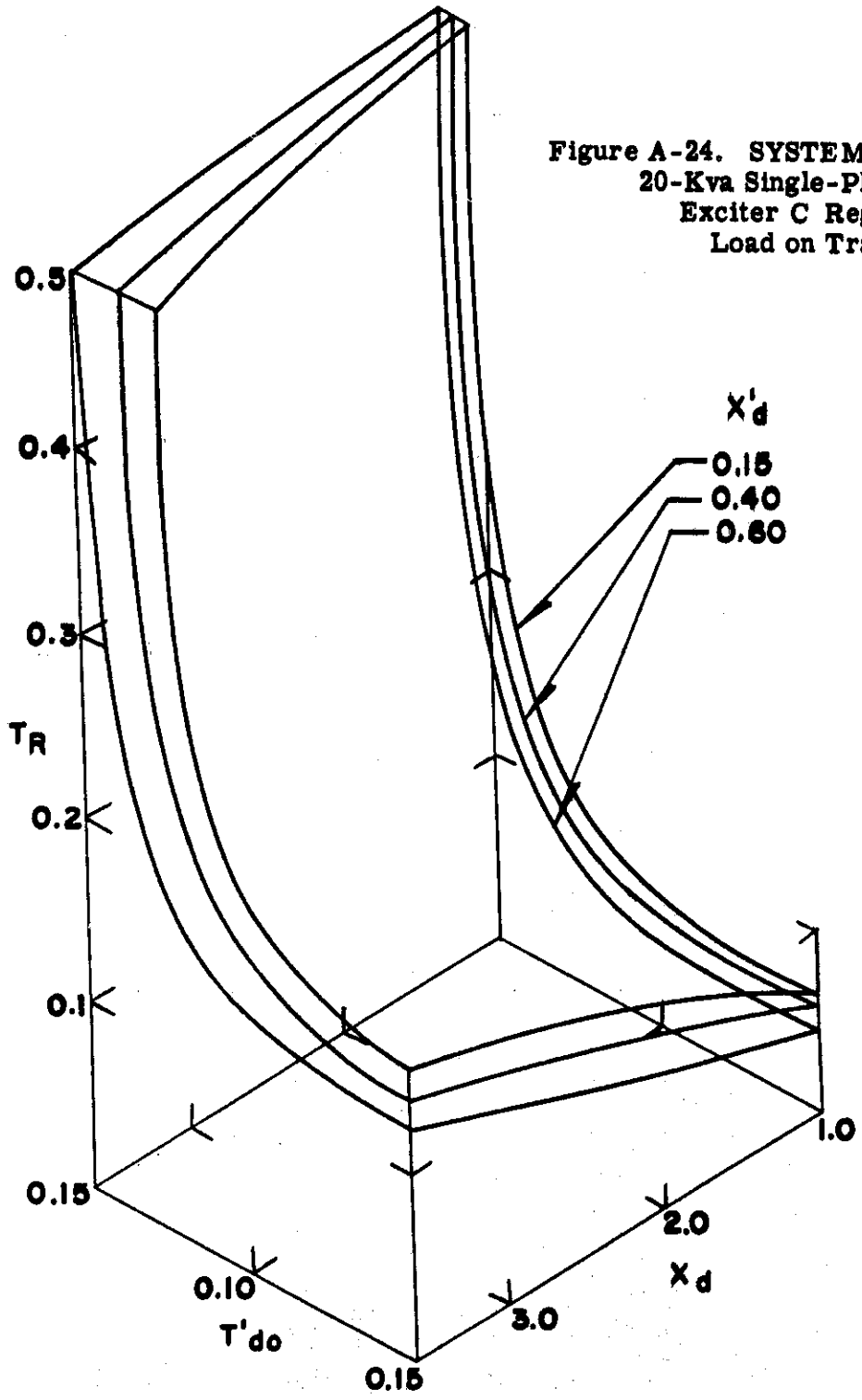

Figure A-24. SYSTEM RECOVERY TIME
20-Kva Single-Phase System
Exciter C Regulator A
Load on Transient

Figure A-25. SYSTEM RECOVERY TIME
20-Kva Single-Phase System
Exciter C Regulator A
Load off Transient

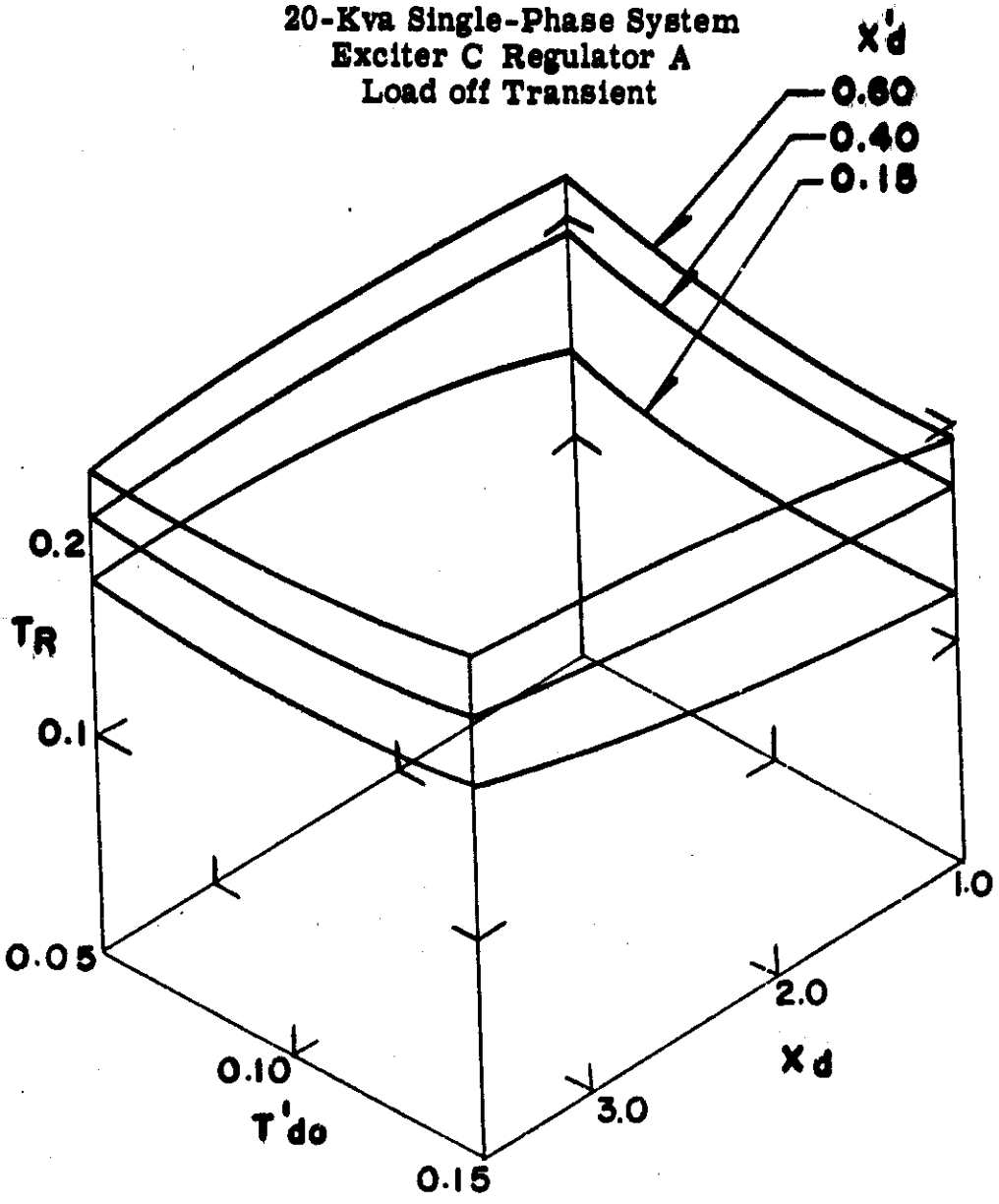

Figure A-26. SYSTEM RECOVERY TIME
20-Kva Single-Phase System
Exciter D Regulator A
Load on Transient

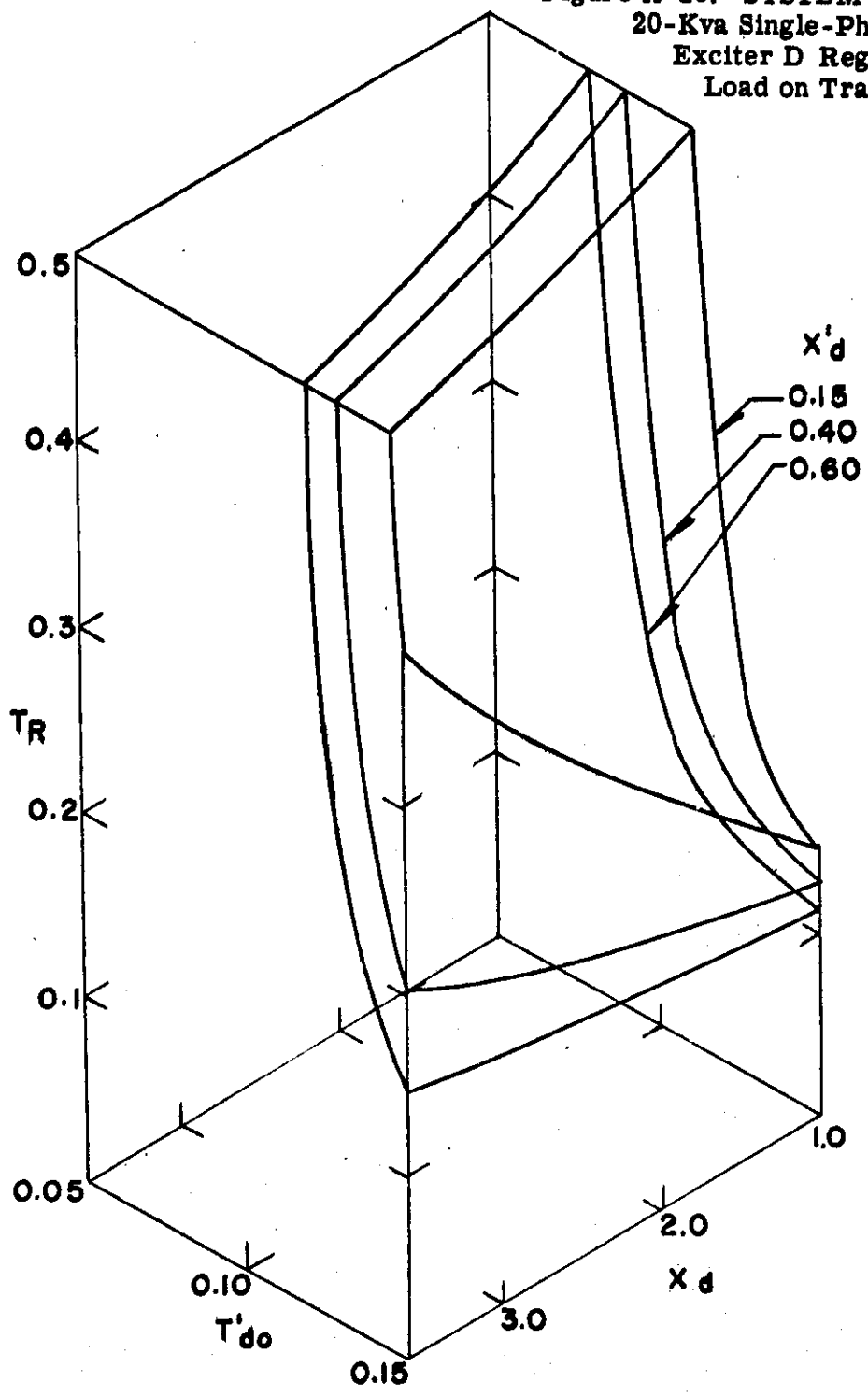

Figure A-27. SYSTEM RECOVERY TIME
20-Kva Single-Phase System
Exciter D Regulator A
Load off Transient

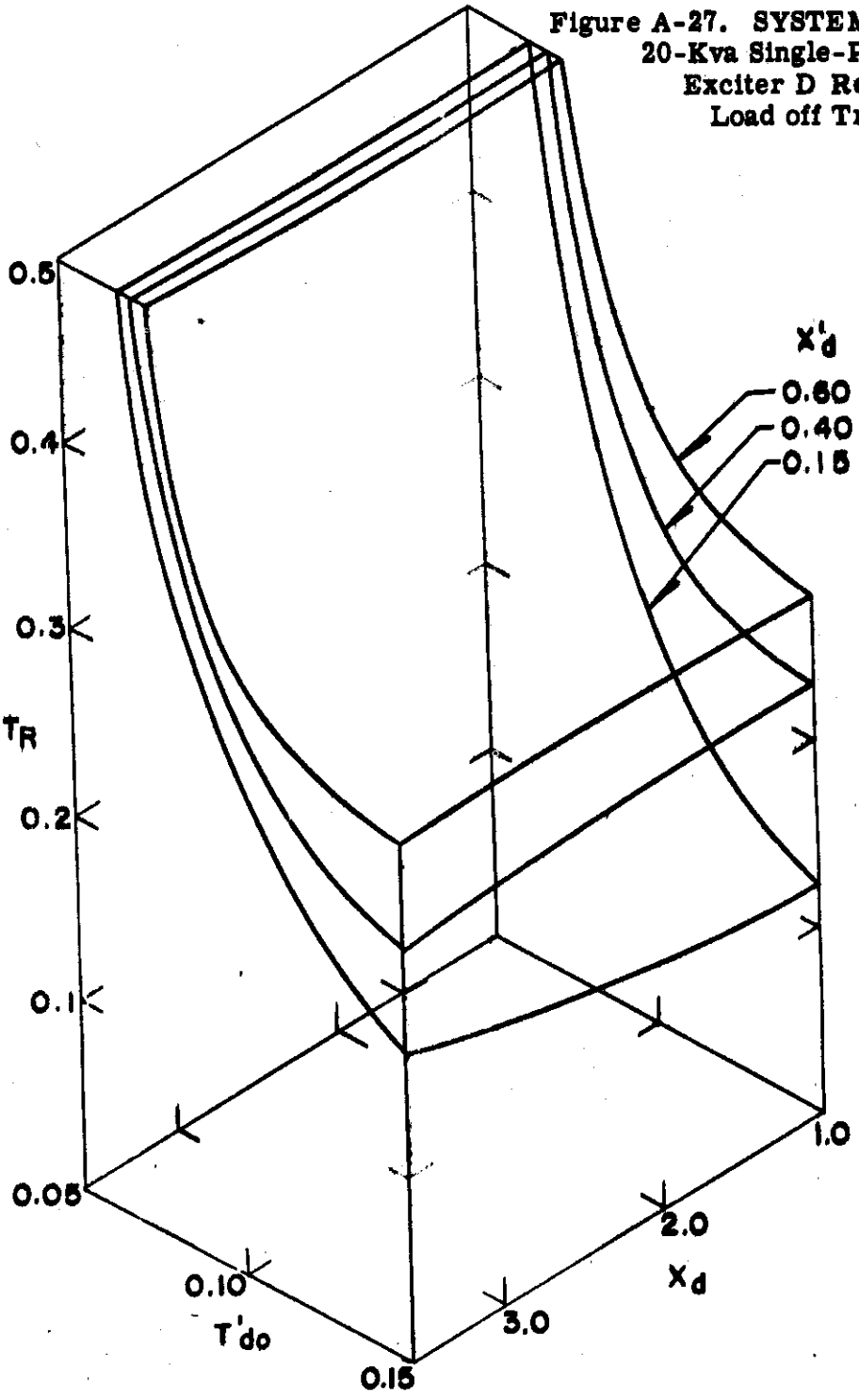

Figure A-28. SYSTEM RECOVERY TIME
20-Kva Single-Phase System
Exciter E Regulator A
Load on Transient X'_d

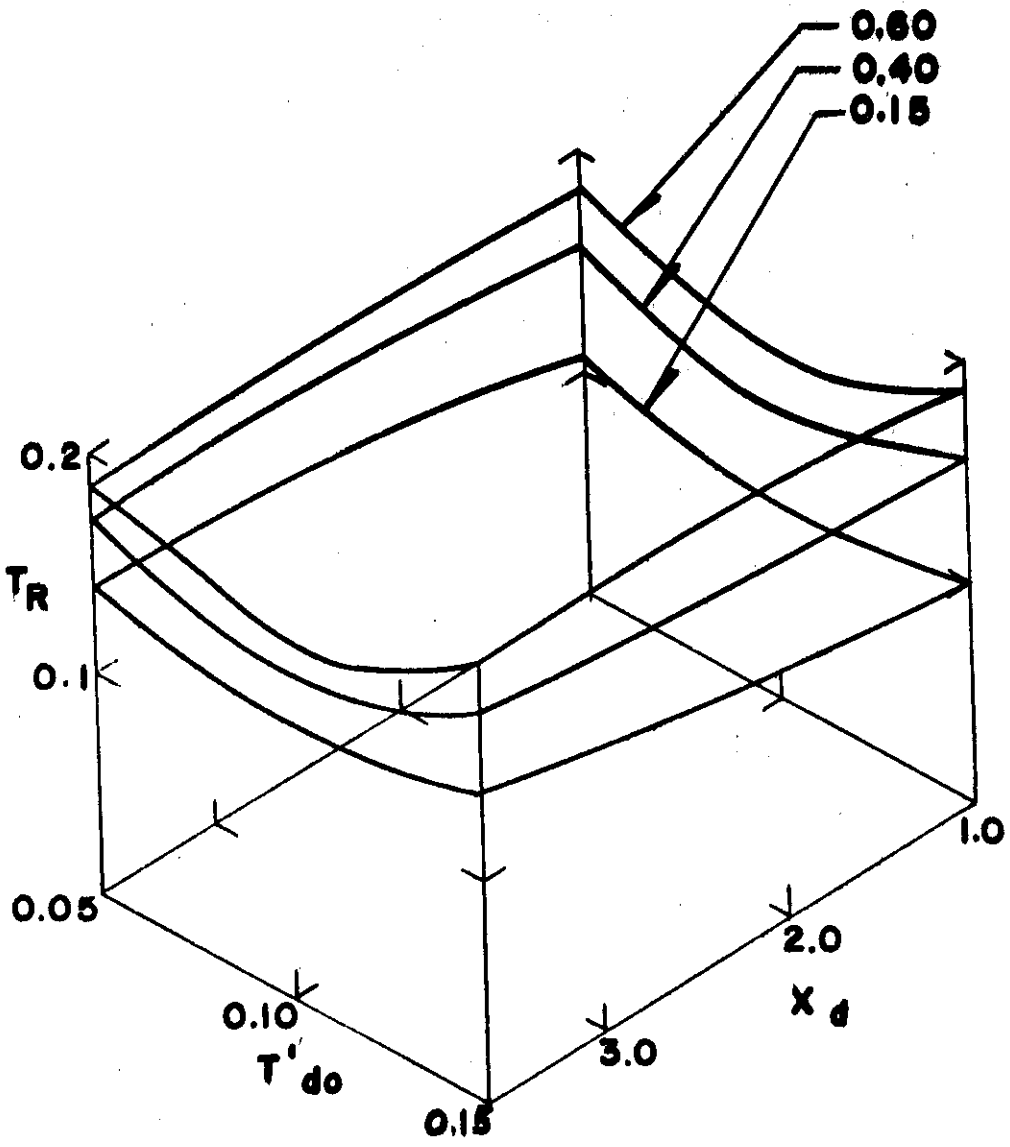

Figure A-29. SYSTEM RECOVERY TIME
20-Kva Single-Phase System
Exciter E Regulator A
Load off Transient

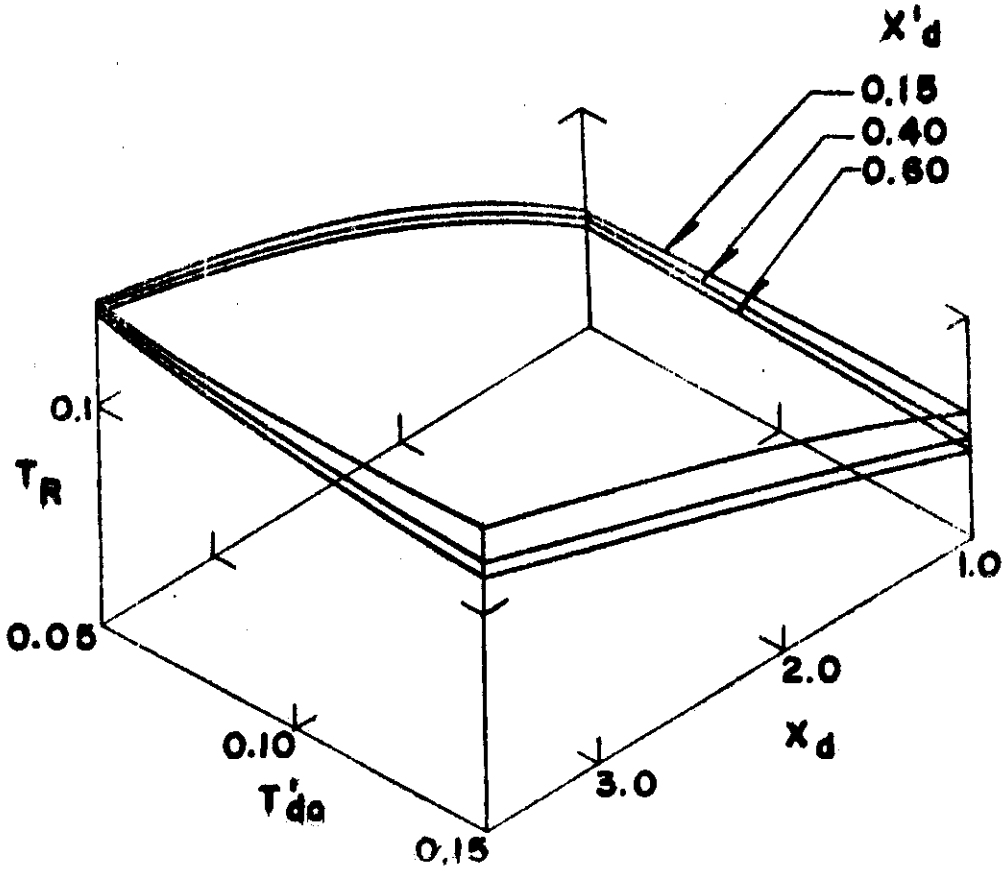

Figure A-30. SYSTEM RECOVERY TIME
20-Kva Single-Phase System
Regulator B
All Exciters
Load on Transient

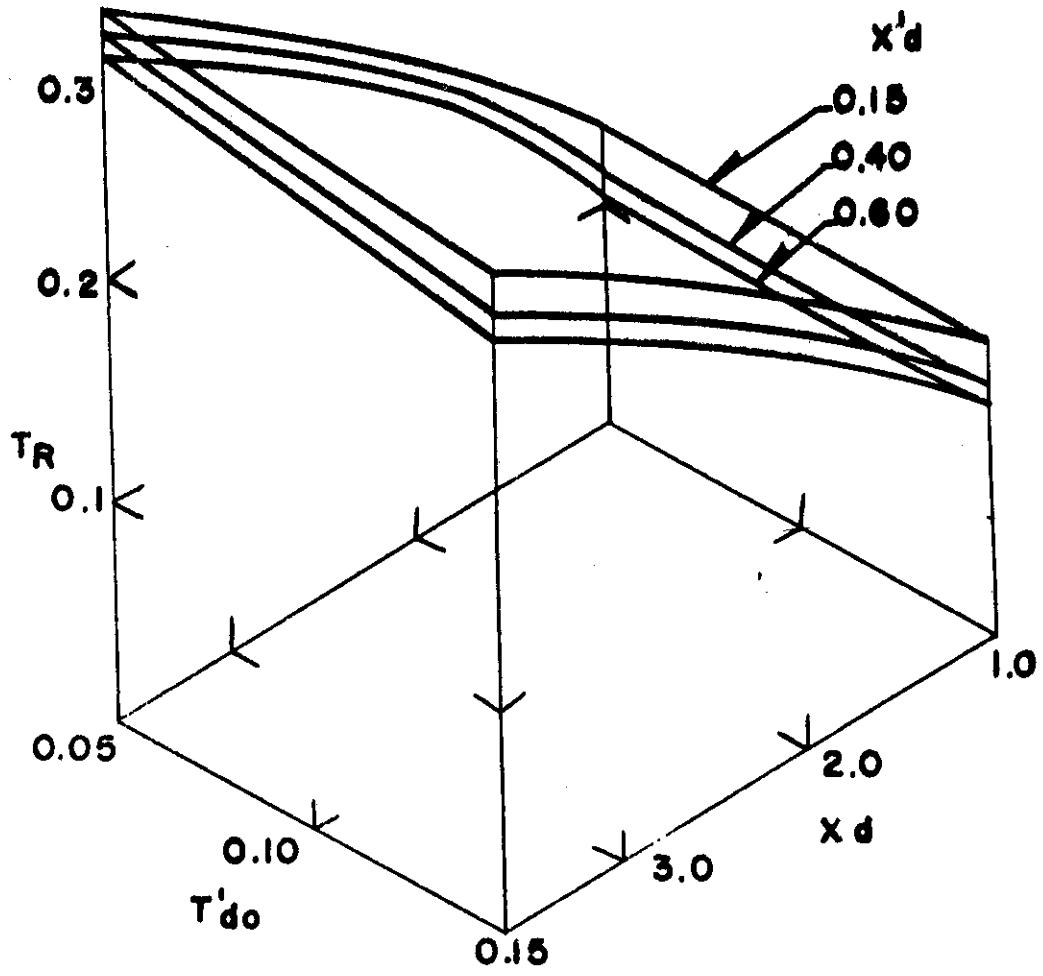

Figure A-31. SYSTEM RECOVERY TIME
20-Kva Single-Phase System
Regulator B
All Exciters
Load off Transient

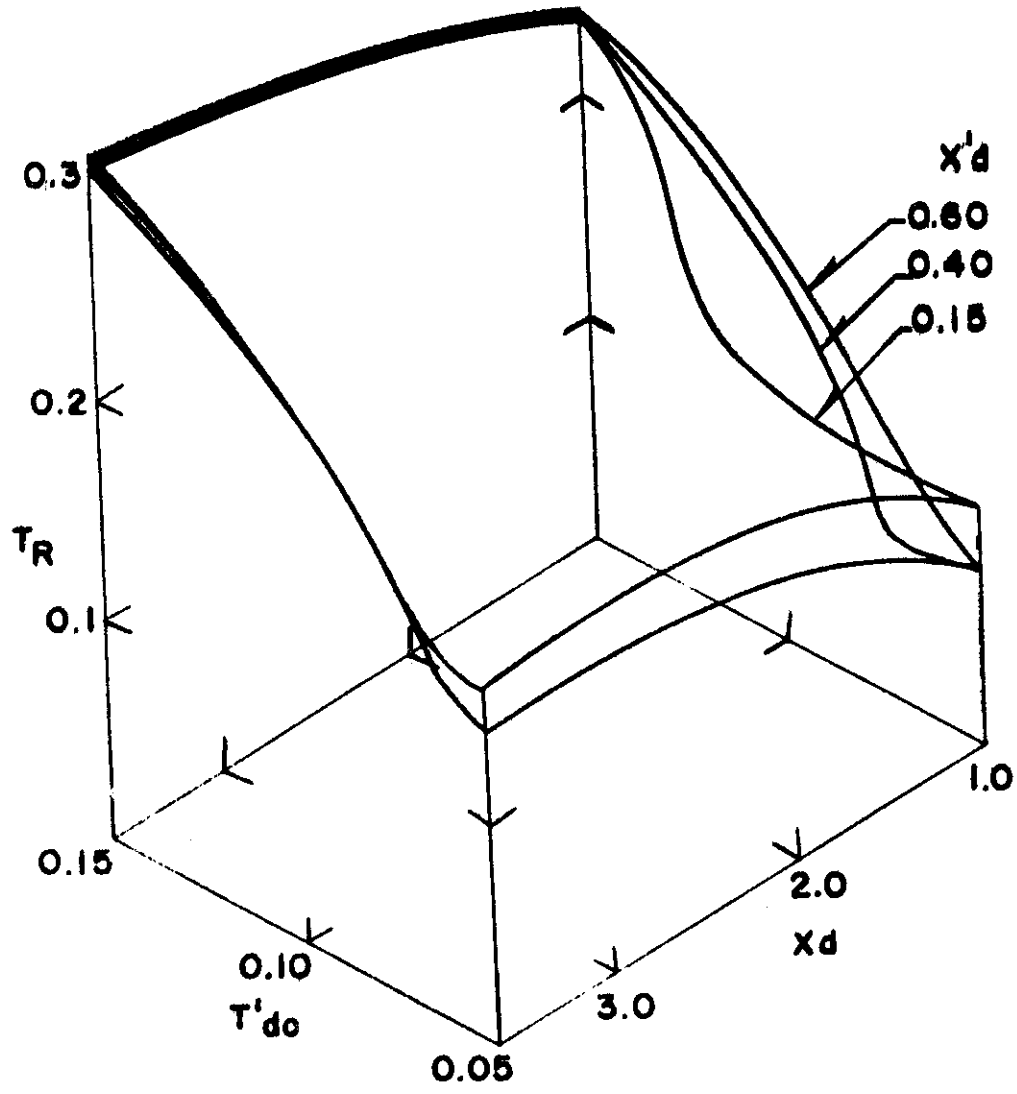

A-4 STUDY OF THREE-PHASE ISOLATED ELECTRIC POWER SYSTEMS (CARBON-PILE REGULATOR).

The two systems used in this part of the report were

(1) the three-phase 60-kva a-c generator-regulator and

(2) the three-phase 40-kva a-c generator-regulator,

both operating isolated. The load used for the 60-kva system was 1.0 per-unit, zero power-factor-lagging, while it was 0.8 per-unit, zero-power-factor-lagging for the 40-kva system. The latter was reduced to better adjust the analogue to the actual results obtained on a true 40-kva generator-regulator.

Saturation was included in both the a-c generator and in the exciter for the two systems. The method used is described in Section A-2 of this appendix. The additional data necessary to adjust the limiter circuits for saturation is given here. First the piece-meal curves as taken from the actual data (see appendix C) are presented and then the analogue curve is shown.

The analogues used for these two three-phase systems are much more elaborate than the one used for the 20-kva system study. This is true both with respect to the effects of saturation and also with respect to the methods of analoging to properly display the transient performance of the system.

The a-c generator analogue is the same as the one shown in figure A-5-b. As shown, it includes the following machine parameters:

(1) Leakage reactance, x_ℓ

(2) Reactance of armature reaction, x_{ad}

(3) Effective field leakage reactance, x'_F

(4) Open-circuit transient time constant, T'_{do}

(5) A-C Generator gain (over-all)

(6) Saturation effects

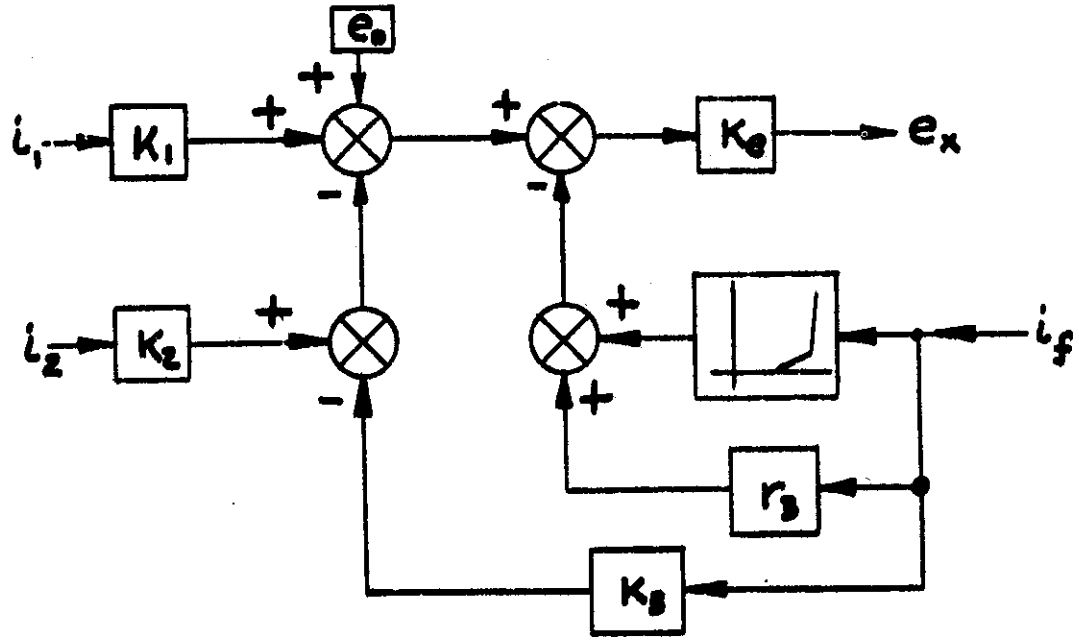

Figure A-32 Block Diagram of Summation of Various Excitations For d-c Exciter

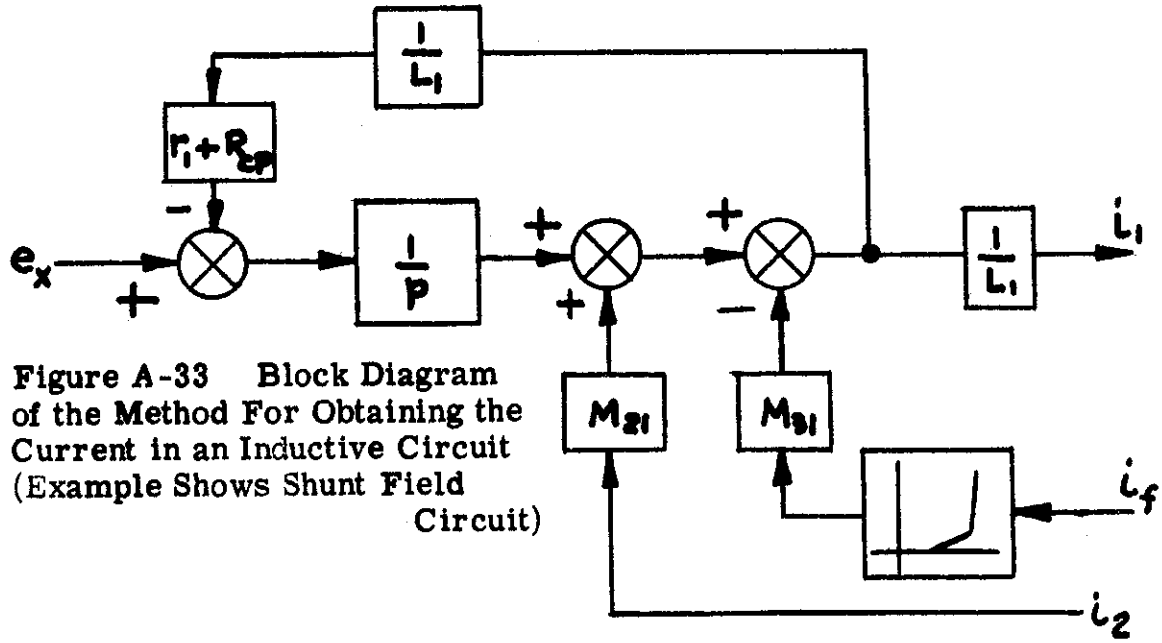

Figure A-33 Block Diagram of the Method For Obtaining the Current in an Inductive Circuit (Example Shows Shunt Field Circuit)

The exciter contains the functions described in Section A-3, but it also includes the effects of saturation. Figure A-32 and A-33 show the block diagram of the operations in the exciter portion of the system. The total exciter includes the following:

(1) Shunt field excitation

(2) Eddy-current effect (omitted from the 40-kva system because it seemed to have little effect)

(3) Voltage drop in armature circuit

(4) Compounding due to interpolar windings, compensating or series windings.

(5) Residual voltage

(6) Effective over-all gain (See figure A-8)

(7) Saturation effects.

The voltage regulator and the stabilizing network were used in their real form, operating in their normal manner. The only change was to apply the terminal voltage signal e_t directly to the rectifier which supplies power to the regulator operating coil circuit. This eliminates the effect of the rectifier and the step-down transformers normally used when a-c voltage is applied. However, this effect is entirely negligible, especially for purposes of this study.

A-4-a 60-Kva System - Figure A-34 shows the complete analogue for the 60-kva system. Tables A-4 and A-5 describe the amplifiers and components. Table A-6 lists pertinent data used for the base system.

Figure A-35 shows the piece-meal saturation curves for the 60-kva a-c generator, both at no load and at 1.0 per-unit zero power-factor (constant impedance). This was used then to set up the computer. Figure A-36 shows how this was applied to amplifier F in the analogue (Figure A-34).

Figure A-37 shows the piece-meal load saturation curve of the exciter. It is interesting to note that at the lower values of this curve the voltage drops in the armature circuit are balanced by the cumulative compounding

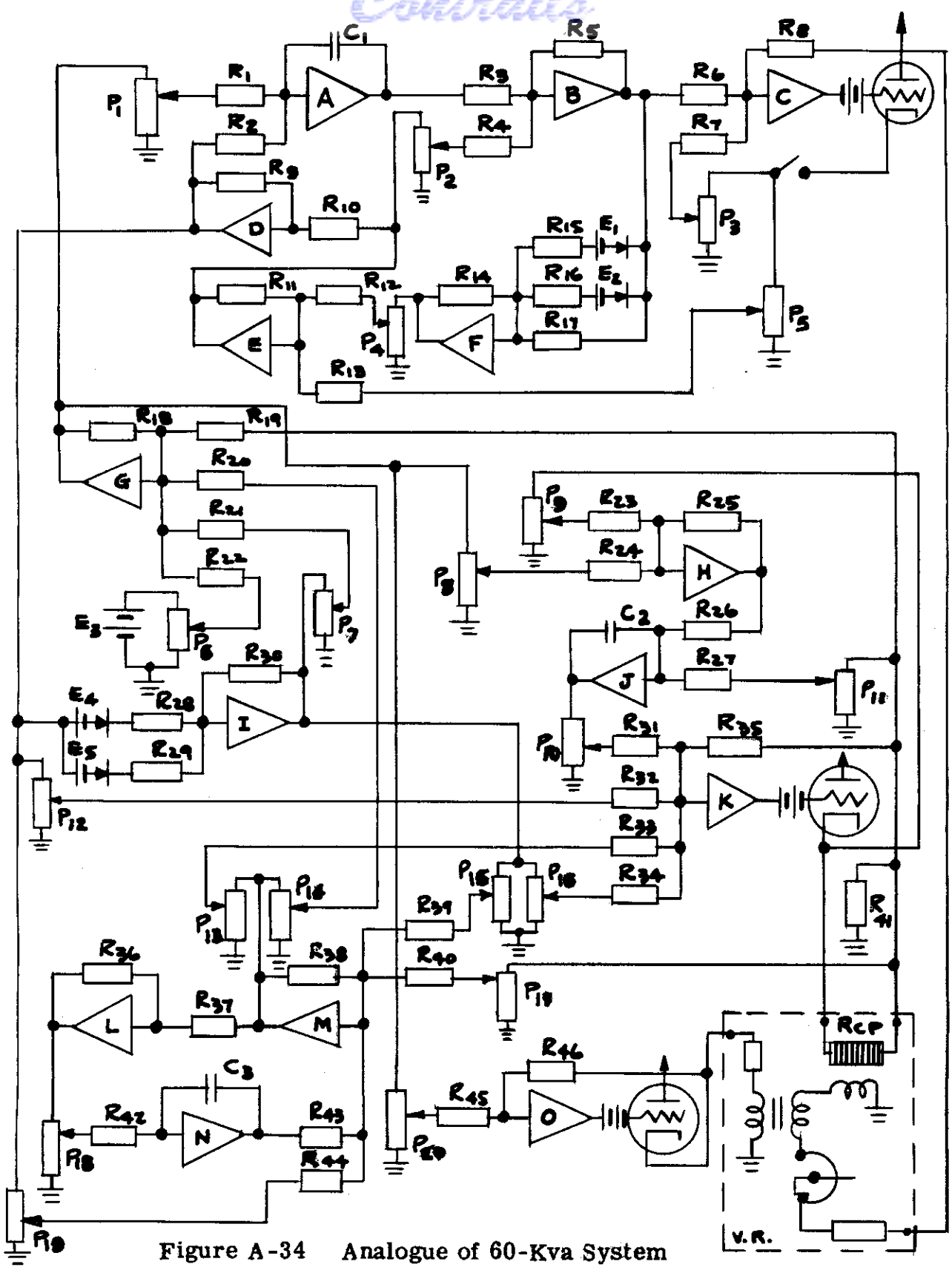

Figure A-34 Analogue of 60-Kva System

Table A-4

Purpose of Each Amplifier in 60-Kva System Analogue

Amplifier	
A	Integration
B	Summation
C	Summation and amplification
D	Sign inversion
E	Amplification and summation
F	Nonlinear a-c generator function generator
G	Summation of exciter excitations
H	Sign inversion
I	Nonlinear exciter function generator
J	Integration
K	Exciter shunt field current generator
L, M, N	Exciter eddy-current generator
O	Sign inversion

Table A-5

Values of Analogue Computer Elements Used For the Base 60-Kva System

A. Resistors

The values are given in megohms, except for R_{41} which is given in ohms.

R	Value	R	Value	R	Value
1	0.500	17	2.000	32	5.02
2	0.500	18	1.95	33	2.49
3	1.000	19	0.760	34	4.98
4	1.000	20	1.860	35	1.000
5	1.000	21	1.000	36	1.000
6	1.000	22	9.60	37	1.000
7	10.00	23	0.510	38	2.000
8	2.46	24	1.000	39	2.020
9	1.000	25	1.000	40	0.500
10	1.000	26	1.000	41	14.75 ohms
11	0.500	27	1.000	42	1.000
12	0.500	28	5.84	43	1.000
13	1.000	29	0.601	44	3.03
14	1.000	30	1.000	45	1.000
15	0.278	31	1.000	46	1.000
16	4.32				

Table A-5 Continued

B. Potentiometers

Values are given in per-unit quantities and are not corrected for the effect of load upon them.

P	Value	P	Value
1	.620	11	.869
2	.370	12	.603
3	.321	13	.644
4	.555	14	.700
5	.406	15	.217
6	.292	16	.400
7	.960	17	.644
8	.750	18	.358
9	.705	19	.490
10	.930	20	.750

C. Condensers

The values are given in microfarads.

C	Value
1	.0531
2	.0202
3	.0042

D. Voltage Sources

E	Value
1	34.0 volts
2	18.15
3	22.5
4	14.15
5	34.9

Table A-6

Data For 60-Kva Base System

x_{ad} = 1.80 p.u.

x_{ℓ} = .08 p.u.

$x_{F'}$ = .185 p.u.

x_L = 1.00 p.u.

$$\frac{\text{voltage applied to } P_1}{\text{actual exciter output}} = 1.333$$

$$\frac{\text{d-c current through } R_{41}}{\text{actual shunt field current}} = 0.723$$

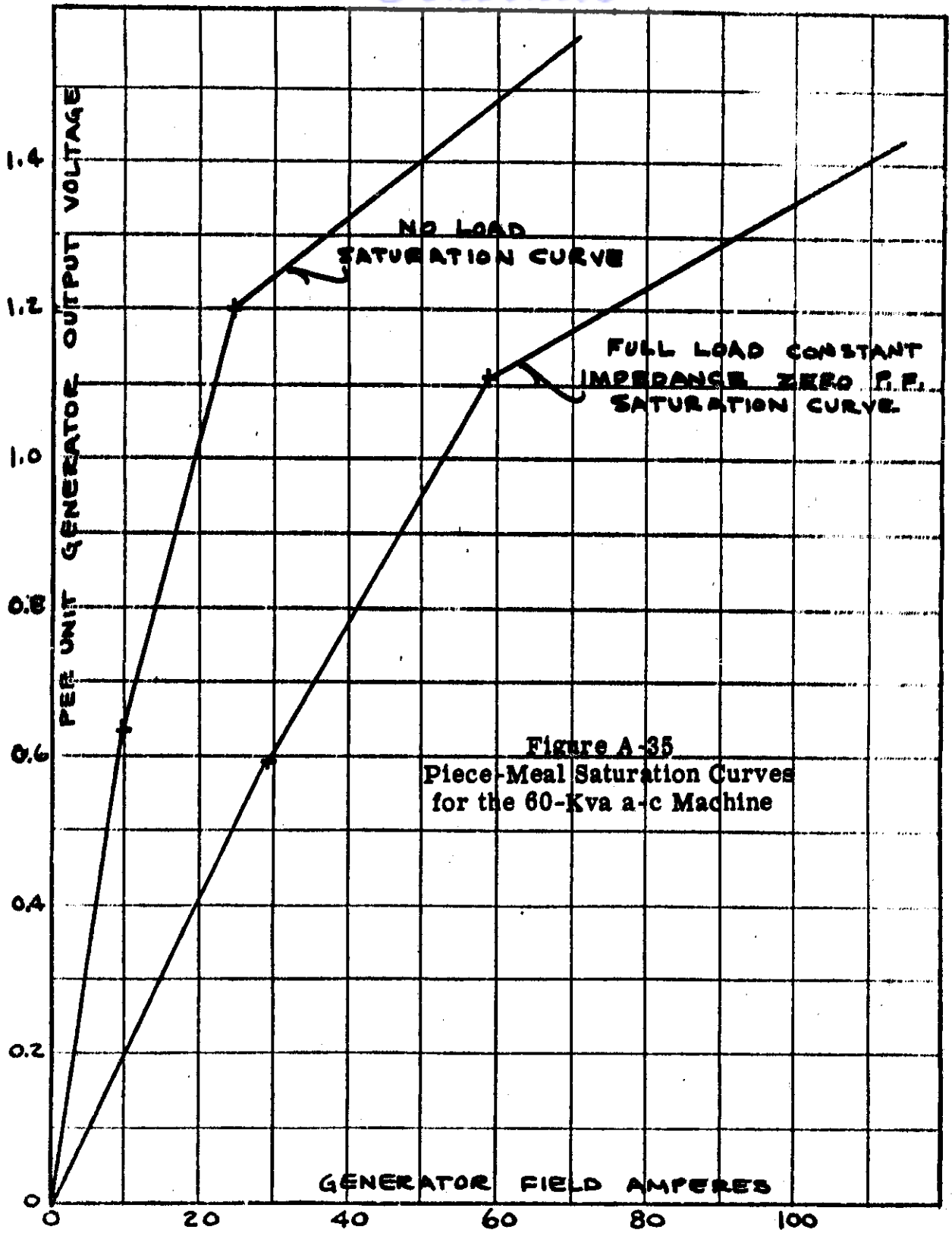

Figure A-35
Piece-Meal Saturation Curves
for the 60-Kva a-c Machine

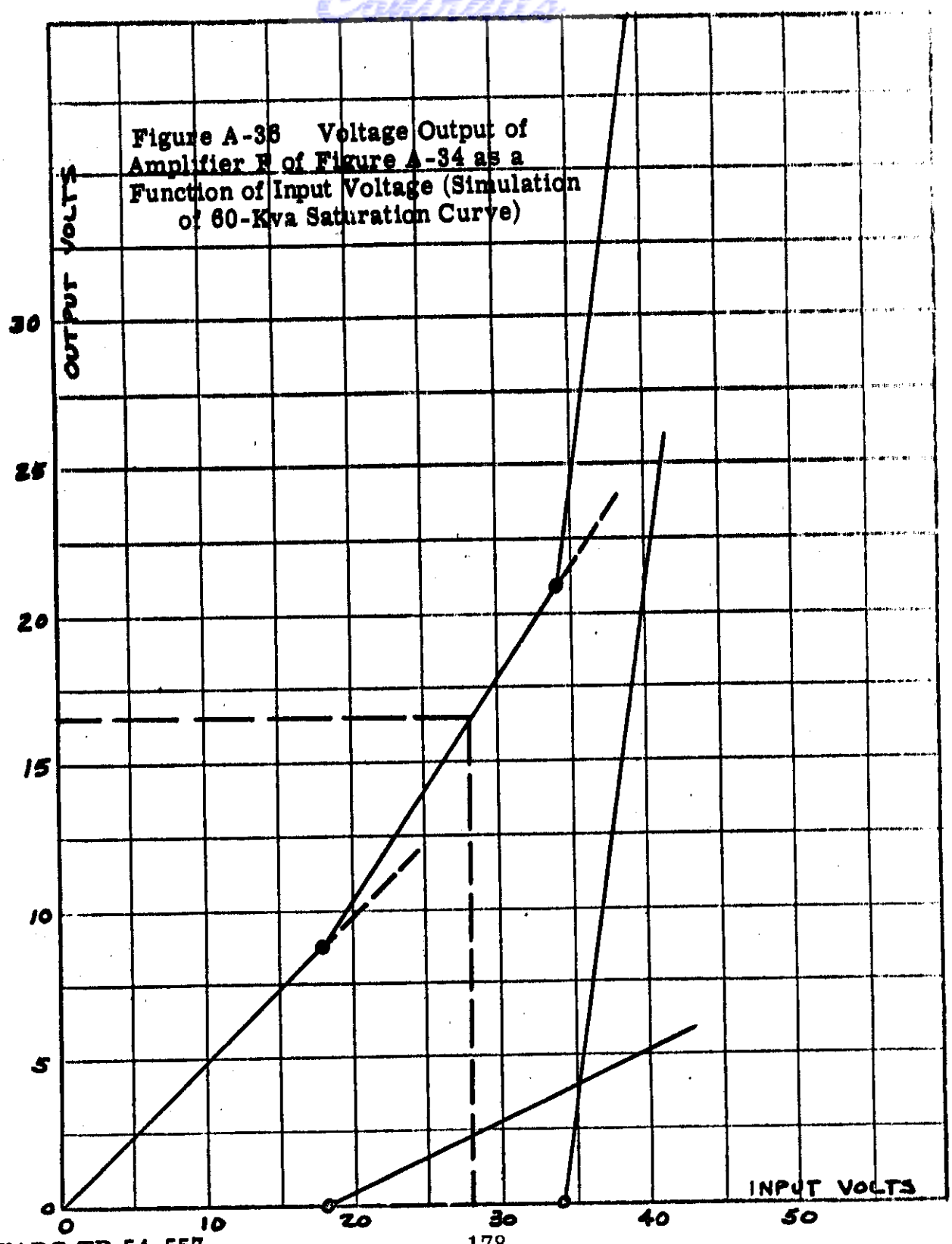

Figure A-38 Voltage Output of Amplifier R of Figure A-34 as a Function of Input Voltage (Simulation of 60-Kva Saturation Curve)

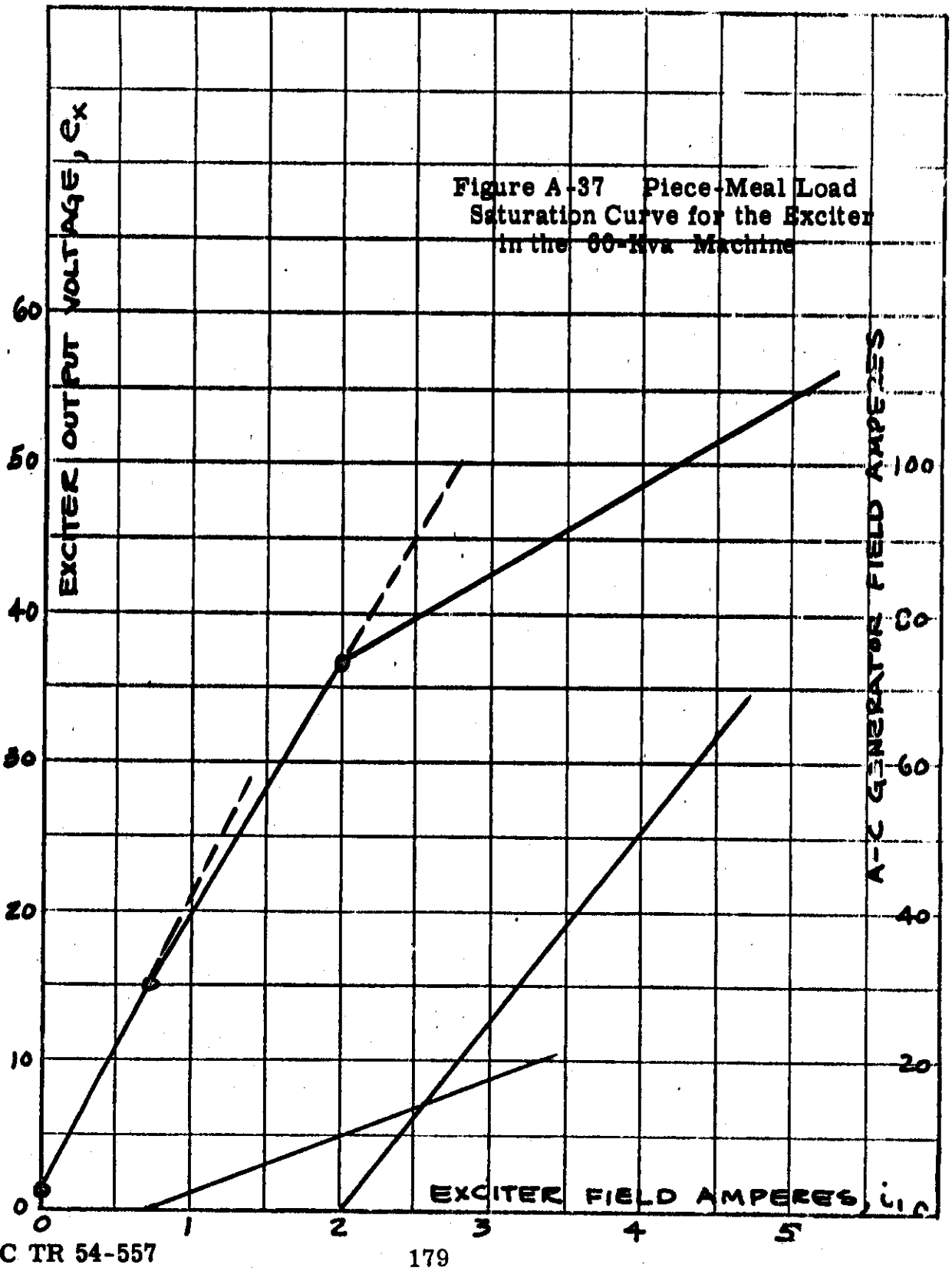

Figure A-37 Piece-Meal Load Saturation Curve for the Exciter in the 60-Kva Machine

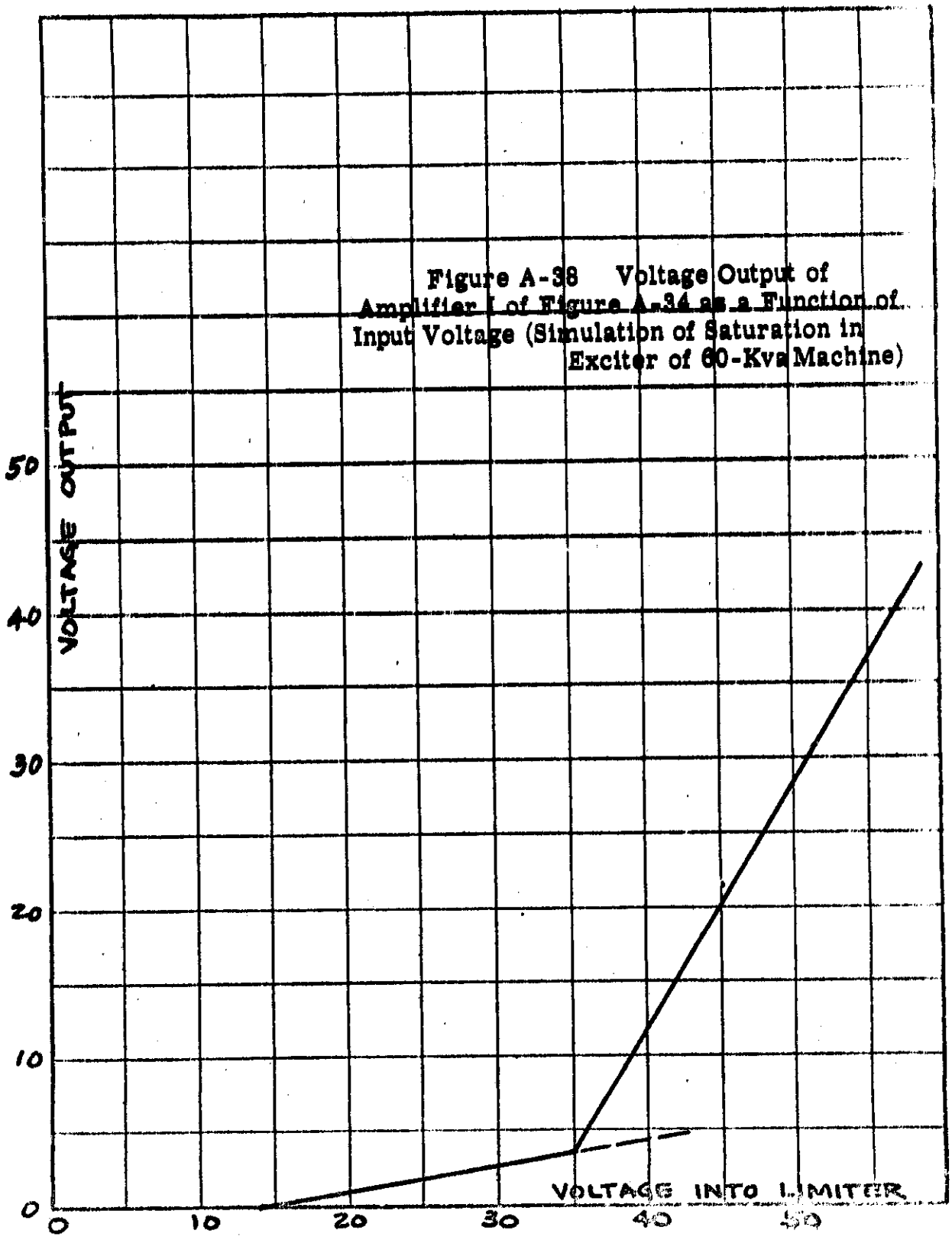

Figure A-38 Voltage Output of Amplifier I of Figure A-34 as a Function of Input Voltage (Simulation of Saturation in Exciter of 60-Kva Machine)

due to the various series fields. Referring to Figure A-32, this means that the two parallel paths for the series current i_f cancel one another, because K_3 and r_3 are equal for this particular machine. Figure A-38 shows how the exciter saturation was simulated in amplifier I (See Figure A-34).

For this study the following parameters were chosen as the independent variables:

(1) Synchronous reactance, x_d

(2) Transient reactance, $x_{d'}$

(3) Open-circuit time constant, $T_{do'}$

(4) a-c Generator gain, K_g

(5) Exciter gain, Ke

(6) Exciter shunt field time constant, T_1

The voltage regulator and the feedback stabilizing transformer remained the same for all the parameter studies made on the 60-kva system.

A-4-b 40-Kva System - Figure A-39 shows the complete analogue for the 40-kva system. Tables A-7 and A-8 describe the amplifiers and components. Table A-9 lists pertinent data used for the base system.

Figure A-40 shows the piece-meal saturation curves for the 40-kva a-c generator. The piece-meal curve in this figure is superimposed on the saturation curve taken from actual data. Figure A-41 shows the piece-meal load saturation curve of the exciter.

For this study the following parameters were chosen as the independent variables:

(1) Synchronous reactance, x_d

(2) Transient reactance, $x_{d'}$

(3) Open-circuit time constant, $T_{do'}$

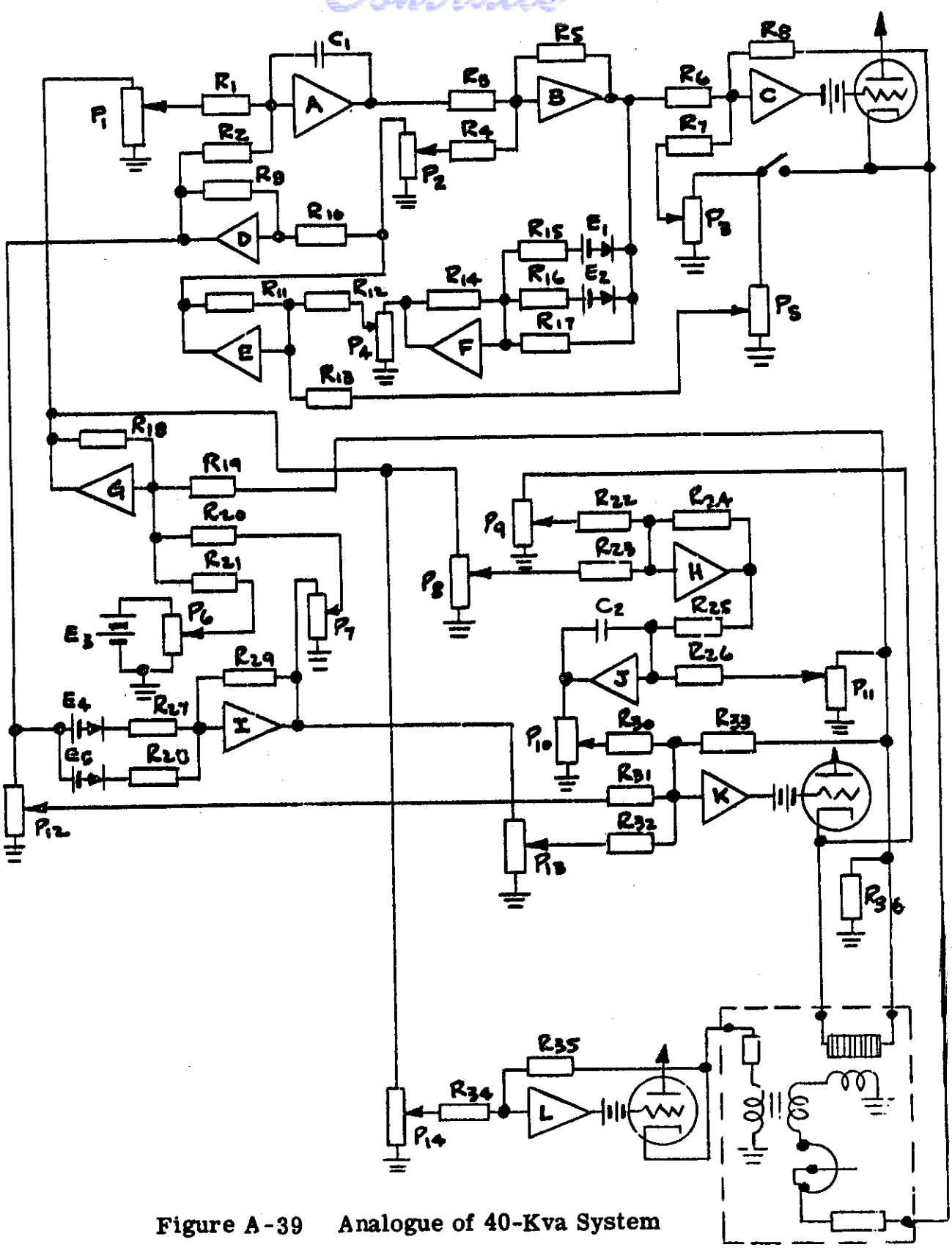

Figure A-39 Analogue of 40-Kva System

Table A-7

Purpose of Each Amplifier in 40-Kva System Analogue

Amplifier	Purpose
A	Integration
B	Summation
C	Summation and amplification
D	Sign inversion
E	Summation and amplification
F	Nonlinear a-c generator function generator
G	Summation of exciter excitations
H	Summation
I	Nonlinear exciter function generator
J	Integration
K	Exciter shunt field current generator
L	Sign inversion

Table A-8

Values of Analogue Computer Elements Used For the Base 40-Kva System

A. Resistors

The values are given in megohms, except for R_{36} which is given in ohms.

R	Value	R	Value	R	Value
1	.239	13	1.000	25	1.000
2	.500	14	1.000	26	.510
3	1.000	15	.239	27	.601
4	1.000	16	.697	28	5.84
5	1.000	17	2.000	29	1.000
6	1.000	18	1.95	30	.500
7	10.00	19	1.23	31	5.00
8	2.46	20	1.000	32	5.00
9	1.000	21	9.60	33	1.000
10	1.000	22	.510	34	1.000
11	.500	23	1.000	35	1.000
12	.500	24	1.000	36	14.75 ohms

Table A-8 Continued

B. Potentiometers

Values are given in per unit quantities and are not corrected for the effect of load upon them.

P	Value	P	Value
1	.563	8	.752
2	.410	9	1.000
3	.244	10	.854
4	.667	11	.752
5	.330	12	.423
6	.292	13	.423
7	.962	14	.757

C. Condensers

The values are given in microfarads.

C	Value
1	.0713
2	.02

D. Voltage Sources

E	Value
1	34.2 volts
2	25.7
3	22.5
4	41.0
5	0

Table A-9

Data For 40-Kva Base System

$x_{ad} = 1.50$ p.u.

$x_{\ell} = .06$ p.u.

$x'_F = .205$ p.u.

$x_L = 1.25$ p.u.

$$\frac{\text{Voltage applied to } P_1}{\text{actual exciter voltage}} = 1.333$$

$$\frac{\text{d-c current through } R_{36}}{\text{actual shunt field current}} = 1.000$$

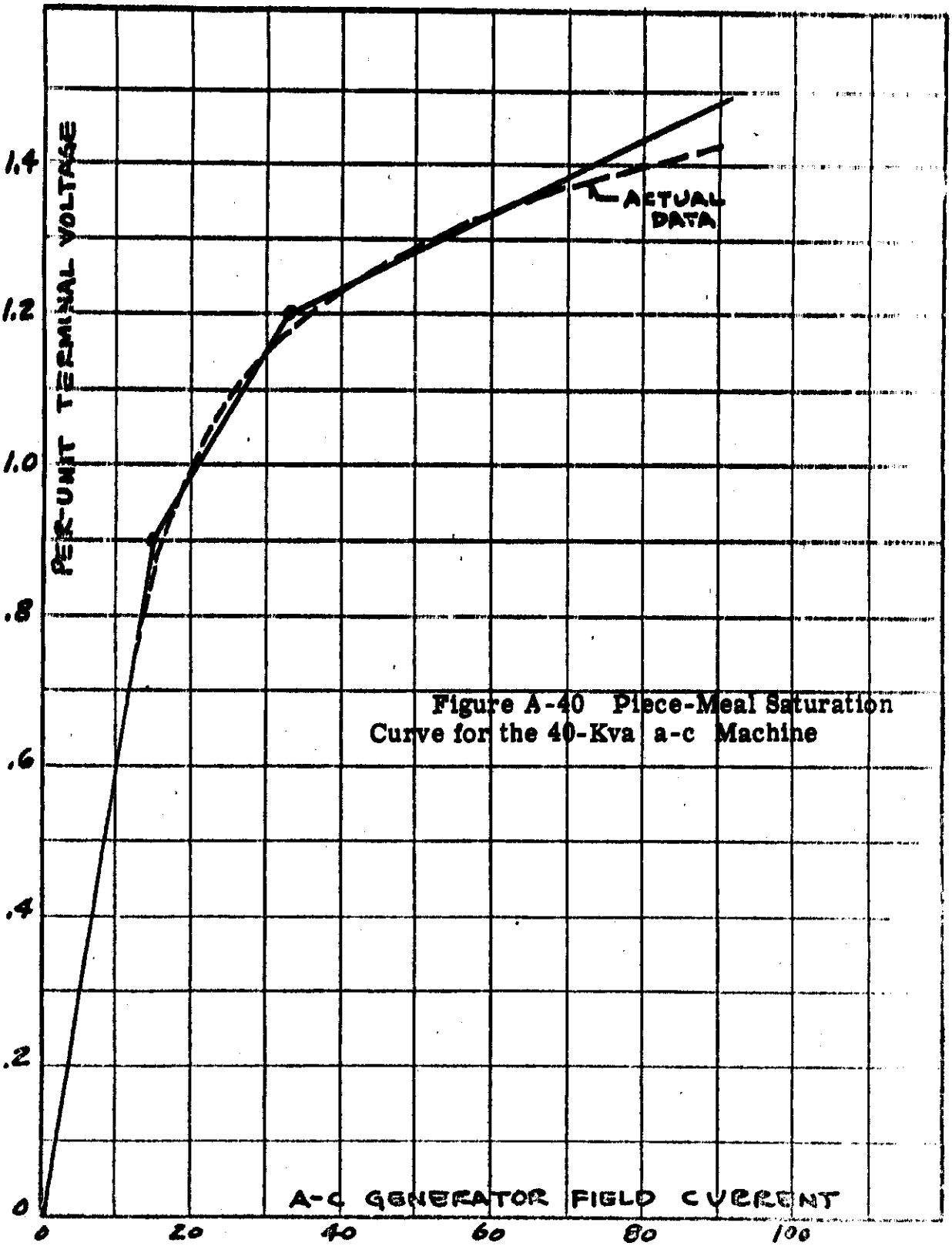

Figure A-40 Piece-Meal Saturation Curve for the 40-Kva a-c Machine

Figure A-41 Saturation Data For Exciter Used in the 40-Kva Machine

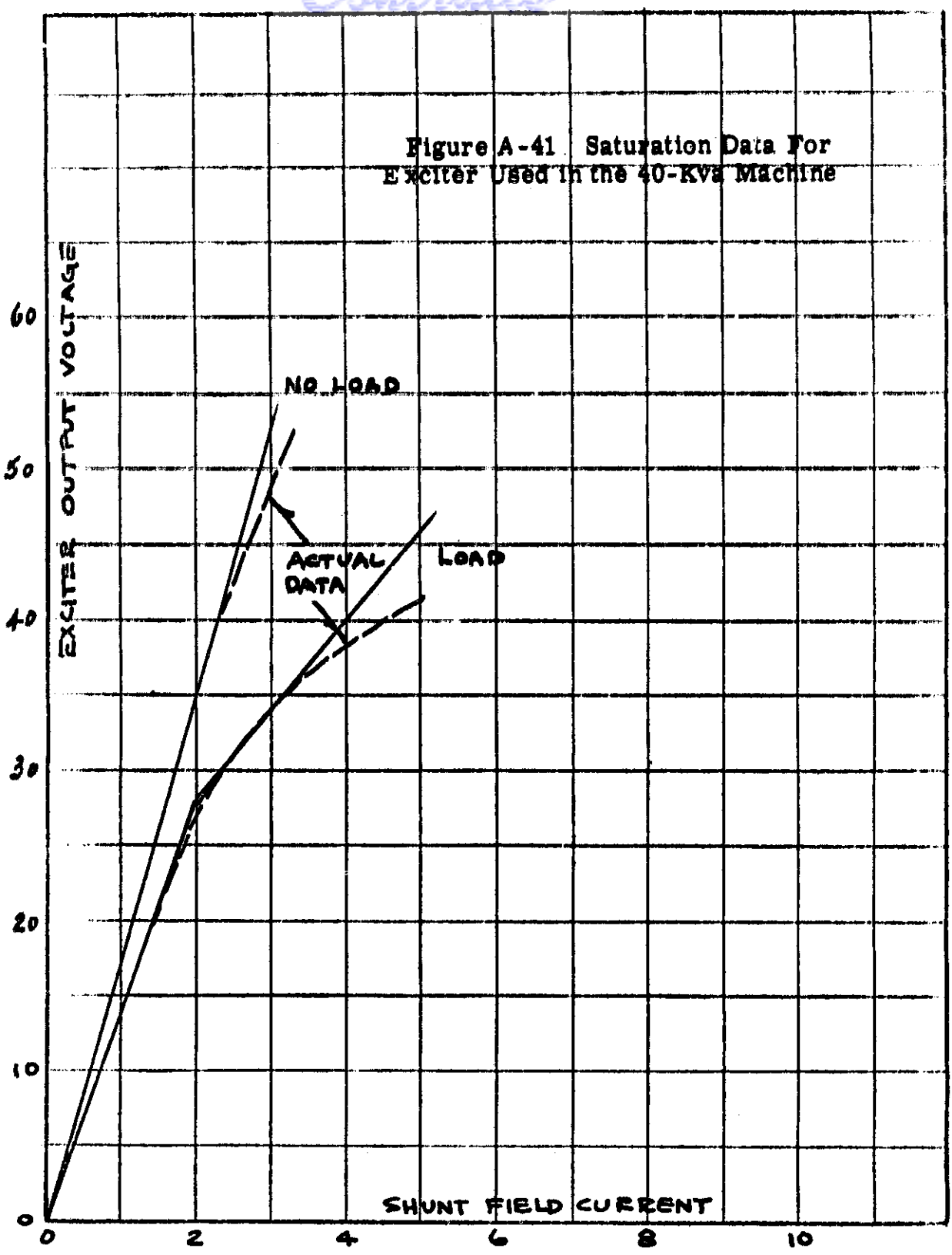

(4) a-c Generator gain, K_g

The exciter was set at the base conditions. Note that there was no eddy-current excitation used in this analogue (See figure A-39).

The voltage regulator and feedback stabilizing transformer remained the same for all the studies made on the 40-kva system.

A-4-c Conclusions - Conclusions will apply to both the 60-kva and 40-kva systems unless otherwise indicated.

Since the degree of stabilization at base conditions for both systems is very near that of optimum damping, the parametric variations do not show the effect on system recovery time as there would be if less damping were used. (This can be readily seen in the 20-kva system studies, comparing regulator A to regulator B.)

Time did not permit as extensive a study of the two three-phase systems as was accomplished on the single-phase system. The parametric variations were therefore confined to the regions of practicality. In other words, the various machine reactances, the gain, and the time constants were limited to those which could be achieved by presently known design practices. The base machine was used as the reference and variations were effected around the values of the parameters describing the base system.

A-4-c-(1) Effect of Practical Variations in the Machine on System Recovery Time - Referring to the material in Chapter II, Section D and in Appendix B, Section 3, the following comments refer to the effect of various practical changes in the a-c generator design on the system recovery time T_r.

(a) Variation of Generator Air Gap (Figure A-42)

The system recovery time increases when the air gap of the a-c generator is reduced. It was noted that the system performance was wholly inadequate even before the absolute minimum practical gap was reached, this being due primarily to the simultaneous increase in x_d, $x_{d'}$, $T_{do'}$ and especially the generator gain K_g. This occurs at both load on and load off conditions.

As the air gap is increased, we do not find the opposite to be true. The effect on system recovery time is negligible when the gap is opened 30 per cent.

(b) Variation of the ratio of Copper to Magnetic Material in the a-c Generator (Figure A-43)

The system recovery time when load is removed is inversely proportional to the ratio of magnetic material to copper material in the field structure of the a-c generator. When a narrow field pole is used the recovery time is higher and when a wide pole is used it is less than that observed with the base system.

The system recovery time when load is applied did not seem to be effected by this change in field structure.

(c) Variation of Armature Conductors in the Stator of the a-c Generator (Figure A-44)

The system recovery time when load is removed increases as the number of conductors in the armature are reduced. However, the effect is almost negligible when the conductors are increased.

Again, as in (b) above, the system recovery time when load is applied is not effected by this change.

(d) Variation of the Cross-Sectional Dimensions of the a-c Generator (Figure A-45) .

The system recovery time when load is removed increases as the generator diameter decreases (length increasing). Again, as in (c) above, the effect of increasing the diameter of the machine (length shortening) was almost negligible on system recovery time.

The system recovery time for the load-on transient does not change appreciably when the diameter of the a-c generator is changed.

(e) Combination Variations (Figures A-46, A-47, A-48, A-49).

When two or more variations are combined simultaneously, the effect on the system recovery time is accentuated by the individual effects. From

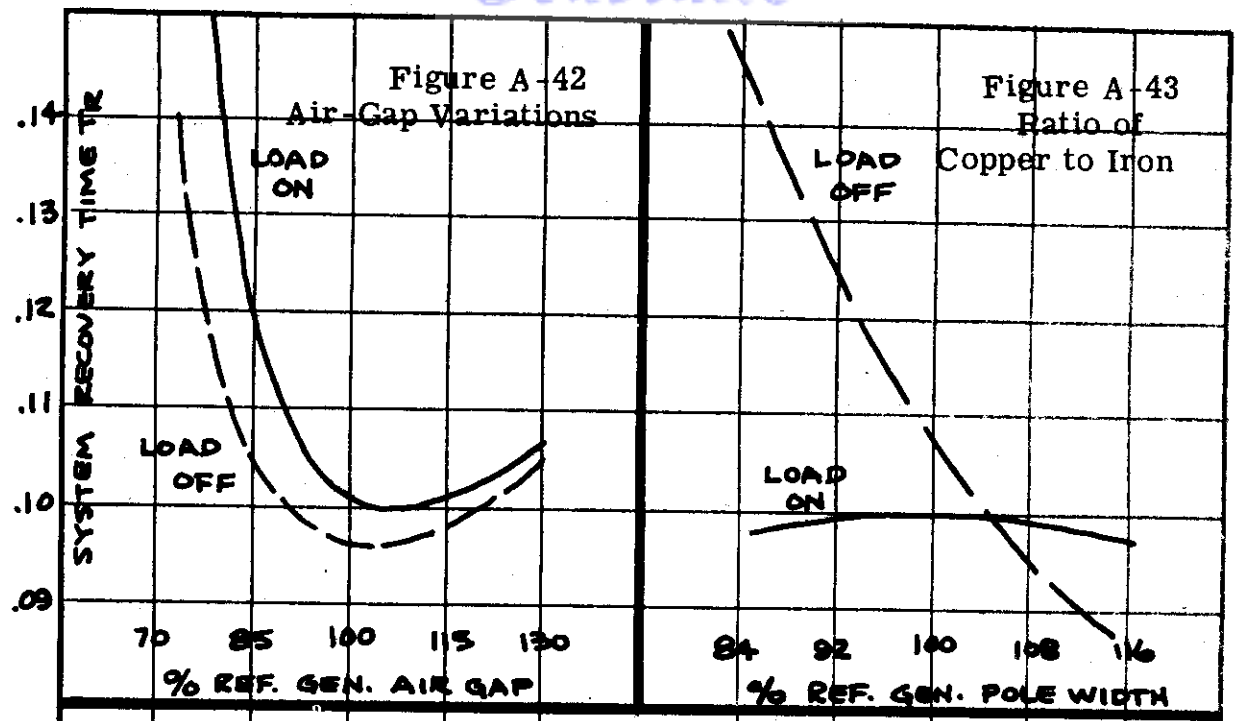

Figure A-42
Air-Gap Variations

Figure A-43
Ratio of
Copper to Iron

System Recovery Time on Three-Phase Systems
as a Function of Dimension and Winding Variations

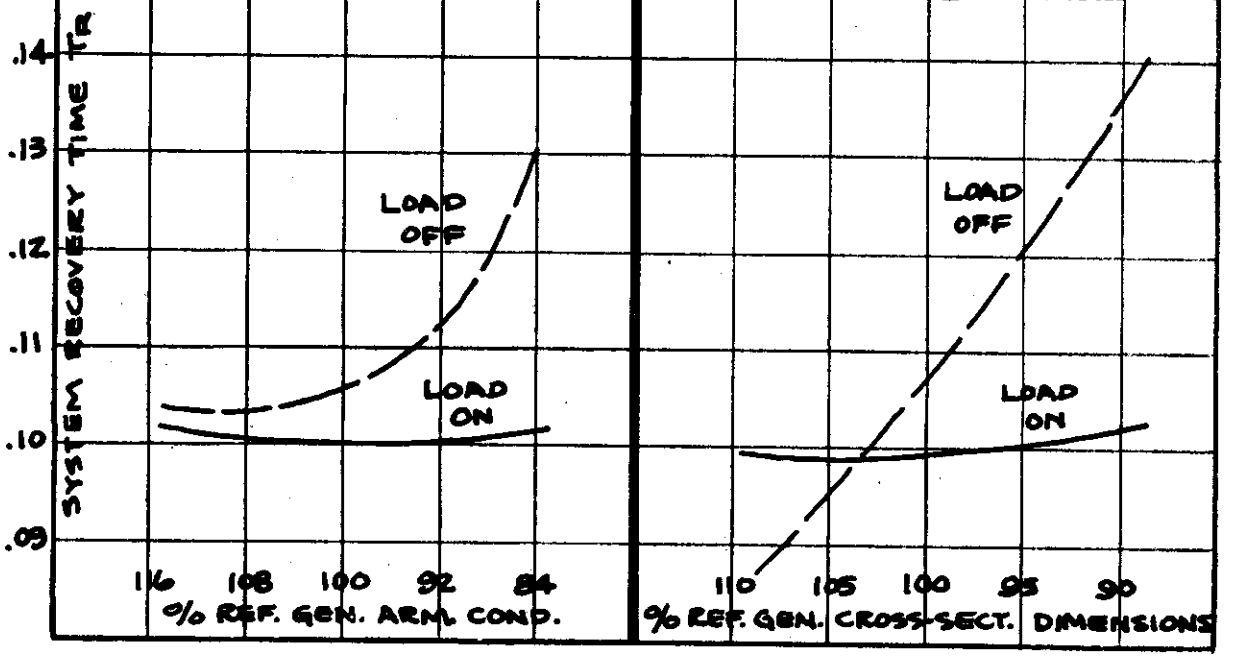

Figure A-44
Armature Conductor Variations

Figure A-45
Variation of Cross-
Section Dimensions

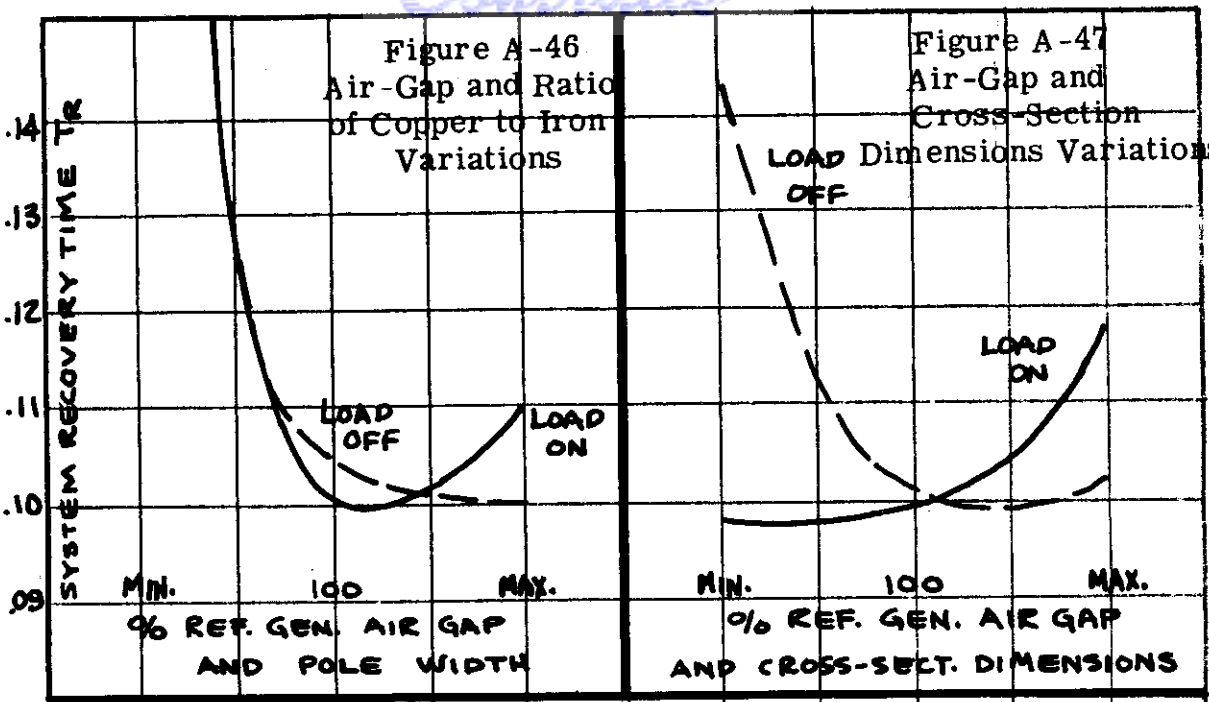

Figure A-46
Air-Gap and Ratio of Copper to Iron Variations

Figure A-47
Air-Gap and Cross-Section Dimensions Variations

System Recovery Time on Three-Phase Systems as a Function of Dimension and Winding Variations

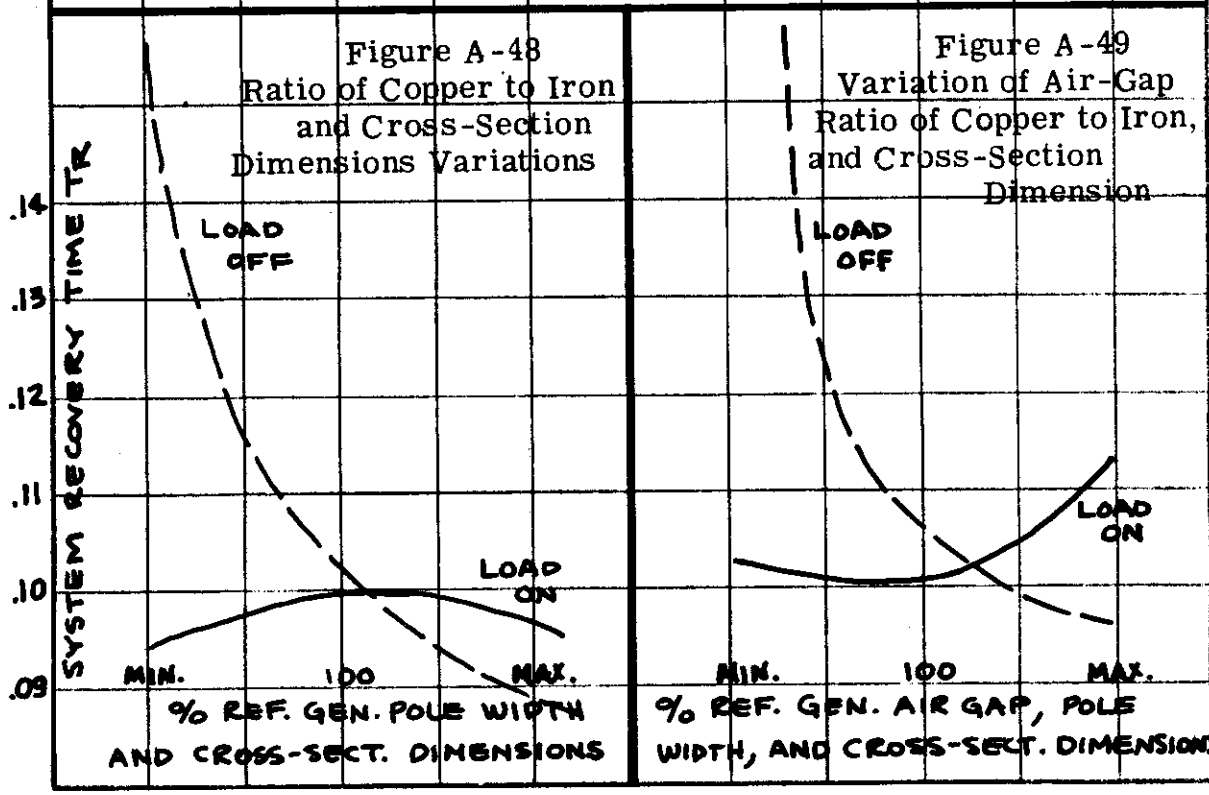

Figure A-48
Ratio of Copper to Iron and Cross-Section Dimensions Variations

Figure A-49
Variation of Air-Gap Ratio of Copper to Iron, and Cross-Section Dimension

a practical standpoint the following combinations were considered:

(i) Air gap and ratio of magnetic material to copper material,

(ii) Air gap and cross-sectional dimensions,

(iii) Ratio of magnetic material to copper material and cross-sectional dimensions, and

(iv) Air gaps, ratio of magnetic material to copper material, and cross-sectional dimensions.

These combinations prove one very important point. All attempts to reduce the weight of the a-c generator to any appreciable amount results in longer system recovery times. Unfortunately though, we do not benefit by increasing the weight, that is, so far as system recovery time is concerned.

The various combinations and the individual changes were made at various exciter gains, all within the practical range for such gain variations. There was no significant difference in system recovery time. This confirms the observations on the 20-kva system where the system stabilization was sufficient to make the transient performance close to or greater than critical damping (Regulator B).

A-4-c-(2) Example of Wide Variations in Machine Parameters and Their Effect on System Recovery Time - In order to show some of the phenomena which occurs when the machine parameters are theoretically varied over wide ranges, a few three-dimensional figures are included showing system recovery time as a function of these parameters.

Figures A-50 and A-51 show the 60-kva system for load on and load off, respectively. These two figures show the basic excitation system only.

Figures A-52 and A-53 show the 60-kva system for load on and load off, respectively, when the exciter time constant is varied. Also in each of these two figures there are three conditions for a-c generator.

The most important factors which were observed in the analogue computer work was the fact that so far as the transient stability is concerned,

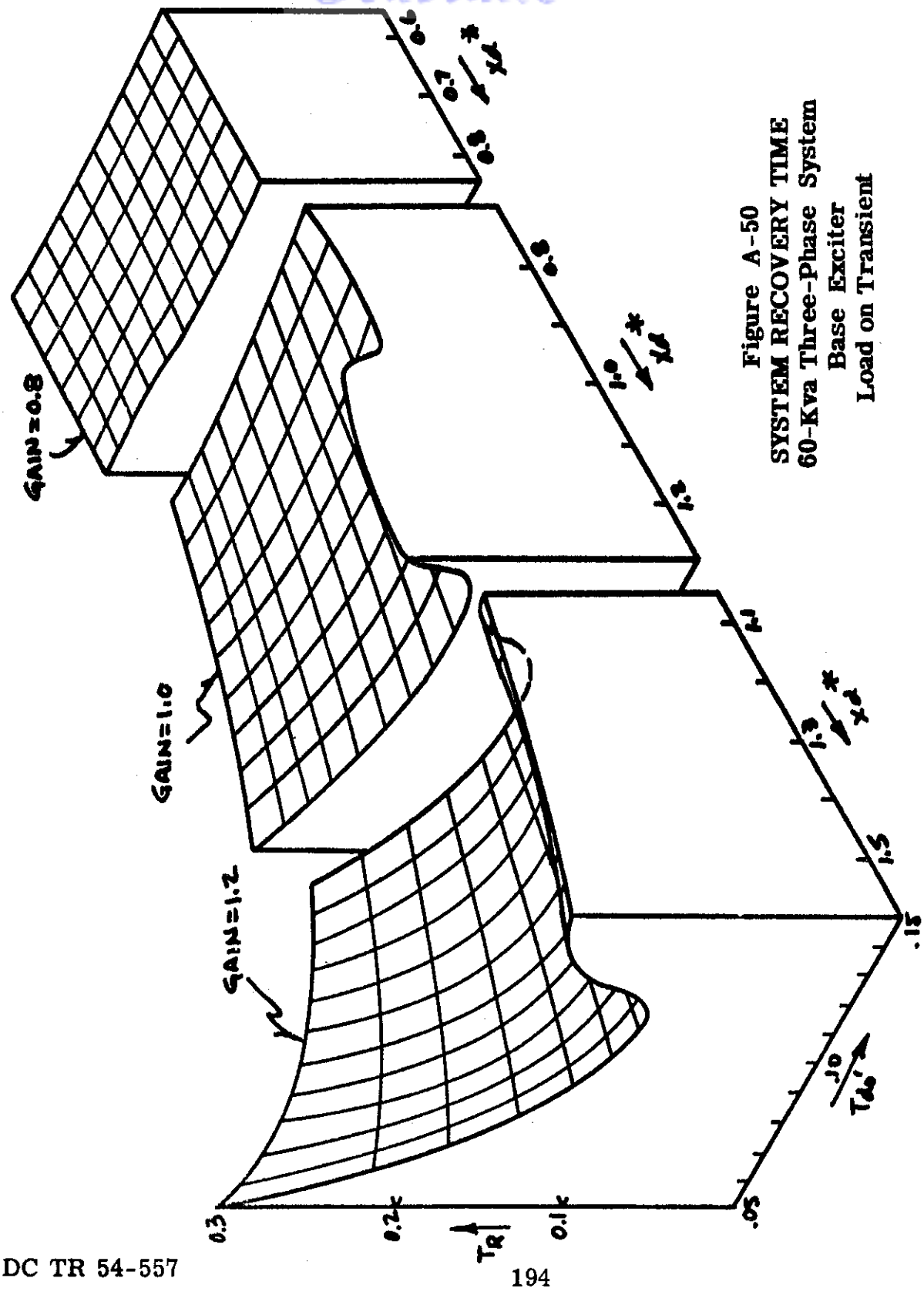

Figure A-50
SYSTEM RECOVERY TIME
60-Kva Three-Phase System
Base Exciter
Load on Transient

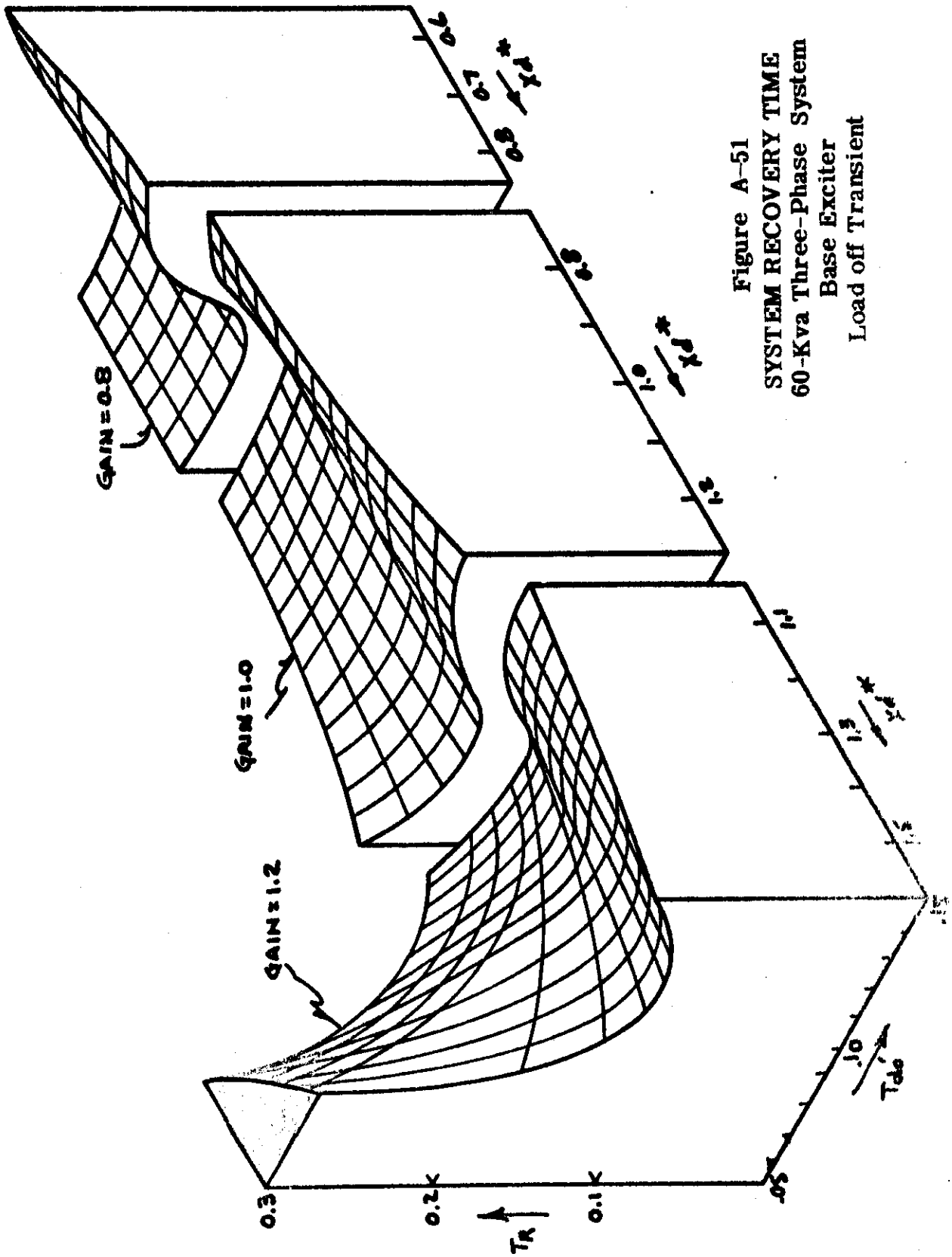

Figure A-51
SYSTEM RECOVERY TIME
60-Kva Three-Phase System
Base Exciter
Load off Transient

Figure A - 52
SYSTEM RECOVERY TIME
60-Kva System
Effect of Varying
the Exciter Time Constant
Load on Transient

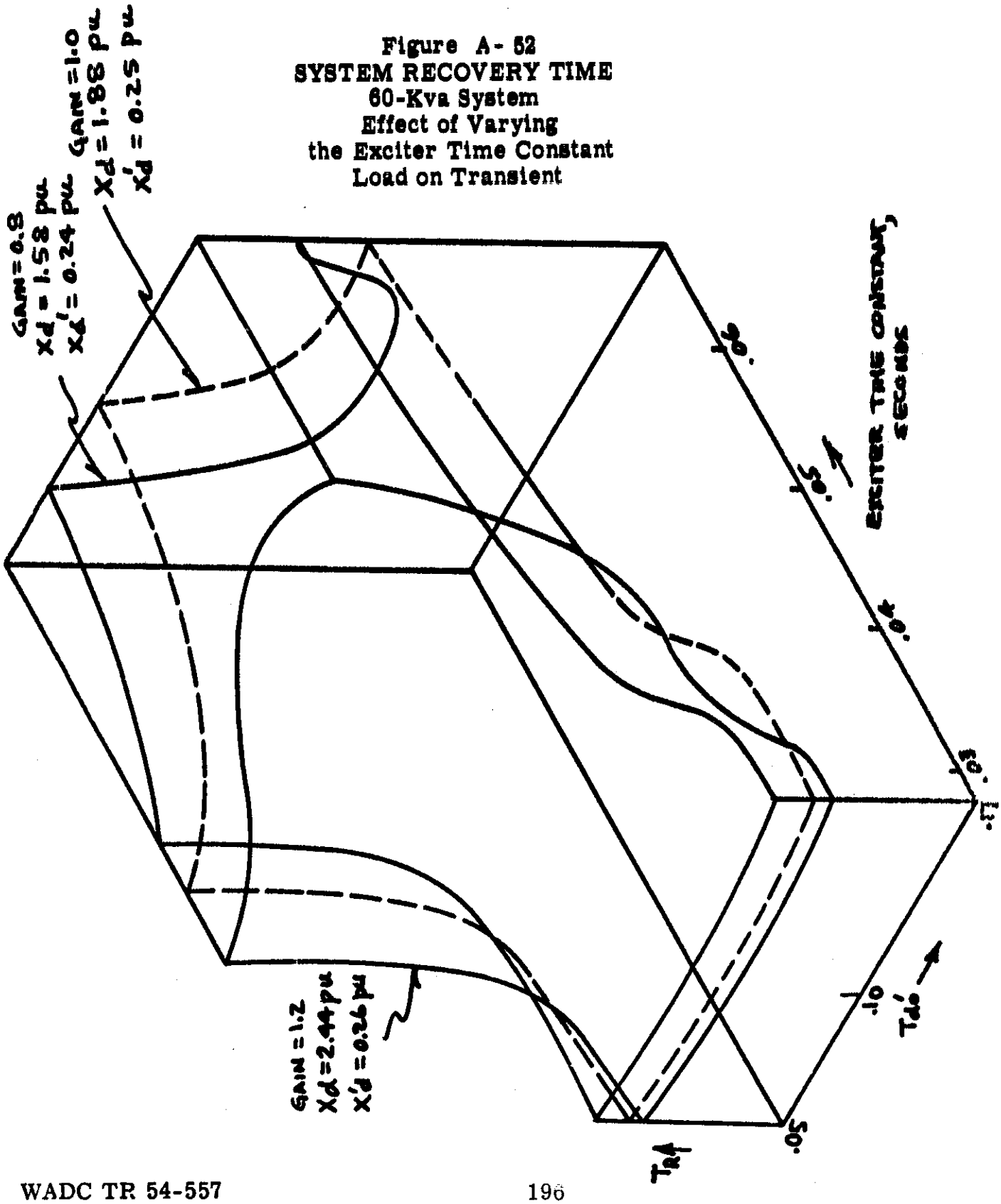

Figure A-53
SYSTEM RECOVERY TIME
60-Kva System
Effect of Varying
the Exciter Time Constant
Load off Transient

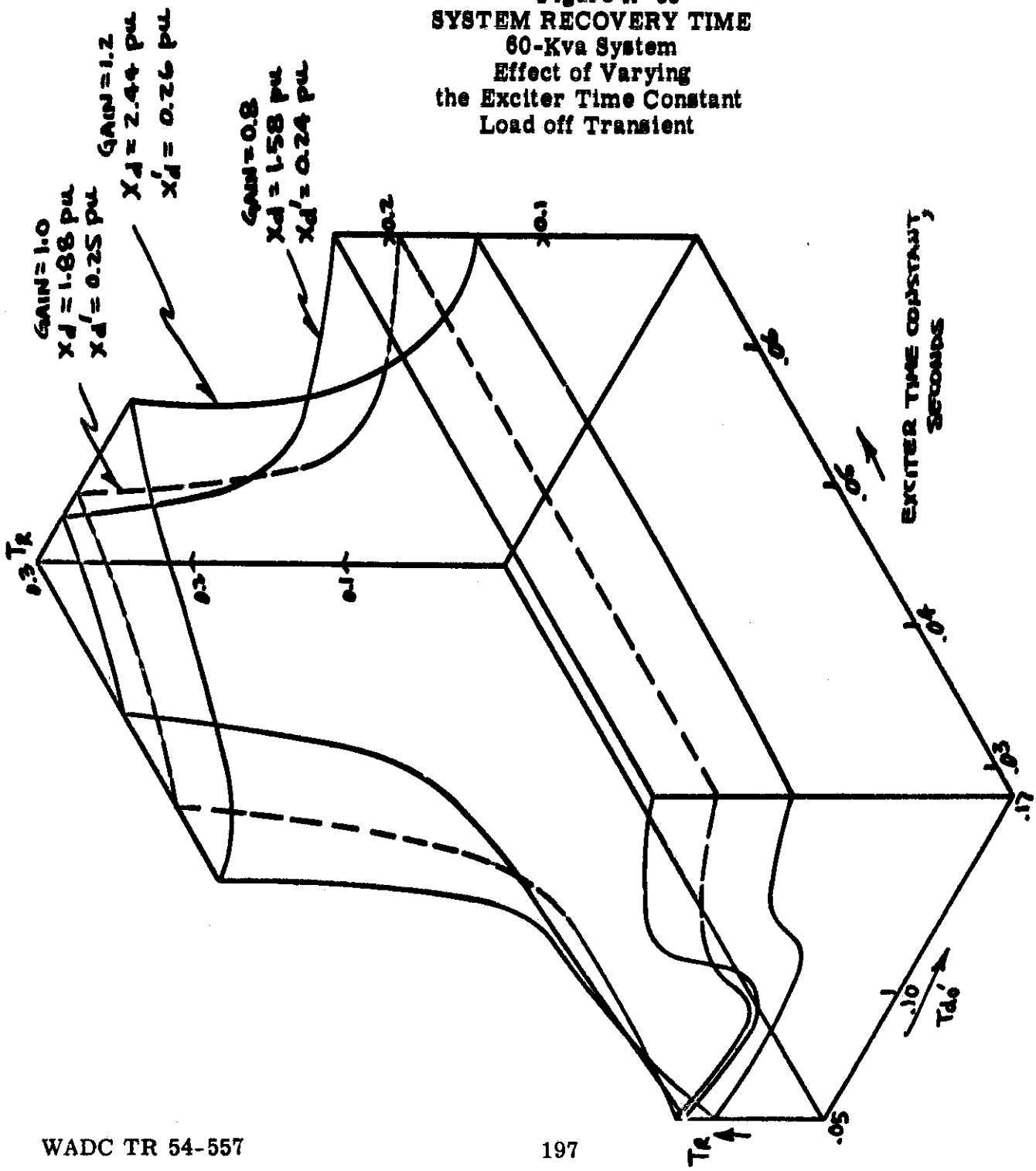

the a-c machine parameters are definitely of secondary effect. The excitation system, and primarily the voltage regulator, will determine to a great extent what the transient performance will be. However, if the stabilization circuits are such as to produce an under-damped system, we do see the machine parameters effecting the transient performance.

A-5 EXCITER REPRESENTATION

This section is added to the other material on the analogue computer to give a more complete understanding of the methods employed in the studies made of the various systems in Sections A-3 and A-4. In this section the exciter portion of the system is covered.

Most of the previous work given in the literature deals with d-c exciters which are separately-excited or are treated with shunt fields having constant impedance. Some work covers the addition of other fields (series, eddy-current effects, etc.), but the problem of a shunt field circuit using parametric forcing is not treated, either analytically or by analogue methods.

First the linear exciter will be covered and then the more complete circuit employing saturation will also be covered.

A-5-a Linear Exciter Representation - For the linear case the analogue representation used in this report was based on a rather simple circuit to start with. Figure A-54 shows the basic arrangement. The equations which describe this circuit are;

$$e_x = R_{cp} i_1 + r_1 i_1 + L_1 p i_1 \tag{1}$$

$$(e_x - R_{cp} i_1) = r_1 i_1 (1 + T_1 p) \tag{2}$$

$$r_1 i_1 = \left[\frac{e_x - R_{cp} i_1}{1 + T_1 p} \right] \tag{3}$$

Using a conventional time-delay circuit in the analogue, one can represent this equation (3) as shown in Figure A-55. The analogue equation is

$$e_o = \frac{-1}{1 + R_f C_f p} \left[\frac{R_3 e_1}{R_1} + \frac{R_3 e_2}{R_2} \right] \tag{4}$$

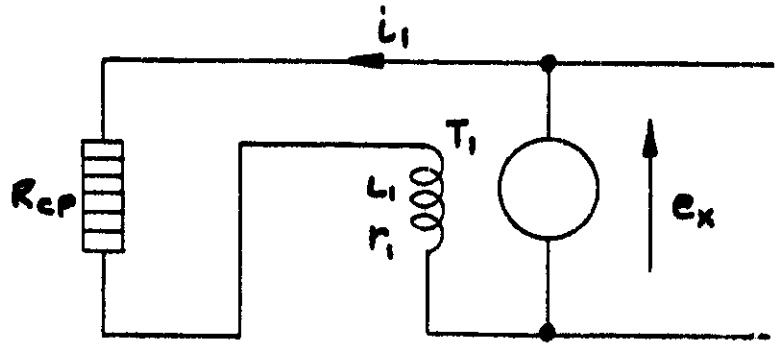

Figure A-54 Linear Exciter With Parametric Forcing

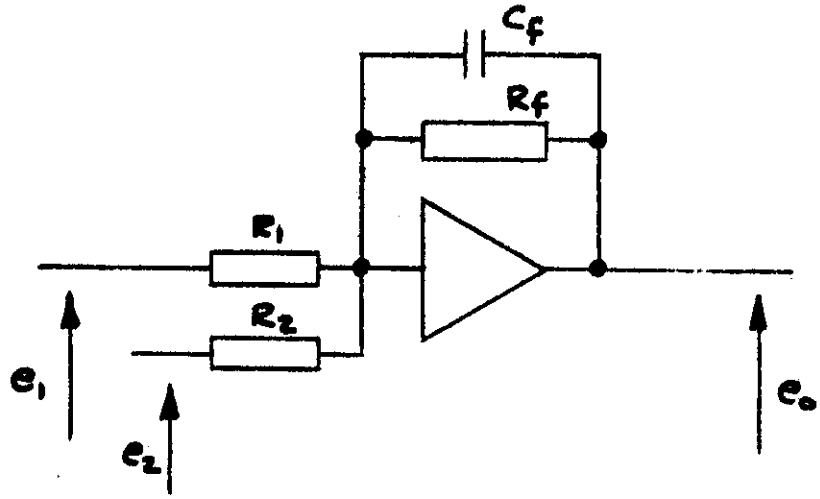

Figure A-55 Analogue Circuit of Simple Time Delay With Two Inputs

Comparing equations (3) and (4) the analogy is correct if the following identities are maintained:

$$\left.\begin{aligned} T_1 &= R_f C_f \\ e_x &= \left[\frac{R_3}{R_1}\right] e_1 \\ -R_{cp} i_1 &= \left[\frac{R_3}{R_2}\right] e_2 \\ -r_1 i_1 &= e_o \end{aligned}\right\} \qquad (5)$$

Note that if it is desired to vary the exciter time constant only, C_f is the element to change.

Next it is necessary to show just how to obtain the signal ($R_{cp} i_1$) which is to be fed into R_2 in the time delay circuit. First we must provide a current i_1 through the carbon pile in sufficient magnitude to properly simulate an actual current flow. This is necessary because the pile characteristics are to a degree a function of this current. Naturally, a d-c amplifier is far too small for such a task. Therefore, some means of power amplification must be employed. A cathode follower (in this case a number of 6AS7 triodes in parallel) is connected to the output of the time delay circuit. The carbon pile is connected in series with the cathode resistor. See Figure A-56. Note that the RC-network used for feedback on the delay amplifier is connected to the positive end of the cathode resistor. This is done to provide a fixed reference point with respect to i_1. If the connection were made to the cathode, the voltage that appears on the feedback network would include the changes in the carbon pile resistance R_{cp} and the field current i_1 .

Refer to the complete analogue for the 20-kva system, Figure A-9, amplifiers G and E. This is the same as the circuit in Figure A-56 above, except for the potentiometers. The extra amplifier (E) is necessary to cancel the $K_1 i_1$ signal.

Since it is seldom that a single field exciter would describe the actual case properly, it is necessary to use this shunt field current signal along with the others, summing them as so many positive and negative excitations to the exciter. This was shown in Figure A-32 in block diagram

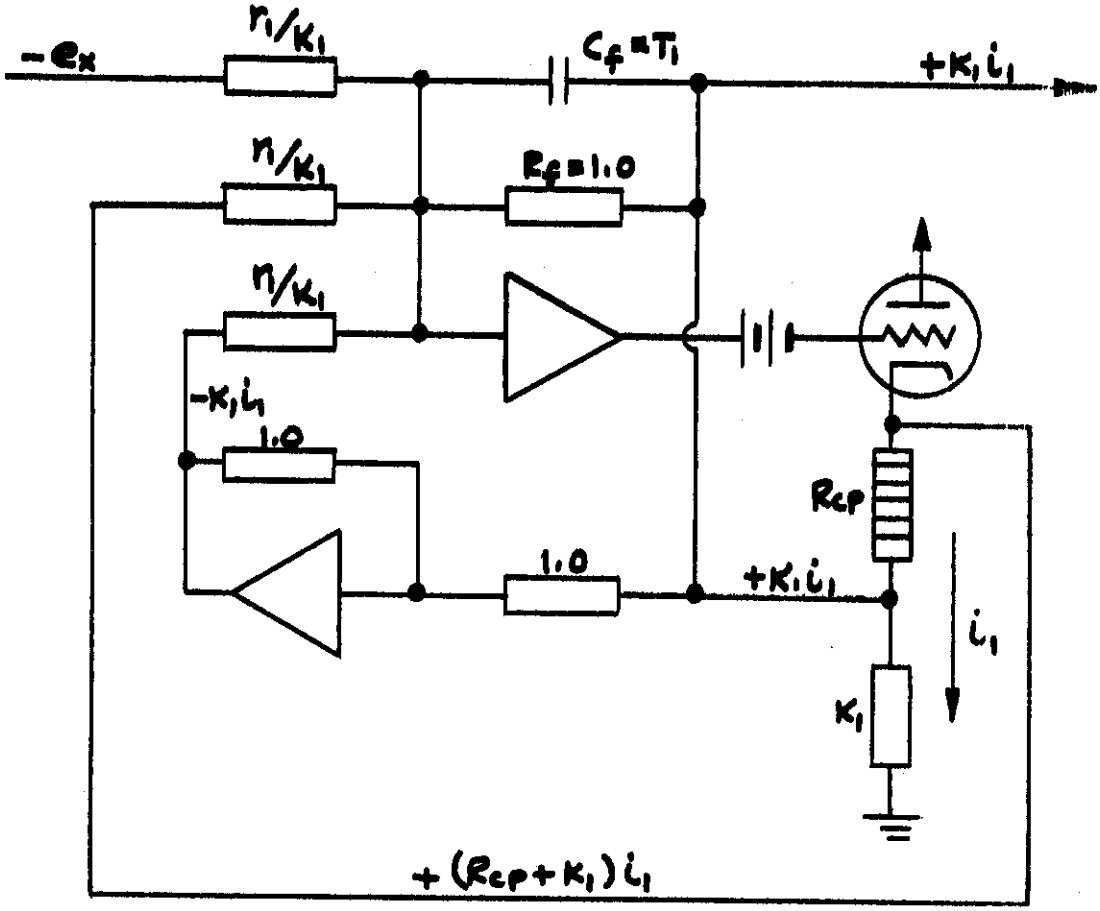

ANALOG: $$K_1 i_1 = \frac{-1}{1+T_1 p}\left[\frac{-K_1 e_x}{r_1} + \frac{K_1(R_{cp}+K_1) i_1}{r_1} - \frac{K_1^2 i_1}{r_1}\right]$$

ACTUAL: $$r_1 i_1 = \frac{e_x - R_{cp} i_1}{1 + T_1 p}$$

Figure A-56 Complete Analogue Circuit
For Linear Exciter With Parameter Forcing
(Single Shunt Field Only)

manner. It is not necessary to show here how this would be done in the analogue. Refer to any one of the complete analogues for this.

One circuit remains in the linear exciter, the circuit to simulate eddy-current effects. The relationship between the shunt field circuit and the eddy-current circuit is

$$i_2 = \frac{M_{21}/r_2 p i_1}{1 + T_2 p} \tag{6}$$

See Figure A-57 and also Figure A-6 . Refer to Chapter III and Appendix B-4 for other material on the subject of eddy-currents. This operation can be simulated in the manner shown in Figure A-58. This analogue circuit can be described as follows:

$$e_o = \frac{-1}{1+R_f C_f p} (R_f C_1 p_1 e_1) \tag{7}$$

Comparing equations (6) and (7) the analogy is correct if the following identities are maintained:

$$\left.\begin{aligned} T_2 &= R_f C_f \\ (M_{21}/r_1) i_1 &= R_f C_1 p_1 e_1 \\ -i_2 &= e_o \end{aligned}\right\} \tag{8}$$

A-5-b Exciter Representation With Saturation - The material that follows covers the type of simulation used in the three-phase system studies which is different from the method used in the single-phase system studies. The latter is described above and covers a more simplified circuit. This simulation is more complex and it also is more flexible, accounting for saturation as well as multiple fields, residual voltage, etc.

Block diagrams of

(1) the method used to sum to various excitations and

(2) the method to produce the field current in a voltage-fed circuit are given in Section A-4 as Figure A-32 and A-33, respectively.

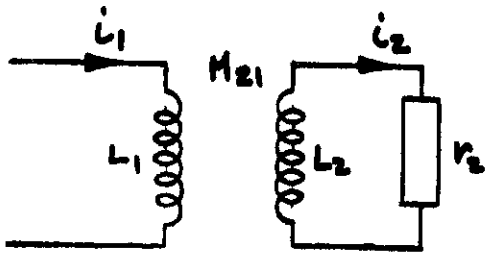

$$e_2 = M_{21} p i_1$$

$$e_2 = r_2 i_2 (1 + T_2 p)$$

$$i_2 = \frac{M_{21}/r_2 \; p \, i_1}{1 + T_2 p}$$

Figure A-57 Relationship Between Shunt Field Circuit and Eddy Current Circuit

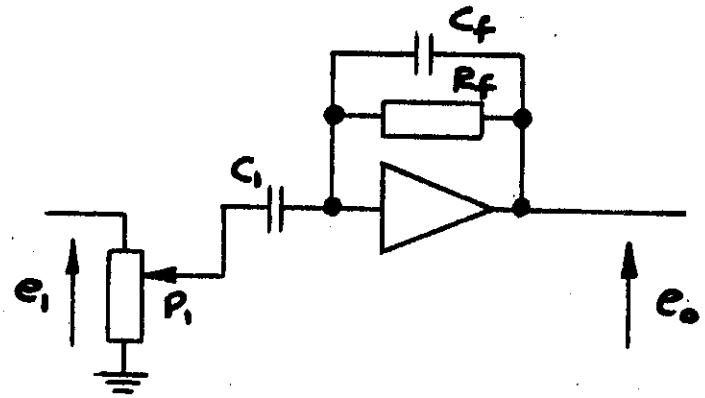

$$e_o = \frac{-1}{1 + R_f C_f p} R_f C_1 P_1 e_1$$

Figure A-58 Analogue Circuit For Eddy-Current Effect in d-c Exciters

(a) Field Currents

For most of the exciters used in aircraft systems the following equations will describe the shunt field circuit adequately,

$$e_x-(R_{cp}i_1 + r_1i_1) = p(L_1i_1 - M_{21}i_2 + M_{31}i_3) \tag{9}$$

Integrating both sides

$$\frac{e_x-(R_{cp}i_1 + r_1i_1)}{p} = L_1i_1 - M_{21}i_2 + M_{31}i_3 \tag{10}$$

Since the object is to obtain a signal proportional to shunt field current i_1 it is necessary to eliminate the two mutual terms. Thus

$$L_1i_1 = \frac{e_x-(R_{cp}i_1 + r_1i_1)}{p} + M_{21}i_2 - M_{31}i_3 \tag{11}$$

This same type of equation can be written for the eddy-current circuit

$$L_2i_2 = -\frac{r_2i_2}{p} + M_{21}i_1 + M_{32}i_3 \tag{12}$$

(b) Saturation

Saturation is taken into account in a number of ways;

(1) the shunt field current at no-load on the exciter may be non-linear, (a circuit similar to the one used for the a-c generator is used),

(2) effect of saturation in the interpoles is accounted for by a circuit which increases the series drop in the exciter faster than the series current increases. (This circuit is shown as amplifier I in both the 60-kva and the 40-kva analogues.)

(c) Other Fields

Series fields in the exciter can be taken into account by a proper change in the summation circuit and in the mutual terms in the field current circuits. Similarly, differential shunt circuits can also be added. Neither of these were used in any of the studies because of the extra complexity, but in many actual machines these are employed to improve performance.

BIBLIOGRAPHY FOR APPENDIX A

1. Harder, E. L., Solution of the General Voltage Regulator Problem by Electrical Analogy; AIEE Transactions, Vol. 66, 1947, pp. 815-825.

2. McCann, Osbon and Kirschbaum, General Analysis of Speed Regulators Under Impact Loads; AIEE Transactions, Vol. 66, 1947, pp. 1243-1252.

3. Carleton, J. T., Analysis of Rototral Voltage Regulators by Electrical Analogy; Proceedings of National Electronics Conference, 1948, pp. 272-278.

4. Carleton, J. T., Transient Behavior of the Two-Stage Rototral Main Exciter Voltage Regulating System as Determined by Electrical Analogy; AIEE Transactions, Vol. 68, 1949, pp. 59-63.

5. Meneley, C. A. and Morrill, C. D., Linear Electronic Analogy Computer Design; Proceedings of National Electronics Conference, 1949, pp. 48-63.

6. Bradley and McCoy, Driftless D-C Amplifiers; Electronics, April 1952, pp. 144-148.

7. Korn and Korn, Electronic Analogue Computers; (McGraw-Hill Book Company, Inc., New York, N. Y., 1952).

8. James, H. B., The Use of an Analogue Computer to Optimize the Transient Response of an Aircraft-Type Generator-Regulator System; AIEE Transactions, Applications and Industry, Vol. 73, November 1953, pp. 363-368.

9 Reswick, James B., Scale Factors for Analog Computers; Product Engineering, March 1954, 197-201.

B-1-d Derivation of Equations - From Park's equations with armature resistance, armature transients and subtransient effects neglected:

$$e_d = -\psi_q$$
$$e_q = \psi_d \qquad (1)$$
$$e_f = p\psi_f + r_f i_f$$

The flux-linkages are:

$$\psi_d = -x_d i_d + x_{ad} i_f$$
$$\psi_q = -x_q i_q \qquad (2)$$
$$\psi_f = -x_{ad} i_d + x_{ff} i_f$$

Eliminating i_f and simplifying:

$$e_q = G(p)E - x_d(p)\, id \qquad (3)$$
$$e_d = x_q i_q \qquad (4)$$

where: $G(p) = \dfrac{1}{1 + T_{do}' p}$; $x_d(p) = \dfrac{x_d + x_d' p T_d' o}{1 + T_{do}' p}$

$$E = \frac{x_{ad} e_f}{r_f} \quad ; \quad T_{do}' = \frac{x_{ff}}{r_f}$$

$$x_d' = x_d - \frac{x_{ad}^2}{x_{ff}}$$

Equations 3 and 4 are the desired relations.

B-1-e Steady State Conditions - Prior to removal of load, the machine is operating in the steady-state at some given power factor (cosØ). Conditions are given by the diagram shown in Figure B-1-1.

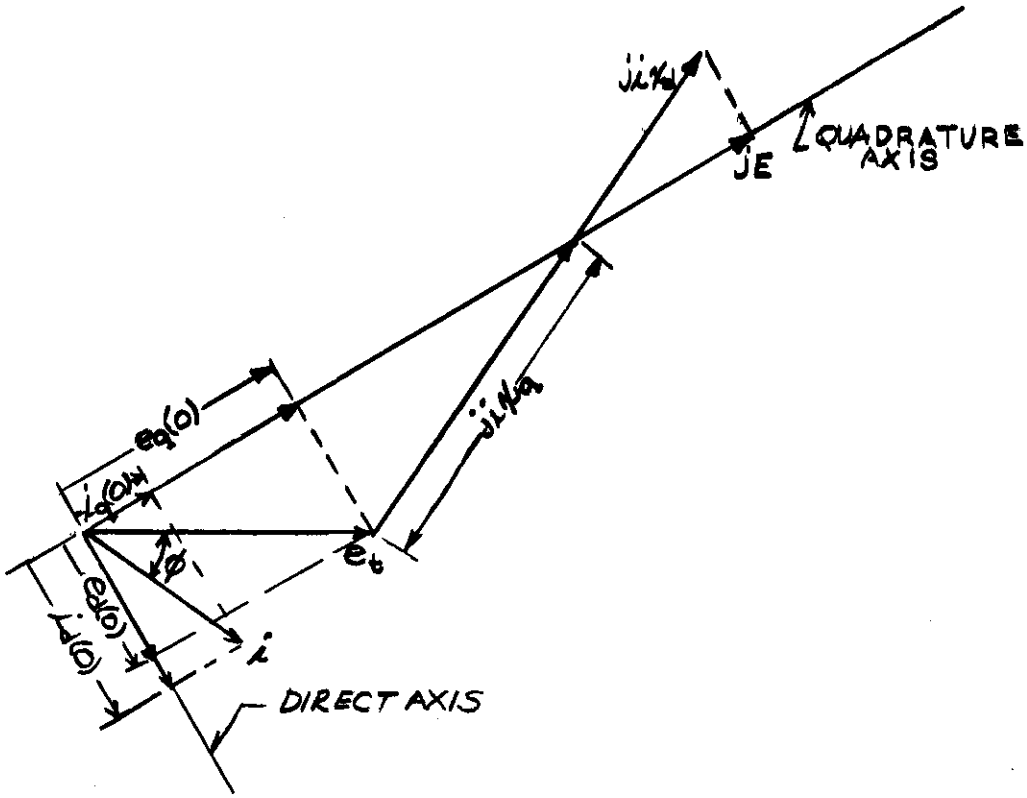

Figure B-1-1 Steady-State Vector Diagram

B-1-f Opening Switch and Use of Incremental Voltage - The equations to be solved are put in Laplace Transform notation by replacing p with s, since zero initial conditions apply. These equations are:

$$E_q(s) = G(s)\, E(s) - x_d(s)\, I_d(s)$$

$$E_d(s) = x_q I_q\,(s)$$

under the conditions that $i_d(t)$ and $i_q(t)$ go from the steady-state values of $i_d(0)$ and $i_q(0)$, respectively, to zero at $t = 0$ and $E(t)$ is a given function of time.

To solve these, use will be made of the principle of superposition. First, the change in voltage will be calculated rather than the total voltage. Thus, $\Delta E_d(s)$ and $\Delta E_q(s)$ will be the Laplace transforms of the

incremental direct-and quadrature-axis voltages, respectively. In solving for $\Delta E_d(s)$, the effect of opening the switch will be replaced by applying a negative step of current. In solving for $\Delta E_q(s)$, superposition will be applied again. Let,

$$\Delta E_q(s) = \Delta E_{q1}(s) + \Delta E_{q2}(s)$$

where: $\Delta E_{q1}(s) = -x_d(s)\ I_d(s)$, the component of incremental quadrature-axis voltage due to opening the switch and $\Delta E_{q2}(s) = G(s)\ \Delta E(s)$, the component of incremental quadrature-axis voltage due to change in excitation voltage. The total quadrature-and direct-axis voltage is obtained by adding the initial voltages to these increments. The envelope of terminal voltage is obtained by combining these total components.

B-1-g Solution for Direct-Axis Component of Terminal Voltage - Equation (4) as a function of time is:

$$e_d(t) = x_q i_q(t)$$

Effect of opening switch is given by:

$$i_q(t) = i_q(0) - i_q(0)\ u(t)$$

where: $u(t) = 0$ for $t < 0$
$u(t) = 1$ for $t > 0$

Therefore,

$$e_d(t) = x_q\left[i_q(0) - i_q(0)\ u(t)\right] \qquad (5)$$

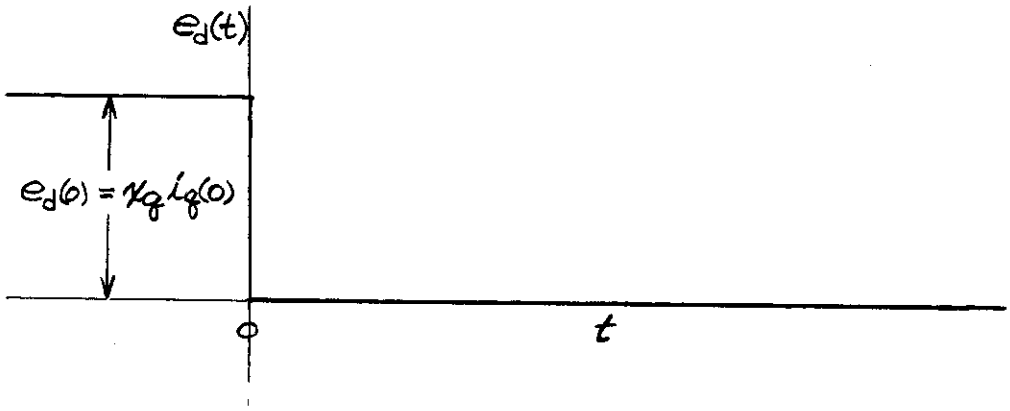

Figure B-1-2 Direct-Axis Component of Terminal Voltage

B-1-h Solution of Quadrature-Axis Component of Terminal Voltage

(i) Component of Incremental Quadrature-Axis voltage due to opening switch with excitation voltage constant.

$$\Delta E_{q1}(s) = -x_d(s)\, I_d(s)$$

Here:
$$I_d(s) = \mathcal{L}\left[-i_d(0)\, u(t)\right] = -\frac{i_d(0)}{s}$$

and
$$x_d(s) = \frac{x_d + x_d'\, T_{do}'(s)}{1 + T_{do}'s}$$

Therefore:
$$\Delta E_{q1}(s) = \left[\frac{x_d + x_d'\, T'_{do}s}{1 + T'_{do}s}\right] \frac{i_d(0)}{s}$$

Expanding this in a partial fraction expansion and taking the inverse transform yields:

$$\Delta e_{q1}(t) = i_d(0)\left[x_d - (x_d - x_d')\, e^{-t/T_{do}'}\right]; t > 0 \quad (6)$$

which is graphically shown in Figure B-1-3.

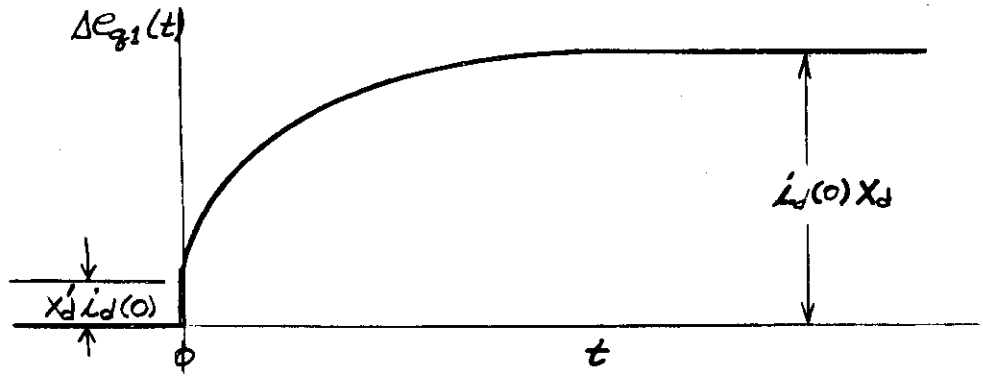

Figure B-1-3 Component of Quadrature-Axis Voltage due to Opening Switch

(ii) Component of Incremental Quadrature-Axis voltage due to change in excitation voltage.

$$\Delta E_{q2}(s) = G(s)\ \ \Delta E(s)$$

Assume:
$$\Delta E(t) = -k(t-t_1)\ u(t-t_1)$$

$$\Delta E(s) = \mathcal{L}\, e(t) = \frac{-k}{s^2}$$

$$G(s) = \frac{1}{1 + T_{do}'s}$$

Therefore:

$$E_q2(s) + \left[\frac{1}{1 + T_{do}'s}\right] \left[\frac{-k}{s^2}\right]$$

Expanding into partial fractions and taking the inverse transform:

$$\Delta e_q2(t) = -k \left\{(t-t_1) - T_{do}' \left[1-e^{\frac{-(t-t_1)}{T_{do}'}}\right]\right\}; \; t > t_1 \qquad (7)$$

which is shown in Figure B-1-4.

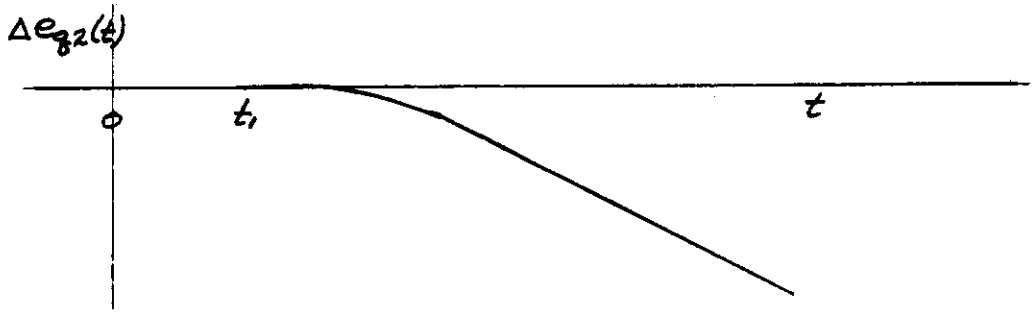

Figure B-1-4 Component of Quadrature-Axis Voltage due to Change in Excitation Voltage.

(iii) Total Quadrature-Axis Voltage

$$e_q(t) = e_q(0) + \Delta e_{q1}(t) + \Delta e_{q2}(t)$$

$$e_q(t) = e_q(0) + i_d(0) \left[x_d - (x_d - x_d') \; e^{-t/T_{do}'}\right]$$

$$-k \left\{(t-t_1) - T_{do}' \left[1-e^{\frac{-(t-t_1)}{T_{do}'}}\right]\right\} \qquad (8)$$

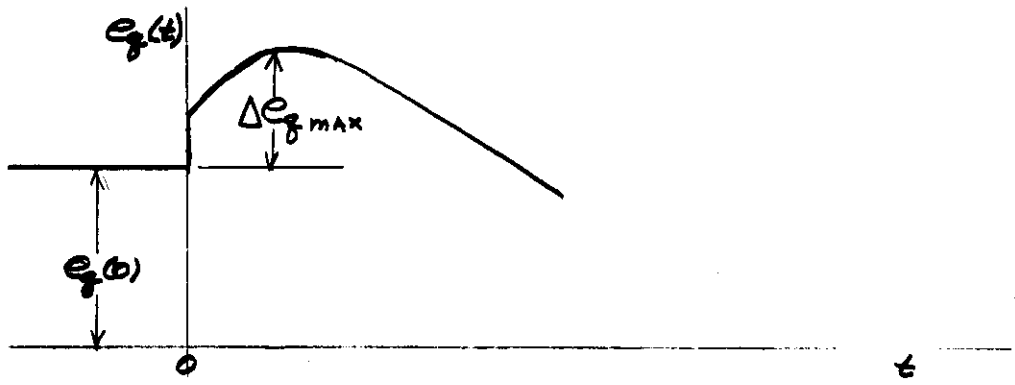

Figure B-1-5 Total Quadrature-Axis Voltage

B-1-i Terminal Voltage - The terminal voltage, e_t, is determined by using the inverse transformation from direct and quadrature-axis components to actual quantities.

$$e_t = e_a = e_d \cos\omega t + e_q \sin\omega t + e_o$$

Considering only the magnitude of the terminal voltage:

$$|e_t| = \sqrt{e_d^2 + e_q^2}$$

Since the expression for e_d and e_q are distinct for before and after the switching operation, the terminal voltage is calculated separately for these two periods. For $t<0$, e_t is given by the steady-state vector diagram and has been assumed to be 1.0 per unit. For $t>0$, $e_d = 0$, consequently, $|e_t| = e_q$.

Therefore the maximum value of $|e_t|$ for $t>0$ is identical with the maximum value of the quadrature-axis component of terminal voltage, e_q maximum.

An expression for the maximum terminal voltage is obtained by differentiating equation (8), setting the results equal to zero and solving for the time of the maximum in equation (8), the following relation for the maximum terminal voltage results:

$$e_{t_{max}} = e_q(0) + i_d(0)\, x_d - k \left\{ T_{do'} \ln \left[\frac{(x_d - x_{d'})}{k} \frac{i_d(0)}{T_{do'}} + e^{t_1/T_{do'}} \right] - t_1 \right\} \qquad (9)$$

B-2 RESUMÉ OF KILGORE'S EQUATIONS FOR CALCULATING SYNCHRONOUS MACHINE CONSTANTS.

The following is a summary of the equations derived by Kilgore in his paper "Calculation of Synchronous Machine Constants - Reactances and Time Constants Affecting Transient Characteristics", AIEE Transactions, 1931. The equations given here cover salient-pole machines with laminated field poles.

The positive sequence reactances are divided into two components, one of which is the armature leakage reactance (x_ℓ).

B-2-a Reactances

(1) Synchronous Reactances (x_d, x_q)

$$x_d = x_\ell + x_{ad}$$

$$x_q = x_\ell + x_{aq} \approx 0.6\, x_d$$

(2) Transient Reactances (x_d', x_q')

$$x_{du}' = x_\ell + x_F'$$

$x_d' = F_{st} x_{du}'$; where $F_{st} = 0.88$, an empirical factor.

x_q' is not calculated by Kilgore since no field winding exists in the quadrature axis of most machines.

$$x_q' = x_q$$

In some studies it is assumed that $x_q' = x_d'$

(3) Subtransient Reactances (x_d'', x_q'')

$x_d'' = x_\ell + x_{Dd}'$; for machines with dampers

$x_d'' = x_d'$; for machines without dampers

$x_q'' = x_\ell + x_{Dq}'$; for machines with dampers

$x_q'' = x_q'$; for machines without dampers.

(4) Negative-Sequence Reactance (x_2)

$$x_2 = 1/2\ (x_d'' + x_q'')$$

(5) Zero-Sequence Reactance (x_o)

See section B-2-b-(5)

B-2-b Component Reactance

Quoting from the reference paper, "All the component reactances are defined as a product of a reactance factor (X) and a specific permeance (λ) for the given component, multiplied by flux distribution coefficients when necessary.

The specific permeance (λ) is defined as the effective flux per pole per inch of core length produced by unit ampere terms per pole.

The reactance factor (X) used here is a group of terms common to all the reactance formulas, but it is chosen in such a way as to have definite physical significance. It is the per cent reactance for unit specific permeance, or the per cent of normal voltage induced by a fundamental flux per pole per inch numerically equal to the fundamental armature ampere terms at rated current. "

(1) Armature Leakage Reactance [6] (x_ℓ)

$$x_\ell = X\ (\lambda i + \lambda b + \lambda e)$$

(2) Reactances of Armature Reaction (x_{ad}, x_{aq})

$$x_{ad} = XC_{dl}\lambda a$$

$$x_{aq} = XC_{ql}\lambda a$$

(3) Effective Field Leakage Reactance (x_F')

$$x_F' = X\lambda_F'$$

(4) Effective Damper Winding Leakage Reactances (x_{Dd}', x_{Dq}')

$$x_{Dd}' = X\lambda_{Dd}$$

$$x_{Dq}' = X\lambda_{Dq}$$

(5) Zero-Sequence Reactance (x_o)

$$x_o = X(\lambda_{lo} + \lambda_{Bo} + 0.2\lambda_e)$$

B-2-c Flux Distribution Factors [7]

Kilgore defines the following coefficients: C_1 is the ratio of the fundamental to the actual maximum of the field form. (The field form is the wave of flux density due to the field only.) The pole constant (C_p) is the ratio of average to maximum of field form. The ratio of equivalent field to armature ampere turns (C_m) is the ratio of fundamental air gap flux produced by the fundamental of armature mmf to that produced by the field for the same maximum mmf. C_{dl} is the ratio of the fundamental air gap flux produced by the direct-axis armature current to that which would be produced with a uniform gap equal to the effective gap over the pole center. C_{ql} is the corresponding coefficient for the quadrature-axis.

C_1 determined by flux map.

C_p determined by flux map.

$$C_m = \frac{(\alpha\pi + \sin\alpha\pi)}{4\sin\alpha\frac{\pi}{2}} \quad \text{or flux plot.}$$

$$C_{dl} = C_m C_l$$

$$C_{ql} = \left[\frac{4\alpha + 1}{5} - \frac{\sin\alpha\pi}{\pi}\right] \quad \text{or flux plot.}$$

B-2-d Reactance Factor, X

In terms of turns, frequency and rated phase voltage and current:

$$X = 100\% \frac{Iph}{Eph} \ell f m P \left[q\left(\frac{n_s}{c}\right) k_p k_d\right]^2 x10^{-8}$$

In terms of effective ampere conductors per inch (Ak_p) and the air gap density (B_g)

$$X = 100\% \left[\frac{k_d}{\sqrt{2}C_1}\right]\left[\frac{Akp}{Bg}\right]$$

B-2-e Specific Permeances

(1) Specific Permeances Related to Leakage Reactance

(a) Specific Permeance for Slot, Tooth Tip and Zig-zag Leakage ($\lambda 1$)

$$\lambda 1 = C_x \frac{20}{mq}\left[\frac{h2}{b_s} + \frac{h1}{3b_s} + \frac{b_t^2}{16\tau_s} + 0.35\frac{bt}{\tau s}\right]$$

$$\text{where: } C_x = 1/4\left[\frac{3y}{mq} + 1\right]\frac{1}{k_p^2 k_d^2}$$

(b) Specific Permeance for Belt Leakage (λ_B)

$\lambda B = 0$ for three-phase

(c) Specific Permeance for End Winding Leakage (λ_e)

$$\lambda_e = \frac{4}{\ell}(2\ell_{e2} + \ell_{el})$$

(2) Specific Permeance of the Air Gap (λ_a)

$$\lambda_a = 3.19\left[\frac{2D}{P_g}\right]$$

(3) Specific Permeance Related to Transient Reactance ($\lambda_{F'}$)

$$\lambda_{F'} = C_{dl}\lambda_a - \frac{\frac{\pi}{4} C_1^2 \lambda_a^2}{\frac{\pi}{2} C_p\lambda_a + \lambda f}$$

where λ_F is the specific permeance for field leakage which is the sum of two components, the side leakage λ_{Fs} and the end leakage λ_{Fe}. That is:

$$\lambda_F = \lambda_{Fs} + \lambda_{Fe}$$

(a) $$\lambda_{Fs} = (3.19)\frac{4}{3}\left[\frac{3(h_h + g - .055\tau_r)}{\tau_r - bh} + \frac{h_{f1} + 3h_{f2} + 0.1\tau_r\left(1 - \frac{10}{p}\right)}{\frac{\pi}{p}(D_r - 2h_h - 0.4h_{f1}) - b_p}\right]$$

(b) $$\lambda_{Fe} = 3.19\left[\frac{4(\ell_h - \ell) + 2h_{f1} + 0.5b_p}{\ell}\right]$$

NOTE: Kilgore points out that a flux map will give accurate results for λ_{Fs} while the above equation is an approximation. Experience on aircraft generators has shown that the results from the above equation differ considerably from that obtained by a flux map. This is particularly true when the underneath side of the pole tip is notched or beveled for wedge fittings. It is recommended that a flux map be made.

(4) Specific Permeance Related to Direct-Axis Transient Reactance (λ_{Dd})

$$\lambda_{Dd} = \left[\cos\frac{(n_b - 1)\tau_b}{\tau_r}\ \frac{\pi}{2}\right]\left[\frac{(\lambda b + \lambda pt)\lambda F}{\lambda b + \lambda pt + \lambda F}\right]$$

where:

$$\lambda_b = 6.38\left[0.5 + \frac{h_{b2}}{b_{b2}} + \frac{h_{b1}}{3b_{b1}}\right]$$

and: $$\lambda_{pt} = 6.38\left[\frac{b_h - \tau_b(n_b - 1)}{3g'}\right]$$

Note: Use dimensions of the slot and bar next to the pole tip. For round bars, use 0.62 instead of $\frac{h_{b1}}{3b_{b1}}$.

(5) Specific Permeance Related to Quadrature-Axis Transient Reactance (λ_{Dq})

$$\lambda_{Dq} = \frac{20\tau_b}{\tau_r}\left[0.5 + \frac{h_{b1}}{3b_{b1}} + \frac{h_{b2}}{b_{b2}} + \frac{g}{\tau_b}\right]$$

Note: Use dimensions of the slot and bar in the pole center. For round bars use 0.62 instead of $\frac{h_{b1}}{3b_{b1}}$

(6) Specific Permeances Related to Zero Sequence Reactance

(a) Specific Permeance for Slot and Tooth Tip Leakage (λ_{lo})

$$\lambda_{lo} = \left[\lambda_l \left(\frac{k_{xo}}{k_x}\right) + \left(\frac{20}{mqk_p^2 k_d^2}\right) \left(\frac{h_1 + 2h_3}{12bs}\right)\right]$$

where: $k_{xo} = \left[\frac{3y}{mq} - 2\right]$, $k_x = \left[\frac{3y}{mq} + \frac{1}{4}\right]$

(b) Specific Permeance for Belt Leakage (λ_{Bo})

$$\lambda_{Bo} = \left[\frac{k_{xo}}{k_x}\right]\lambda_{Dq}, \text{ for machines with dampers.}$$

$$\lambda_{Bo} = \frac{k_{xo}}{k_p^2} \ (.07\lambda_a), \text{ for machines with no dampers.}$$

B-2-f Time Constants

(1) Open-circuit Time Constant (T_{do}')

$$T_{do}' = \frac{L_f}{r_f}$$

where: $L_f = N_p^2 P \ell 10^{-8} \left(\frac{\pi}{2} C_p \lambda_a + \lambda_F\right)$

(2) Short-circuit Transient Time Constant (T_d')

$$T_d' = \frac{x_d'}{x_d} T_{do}'$$

(3) Armature Time Constant (T_a)

$$T_a = \left[\frac{x_2}{2\pi f r_a}\right]$$

B-2-g Symbols Used in Appendix B-3

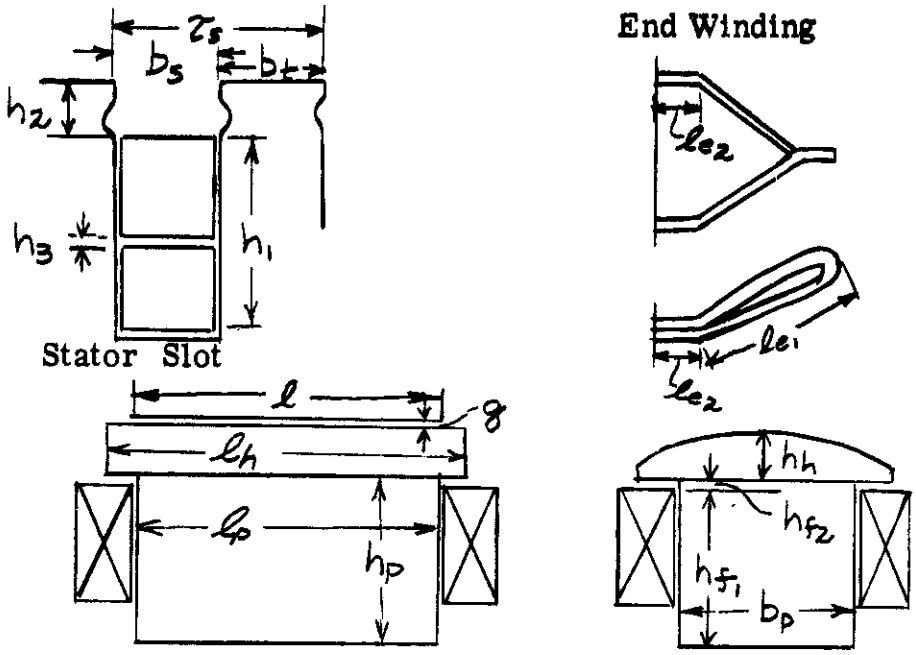

Figure B-2-1 Symbols Representing Machine Dimensions

A - ampere conductors per inch (amperes per slot÷ slot pitch)
b_{b1} - width of damper bar
b_{b2} - width of slot above damper bar
Bg - air gap density over pole center (at rated voltage)
B_1 - maximum fundamental density at rated voltage
D - inside diameter of armature (armature bore)
E_{ph} - rated phase voltage (phase winding voltage)
f - rated frequency
F_{st} - ratio of saturated to unsaturated transient reactance (an empirical constant used here as 0.88)
g - actual (single) air gap in pole center
g' - effective air gap, including increase in gap due to stator slots and vents and end fringing
h_{b1} - depth of damper bar
h_{b2} - depth of slot above the damper bar
I_{ph} - rated phase winding current
k_d - distribution factor for stator winding
k_p - chord factor of the stator winding

k_x - reduction of slot reactance due to chording
k_{xo} - reduction of zero sequence slot reactance due to chording
L_f - total self inductance of the field
m - number of phases
n_b - number of damper bars per pole
n_s - number of conductors per slot
N_p - number of field turns per pole
P - number of poles
q - slots per phase per pole
r_f - field resistance in ohms at 75 deg. cent.
X - reactance factor, per cent reactance for unit specific permeance
y - coil throw (number of slots spanned)
α - "pole embrace" ratio of pole arc to pole pitch
λ - "specific permeance" effective flux per pole per inch of length for unit ampere turns.
τ - pole pitch on stator diameter
τ_b - pitch of damper bars
τ_r - pole pitch on rotor diameter

B-3 A-C GENERATOR ELECTRICAL MACHINE CONSTANTS AS AFFECTED BY DESIGN VARIATIONS.

Some simplifying assumptions in the design calculation will be made and the machine constants and characteristics will be determined for eight different machines. The following variations will be studied:

(a) length of the air gap,

(b) the ratio of copper to magnetic material,

(c) the number of armature conductors, and

(d) the cross-sectional dimensions keeping the same configuration proportions.

All new designs are similar to a common existing machine, referred to hereafter as the "reference" machine. It is rated at: 60 kva, 120/208 volts, 5400/6000 rpm, and 360/440 cps. In addition, it must be capable of delivering 150 per cent load at .75 power factor and minimum speed for five minutes. In all cases, the new designs have the reference machine rating. The stack length is adjusted to give the proper output voltage.

The designs considered here are for salient-pole machines. An extension of the work could include distributed-field windings. It is also important to point out that these machines are for blast-air cooling.

B-3-a Variation of Effective Air-Gap Length - Assumptions for Air-Gap Calculations:

(a) The reference machine has an actual air-gap length of .030 inches on one side. The calculation for the smaller gap was made at .0185 inches, and for the larger gap at .043 inches.

(b) The field form is identical with that of the reference machine. For the reduced air-gap calculation, this necessitates increasing the pole enclosure and a substantial reduction of the pole-tip air-gaps. For the increased air-gap calculation, the converse is required. Flux plots were made to assure that practical poles could be built with this assumption.

(c) The armature punchings and windings are identical with the refer-

ence machine.

(d) All designs are based upon a 150 per cent load, at zero power factor and at minimum speed. This requires more excitation than the specification requirement of .75 power factor for the reference machine. It is a simplifying assumption, but should serve as a satisfactory base condition, since all designs are compared at the same load.

(e) It is assumed that the reference machine field ampere-turns, for the load mentioned above, may be applied on the new designs and cause the same temperature rise. The cross-sectional dimensions are identical, but differences in stack length may slightly affect the heat conducted out to the air stream through the pole body. The armature heating is much easier to control, since a large volume of air may be circulated over the outside diameter.

Air-Gap Calculation Procedure:

The calculating procedure for the air-gap variations is given below to illustrate the methods used.

(a) A no-load and zero-power-factor saturation curve was calculated for the reference machine at minimum speed. Also, machine constants, x'_d , and T'_{do} were calculated using L. A. Kilgore's and P. L. Alger's papers as references. Close agreement with test values was obtained. The no-load saturation curve at minimum speed is then corrected for increased pole leakage at 150 per cent load and shown as curve A in Figure B-3-1.

(b) For the 133.3 per cent effective air-gap calculation, as an example, a new air-gap line is drawn with 33.3 per cent greater ampere-turns for a particular voltage then that of curve A. The saturation ampere-turns are then taken from curve A and added to the new air-gap line, giving curve B.

(c) The final no-load saturation curve can be drawn when the new stack length is determined. First, the ampere-turns AT_1 necessary to generate e_p is calculated as the total ampere-turns minus the demagnetizing ampere-turns. Two equations can be written relating e_p to stack length. They are:

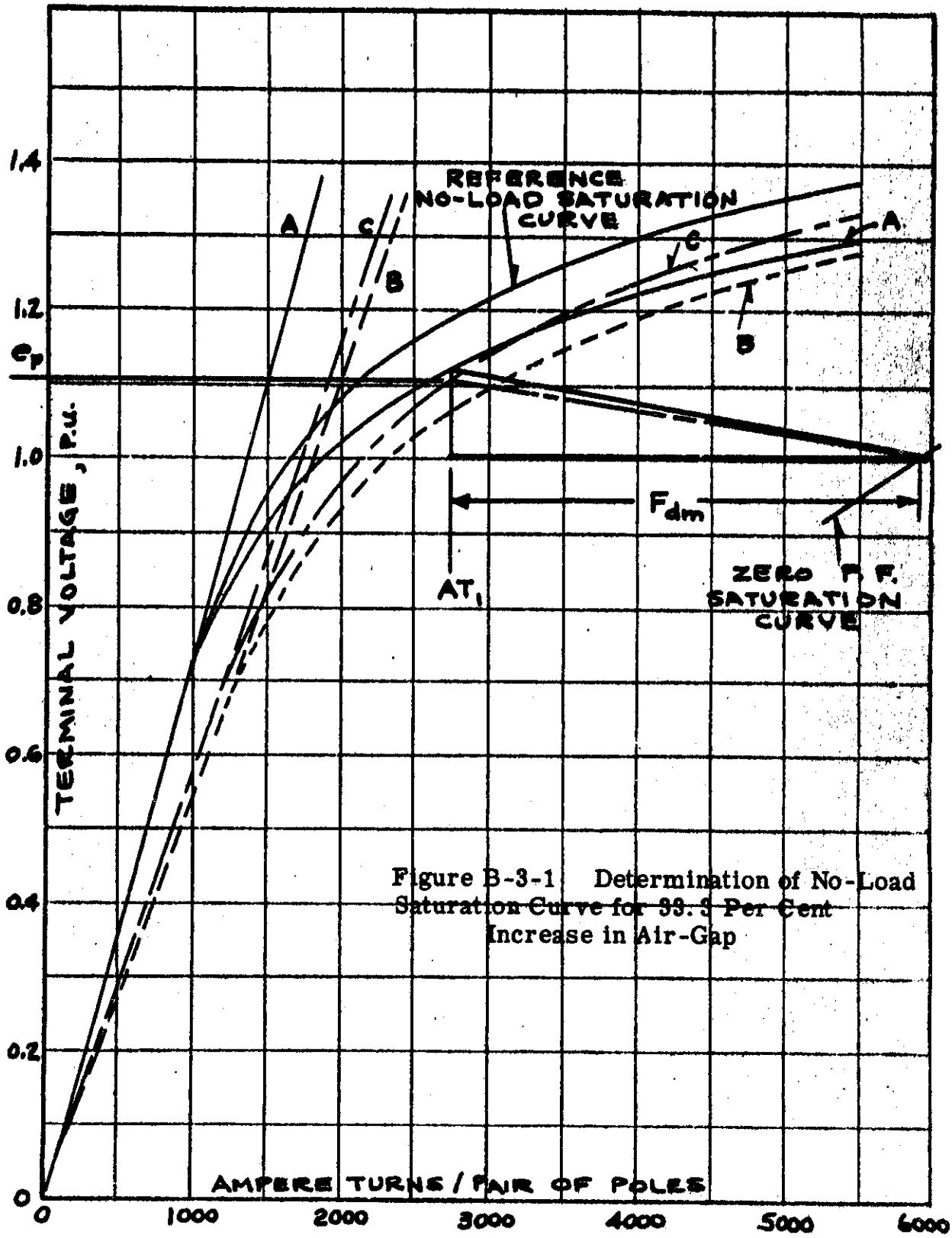

Figure B-3-1 Determination of No-Load Saturation Curve for 33.3 Per Cent Increase in Air-Gap

(1) $e_p = e_o + 1.5\, x_\ell = e_o + K_a + K_b \ell$

(2) $e_p = e_1 \, \ell/\ell_o$

where: e_p is per cent rated voltage plus x_ℓ

e_o is per cent rated voltage

e_1 is per cent voltage from curve B at ampere-turns AT_1

x_ℓ is per cent armature leakage reactance drop

ℓ is the new design stack length

ℓ_o is the reference machine stack length

K_a and K_b constants from machine dimensions times 1.5

The new stack length ℓ is obtained by solving equations (1) and (2). The final saturation curve C may be drawn by multiplying curve B by ℓ/ℓ_o.

(d) Curve C is for 360 cps. The machine constants are calculated at the nominal frequency of 400 cps. Curve C can be multiplied by 400/360 to give the 400-cps saturation curve.

B-3-b Variation of the Ratio of Copper to Magnetic Material - Assumptions for the Ratio of Copper to Magnetic Material Calculations:

(a) A calculation is made for a pole body 85 per cent of the width of that of the reference machine, and another at 115 per cent. The armature slots are kept the same size and the number adjusted to give a balanced magnetic circuit. This results in a 15.3 per cent increase for the narrow-pole design, and a 15.3 per cent decrease for the wide-pole design.

(b) The maximum field ampere-turns are assumed to equal that of the reference machine times the ratio of the new winding cross-section to that of the reference machine cross-section.

(c) The winding cross-section is obtained, on the slender-pole machine,

for example, on the following basis: since there is more winding space available than on the reference machine, the cross section may be increased, keeping the same current density. The additional copper must also be cooled, so it is assumed that the temperature rise will be the same as the reference machine's if the ratio of ventilating space to copper is kept constant. Figure II-12 shows how this may be done in practice.

(d) The field form is assumed to be identical with that of the reference machine.

The calculating procedure for obtaining the saturation curves is similar to that described for the air-gap calculations.

B-3-c Variation of Armature Conductors - Assumptions for Variation of Conductors Calculations:

(a) Conductors per slot is the same as that of the reference machine, while the number of slots is changed to 115.3 per cent. Another calculation is made for 84.7 per cent of the slots of the reference machine.

(b) The cross-sectional area of the teeth, per inch of stack, is kept the same as that of the reference machine.

(c) The field structure is unchanged except for stack length and it is assumed the temperature rise will be the same as that of the reference machine with the same ampere-turns applied.

(d) The field form remains the same as that of the reference machine.

(e) The core cross-sectional area is the same as that of the reference machine.

Obtaining the no-load saturation curve is carried out in a manner similar to that for the variation of air-gap study.

B-3-d Variation of Dimensions Perpendicular to the Shaft Holding the Same Proportions - Assumptions for the "Variation of Dimensions Perpendicular to the Shaft" Calculations:

(a) One calculation was made where each dimension was 107.5 per

cent of that for the reference machine. This gives 15.3 per cent increase in the areas in a plane perpendicular to the shaft. Another calculation was made with the dimensions at 92 per cent, giving a 15.3 per cent decrease in areas.

(b) Considering the increased dimension calculation, for example, the field winding is assumed to have the same temperature rise as the reference machine when it has 115.3 per cent of the reference machine ampere-turns applied. This is the same assumption discussed previously where the cooling-air cross-sectional area is kept proportional to copper.

(c) The effective air-gap length is taken at 107.5 per cent of that for the reference machine in one calculation, and 92 per cent in the other. If the stack length is not changed, this results in the same permeance for the air-gap because the pole-face area is increased proportionately.

(d) The field form is identical with that of the reference machine.

(e) The number of slots are increased 15.3 per cent in one calculation and decreased the same amount in the other. This can be done and still maintain the same flux densities in the teeth as that of the reference machine.

To obtain the no-load saturation curve, the reference machine corrected curve was taken, a correction made for the 7.5 per cent increase in flux (in the case of the 107.5 per cent dimensions), one for 7.5 per cent increase in the length of the flux path, and another for a 15.3 per cent increase in the number of armature conductors. Finally, the new stack length is determined and a final correction is made for the decreased length. The remainder of the calculations are similar to those discussed previously.

B-3-e Calculation of Machine Constants - The assumptions and calculations which have been discussed set the physical dimensions and windings of the respective designs. It is possible to calculate the machine constants using Kilgore's equations which are summarized in Appendix B-2.

B-3-f Results - Tables B-1 and B-2 summarize the machine and design constants for the various new designs and the reference machine. The

TABLE B-1

Design and Machine Constants
at 400 CPS Rated Load

	Ref. Gen.	Air-Gap		Ratio Copper to Iron	
		133.3%	66.6%	85% Fe	115% Fe
X	.0141	.0147	.0133	.0174	.0118
λ_i	3.69	3.59	3.90	3.05	4.78
λ_e	1.84	1.76	1.95	1.96	1.54
x_ℓ	.078	.078	.078	.087	.075
λ_a	143.00	107.00	214.00	143.00	143.00
x_{ad}	1.80	1.42	2.55	2.33	1.51
λ_{FS}	6.17	5.98	5.98	6.74	5.98
λ_{FE}	2.41	2.31	2.19	2.48	2.10
x'_F	.180	.171	.230	.256	.158
x'_d	.259	.249	.308	.343	.236
x_d	1.88	1.49	2.63	2.34	1.46
L_f	.0525	.0418	.0724	.0767	.0359
r_f	.500	.516	.484	.600	.419
T'_{do}	.105	.081	.150	.128	.086
Gen. Gain	.082	.064	.116	.089	.074
Stack	3.37	3.52	3.18	3.16	4.01
Gen. $D^2\ell$	318.00	332.00	300.00	286.00	394.00
Exc. $D^2\ell$	66.90	69.00	64.70	80.20	56.00
Total $D^2\ell$	385.00	401.00	365.00	366.00	450.00

TABLE B-2

Design and Machine Constants at 400 CPS Rated Load

	Ref. Gen.	Armature Conductors		Diameter Changes	
		115.3%	84.7%	107.5%	92%
X	.0141	.0176	.0110	.0150	.0132
λ_i	3.369	3.81	3.64	3.52	3.97
λ_e	1.84	2.15	1.60	2.70	1.21
x_ℓ	.078	.105	.058	.093	.068
λ_a	143.00	143.00	143.00	143.00	143.00
x_{ad}	1.80	2.25	1.41	1.92	1.69
λ_{FS}	6.17	6.17	6.17	6.17	6.17
λ_{FE}	2.41	2.41	2.41	3.24	1.69
x'_F	.180	.229	.144	.207	.169
x'_d	.259	.334	.201	.300	.237
x_d	1.88	2.36	1.46	1.98	1.67
L_f	.0525	.0492	.0565	.056	.049
r_f	.500	.483	.521	.528	.485
T'_{do}	.105	.102	.108	.107	.101
Gen. Gain	.082	.089	.073	.075	.085
Stack	3.37	3.16	3.63	2.70	4.42
Gen. $D^2\ell$	318.00	306.00	334.00	293.00	353.00
Exc. $D^2\ell$	66.90	64.70	69.70	70.60	64.90
Total $D^2\ell$	385.00	371.00	404.00	364.00	418.00

symbols used are defined in the nomenclature for the main text with the exception of "Generator Gain". It is defined as the per cent air-gap voltage per ampere-turn per pair of poles.

B-4 EXCITER EDDY-CURRENT STUDY

Derivation of the eddy-current equations for solid iron are given here following Pohl's work in general. There are some differences in details which are intended to add clarity. A sample calculation for the resistance and inductance of the eddy current circuit is included.

B-4-a Calculation of Eddy-Current Effects – Let it be assumed that an exciting mmf is applied to a sheet of iron, shown in Figure B-4-1, so that the net flux per unit width, ϕ_n, is building up at a constant rate. For uniform flux distribution in the iron the incremental voltage, e_s, and current density, g_s, in the iron would be linear with the distance s as shown in Figure B-4-2. This is also true when the flux is not uniformly distributed but as indicated in Figure B-4-3. It is necessary that the slope of the curves for different times t_1, t_2, etc. must be parallel at any value of s. It is believed in reality the curves do meet these requirements though proof cannot be offered. If so,

$$\frac{d\phi s}{dt} = k_1 s$$

$$e_s = k_1 s \, 10^{-8}$$

$$g_s = \frac{e_s}{\rho} = k_1 \frac{s \, 10^{-8}}{\rho}$$

where: ϕs = flux between plus and minus s

k_1 = some undefined constant

e_s = voltage generated in the incremental conductors at s

s = distance from center-line of iron sheet

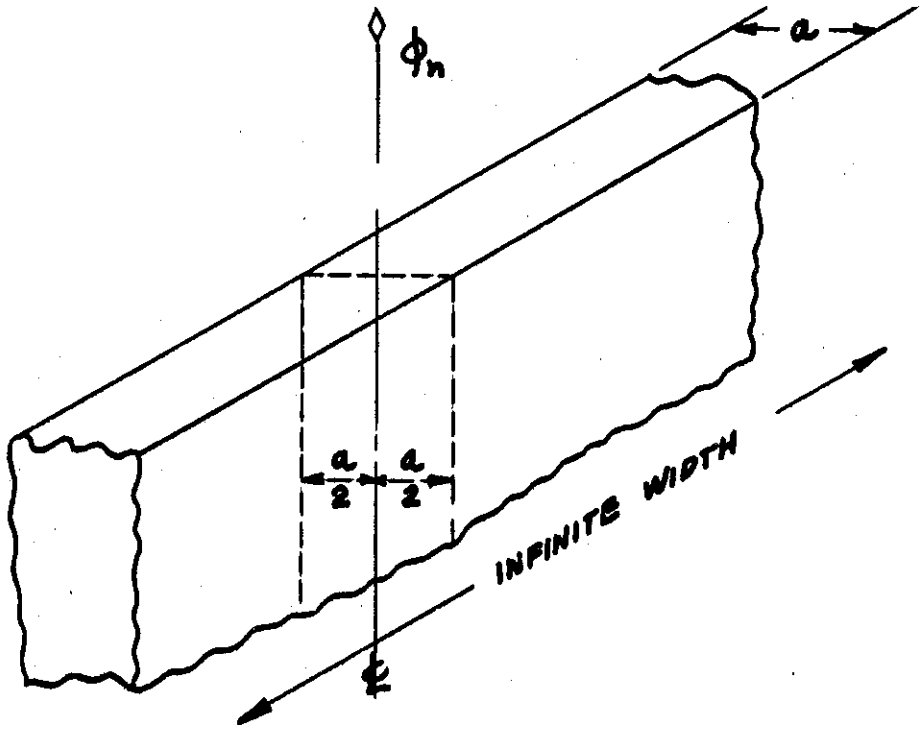

Figure B-4-1 Net Flux Direction in Iron Sheet

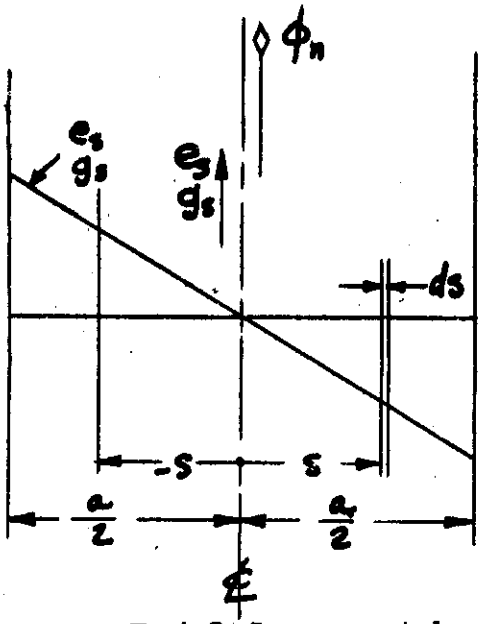

Figure B-4-2 Incremental Voltage and Current

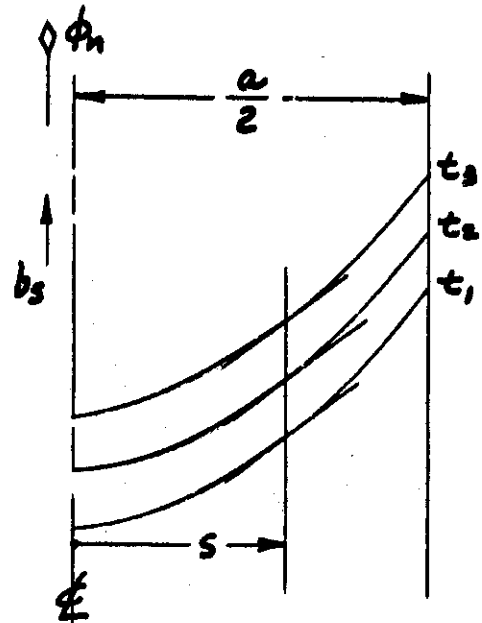

Figure B-4-3 Flux Density With Constant dϕn/dt

g_s = current density in incremental conductors at s - amp./cm^2

ρ = resistivity of magnetic material-ohm-cm

The ampere-turns outside $\pm$ s, AT_s, determine the counter flux density b_s at s. Expressions for these are:

$$AT_s = \int_s^{a/2} \frac{k_1 \, s}{\rho \, 10^8} \, ds = \frac{k_1}{2 \rho \, 10^8} \left[\frac{a^2}{4} - s^2 \right]$$

$$b_s = k_2 \, AT_s = \frac{k_1 \, k_2}{2 \rho \, 10^8} \left[\frac{a^2}{4} - s^2 \right]$$

where: k_2 = permeance of magnetic circuit.

This is the equation for a parabola with its focus on the centerline of the iron (s = o).

The total counter flux caused by the eddy-currents per unit width of the sheet of iron is

$$\phi c = \int_0^{a/2} b_s \, ds = \frac{k_1 \, k_2}{2 \rho \, 10^8} \int_0^{a/2} \left[\frac{a^2}{4} - s^2 \right] ds$$

$$= \frac{k_1 \, k_2 \, a^3}{24 \, \rho \, 10^8}$$

For a substitute winding, outside of the iron, having the same counter flux strength as the actual eddy currents the following expressions can be written:

$$b_{s2} = k_2 \, i_2$$

$$\phi c2 = b_{s2} \int_0^{a/2} ds = \frac{a}{2} \, k_2 \, i_2$$

where: b_{s2} = flux density throughout the iron,

i_2 = current flow in the substitute winding, and

ϕ_{c2} = counter flux caused by the substitute winding.

The substitute winding (one turn) must give the same counter flux as the actual eddy currents so ϕ_c must equal ϕ_{c2} or

$$\frac{k_1 \; k_2 \; a^3}{24 \; \rho \; 10^8} = \frac{a}{2} \; k_2 \; i_2$$

and $$i_2 = \frac{k_1 \; a^2}{12 \; \rho \; 10^8} \text{ amperes}$$

The voltage generated in the substitute winding is

$$e_2 = k_1 \frac{a \; 10^{-8}}{2} \text{ volts/cm width of iron.}$$

The conductance of the substitute winding per cm of its length and per cm length of flux path is

$$G'_2 = \frac{i_2}{e_2} = \frac{k_1 \; a^2}{12 \; \rho \; 10^8} \; \frac{2}{k_1 \; a \; 10^{-8}} = \frac{a}{6\rho} \text{ mhos.}$$

Now, the length of the substitute winding would be 2 (a + b) and the length of the magnetic circuit is ℓ_2 so the conductance would be

$$G_2 = G'_2 \; \frac{\ell 2}{2(a+b)} = \frac{a \; \ell 2}{12 \; \rho \; (a+b)} \text{ mhos.}$$

This is Pohl's equation for the case of an infinitely wide sheet of iron. He gives the following equation for a rectangular cross section of iron:

$$G_2 = \frac{a \cdot \ell \cdot 2}{\rho \; (20a + 12b)} \text{ mhos.}$$

It was pointed out in Chapter III-C-3-a that the factor 1/2 P must be applied to give the conductance for a substitute winding on an exciter with P poles. The "2" enters in because the flux has two paths in the frame and the length of the solid iron is defined as one-half the distance on the frame between main poles. The substitute winding resistance for an exciter is therefore

$$r_2 = \frac{2P}{G_2} = \frac{2P\,\rho\,(20a + 12b)}{a\,\ell_2} \quad \text{ohms.}$$

B-4-b Sample Calculation for Eddy-Current Constants in an Exciter

Suppose the following information is at hand:

$L_1 = .157$ henrys $\qquad \ell_2 = 3.48$ cm

$a = .800$ cm $\qquad P = 6$

$b = 3.65$ cm $\qquad \rho = 10.0 \times 10^{-6}$ ohm-cm

then the resistance of a one turn substitute winding may be determined from the equation given previously:

$$\text{or } r_2 = 2 \times 6 \times 10^{-5}\ \frac{(20 \times .800 + 12 \times 3.65)}{.800 \times 3.48} = .00258 \text{ ohms.}$$

The self-inductance of the substitute winding is calculated by the equation given in Chapter III-C-3-a:

$$L_2 = 1.22\ L_1\ \frac{\phi_{12} \cdot n_2^{\,2}}{\phi_{11} \cdot n_1^{\,2}}$$

The ratio of ϕ_{12} to ϕ_{11} is determined from a flux map of the exciter stator interpolar region, as shown in Figure B-4-4.

Referring to the figure, the permeance, P, for the flux path under the pole is $P_{ag} = \frac{W}{g'} = \frac{.575}{.0335} = 17.75$

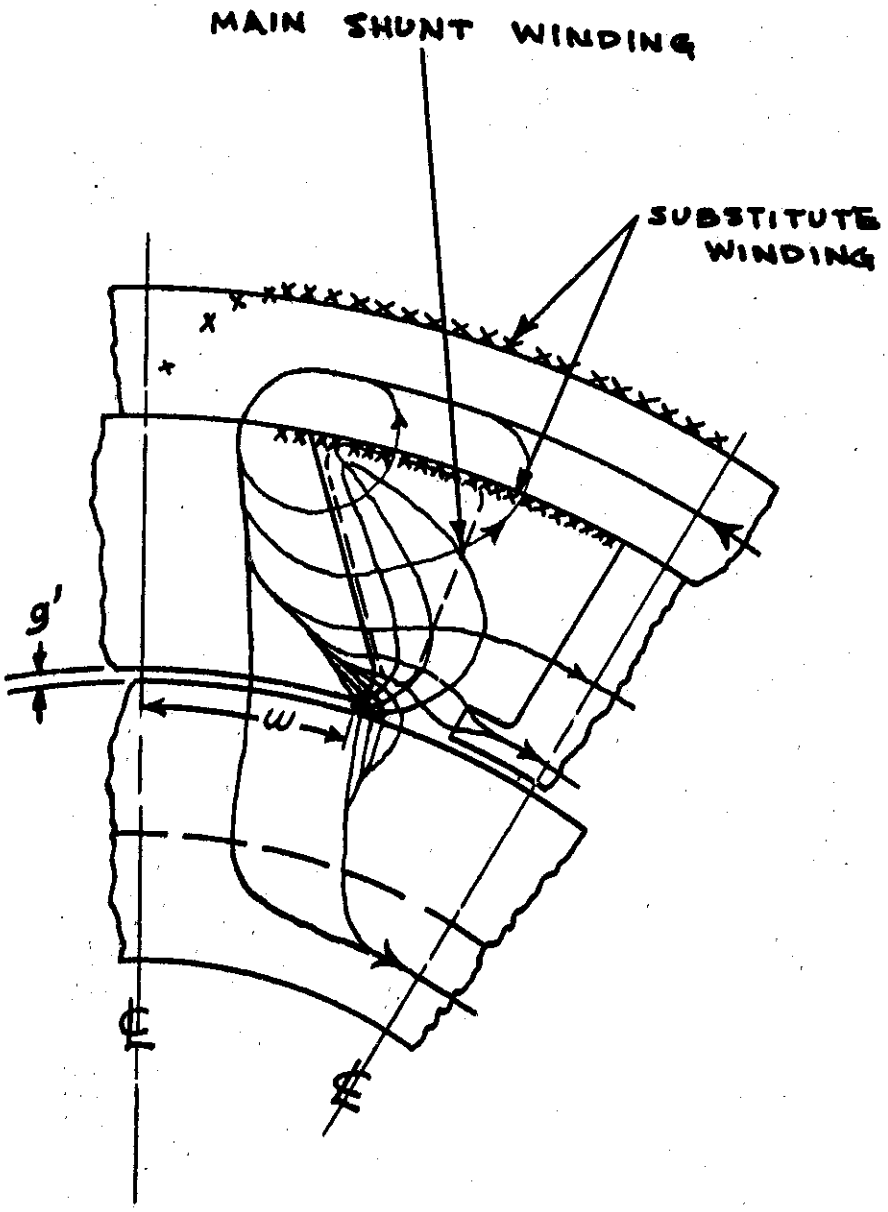

Figure B-4-4 Flux Map for Exciter Interpolar Region

The effective permeance for the flux at the side of the pole linking the main shunt (some tubes of flux do not link all of the turns) is

$$P_{s1} = \frac{7.1}{4} = 1.775$$

The effective permeance for the flux at the side of the pole linking the substitute winding is $P_{s2} = 7.05/4 = 1.762$

Now, ϕ_{12} is proportional to $P_{ag} + P_{s2}$

and ϕ_{11} is proportional to $P_{ag} + P_{s1}$

so $\frac{\phi 12}{\phi 11} = \frac{17.75 + 1.762}{17.75 + 1.775} = .995$, or say unity.

It is rather apparent from the flux map that approximately the same flux links the substitute winding that links the main shunt winding without the above calculations. It is included to show the method.

The self inductance may be calculated as:

$$L_2 = 1.22 \times .157 \times 1.0 \times \frac{1}{(125)^2} = 1.228 \times 10^{-5} \text{ henrys}$$

The time constants of the eddy-currents is L_2/r_2 or

$$T_2 = \frac{1.228 \times 10^{-5}}{258 \times 10^{-5}} = .00475 \text{ secs.}$$

BIBLIOGRAPHY FOR APPENDIX B

1. Park, R. H., Definition of an Ideal Synchronous Machine and Formula for the Armature Flux Linkages, General Electric Review, Vol. 31, June 1928, pp 332-334.

2. Park, R. H., Two-Reaction Theory of Synchronous Machines - Generalized Method of Analysis - Part I, AIEE Transactions, Vol. 48, 1929, pp 716-727.

3. Harder, E. L. and Cheek, R. C., Regulation of A-C Generators with Suddenly Applied Loads, AIEE Transactions, Vol. 63, 1944, pp 310-318.

4. Anderson, H. C. Jr., Voltage Variation of Suddenly Loaded Generators, General Electric Review, August 1945, pp 25-33.

5. Kilgore, L. A., Calculation of Synchronous Machine Constants, AIEE Transactions, Vol. 50, 1931, pp 1201-1213.

6. Alger, P. L., Calculation of Armature Leakage Reactance of Synchronous Machines, AIEE Transactions, Vol. 47, 1928, pp 493-513.

7. Wiseman, R. W., Graphical Determination of Magnetic Fields, AIEE Transactions, Vol. 46, 1927, pp 141-154.

APPENDIX C

TEST CHARACTERISTICS AND MACHINE CONSTANTS ON ACTUAL A-C GENERATORS

This appendix presents the data and characteristics of the five machines used for this report. These machines are rated as follows:

(1) 20-kva, single-phase, 120 volts, 0.90 P.F., 400/800 cps, 4000/8000 rpm
USAF Type C-2

(2) 60-kva, three-phase, 120/208 volts, 0.75 P.F., 360/440 cps, 5400/6600 rpm
USAF Spec. MCREXE 21-48

(3) 40-kva, three-phase, 120/208 volts, 0.75 P.F., 380/420 cps, 5700/6300 rpm
USAF Type MB-1

(4) 30-kva, three-phase, 120/208 volts, 0.90 P.F., 400/800 cps, 4000/8000 rpm
USAF Spec. MIL-G-6099

(5) 8-kva, single-phase, 120 volts, 0.90 P.F., 380/1000 cps, 3800/10000 rpm
USAF Type B-1

The data is arranged as follows:

(1) Various winding resistances in the a-c generator and exciter (25^{o} C)

(2) Per-unit reactances at average rated speed

(3) Time constants at room ambient conditions

(4) A-C generator saturation curves

(5) Exciter saturation curves

Under Part C-3 there are also a number of oscillograms showing the operation of the 40-kva a-c generator under the control of a Westinghouse Type AVR-370-E carbon-pile voltage regulator. These oscillograms show system transients for:

(1) Voltage build-up

(2) Short F to A+

(3) Open T_1 sensing lead

(4) A-C generator load switching transients (0.75 P.F. load)

C-1 WESTINGHOUSE AIRCRAFT A-C GENERATOR
TYPE 12RD20 S# 1172461
20-KVA, SINGLE-PHASE, 120 VOLTS, 9 P. F.
400/800 CPS, 4000/8000 RPM
USAF TYPE C-2

WINDING RESISTANCES (Ohms at 25° C)

A-C Generator armature per phase (d-c)	.022
A-C Generator field	.521
Exciter armature	.053
Exciter shunt field	2.42
Exciter differential field	24.2
Exciter series plus interpole plus comp.	.078

REACTANCES (Per-unit) 6000 rpm, 600 cps

D - axis synchronous	(x_d)	1.28
D - axis synchronous (slip test)	(x_d)	1.32
D - axis transient (s.c. test)	(x'_d)	.442
D - axis subtransient (s.c. test)	(x''_d)	.357
D - axis subtransient (locked rotor test)	(x''_d)	.336
Q - axis synchronous (slip test)	(x_q)	.789
Q - axis subtransient (locked rotor test)	(x_q'')	.394

TIME CONSTANTS (in seconds)

Open-circuit transient	(T'_{do})	.0833
Short-circuit transient	(T'_d)	.0250
Short-circuit subtransient	(T''_d)	.0024
Exciter shunt field	(T_1)	.026

Figure C-1 A-C Generator Saturation Characteristics
20-Kva, single-phase .9 pf, 120 volts
(for 4000 rpm)

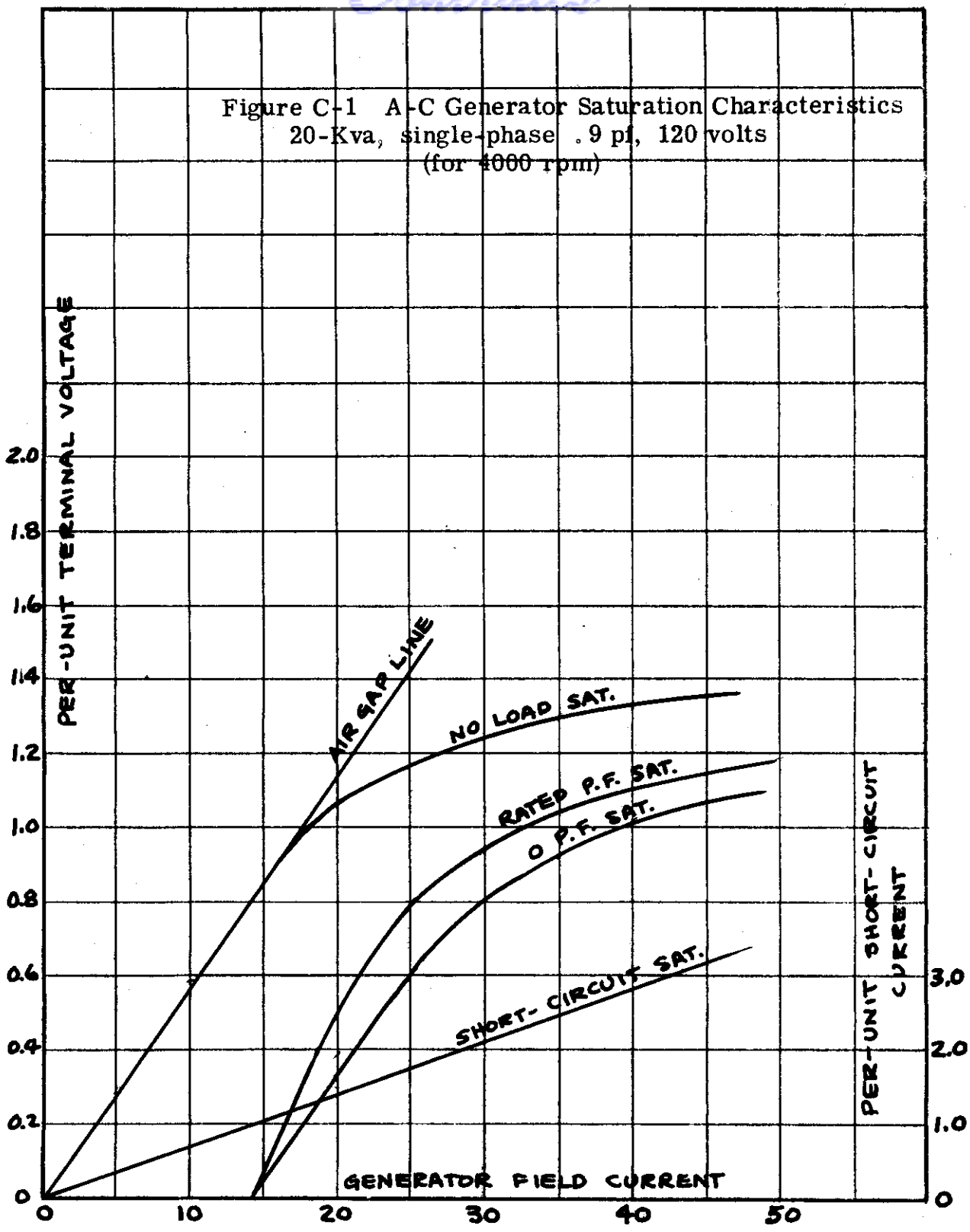

Figure C-2 A-C Generator Exciter Saturation Characteristics
20-Kva, single-phase, 9 pf, 120 volts
(for 8000 rpm)

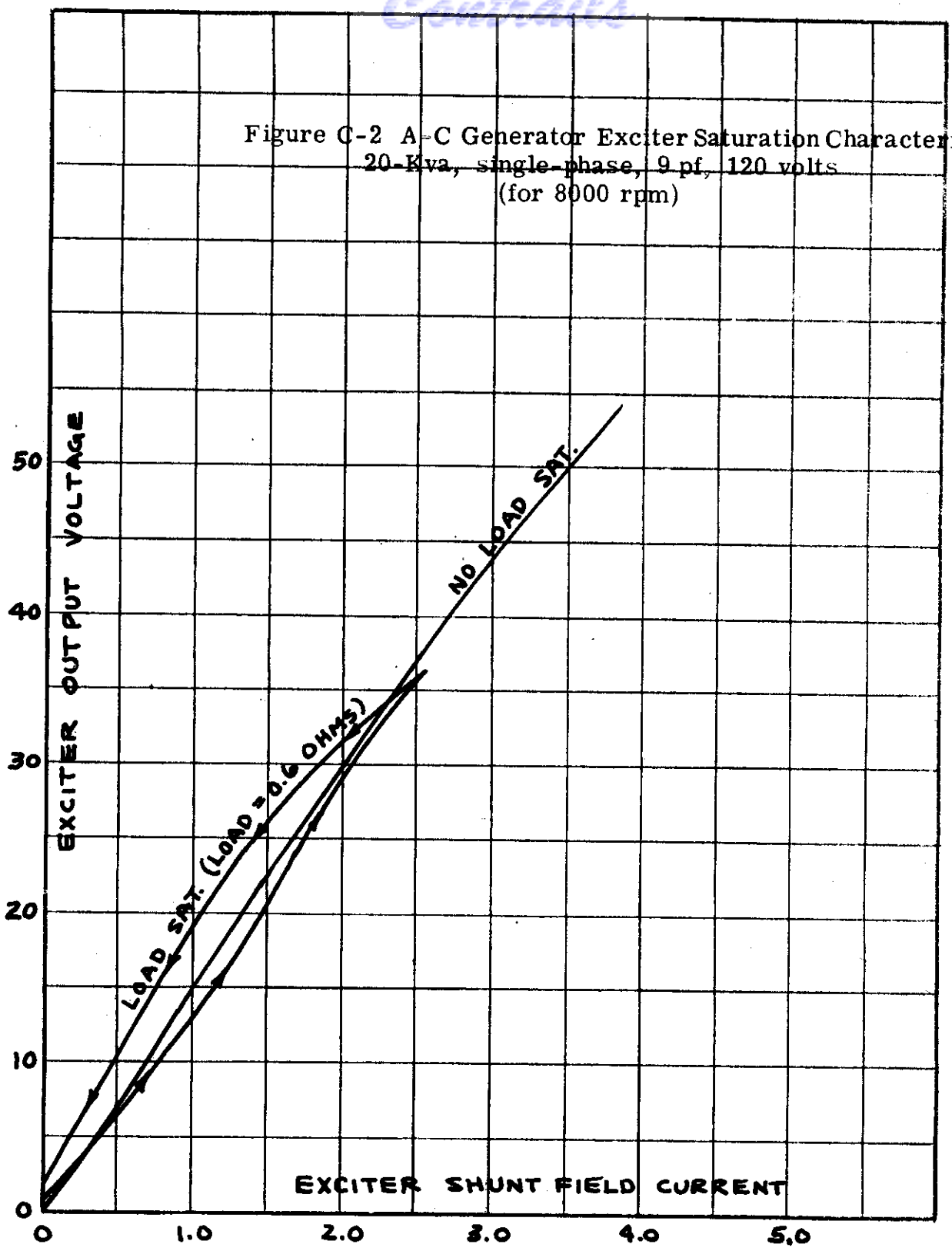

C-2 WESTINGHOUSE AIRCRAFT A-C GENERATOR
TYPE 8QL60C, S# 1172473
60-KVA, THREE-PHASE, 120/208 VOLTS, 75 P.F.
360/440 CPS, 5400/6600 RPM
USAF SPEC. MCREXE 21-48

WINDING RESISTANCES (Ohms at 25° C)

A-C Generator armature per phase (d-c)	.014
A-C Generator field	.386
Exciter armature	.057
Exciter shunt field	4.53
Exciter differential shunt field	24.4

REACTANCES (Per-unit) 6000 rpm, 400 cps

D - axis synchronous	(x_d)	1.88
D - axis transient	(x'_d)	.246
D - axis subtransient (s.c. test)	(x''_d)	.169
Negative sequence (L-L s.c. test)	(z_2)	.0748 +j .217
Zero sequence (single phase test)	(z_0)	.0241 +j .0402

TIME CONSTANTS (in seconds)

Open-circuit transient	(T'_{do})	.099
Short-circuit transient	(T'_d)	.0124
Short-circuit subtransient	(T''_d)	.0016
Exciter shunt field	(T_1)	.045

Figure C-3 A-C Generator Saturation Characteristics
60-Kva, three-phase .75 pf, 120/208 volts
(for 6000 rpm)

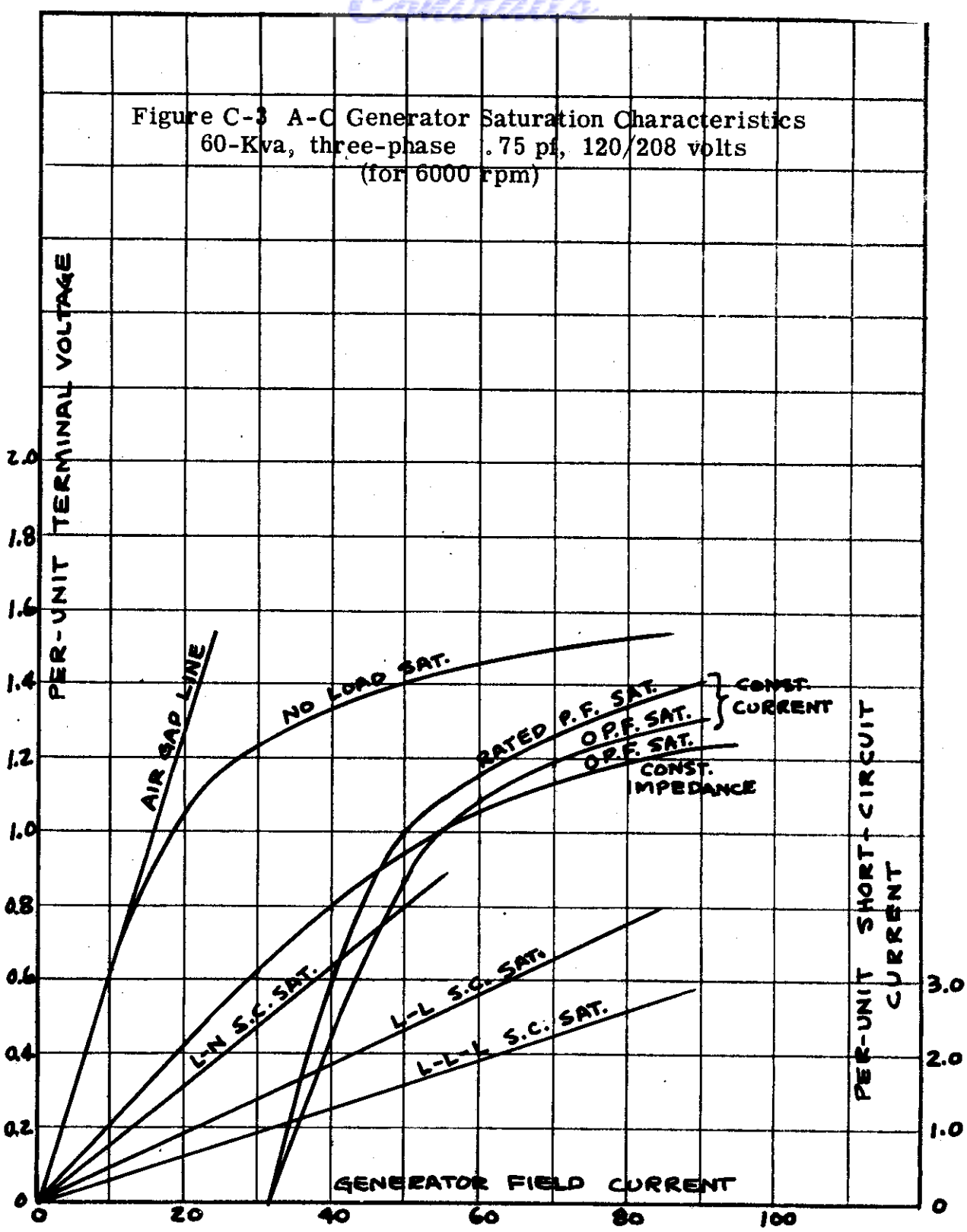

Figure C-4 A-C Generator Exciter Saturation Characteristics
60-Kva, three-phase, .75 pf, 120/208 volts
(for 6000 rpm)

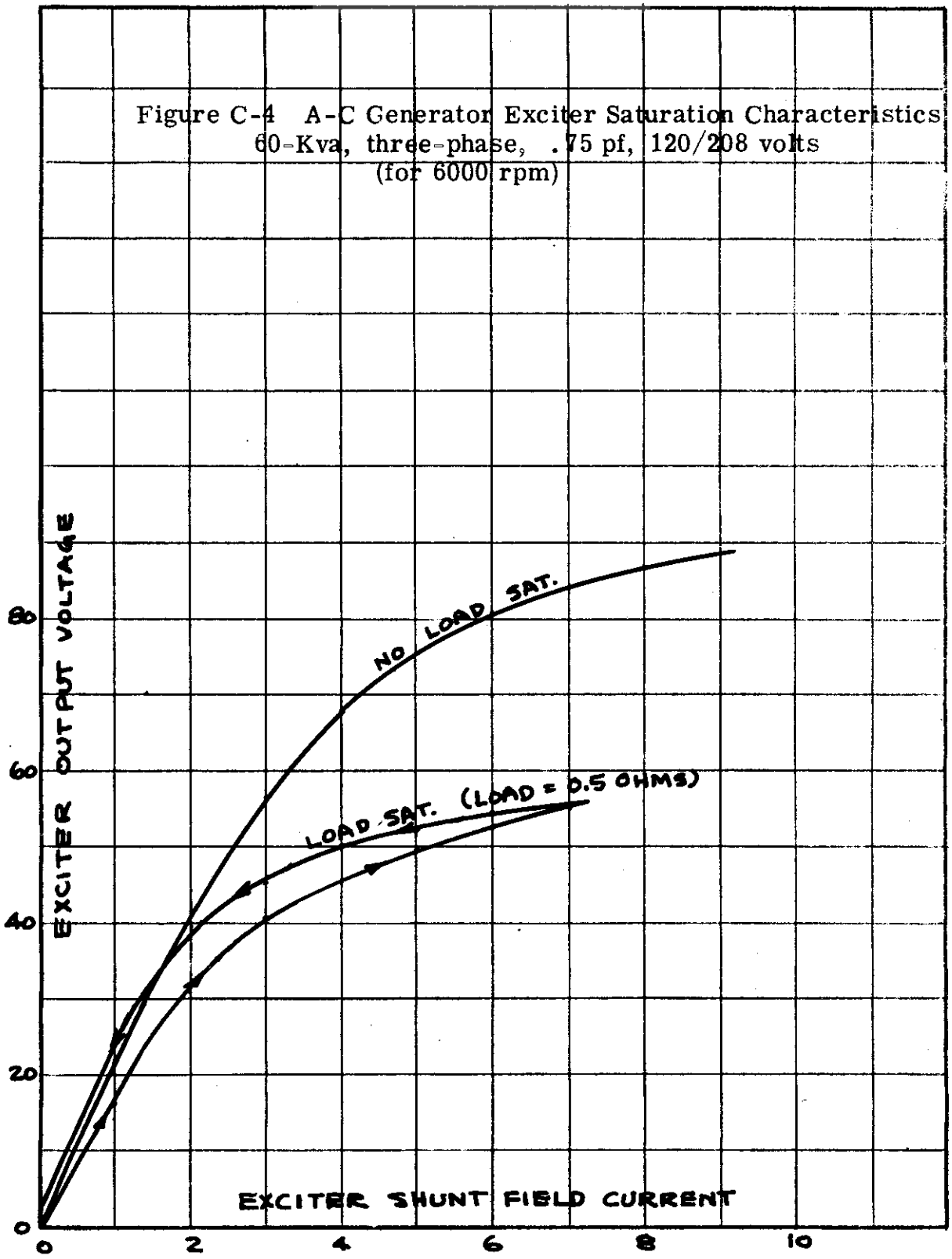

C-3 WESTINGHOUSE AIRCRAFT A-C GENERATOR
TYPE 8QL40H, S# 1639124
40-KVA, THREE-PHASE, 120/208 VOLTS, 75 P.F.
380/420 CPS, 5700/6300 RPM
USAF TYPE MB-1

WINDING RESISTANCES (Ohms at 25° C)

A-C Generator armature per phase (d-c)	.0265
A-C Generator field	.305
Exciter armature	.057
Exciter series	.017
Exciter interpole and comp.	.067
Exciter differential shunt field	30.0
Exciter shunt field	6.33

REACTANCES (Per-unit) 6000 rpm, 400 cps

D - axis synchronous	(x_d)	1.61
D - axis transient (s.c. test)	(x'_d)	.239
D - axis subtransient (s.c. test)	(x''_d)	.160
D - axis subtransient (locked rotor test)	(x''_d)	.161
Q - axis synchronous (motor test)	(x_q)	.673
Q - axis subtransient (locked rotor test)	(x_q'')	.175
zero sequence (single phase test)	(z_0)	.020 + j .020
Negative sequence (L-L s.c. test)	(z_2)	.0608 + j .1521

TIME CONSTANTS (in seconds)

Open-circuit transient	(T'_{do})	.127
Short-circuit transient	(T'_d)	.0122
Short-circuit subtransient	(T''_d)	.0016
Exciter shunt field	(T_1)	.027

Figure C-5 A-C Generator Saturation Characteristics
40-Kva, three-phase, .75 pf, 120/208 volts
(for 6000 rpm)

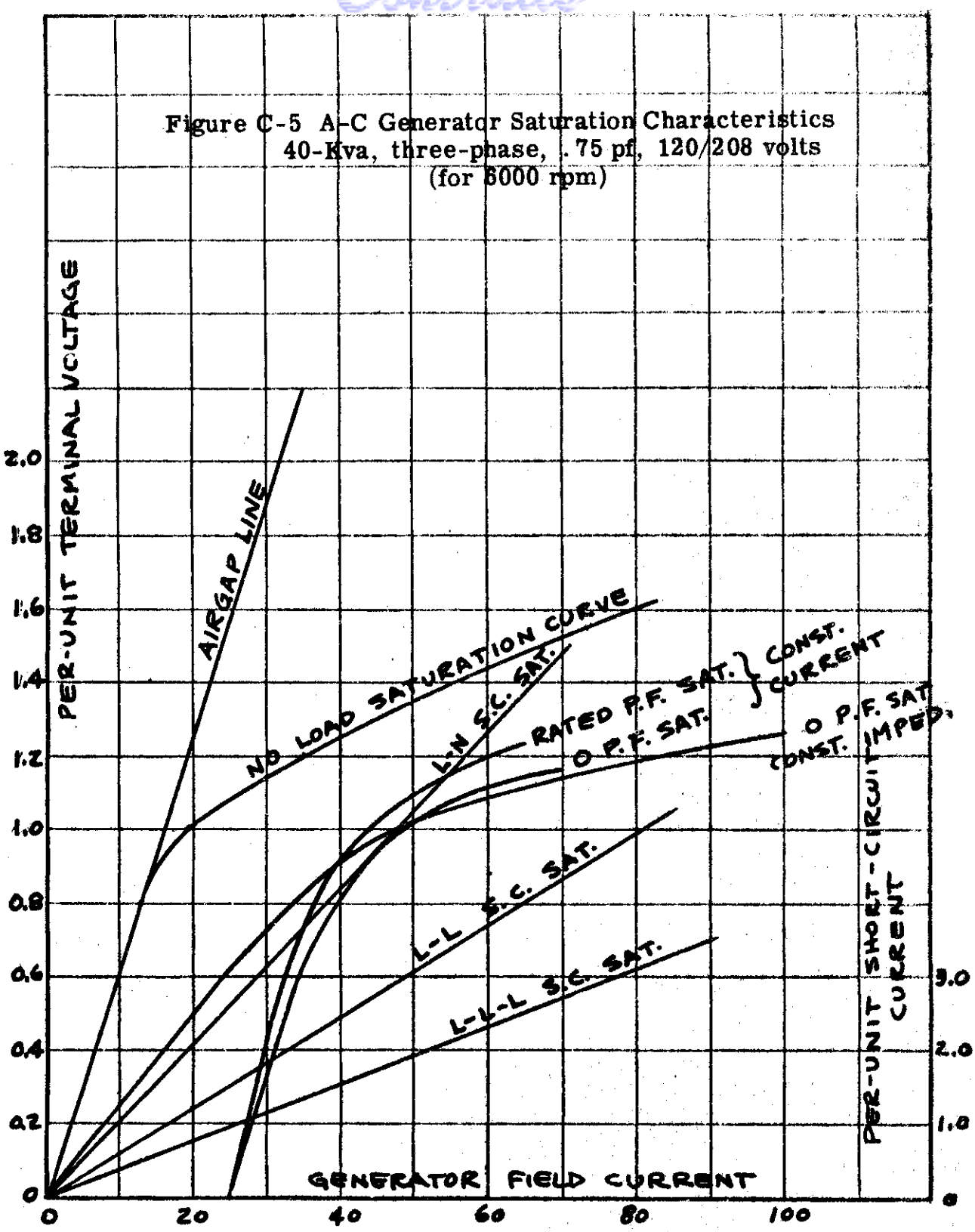

Figure C-6 A-C Generator Exciter Saturation Characteristics
40-Kva, three-phase, .75 pf, 120/208 volts
(for 6000 rpm)

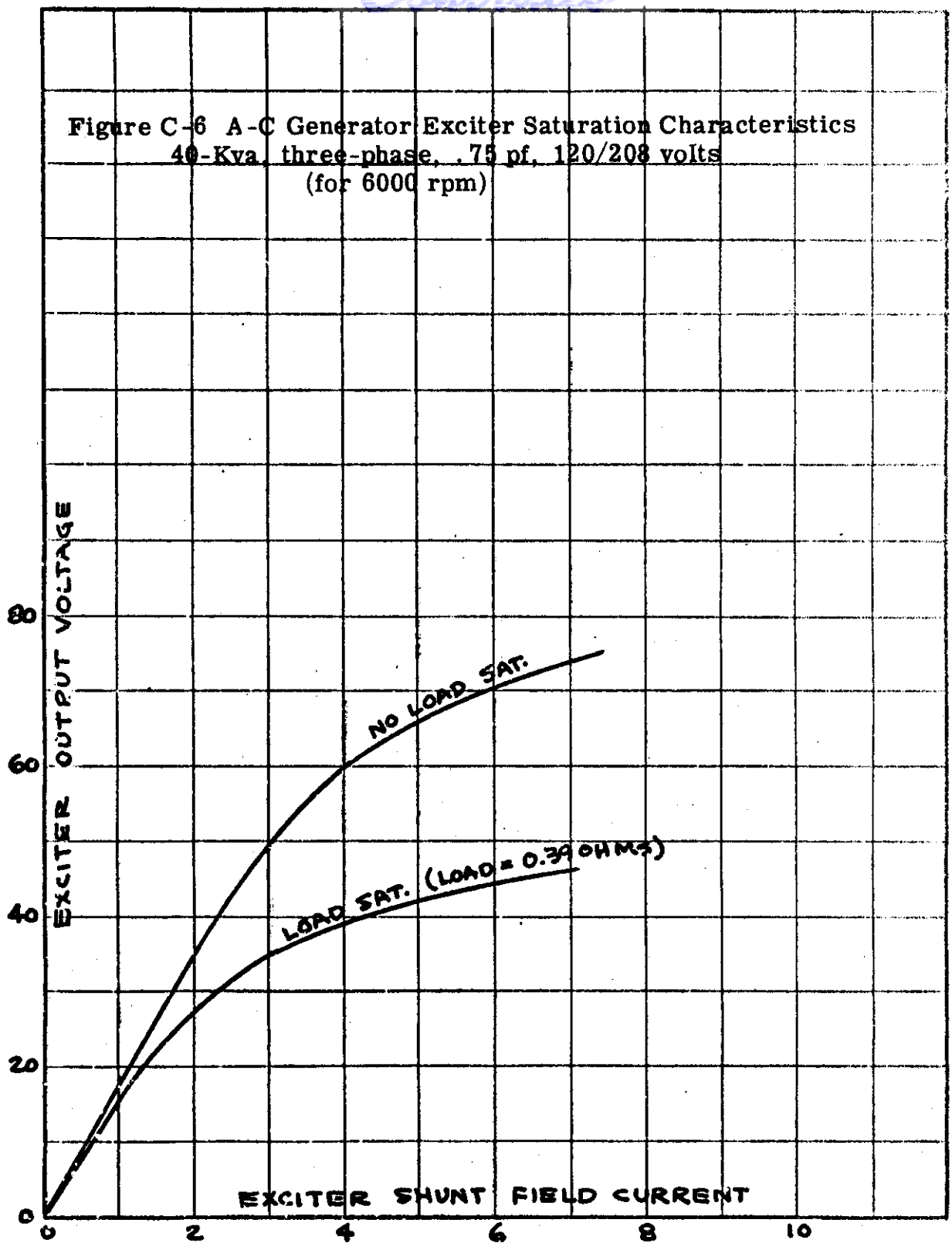

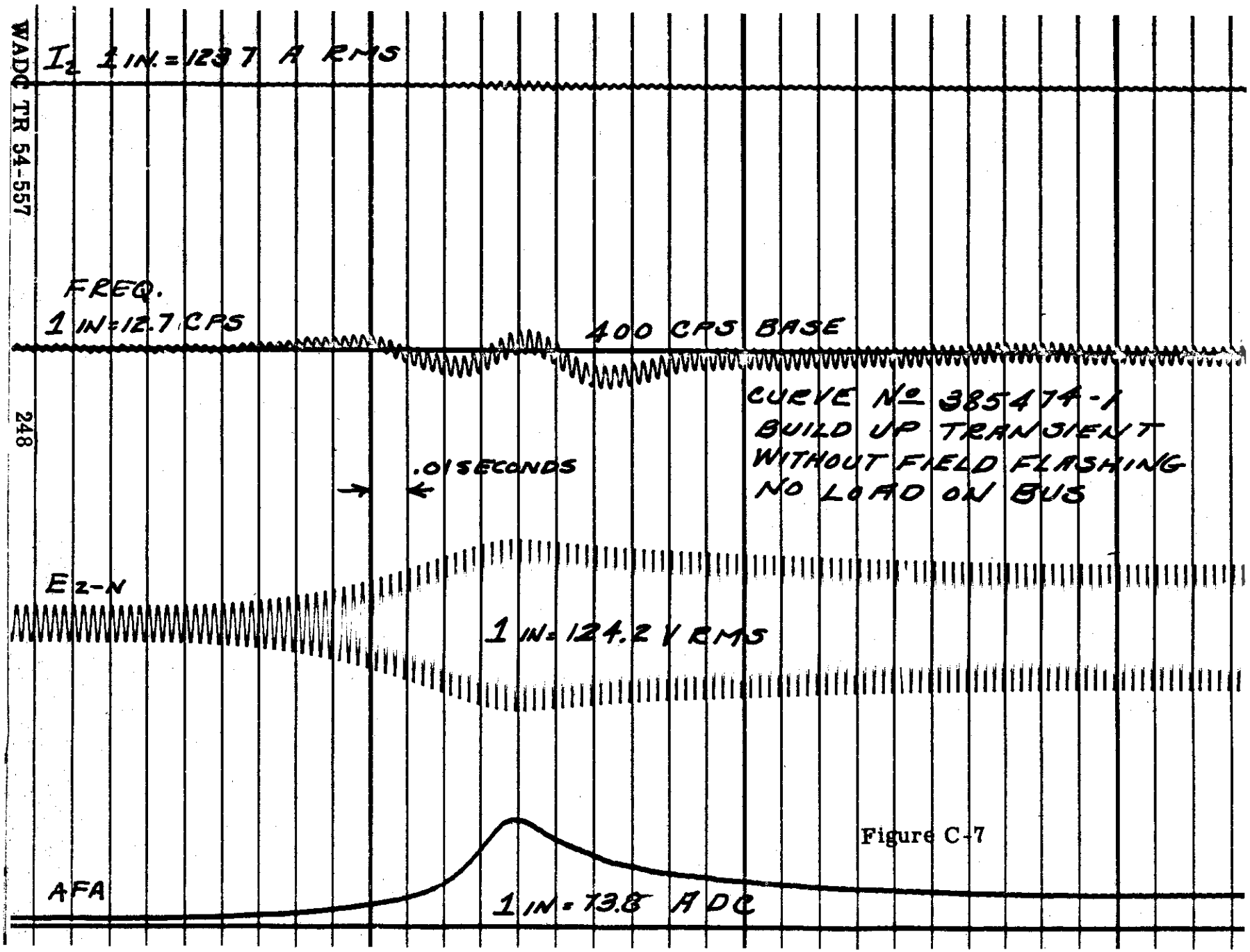

Figure C-7

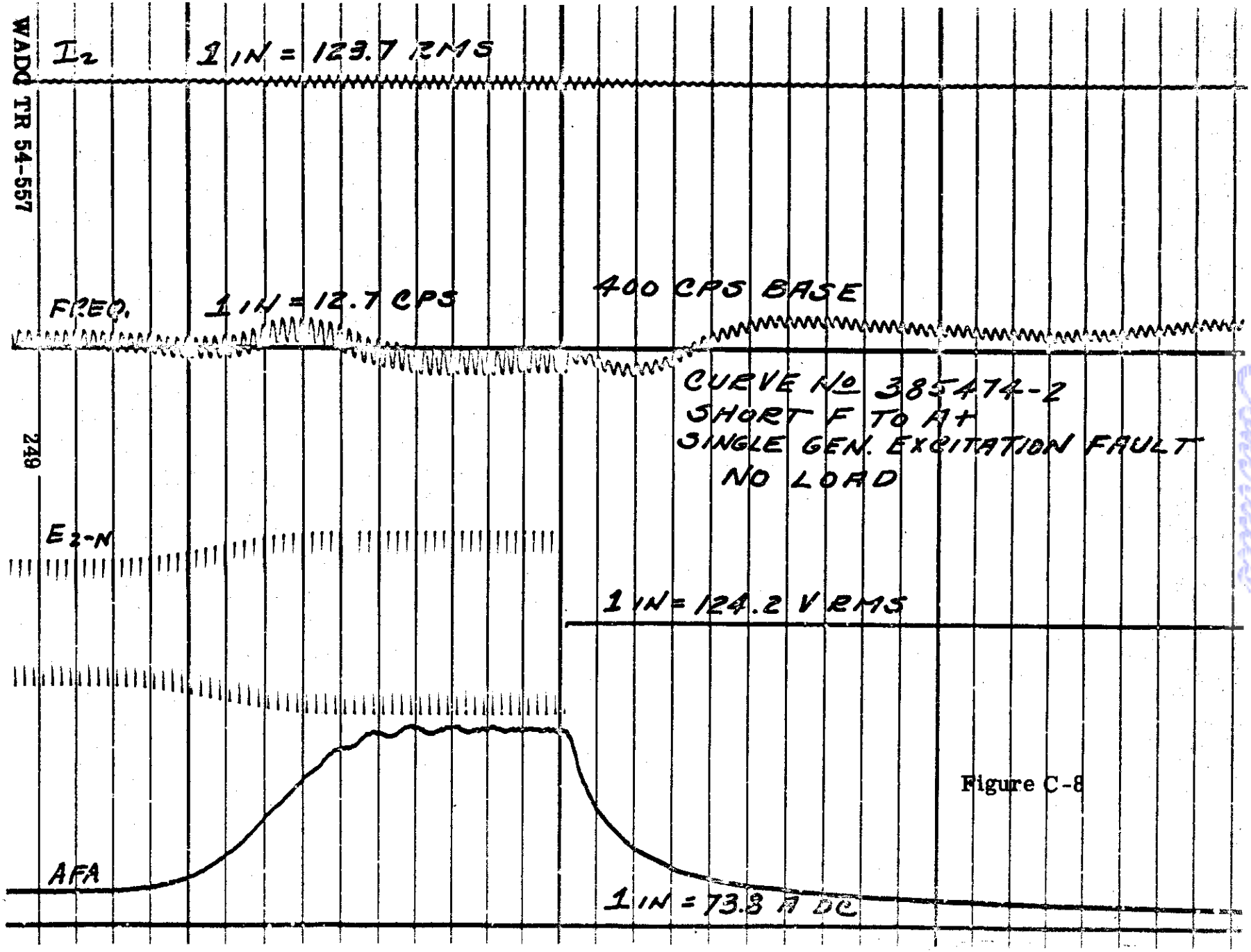

Figure C-8

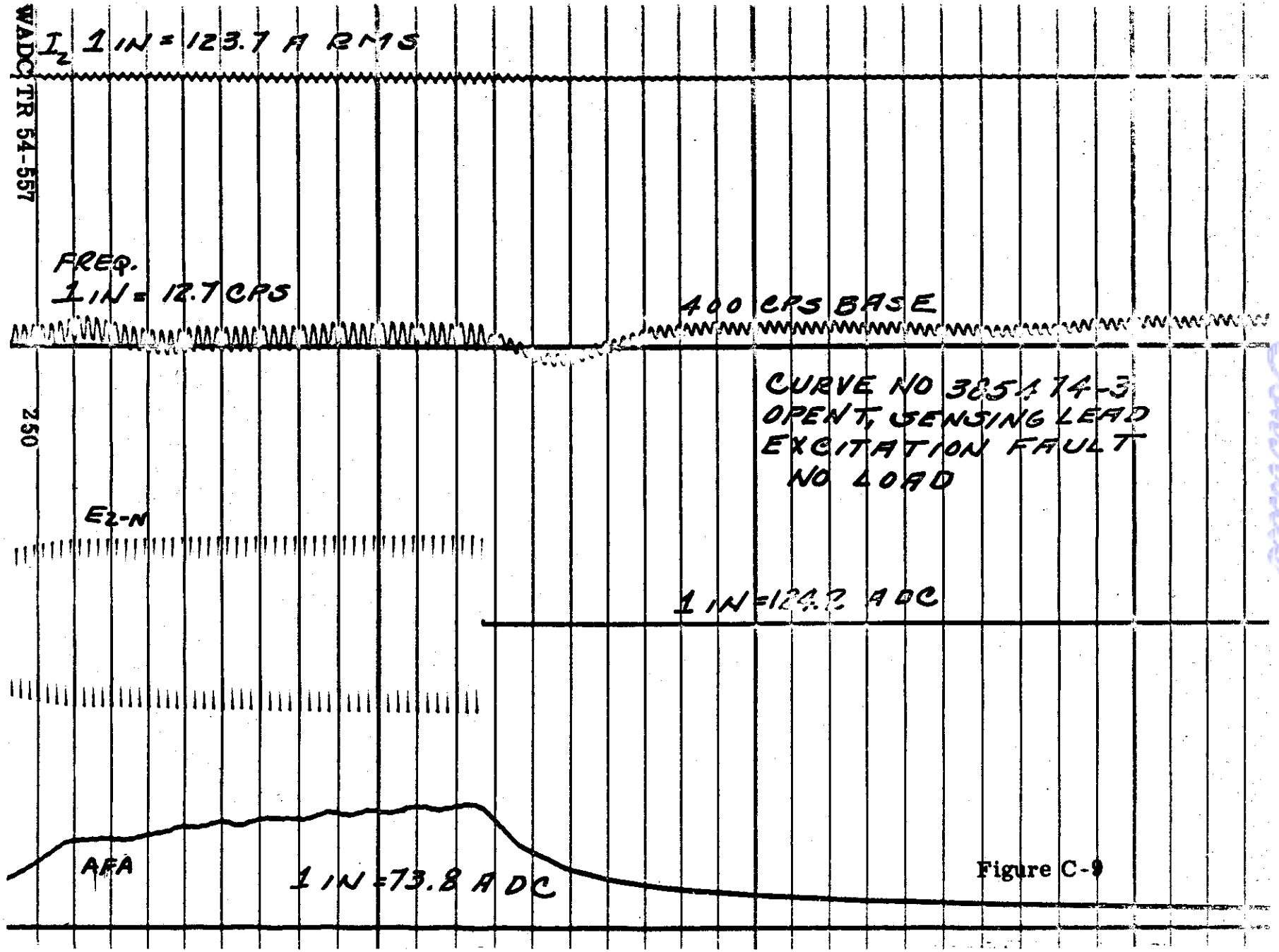

Figure C-9

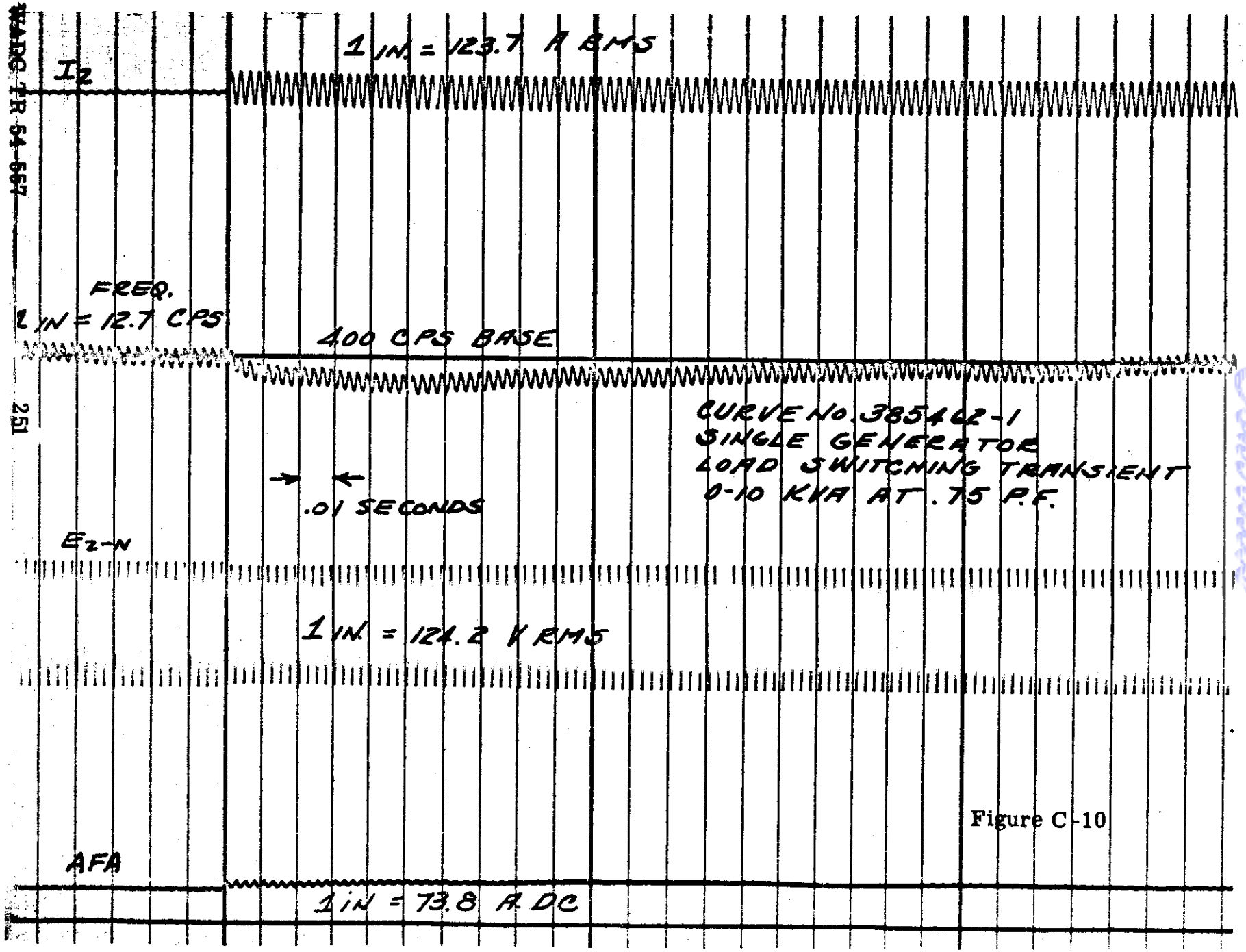

Figure C-10

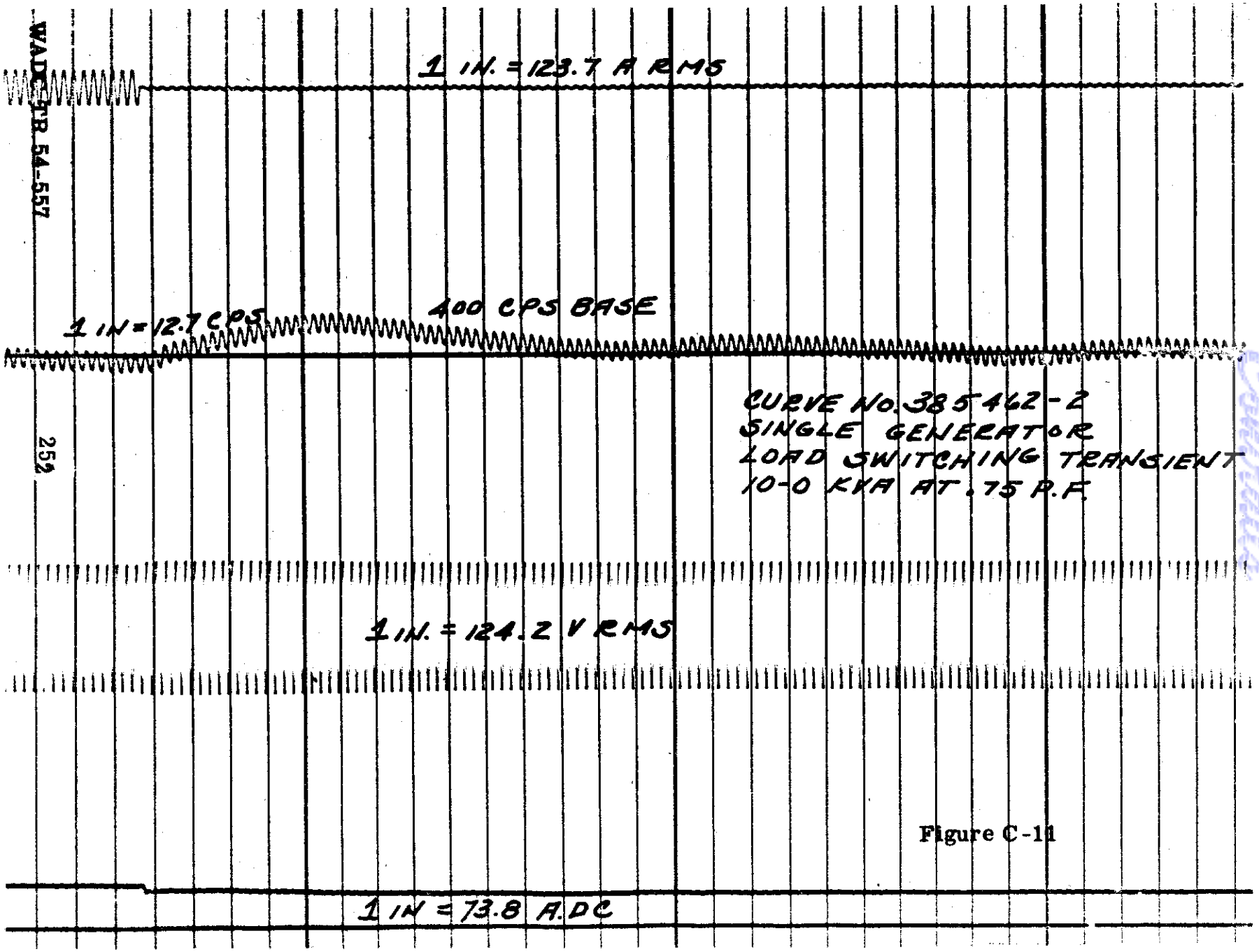

Figure C-11

Figure C-12

Figure C-13

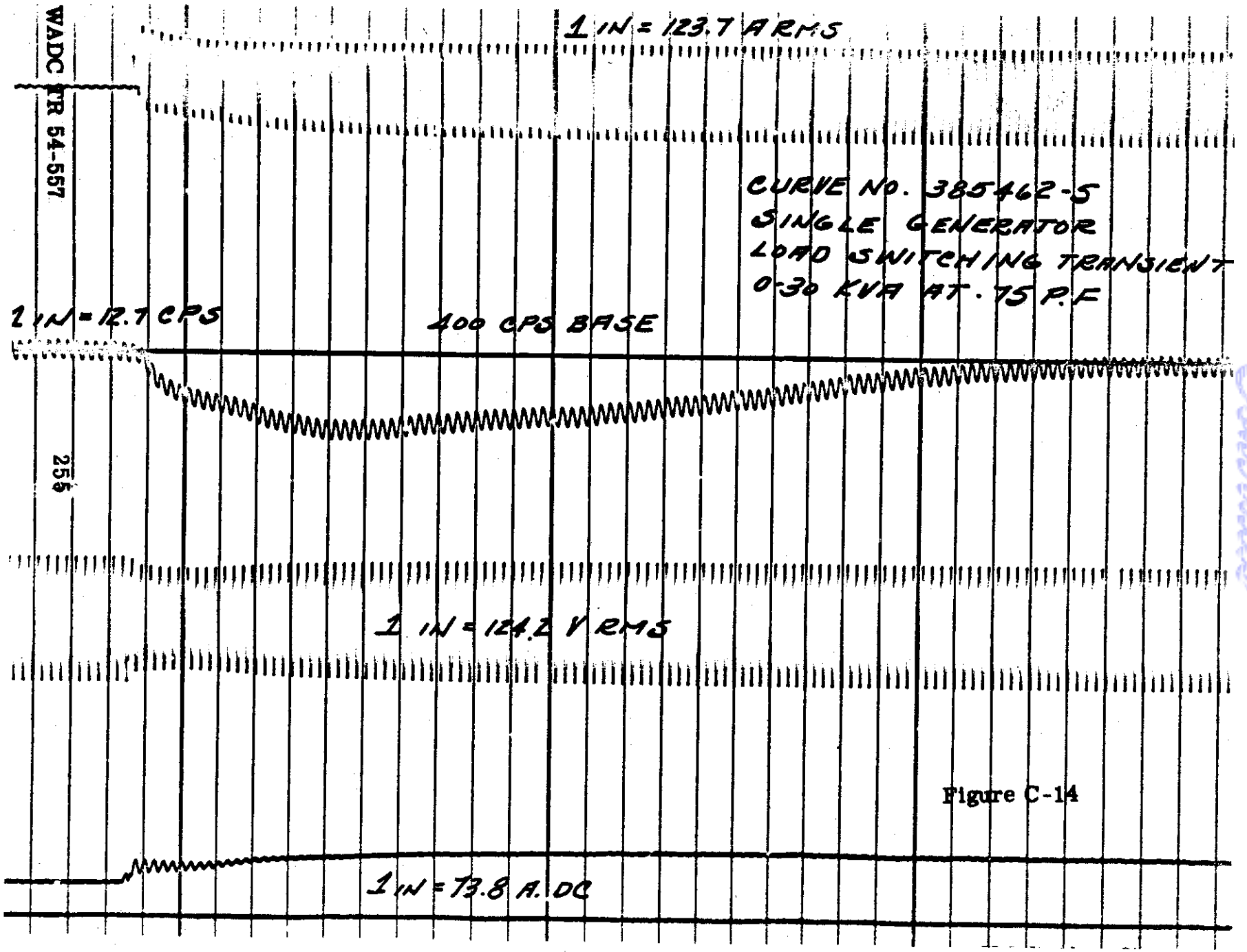

Figure C-14

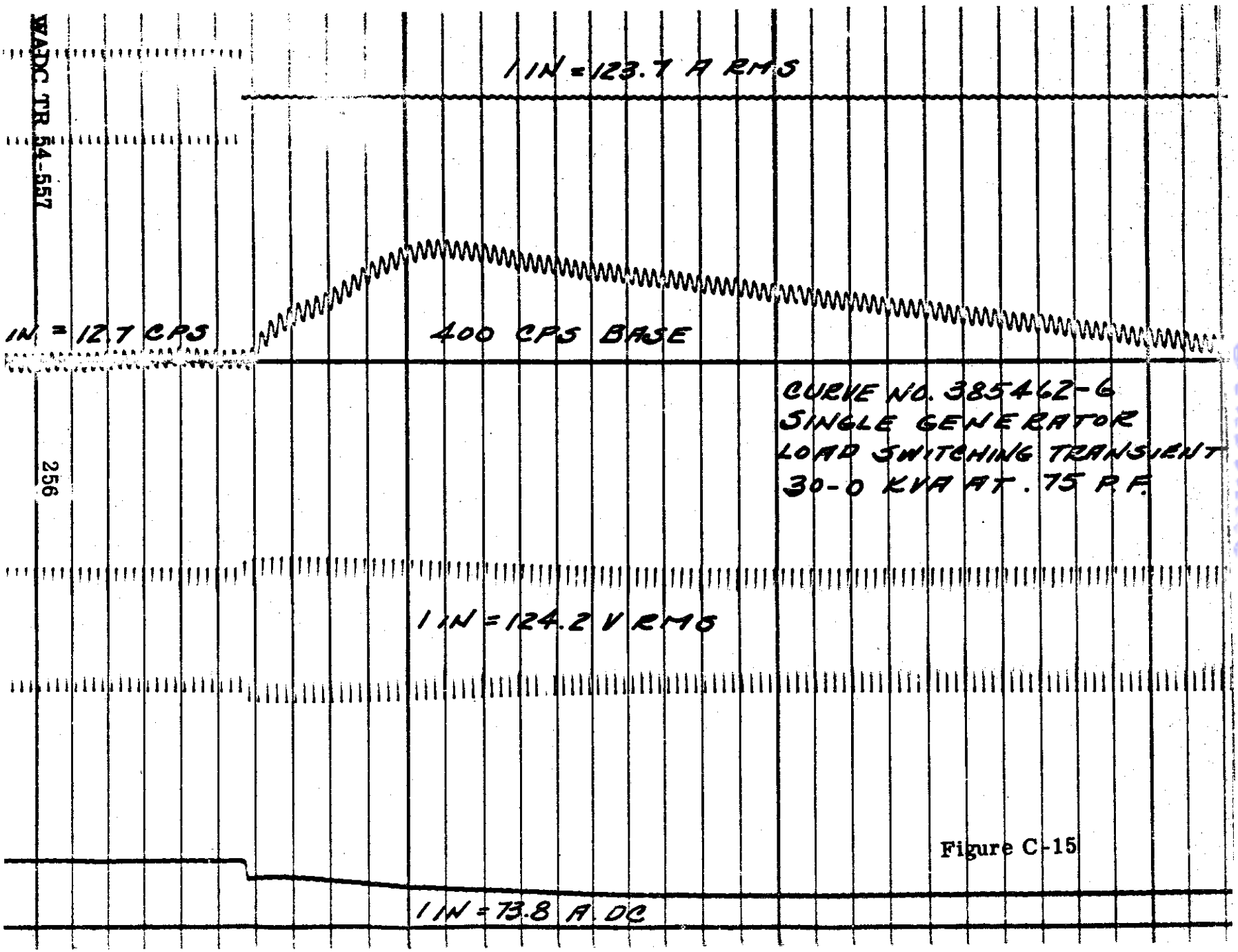

Figure C-15

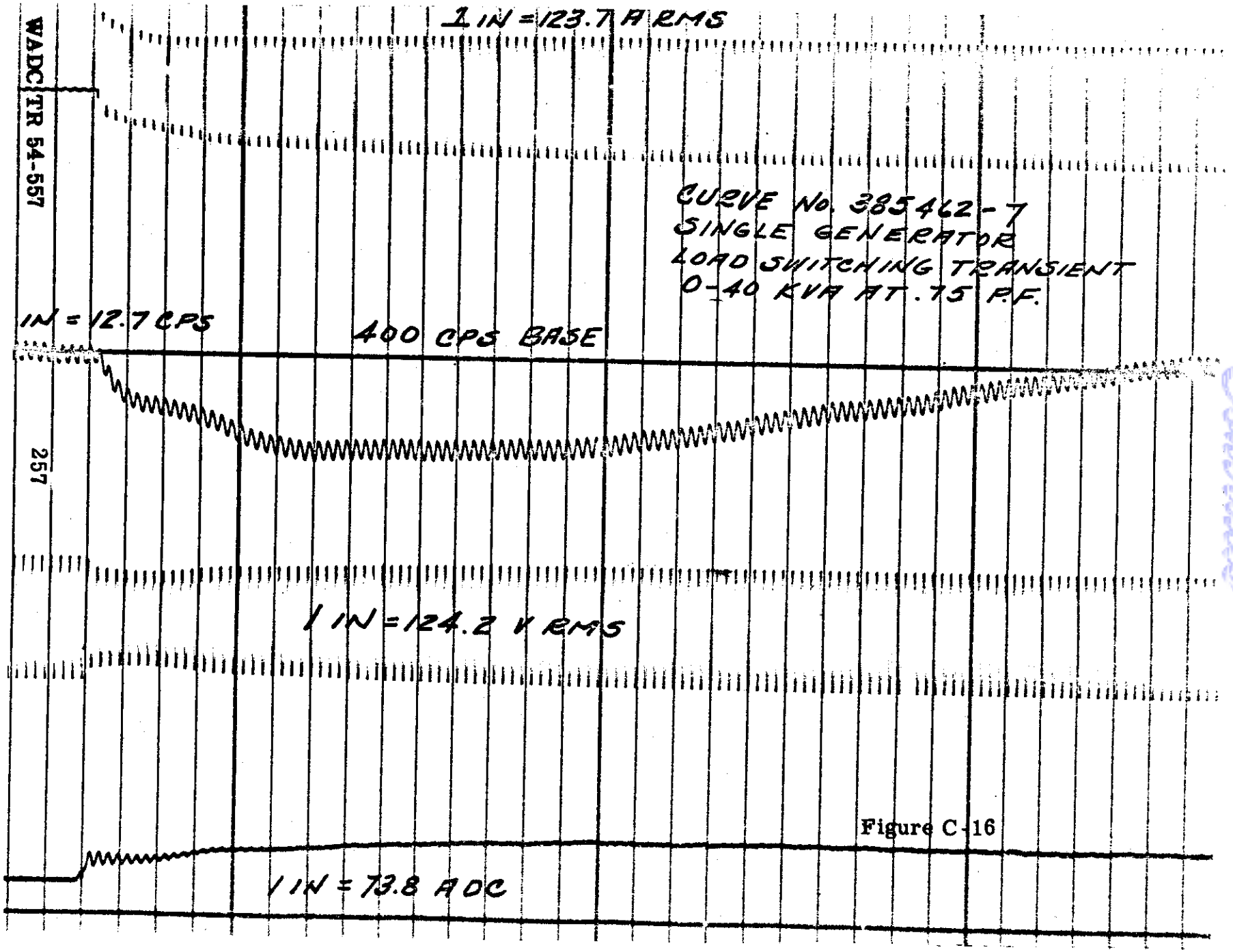

Figure C-16

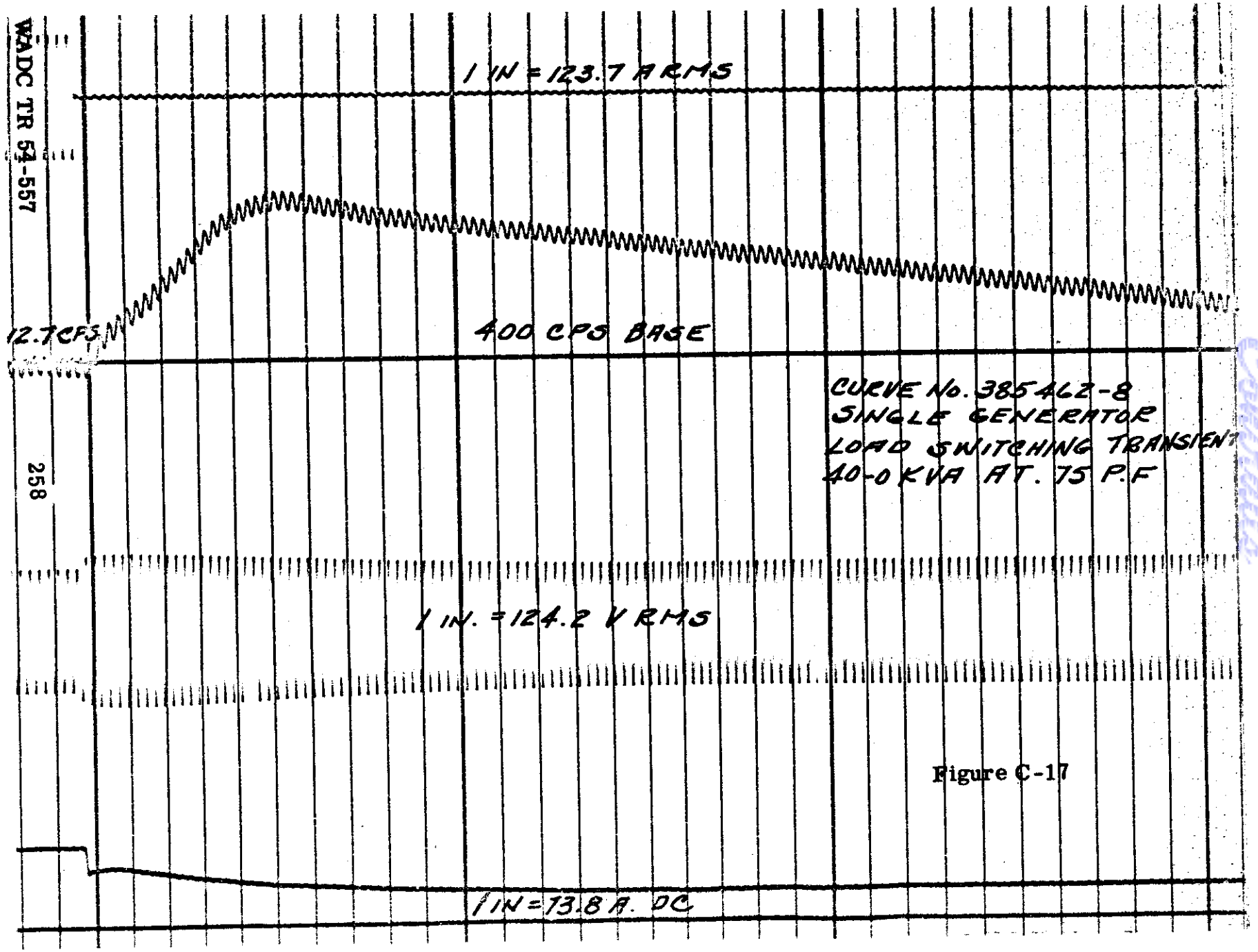

Figure C-17

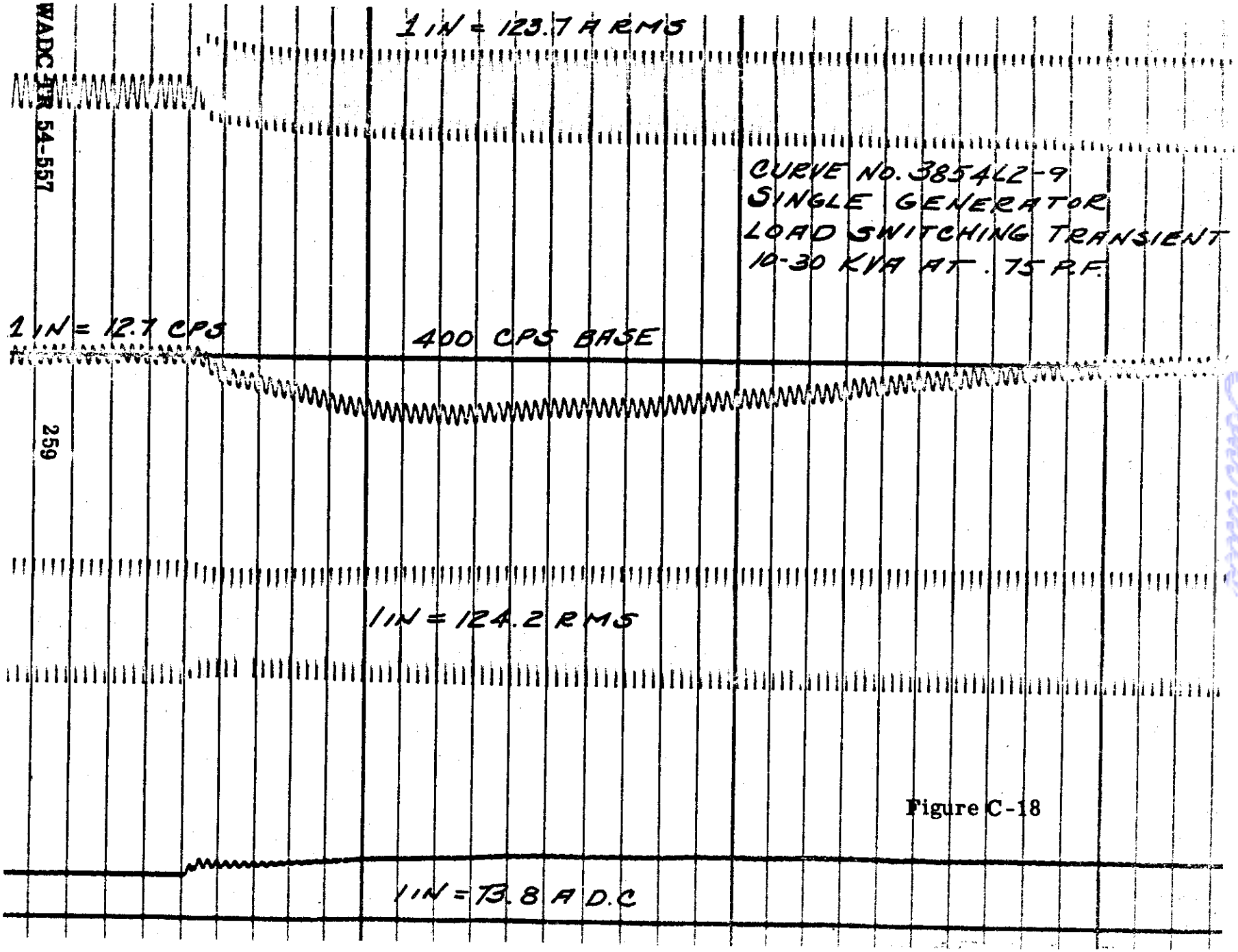

Figure C-18

Figure C-19

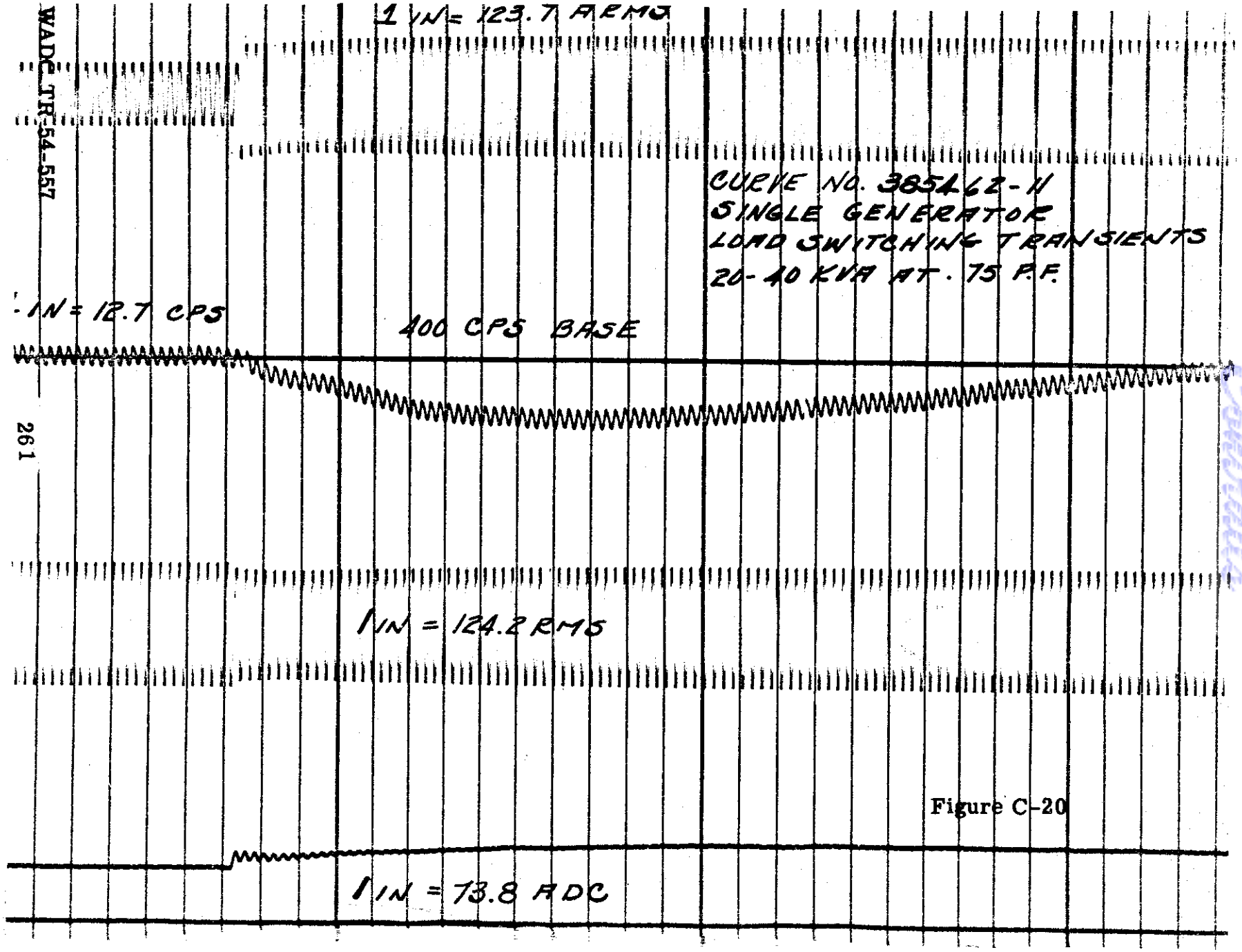

Figure C-20

C-4 WESTINGHOUSE AIRCRAFT A-C GENERATOR
TYPE 12QD30H, S# 1172465
30-KVA, THREE-PHASE, 120/208 VOLTS, 0 P.F.
400/800 CPS, 4000/8000 RPM
USAF SPEC. MIL-G-6099

WINDING RESISTANCES (Ohms at 25° C)

A-C Generator armature per phase (d-c)	.044
A-C Generator field	.521
Exciter armature	.053
Exciter shunt field	2.42
Exciter differential field	23.9
Exciter series plus interpole plus comp.	.078

REACTANCE (Per-unit) 6000 rpm, 600 cps

D - axis synchronous	(x_d)	1.98
D - axis transient (s.c. test)	(x'_d)	.392
D - axis subtransient (s.c. test)	(x''_d)	.301
D - axis subtransient (locked rotor test)	(x''_d)	.312
Q - axis synchronous (slip test)	(x_q)	1.13
Q - axis subtransient (locked rotor test)	(x_q'')	.356
Zero sequence (single phase test)	(z_0) .034 + j	.020
Negative sequence (L-L short)	(z_2) .104 + j	.290

TIME CONSTANTS (in seconds)

Open-circuit transient	(T'_{do})	.0833
Short-circuit transient	(T'_d)	.0218
Short-circuit subtransient	(T''_d)	.0022
Exciter shunt field	(T_1)	.026

Figure C-21 A-C Generator Saturation Characteristics
30-Kva, three-phase, .9 pf, 120/208 volts
(for 6000 rpm)

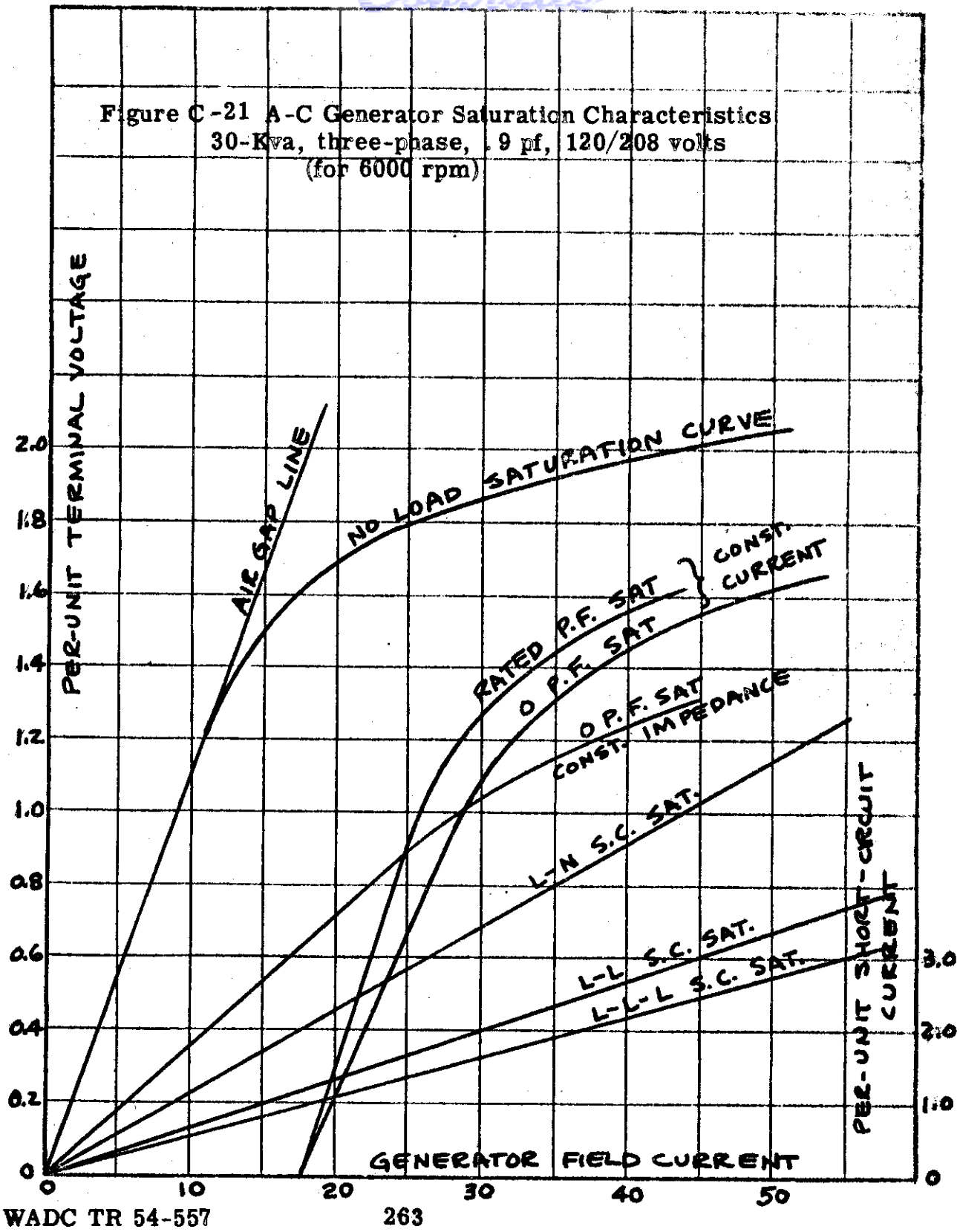

Figure C-22 A-C Generator Exciter Saturation Characteristics
30-Kva, three-phase, .9 pf. 120/208 volts
(for 8000 rpm)

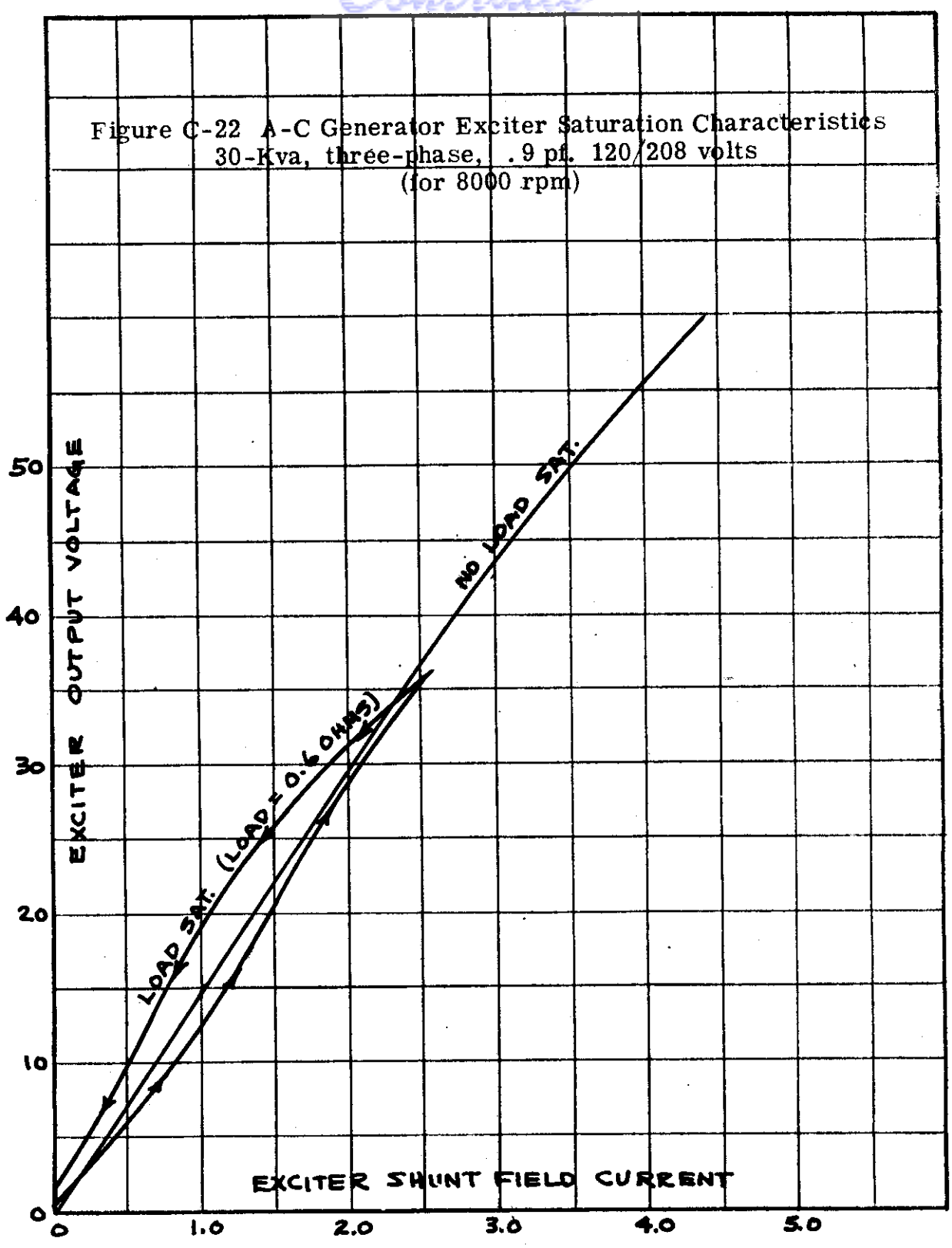

C-5 WESTINGHOUSE AIRCRAFT A-C GENERATOR
TYPE 12RD8E, S# 1172429
8-KVA, SINGLE-PHASE, 120 VOLTS, 9 P.F.
380/1000 CPS, 3800/10,000 RPM
USAF TYPE B-1

WINDING RESISTANCES (Ohms at 25° C)

A-C Generator armature per phase (d-c)	.18
A-C Generator field	20.2

REACTANCES (Per-unit) 6000 rpm, 600 cps

D - axis synchronous	1.26
D - axis transient	.334
D - axis subtransient	.297

TIME CONSTANTS (in seconds)

T_{do}' - Open-circuit transient	.095
T_{d}' - Short-circuit transient	.027
T_{d}'' - Short-circuit	.003

Figure C-23 A-C Generator Saturation Characteristics
8-Kva, single-phase, .90 pf, 120 volts
(for 6000 rpm)

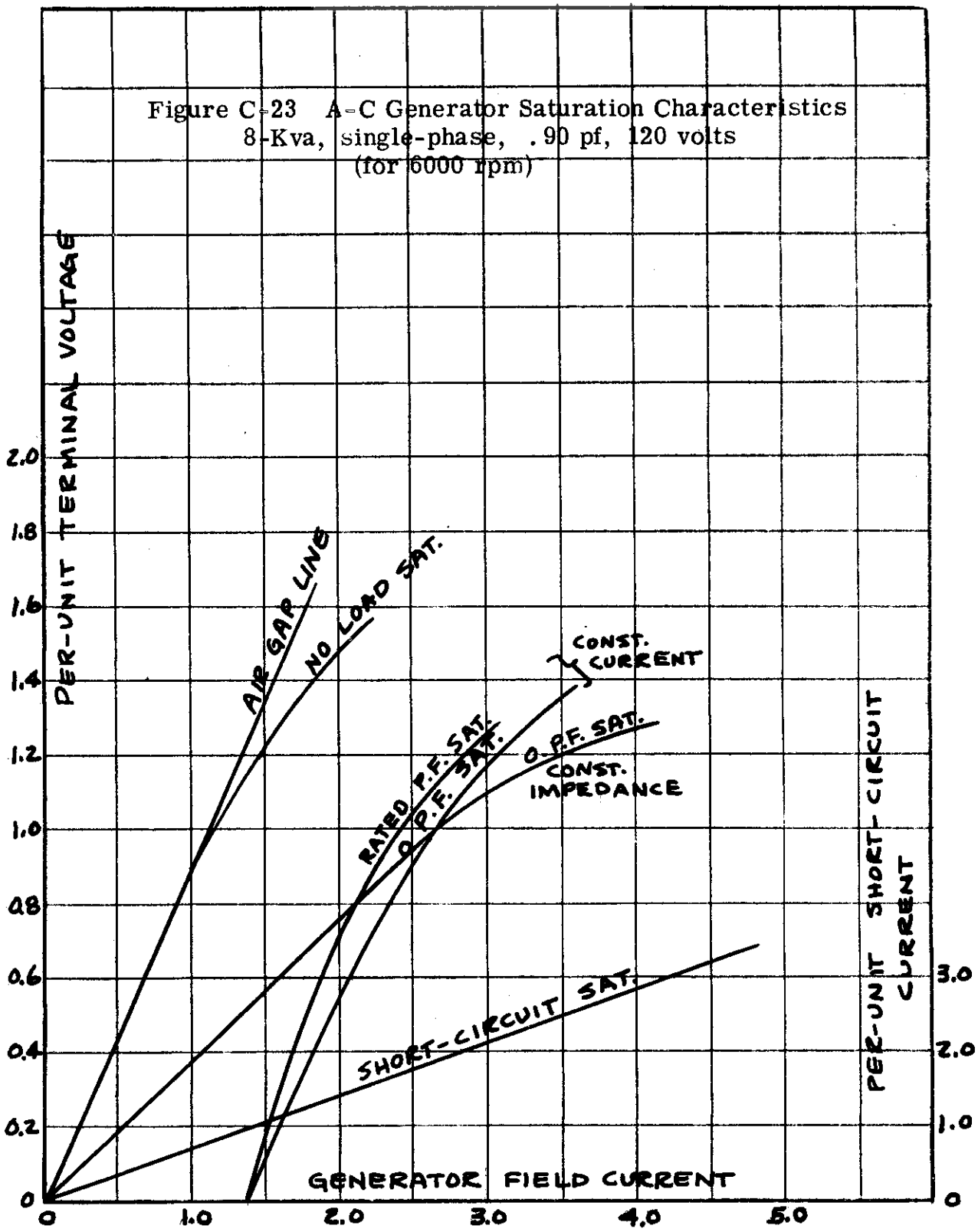

APPENDIX D

ACTUAL MOCK-UP TESTS OF PARALLEL A-C GENERATORS

This appendix is a collection of oscillograms taken of the operation of a two-generator parallel system. The purpose for including this material into the report is to demonstrate the operation of such a parallel system and also to show the differences that exist between generators operated by carbon-pile regulators and those operated by magnetic-amplifier regulators. Part 1 of this appendix covers the operations with carbon-pile regulator control, while Part 2 covers the same operations but with a magnetic-amplifier regulator instead.

The following tests were conducted on the mock-up:

(1) Paralleling, both automatic and manual
(2) Load switching, both on and off
(3) A-C generator feeder faults
(4) Excitation faults
(5) Manual application and removal of bus faults.

It will be noted that the actual number of individual tests is much greater in the case of the magnetic-amplifier regulator than that of the carbon-pile regulator. This was a necessity because of the fact that faults occurring on different phases where a magnetic amplifier control is used may produce different operating conditions. In the case of the carbon-pile regulator this is not true.

The following equipment was used as a part of the two-generator system (two complete sets):

(1) Westinghouse Type 8QL40H a-c generator
40 KVA, three-phase, 120/208 volts, 0.75 P.F.
380/420 cps, 5700/6300 rpm, USAF Type MB-1
(See Appendix C-3 for a description of the characteristics of this machine)

(2) Sundstrand Constant Speed Drive, Type 609179

(3) Westinghouse Type AVP-39 control and protective panel

(4) Westinghouse Type AVA-5 automatic paralleling relay

(5) Westinghouse Type AVR-10B circuit breakers
USAF Type A-1

(6) Voltage Regulators:

(a) Westinghouse Type AVR-370-E carbon-pile voltage regulator

(b) Westinghouse Type AVR-22-A magnetic-amplifier voltage regulator

The bus arrangement used for these tests is shown in Figure D-1 with a more complete circuit in Figure D-2 which also shows the reactive load division network.

The frequency of the bus voltage is shown in all oscillograms and is an indication of the transient performance of the drive system used to operate the a-c generators.

In each figure the small timing intervals are 0.01 seconds while the large heavier lines indicate every 0.10 seconds.

This data is presented to show the typical operation of a two-generator system with either carbon-pile regulator control or magnetic-amplifier control. At the same time, these oscillograms demonstrate the performance of a typical a-c generator for which the essentials constants are given in Appendix C-3.

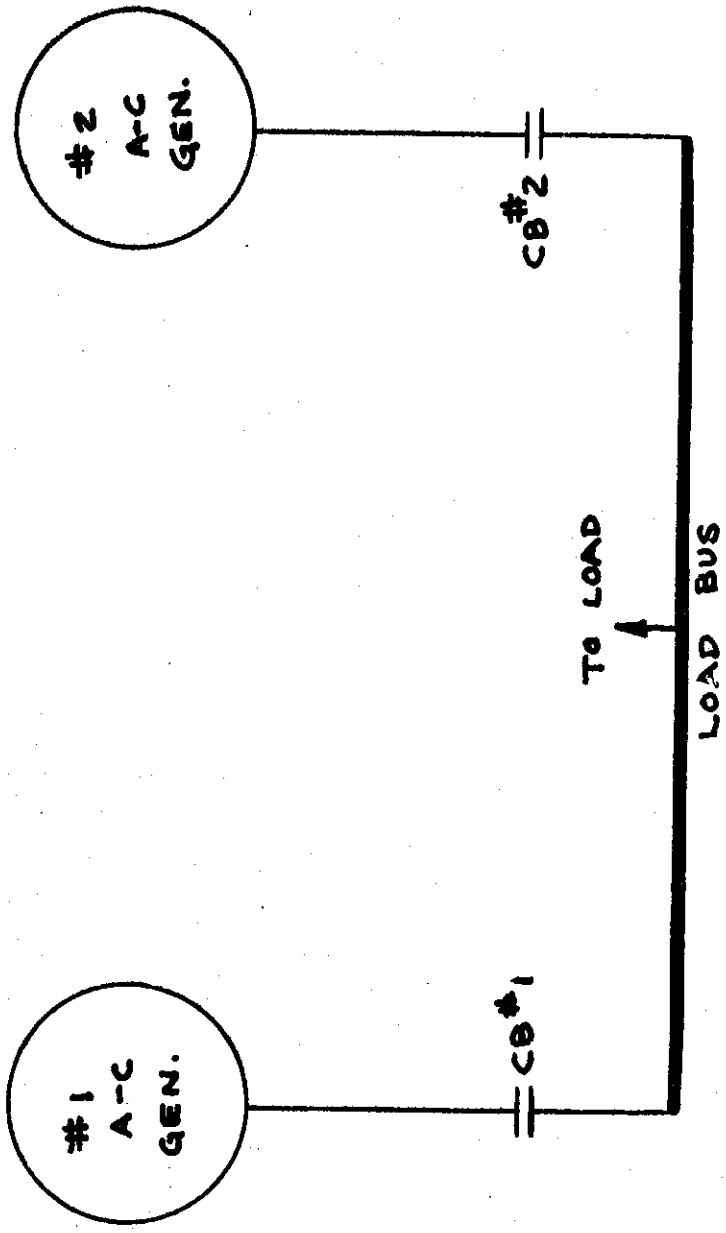

Figure D-1 Bus Arrangement Used For Parallel Tests

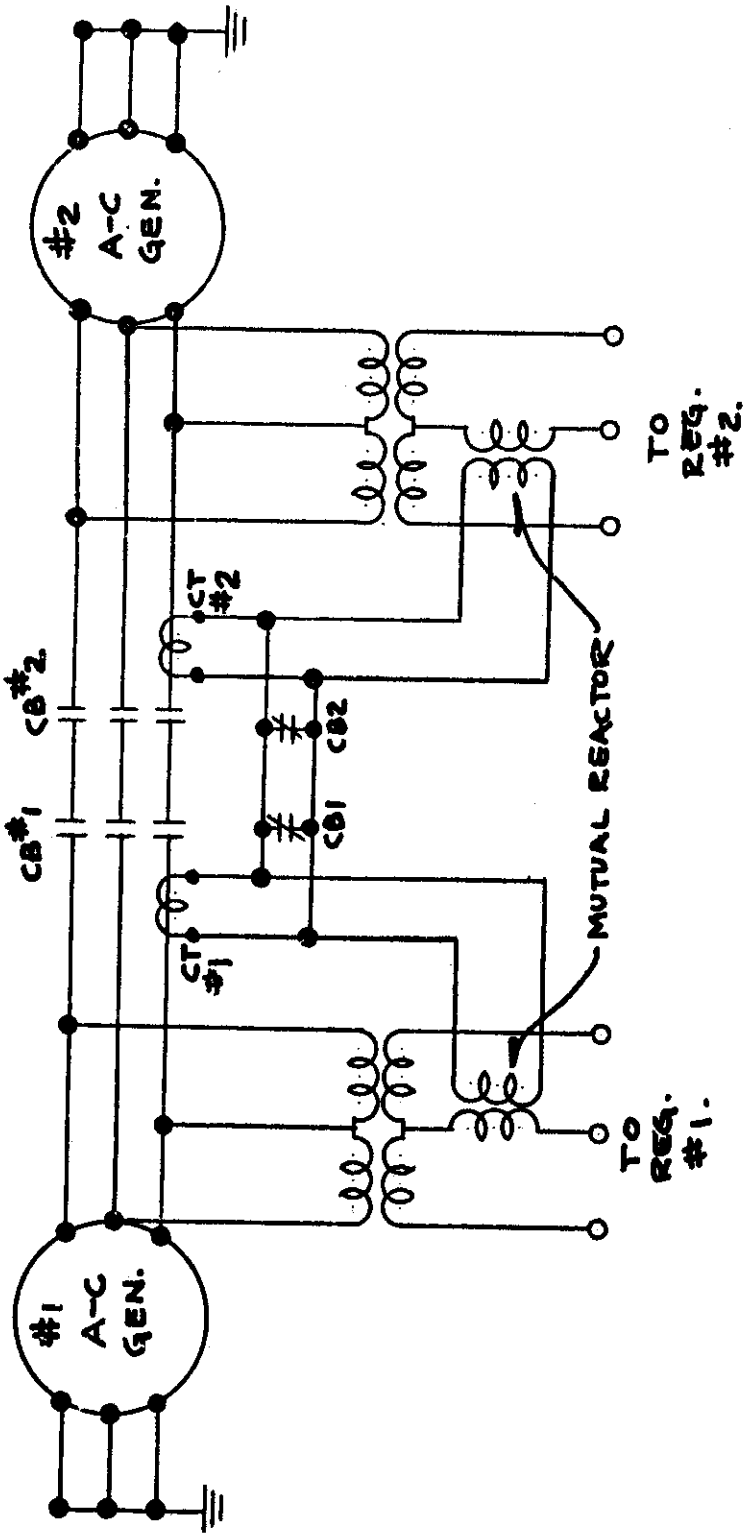

Figure D-2 Parallel System Schematic Showing Reactive Load Division Circuit

TABLE D-1

Symbols Used On Oscillograms

I_1	-	current in phase 1
I_2	-	current in phase 2
I_3	-	current in phase 3
E_{1-N}	-	line-to-neutral voltage on phase 1
E_{2-N}	-	line-to-neutral voltage on phase 2
E_{3-N}	-	line-to-neutral voltage on phase 3
I_{FAULT} (I_{TOTAL})	-	total fault current
AFA	-	a-c generator field current
FREQ	-	frequency of the bus voltage
#1	-	refers to number 1 machine
#2	-	refers to number 2 machine

D-1 PARALLEL SYSTEM TESTS USING TWO 40-KVA A-C GENERATORS WITH CARBON-PILE VOLTAGE REGULATOR CONTROL

D-1-a Paralleling Transients

(1) Test Procedure

With number 1 generator connected to the bus, number 2 was also connected to the bus under the following conditions:

(a) Automatic paralleling, no load on bus

(b) Automatic paralleling, 40-kva on bus

(c) Manual paralleling, 120 degrees out of phase, no load on bus

(d) Manual paralleling, 180 degrees out of phase, no load on bus

(2) Test Results

The results of this test are shown on the attached oscillograms as follows:

Load	Paralleling	Figure No.
0	Automatic	D-3
40	Automatic	D-4
0	Manual (120 degrees)	D-5
0	Manual (180 degrees)	D-6

D-1-b Load Switching Transients

(1) Test Procedure

With two generators operating in parallel, various loads were applied and removed on the system bus to determine the load switching transients.

(2) Test Results

The results of these tests are shown on oscillograms as follows:

Load, KVA	P. F.	Figure No.
0-20	.75	D-7
20-0	.75	D-8
0-40	.75	D-9
40-0	.75	D-10
0-60	.75	D-11
60-0	.75	D-12
0-80	.75	D-13
80-0	.75	D-14
20-60	.75	D-15
60-20	.75	D-16
40-80	.75	D-17
80-40	.75	D-18

D-1-c Generator Feeder Faults Within Differential Protection Zone

(1) Test Procedure

With two generators operating in parallel with zero and 40 KVA at 75% P. F. bus loads, line-to-ground, line-to-line and three phase symmetrical faults were imposed on the system within the differential protection zone of one of the generators. The total fault impedance was about 0.03 ohms. In all cases number 1 generator was faulted. See Figure D-19.

(2) Test Results

The results of these tests are shown on oscillograms as follows:

Type of Fault	Bus Load	Figure No.
T_1 - N	0	D-20
T_1 - T_2	0	D-21
T_1 - T_2 - T_3	0	D-22
T_1 - N	40	D-23
T_1 - T_2	40	D-24
T_1 - T_2 - T_3	40	D-25

D-1-d Excitation Faults

(1) Test Procedure

With two generators operating in parallel, various excitation type faults were applied to the system while the system load was zero and 40 KVA at .75 P.F. The faults included the opening of regulator sensing leads and shorting F to A+ on the exciter. See Figure D-26 for pictorial explanation of faults.

(2) Test Results

The results of these tests are shown on oscillograms as follows:

Type of Fault	Bus Load	Figure No.
Short F to A+	0	D-27
Short F to A+	40	D-28
Open T_1 Sensing Lead	0	D-29
Open T_1 Sensing Lead	40	D-30

D-1-e Manual Application and Removal of Bus Faults Test Procedure

(1) Test Procedure

With two generators operating in parallel and with zero and 40 KVA at 75% P.F. load line-to-line, line-to-neutral and three phase symmetrical faults on the bus were manually applied and removed. See figure D-19. Faults are outside of the differential protection zone.

(2) Test Results

The results of these tests are shown on oscillograms as follows:

Type of Fault	Bus Load	Figure No.
Application T_1-N	0	D-31
Removal T_1-N	0	D-32
Application T_1-T_2	0	D-33
Removal T_1-T_2	0	D-34
Application T_1-T_2-T_3	0	D-35
Removal T_1-T_2-T_3	0	D-36
Application T_1-N	40	D-37
Removal T_1-N	40	D-38
Application T_1-T_2	40	D-39
Removal T_1-T_2	40	D-40
Application T_1-T_2-T_3	40	D-41
Removal T_1-T_2-T_3	40	D-42

D-2 PARALLEL SYSTEM TESTS USING TWO 40-KVA A-C GENERATORS WITH MAGNETIC AMPLIFIER VOLTAGE REGULATOR CONTROL

D-2-a Paralleling Transients

(1) Test Procedure

With number 1 generator connected to the bus, number 2 was also connected to the bus under the following conditions:

1. Automatic paralleling, no load on bus
2. Automatic paralleling, 40 KVA on bus
3. Manual paralleling, 120 degrees out of phase, no load on bus
4. Manual paralleling, 180 degrees out of phase, no load on bus

(2) Test Results

The results of this test are shown on oscillograms as follows:

Load	Paralleling	Figure No.
0	Automatic	D-43
40	Automatic	D-44
0	Manual (120 degrees)	D-45
0	Manual (180 degrees)	D-46

D-2-b Load Switching Transients

(1) With two generators operating in parallel, various loads were applied and removed on the system bus to determine the load switching transients.

(2) Test Results

The results of these tests are shown on oscillograms as follows:

Load, KVA	P. F.	Figure No.
0-20	.75	D-47
20-0	.75	D-48
0-40	.75	D-49
40-0	.75	D-50
0-60	.75	D-51
60-0	.75	D-52
0-80	.75	D-53
80-0	.75	D-54
20-60	.75	D-55
60-20	.75	D-56
40-80	.75	D-57
80-40	.75	D-58

D-2-c Excitation Faults

(1) Test Procedure

With two generators operating in parallel, various excitation type faults were applied to the system while the system load was zero and 40 KVA at .75 P.F. The faults included the opening of regulator sensing leads, shorting F to A+ on the exciter and opening F from the regulator to the exciter. See Figure D-59 for pictorial explanation of faults.

(2) Test Results

The results of these tests are shown on oscillograms as follows:

Type of Fault Load	KVA	Figure No.
Open T_1 sensing lead	0	D-60
Open T_1 sensing lead	40	D-61
Open T_2 sensing lead	0	D-62
Open T_2 sensing lead	40	D-63
Open T_3 sensing lead	0	D-64
Open T_3 sensing lead	40	D-65
Short F to A+	0	D-66
Short F to A+	40	D-67
Open F lead (start)	0	D-68
Continuation of Figure D-68	0	D-69
Open F lead (start)	40	D-70
Continuation of Figure D-70	40	D-71

D-2-d Generator Feeder Faults Within Differential Protection Zone

D-2-d-1 No Load on Bus

(1) Test Procedure

With two generators operating in parallel, line-to-ground, line-to-line and three phase symmetrical faults were imposed on the system within the differential protection zone of one of the generators. The total fault impedance was about 0.03 ohms. In all cases number 1 generator was faulted. See Figure D-72.

(2) Test Results

The results of these tests are shown on oscillograms as follows:

Type of Fault	Figure No.
T_1 - N	D-73
T_2 - N	D-74
T_3 - N	D-75
T_1 - T_2	D-76
T_2 - T_3	D-77
T_3 - T_1	D-78
T_1 - T_2 - T_3	D-79
T_1 - T_2 - N	D-80
T_1 - T_2 - T_3 - N	D-81

D-2-d-2 Rated Load on Bus

(1) Test Procedure

With two generators operating in parallel, line-to-ground, line-to-line and three phase symmetrical faults were imposed on the system within the differential protection zone of one of the generators. The total fault impedance was about 0.03 ohms. In all cases number 1 generator was faulted. See Figure D-72.

(2) Test Results

The results of these tests are shown on oscillograms as follows:

Type of Fault	Figure No.
T_1 - N	D-82
T_2 - N	D-83
T_3 - N	D-84
T_1 - T_2	D-85
T_2 - T_3	D-86
T_3 - T_1	D-87
T_1 - T_2 - T_3	D-88
T_1 - T_2 - N	D-89
T_1 - T_2 - T_3 - N	D-90

D-2-e Manual Application and Removal of Bus Faults

D-2-e-1 No Load on Bus

(1) Test Procedure

With two generators operating in parallel, line-to-line, line-to-neutral and three phase symmetrical faults on the bus were manually applied and removed.

(2) Test Results

The results of these tests are shown on oscillograms as follows:

Type of Fault	Figure No.
Application T_1-N	D-91
Removal T_1-N	D-92
Application T_2-N	D-93
Removal T_2-N	D-94
Application T_3-N	D-95
Removal T_3-N	D-96
Application T_1-T_2	D-97
Removal T_1-T_2	D-98
Application T_2-T_3	D-99
Removal T_2-T_3	D-100
Application T_3-T_1	D-101
Removal T_3-T_1	D-102
Application T_2-T_3-N	D-103
Removal T_2-T_3-N	D-104

Application T_1-T_2-T_3	D-105
Removal T_1-T_2-T_3	D-106
Application T_1-T_2-T_3-N	D-107
Removal T_1-T_2-T_3-N	D-108

D-2-e-2 Rated Load on Bus

(1) Test Procedure

With two generators operating in parallel, line-to-line, line-to-neutral and three phase symmetrical faults on the bus were manually applied and removed.

(2) Test Results

The results of these tests are shown on oscillograms as follows:

Type of Fault	Figure No.
Application T_1-N	D-109
Removal T_1-N	D-110
Application T_2-N	D-111
Removal T_2-N	D-112
Application T_3-N	D-113
Removal T_3-N	D-114
Application T_1-T_2	D-115
Removal T_1-T_2	D-116
Application T_2-T_3	D-117
Removal T_2-T_3	D-118

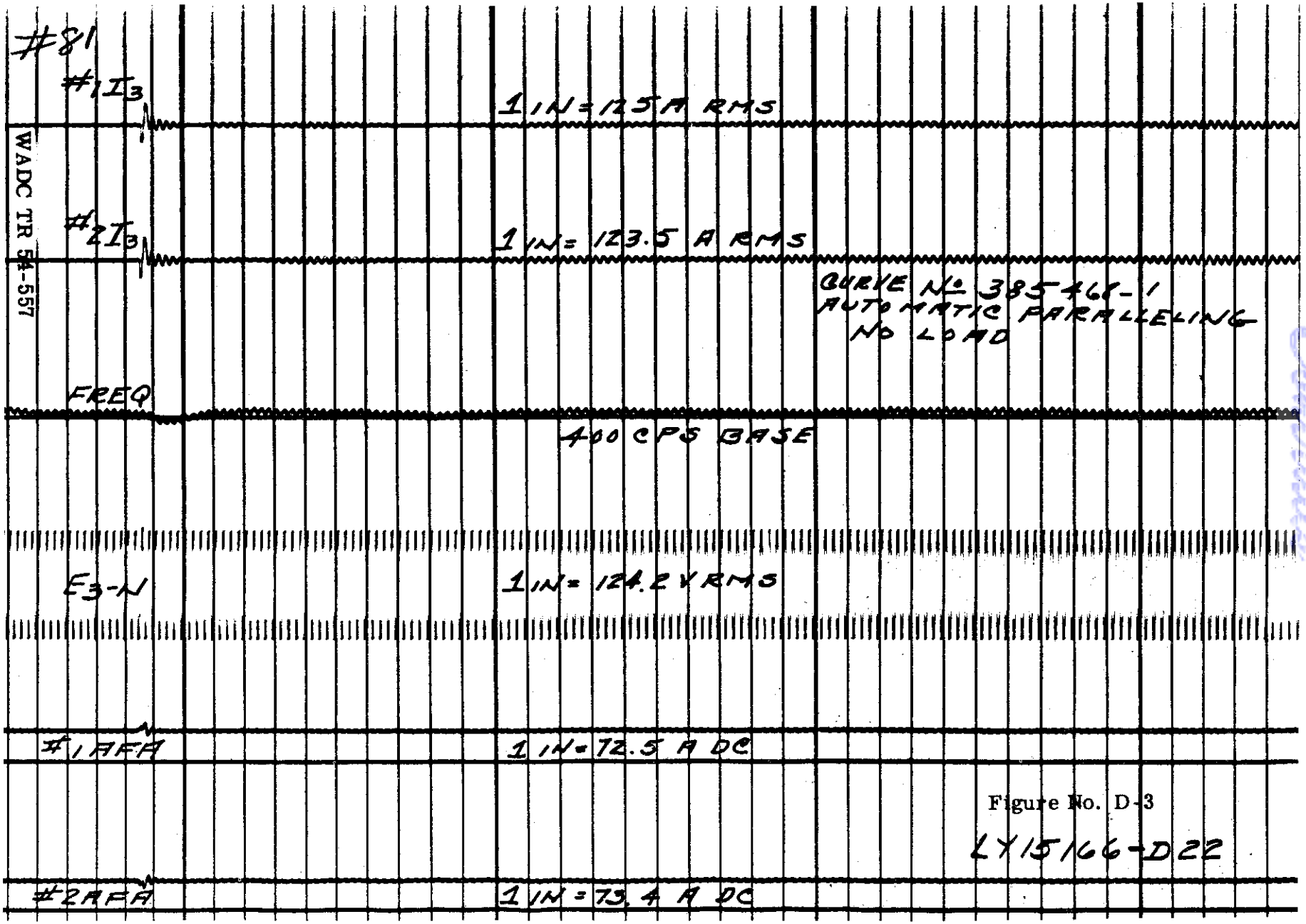

Figure No. D-3

LY15166-D22

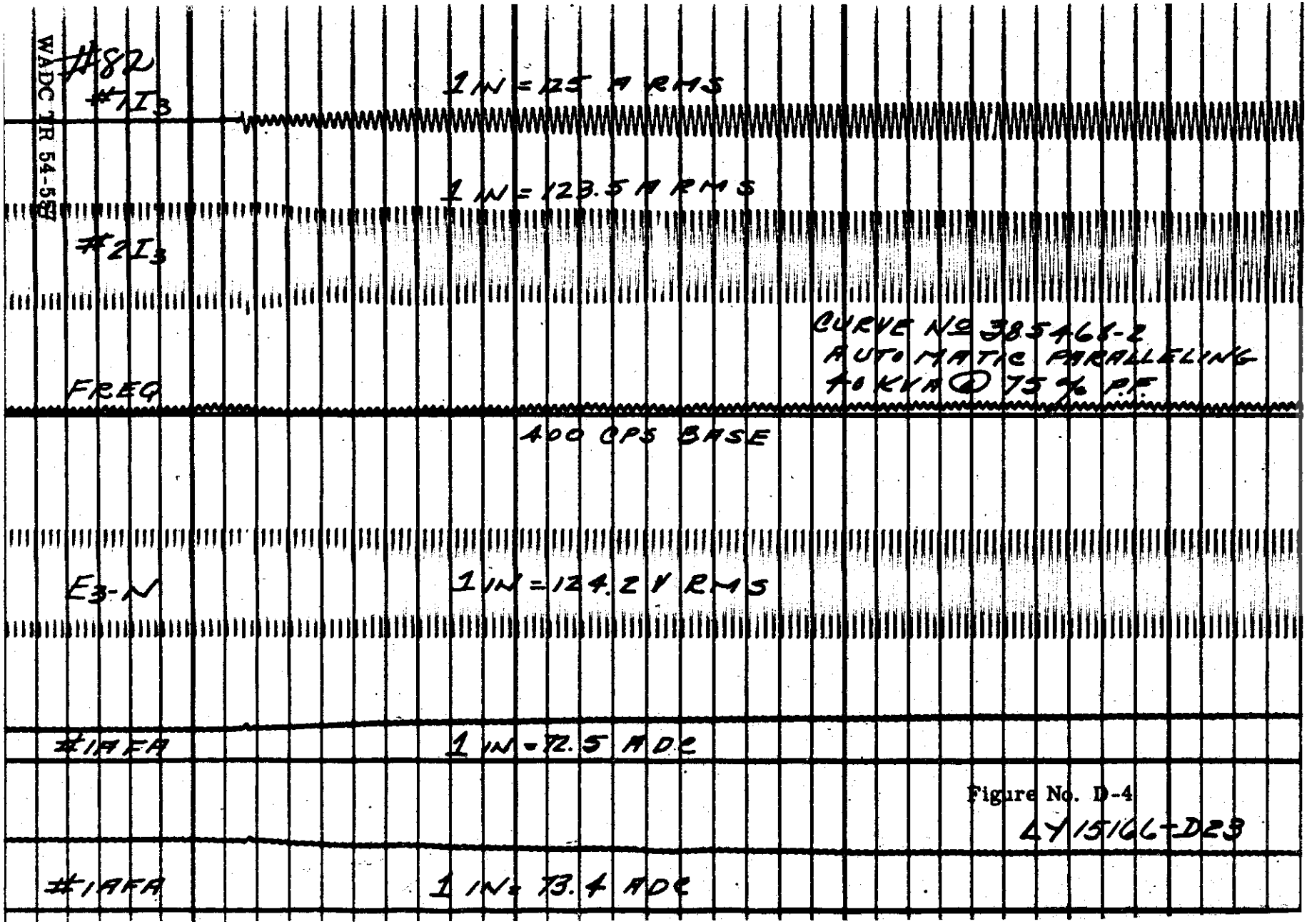

Figure No. D-4

4Y1516C-D23

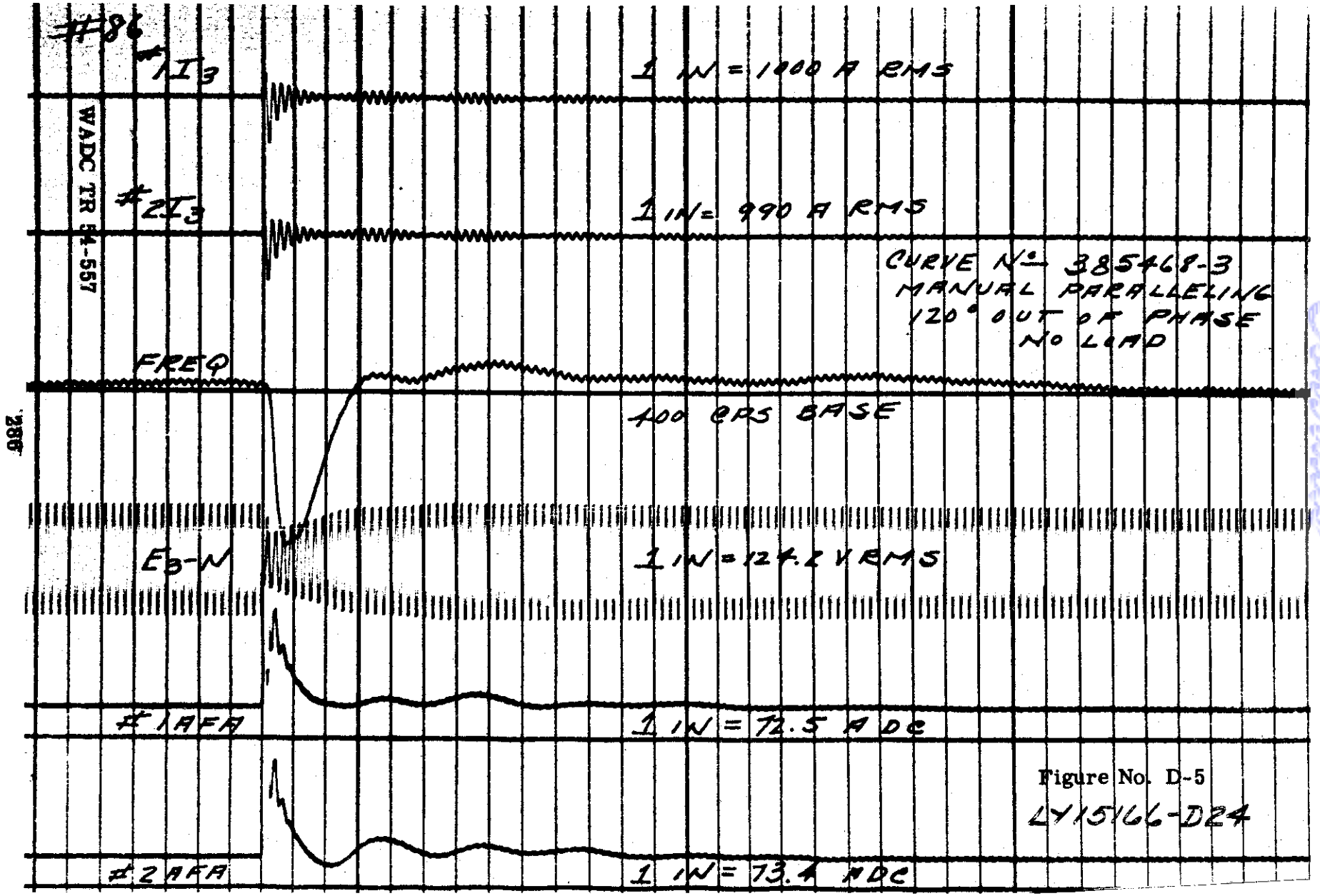

Figure No. D-5

LY15166-D24

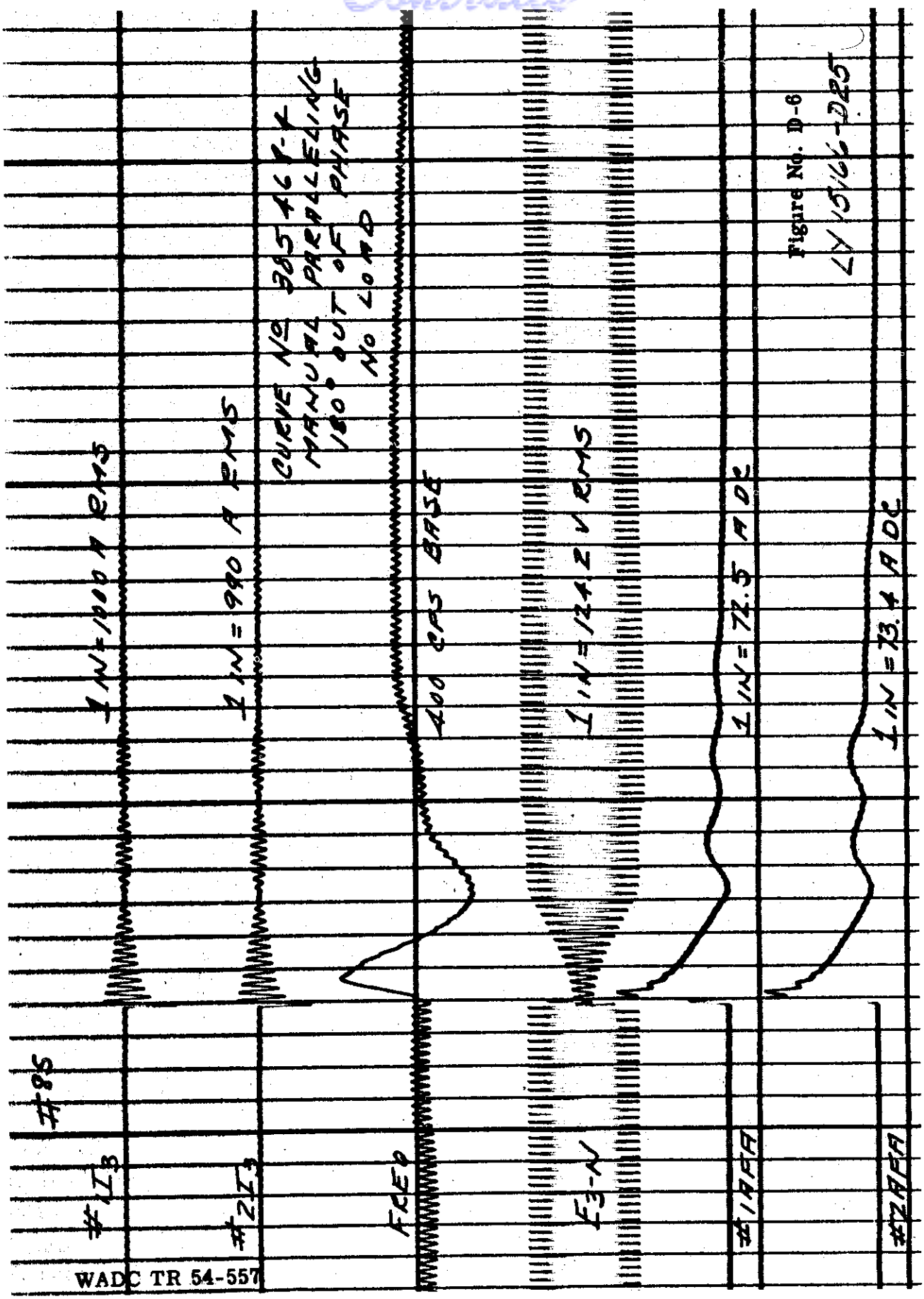

Figure No. D-6

Figure No. D-7
LY-5764-226

Figure No. D-8

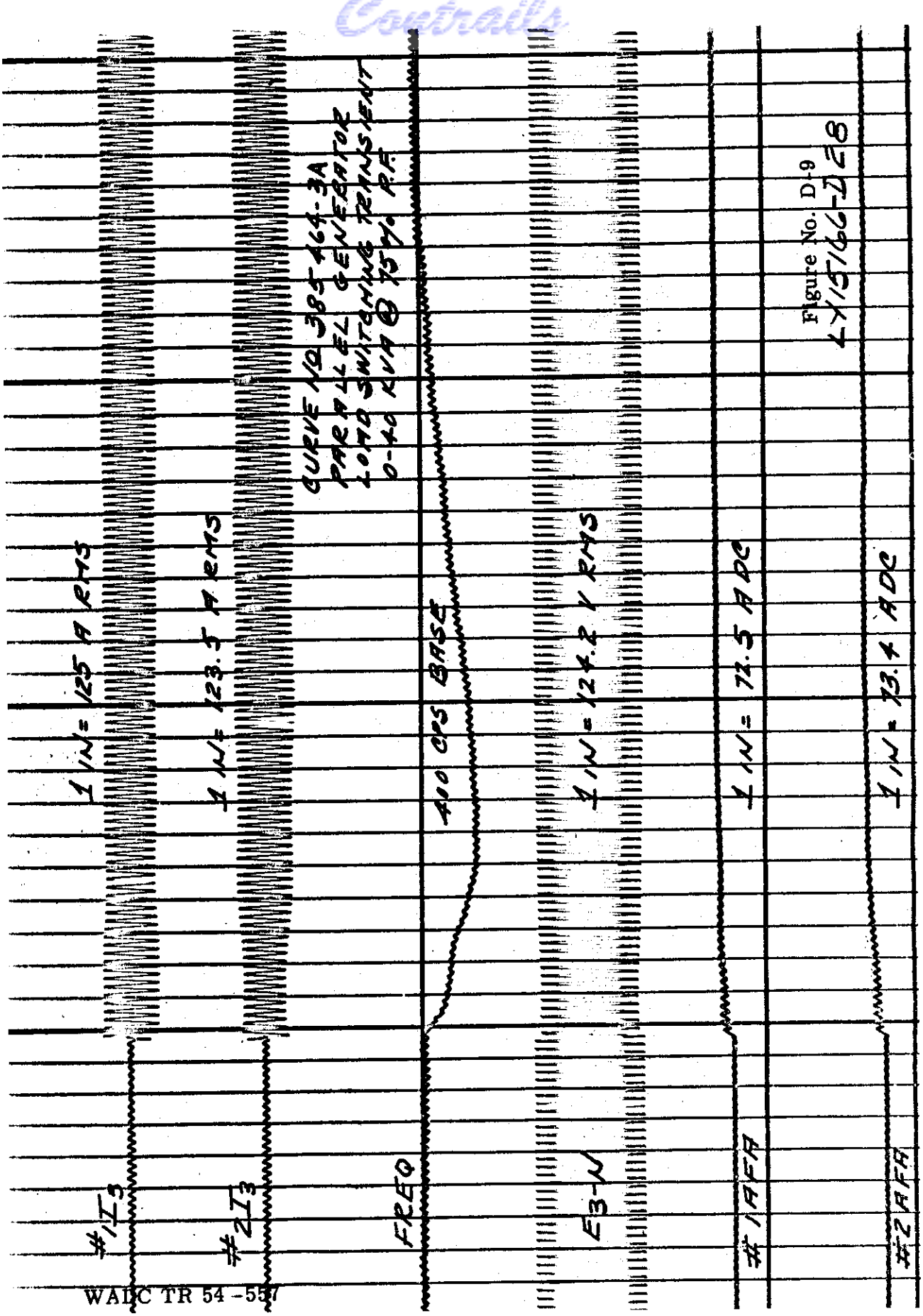

Figure No. D-9

WADC TR 54 -557

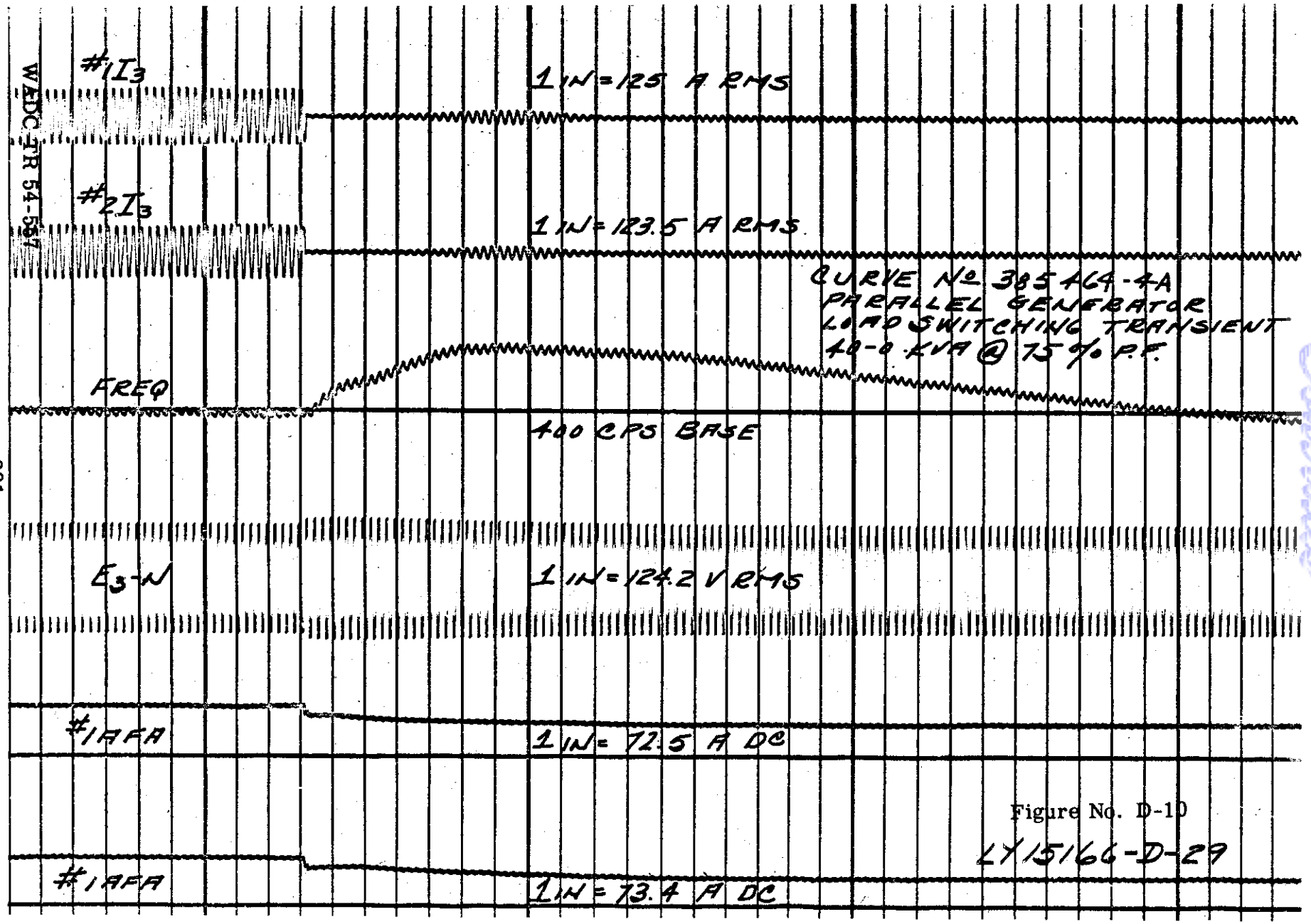

Figure No. D-10

LY15166-D-29

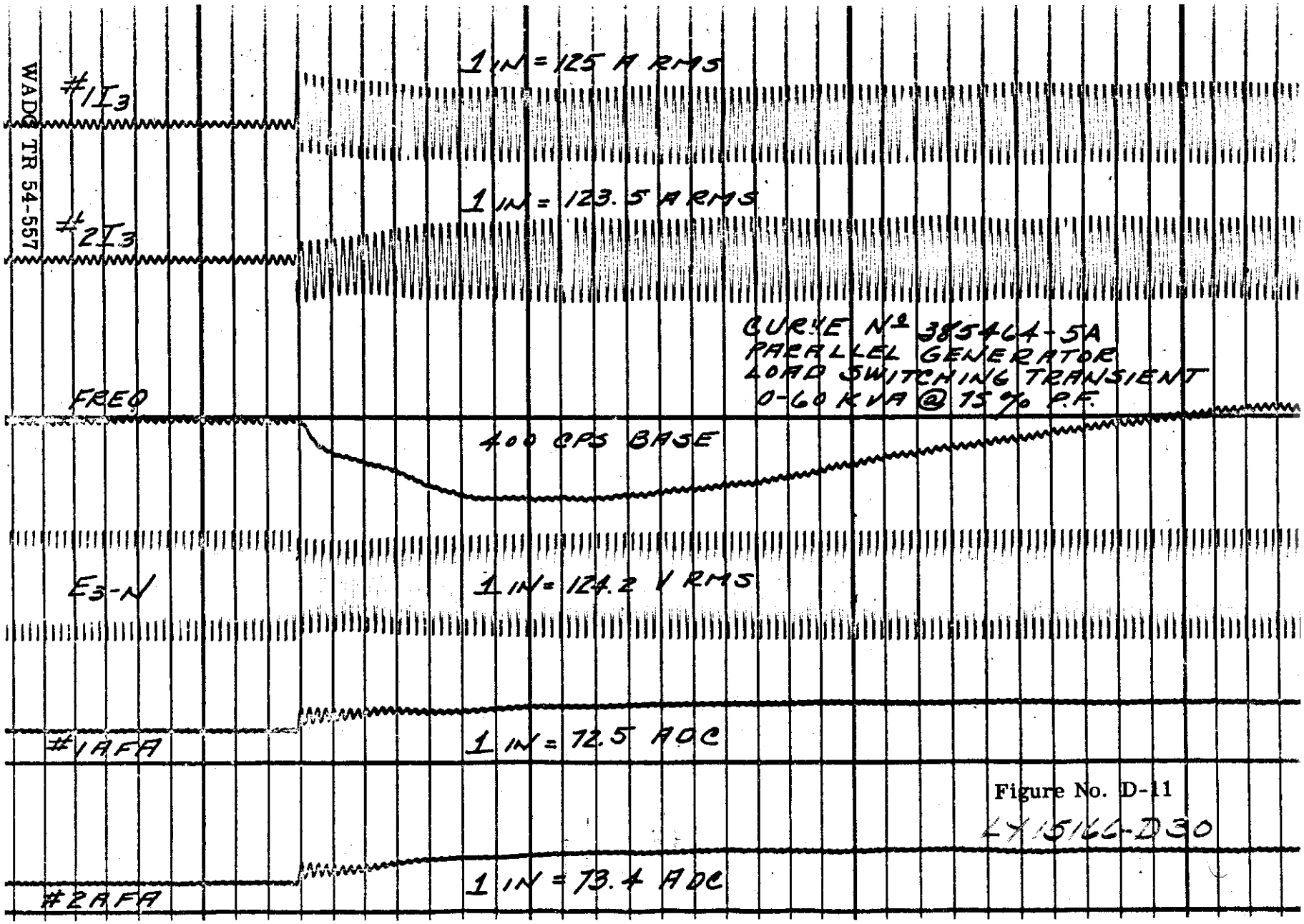

Figure No. D-11

LX15166-D30

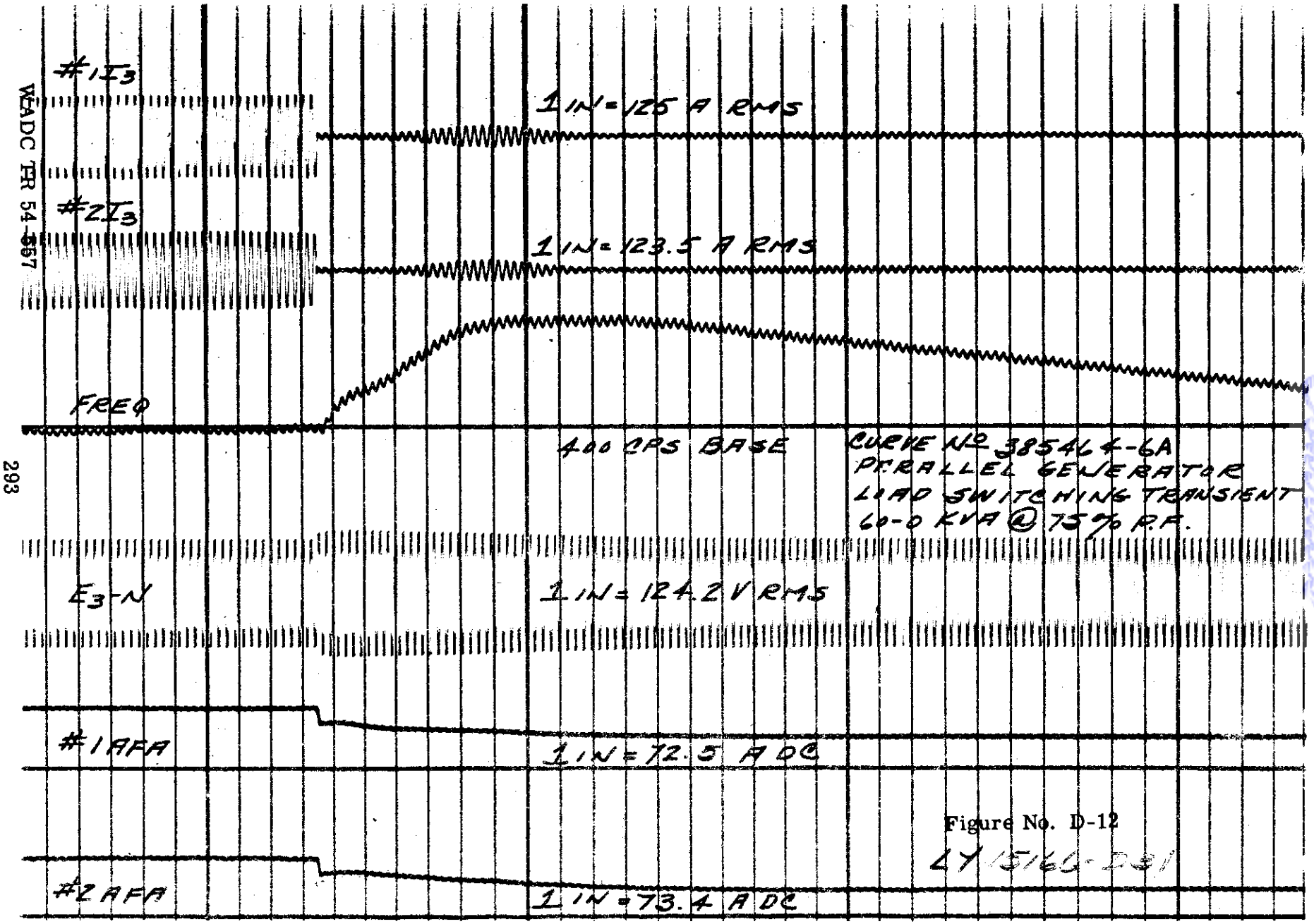

Figure No. D-12

47 5169-291

Figure No. D-13

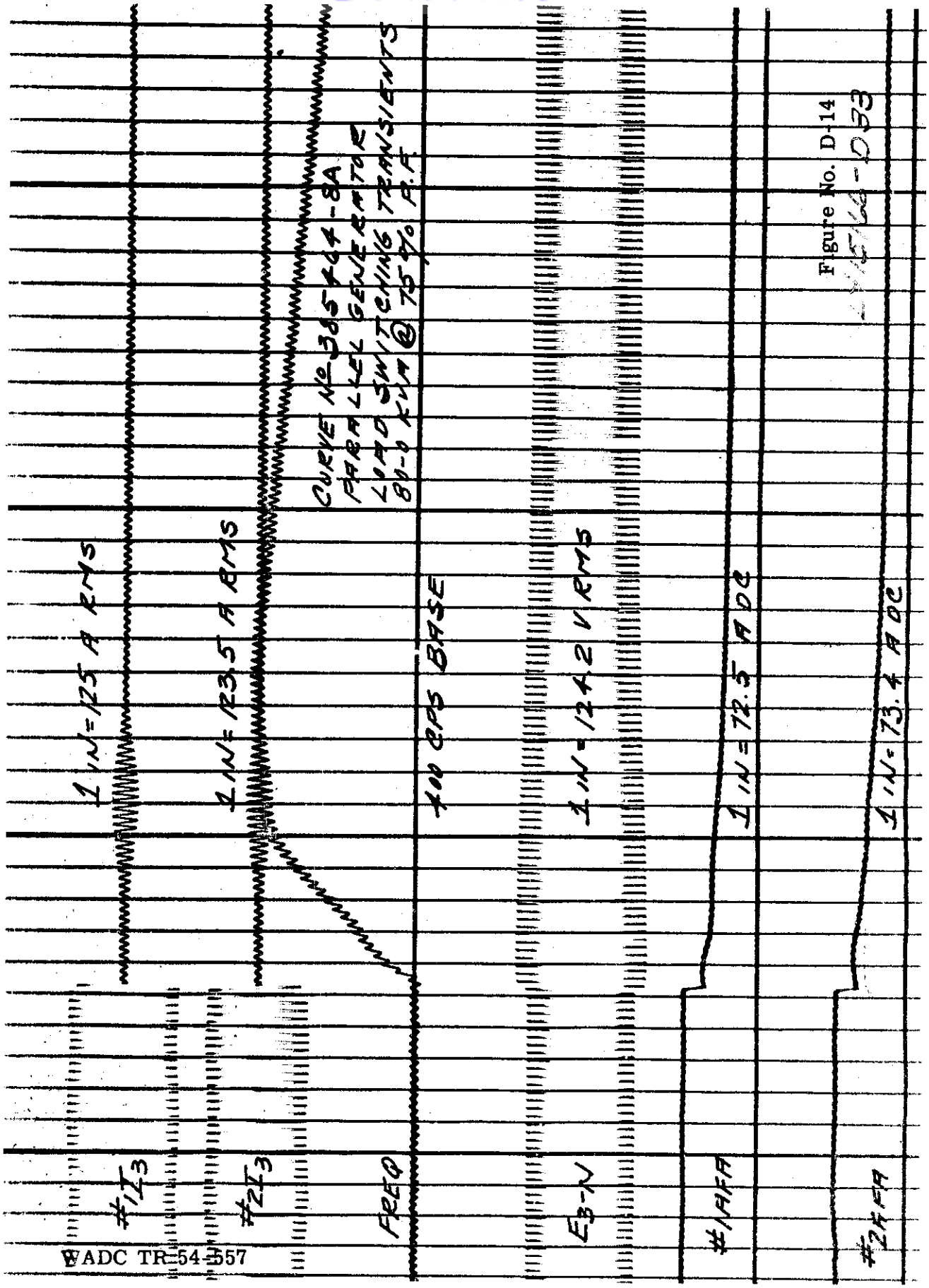

Figure No. D-14

WADC TR 54-557

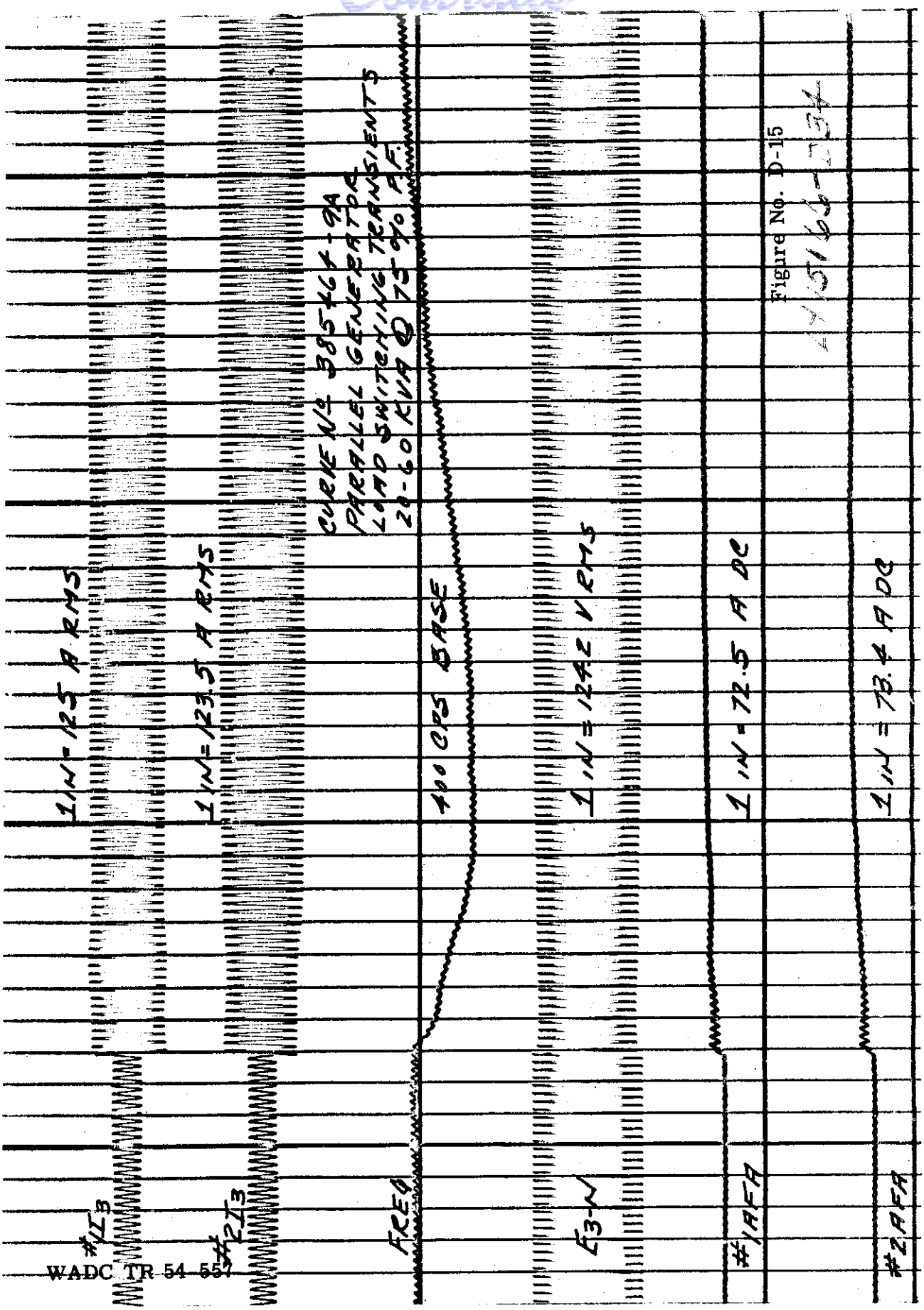

Figure No. D-15

Figure No. D-16

Figure No. D-17

Figure No. D-18

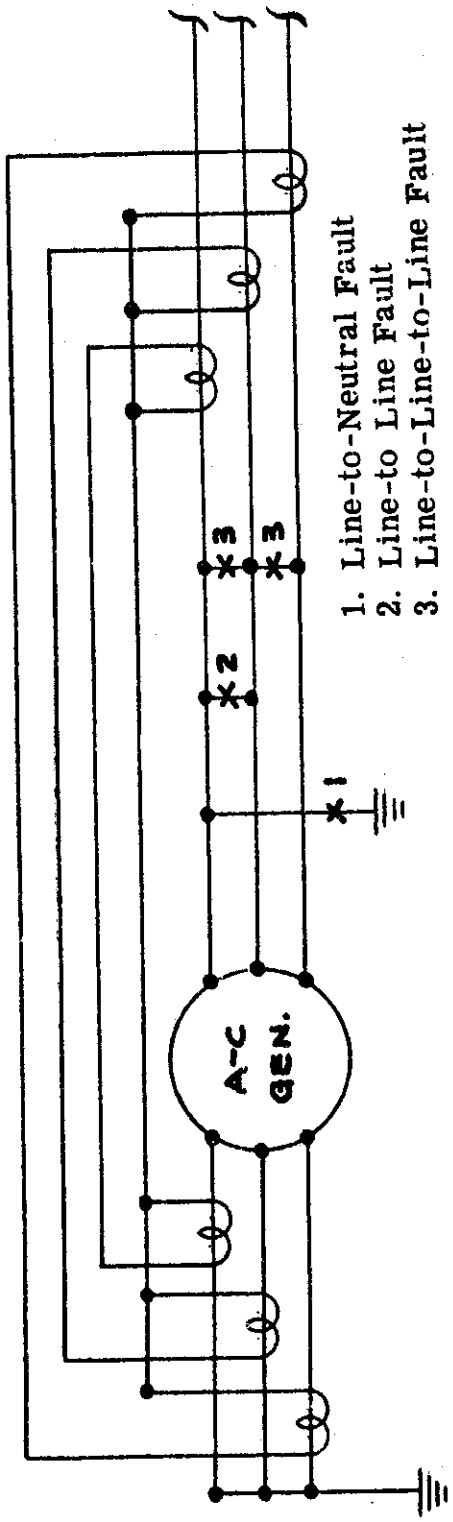

Figure D-19 Schematic Diagram Showing Where Feeder Faults Are Applied

Figure No. D-20

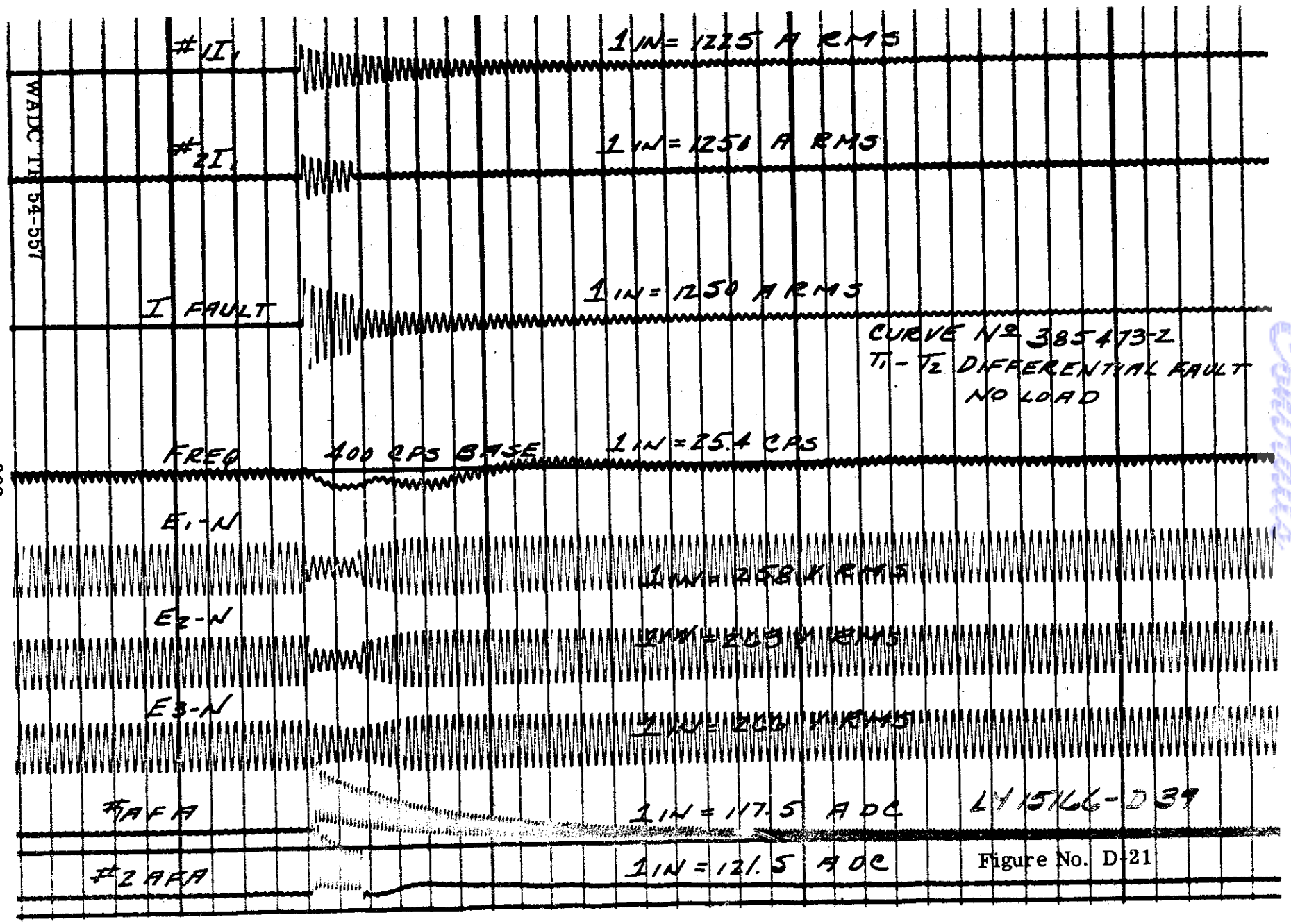

Figure No. D-42

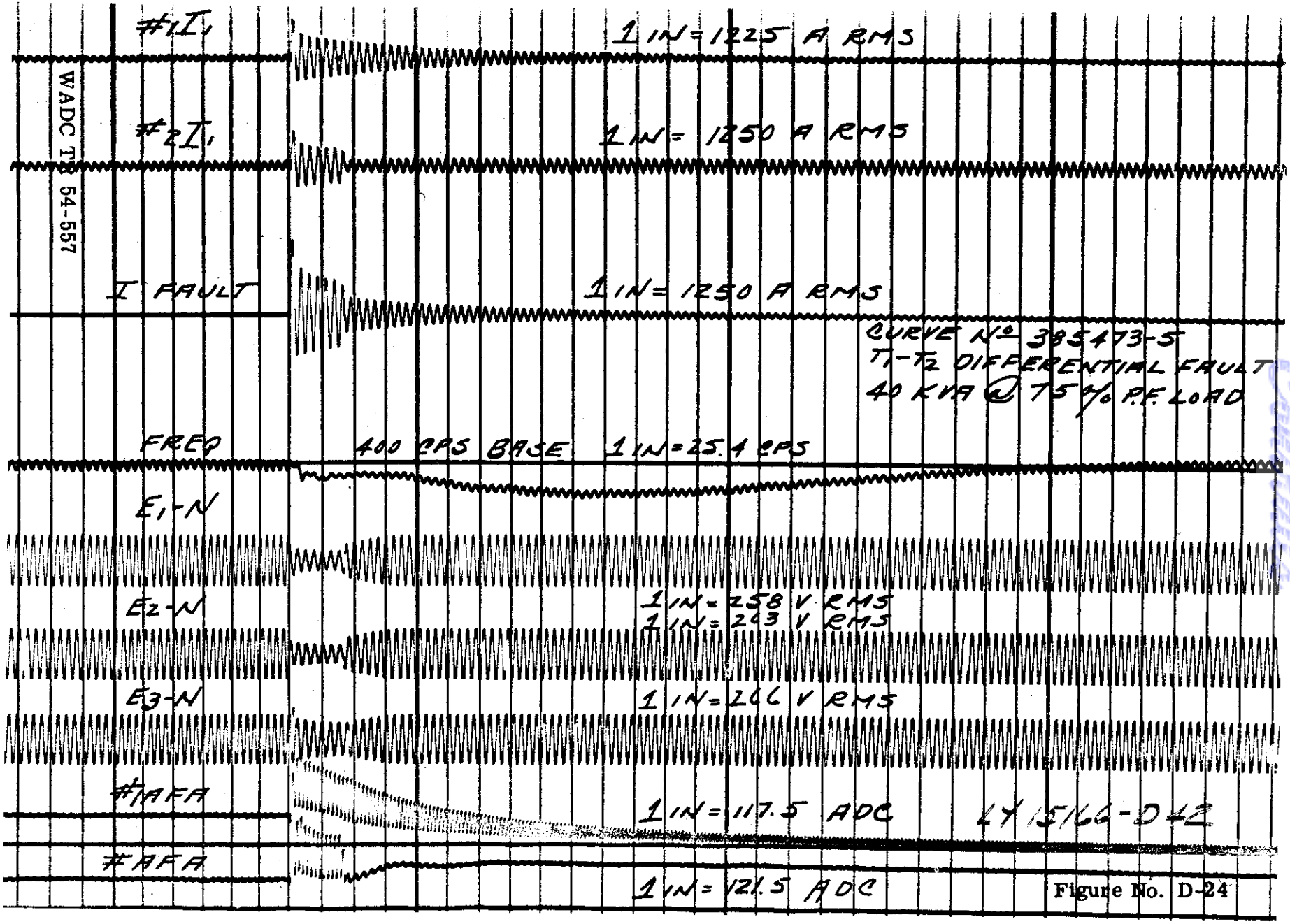

Figure No. D-24

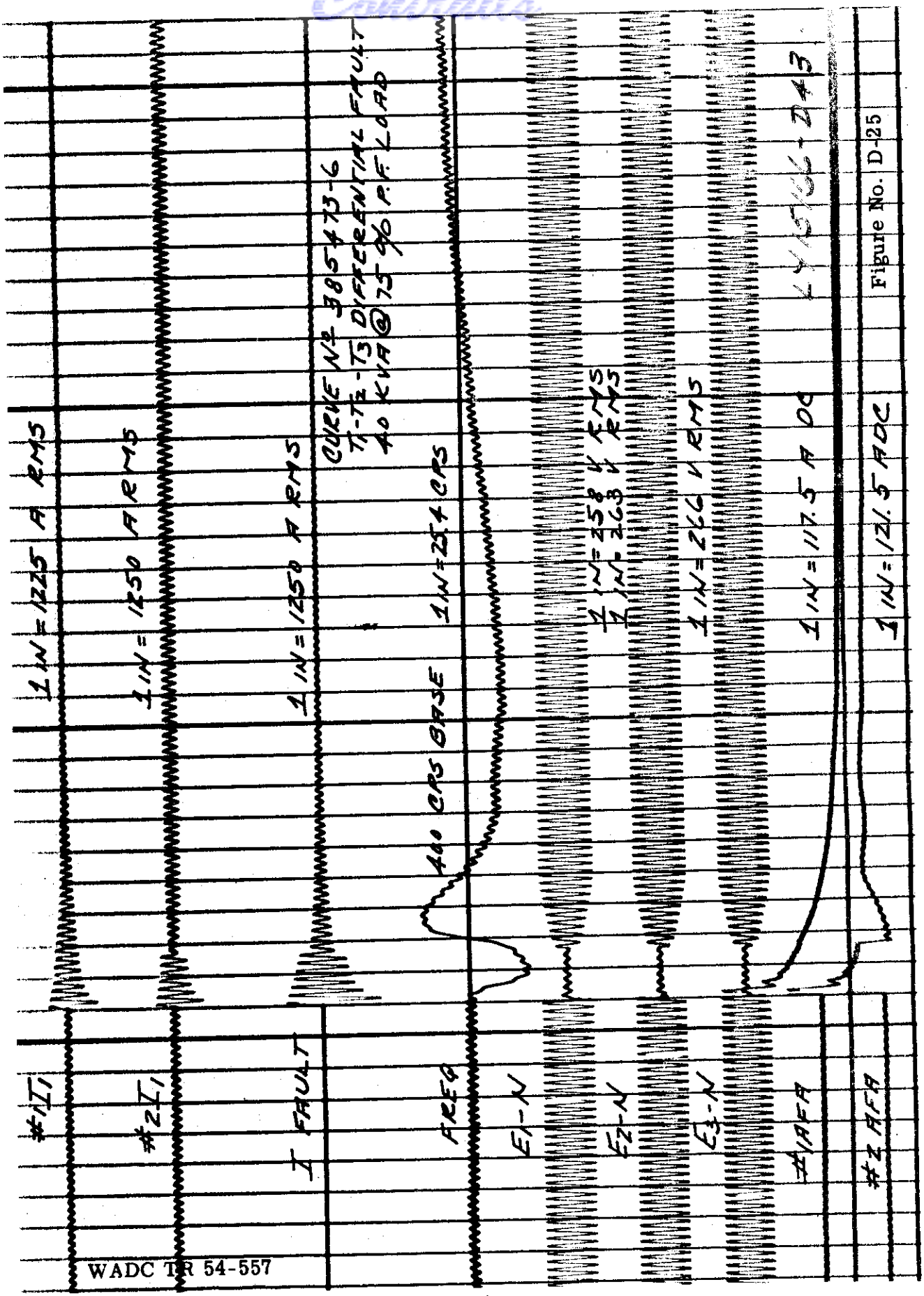

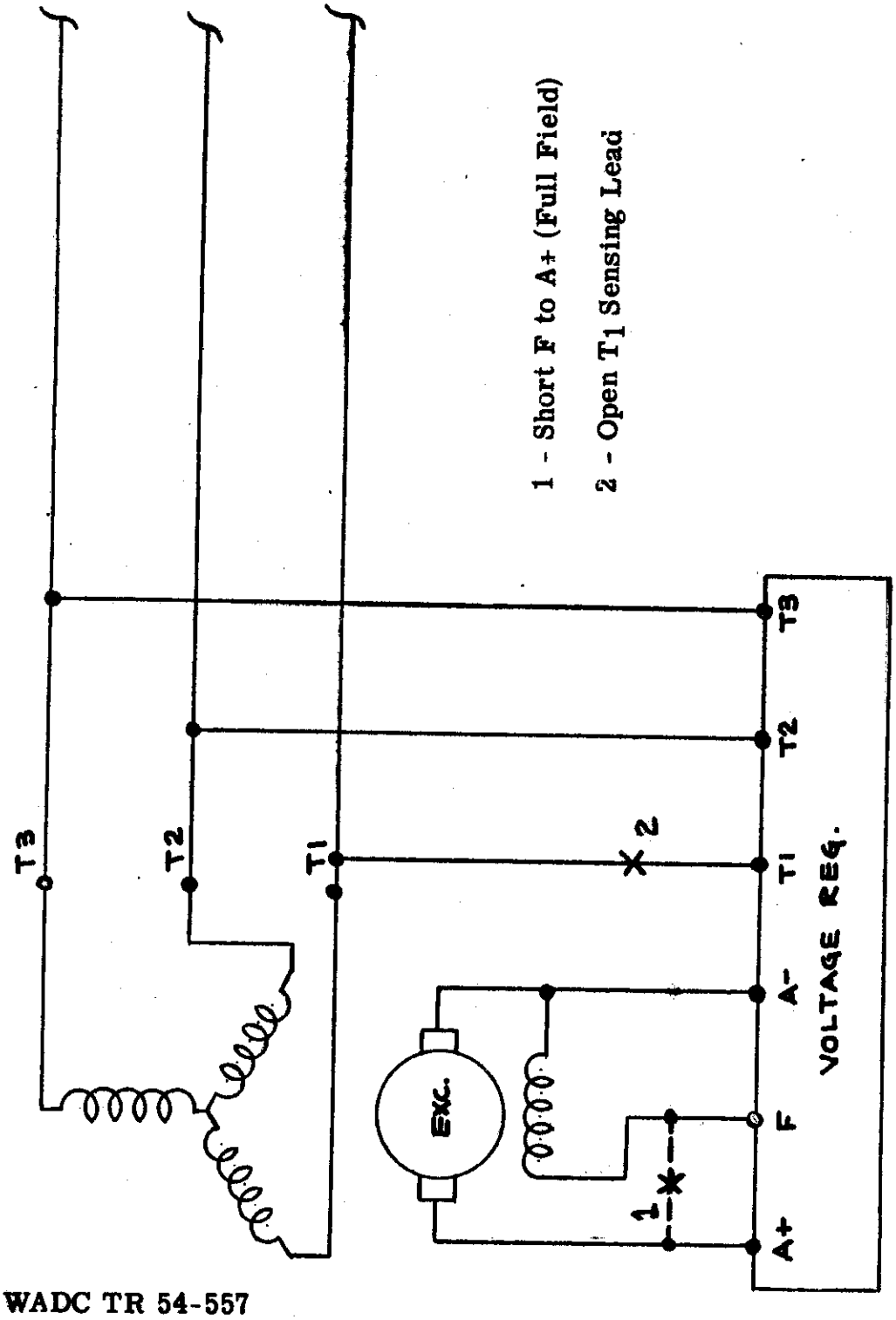

Figure D- 26 Schematic Showing Where Excitation Faults Are Applied

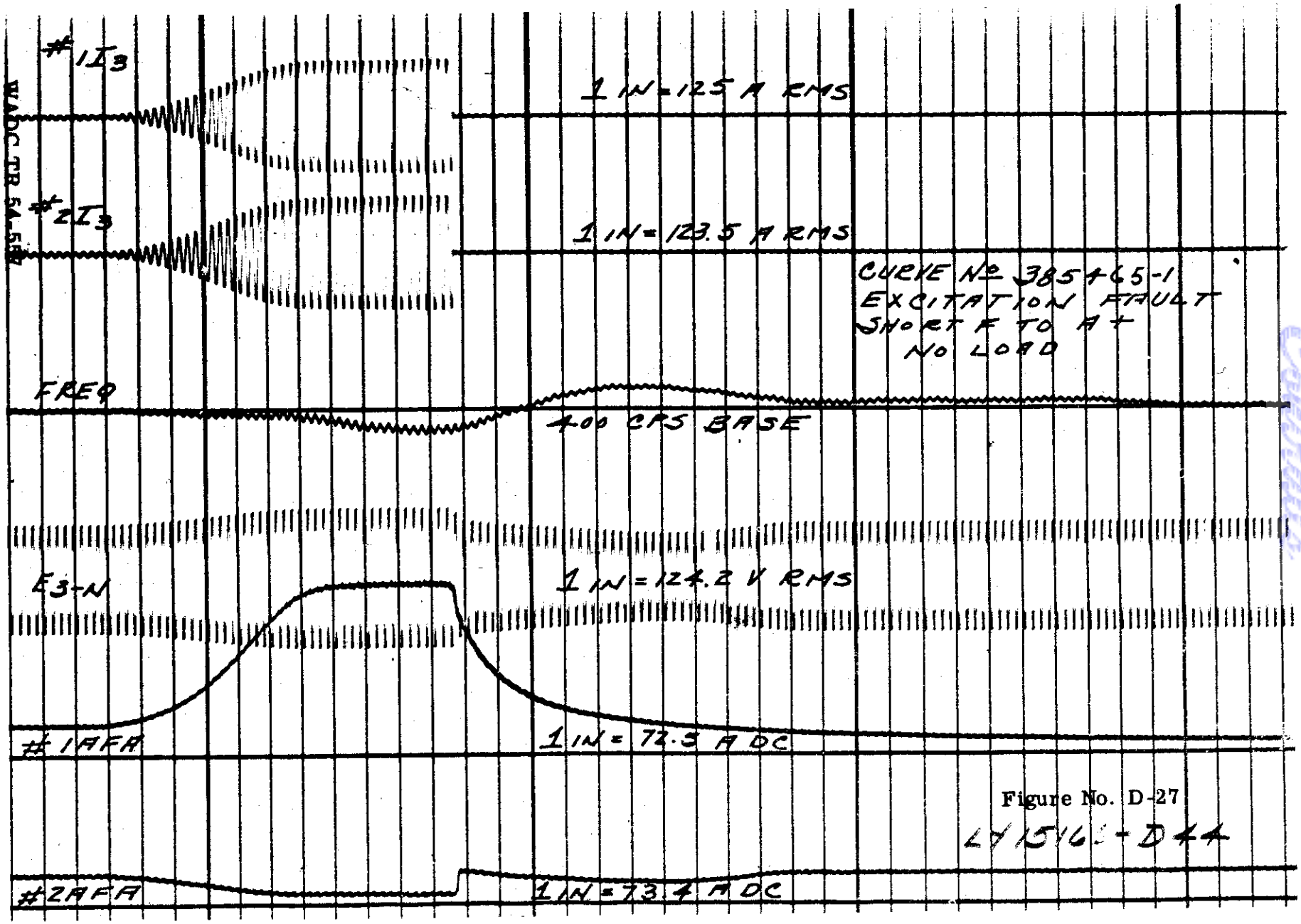

Figure No. D-27

LA 15463-D44

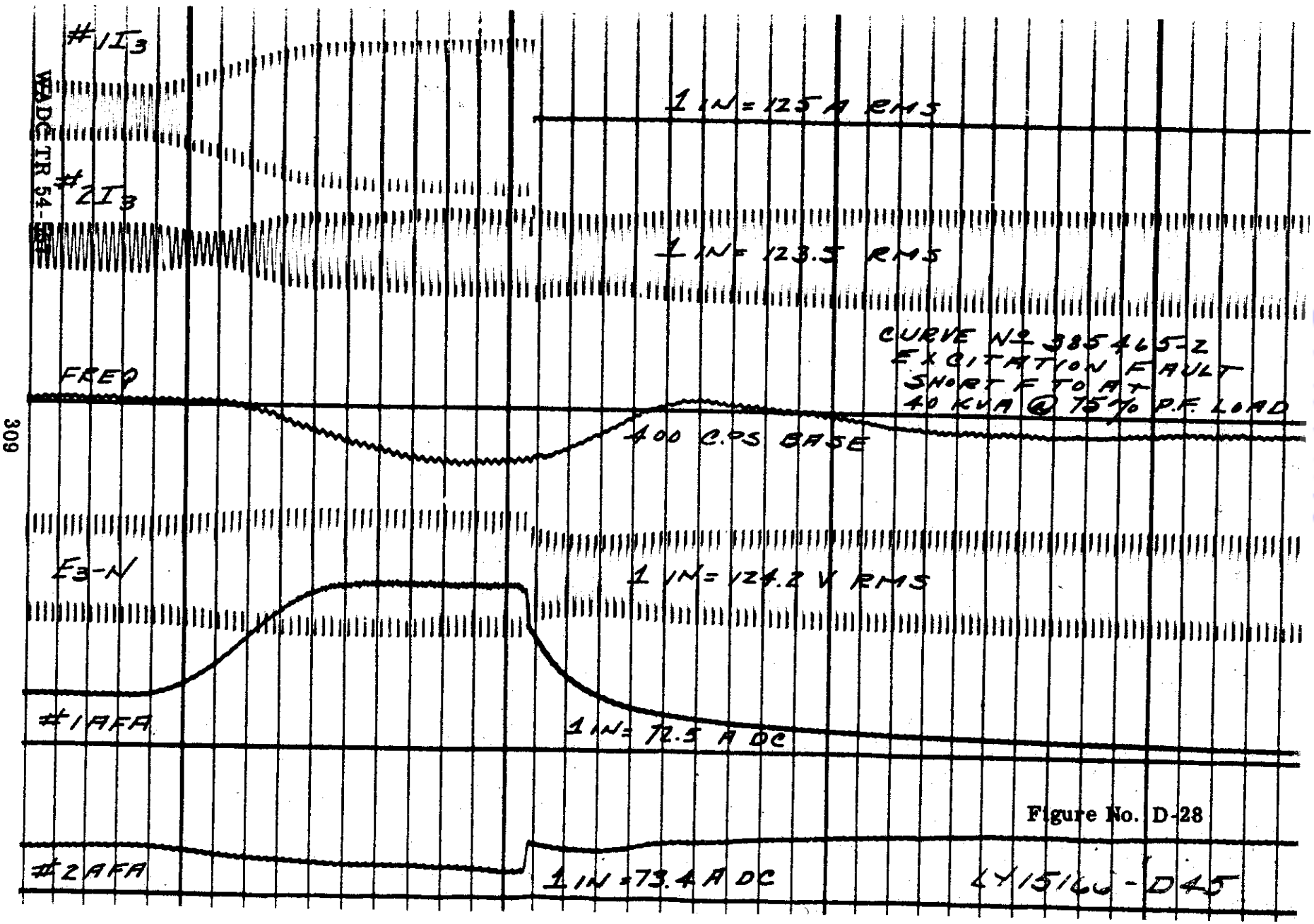

Figure No. D-28

4Y151C5 - D45

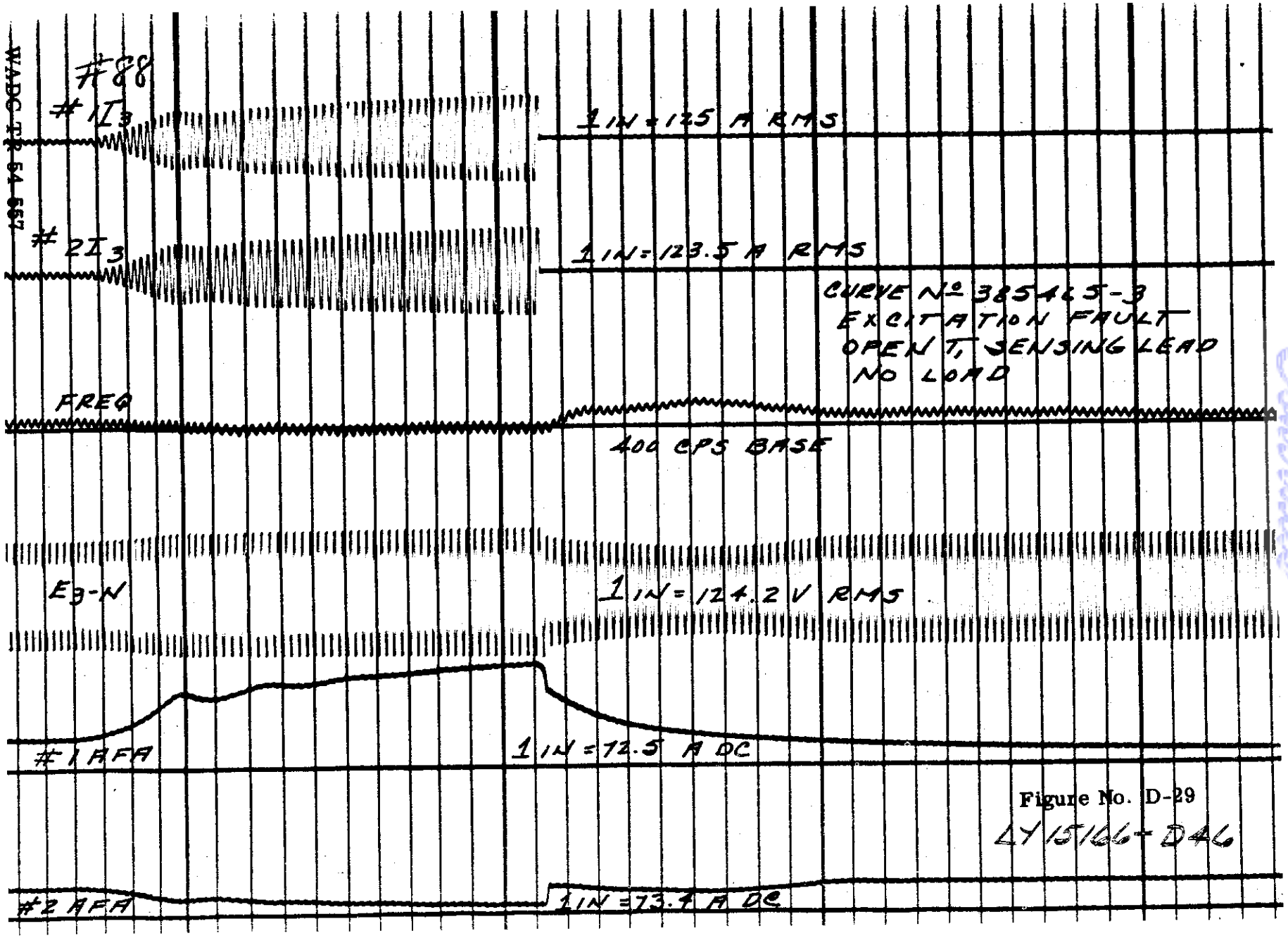

Figure No. D-29

AY 15166-D46

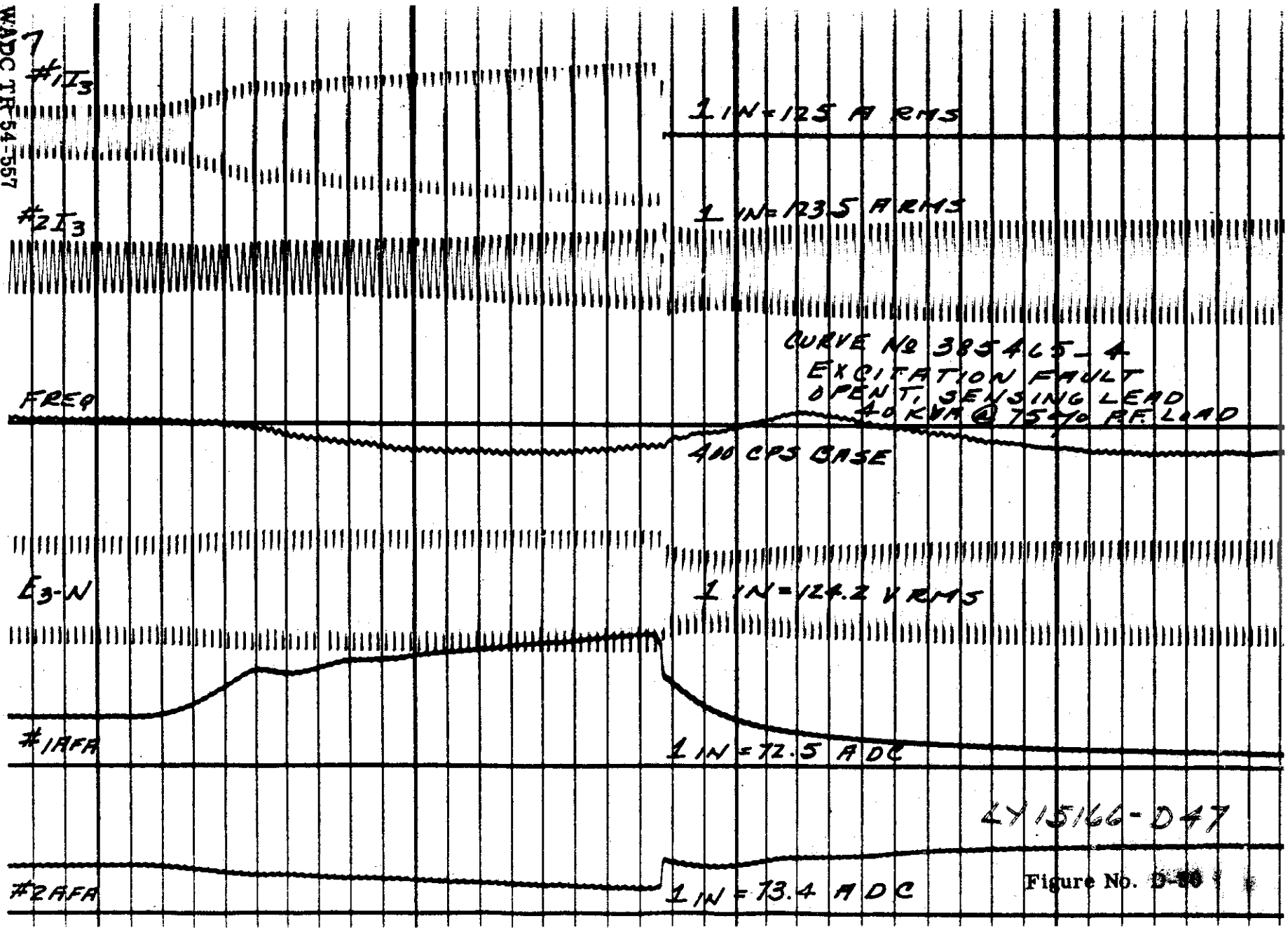

4Y 15166-D47

Figure No. 3-88

Figure No. D-31

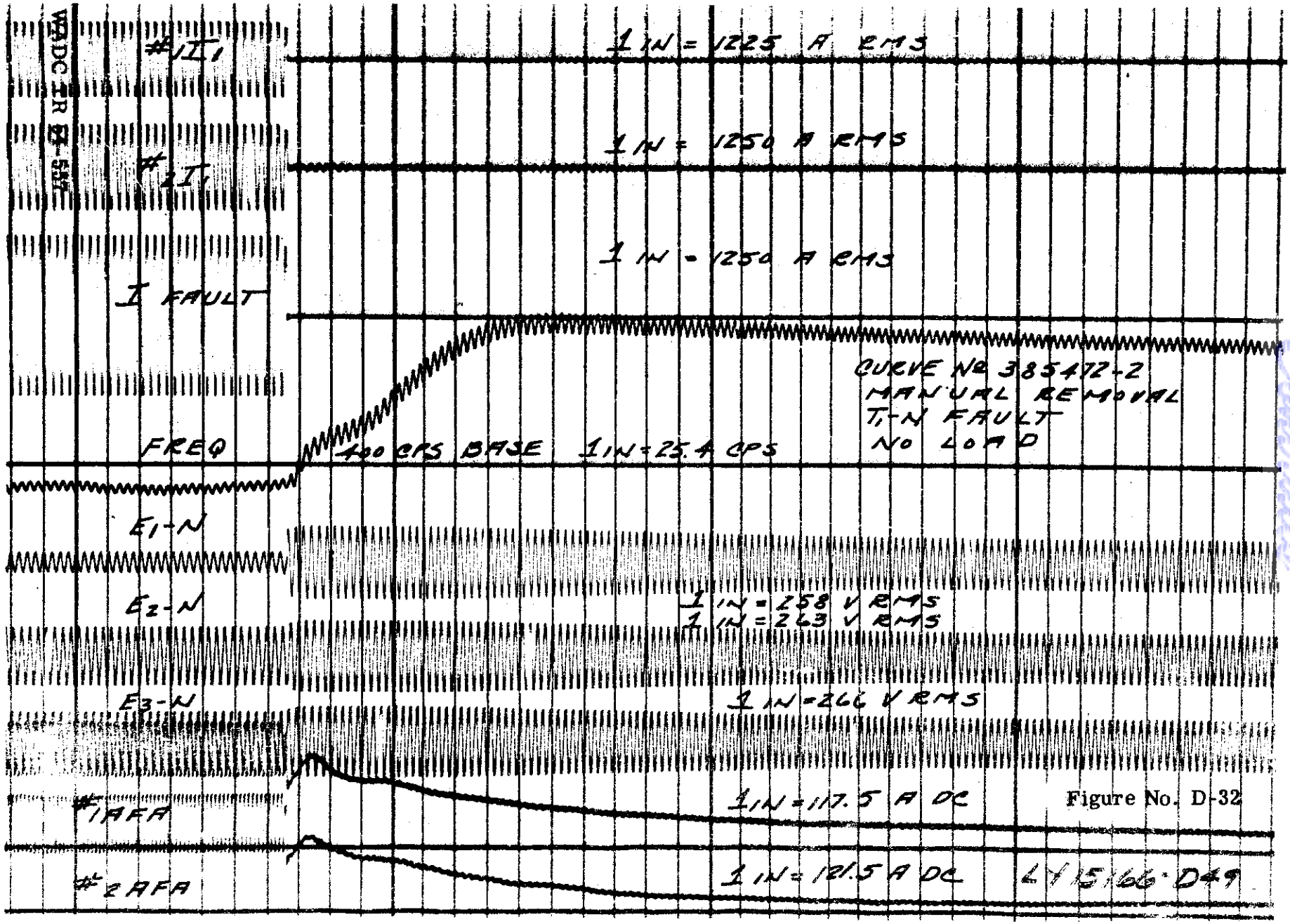

Figure No. D-32

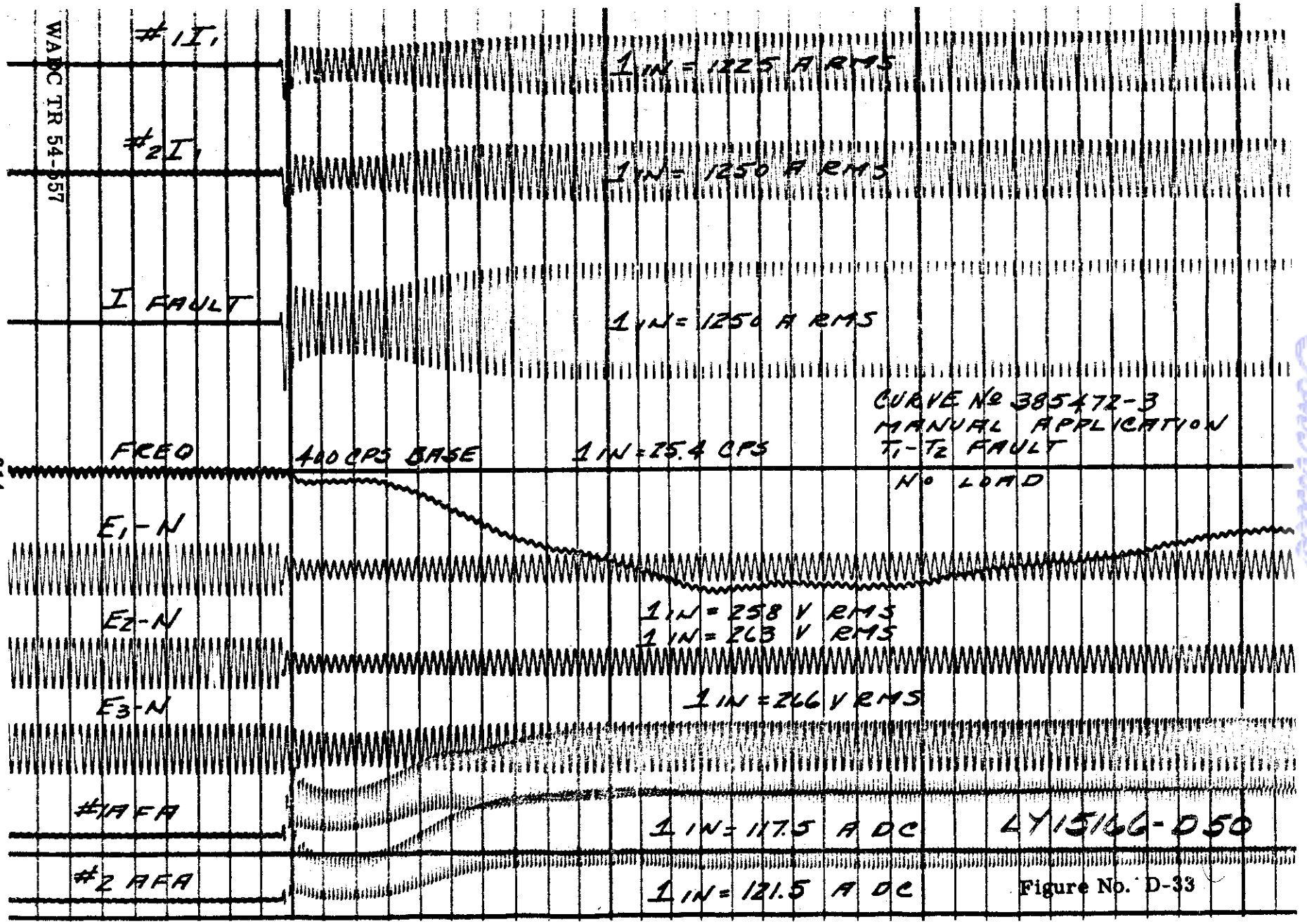

Figure No. D-33

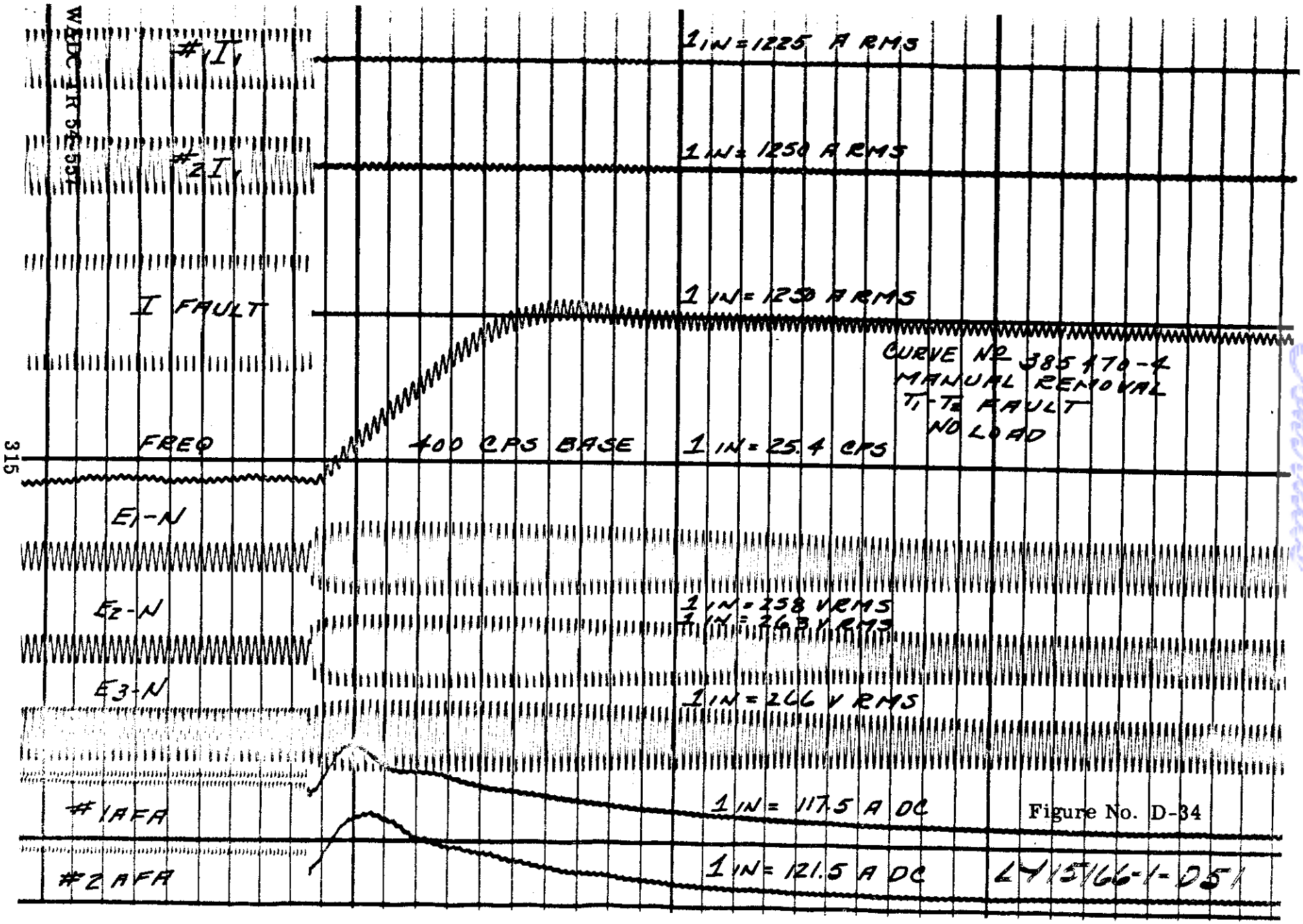

Figure No. D-34

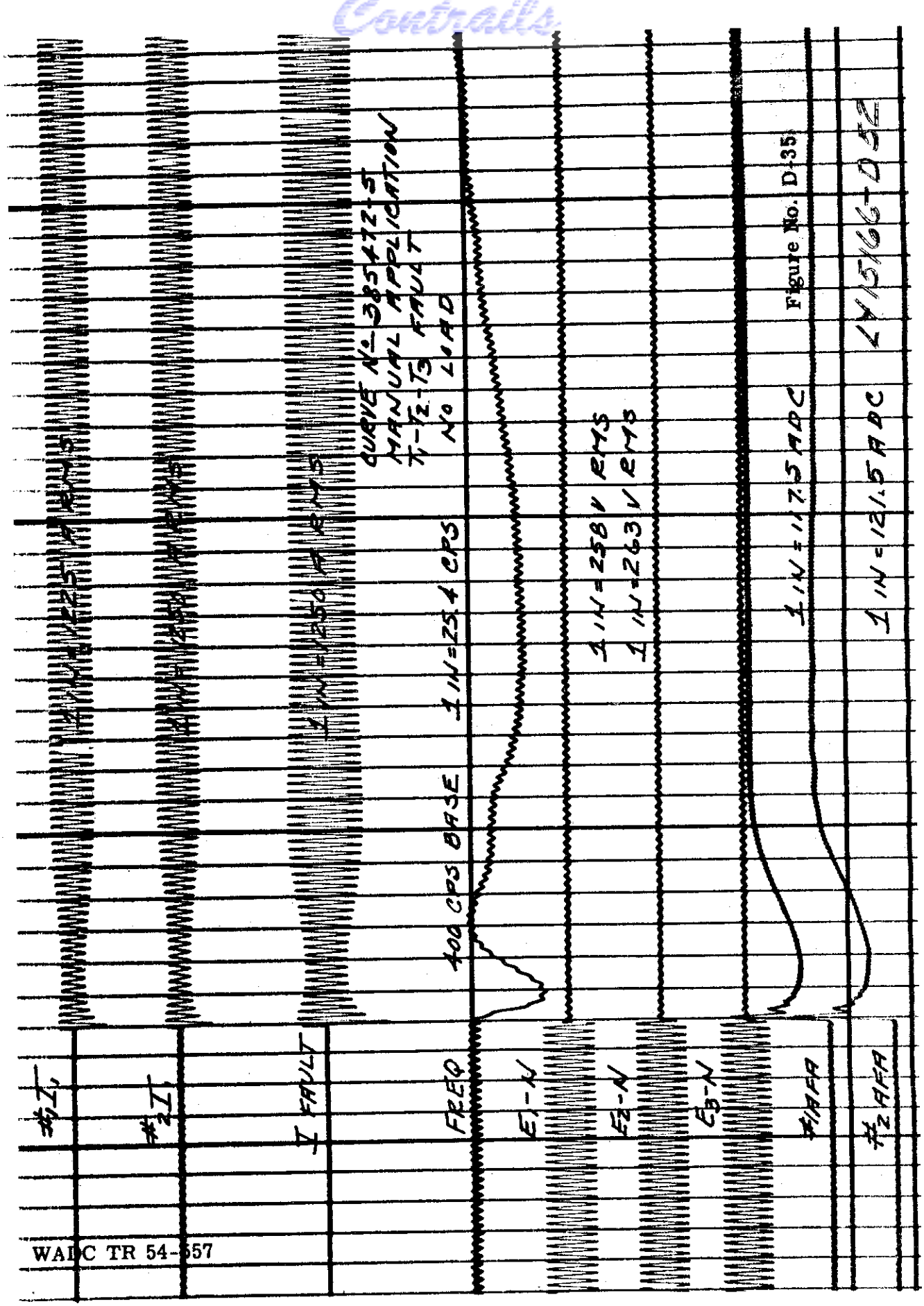

Figure No. D-35

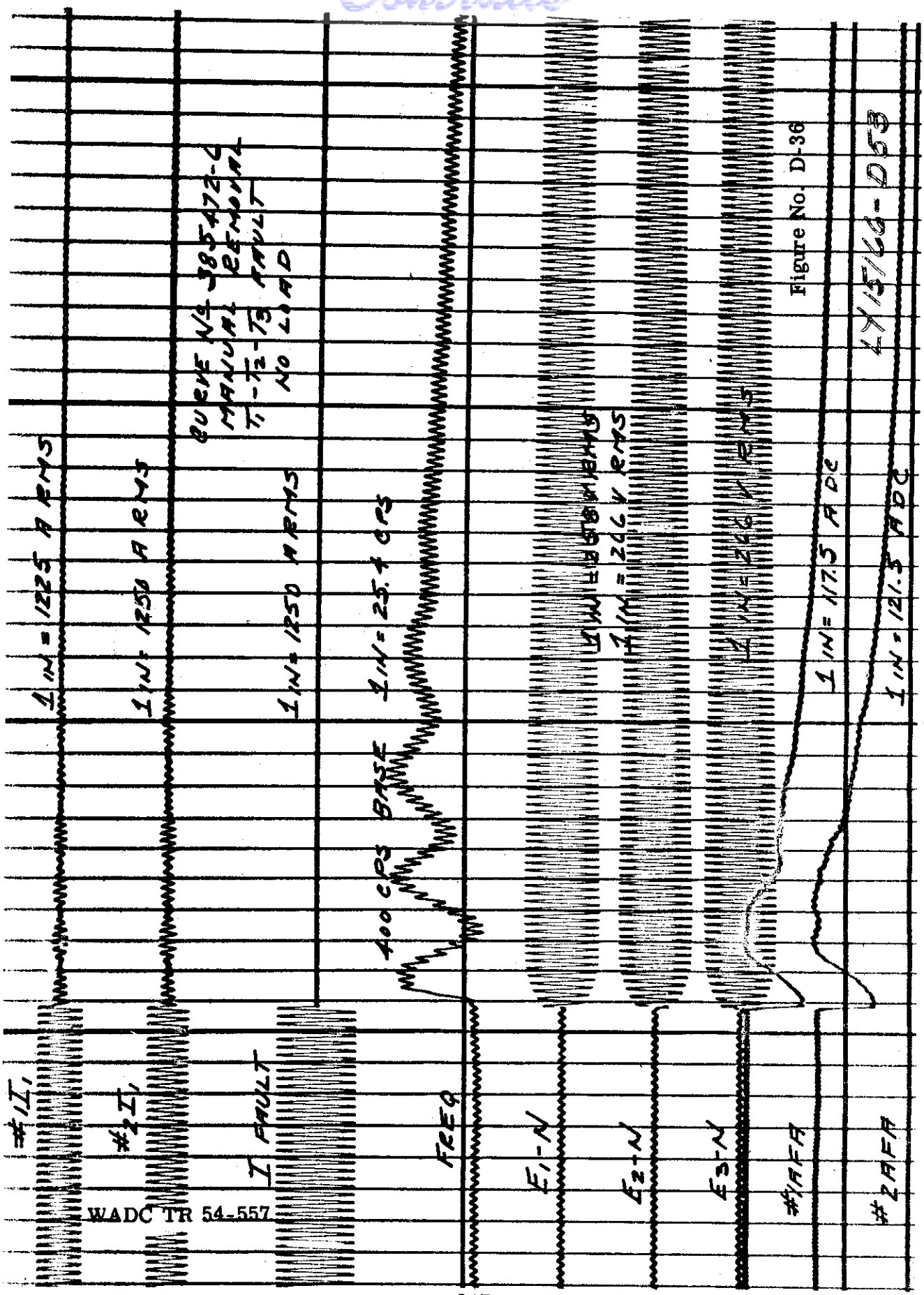

Figure No. D-36

Figure No. D-37

Figure No. D-38

47151A-D55

Figure No. D-39

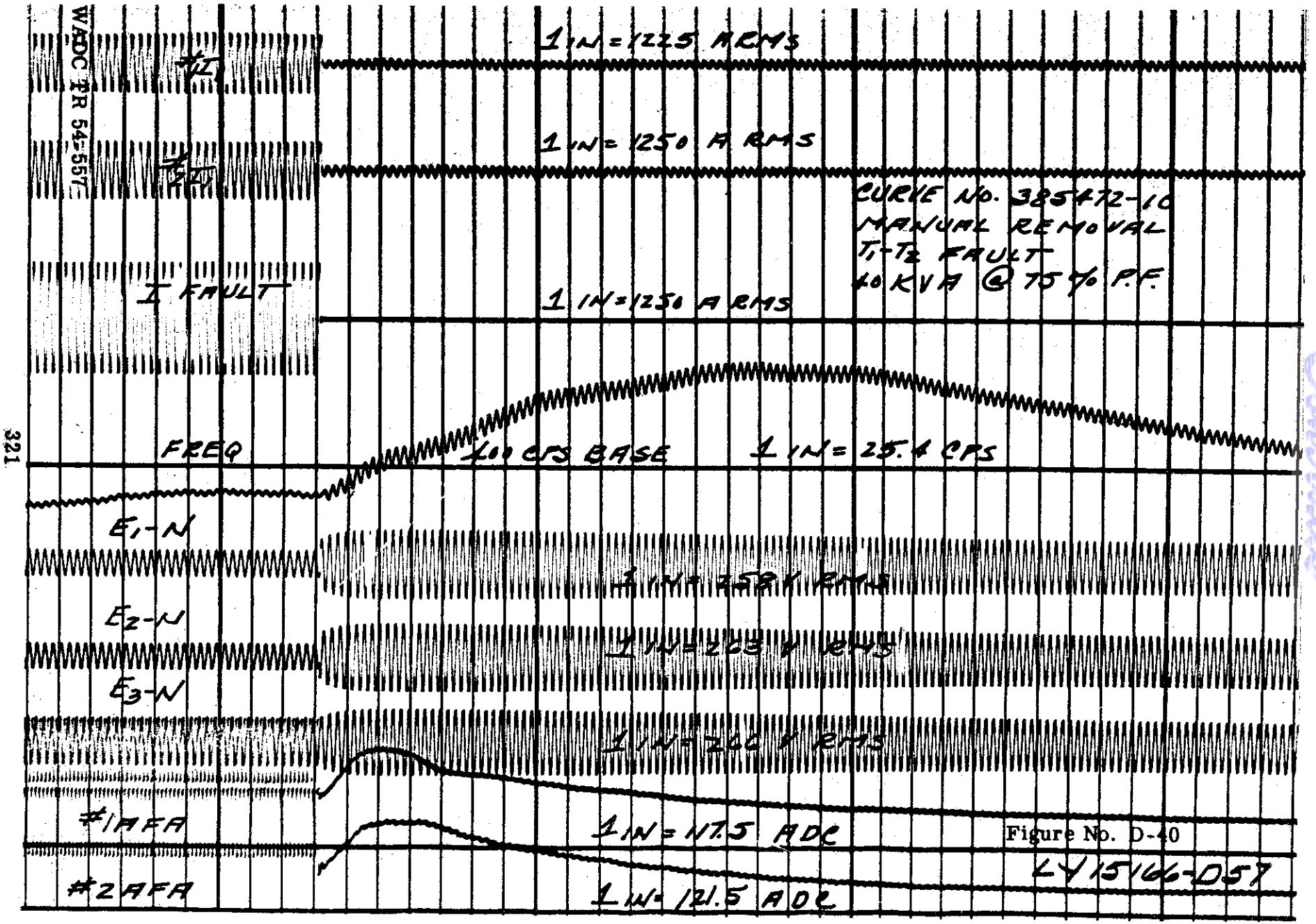

Figure No. D-40

LY15166-057

Figure No. D-41

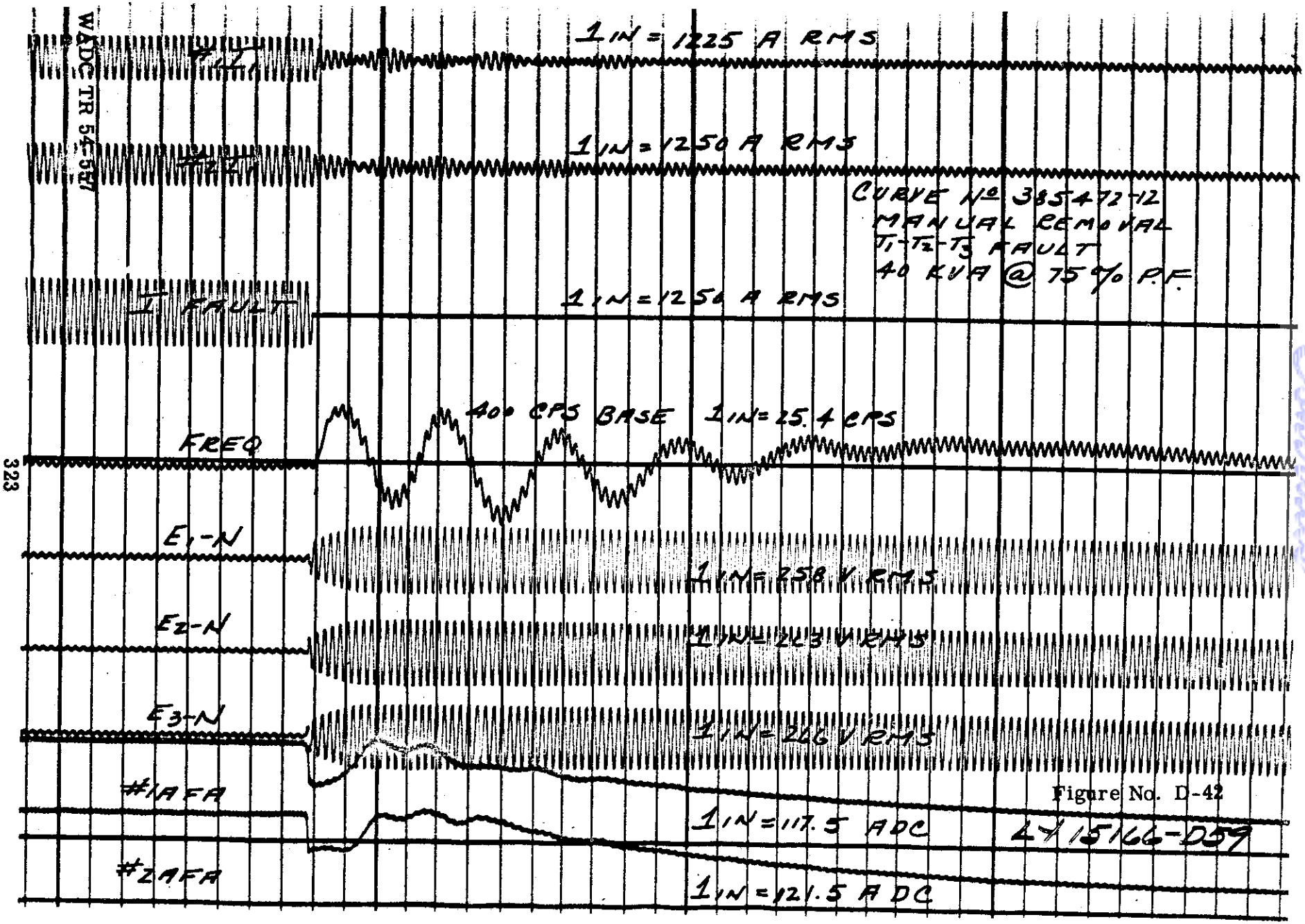

Figure No. D-42

47 15166-059

323

Figure No. D-48
LY 15073-025

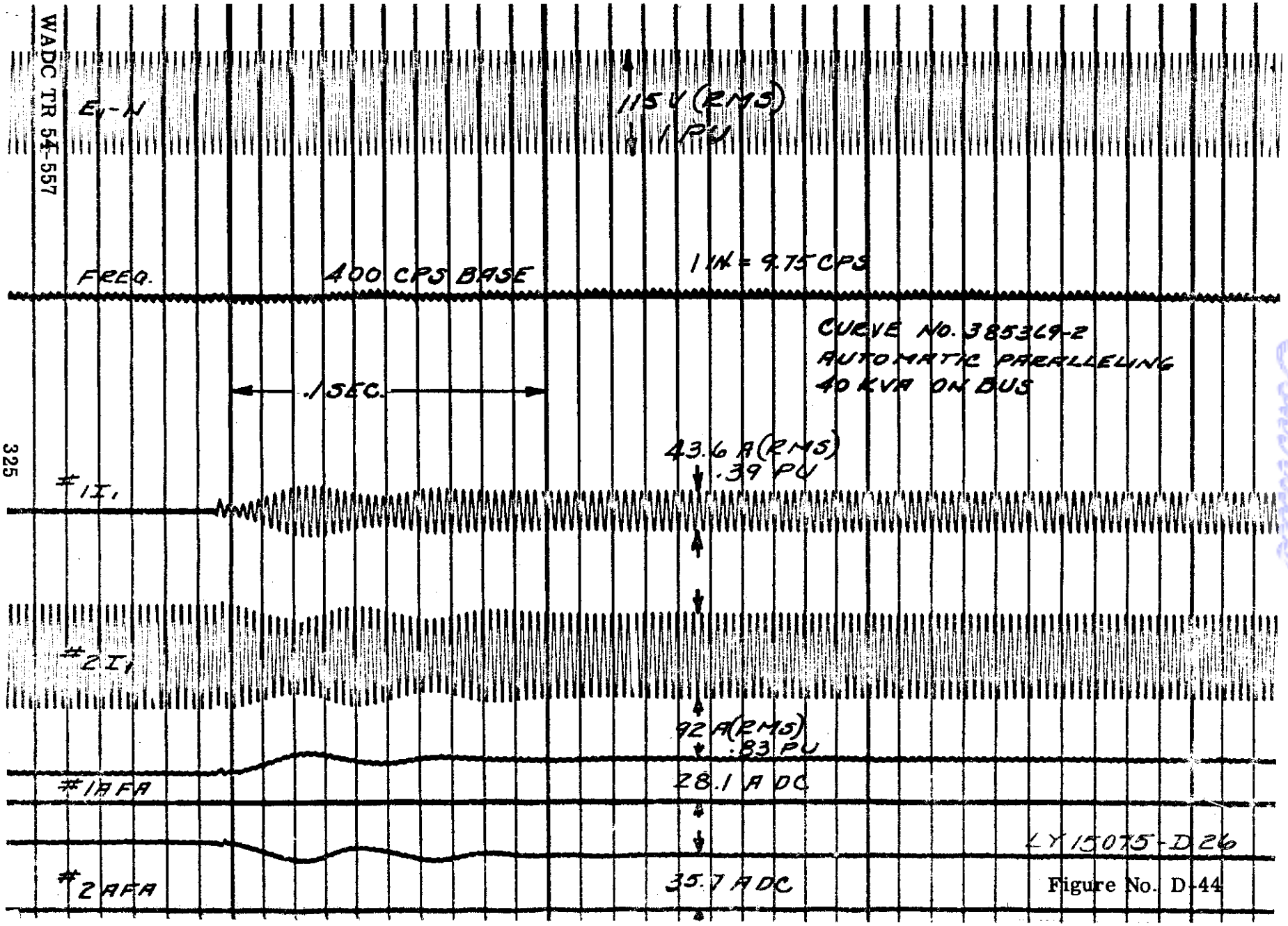

Figure No. D-44

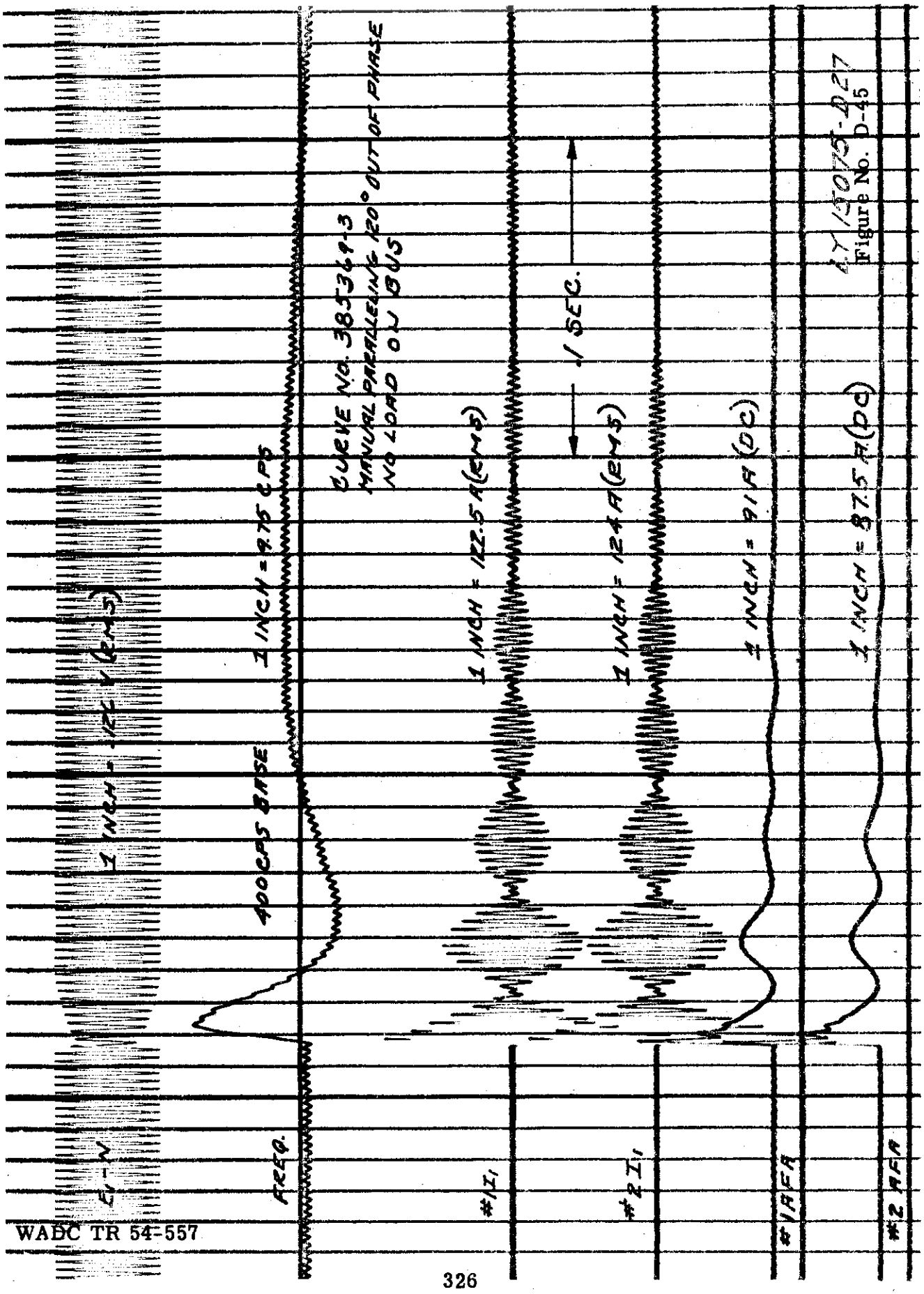

Figure No. D-45

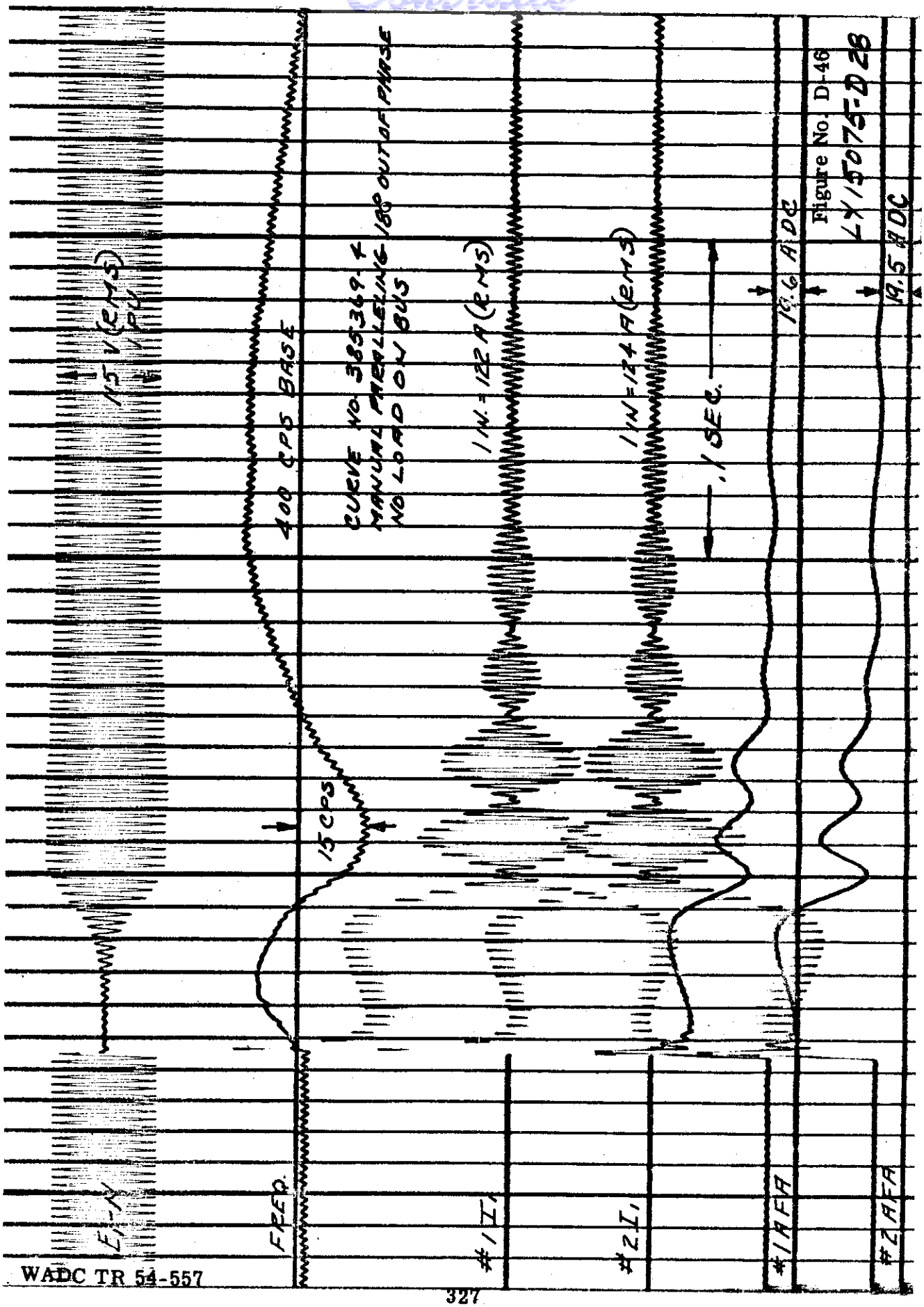

Figure No. D-46

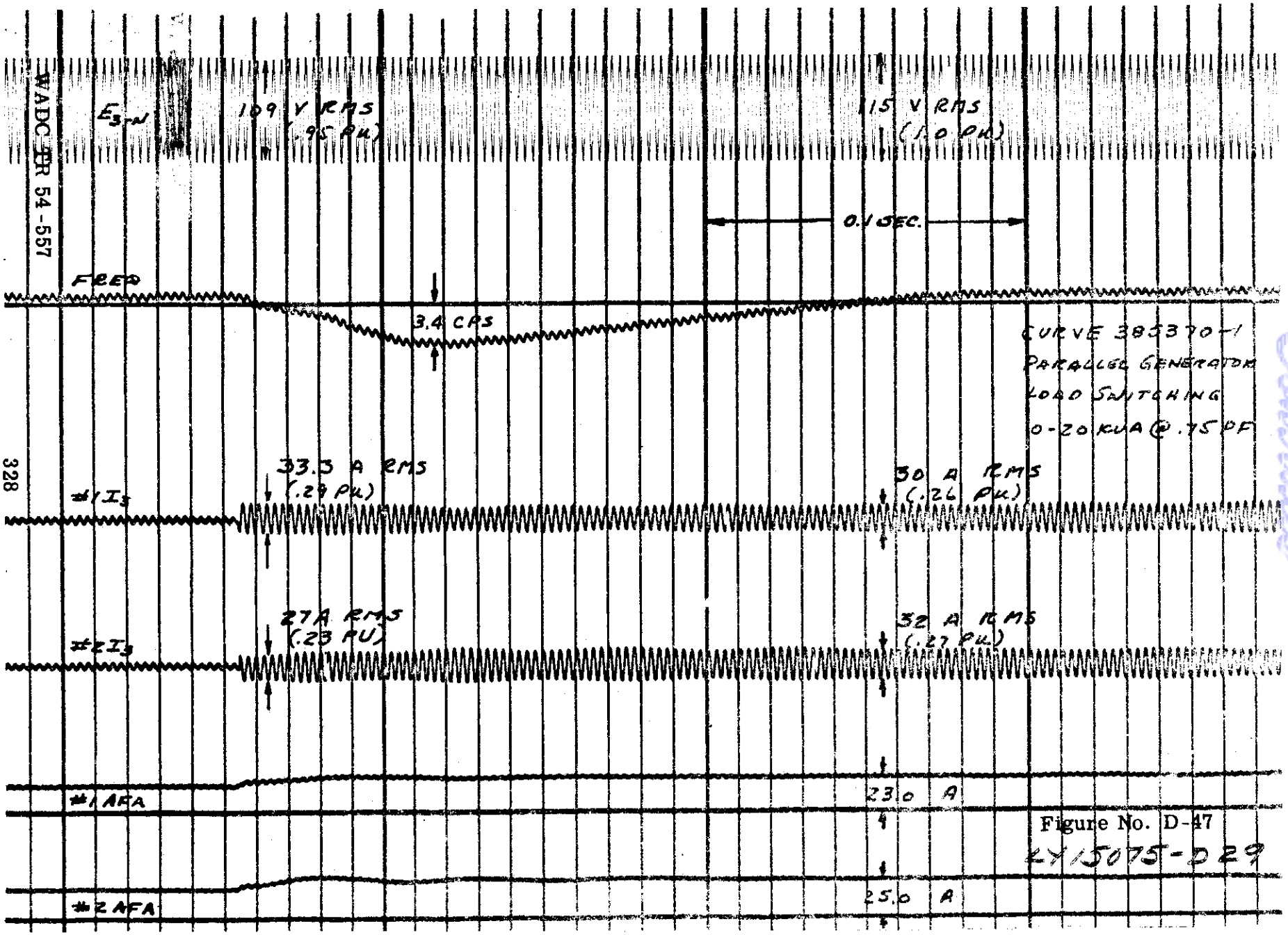

Figure No. D-47

4Y15075-D29

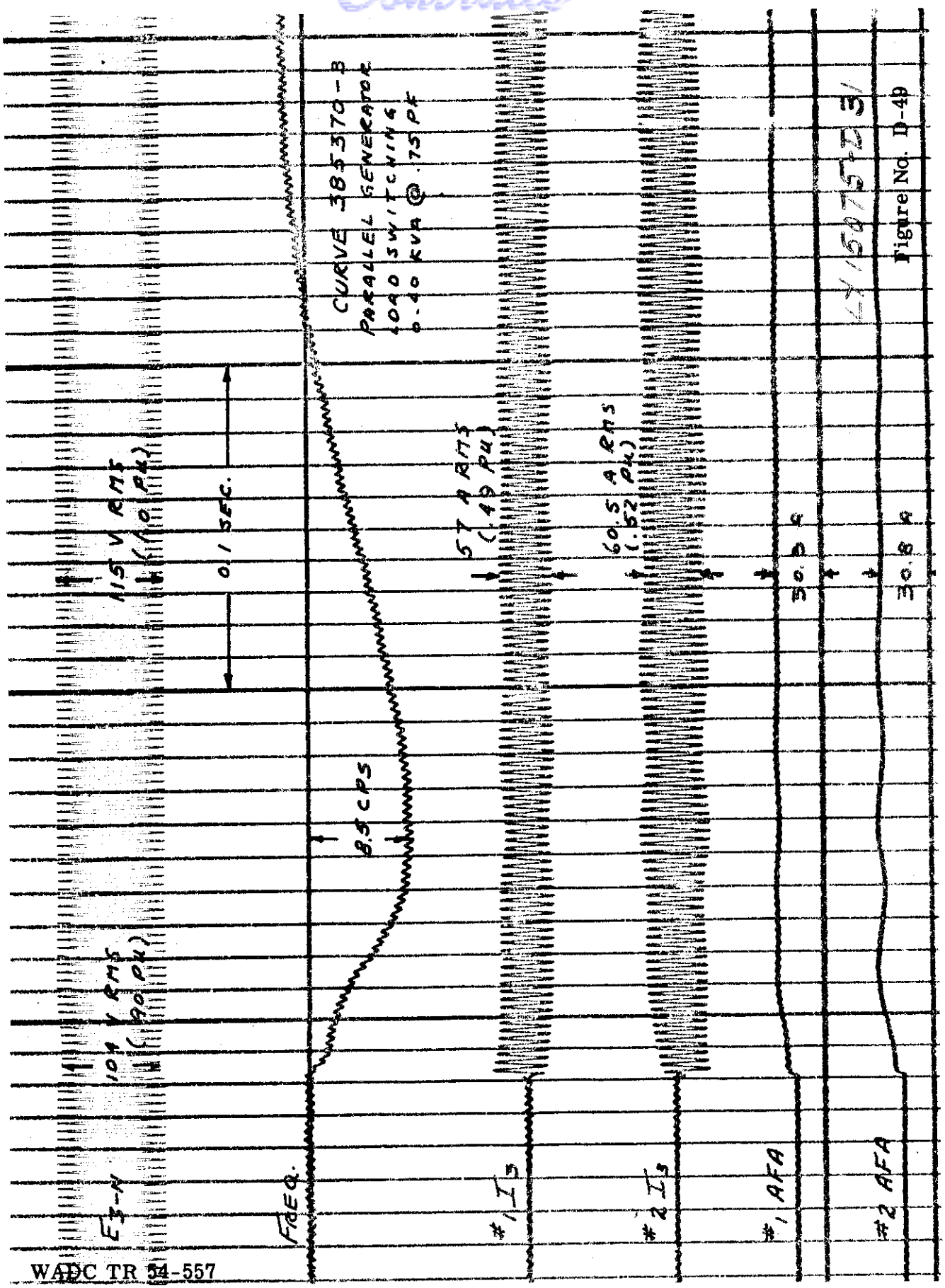

Figure No. D-4b

Figure No. D-50

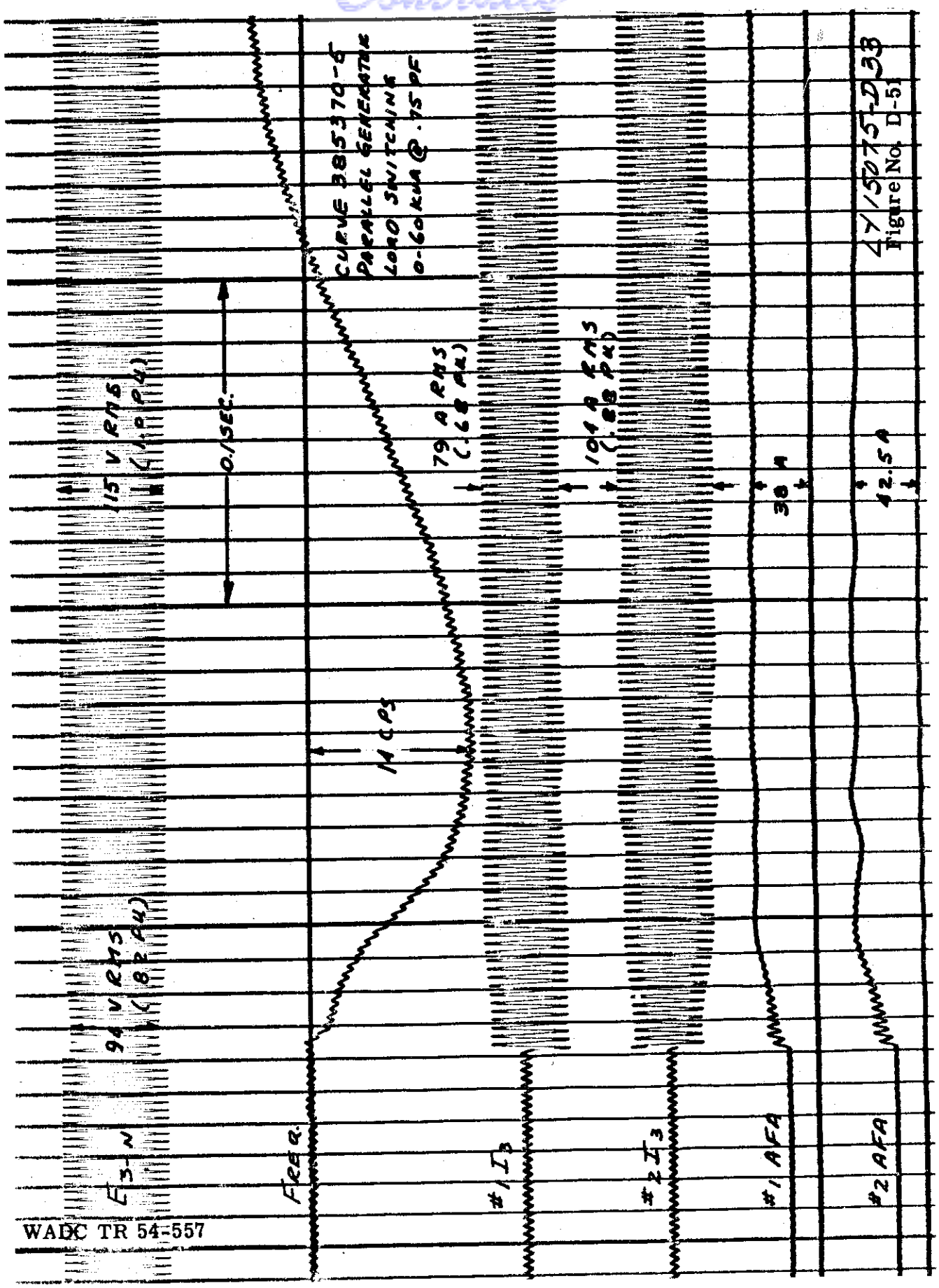

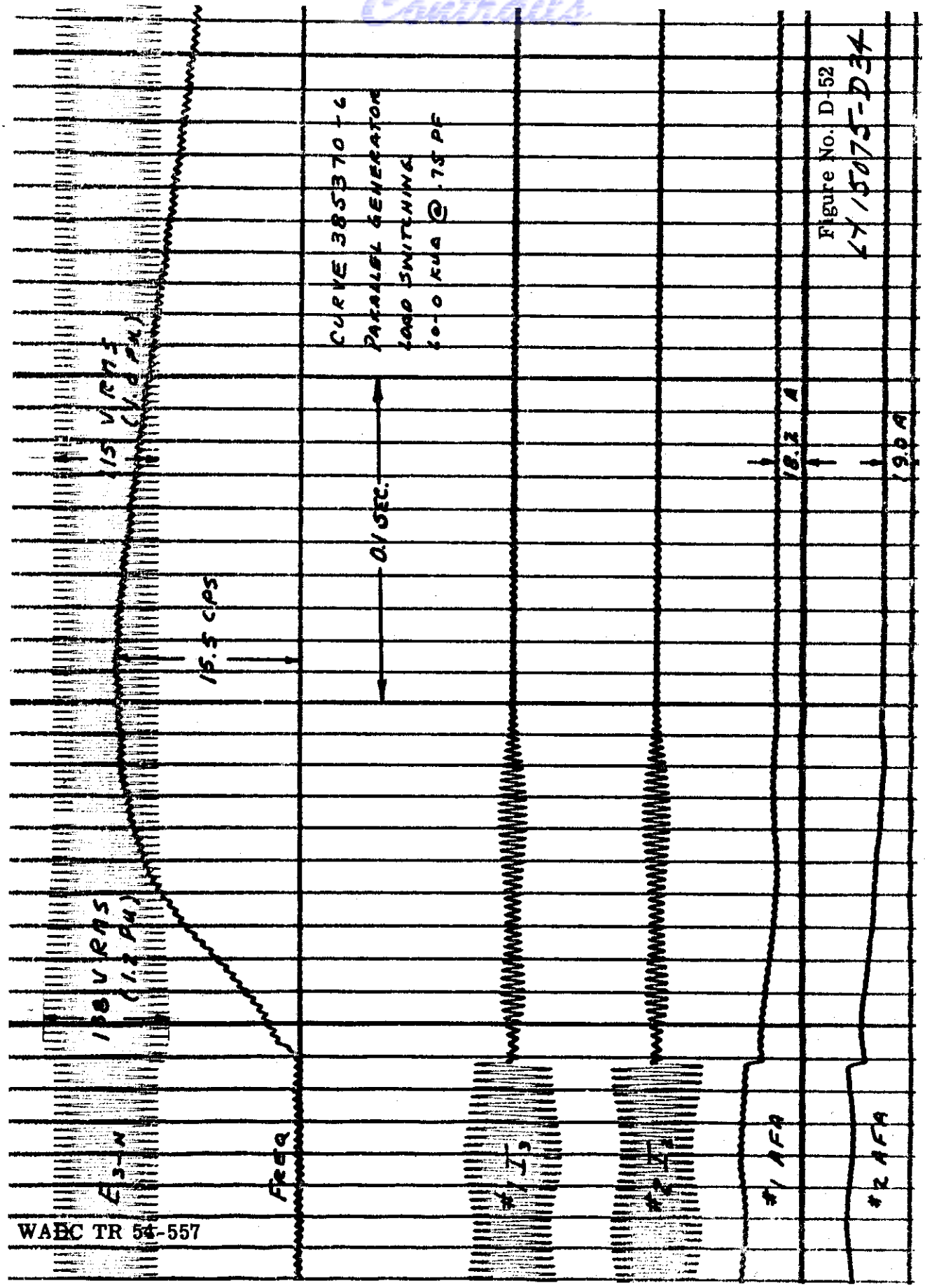

Figure No. D-52
47/38537-D34

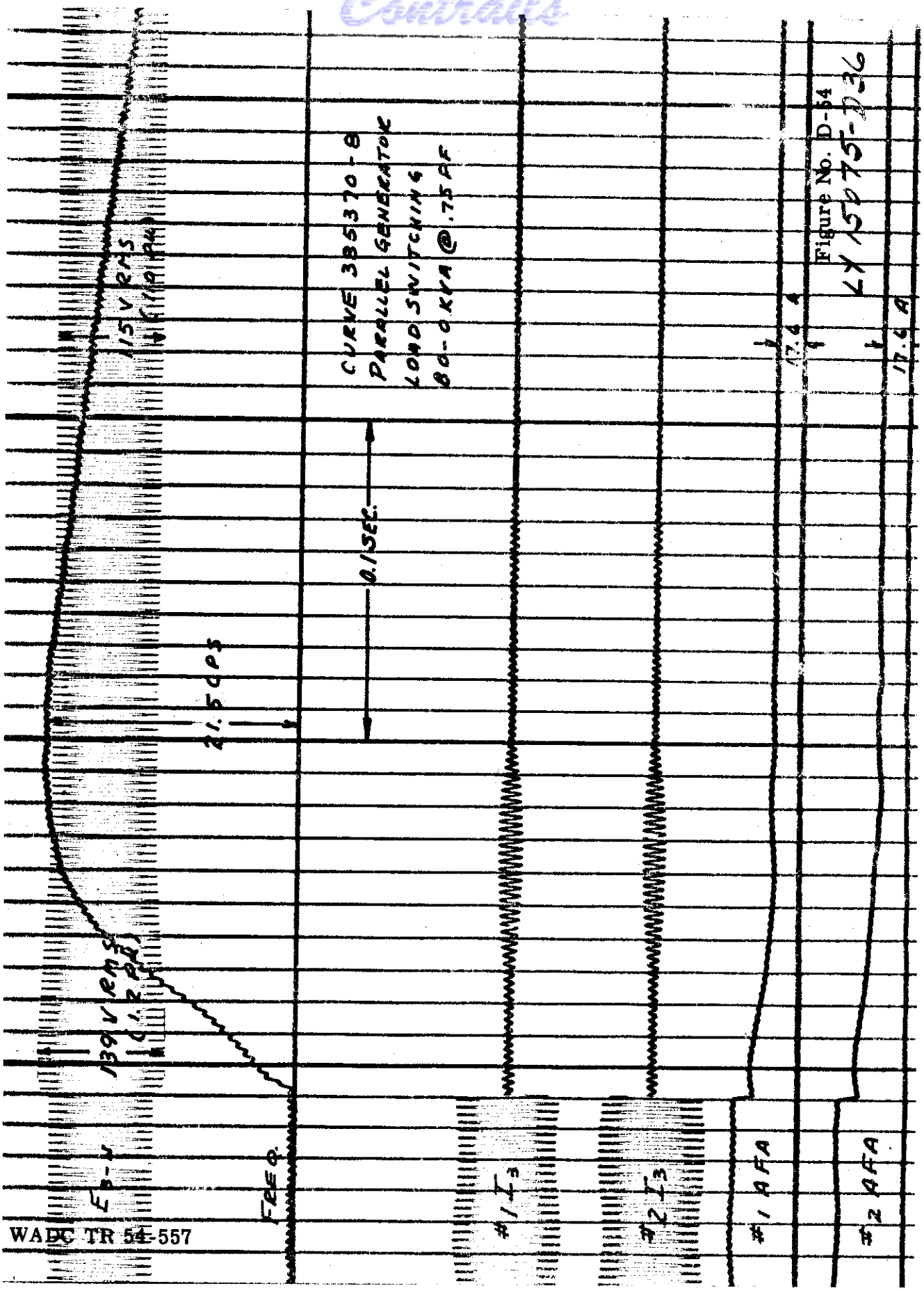

Figure No. D-54
LY 15D 75-D-36

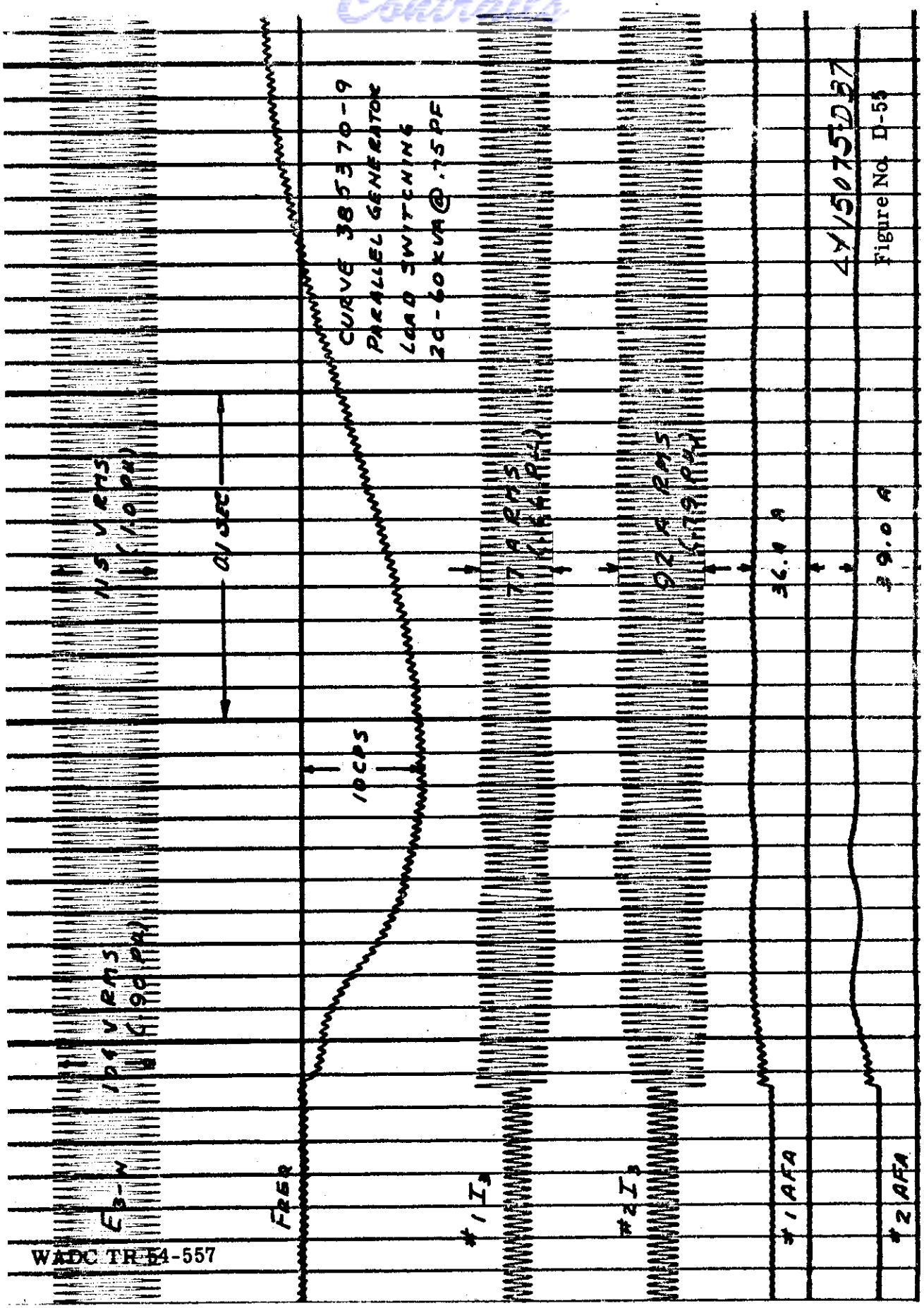

Figure No. D-53

Figure No. D-56
47150 TS-D 38

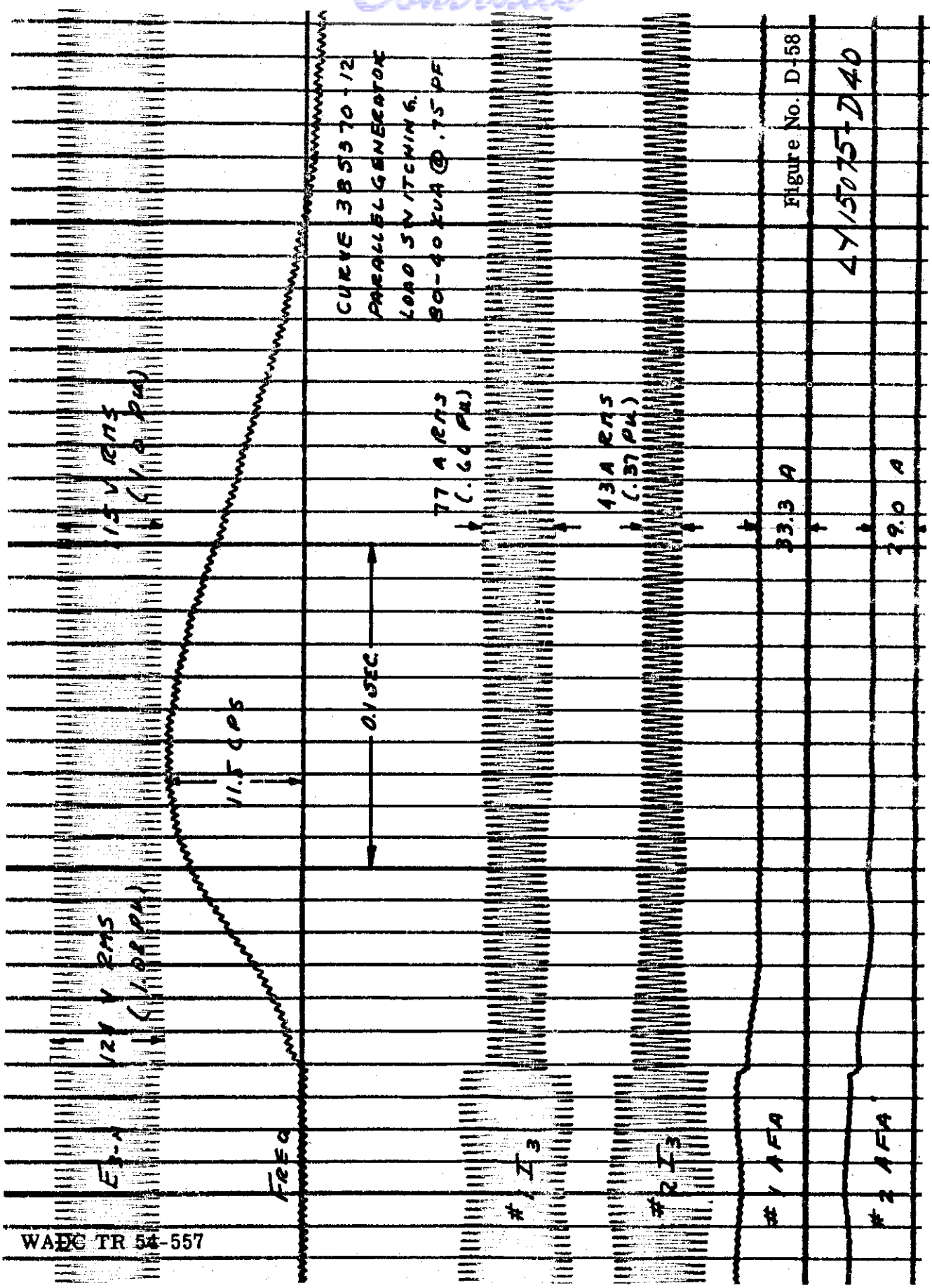

Figure No. D-58

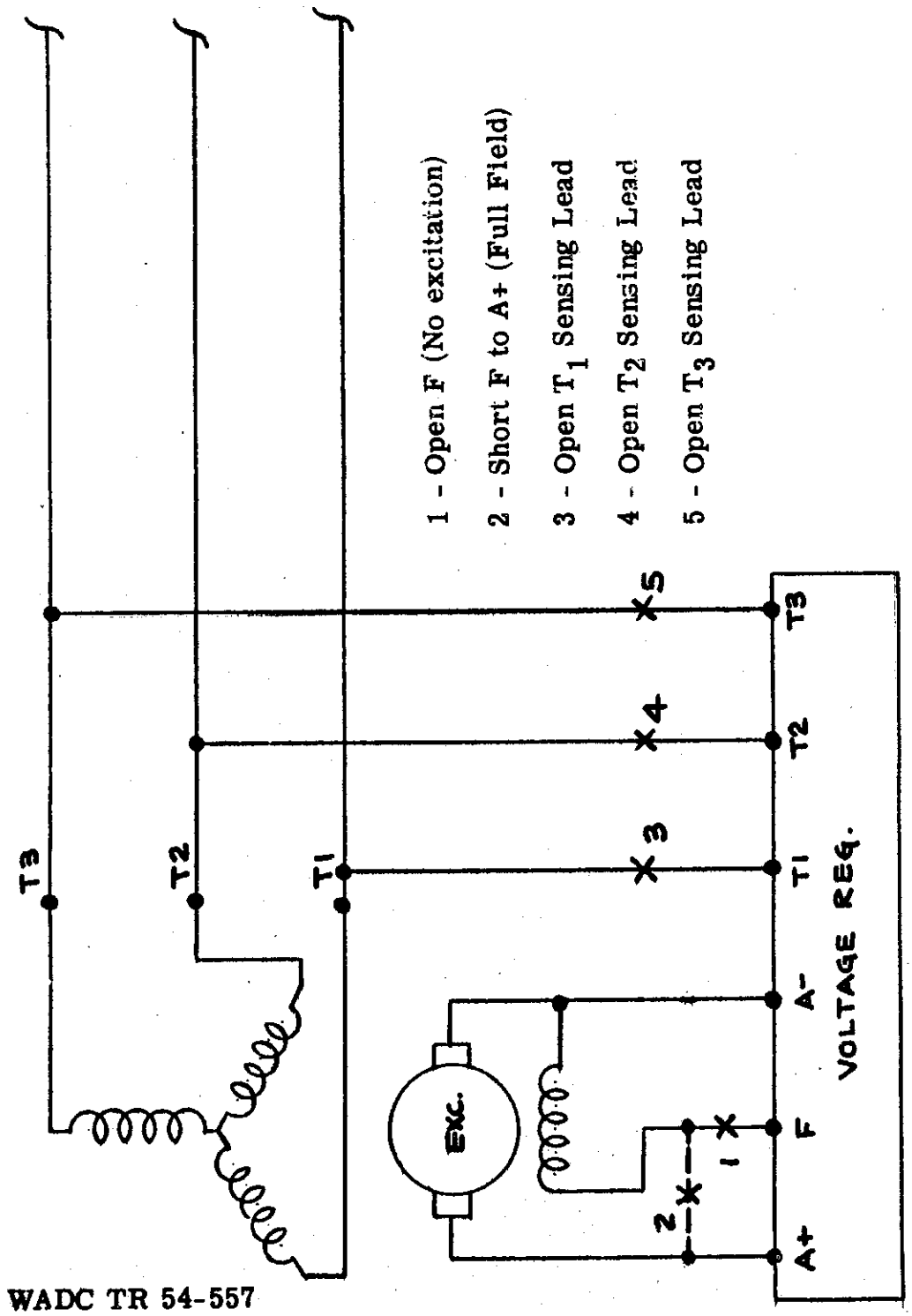

Figure D-59 Schematic Diagram Showing Where Excitation Faults are Applied

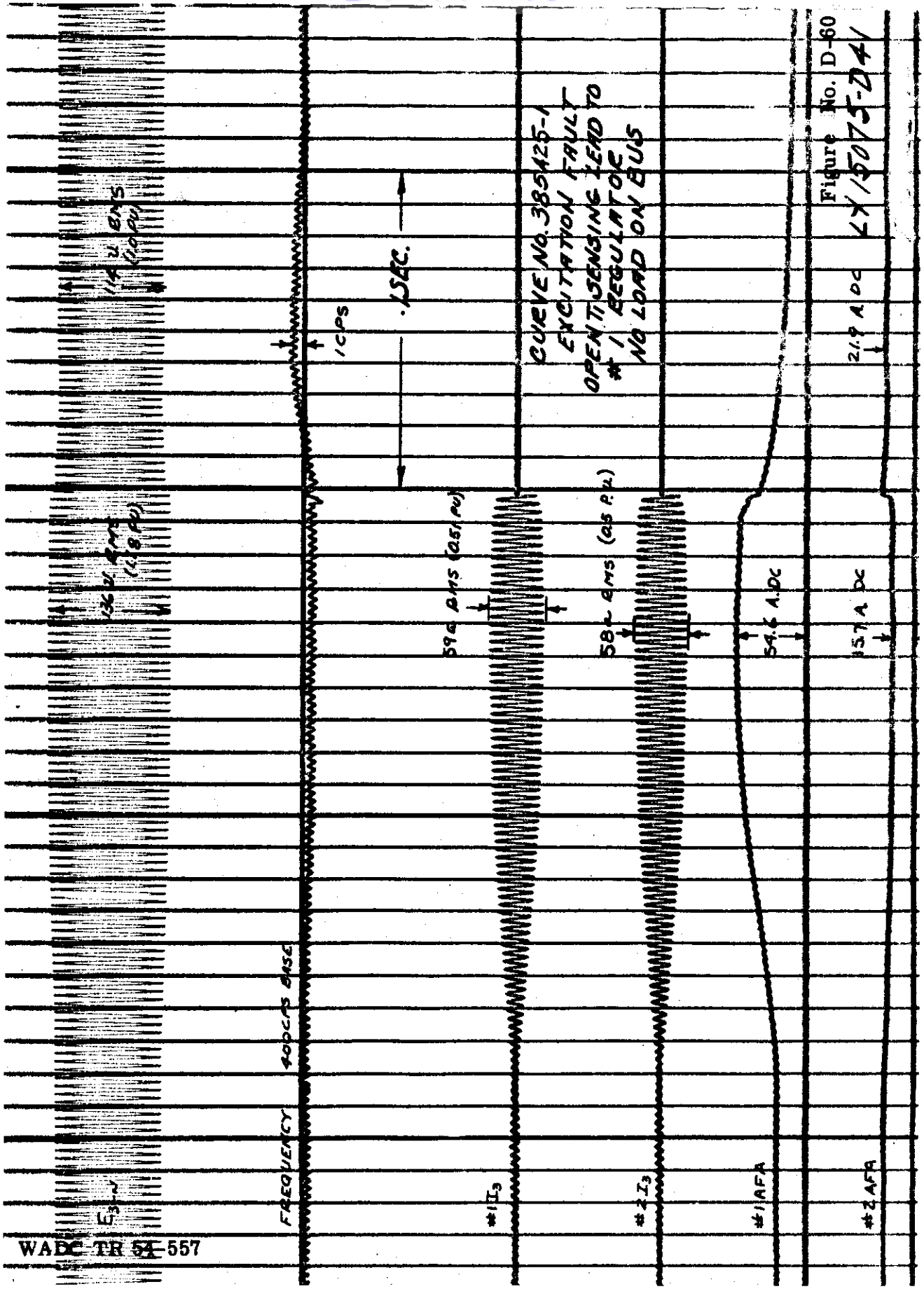

Figure No. D-60

LY/5075-241

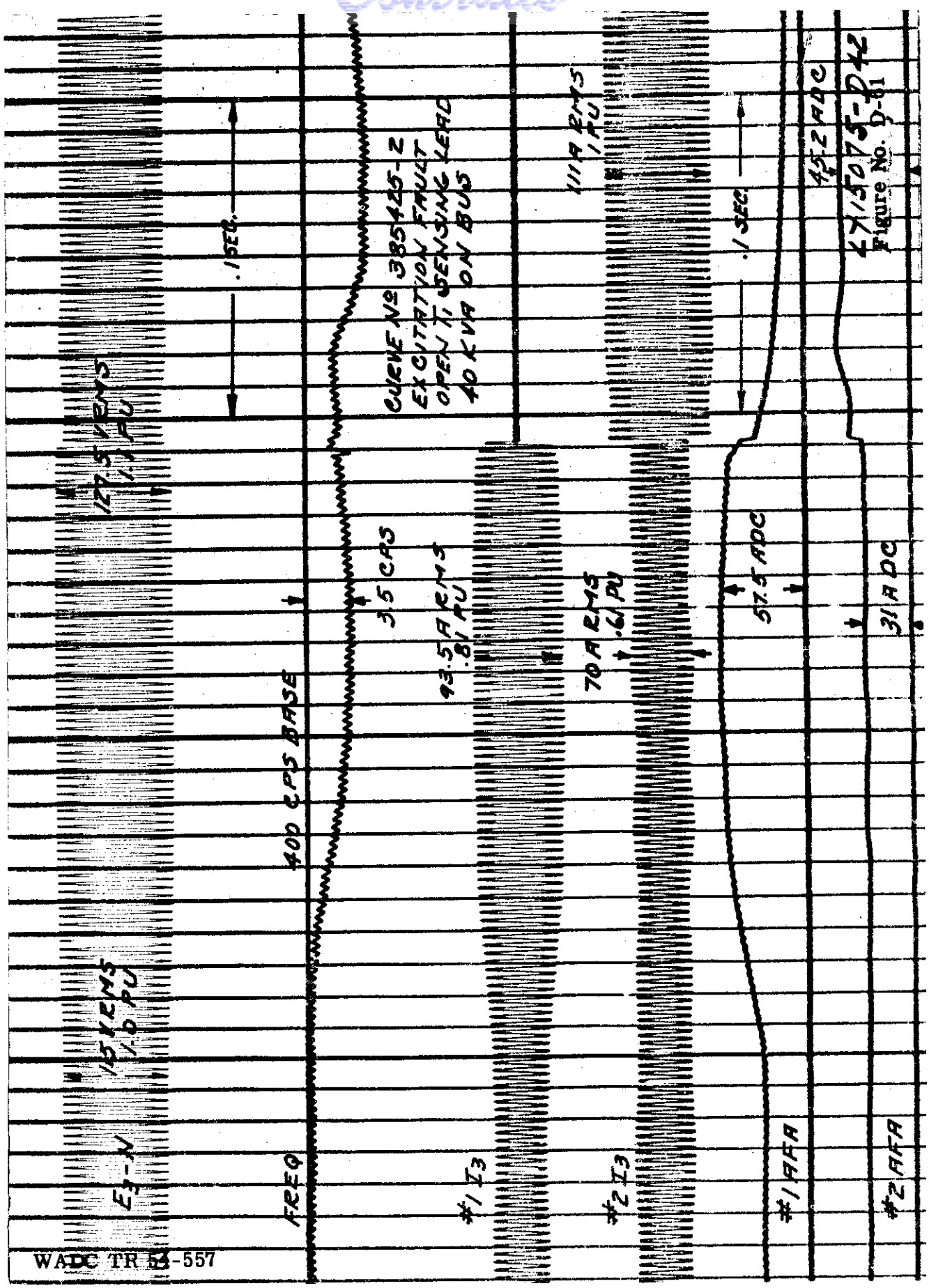

Figure No. D-62

LY 15D75-D43

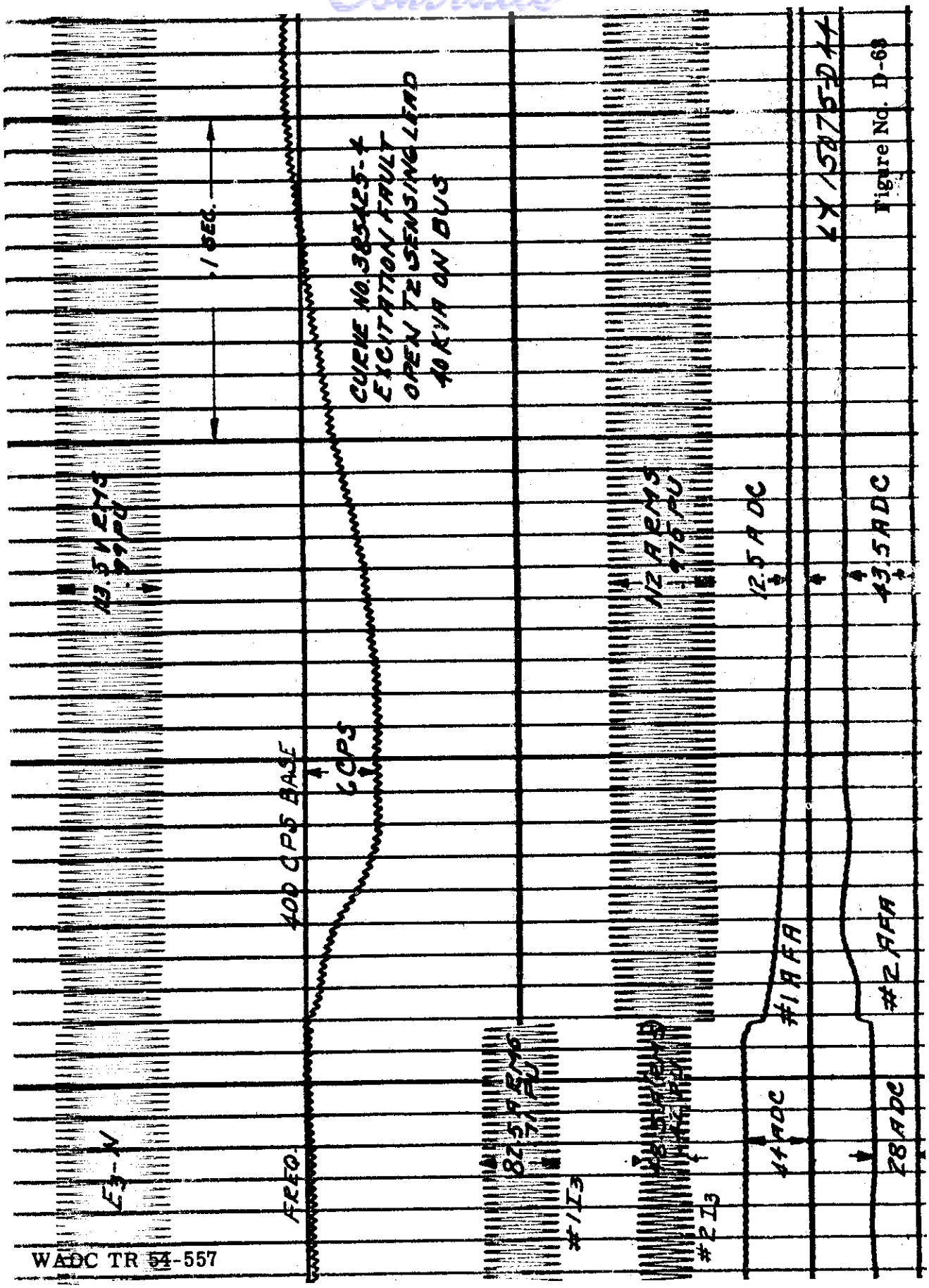

Figure No. D-68

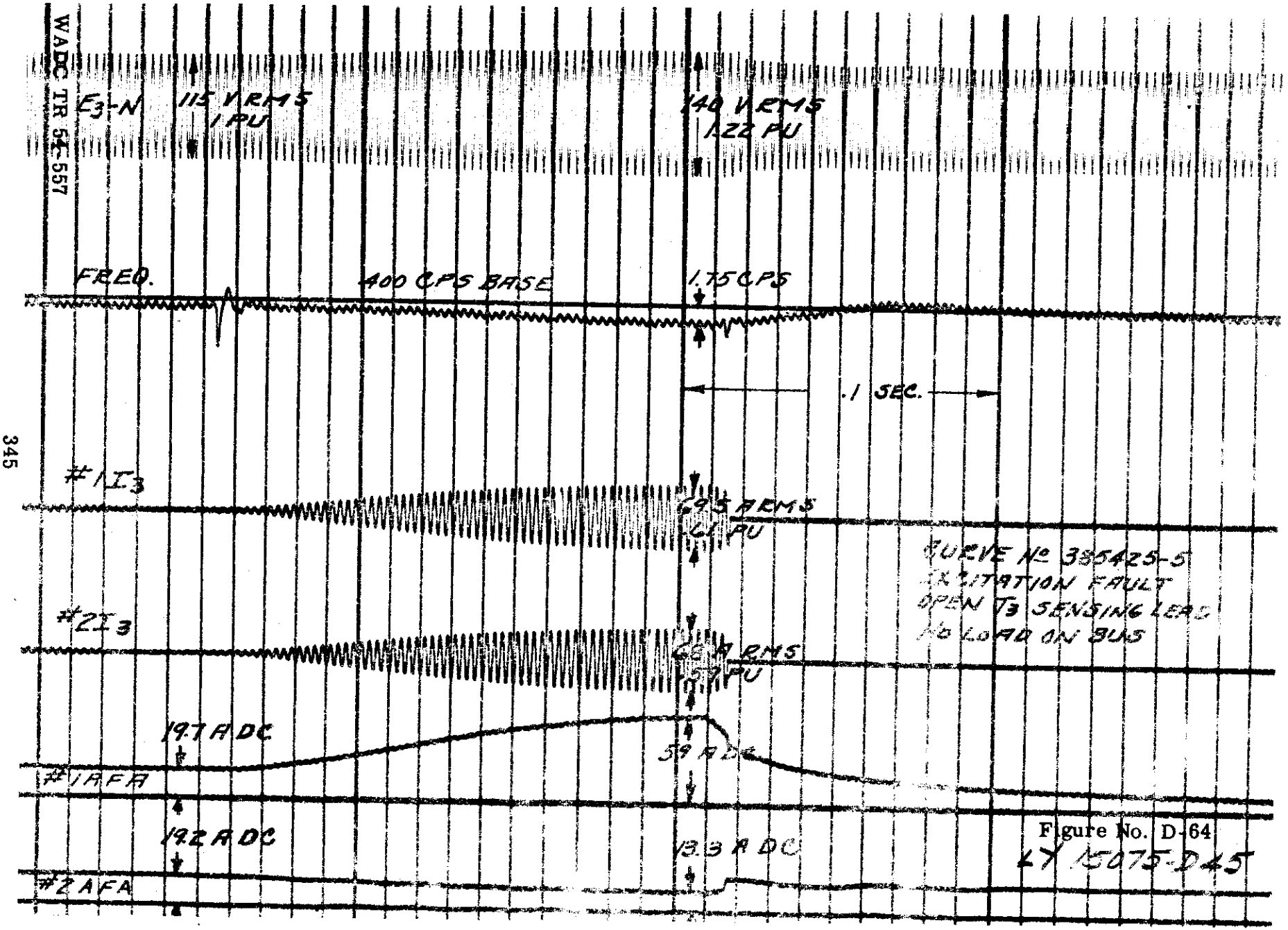

Figure No. D-64

47 5075-245

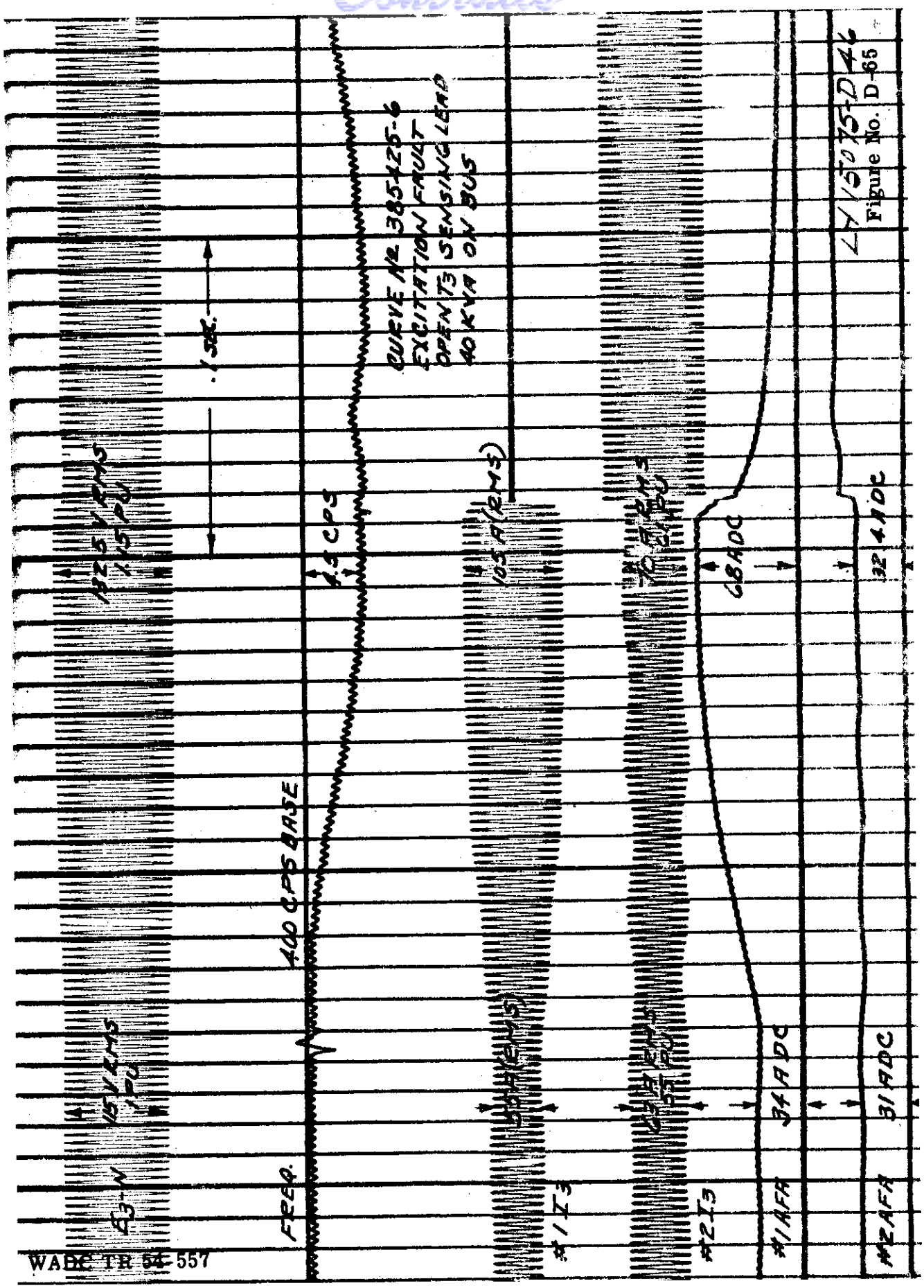

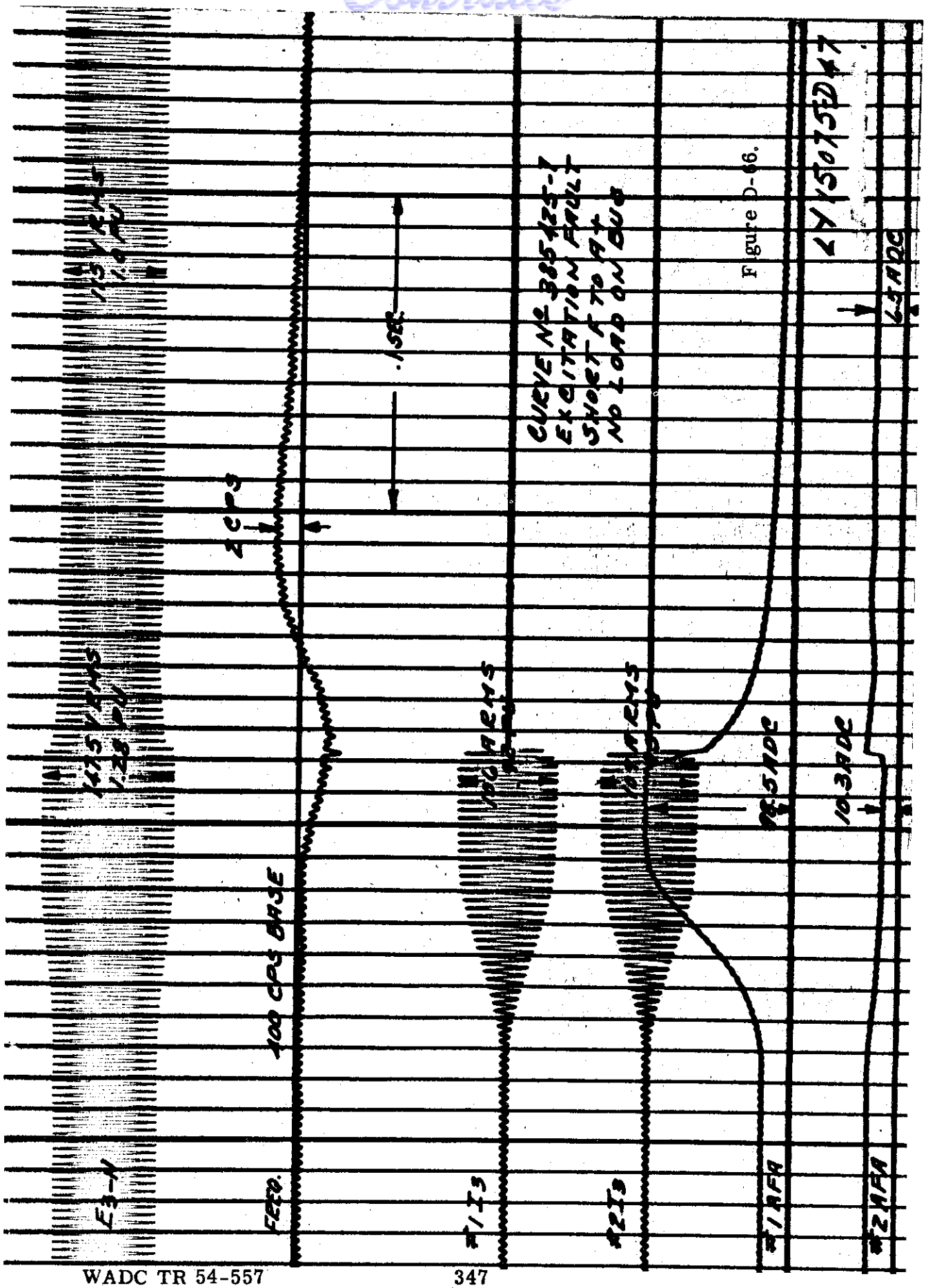

Figure D-66.

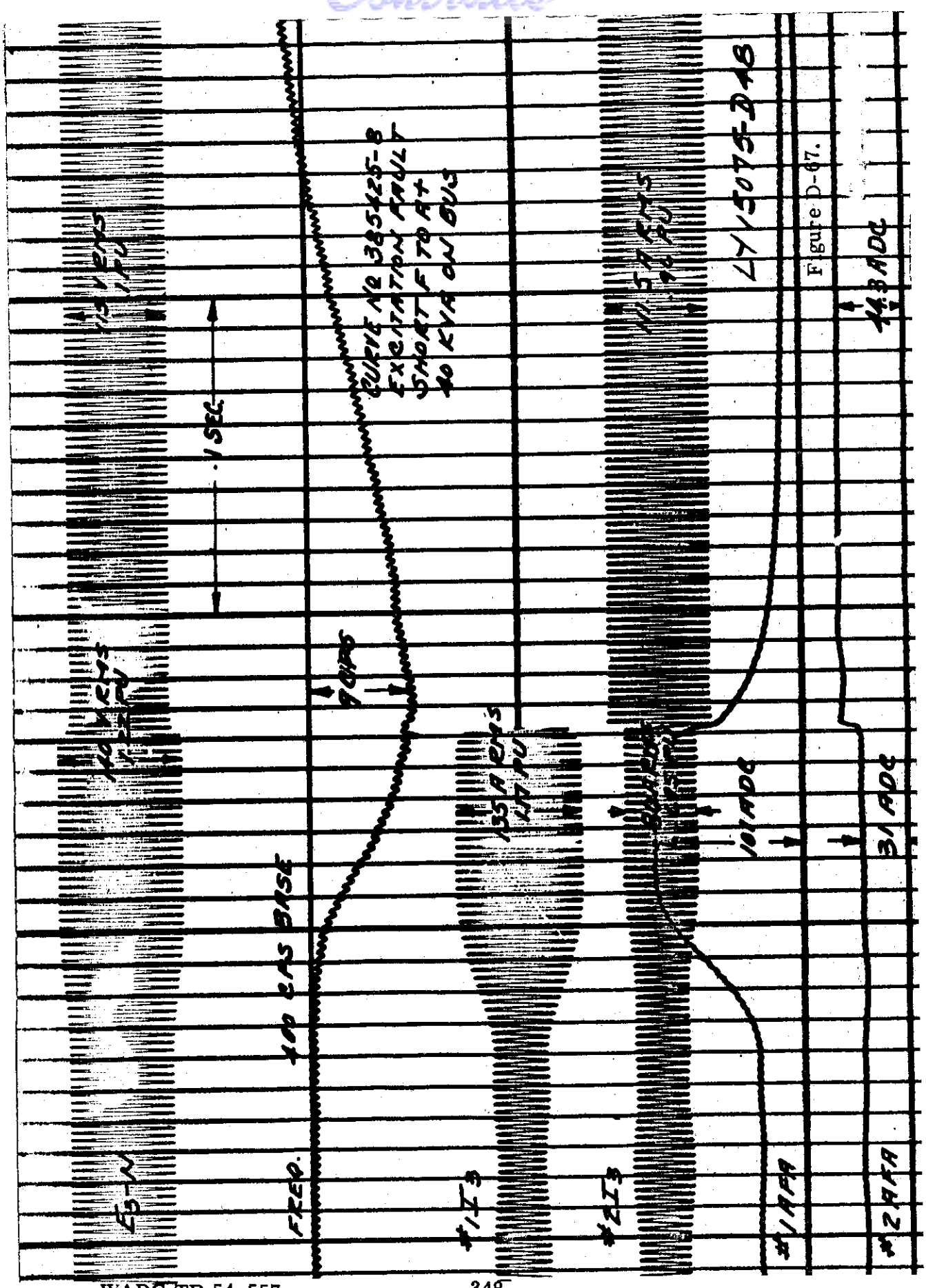

Figure D-67.

Figure No. D-68

Figure No. D-69

Figure No. D-70

Figure No. D-11

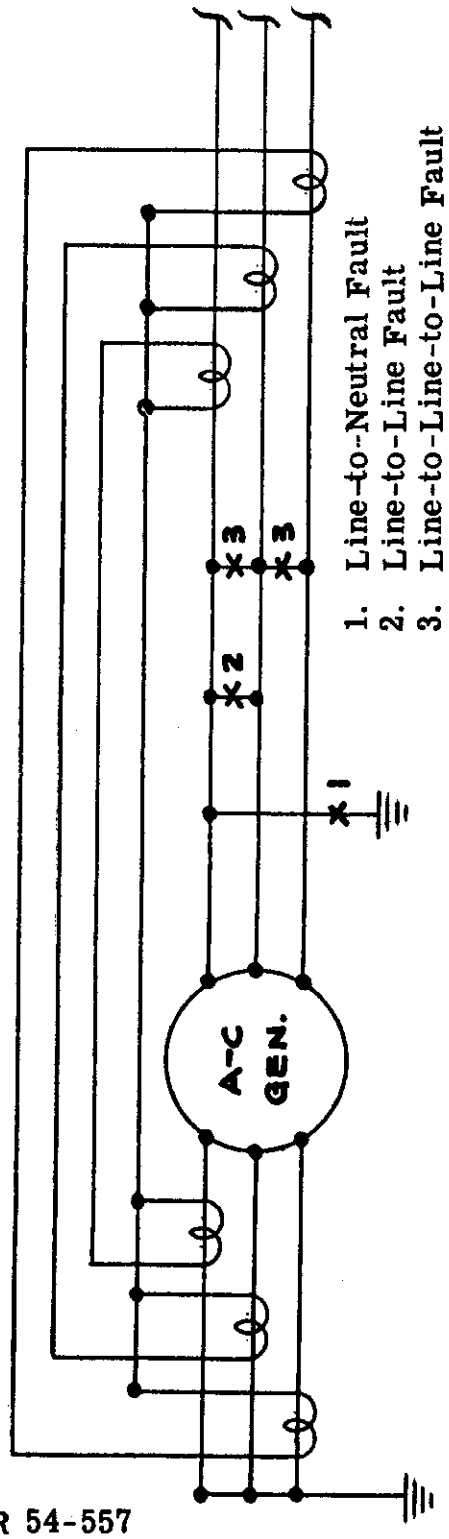

Figure D-72 Schematic Diagram Showing Where Feeder Faults Are Applied

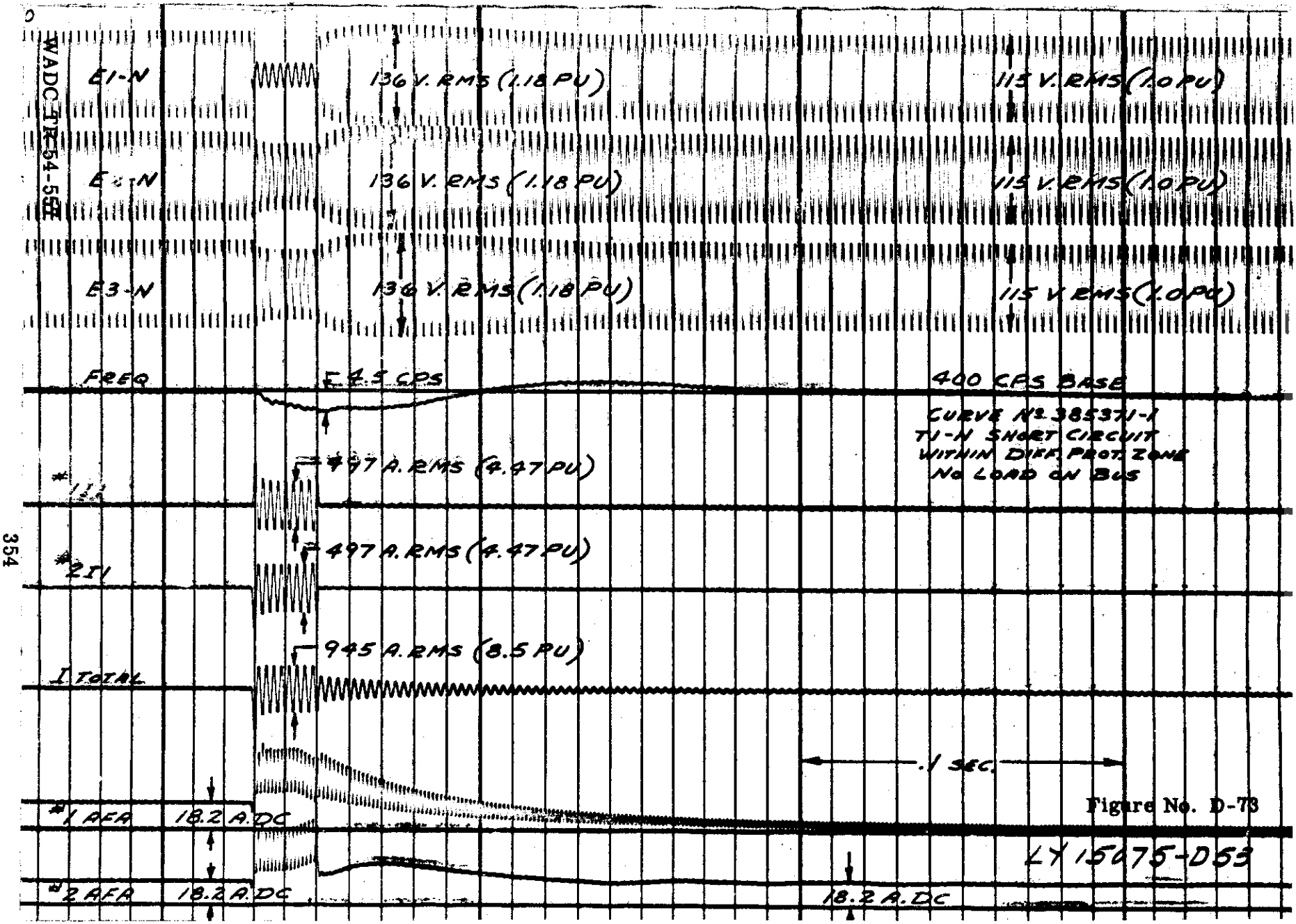

Figure No. D-73

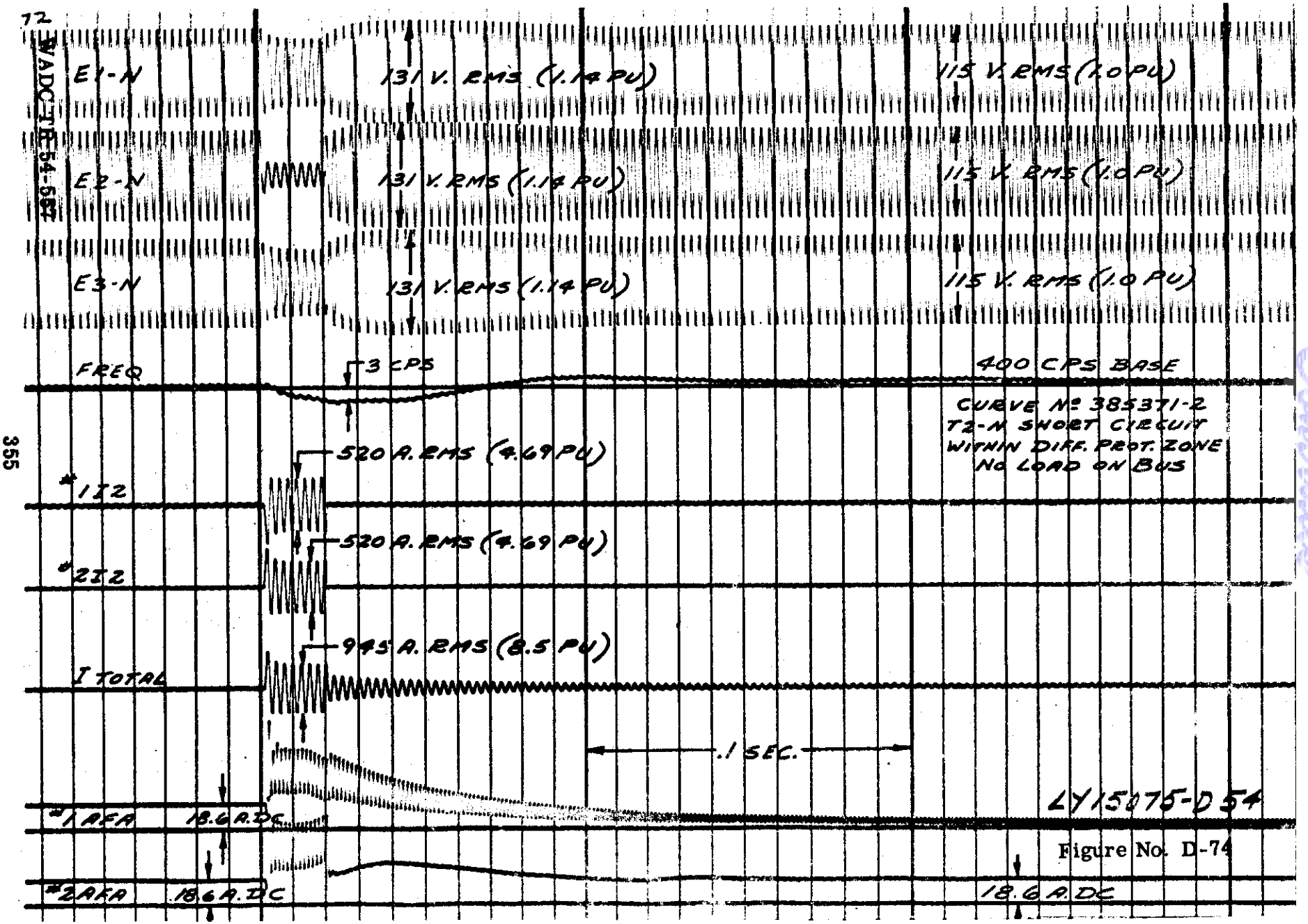

Figure No. D-74

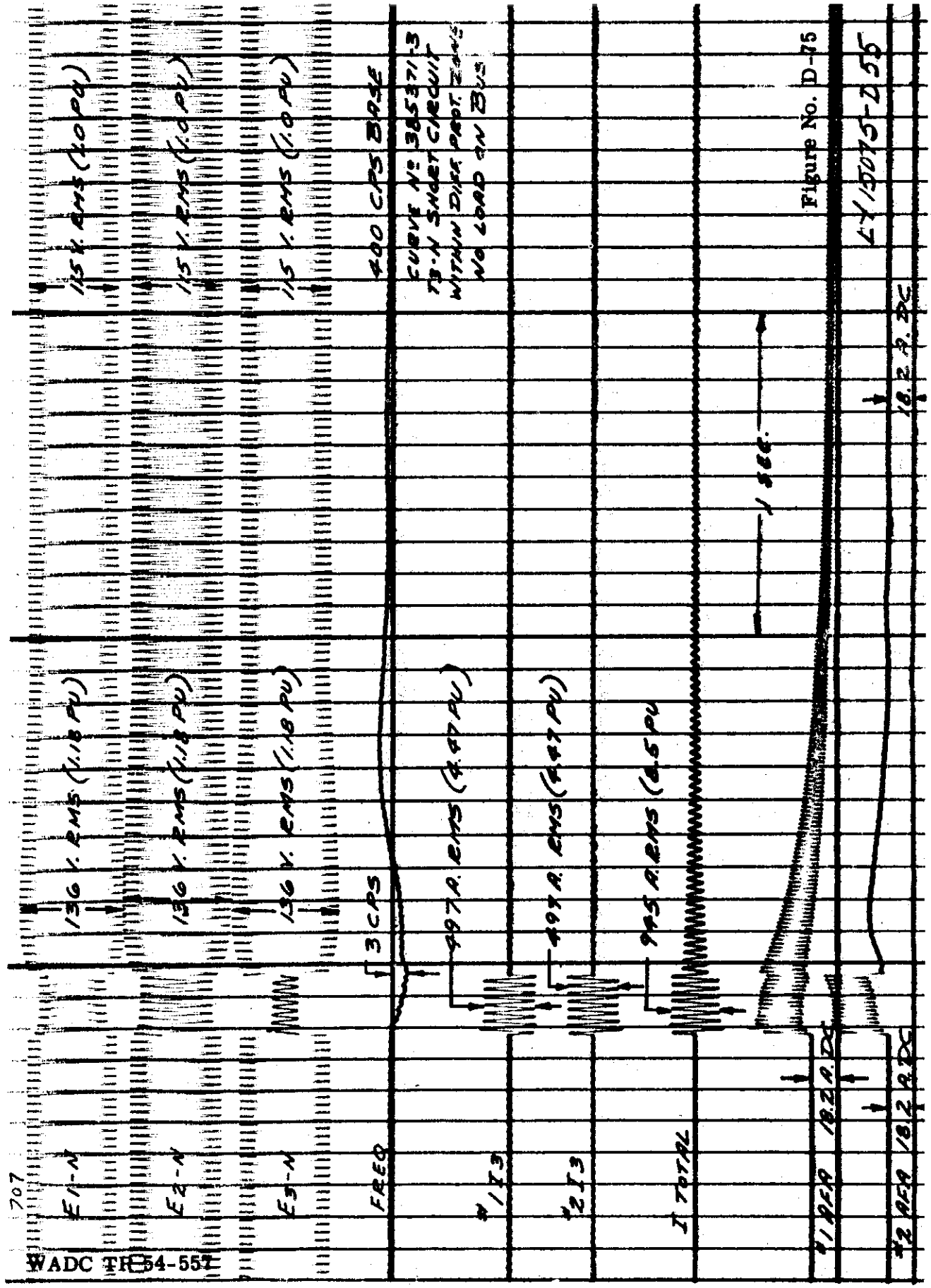

Figure No. D-75

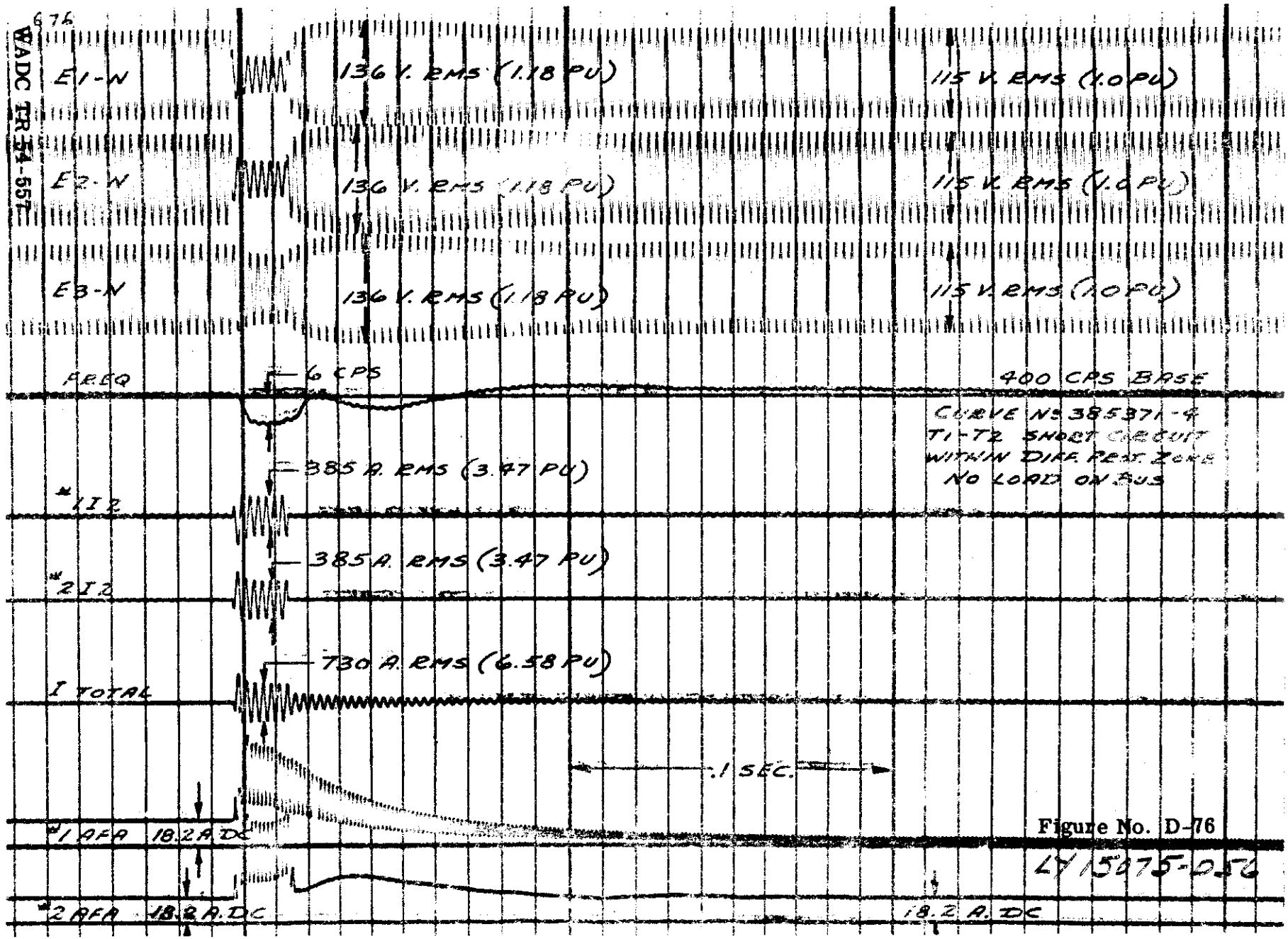

Figure No. D-76

LY 15075-D-76

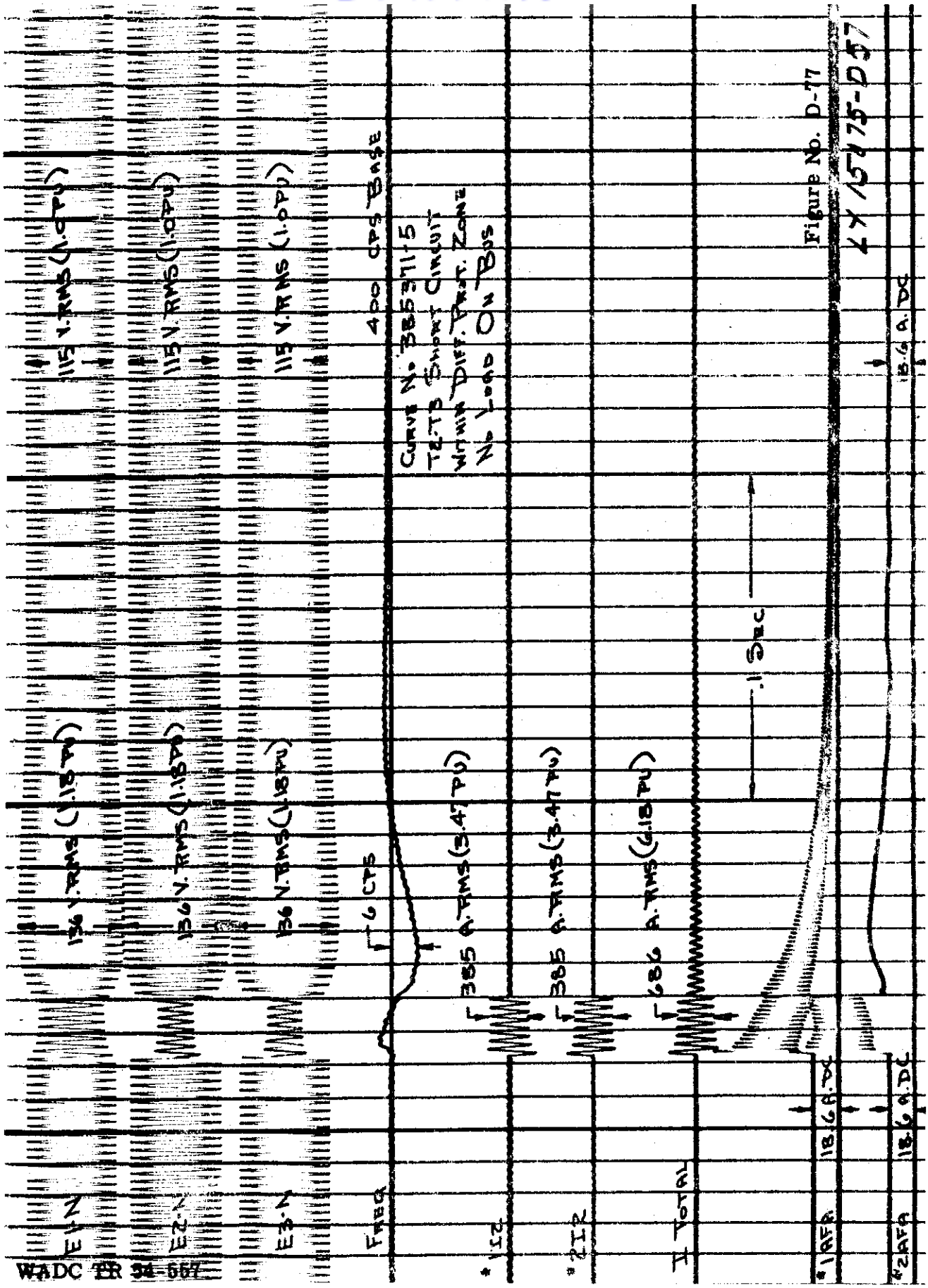

Figure No. D-77

47 157 75-D 57

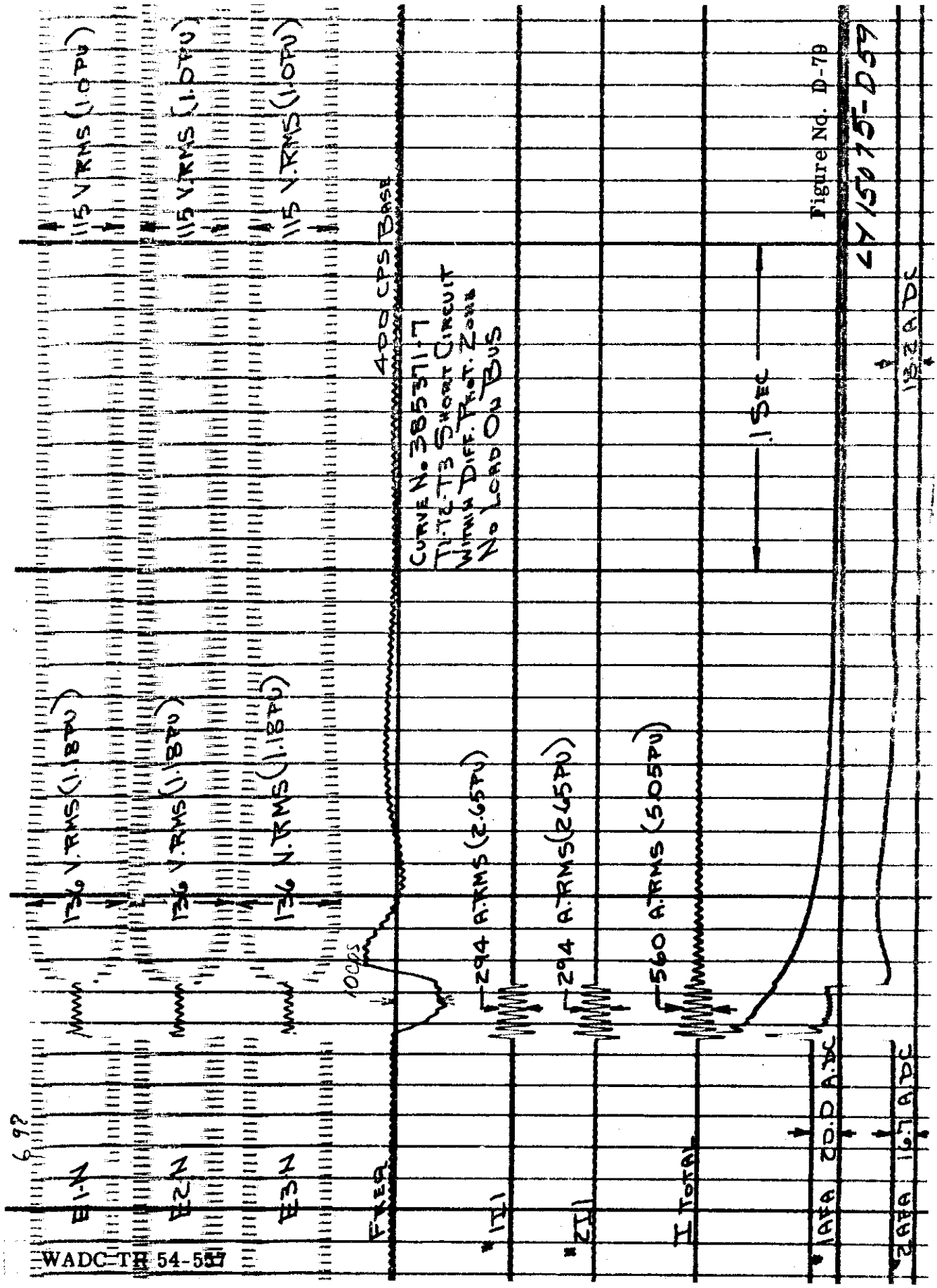

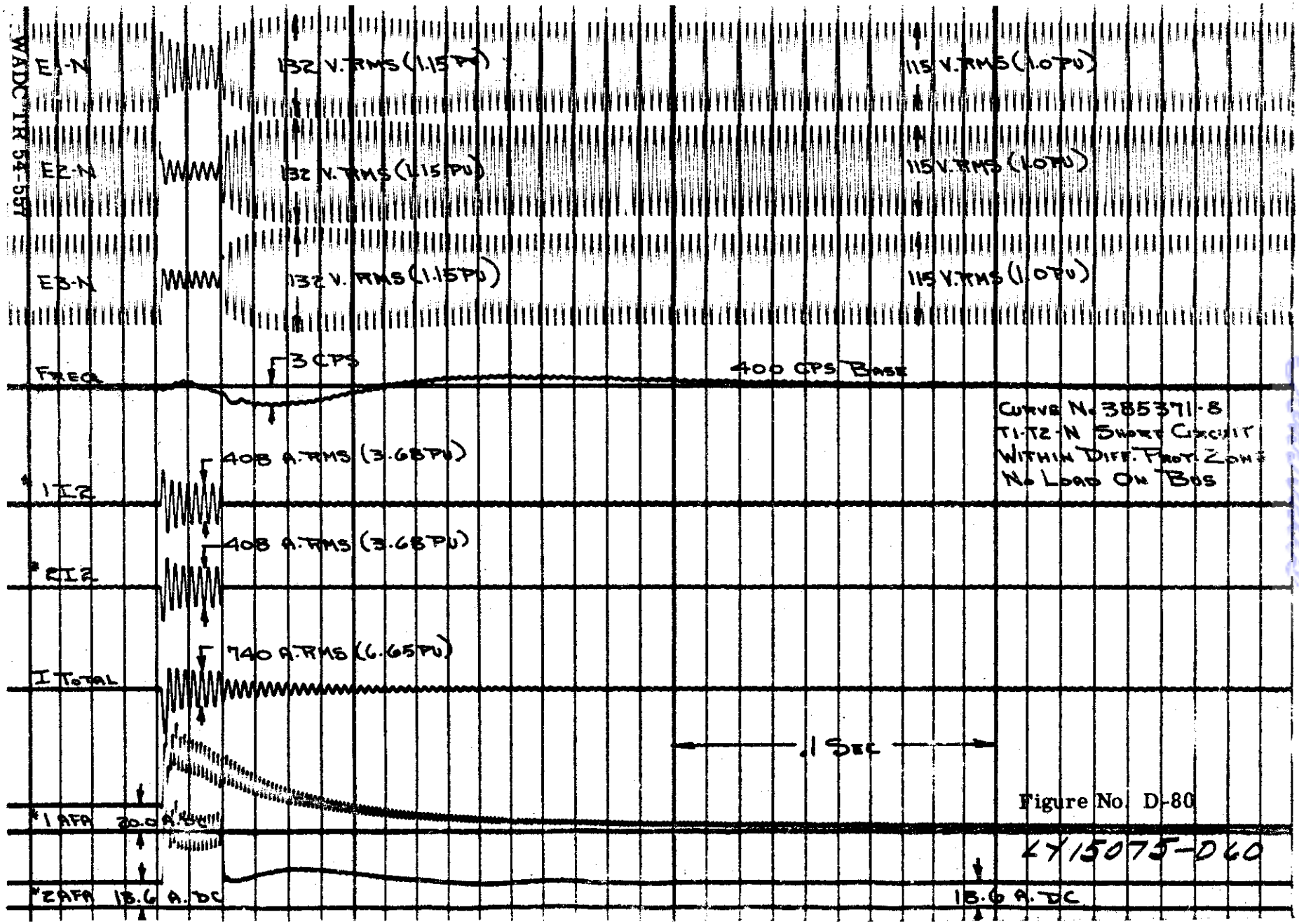

Figure No. D-80

KY15075-060

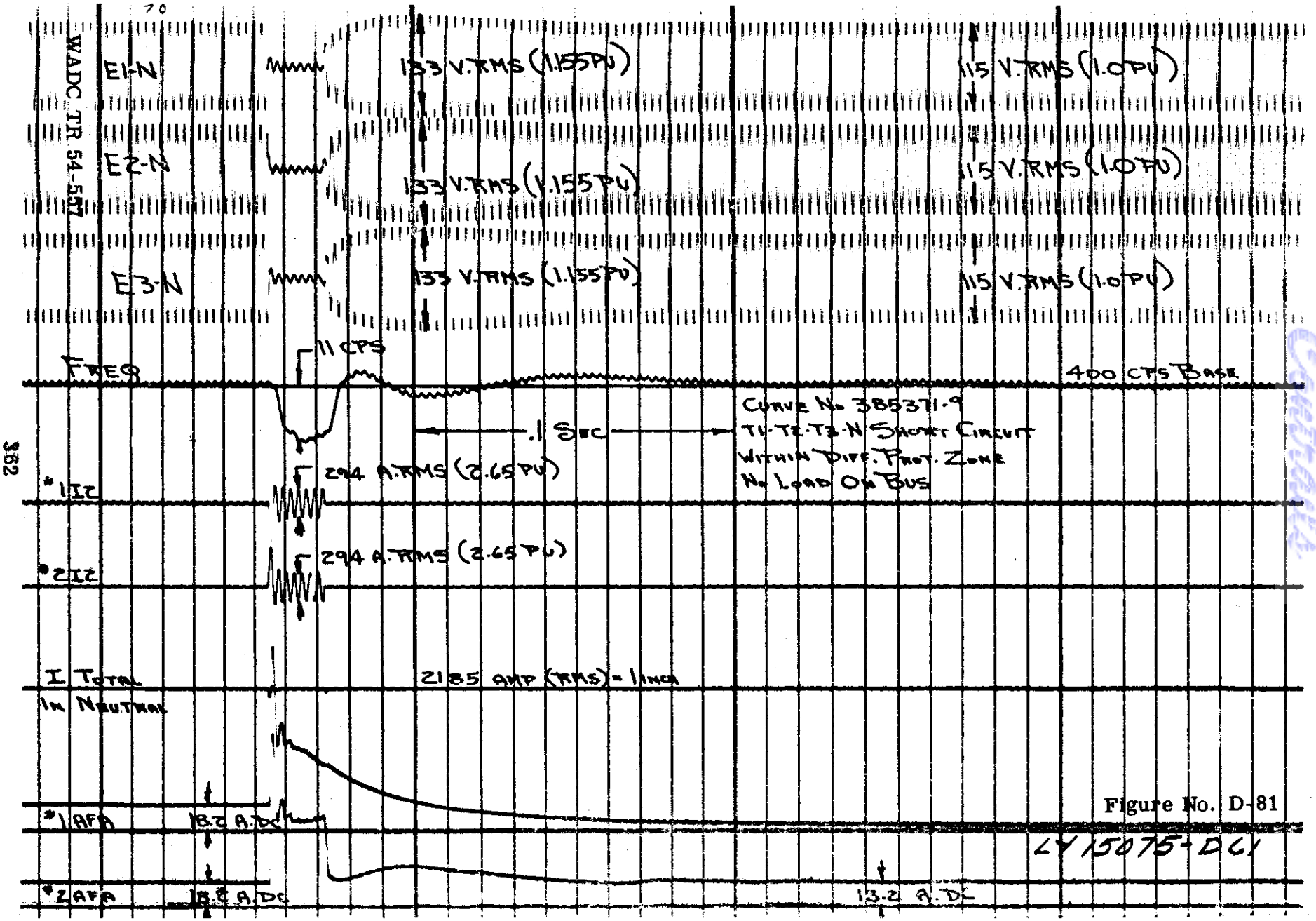

Figure No. D-81

LY 15075-DC1

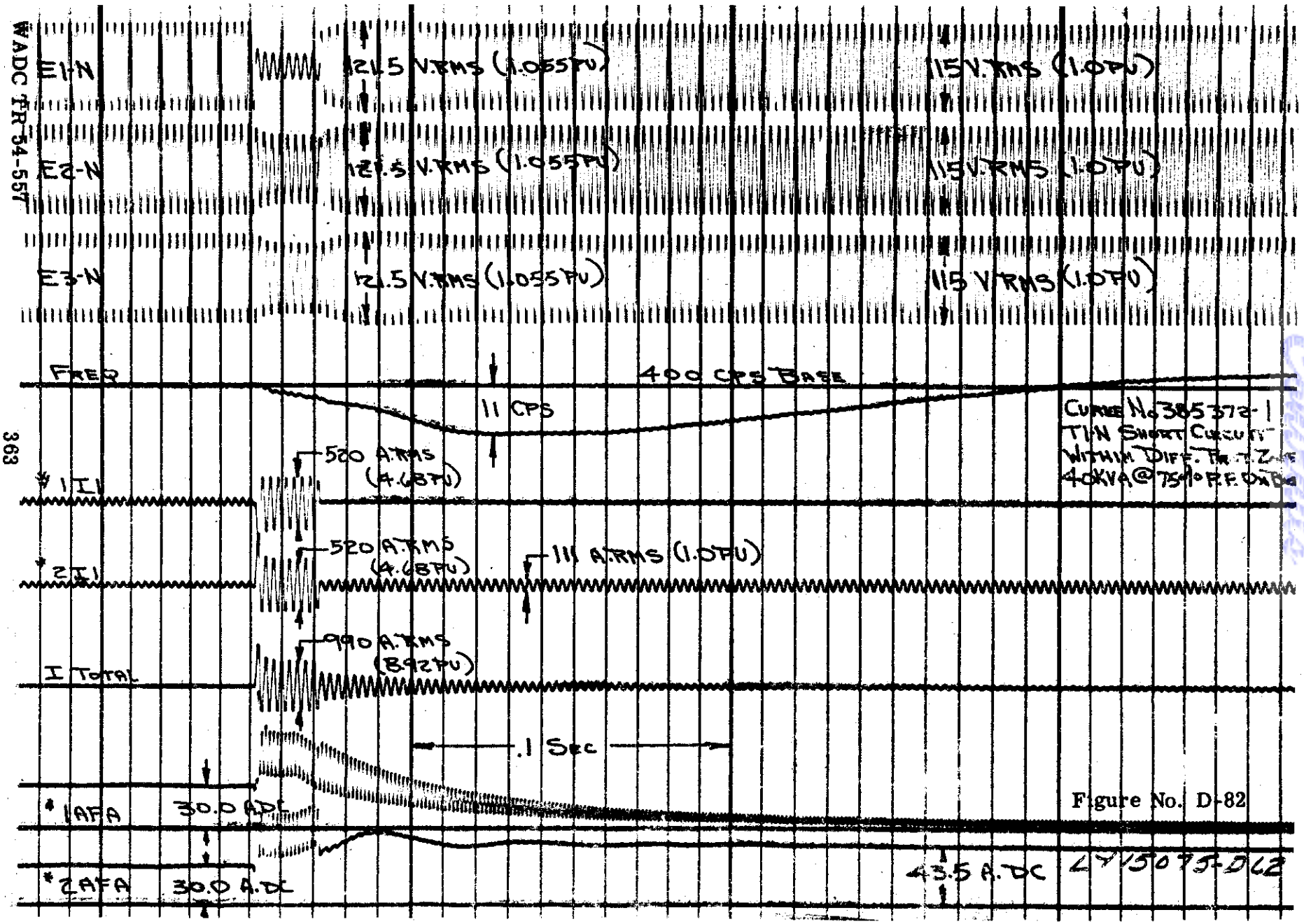

Figure No. D-82

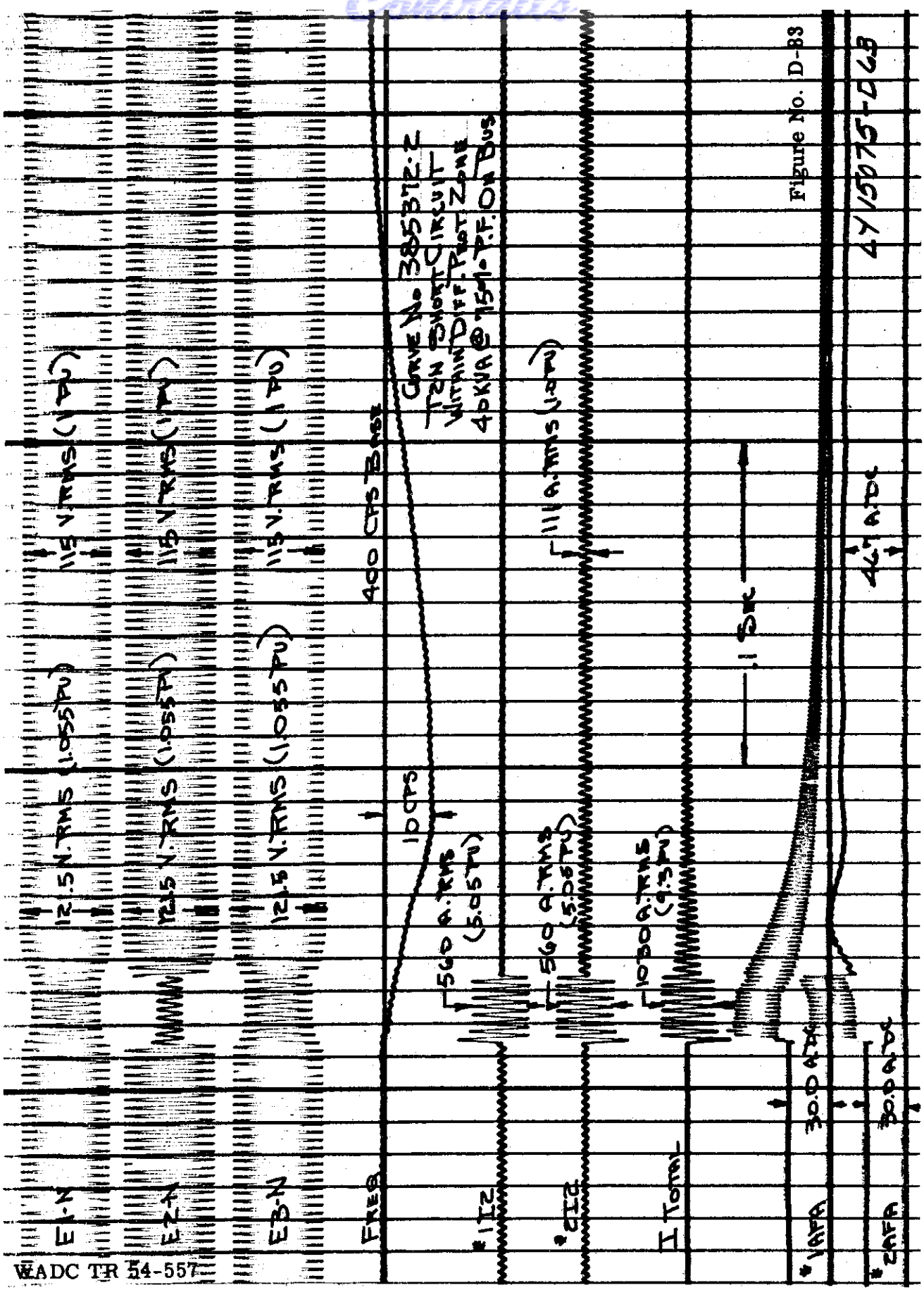

Figure No. D-83

47/15975-043

Figure No. D-84

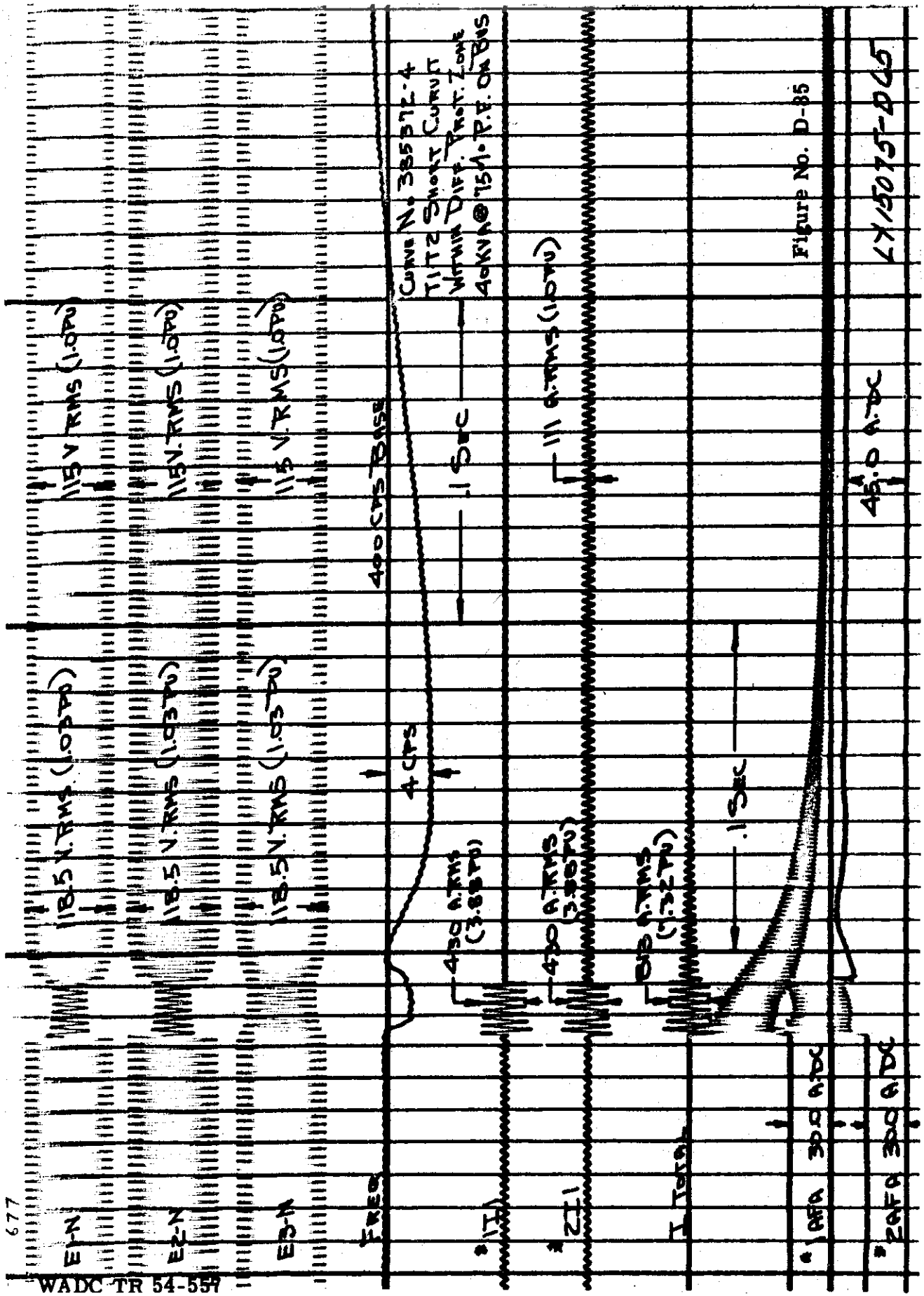

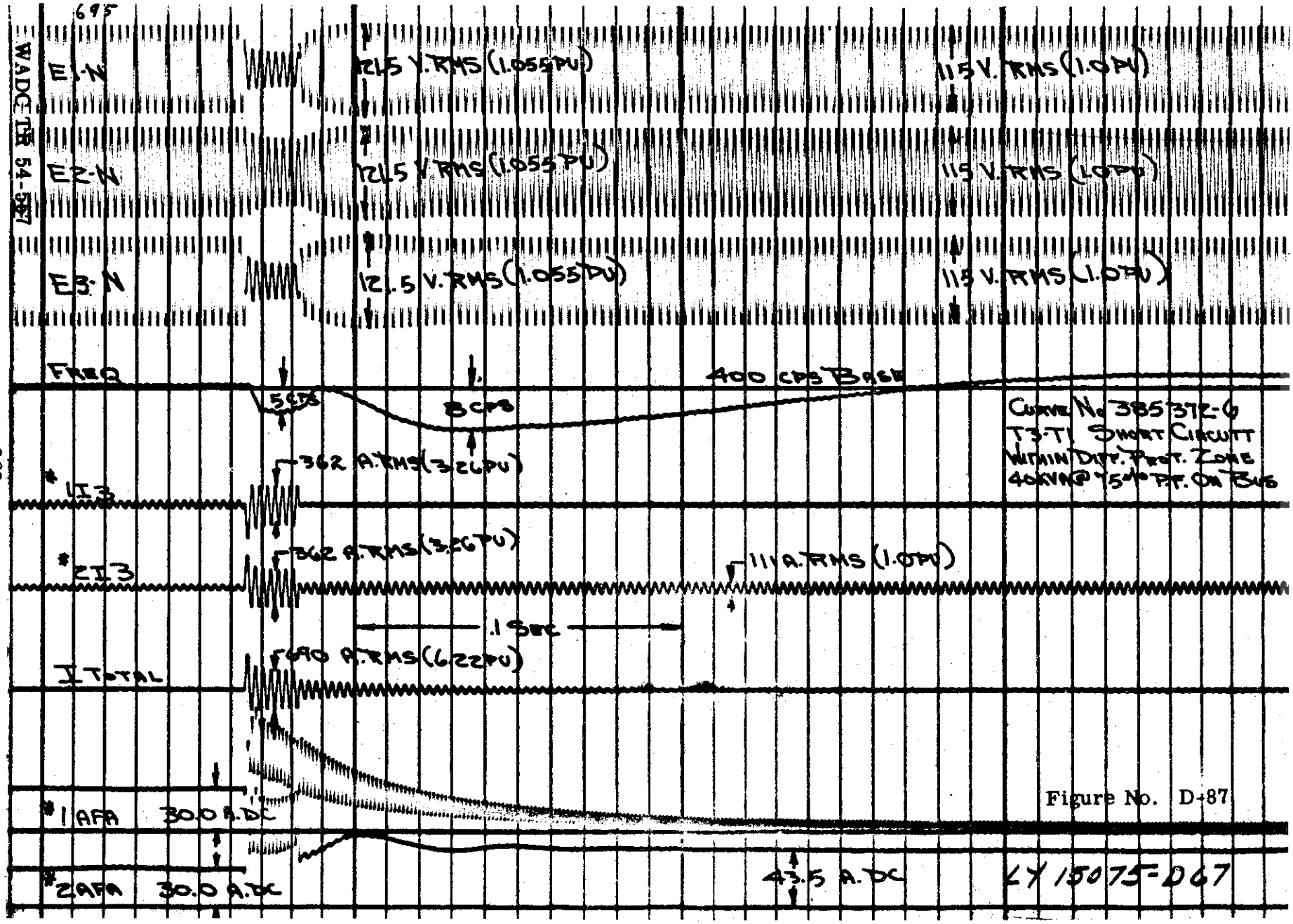

Figure No. D-87

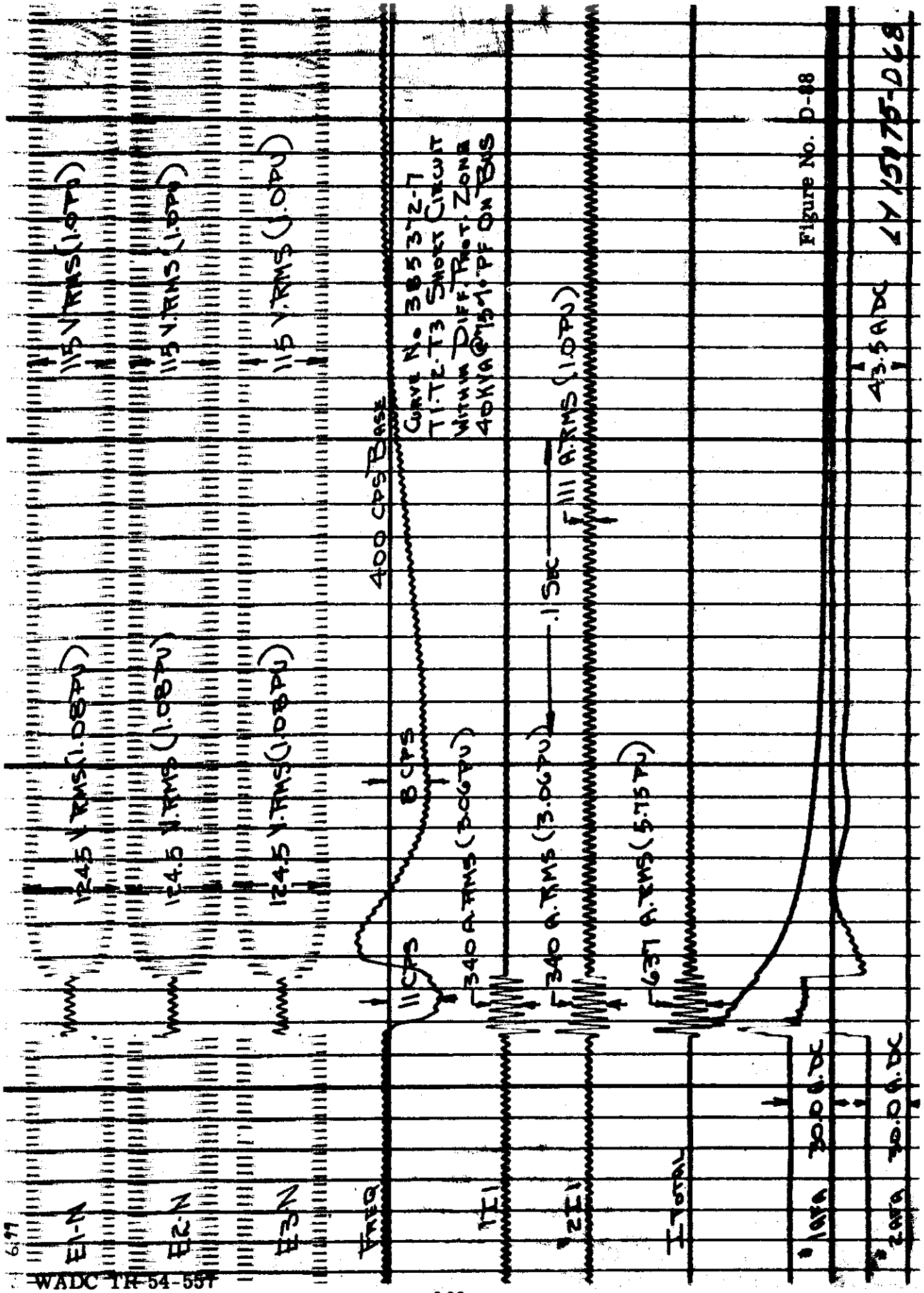

Figure No. D-89

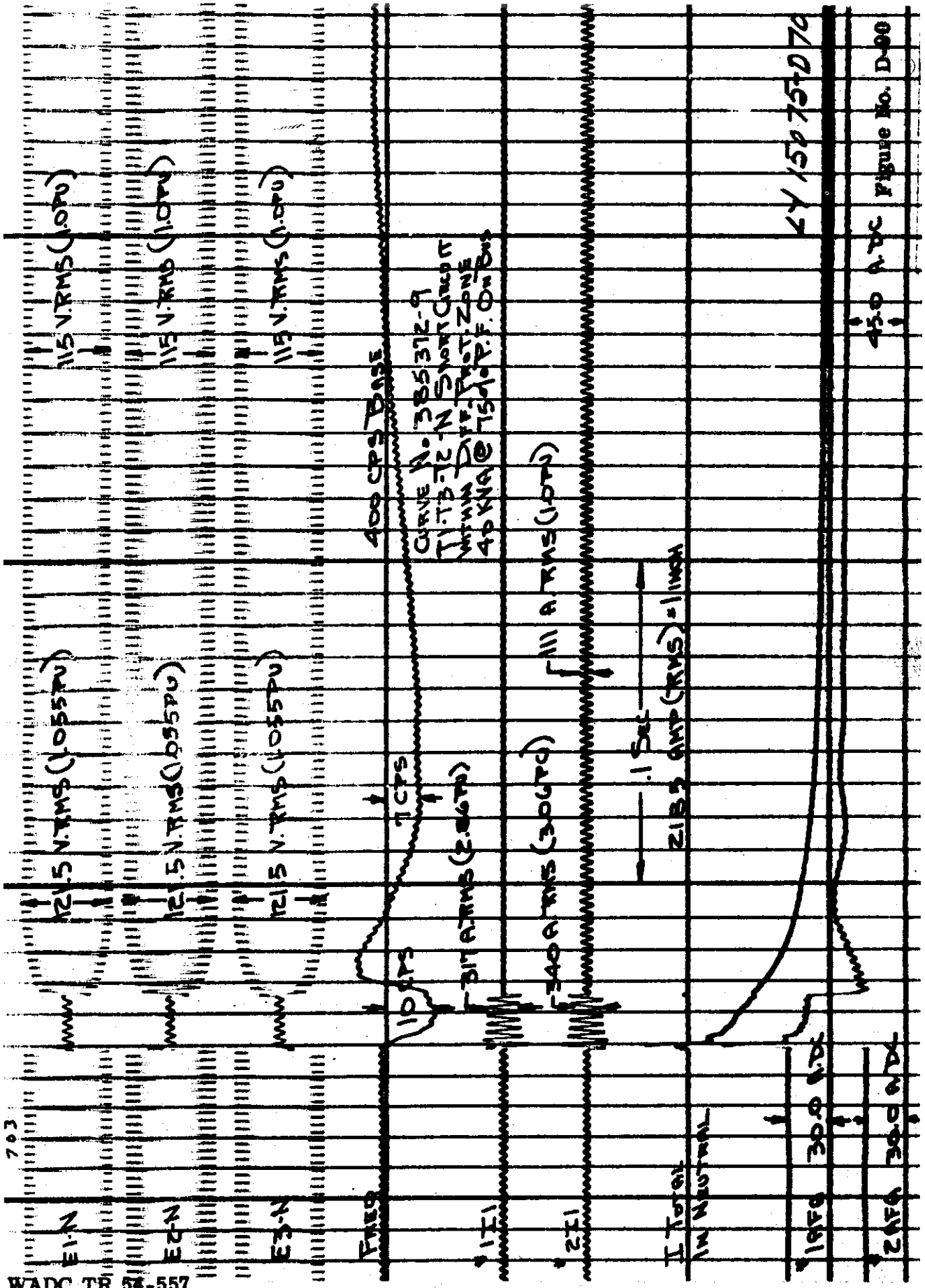

Figure No. D-91

47/5475-D71

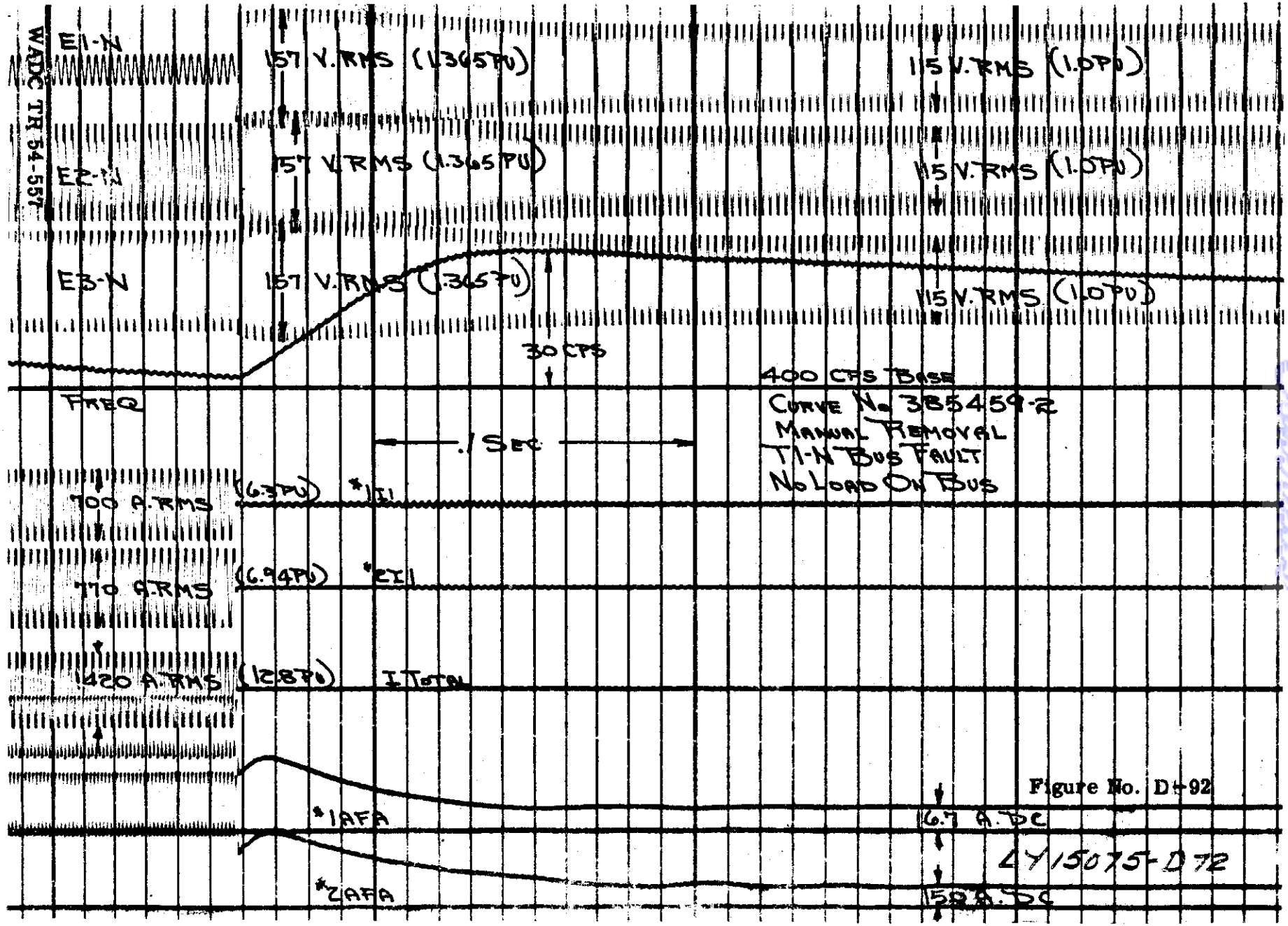

Figure No. D-92

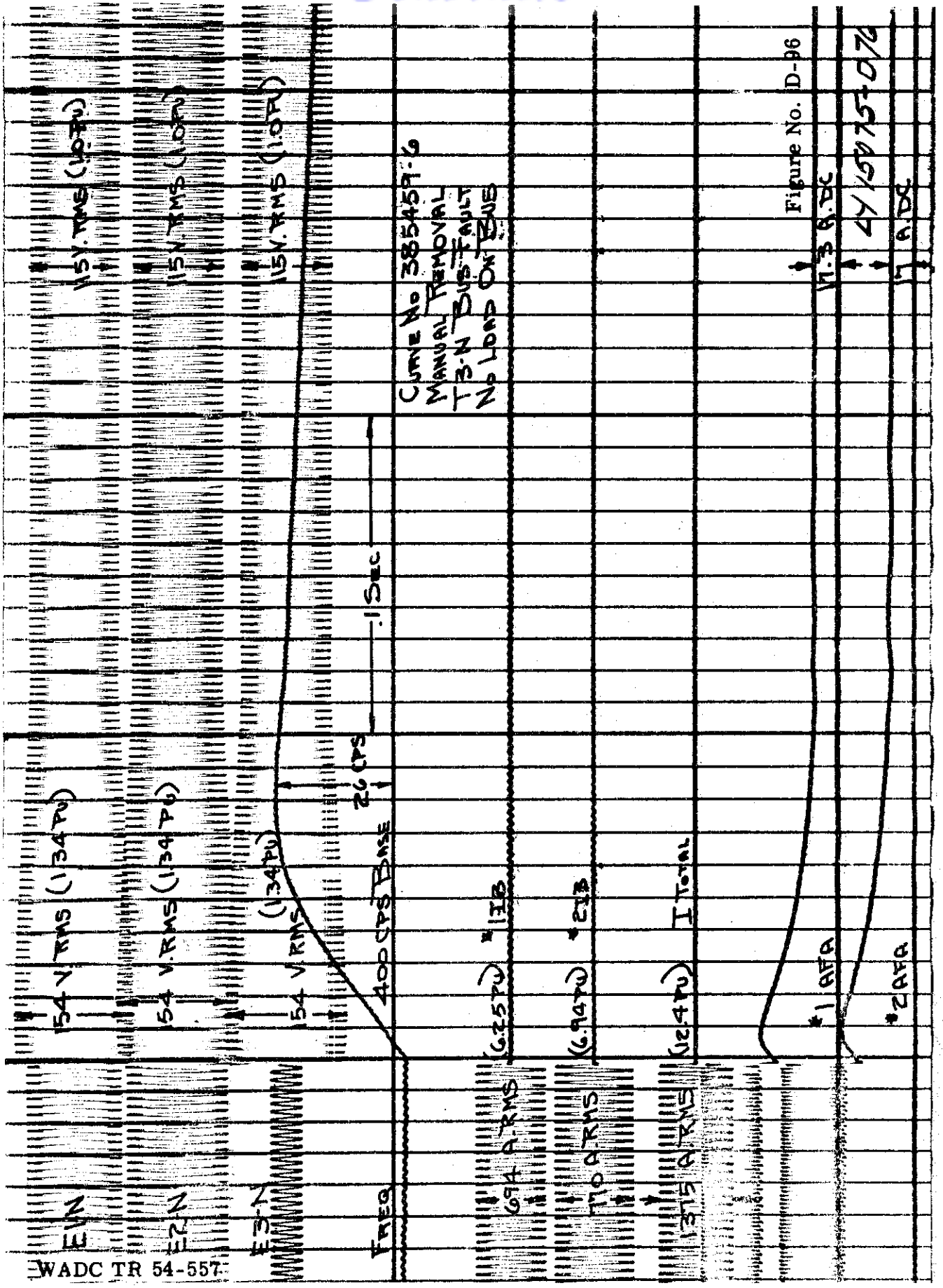

Figure No. D-97

47/45T-77

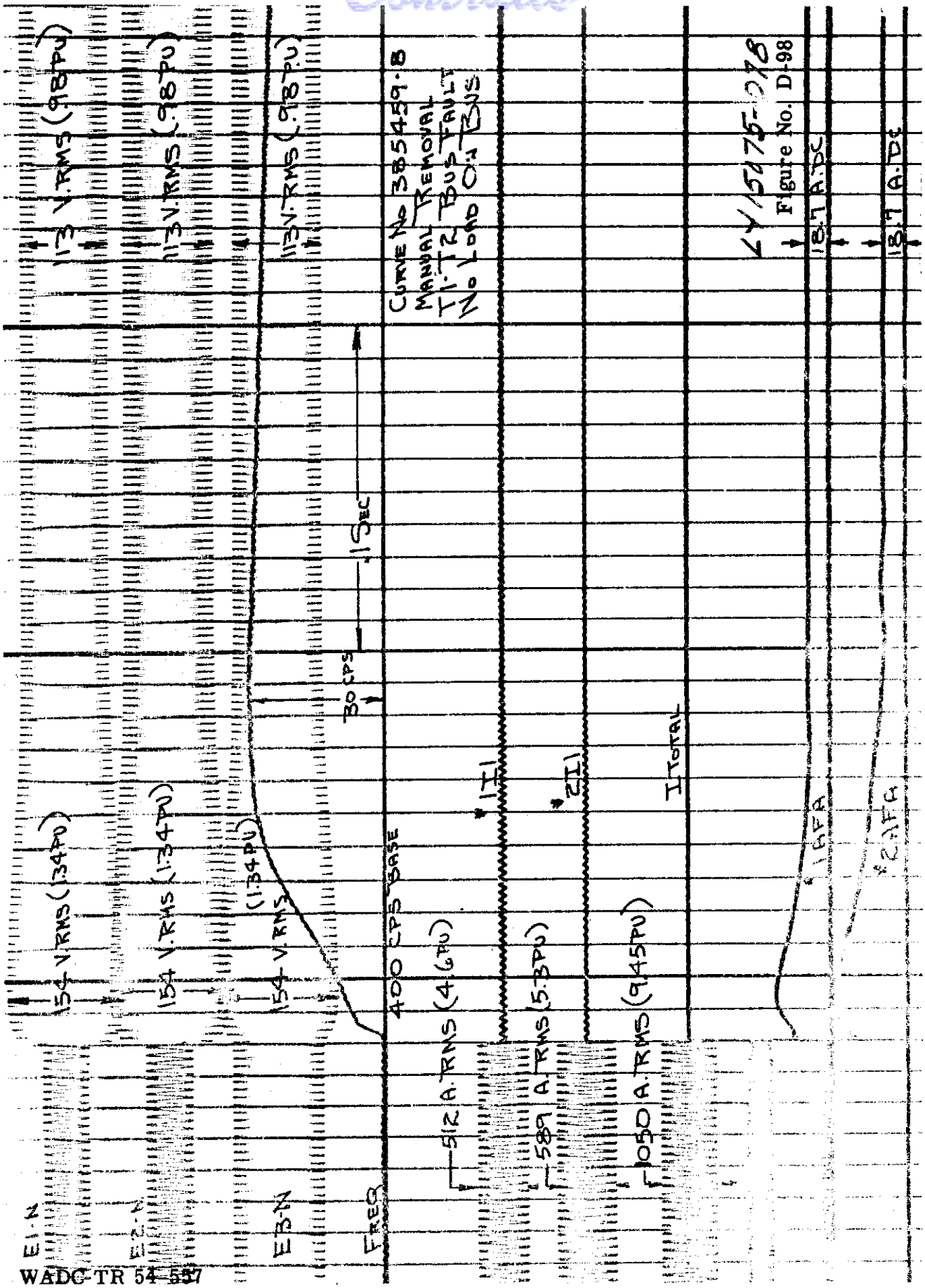

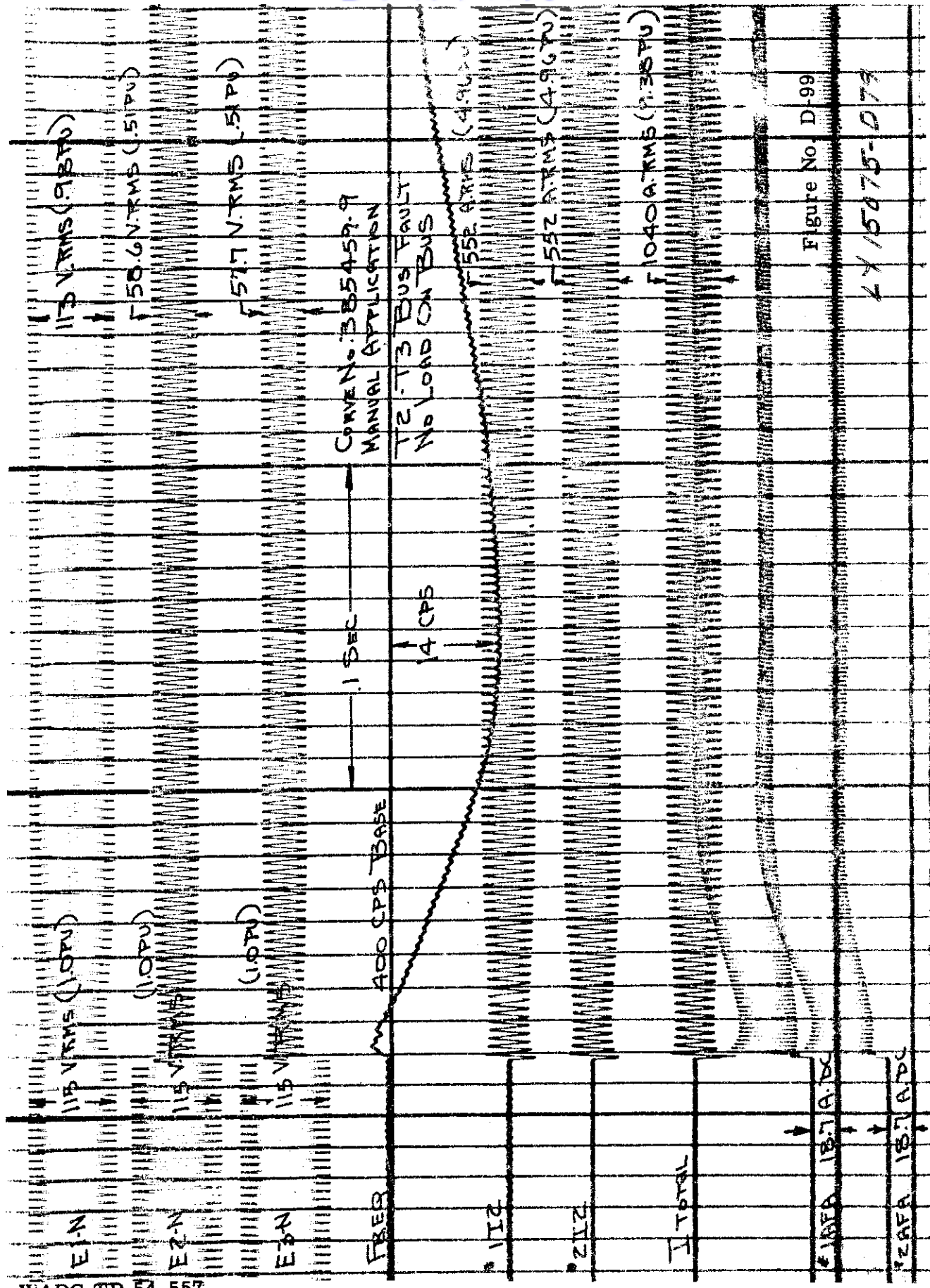

Figure No. D-69

4Y/15475-D-74

Figure No. D-101

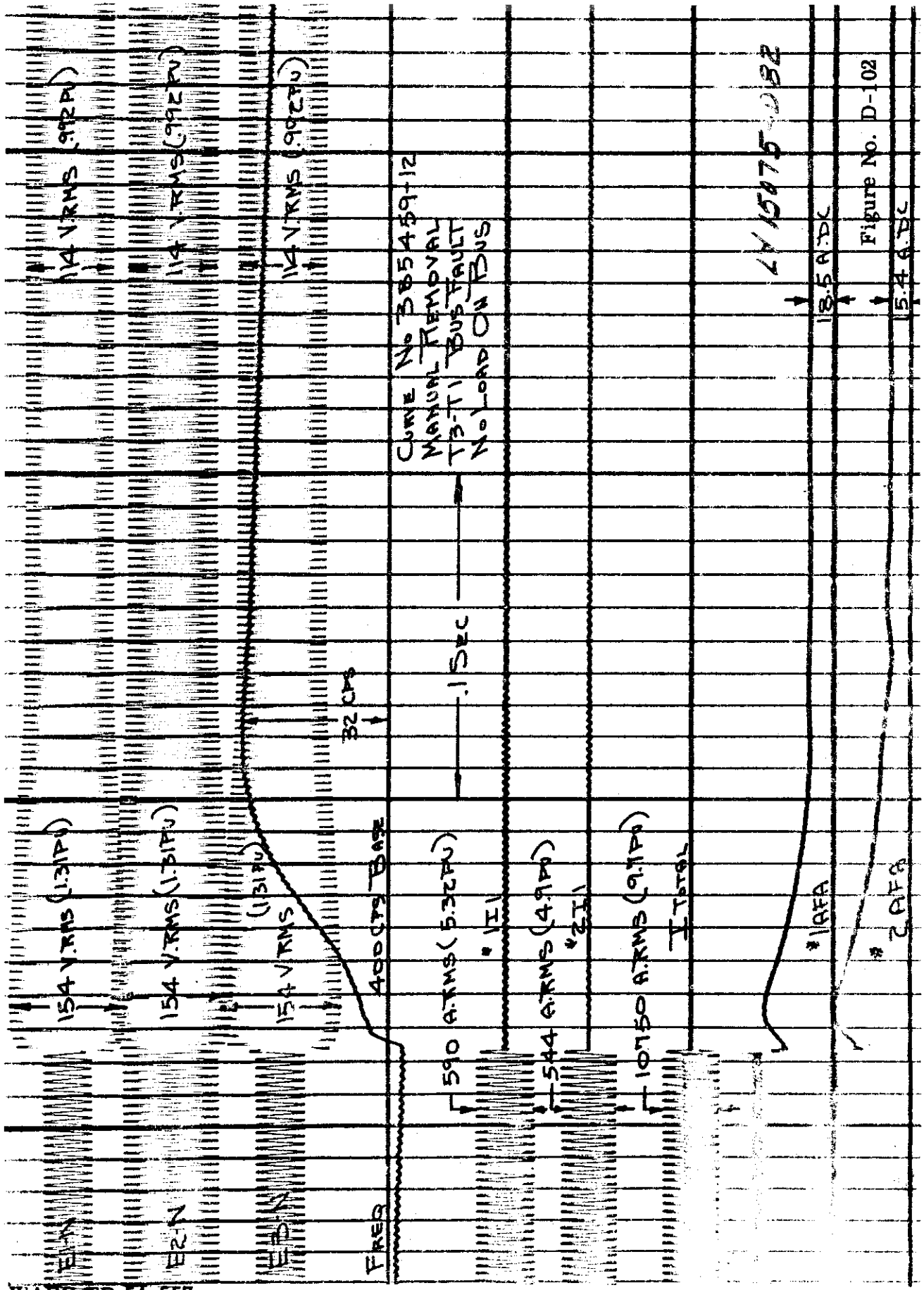

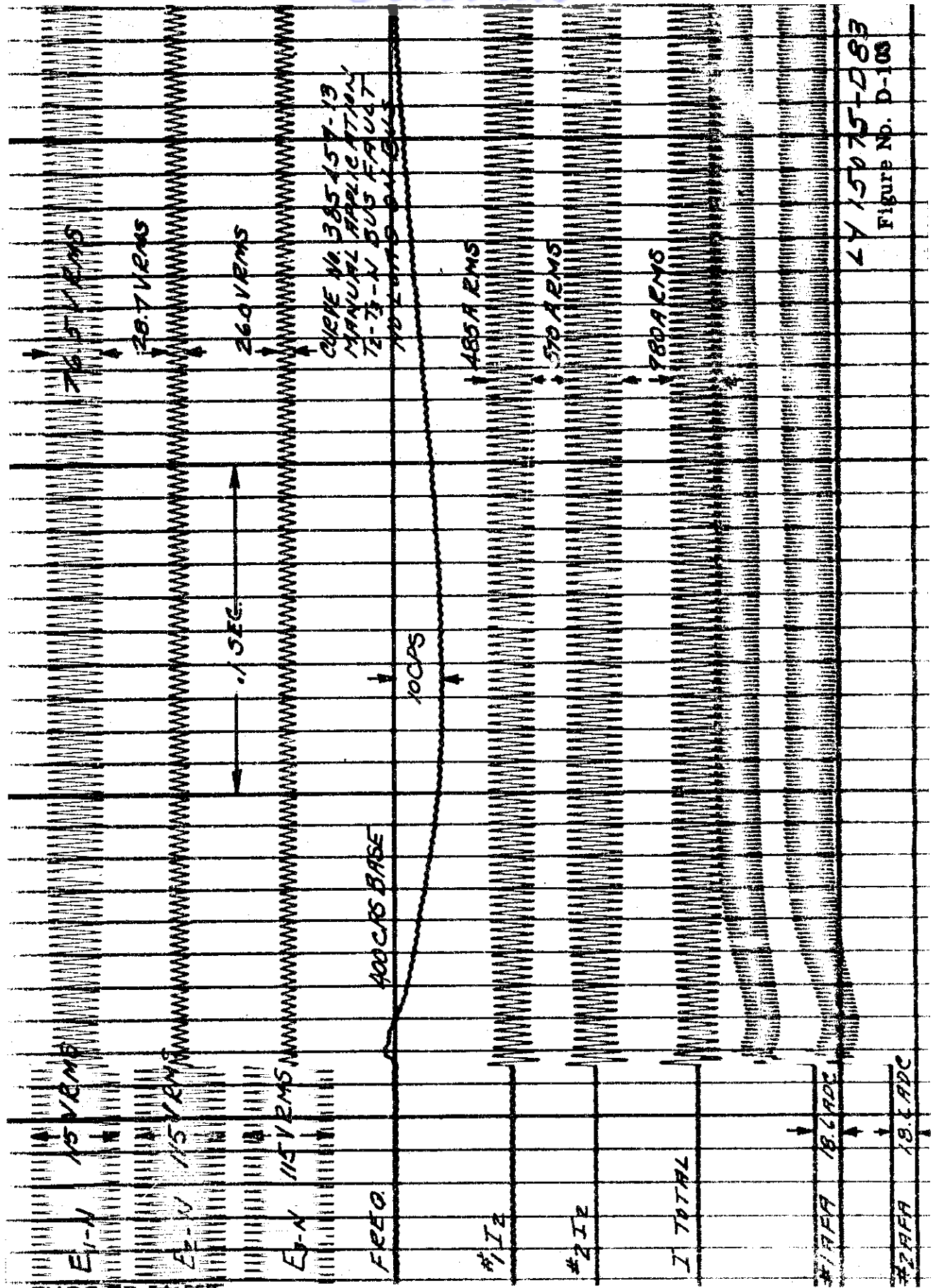

Figure No. D-18

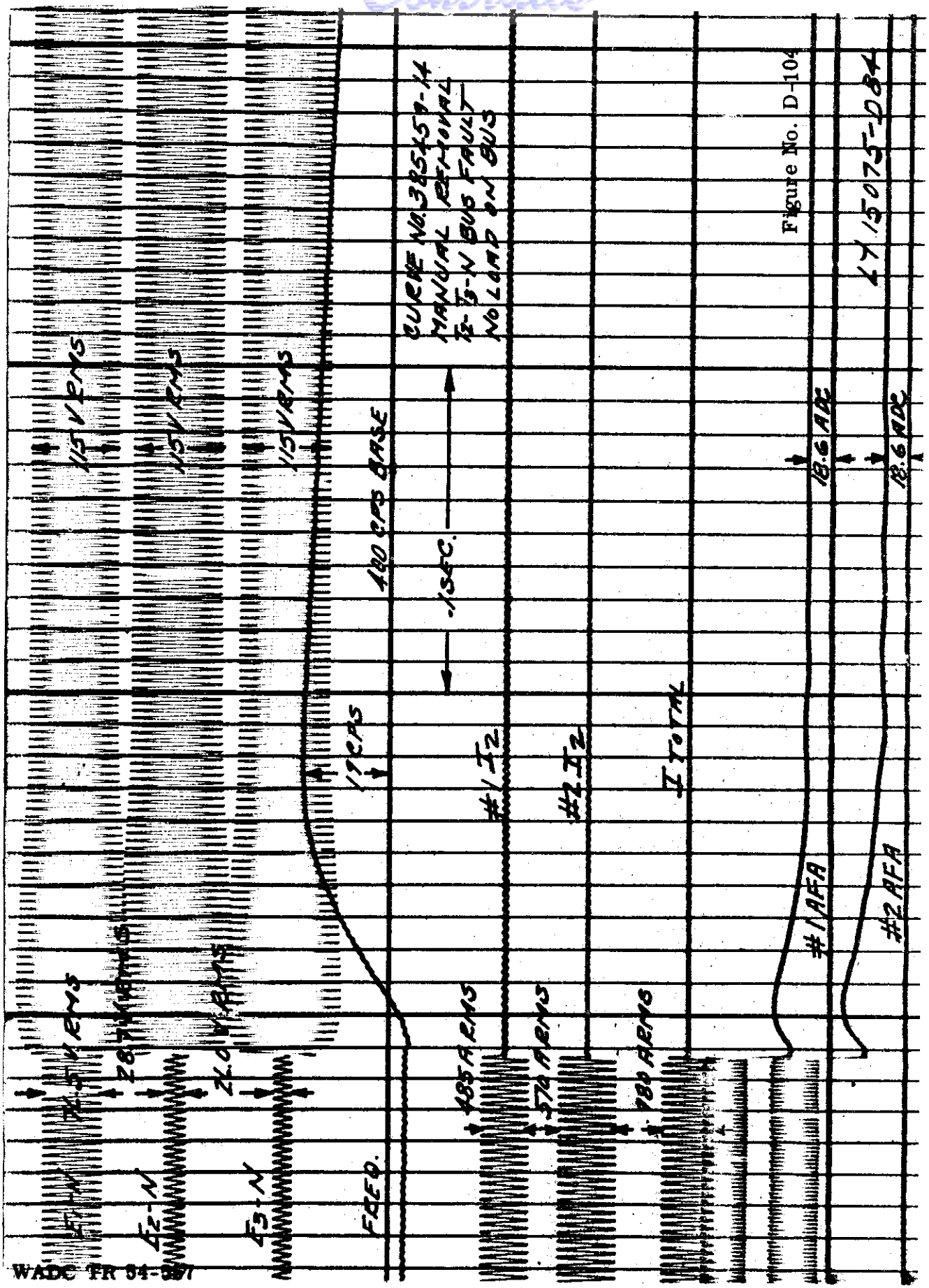

Figure No. D-104

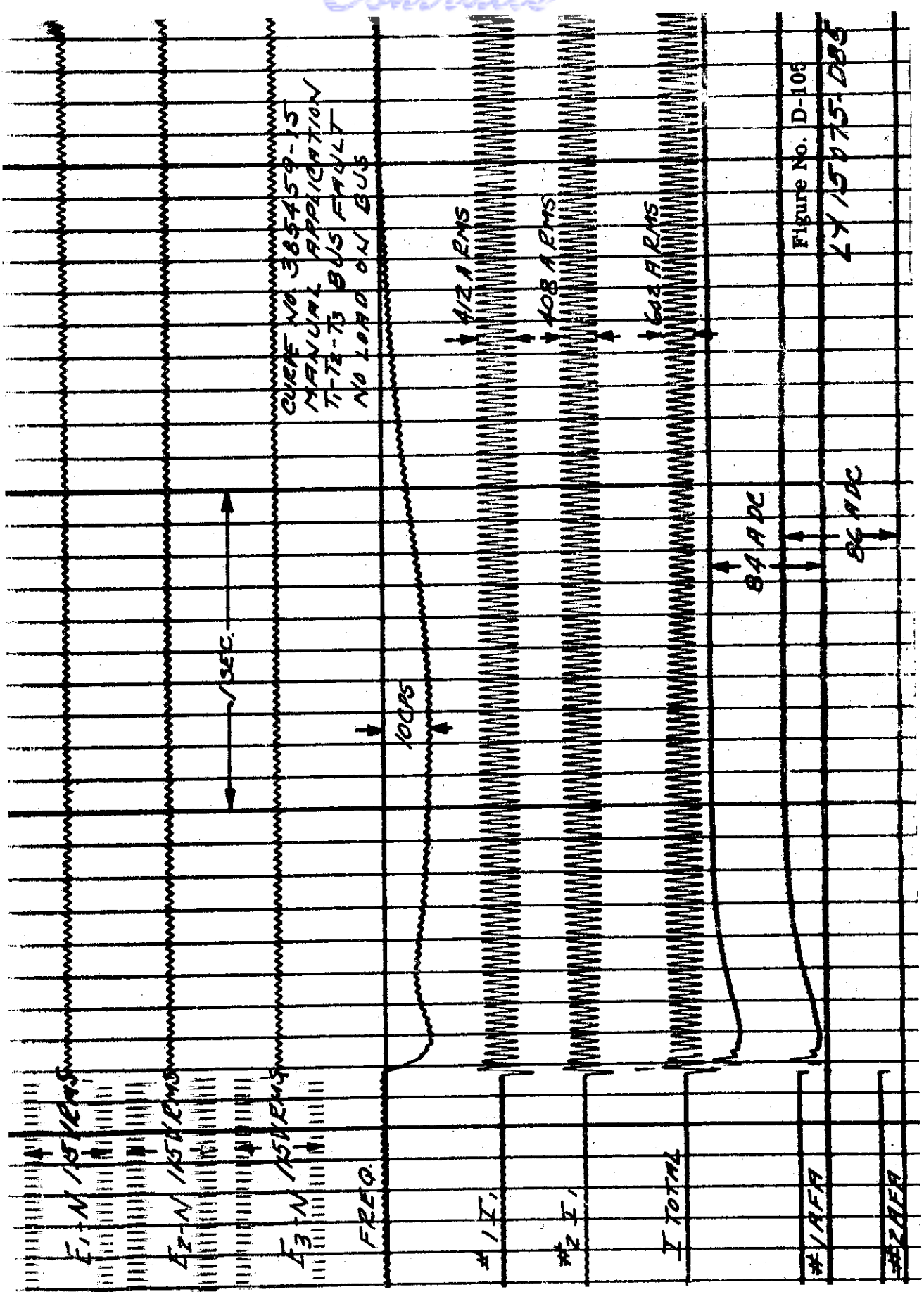

Figure No. D-105

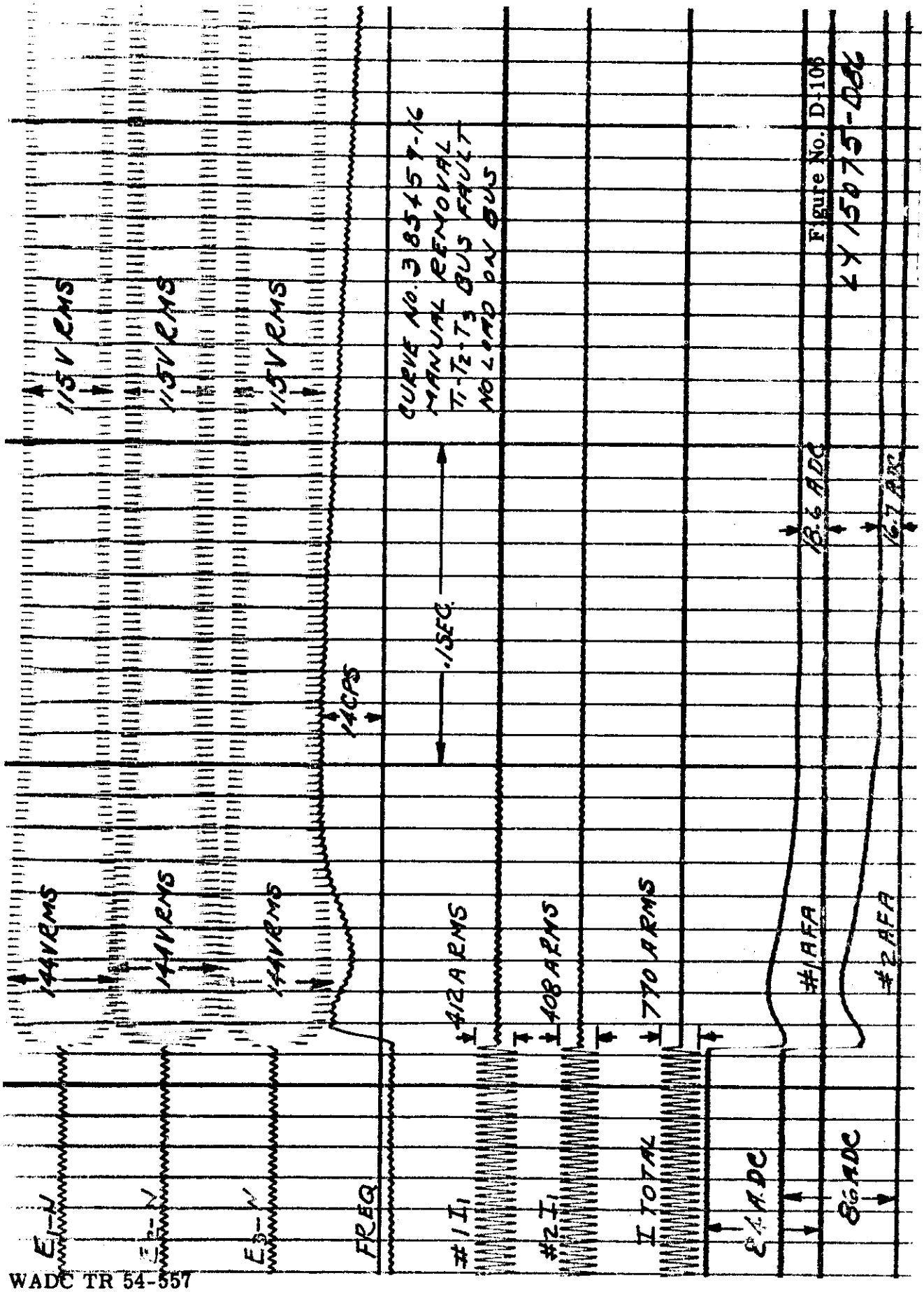

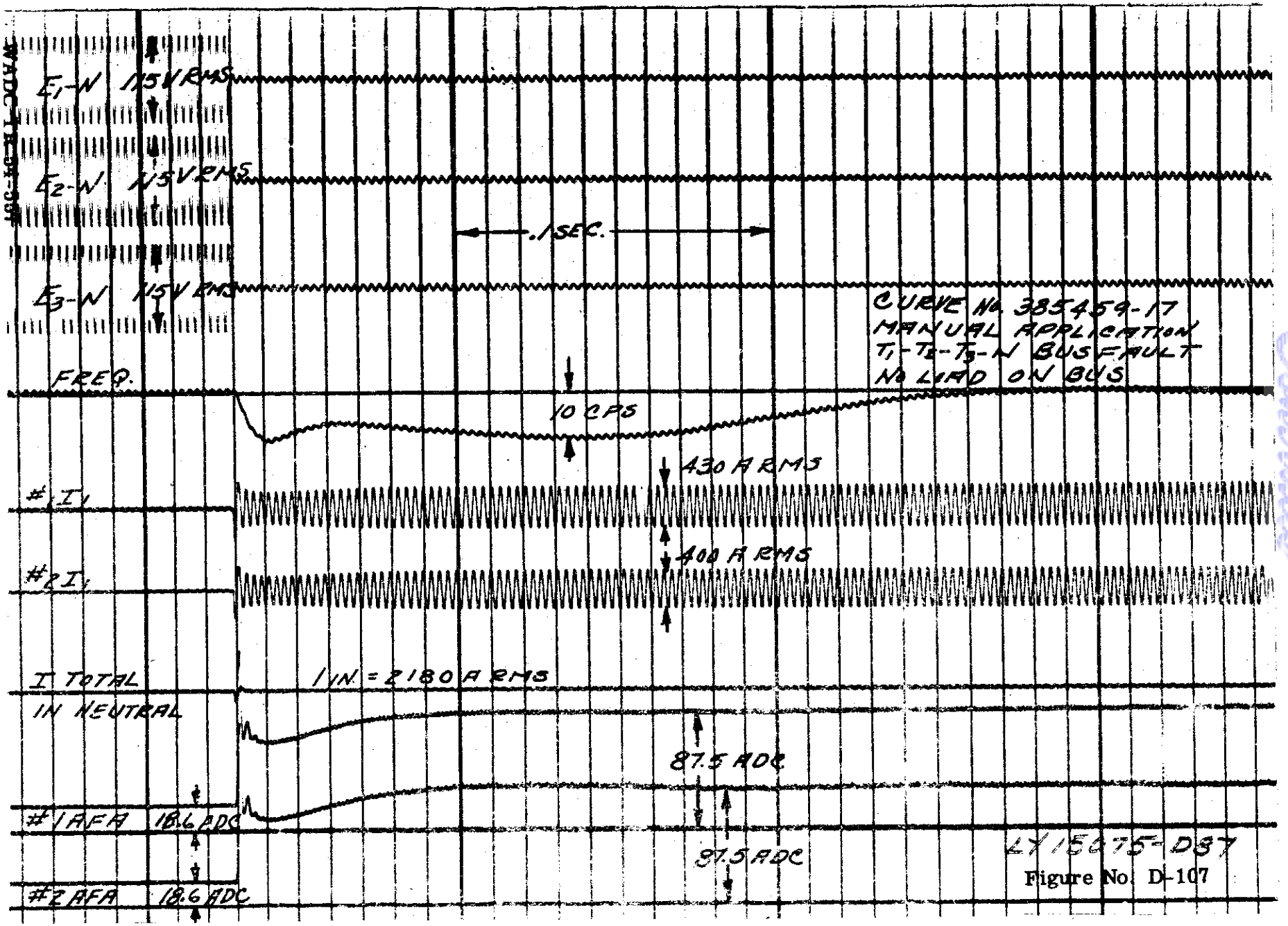

Figure No. D-107

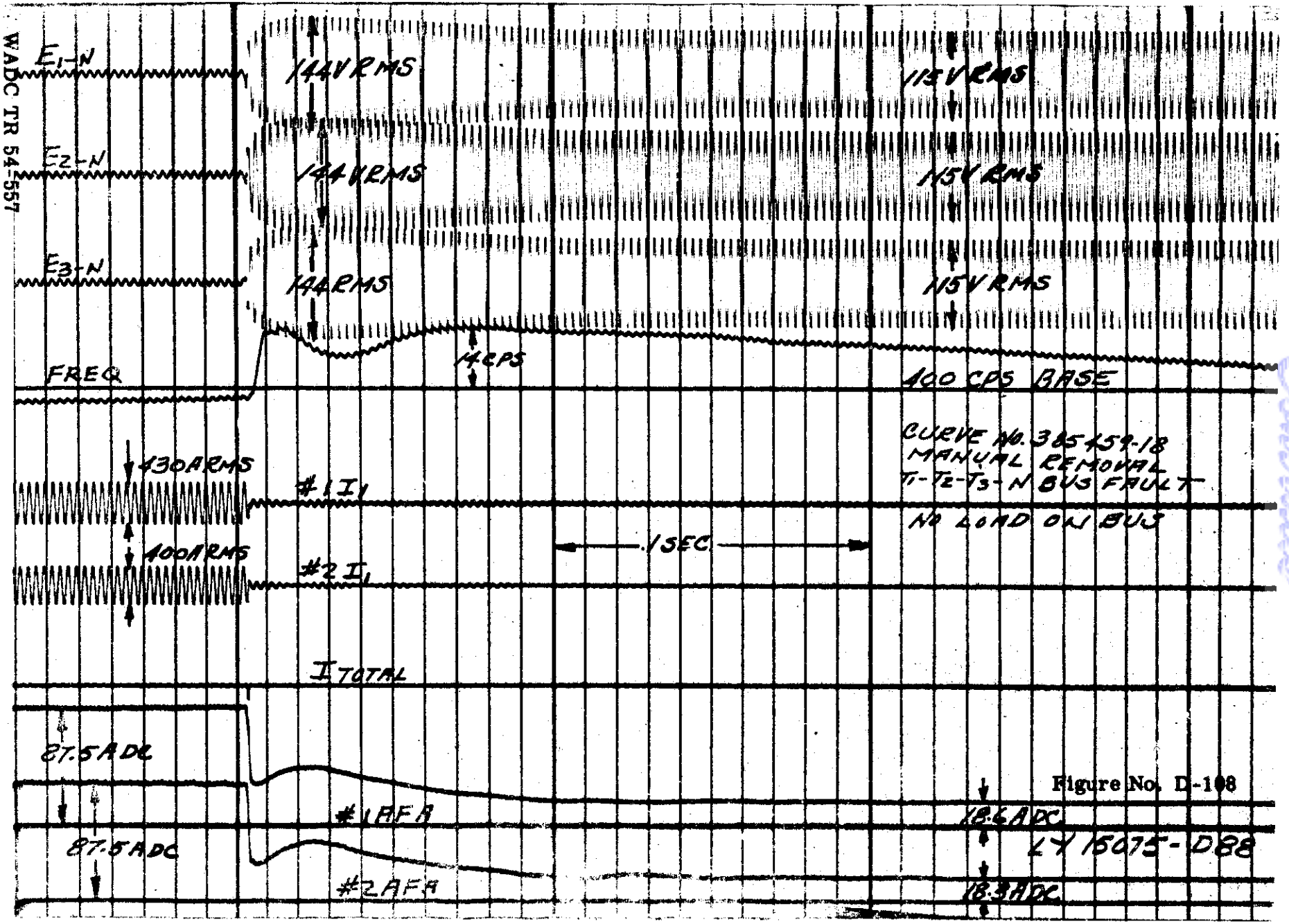

Figure No. D-108

↙ 15075-09
Figure No. D-10

Figure No. D-111
AF 15075-57

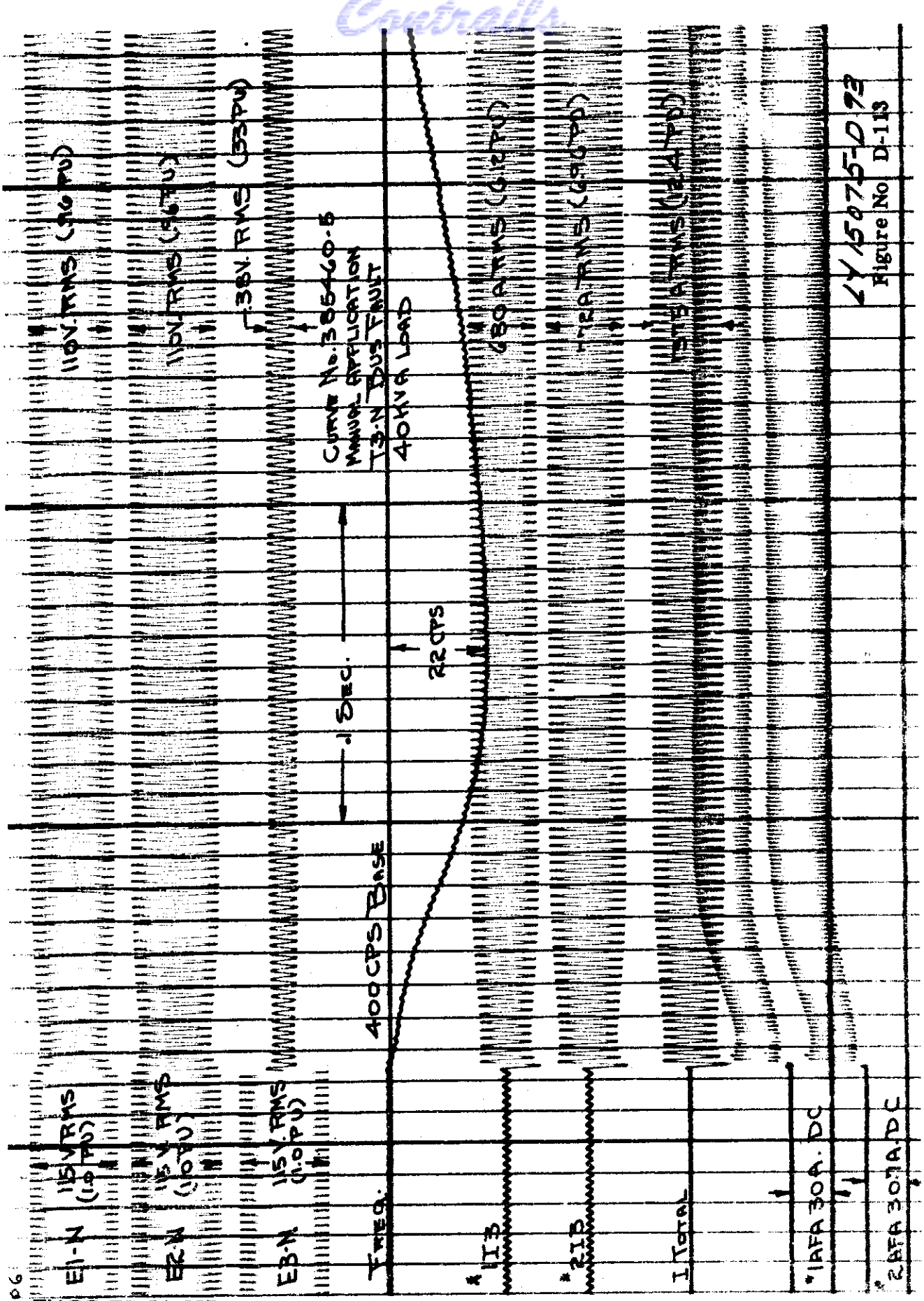

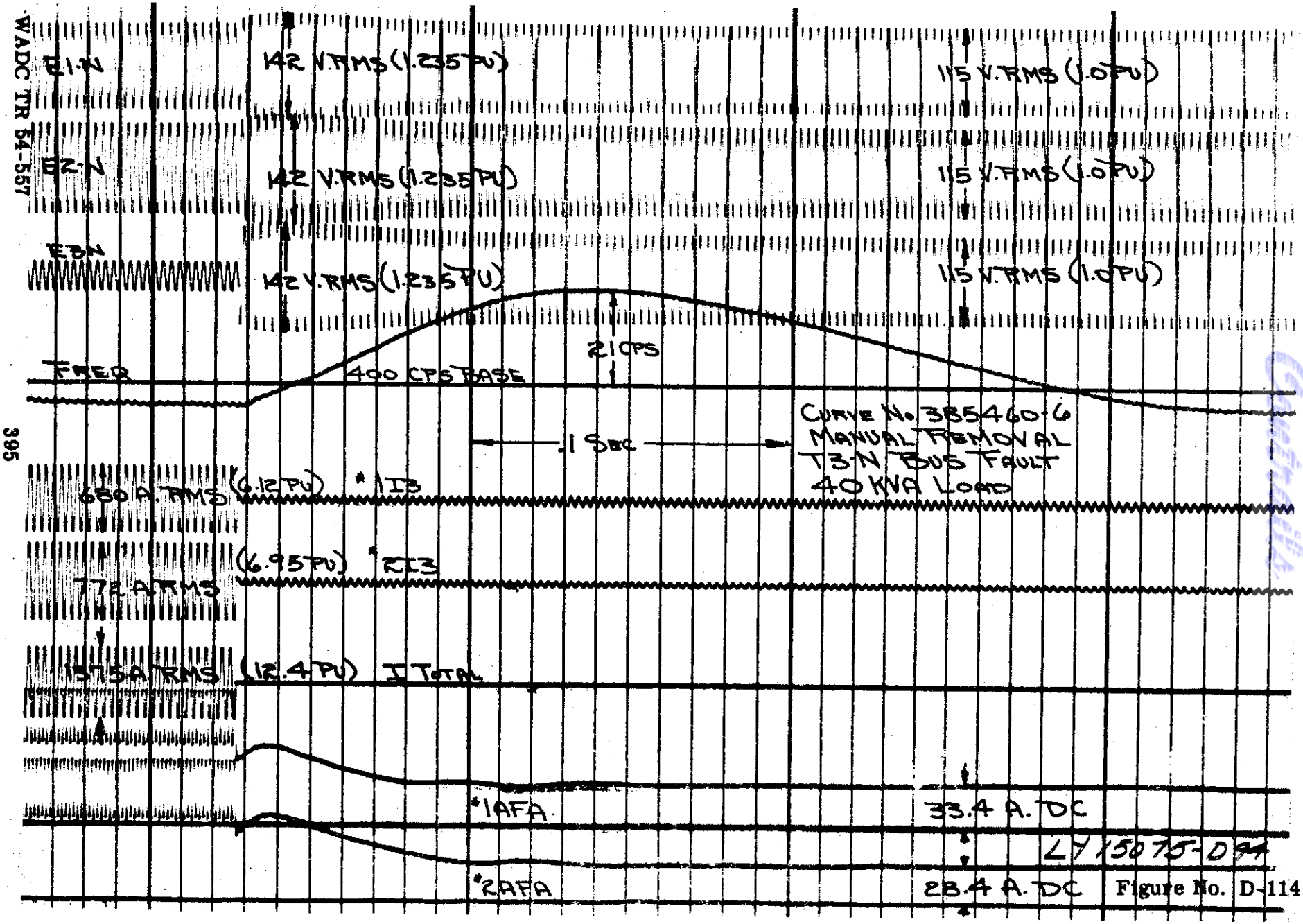

Figure No. D-114

4Y 19675-A 95
FIGURE NO. D-115

Figure No. D-117

4Y1507F-047

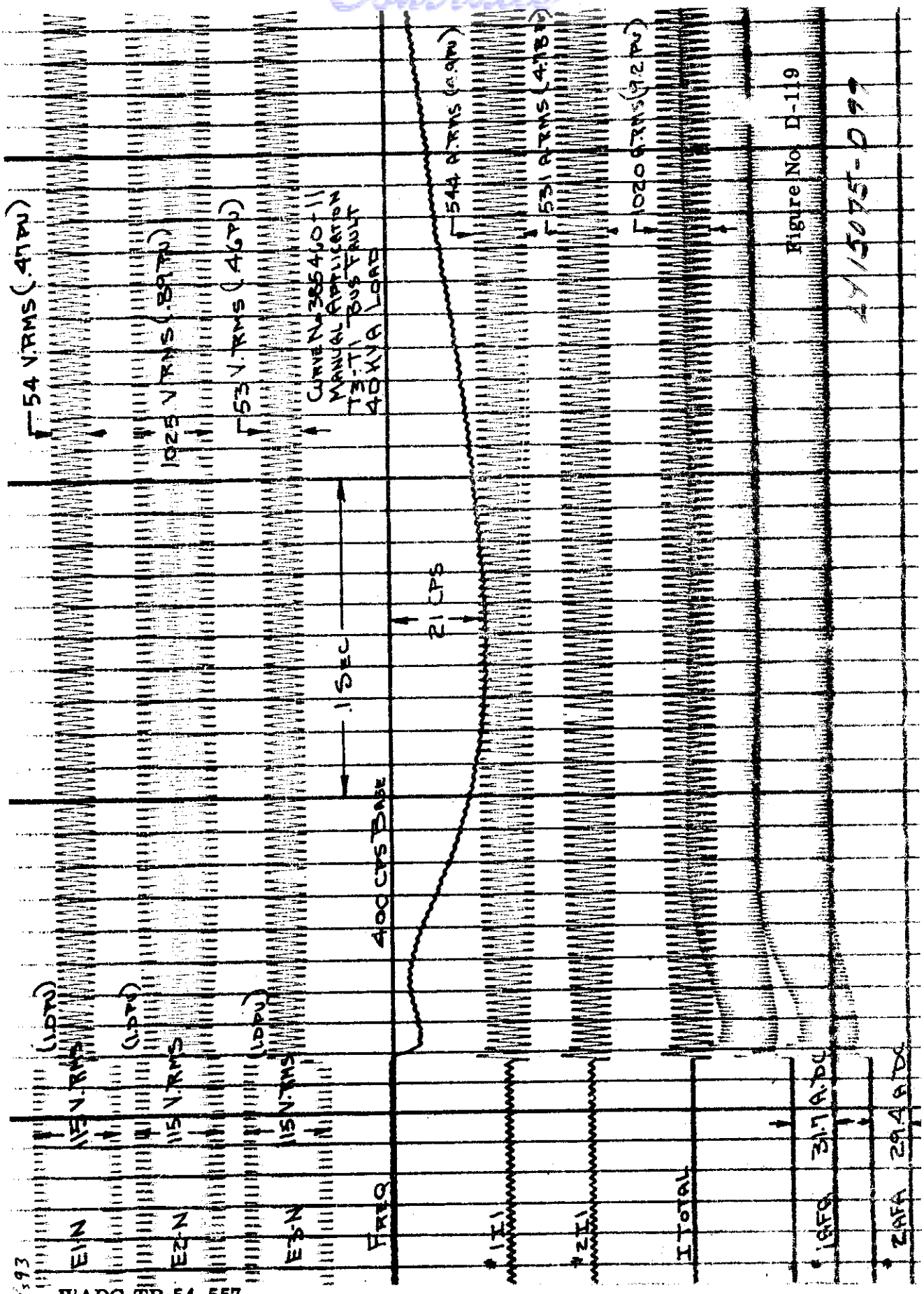

Figure No. D-119

4/1/54 T-D 99

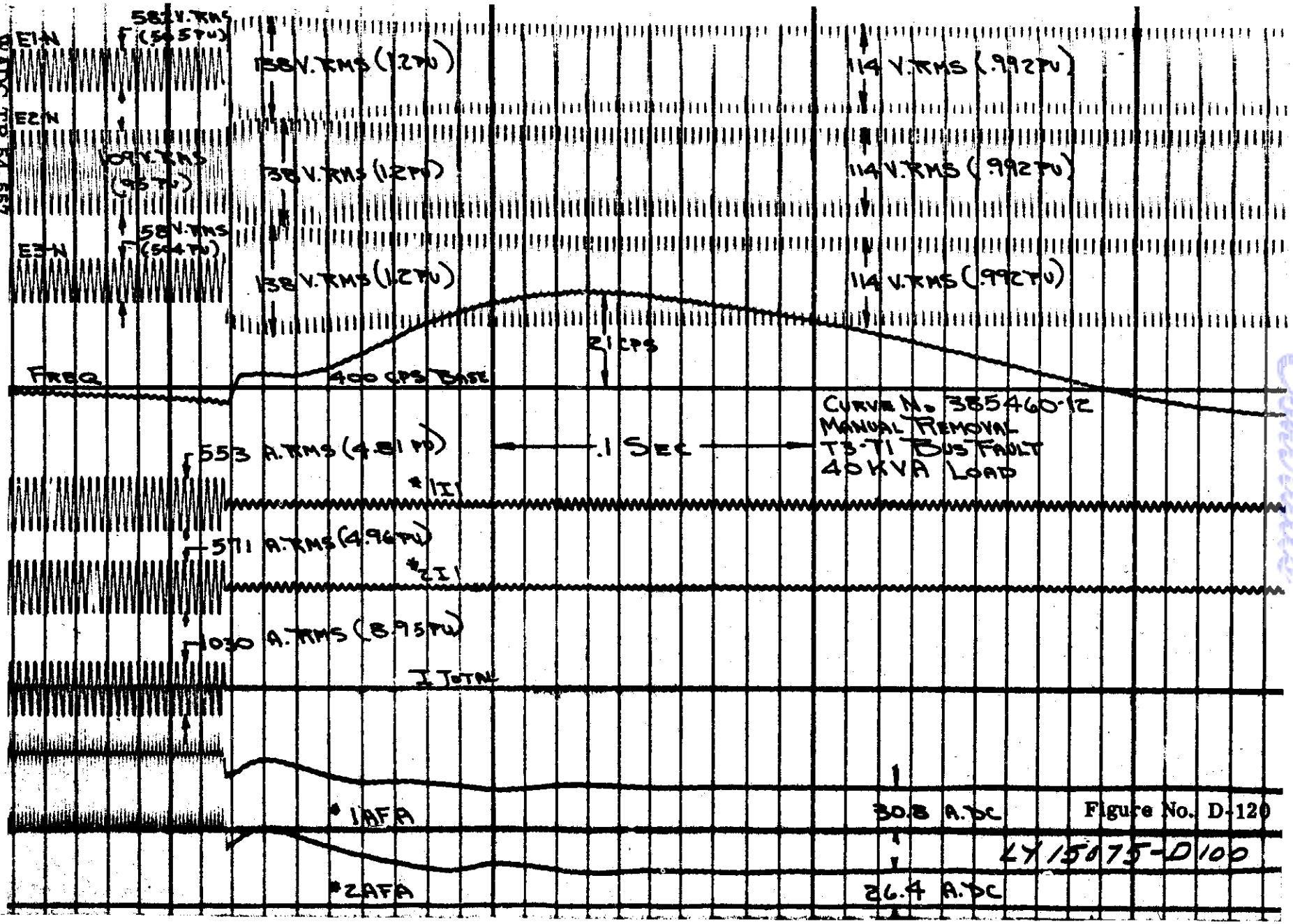

Figure No. D-120

LY15075-D100

401

Figure No. D-121

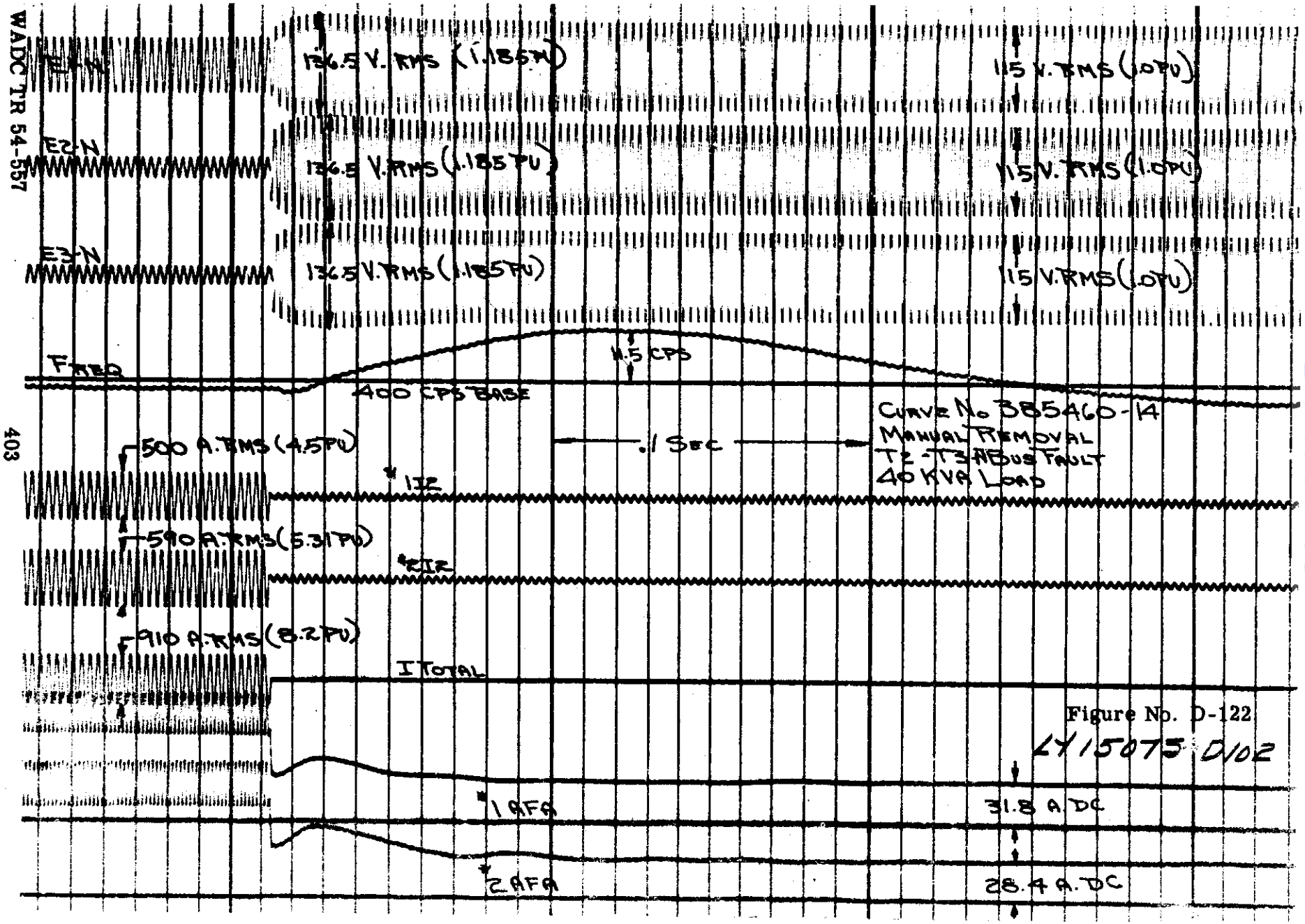

Figure No. D-122

LY15075 D102

Figure No. D-123

17 15075-D103

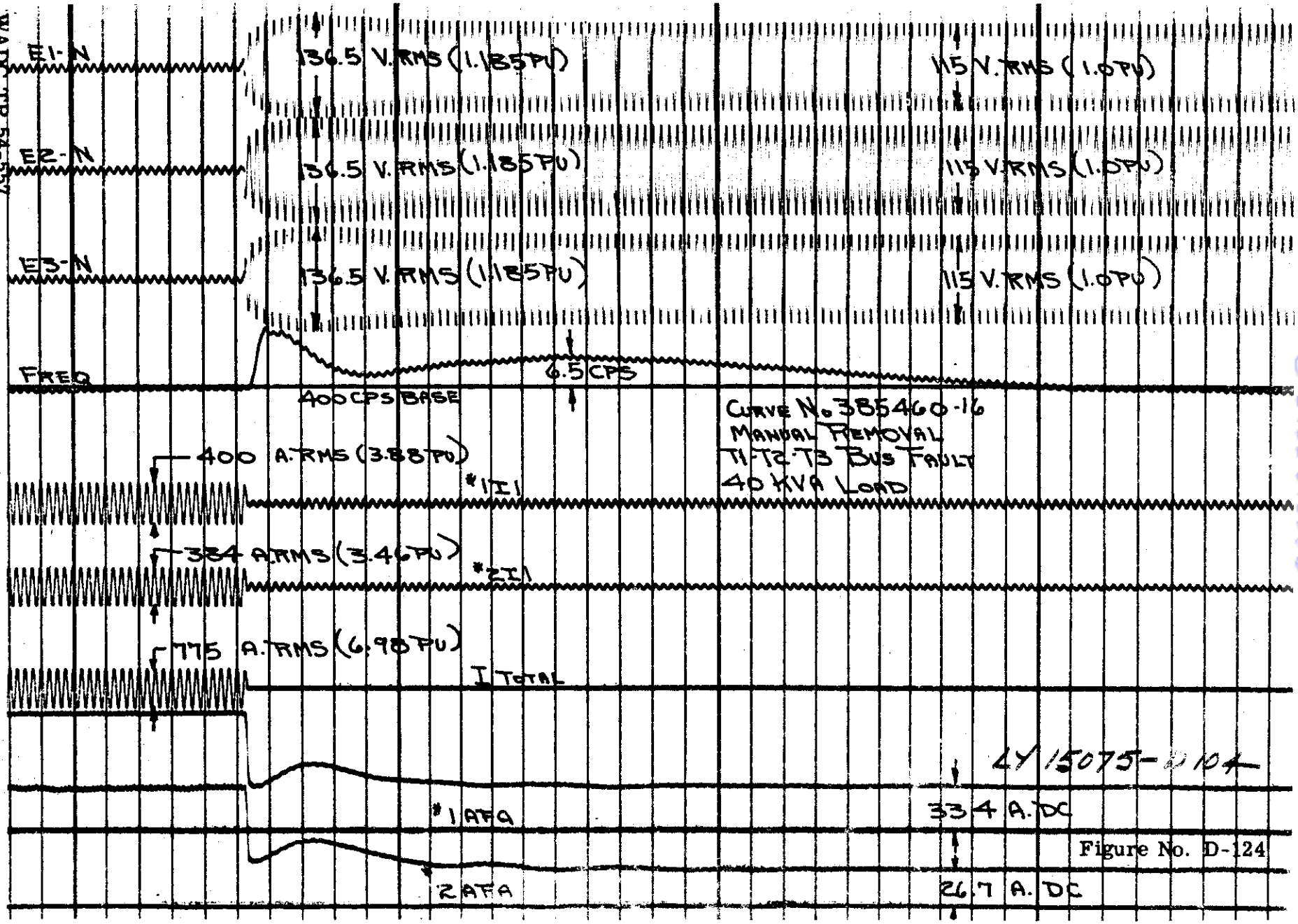

Figure No. D-124

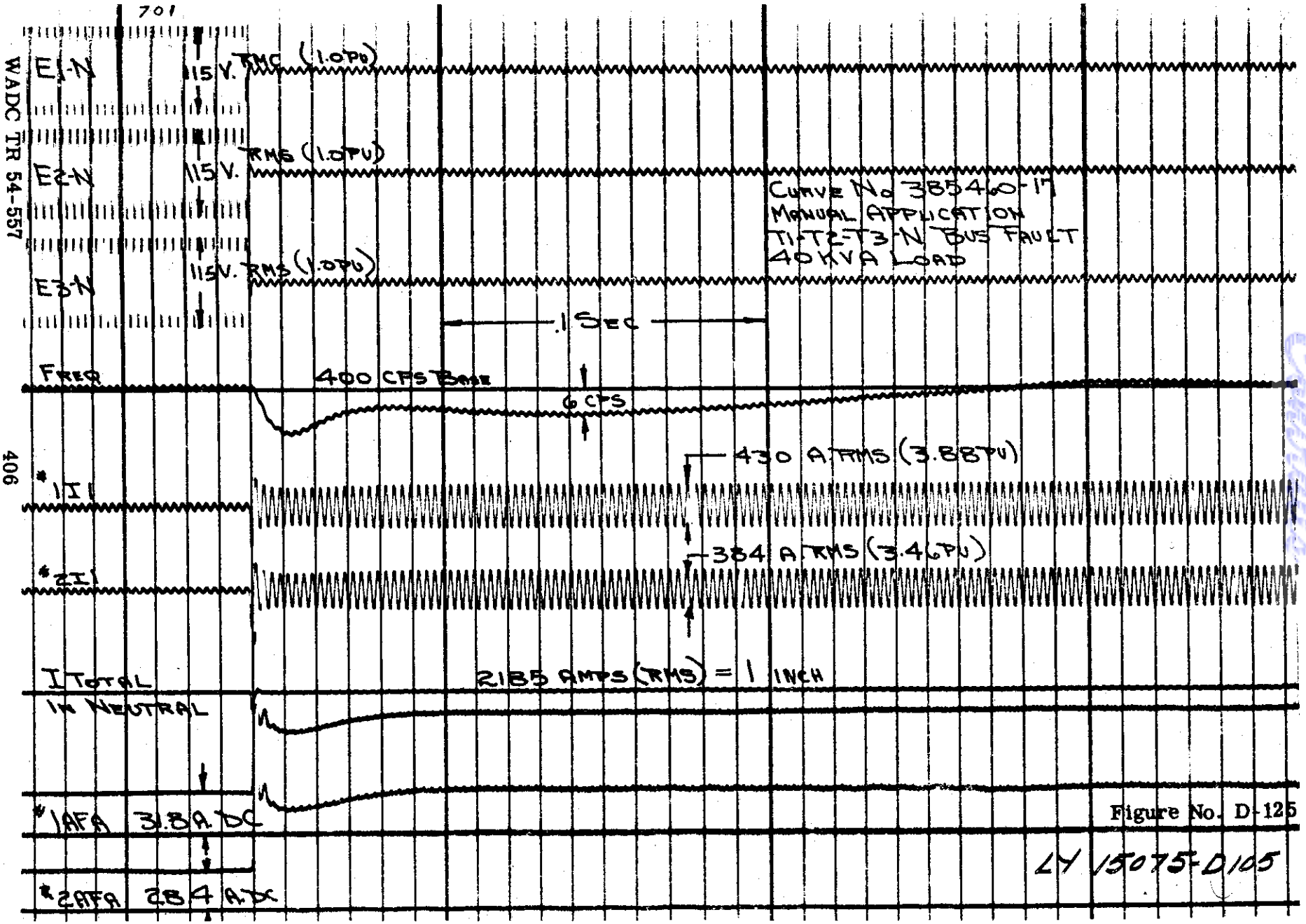

Figure No. D-125

LY 15075-D105

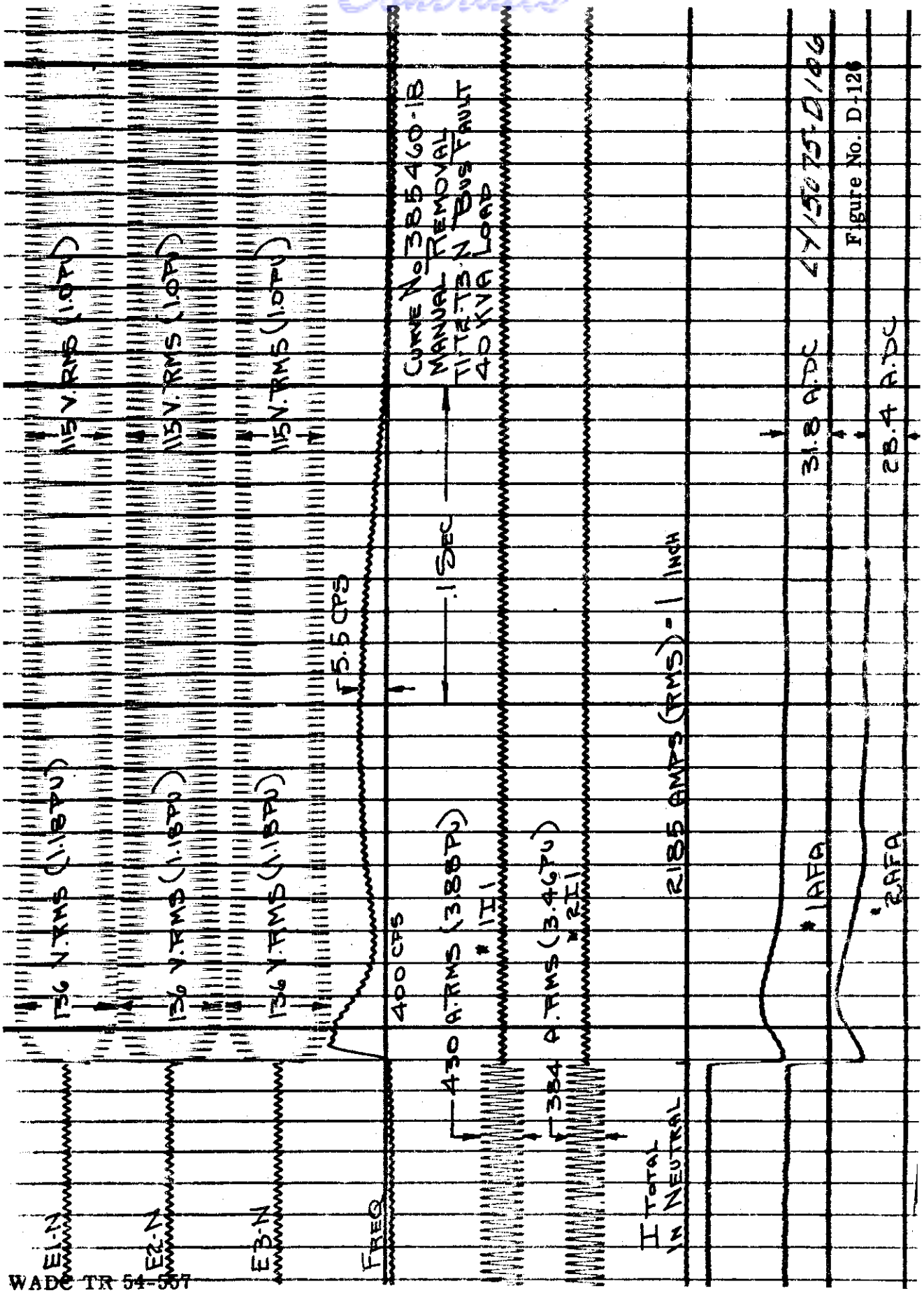

Figure No. D-126

APPENDIX E

A-C SYSTEM SURVEY

E-1 INTRODUCTION

A study of a-c machine characteristics for aircraft electric systems would be broadened if the electric system performance requirements could be determined. A questionnaire was circulated to air-frame manufacturers, utilization equipment and systems manufacturers, commercial airlines and branches of the military service.

The questionnaire was prepared using military specifications MIL-E-7894 and MIL-G-6099 for reference. Where possible, the requirements were broadened by adding certain detail questions covering requirements not presently included in the specifications. The questionnaire covered the 400-800 cps, single-generator system, 380-420 cps, single-generator system and the 380-420 cps, parallel a-c generator system.

E-2 DISCUSSION OF THE A-C SYSTEM SURVEY

Fifteen questionnaires were answered, and the number of returned questionnaires per category were:

Air-Frame Manufacturers	7
Utilization Manufacturers	3
Commercial Airlines	3
Military Services	2

The answers received from the commercial airlines are not included in the survey summary because the response indicated very little experience with a-c electric power. The Navy indicated more interest in the 380-420 cps a-c power system than the 400-800 cps a-c power system.

The response of the aircraft industry was not sufficient to consider the results of the survey to be conclusive. About 15 per cent of the questionnaires sent out were returned. In an effort to maximize the value of the survey, the answers to the questions will be broken into three parts; the answer indicated by the air-frame manufacturer, by the utilization equipment or system manufacturer and by the power equipment or

system manufacturer. The questions will be listed as originally sent out in the survey, with the answers after each question identified by:

A - Air-frame Manufacturers
B - Utilization Equipment or System Manufacturers
C - Power Equipment or System Manufacturers

E-3 A-C SYSTEM QUESTIONNAIRE

1.0 Record:

Name
Title
Company Affiliation
Address
Interview Date
Interviewed by
Date

1.1 In preparing this questionnaire reference to MIL-G-6099 and MIL-E-7894 is used. It is requested the above specifications be used as references when making replies.

2.0 115/200 Volt, Three Phase, 400/800 CPS
Single Generator A-C System

2.1 Voltage Regulation

2.1.1 MIL-E-7894 (Para. 4.7) permits 115 ± 5 volts regulation.
Satisfactory .....Your requirement ±..... volts.

A. Satisfactory
B. Satisfactory
C. Satisfactory

2.1.2 Figure 1 (Curves B and C) defines the normal switching transients.
Satisfactory ..... Your requirement (Add to curve)

A. Satisfactory
B. Satisfactory
C. Satisfactory

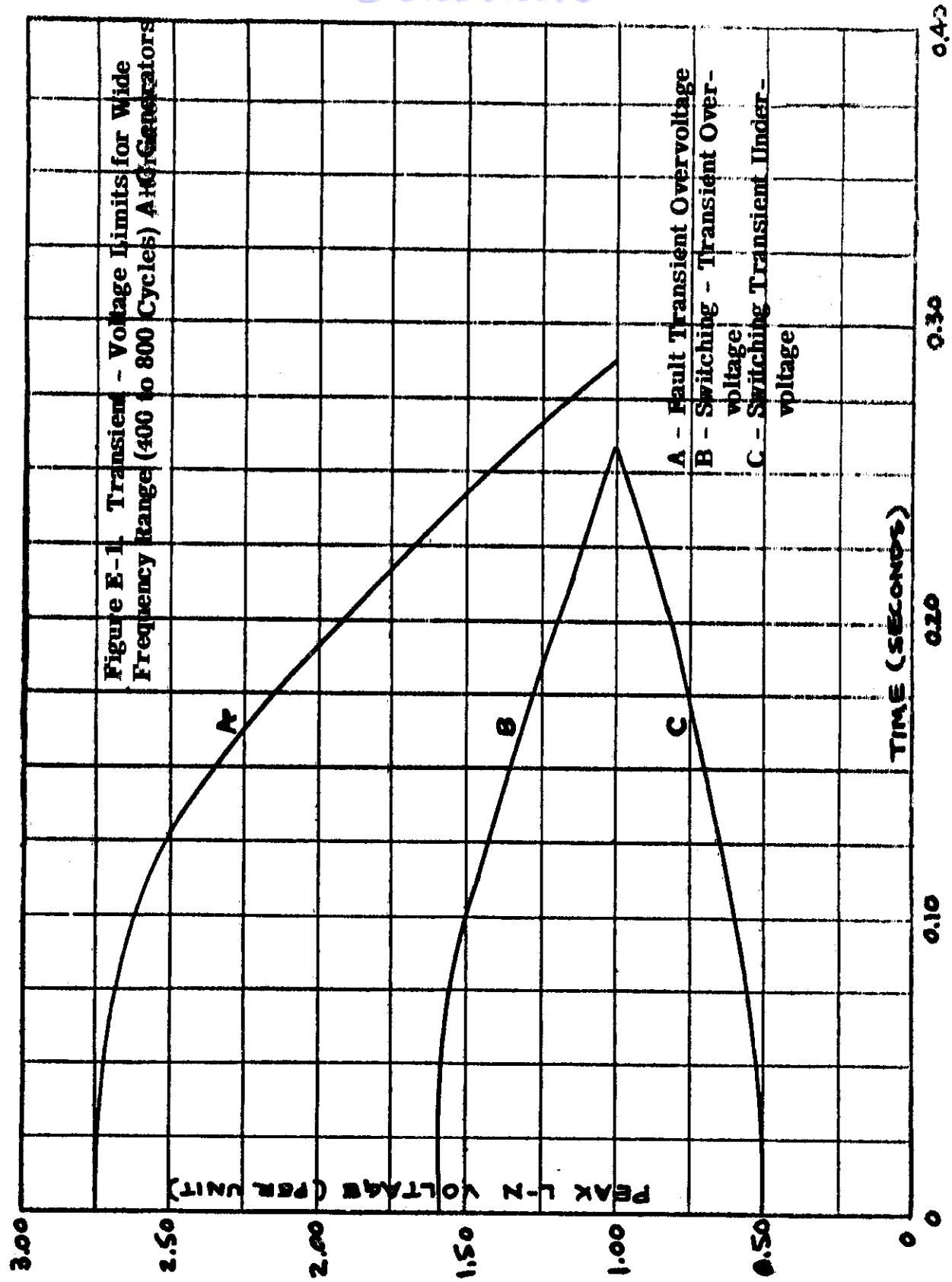

2.1.3 Figure 1 (Curve A) defines the maximum fault transient overvoltage.
Satisfactory ..... Your requirement (Add to curve)

A. Satisfactory
B. Satisfactory
C. Satisfactory

2.2 Voltage Unbalance

2.2.1 MIL-E-7894 (Para. 3.2.1.2.2) permits 4 percent voltage unbalance.
Satisfactory ..... Your requirement ..... percent.

A. Satisfactory
B. Satisfactory
C. Satisfactory

2.2.2 For your answer in 2.2.1 what loads are used.
Three Phase ..... percent rated
Single Phase ..... percent rated
Power Factor ..... percent for 3 phase
Power Factor ..... percent for 1 phase

A. No answer indicated
B. No answer indicated
C. Requirements of MIL-E-7894 and MIL-G-6099 should be used except 2/3 rated single-phase load should not be required in meeting four percent voltage unbalance.

2.3 Voltage Phase Displacement

2.3.1 MIL-E-7894 (Para. 3.2.1.2.4) specified the angle between fundamental phase voltage shall be within the limits of 115 to 125 degrees.
Satisfactory ..... Your requirement

A. Satisfactory
B. Satisfactory
C. Satisfactory

2.3.2 For your answer in 2.3.1 what loads are used.
Three Phase ..... percent rated
Single Phase ..... percent rated
Power Factor ..... percent for 3 phase
Power Factor ..... percent for 1 phase

A. No answer indicated.
B. No answer indicated
C. Should be specified within the requirements of MIL-G-6099.

2.4 Wave Form

2.4.1 MIL-E-7894 (Para. 3.2.1.2.5) specified the phase voltage wave form shall be within the following limits:

1. Amplitude factor: 1.41 ± 0.14
2. Harmonic content: 5 percent of fundamental

Satisfactory ..... Your requirement .....

A. No answer indicated
B. No answer indicated
C. Amplitude factor: $1.41 \pm .05$
Harmonic content: The root mean square of all harmonic percentages referred to the fundamental should not exceed two percent.

2.4.2 For your answer in 2.4.1, what percent of system load would be rectifier loads (electronic or power rectifiers).
Three phase rectifiers ..... percent
Single phase rectifiers ..... percent

A. No answer indicated
B. Approximately 35 percent of utilization-equipment load is a single-phase rectifier load. No three-phase rectifier load indicated.
C. No answer indicated

2.5 Amplitude Modulation

2.5.1 MIL-E-7894 (Para. 3.2.1.2.6) requires the amplitude modulation shall not exceed 2 percent at any frequency.
Satisfactory ..... Your requirement ..... percent

A. The frequency of modulation should be specified as well as the amplitude of the modulation.
B. No answer indicated
C. Both air-frame and utilization manufacturers have indicated a requirement for specifying the frequency of voltage modulation, as well as the amplitude of voltage modulation.

2.6 Fault Conditions

2.6.1 Three Phase Symmetrical Short Circuits -
MIL-E-7894 and MIL-G-6099 does not specify the short circuit capacity of an a-c generator and voltage regulator. A-C machines designed to meet 400/800 cps frequency range usually have a minimum short circuit capacity of 250 percent rated load current measured at minimum rated speed, at approximately 25 degrees centigrade ambient and at sea level conditions.
Satisfactory ..... Your requirement ..... percent

A. No answer indicated
B. Satisfactory
C. Satisfactory

2.6.1.1 The equipment referenced in paragraph 2.6.1 will supply 250 percent short circuit current for 5 seconds.
Satisfactory ..... Your requirement ..... seconds

A. No answer indicated
B. Satisfactory
C. Satisfactory

2.6.1.2 The test for short circuit capacity should be measured at the terminals of the a-c generator. The terminal voltage (measured line to line) should not exceed 25 volts during the test.
Satisfactory ..... Your requirement ..... volts
(Zero fault impedance is not obtainable)

A. No answer indicated
B. Satisfactory
C. Satisfactory

2.7 Overloads

2.7.1 MIL-G-6099 (Para. 4.5.3.2) specifies that the generator shall demonstrate its ability to produce overloads in ambients of 15 to 40 degrees Centigrade at 115 percent minimum rated speed.

Load	Time
150 percent	5 minutes
200 percent	5 seconds

Satisfactory ..... Your requirements .....

A. Satisfactory
B. No answer indicated
C. Satisfactory

2.8 System Impedance

2.8.1 Do you consider a-c generator feeder impedance when evaluating faults and fuse co-ordination.

A. Mainly considered by manufacturers of large aircraft
B. Do not consider
C. Mainly considered by manufacturers of large aircraft

2.8.2 If the answer is yes in 2.8.1, what values are representative.

Z_1 (Pos. Sequence) ..... Ohms
Z_2 (Neg. Sequence) ..... Ohms
Z_0 (Zero Sequence) ..... Ohms
Frequency Base ..... CPS

(Give answer in R + JX form)

A. No answer indicated. Depends on size of aircraft.
B. No answer indicated
C. On aircraft with long a-c generator feeders, the impedance is important in determining the fault-clearing capabilities of the a-c generator. The short-circuit capacity of an a-c generator to be used on long feeder may need to be greater than one used on a relatively short feeder.

2.9 System Capacity

2.9.1 On initial aircraft design, what percent of system capacity is actual average load? ..... percent.

A. No answer indicated
B. No answer indicated
C. No answer indicated

2.9.2 What percent of actual average load would be motor loads? ..... percent. What types predominate?

A. No answer indicated
B. No answer indicated
C. No answer indicated

2.9.3 What percent of actual average load would be rectifier loads? ..... percent.

A. No answer indicated
B. No answer indicated
C. No answer indicated

2.9.4 What minimum lagging power factor would be representative of your requirements?

A. No answer indicated
B. No answer indicated
C. .75 power factor seems to cover all needs.

2.10 Additional Comments or Questions on 400/800 CPS A-C Systems.

A. None given
B. None given
C. It appears that very little general consideration is being given to the 400/800 cps, a-c system.

3.0 115/200 Volt, Three Phase, 380/420 CPS, Single Generator and Parallel Generator A-C System

3.1 Voltage Regulation

3.1.1 MIL-E-7894 (Para. 4.7) permits 115 ± 5 volts regulation.
Satisfactory ..... Your requirement ± ..... volts.

A. Average requirement about ± 2.5 percent regulation. ± 1.5 percent regulation would cover all requirements.
B. Satisfactory. ± 1 volt was minimum indicated.
C. ± 2 percent appears to cover the majority of requirements made. ± 1 volt has been requested.

3.1.2 Figure 2 (Curves B and C) defines the normal switching transients.
Satisfactory ..... Your requirement (Add to curve)

A. Satisfactory
B. Satisfactory
C. Satisfactory

3.1.3 Figure (Curve A) defines the maximum fault transient overvoltage.
Satisfactory ..... Your requirement (Add to curve)

A. Satisfactory
B. Satisfactory
C. Satisfactory

3.2 Voltage Unbalance

3.2.1 MIL-E-7894 (Para. 3.2.1.2.2) permits 4 percent voltage unbalance.
Satisfactory ..... Your requirement ..... percent.

A. Satisfactory
B. No answer indicated
C. Satisfactory

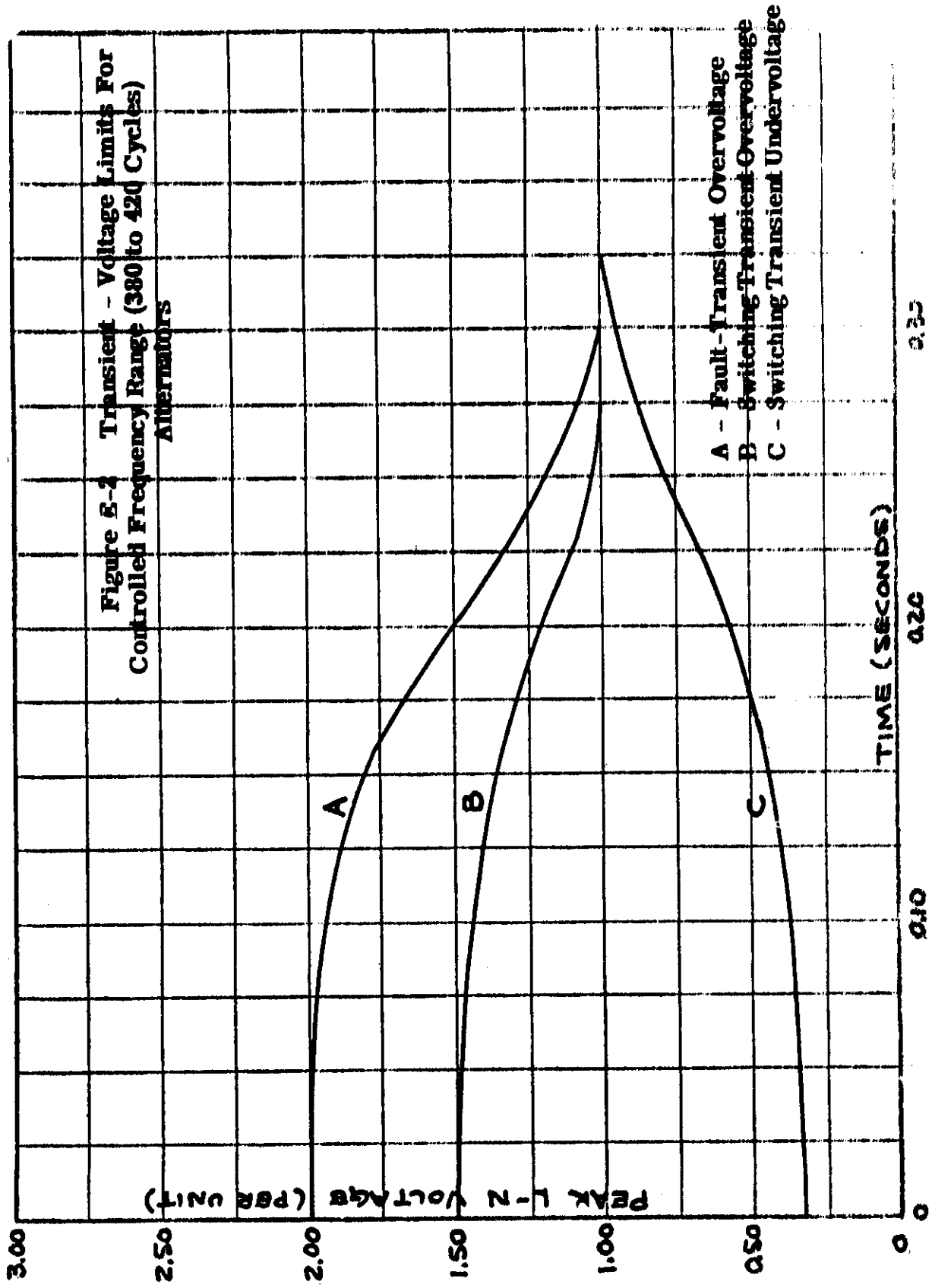

Figure 5-4 Transient - Voltage Limits For Controlled Frequency Range (380 to 420 Cycles) Alternators

3.2.2 For your answer in 3.2.1 what loads are used.
Three Phase ..... percent rated
Single Phase ..... percent rated
Power Factor ..... percent for 3 phase
Power Factor ..... percent for 1 phase

A. Satisfactory
B. No answer indicated
C. Requirements of MIL-E-7894 and MIL-G-6099 should be used except 2/3 rated single-phase load should not be required in meeting 4 percent voltage unbalance.

3.3 Voltage Phase Displacement

3.3.1 MIL-E-7894 (Para. 3.2.1.2.4) specified the angle between fundamental phase voltage shall be within the limits of 115 to 125 degrees.
Satisfactory ..... Your requirement .....

A. Satisfactory
B. Satisfactory
C. Satisfactory

3.3.2 For your answer in 3.3.1, what loads are used.
Three Phase ..... percent rated
Single Phase ..... percent rated
Power Factor ..... percent for 3 phase
Power Factor ..... percent for 1 phase

A. No answer indicated
B. No answer indicated
C. Should be specified within the requirements of MIL-G-6099.

3.4 Wave Form

3.4.1 MIL-E-7894 (Para. 3.2.1.2.5) specified the phase voltage wave form shall be within the following limits:
1. Amplitude factor: 1.41 ± 0.14
2. Harmonic content: 5 percent of fundamental

Satisfactory ..... Your requirement .....

A. Amplitude factor: 1.41 ± .05.
Harmonic Content: The root mean square of all harmonics percentages referred to the fundamental should not exceed 2 percent.

B. No answer indicated

C. Amplitude factor: 1.41 ± .05.
Harmonic Content: The root mean square of all harmonics percentages referred to the fundamental should not exceed 2 percent.

3.4.2 For your answer in 3.4.1, what percent of system load would be rectifier loads (electronic or power rectifiers).
Three phase rectifiers ..... percent
Single phase rectifiers ..... percent

A. 10-20 percent indicated for three-phase rectifiers.
3-5 percent indicated for single-phase rectifiers.

B. No answer indicated for three-phase rectifiers.
30-50 percent indicated for single-phase rectifiers.

C. Have not determined a value.

3.5 Amplitude Modulation

3.5.1 MIL-E-7894 (Para. 3.2.1.2.6) requires the amplitude modulation shall not exceed 2 percent at any frequency.
Satisfactory ..... Your requirement ..... percent.

A. Need maximum amplitude of 1 percent.

B. Satisfactory

C. Both air-frame and utilization manufacturers have indicated a requirement for specifying the frequency of voltage modulation, as well as the amplitude of modulation.

3.6 Fault Conditions

3.6.1 Three Phase Symmetrical Short Circuit
MIL-E-7894 and MIL-G-6099 does not specify the short circuit capacity of an a-c generator and voltage regulator. A-C machines designed to meet 380/420 cps frequency range usually have a minimum short circuit capacity of 300 percent rated load measured at minimum rated speed, at approximately 25 degrees centigrade ambient and at sea level conditions.
Satisfactory ..... Your requirement ..... percent.

A. Satisfactory
B. Satisfactory
C. Satisfactory

3.6.1.1 The equipment referenced in paragraph 3.6.1 will supply 300 percent short circuit current for 5 seconds.
Satisfactory ..... Your requirement ..... seconds.

A. Satisfactory
B. Satisfactory
C. Satisfactory

3.6.1.2 The test for short circuit capacity should be measured at the terminals of the a-c generator. The terminal voltage (measured line to line) should not exceed 25 volts during the test.
Satisfactory ..... Your requirement ..... volts.
(Zero fault impedance is not obtainable)

A. Satisfactory
B. Satisfactory
C. Satisfactory

3.7 MIL-G-6099 (Para. 4.5.3.2) specified that the generator shall demonstrate its ability to produce overloads in ambients of 15 to 40 degrees centigrade of 115 percent minimum rated speed. We believe conformance should be shown at nominal rated speed.

Load	Time
150 percent	5 minutes
200 percent	5 seconds

Satisfactory ..... Your requirement .....

A. Believe the overload rating should be specified at a minimum rated speed.
B. Satisfactory
C. Satisfactory

3.8 System Impedance

3.8.1 Do you consider a-c generator feeder impedance when evaluating faults and fuse co-ordination.

A. Yes
B. No
C. More important on large aircraft than on small aircraft.

3.8.2 If the answer is yes in 3.8.1, what values are representative.
Z_1 (Pos. Sequence) ..... Ohms
Z_2 (Neg. Sequence) ..... Ohms
Z_3 (Zero Sequence) ..... Ohms
Frequency Base ..... Ohms
(Give answer in R + JX form)

A. No answer indicated
B. No answer indicated
C. On aircraft with long a-c generator feeders, the impedance is important in determining the fault-clearing capabilities of the a-c generator. The short-circuit capacity of an a-c generator to be used on long feeder may need to be greater than one used on a relatively short feeder.

3.9 System Capacity

3.9.1 On initial aircraft design, what percent of system capacity is actual average load? ..... percent.

A. Fifty percent
B. No answer indicated
C. Forty percent

3.9.2 What percent of actual average load would be motor loads? ..... percent. What types predominate?

A. Fifty percent. No answer given as to type.
B. Thirty-Forty percent. No answer given as to type.
C. Have not determined an answer.

3.9.3 What percent of actual average load would be rectifier loads? ..... percent.

A. Fifteen-twenty-five percent.
B. Forty-fifty percent of equipment load.
C. Twenty-five to thirty-five percent where transformer - rectifiers are used to obtain d-c power.

3.9.4 What minimum lagging power factor would be representative of your requirements?

A. .75 power factor lagging.
B. .75 to .90 lagging power factor.
C. .75 lagging power factor to .95 leading power factor should be specified.

3.10 Frequency

3.10.1 Should the frequency for the parallel a-c system be specified as 380/420 CPS?
Satisfactory ..... Your requirement .....

A. Satisfactory
B. Satisfactory
C. Satisfactory

3.10.2 What frequency recovery time should be specified for the parallel a-c system after 50 percent system load change?

A. The requirements indicated ranged from 0.1 seconds to 1.2 seconds.
B. The requirements indicated ranged from 0.3 seconds to no frequency change.
C. The requirement must vary with rating of the drive-generator combination. No definite values have been determined as yet.

3.10.3 What maximum or minimum frequency change should be allowed when 50 percent system load change is applied or removed from the system?

A. The requirements indicated ranged from a maximum of 5 cps to a maximum of 40 cps.
B. The requirements indicated ranged from no frequency change to a maximum of 20 cps.
C. No definite values have been determined.

3.11 For Parallel Systems Only

3.11.1 Kilowatt Load Division

3.11.1.1 What should be the permissible steady state kilowatt load unbalance between any two a-c generators in a parallel a-c system?

A. Ten percent of a single a-c generator capacity
B. No answer indicated
C. Have not determined a definite requirement. Would recommend maximum unbalance in kilowatt load not exceed 20 percent of a single a-c generator rating.

3.11.1.2 What should be the recovery time allowed for kilowatt load division to become stabilized?

A. One second
B. No answer indicated
C. Should be greater than the value specified for frequency recovery.

3.11.2 Reactive Load Division

3.12.2.1 What should be the permissible steady state kilovar load unbalance between any two a-c generators in a parallel a-c system?

A. Ten percent of a single a-c generator capacity.
B. No answer indicated
C. The unbalance in kilovar load not exceed 20 percent of single a-c generator rating.

3.12.2.2 What should be the recovery time allowed for kilovar load division to become stabilized?

A. The requirements indicated ranged from 0.1 second to 1.0 second.
B. No answer indicated
C. .5 second should be satisfactory.

3.13 Auto Paralleling

3.13.1 Do you believe auto-paralleling is needed on the parallel a-c system?

A. Yes, particularly where crew members are limited.
B. No answer indicated
C. Yes. Present manual paralleling methods cannot produce performance, frequency and voltage, equal to that when an auto-paralleling relay is used.

3.13.2 If auto-paralleling is used should the maximum frequency and voltage changes at paralleling be limited to that obtain when 100 percent system load is applied?
Satisfactory ..... Your requirement .....

A. Satisfactory, but lesser system disturbance desirable.
B. No answer indicated
C. Since the question was written, it has been proven that auto-paralleling can be accomplished with a lesser transient. The lesser system transient is desirable.

3.14 Additional Comments or Questions on 380/420 CPS a-c systems.

The following are the detailed comments as taken from the survey:

A. 1. Frequency modulation should not exceed 0.5 percent.
2. Increase machine capacity with no blast air (120-degree C machines).

B. It is becoming more and more essential in present day electronic computers, etc. that precise frequency supplies be incorporated in aircraft. Rate finding devices are dependent on precise frequencies, and are being used in our equipment as well as many armament systems. MIL-E-7894, paragraph 3.3.1.2 states that such precise

frequencies will be supplied by utilization equipment. The airframe and power equipment manufacturers are merely postponing the day when 400± 1 or .1 cps supplies of considerable capacities are a common aircraft power source. The development of such supplies will save considerable development and engineering time required of utilization equipment manufacturers.

C. We have two major systems problems: First the electrical performance of an a-c power system and secondly, the cooling system required for any electrical system.

E-4 CONCLUSIONS

Approximately 15 percent of the questionnaires sent out were returned answered. It is concluded from the comments returned that the small percentage of returns was due to:

(1) Many manufacturers of small aircraft such as helicopters and fighters have not used a-c electric power systems as described by the survey and therefore abstained from answering.

(2) Many manufacturers could not justify the engineering time required to answer the survey. We were not permitted to take cognizance of the fact that this was a government study contract.

Therefore the results of the survey can not be considered conclusive because of limited coverage.

Detailed conclusions have been formulated for each question presented in the survey. The conclusions identified by "C" after each question does not signify the state of the engineering art with respect to a-c electric power systems but is added so another viewpoint might broaden the results. The broader conclusions that are indicated by the survey are:

(1) The manufacturers of large airframes are more interested in a-c electric power systems than the manufacturers of small airframes.

(2) There is more interest in and need for the 380/420-cps, a-c power system than the 400/800-cps, a-c power system.

(3) There are many divergent opinions on detail requirements for a-c power systems, but much agreement is found if the requirement is in MIL-E-7894 or MIL-G-6099.

It is recommended that the specifications made available to the airframe industry be studied, first, from an electric-system viewpoint; second, from the power, distribution, and utilization system viewpoint, and then supported by detail apparatus specifications.

APPENDIX F

GLOSSARY OF DEFINITIONS AND SYMBOLS

Unless otherwise indicated in the report, the following definitions and symbols will apply. The definitions are all taken from the American Standard Definitions of Electrical Terms, AIEE, ASA C42-1941.

F-1 A-C GENERATOR

Direct Axis

The direct axis is the axis of magnetization of the main field winding usually coinciding with the polar axis.

Quadrature Axis

The quadrature axis is the interpolar axis.

Direct-Axis Voltage

A direct-axis voltage is a voltage generated by a flux in the direct axis.

Quadrature-Axis Voltage

A quadrature-axis voltage ia a voltage generated by a flux in the quadrature axis.

Direct-Axis Component of Armature Current

A direct-axis component of armature current is one which magnetizes in the direct axis.

Quadrature-Axis Component of Armature Current

A quadrature-axis component of armature current is one which magnetizes in the quadrature axis.

Air-Gap Line

The air-gap line is the extended straight line portion of the no-load saturation curve.

Short-Circuit Ratio (SCR)

The short-circuit ratio is the ratio of the field current for rated open-circuit armature voltage and rated frequency to the field current for rated armature current on sustained symmetrical short-circuit at rated frequency.

Direct-Axis Synchronous Reactance (x_d)

The direct-axis synchronous reactance is the ratio of the fundamental component of reactive armature voltage, due to the fundamental direct-axis component of armature current, to this component of current under balanced steady-state conditions and at rated frequency.

Unless otherwise specified the value of synchronous reactance will be that corresponding to the rated armature current.

Synchronous Impedance

The per-unit direct-axis synchronous impedance equals the ratio of the field current at rated armature current on sustained symmetrical short-circuit to the field current at normal open-circuit voltage on the air-gap line. (Note: This definition of synchronous impedance is used to a great extent in electrical literature and corresponds to the definition of direct-axis synchronous reactance as determined from open-circuit and sustained short-circuit tests.)

Direct-Axis Transient Reactance (x'_d)

The direct-axis transient reactance is the ratio of the fundamental component of reactive armature voltage, due to the fundamental direct-axis alternating-current component of the armature current, to this component of current under suddenly applied load conditions and at rated frequency, the value of current to be determined by the extrapolation of the envelope of the alternating-current component of the current wave to the instant of the sudden application of load, neglecting the high-decrement currents during the first few cycles.

The rated current value of the direct-axis transient reactance will be that obtained from a three-phase sudden short-circuit test at the terminals of the machine at no-load and rated speed, and with an initial voltage such as to give a transient value of short-circuit current plus the sustained value

equal to the rated current, neglecting the high-decrement current during the first few cycles. This requirement means that the test voltage (per-unit) is equal to the rated current value of transient reactance (per-unit). In actual practice, the test voltages will seldom result in transient currents of exactly the rated value, and it will usually be necessary to determine the rated current value of transient reactance from a curve of reactances plotted against voltage.

The rated voltage value of the direct-axis transient reactance will be that obtained from a three-phase sudden short-circuit test at the terminals of the machine at no-load and rated armature voltage. (Note: Refer to Anderson's paper on voltage dips for the concept of the rated current value of the direct-axis transient reactance.)

Direct-Axis Subtransient Reactance (x''_d)

The direct-axis subtransient reactance is the ratio of the fundamental component of reactive armature voltage, due to the initial value of the fundamental direct-axis component of the alternating-current component of the armature current, to this component of current under suddenly applied load conditions and at rated frequency.

The rated current value of direct-axis subtransient reactance will be that obtained from the tests for the rated current value of direct-axis transient reactance.

The rated voltage value of direct-axis subtransient reactance will be that obtained from a short-circuit test at the terminals of the machine at no-load and rated speed and at rated armature voltage.

Quadrature-Axis Synchronous Reactance (x_q)

The quadrature-axis synchronous reactance is the ratio of the fundamental component of reactive armature voltage, due to the fundamental quadrature-axis component of armature current, to this component of current under steady-state conditions and at rated frequency.

Unless otherwise specified, the value of quadrature-axis synchronous reactance will be that corresponding to rated armature current.

Quadrature-Axis Transient Reactance (x'_q)

The quadrature-axis transient reactance is the ratio of the fundamental component of reactive armature voltage, due to the fundamental quadrature-axis component of the alternating-current component of the armature current, to this component of current under suddenly applied load conditions and at rated frequency, the value of current to be determined by the extrapolation of the envelope of the alternating-current component of the current wave to the instant of the sudden application of load, neglecting the high-decrement currents during the first few cycles: (Note: The quadrature-axis transient reactance usually equals the quadrature-axis synchronous reactance except in solid-rotor machines, since in general there is no really effective field current in the quadrature axis.)

Quadrature-Axis Subtransient Reactance (x''_q)

The quadrature-axis subtransient reactance is the ratio of the fundamental component of reactive armature voltage, due to the initial value of the fundamental quadrature-axis component of the alternating-current component of the armature current, to this component of current under suddenly applied balanced load conditions and at rated frequency.

Unless otherwise specified, the quadrature-axis subtransient reactance will be that corresponding to rated armature current.

Negative-Sequence Reactance (x_2)

The negative-sequence reactance is the ratio of the fundamental component of reactive armature voltage, due to the fundamental negative sequence component of armature current, to this component of armature current at rated frequency.

Negative-Sequence Resistance (r_2)

The negative-sequence resistance is the ratio of the fundamental component of in-phase armature voltage, due to the fundamental negative-sequence component of armature current, to this component of current at rated frequency. (Note: This resistance, which forms a part of the negative sequence impedance for use in circuit calculations to establish relationships between voltages and currents, is not directly applicable in the calculations of the total loss in the machine caused by the flow of negative-

sequence currents. This loss is the product of the square of the fundamental component of the negative-sequence current and the difference between twice the negative-sequence resistance and the positive-sequence resistance, i. e. $I_2^2 (2r_2 - r)$.

Zero-Sequence Reactance (x_0)

The zero-sequence reactance is the ratio of the fundamental component of reactive armature voltage, due to the fundamental zero-sequence component of armature current, to this component at rated frequency.

Unless otherwise specified, the value of zero-sequence reactance will be that corresponding to a zero-sequence current equal to rated armature current.

Potier Reactance (x_p)

Potier reactance is a synchronous machine quantity determined from a no-load saturation curve, and a zero power factor (over excited) excitation. It is useful for the calculation of excitation of the machine at other loads and power factors. The excitation results in the range from zero power factor over excited to unity power factor are close enough to the test values for most practical applications. The height of a Potier reactance triangle determines the reactance drop, and the reactance x_p is equal to the reactance drop divided by the current.

Unless otherwise specified, the value of Potier reactance shall be that obtained from the no-load normal frequency saturation curve; and the excitation for rated voltage and current at zero power factor (over excited), and at rated frequency.

Approximate values of Potier reactance may be obtained from test-load excitations at loads differing from rated load, and at power factors other than zero.

Direct-Axis Transient Open-Circuit Time Constant (T'_{do})

The direct-axis open-circuit time constant is the time in seconds required for the rms alternating-current value of the slowly decreasing component present in the direct-axis component of symmetrical armature voltage on open-circuit to decrease to 0.368 of its initial value when the field winding is suddenly short-circuited with the machine running at rated speed.

Direct-Axis Transient Short-Circuit Time Constant (T'_d)

The direct-axis transient short-circuit time constant is the time in seconds required for the rms value of the slowly decreasing component present in the direct-axis component of the alternating-current component of the armature current under suddenly applied symmetrical short-circuit conditions with the machine running at rated speed, to decrease to 0.368 of its initial value.

The rated current value of the direct-axis transient short-circuit time constant will be that obtained from the test for the rated current value of the direct-axis transient reactance.

Direct-Axis Subtransient Open-Circuit Time Constant (T''_{do})

The direct-axis subtransient open-circuit time constant is the time in seconds required for the rapidly decreasing component (negative) present during the first few cycles in the direct-axis component of symmetrical armature voltage under suddenly removed symmetrical short-circuit conditions, with machine running at rated speed, to decrease to 0.368 of its initial value.

Direct-Axis Subtransient Short-Circuit Time Constant (T''_d)

The direct-axis subtransient short-circuit time constant is the time in seconds required for the rapidly decreasing component present during the first few cycles in the direct-axis component of the alternating-current component of the armature current under suddenly applied short-circuit conditions, with the machine running at rated speed decreased to 0.368 of its initial value.

The rated current value of the direct-axis subtransient short-circuit time constant will be that obtained from the test for the rated current value of the direct-axis transient reactance.

The rated voltage value of the direct-axis subtransient short-circuit time constant will be that obtained from the test for the rated voltage value of the direct-axis transient reactance.

Quadrature-Axis Transient Open-Circuit Time Constant (T'_{qo})

The quadrature-axis open-circuit time constant is the time in seconds required for the rms alternating-current value of the slowly decreasing

component present in the quadrature-axis component of symmetrical armature voltage on open-circuit to decrease to 0.368 of its initial value when the quadrature field winding (if any) is suddenly short-circuited with the machine running at rated speed. (Note: This time constant is important only in turbine generators.)

Quadrature-Axis Transient Short-Circuit Time Constant (T'_q)

The quadrature-axis transient short-circuit time constant is the time in seconds required for the rms alternating-current value of the slowly decreasing component present in the quadrature-axis component of the alternating-current component of the armature current under suddenly applied short-circuit conditions with the machine running at rated speed to decrease 0.368 of its initial value.

Quadrature-Axis Subtransient Open-Circuit Time Constant (T''_{qo})

The quadrature-axis subtransient open-circuit time constant is the time in seconds required for the rapidly decreasing component (negative) present during the first few cycles in the quadrature-axis component of symmetrical armature voltage under suddenly removed symmetrical short-circuit conditions with the machine running at rated speed, to decrease 0.368 of its initial value.

Quadrature-Axis Subtransient Short-Circuit Time Constant (T''_q)

The quadrature-axis subtransient short-circuit time constant is the time in seconds required for the rapidly decreasing component present during the first few cycles in the quadrature-axis component of the alternating-current component of the armature current under suddenly applied symmetrical short-circuit conditions, with the machine running at rated speed, to decrease to 0.368 of its initial value.

Short-Circuit Time Constant of Armature Winding (T_a)

The short-circuit time constant of the armature winding is the time in seconds for the asymmetrical (direct-current) component of armature current under suddenly applied short-circuit conditions, with the machine running at rated speed, to decrease to 0.368 of its initial value.

The rated current value of the short-circuit time constant of the armature winding will be that obtained from the test specified for the rated current value of direct-axis transient reactance.

The rated voltage value of the short-circuit time constant of the armature winding will be that obtained from a short-circuit test at the terminals of the machine at no-load and rated speed and at rated armature voltage.

The following symbols are used for the a-c generator:

T'_{dz} - load-circuit transient time constant
K_g - volts generated per volts applied to input (voltage gain of generator
K_t - field current amperes per volt of terminal at no-load
K_S - additional field current amperes per ampere of load-current under zero-power-factor load
i_f - total a-c generator field current
r_f - a-c generator field resistance
x_L - load reactance
i_L - load current (zero-power-factor load)
T_R - system recovery time

F-2 EXCITER

Exciter

An exciter is an auxilary generator which supplies energy for the field excitation of another electric machine.

Exciter Response

The exciter response is the rate of increase or decrease of the main exciter voltage when resistance is suddenly removed from or inserted in the main exciter field circuit.

Note: The response of an exciter may be expressed in volts per second or may be represented by the numerical value obtained by dividing the volts per second by some designated value of voltage, such as the nominal collector ring voltage.

Nominal Exciter Response

The nominal exciter response is defined as the numerical value obtained when the nominal collector ring voltage is divided into the slope, expressed in volts per second, of that straight line voltage-time curve, which begins at nominal collector ring voltage and continues for one-half second, under which the area is the same as the area under the no-load voltage increase-time curve of the exciter starting at the same initial voltage, and continuing for the same length of time.

Exciter Response, k (as used in Chapter II and Appendix B-1)

The exciter response k is similar to the one defined above except that the rate in volts per second is divided by the no-load per-unit collector ring voltage as determined from the air gap line of the a-c generator.

The following symbols are used for the exciter:

e_x --- exciter output voltage
e_o --- exciter residual voltage
K_1 --- generated volts per ampere of shunt field current
K_2 --- generated volts per ampere of equivalent eddy current
K_3 --- generated volts per ampere of series field current
K_x --- generated volts per volts input of exciter (relative exciter gain)
r_1 --- Resistance of shunt field
L_1 --- Inductance of shunt field
T_1 --- Time constant of shunt field (L_1/r_1)
r_2 --- Equivalent resistance of eddy currents circuit
L_2 --- Equivalent inductance of eddy currents circuit
T_2 --- Time constant of eddy currents circuit (L_2/r_2)
M_{2_1}/r_2 --- Mutual time constant between eddy currents circuit and shunt field circuit
i_1 --- exciter shunt field current
i_2 --- exciter eddy current
i_f --- exciter load current (series field)
r_3 --- resistance of exciter armature, brushes and compensating and interpole fields

F-3 VOLTAGE REGULATOR

The following symbols are used for the voltage regulator:

e_c --- Voltage applied to regulator operating coil
$R_{cp}(e_c, i_1)$ --- Resistance of the carbon pile as a function of both e_c and i_1
T_p --- Feedback stabilizing transformer primary time constant
T_t --- Feedback stabilizing transformer mutual time constant
i_c --- Regulator coil current
t_1 --- Effective regulator time delay